AD NUMBER
AD020131
CLASSIFICATION CHANGES
TO: **unclassified**
FROM: **confidential**
LIMITATION CHANGES
TO: **Approved for public release; distribution is unlimited.**
FROM: **Distribution authorized to U.S. Gov't. agencies and their contractors; Administrative/Operational Use; 22 DEC 1952. Other requests shall be referred to Office of Naval Research, Attn: Code 441, Washington, DC.**
AUTHORITY
ONR ltr dtd 15 Augt 1968; ONR ltr dtd 15 Augt 1968

PROGRESS REPORT ON
HIGH ALTITUDE PLASTIC BALLOONS
CONTRACT NONR-710 (01)
JUNE 15, 1952 to DECEMBER 22, 1952
VOLUME V
CONFIDENTIAL SECURITY INFORMATION

Copy No. 5-3

ERRATA SHEET

University of Minnesota
Physics Department

Balloon Project Progress Report No. 2

Volume V

Page II-7 - line 1. Insert the word "center" between "the" and "position".
Page II-7 - line 4. Delete ", the use of the" and insert "a".
Page III-A-10 - line 22. Delete "sec θ" and insert "cos $\theta/2$".
Page III-A-10 - line 24. Delete "θ" and insert "$\theta/2$".
Page III-A-10.- line 24. Insert the words "near the bottom" between "angle" and "between".
Page III-A-12 - line 8. Insert the words "the full meridian stress extends further up and" between the words "therefore" and "the".
Page III-A-12 - line 9. Insert the words "of a conventional shaped balloon" after the word "ascension".
Page III-A-12 - line 13. Insert "cos $\theta/2$" after "$2\pi rt_m$".
Page III-B-17 - line 4. Delete "0.143" and insert "0.125".
Page III-B-17 - line 6. Delete "0.143" and insert "0.125".
Page III-B-17 - line 7. Delete "41.5" and insert "73.7".
Page III-B-23 - line 17. Insert "$(\dot{r}^2+\dot{z}^2)$" in place of "$(\dot{r}+\dot{z}^2)$".
Page III-C-27 - line 6. Insert "half" between the words "the" and "cone".
Page III-C-27 - line 7. Delete "1800" and insert "1300".
Page III-E-75 - line 15. Delete "III-D" and insert "III-C"
Page VI-181 - lines 26 & 27. Delete the words "almost spherical." and insert "at approximately its designed shape."
Page VI-184 - line 3. Insert the word "difference" between "pressure" and "at".
Page VI - 184 - line 12. Should read " or $v=\sqrt{\frac{2gz}{K}}$ ".
Page VI-195 - line 24. Delete "into" and insert "out of".
Page VI-195 - line 25. Delete "into" and insert "from".
Page VI-204 - line 4. Insert the word "helium" between "our" and "results".
Page VI-204 - line 6. Delete the words "per cent" and insert the words "expressed as fraction" between the word "lift" and "of".
Page VI-204 - line 7. Insert the words "gradient (negative" between the words "atmospheric" and "lapse". Insert a parenthesis mark after "rate".
Page VI-197 - line 1. Insert the words "in the stratosphere" between the words "that" and "rising".
Page IV-118 - Caption-Figure 31. Should read "(See Figure 7-B)" instead of "(See Figure 7-D)".

PROGRESS REPORT ON RESEARCH AND DEVELOPMENT IN THE FIELD OF HIGH ALTITUDE PLASTIC BALLOONS

CONDUCTED UNDER
CONTRACT NONR-710(01), NR 211 002
FOR PERIOD JUNE 15, 1952, to DECEMBER 22, 1952
WITH THE
OFFICE OF NAVAL RESEARCH

AND SPONSORED JOINTLY
BY THE ARMY, NAVY AND AIR FORCE

PREPARED BY THE
DEPARTMENT OF PHYSICS
UNIVERSITY OF MINNESOTA
MINNEAPOLIS 14, MINNESOTA

5-3

PROGRESS REPORT ON CONTRACT #710(01)

From June 15, 1952 to December 22, 1952

VOLUME V

CONFIDENTIAL SECURITY INFORMATION

Table of Contents

SECTION I

ORGANIZATION

Personnel, space and equipment for the Balloon Project remain essentially the same as reported in the first Progress Report. A few changes have occurred in personnel; Mr. William Huch, experienced balloon designer has been added to the senior staff as a consultant and the nominal Scientific Director now divides his time between the Balloon Project and Los Alamos. In effect much of the responsibility for the direction of the work falls upon Dr. Edward P. Ney and Dr. John R. Winckler.

The current personnel falls into the following categories:

Experienced Research men (Ph.D)	5
Assistant Scientists	2
Junior Scientists	3
Research Fellows	3
Research Assistants	1
Electronics Mechanics	4
Engineering Assistants	14
Statistical Clerks	1
Photographers	1
Non-scientific, miscellaneous, etc., equivalent	6
Total	40

The names and experience of the senior men are:

Charles L. Critchfield, Professor of Physics
Scientific Director of Project, Ph.D., 1939 (half-time)

Edward P. Ney, Associate Professor of Physics
Alternate Scientific Director, Ph.D., 1947

John R. Winckler, Associate Professor of Physics
Ph.D., 1946

Homer T. Mantis, Assistant Professor, Mechanical Engineering
Ph.D., (Meteorology), 1949

Gilbert Perlow, Research Associate, Ph.D. 1940

Raymond Maas, Consultant in Electronics and Instrumentation
B.E.E., 1948

William O. Huch, Consultant in Design and Operations
BS, (Aeronautical Engineering), 1942

A complete list of laboratory and office personnel, in addition to the five senior men listed above is as follows:

Leland Bohl, Research Fellow (half-time)
John Linsley, Research Fellow (half-time)
Kinsey Anderson, Research Assistant (half-time)
Robert L. Howard, Assistant Scientist
(Section Leader, Electronics Section)
Logan D. Gilman, Assistant Scientist
(Section Leader, Instrumentation Section)
Eugene Byrne, Junior Scientist
Willard Lewis, Junior Scientist
John Gergen, Junior Scientist
James Stoddart, Electronics Mechanic
Wilmer Kurth, Electronics Mechanic
Robert Anderson, Electronics Mechanic
Phillip Erickson, Electronics Mechanic (half-time)
Sam Brinda, Engineering Assistant
Charles K. France, Engineering Assistant
Donald F. Kruse, Engineering Assistant
Joseph LeClair, Engineering Assistant
Bernard Welinski, Engineering Assistant
Paul W. Chase, Engineering Assistant (half-time)
Robert E. Danielson, Engineering Assistant (half-time)
Evan E. Day, Engineering Assistant (half-time)
Theodean Erickson, Engineering Assistant
Idar Anderson, Engineering Assistant
Lester Beckland, Engineering Assistant
Roswell Wahl, Engineering Assistant
Richard Hendricks, Engineering Assistant
Arthur Walseth, Engineering Assistant
Charles Wilson, Utility Man
Robert Newton, Utility Man
Irwin M. Fine, Photographer
Joan Markham, Senior Clerk
Shirley Whitmore, Senior Statistical Clerk
Ferdinand Ohnsorg, Research Fellow
Marlene Besaw, Secretary
Berton Atkinson, Draftsman
Ewald Eckland, Assistant Foreman
Rudolph Thorness, Machine Shop Foreman
Donald Hanson, General Mechanic
Charles Edwards, General Mechanic
Cecil Smith, General Mechanic
Roy Lahti, General Mechanic
Victor Hoberg, Sr. General Mechanic

Winter operations have been made practical by flying from Pierre, South Dakota . A mobile communications unit has been installed in a Navy trailer van and used at Pierre. Prevailing westerlies prevent complete tracking of sustained flight when launched at Minnesota.

The program on liquefaction of hydrogen and helium has been dropped as unnecessary duplication in the face of the rapid progress being made elsewhere. In addition, the present trend in balloon design is to minimize ballast requirements.

Data of value to the project were gathered on cosmic ray flights in Texas, financed by a separate contract with ONR.

In general, the project is enjoying full cooperation on the part of the University and Department Administration, the representatives of ONR and CAA, the manufacturers of balloons and the hundreds of people who have found gear and balloons and have helped in their recovery.

SECTION II

LAUNCHING SUMMARY

This section of the report will summarize our experiences with 55 launchings which constitutes the number of flights made on the project to date. The launching method is described in detail in the first Progress Report, Volume I, pages 2-1 to 2-29. The method is still carried out as described in that report with a few minor modifications which are necessitated by changes in the balloon design and a few minor changes which were found to be advisable in the launching method itself. The spun aluminum girdle shown in Figure 2, Page 2-13, is customarily covered with nylon cloth in the form of a stocking instead of taping transversely with nylon tape. The nylon cloth has been found to give the proper frictional coefficient so that the girdle stays on the balloon and slips smoothly down as the balloon fills out during ascent. It was found advisable to protect the balloon underneath the position corset found in Figure 5, Page 2-16 of Volume I, by a layer of sponge rubber wrapped in polyethylene. This provides a cushion between the stiff parts of the corset and the canopy of the balloon which is secured down over the inflation thimble by this corset. The sponge rubber cushion is attached to the corset on one end and falls off just before take-off when the corset is removed. The invention of the duct appendix which is customarily installed directly in the top of the balloon necessitated a different rigging arrangement for packing. The suspension clamp shown in Figure 3, Page 2-14, Volume I, is replaced by a simple clamp which merely provides a feed through for the top rope. No effort is made to hang the balloon by this feed through. The balloon is hung by a harness connected to the point where the duct appendix is inserted. A discussion of the method of inserting the duct appendix in the balloon will be found in another section of this report where the duct appendix is described in detail. The changes in the suspension ring can also be understood by references to Pages 2-21 and 2-22 in Volume I which show how the suspension ring was formerly used. The duct appen-

dix occupies the position where the suspension ring was formerly clamped in and as the tapes no longer converge across the ring when it is placed off center on the edge of the duct, it is not a satisfactory point from which to hang the entire balloon. Therefore, the use of the harness connected to the periphery of the point at which the duct is inserted was used.

An experience with one flight which failed, because the top rope which used to be left long and was pulled through as the top ascended, became snarled around the suspension ring, made it seem advisable to cut this rope short after the balloon was erected. This is done by using a knot called a slippery sheet bend which can be released from the ground by a side rope and which removes the main tie rope from the balloon. Then only about 3 or 4 feet of rope has to pass through the fitting as the top of the balloon erects and this avoids possibility of snarling or catching in the folds of the fabric. These improvements just described were made as a result of difficulties of one kind or another in the launchings. A survey of the flights made to date shows that in the first ten flights, there was a total of four cases of which failures of one kind or another due strictly to launching technique resulted. In flights #10 to #20 there were three cases of failure. In flights #21 to #30 there were five, and in flights #31 to #40 there were none. In flights #41 to #50 there were none and in flights #51 up to the present there was but one case of failure, which was not a failure of apparatus but represented an error in judgement and is probably not representative of the others.

All of these cases do not result in complete failure of the flight for scientific purposes of the project but are listed because something went wrong with some feature of the launching method. As pointed out many times, this launching method is very suitable for the purposes of this project because it enables one to weigh the balloon off as one does a vertical inflation generally used only with smaller balloons. It was found that with a combination of this

launching technique with the use of a large windscreen available near Minneapolis, launchings were very seldom held up because of wind. Even with the windscreen, however, launchings must be limited to winds of less than 35 miles per hour but this wind speed does not occur very often. The weigh-off data has been analyzed and it appears that the scatter of this data indicates an accuracy in weigh-off of about ± 2% of the gross load involved. (See Section VI Page 178 and Figure 3) This scatter is obtained from an analysis of a large number of flights in terms of the initial ascent rate as a function of the measured weigh-off. If one tries to make an estimate from looking at the weigh off measurements and also by comparing the weigh off at two points during the launchings, namely when the inflated balloon was secured at both ends to the ground and weighed off and then when the balloon was erected and weighed off just at the bottom, and considering fluctuations in readings due to wind burbles around the windscreen, etc., one concludes that the measured values are within ±10% of the free lift. The free lift varies, of course, from one flight to another but free lift is something like 10% of gross load so that the order of accuracy is from 1% to 2% of the gross load from this consideration.

The expenses involved in the packing operation have been itemized and a cost estimate made. The cost of balloon hardware, including a special bag to wrap the balloon in once it is packed, corset, harness, inflation thimble, specially prepared automobile inner tube, the aluminum girdle, etc., total about $330. This includes about 26 man hours of time in the packing which is probably on the high side. There are some special items involved in this launching method such as an antenna dropper to unwind the radio antenna once the balloon is in the air and the cost of packed parachutes, etc., which probably brings the total cost up to about $400. It is felt that this is a small expense compared to the loss of flight due to inaccurate weigh-offs or the cost of keeping project personnel

inactive while waiting for weather which is suitable for other launching methods. Experiences in the field with this launching method have proven very successful. A joint operation with General Mills, Inc. was conducted at Pyote, Texas, in July of 1952 in which three flights were launched in 10 days. Most of the 10 days were occupied in recovering gear and getting ready for the next flight. The winter, 1952-53, launching site has been moved from Minneapolis to Pierre, South Dakota, so that the trajectories would give us an extra day of flight time and in some cases prevent the loads from being lost in the Great Lakes. This operation has been carried forward very satisfactorily using simply the facilities available at the Pierre Muncipal Airport. One of the square hangars was used as a windscreen. Five series of three launchings each have been made and each series conducted in considerably less than a week. So far there were no hold-ups because of weather. A series of flights which are not reported in this report were made in Pyote, Texas, in January of 1953, in conjunction with the SKYHOOK project of Winzen Research in which the Minnesota technique was used throughout for 15 launchings which were extremely successful.

SECTION III-A

CONSIDERATIONS ON BALLOON SHAPE

Since balloons can be manufactured in any desired shape of closed surface, it appears reasonable that there is a most desirable shape. It is one of the objectives of the High Altitude Balloon Project to solve this problem. The main difficulty is that the problem has never been adequately formulated; hence the project is currently engaged in identifying the significant features that can be improved by changing the design of the cell. Theoretical work on the nature of stresses in static axially symmetric cells has been completed and electronic computer runs on a large variety of given conditions have been made. But it remains to deduce from field and hangar tests the relative importance of the features that can be effected by balloon design. (In the following, the distinction between design on the table and shape in the air must be kept in mind.)

The principal quantities to be considered are the stresses, the consequent strain or plastic flow, and the relationship between surface area and volume contained. The considerations are on the general shape not including appendices, valves, attachments, etc. Stresses on the surface arise from supporting the payload and the lower portions of the balloon and from gas pressure. Those stresses that have a direction which is tangent to the surface and that lies in a vertical plane are called meridional stresses, t_m. If the balloon weight and differential gas pressure can be ignored $2\pi r t_m \sec\theta$ = payload at a point near the bottom where the radius of a horizontal section of an axially symmetric balloon is r and θ is the angle between the vertical and the tangent plane. Hence, as one nears the bottom apex the stresses become very high and will

exceed the strength of the film if its thickness does not increase also. Hitherto, this difficulty has been surmounted by applying meridional 'load bearing' tapes over the heat seals, thus relieving the plastic film near the apex.

Tests at Weeksville showed that the meridional stress is rapidly transferred from the tapes alone into the film. This is indicated also in up-pictures in flight in which tapes often appeared to be wrinkled. The safest assumption is therefore that the meridional stress is distributed uniformly over the surface everywhere above a few tens of feet from the apex of a large balloon.

Curvature in a stressed surface produces an 'inward' force per unit area. By 'inward' is meant: towards the concave side. In the balloon this force is opposed by the difference in pressure of gas inside and outside the balloon. If the 'inward' pressure created by the meridional stress is nullified everywhere by the gas pressure, the balloon is said to have a "natural shape". For a given ratio of balloon weight to gross weight there is a doubly infinite family of natural shapes for one-cell balloons, corresponding to the choice of the cone angles at top and bottom, for example. All such shapes have axial symmetry.

Since the pressure difference in a natural shape is balanced entirely by the meridional stress, and since the balloon is concave inward in every horizontal section, the circumferential tension is zero everywhere for those shapes. It was to achieve no circumferential tension in the design that General Mills, Inc. set out originally to find such a shape. The theory was that it is better to have the fabric stressed uniaxially than to have it stressed biaxially. Their success in flying very heavy loads may depend partly on the more efficient stressing in the natural shape.

Zero circumferential tension everywhere means that there is no tendency to stretch the fabric into a form of larger 'radius' r at any point. If excess girth of fabric is provided at any point along the length of the balloon the fabric will overlap at that point. Hence, during ascension most of any balloon tends to the natural shape for the existing distribution of weight of fabric and for the particular payload carried. Moreover, the curvature of the balloon surface is higher when the outside pressure is higher and therefore the stresses are greatest in the early stages of ascension. Consequently, there is little direct relationship between the design of the fully inflated cell and the minimization of stresses except at the very top and bottom and at points of discontinuity of curvature.

At the very top of a natural shape $2\pi r t_m$ = gross load, so that t_m again diverges as $r \to 0$ at the top and the fabric must be reinforced. In a flat-top natural shape r increases with the cube root of the distance from the top. Balloons designed with a spherical top have a 'radius' r that increases with the square root of the distance from the top and the circumferential tension becomes equal to the meridional tension at the top. Thus, the presence of meridional tapes restricts plastic deformation in the direction in which they lie and permits enlargement of the circumference. The result is that spherical balloons tend to develop a flat top and this was evident on the fully inflated cells at Weeksville. Since nothing can be gained by permitting a cell to <u>stretch</u> into a natural shape near the top the conclusion is that it is better to design the cells with more fabric in the crown so as to conform to a cubical parabola rather than an ordinary one.

The principal difficulty with applying the theory of the natural shape is that the design depends upon the ratio of balloon weight to

gross load. This ratio may be expected to vary with different uses of the balloon and even varies during flight, if ballast is dropped. One has then either to make compromises or produce a balloon that automatically assumes a natural shape. As mentioned above, the circumferential stress goes to zero wherever there is excess fabric. To utilize this in design Winckler suggested making a balloon out of a cylinder of fabric of radius about that (or a little greater than that) of the desired radius of the fully inflated cell and of length equal to the total "gore length". The cell is completed by gathering the fabric together into folds and clamping with suitable rings at top and bottom. If this is done with reasonable care the cell will have excess fabric everywhere except possibly just at the equator and the strength per foot will increase inversely proportionately to π as it should. The remaining care to be taken in design is that of the valving mechanism. This design was originally conceived to eliminate the tapes which seem to contribute inordinately to solar super heat but it automatically solves the shape problem for any load ratio and at all stages of flight.

There is one danger in having excess fabric on the surface and that is that the volume of the balloon then depends upon the pressure differential. Hence, at ceiling, the valving superpressure might enlarge the cell and cause it to overvalve by overshooting its ceiling for the natural shape at regular pressure. This effect has not appeared in flights where cone-on-sphere balloons are valved to operate at a sub-pressure, however, and it seems that the warming of gas after the valving pressure is relieved is more than adequate to compensate it. Obviously these points are subject to more detailed experimentation and analysis.

SECTION III-B

CALCULATION OF CYLINDER BALLOON SHAPES

The so-called "cylinder balloon" is made from a cylinder of balloon fabric gathered together at each end. The cylinder is then inflated, and the shape of the balloon depends only on the gore length (which is constant) and the degree of inflation, so long as the radius of the balloon does not approach the radius of the original cylinder.

As the balloon is inflated, there will be a volume at the top of the balloon where the pressure of the gas at each point exceeds the pressure of the outside air at the same vertical height above the bottom apex of the balloon. In the remainder of the balloon volume, the gas pressure will be less than the corresponding air pressure. The former region can be said to have "super-pressure" and the latter, "sub-pressure". The height above the bottom of the balloon of the horizontal plane that separates the sub- and super-pressure regions is called the "sub-pressure height", and it is this length that characterizes the degree of inflation of the balloon. As the inflation continues, the sub-pressure height goes to zero. If an appendix is put on the balloon, the super-pressure region can extend down into the appendix, and the appendix will be collapsed below the super-pressure region. The distance from the bottom apex of the balloon (where the load is attached) to where the appendix is collapsed is the "super-pressure height". The balloon could, of course, be super-pressured without the appendix by means of an appropriate gas fitting.

For a given gore length, the shape and volume of the cylinder balloon will be uniquely determined as a function only of the sub- or super-pressure height (pressure difference head at bottom apex). This section of the report presents the results of a calculation of cylinder balloon shapes and volumes. The shapes are described by giving the height of the balloon from top apex to bottom apex,

the radius of the balloon at its biggest part, and the total opening cone angle at the bottom of the balloon:

Sub-pressure balloon

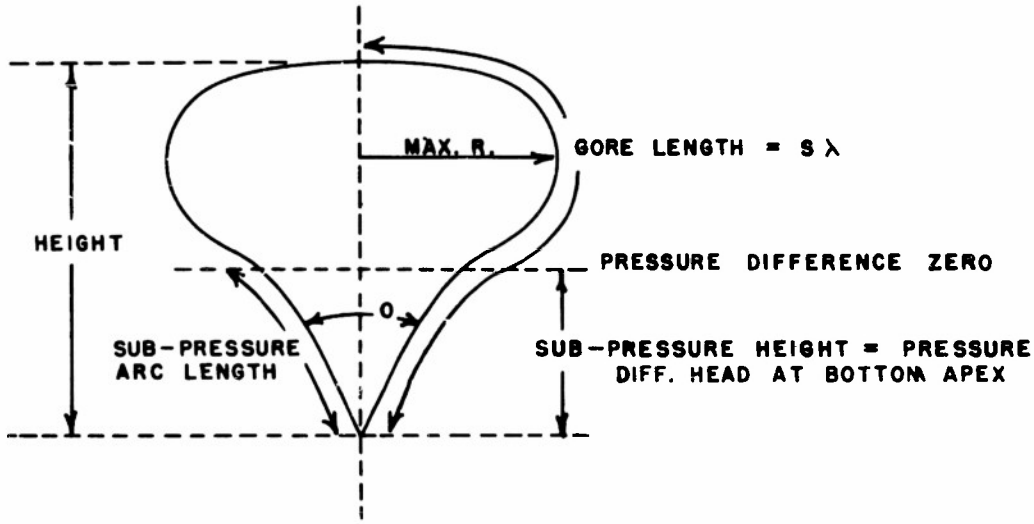

Super-pressure balloon

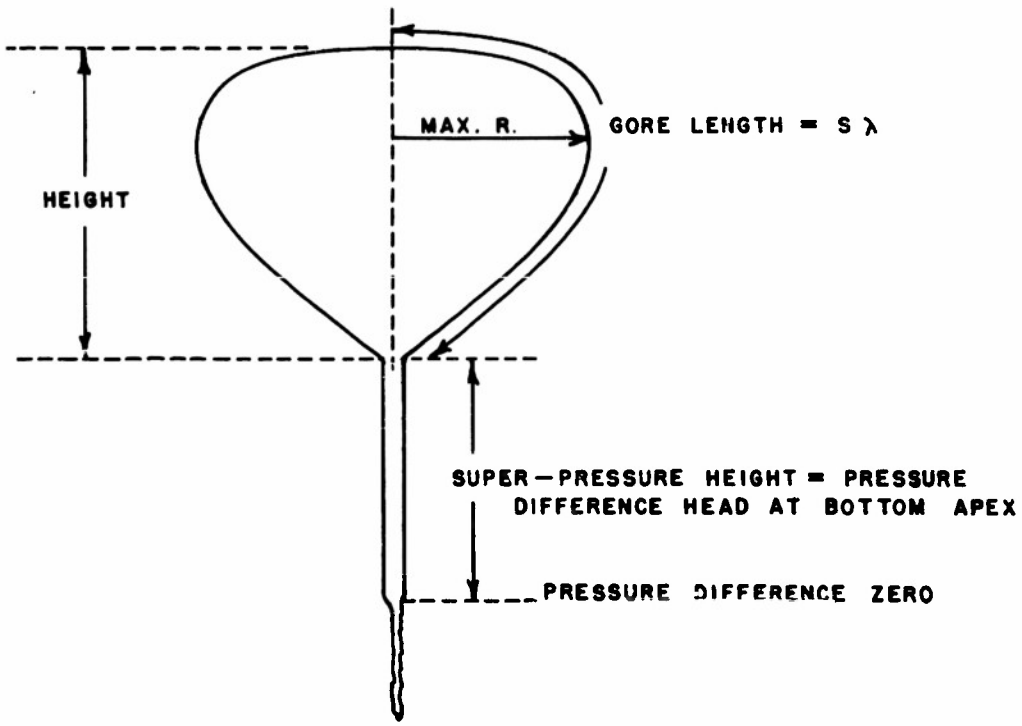

The volume is computed for each shape, and, for the sub-pressure balloons, the distance along the gore between the bottom apex and the pressure difference zero is computed as "sub-pressure arc length". It is this length that determines, for instance, how far from the bottom apex one would want to terminate a duct appendix to get a certain degree of "sub-pressure" with its attendant volume defect and cone angle. The shape and volume are given in terms of a balloon whose gore length is one unit. The height, maximum radius, volume, and pressure head at bottom apex are to be scaled up to the appropriate gore length.

The purpose of the following examples is to illustrate the use of the curves:

(1) A duct balloon has its duct cut off 25% of the way up from the bottom apex. The gore length of the balloon is 75 feet.

For a unit-gore-length balloon, the sub-pressure arc length would be 0.250. From the curves, the pressure head at bottom apex would be -0.205 (Fig.2). This corresponds to a cone angle of 68°(Fig.2), a radius of 0.300 (Fig.3), a height of 0.708 (Fig.3), and a volume of 0.103 (Fig.1). Thus the 75-foot gore length balloon would have

height = 53 feet

radius = 22.5 feet

volume = 43,000 cubic feet

(2) A cylinder balloon of gore length 90 feet is to have a 90° cone angle at the bottom.

A 90° cone angle corresponds to a pressure head of -0.080 at the bottom apex (Fig.2), which in turn implies a sub-pressure arc length of 0.100 (Fig.2) for a unit gore length balloon. The duct should thus be cut 10% up from the bottom, or 9 feet from bottom apex.

(3) A balloon with an appendix of negligible length at the bottom apex is to have a volume of 50,000 cubic feet.

A balloon of unit gore length and zero pressure head at bottom apex would have a volume of 0.143 (Fig.1). For gore length S_λ the volume would be

$$0.143\ S_\lambda^3$$

Hence, the gore length of the balloon should be $S_\lambda = 41.5$ feet.

(4) A balloon has a gore length of 75 feet and an appendix that extends 45 feet below the bottom apex of the balloon.

On valving, the pressure difference head at bottom apex on a similar balloon of unit gore length would be +0.600. From the curves the volume would be 0.147 (Fig.1), the height 0.555 (Fig.3), radius 0.360 (Fig.3), and total cone angle at apex of 141° (Fig.2). The 75 foot gore length balloon would have

height = 41.6 feet

radius = 27.0 feet

volume = 62,000 cubic feet

In comparison with the balloon of example (1), this balloon is bigger in volume and more oblate in shape.

The curves given below were calculated under the assumptions that there is cylindrical symmetry about the vertical axis and that the fabric weight is small compared to the weight of the load.

The fabric tension in a cylinder balloon is entirely meridional and is constant everywhere on the balloon. If R is the radius of the cylinder from which the balloon was made, then the tension per unit length in the balloon fabric is:

$$t = \frac{L}{2\pi R} \sec\frac{\theta}{2}$$

where L is the load attached to the bottom apex and θ is the total opening cone angle at that apex. A curve showing sec $\frac{\theta}{2}$ is given.

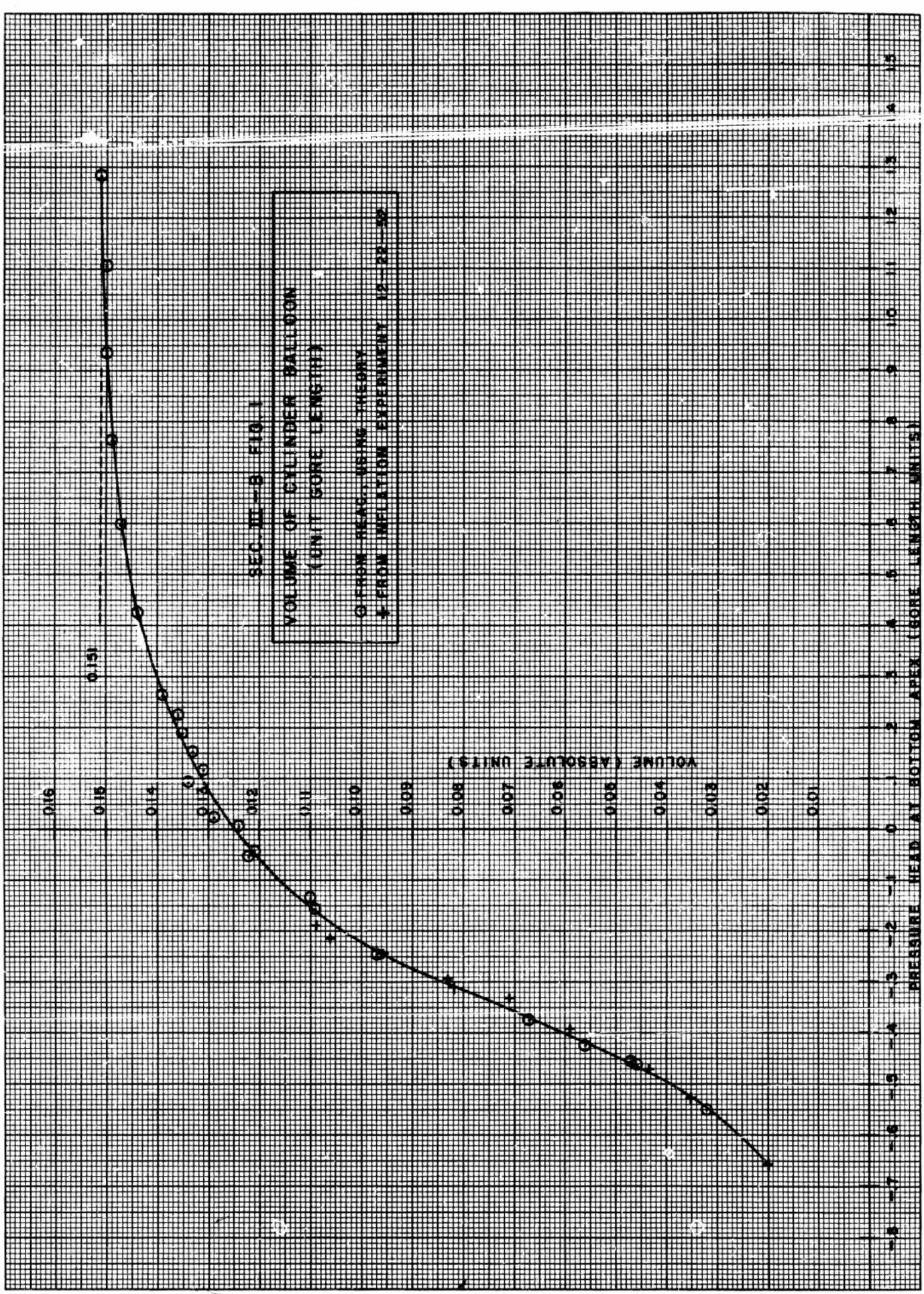
SEC-IE-8 F10.1
VOLUME OF CYLINDER BALLOON
(UNIT CORE CONCEPT)
O FROM REAC-IDEAL THEORY
+ FROM INTERLOM EXPERIMENT 12-22-59
VOLUME (ABSOLUTE UNITS)
0.16
0.15
0.14
0.13
0.12
0.11
0.10
0.09
0.08
0.07
0.06
0.05
0.04
0.03
0.02
0.01
0
PRESSURE HEAD AT BOTTOM APEX (CORE LENGTH UNITS)

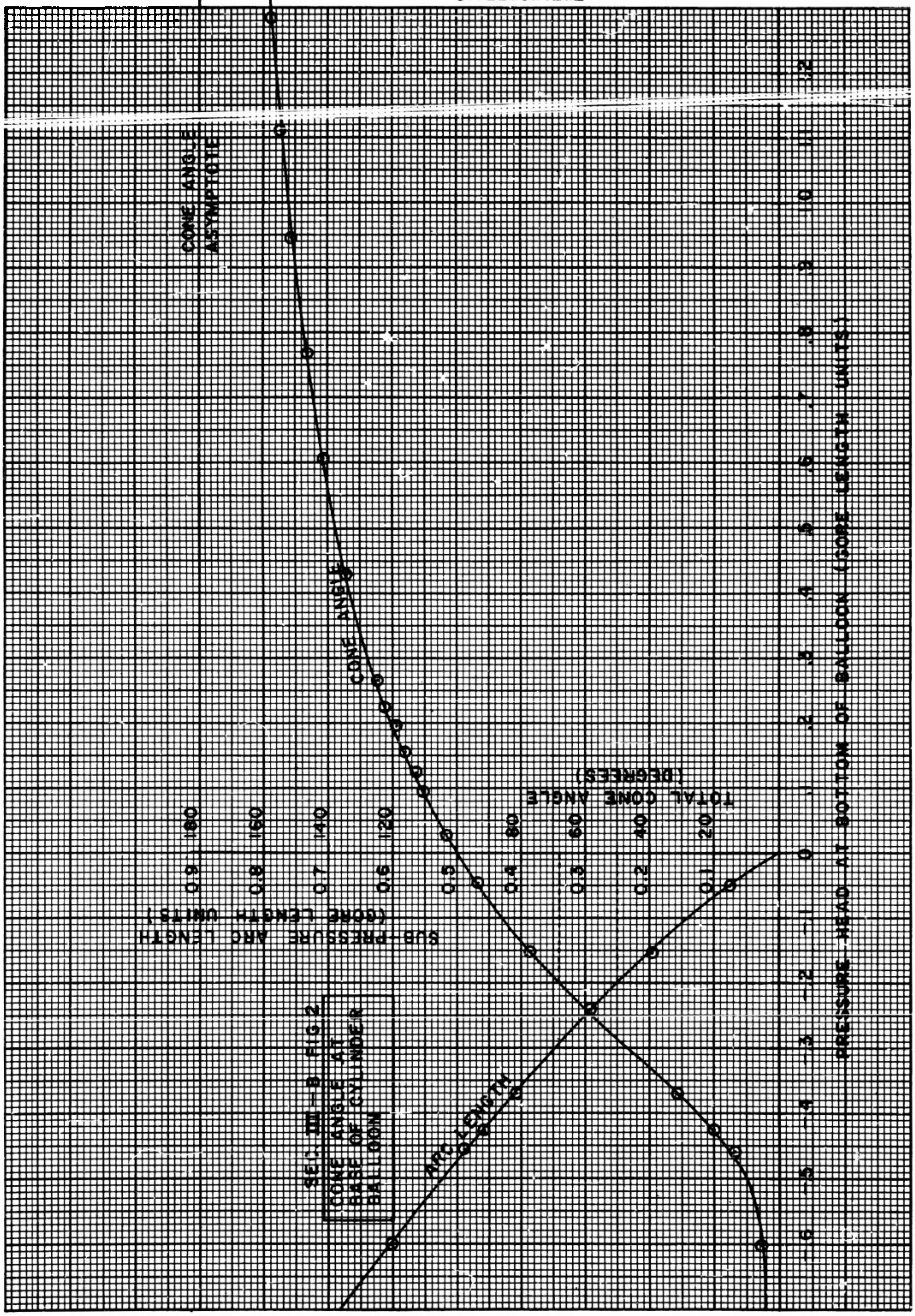

SEC. III-B FIG. 2
CONE ANGLE AT BASE OF CYLINDER BALLOON

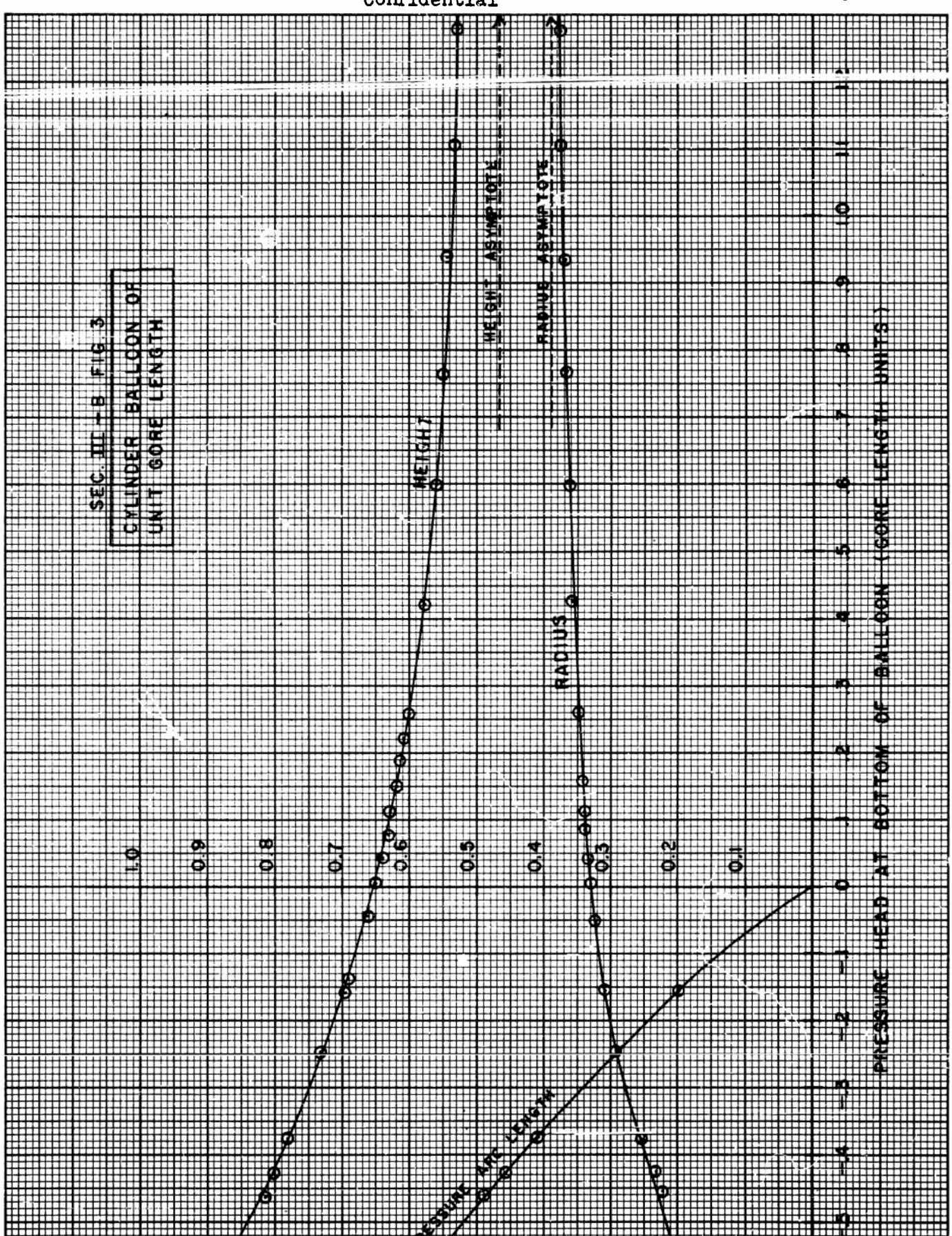
SEC. III-B FIG 3
CYLINDER BALLOON OF UNIT GORE LENGTH
HEIGHT
HEIGHT ASYMPTOTE
RADIUS
RADIUS ASYMPTOTE
SUB-PRESSURE ARC LENGTH
PRESSURE HEAD AT BOTTOM OF BALLOON (GORE LENGTH UNITS)
1.0
0.9
0.8
0.7
0.6
0.5
0.4
0.3
0.2
0.1
0
-1
-2
-3
-4
-5
-6
1
2
3
4
5
6
7
8
9
10
11

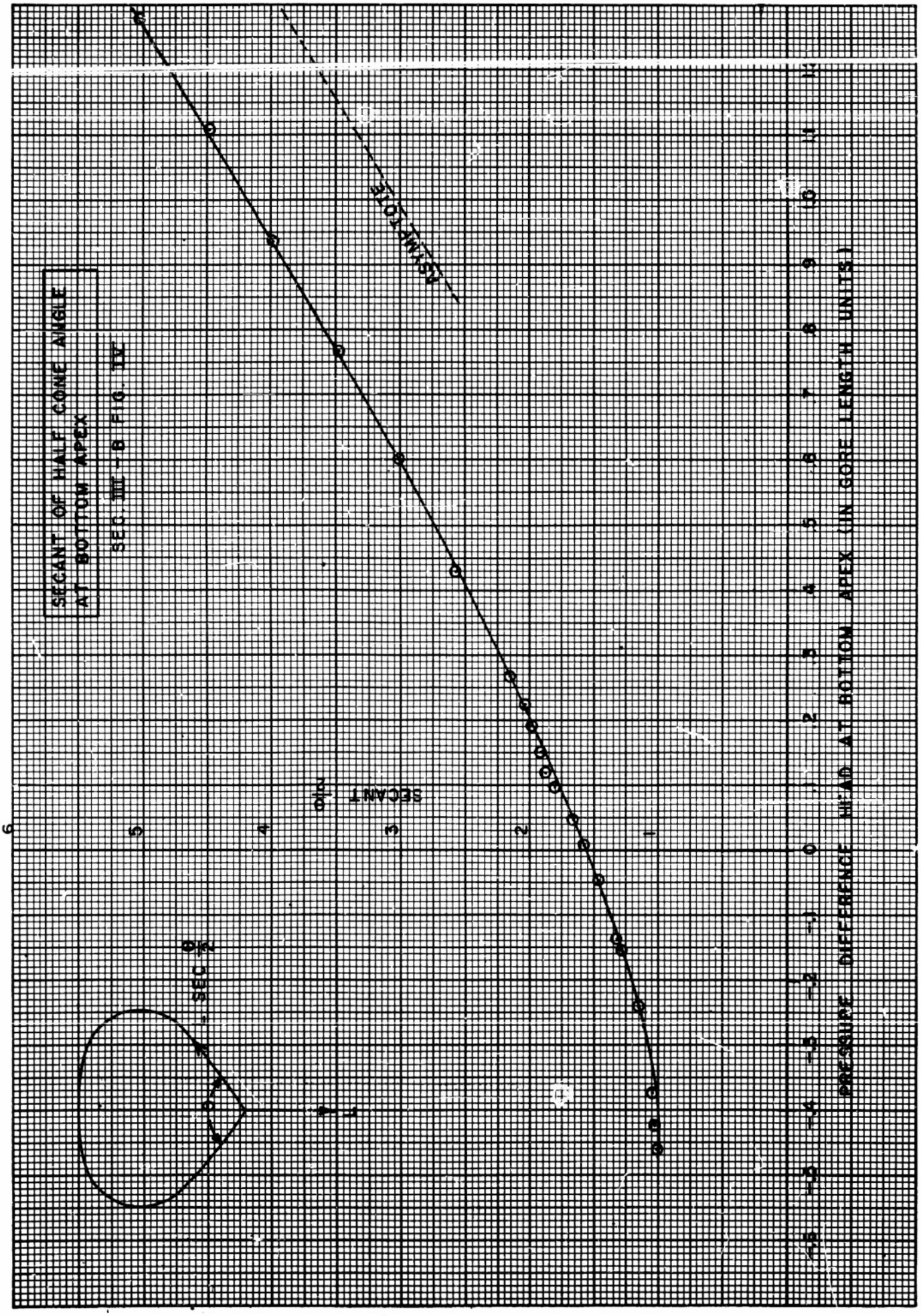
SECANT OF HALF CONE ANGLE AT BOTTOM APEX
SEC. III-B FIG. III
SECANT $\frac{\theta}{2}$
PRESSURE DIFFERENCE HEAD AT BOTTOM APEX (IN GORE LENGTH UNITS)
SEC. θ/2

Derivation of Equations

With each shape of balloon there is associated a potential energy. The shape that actually obtains in a cylinder balloon is the shape that minimizes the potential energy under given boundary conditions. This is clearly a problem in the calculus of variations. Thus we seek the curve, whose parametric representation is $r = r(s)$ and $z = z(s)$, that is an extremal to the variation problem:

$$\delta \int_0^{s_\lambda} z r^2 \dot{z}\, ds = 0$$

where the integral is proportional to the balloon's potential energy, r and z are as shown below, and the dot indicates differentiation with respect to the arc length s.

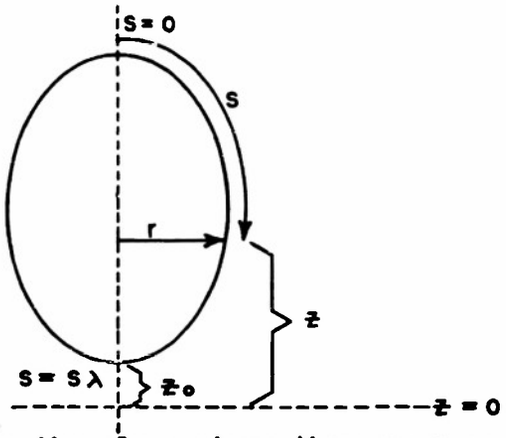

For convenience, $z = 0$ corresponds to the plane where the pressure difference across the fabric is zero. Thus the pressure difference at any point is βz where β is the difference in density between the outside air and the lifting gas. The pressure difference at the bottom apex is βz_0.

As stated, the variation problem implies that the arc length (gore length) is constant. The variation is subject to the condition that $\dot{r}^2 + \dot{z}^2 = 1$, and that $r(0) = r(s_\lambda) = 0$ and $z(s_\lambda)$ is given as z_0. Accordingly, our problem is the minimization of the integral:

$$\int_0^{s_\lambda} [z r^2 \dot{z} + (\dot{r} + \dot{z}^2) K]\, ds$$

where K is a function of s, but does not participate in the variation. The Euler equations for this problem are obtained immediately as:

$$\begin{cases} \frac{d}{ds}(2K\dot{r}) - 2r z \dot{z} = 0 \\ \\ \frac{d}{ds}(z r^2 + 2K\dot{z}) - r^2 z = 0 \end{cases}$$

Using the relation $\dot{r}^2 + \dot{z}^2 = 1$, the equations can be written:

$$K\ddot{r} - r z \dot{z} = 0 \qquad (1)$$

$$K\ddot{z} + r z \dot{r} = 0 \qquad (2)$$

$$\dot{K} = 0 \qquad (3)$$

The equation (3) gives K = constant.

The volume of the balloon can be obtained directly from equation (2) as follows:

$$V = -\pi \int_0^{s_\lambda} r^2 \dot{z}\, ds = -\pi \left[r^2 z\right]_0^{s_\lambda} + \pi \int_0^{s_\lambda} 2 r \dot{r} z\, ds,$$

using equation (2)

$$V = -2\pi \int_0^{s_\lambda} K\ddot{z}\, ds = -2\pi K \left[\dot{z}\right]_0^{s_\lambda}$$

If the load ($= pV$) is supported entirely at the bottom apex, then $\dot{z}(0) = 0$, and

$$V = -2\pi K \dot{z}(s_\lambda) = 2\pi K \cos\frac{\theta}{2}$$

if θ is the total opening cone angle at the bottom apex.

As a result of the variation, there is a boundary term:

$$\left[(z r^2 + 2K\dot{z})\,\delta z + 2K\dot{r}\,\delta r\right]_0^{s_\lambda}$$

which must vanish. It does vanish by virtue of the conditions:

$$\delta r(0) = \delta r(s_\lambda) = \delta z(s_\lambda) = 0$$

(The quantity $\zeta \bar{z}(o)$ is arbitrary, but $\pi(o) = O$ and $\dot{\bar{z}}(o) = O.$)

The result of the solution of the set of differential equations (1) and (2) can be expressed as a family of solutions with parameter $\bar{z}_o$ (pressure difference head at bottom apex) with unit gore length $S_{\lambda=1}$. From these solutions, the volume, cone angle, height and maximum radius of the unit gore length balloon can be obtained.

The solution of the differential equations was done with the aid of a Reeves Analogue computer.

SECTION III-C

CYLINDER BALLOONS

A critical study of the balloon shape problem has been carried out on the REAC computer. A consequence of this study is that a balloon which has adequate material in it will take on the natural shape and thereby become a balloon which has a zero circumferential stress. It was this fact made evident by the study of the physics of balloon shape that lead us to the idea of making a balloon without tapes and having the load carried by the plastic itself. For such a balloon the question was asked as to what shape or configuration one should begin with in order to have the stress in the plastic everywhere the same. The answer to this question turns out to be that a balloon which is made of a cylinder tied together at the ends will have everywhere the same meridional stress and at the same time, if it has enough gores in it so that it can become natural shape, will everywhere have zero circumferential stress. There are various possibilities for such a balloon. One can use the duct appendix cut at some position above the bottom of the balloon as with the cone-on-sphere balloons and in this case one has a sub-pressure balloon. If one brings the duct to the bottom of the balloon or if one has an open skirt appendix at the bottom one may have such a balloon with so-called zero pressure or with the pressure at the bottom of the balloon equal to outside atmospheric pressure. Finally if one brings the duct well below the bottom of the balloon it is possible to have a balloon which is a super-pressure balloon and which, therefore, is relatively independent of fluctuations in temperature provided these fluctuations do not correspond to more than the amount the balloon is super-pressured. It is easy to see what the ultimate requirement on such a balloon is from the standpoint of carrying a heavy load. Since the stress in the plastic is all meridional and since it must lift the load, the vertical component of this stress

at the bottom of the balloon must be equal to the weight of the load. Let us take an example. For a 25' diameter cylinder tied together at the ends, of 45' gore length a balloon made of 1-mil polyethylene material contains approximately 1 square inch of material. The ultimate tensile strength of polyethylene is 2000 pounds per square inch and consequently this 25' balloon will lift a load at ultimate tensile somewhere in this vicinity. Because the cone angle is not zero but is more like 50° the ultimate load is reduced by the appropriate geometric factor to about 1800 pounds. It would not be possible to test such a balloon to ultimate as a sub-pressure balloon or as a zero-pressure-at-the-bottom balloon because of the fact that its volume at sea level is not large enough to lift the required load.

The first cylinder balloon made under these circumstances was tested at the time of the Balloon Meeting held here at Minnesota, December 11 and 12, 1952, and various members of the audience were invited to look at it.* It consisted of a 12' diameter cylinder with a duct appendix on the top and it was inflated behind the lecture room. It took on the natural shape as expected and did this without the introduction of any circumferential stress. The position of the zero pressure level could be readily varied by raising the duct and allowing the balloon to valve and the position of the zero pressure level was evident by looking at the balloon to be the place where the curvature of the balloon changed its direction. Since this preliminary test was so successful it was decided to go ahead and attempt larger cylinder balloons and the next size which was studied was one which was 25' in diameter, 45' long. This ratio of diameter to length is such that one can obtain natural shape balloons only for sub-pressure balloons since if the zero pressure level is placed at the bottom, the diameter of the balloon is not quite large enough to allow the balloon to take the natural shape without the introduction of circumferential stress.

*The polyethylene cylinders were manufactured by General Mills, Inc.

Figure 1 shows a series of shots of the smaller cylinder inflated in the lecture room. Figure 2 to Figure 4 show a similar series of shots of the 25' diameter cylinder inflated in Williams Arena. These pictures were taken as the inflation of the balloon is continued and the last picture corresponds to a balloon lifting 570 pounds gross. The material carried the load very well, in the absence of tapes, and there was no evidence that any of the components of the system were failing. Actually two tests were made with the 25' polyethylene 1-mil cylinders. One of these was a test in which the inflation consisted of half air and half helium, and the second consisted of an inflation of pure helium (Figures 2 to Figures 4). Both tests were a complete success and it was felt that at least with this load which was well below ultimate in the material the balloon performed satisfactorily. Figure 9 shows the measured gross lift obtained for the 25' polyethylene cylinder as a function of the duct length along the gore from the bottom to the zero pressure level. As can be seen, there is a very large volume defect if the duct is cut short on a sub-pressure natural shape balloon as the balloon immediately begins to shrink at the point of maximum diameter if the duct is cut higher than the point at which circumferential tension sets in. The comparison of this curve and the theoretical results are given in Section III-B, and the result of the theory for this balloon is shown in Figure 9. The comparison with theory is on an absolute volume basis and the two curves have not been normalized.

One of the principal advantages of the cylinder balloon aside from its ease of manufacture and cheapness of construction lies in the fact that tthe balloon material itself carries the load rather than having to transfer it to the tapes which then carry it to the load. In order to utilize this property to the greatest extent it is desirable to have a balloon constructed of material of as high a tensile strength as possible. Polyethylene does not really satisfy these requirements since its ultimate tensile is only 2000 pounds per square inch. Consequently we began to investigate the possibility of using Mylar, a material

A. A group of visitors inspecting the duct on the first small cylinder.

B. View showing the zero pressure level in the duct.

C. Examination of the balloon to determine its circumferential stress.

D. Examination of the balloon to determine its circumferential stress.

Sec III-C Fig 1

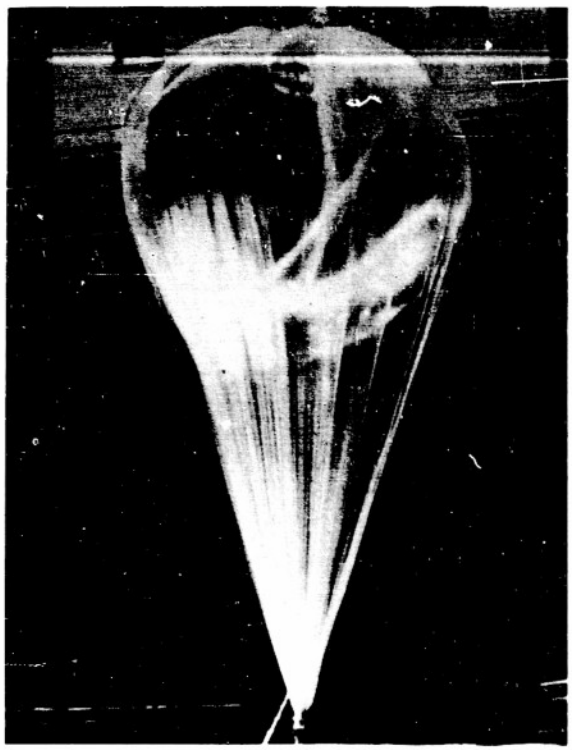

A. Gross load equals 153 pounds.

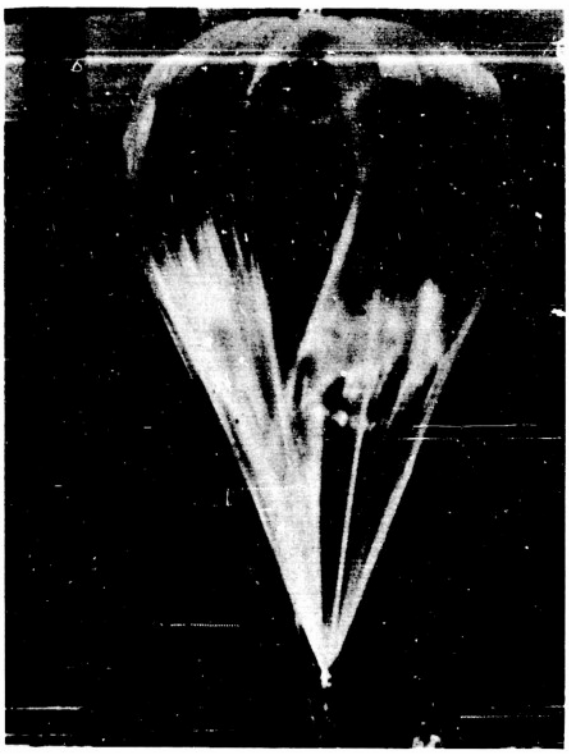

B. Gross load equals 253 pounds.

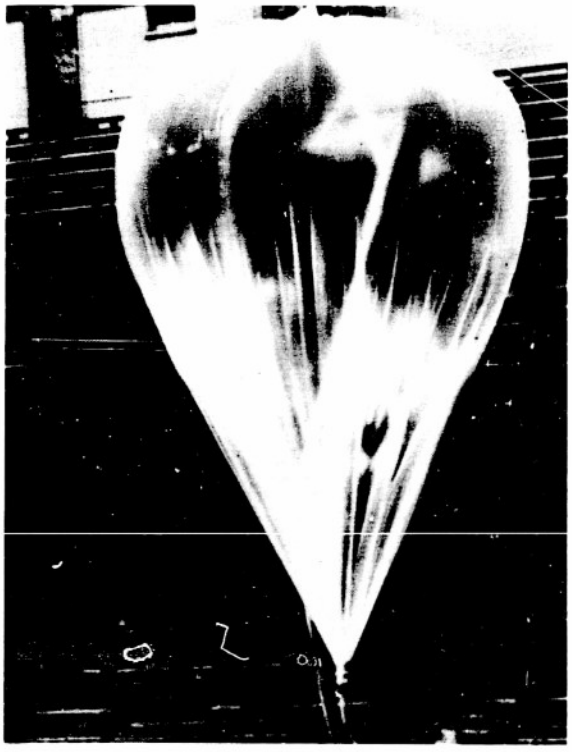

C. Gross load equals 303 pounds.

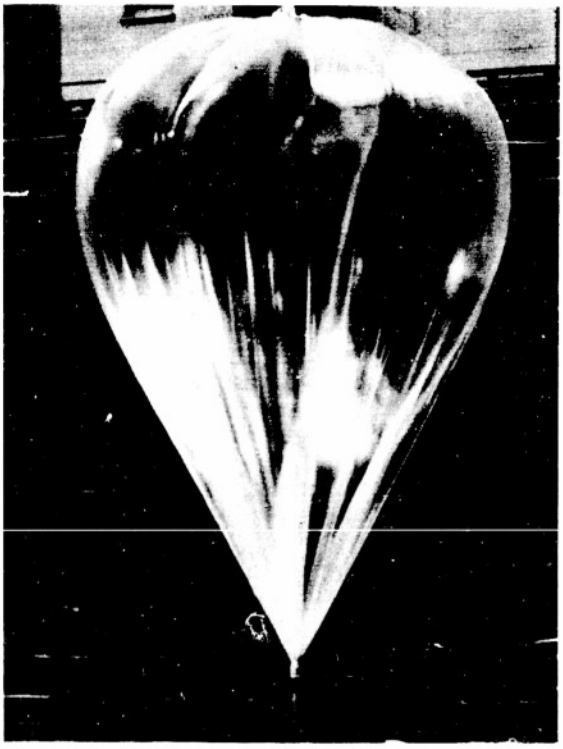

D. Gross load equals 353 pounds.

Sec III-C Fig 2. A 25' diameter by 45' gore length polyethylene cylinder at various stages of inflation with pure helium. The gross load lifted is indicated in each photograph. Because of the slack material near the bottom the true cone angle of the natural shape balloon is not necessarily the observed cone angle in the photograph.

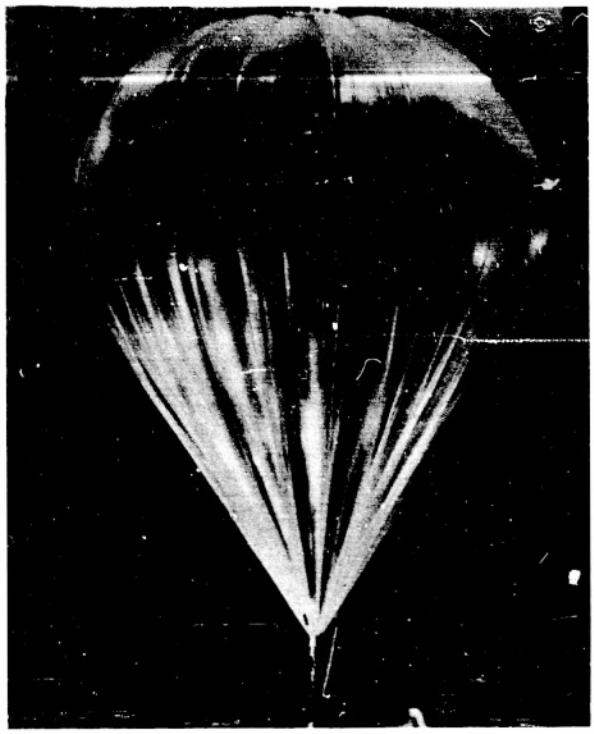

A. Gross load equals 415 pounds.

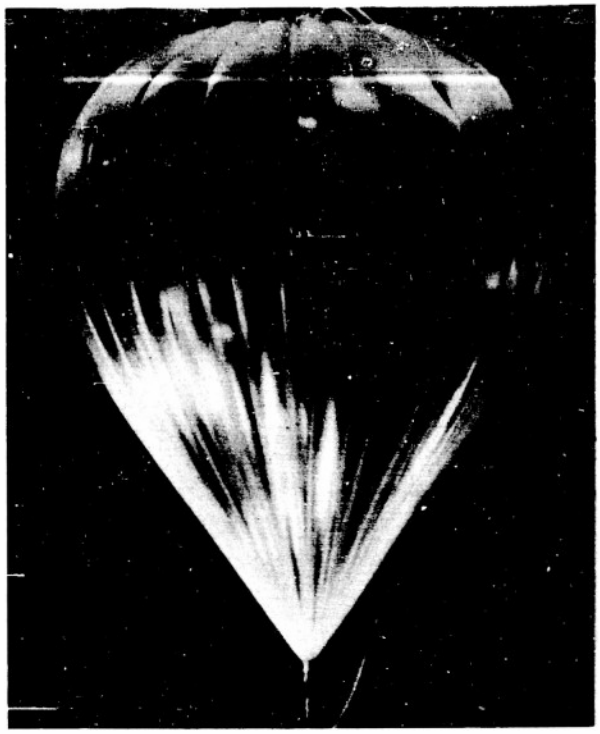

B. Gross load equals 465 pounds.

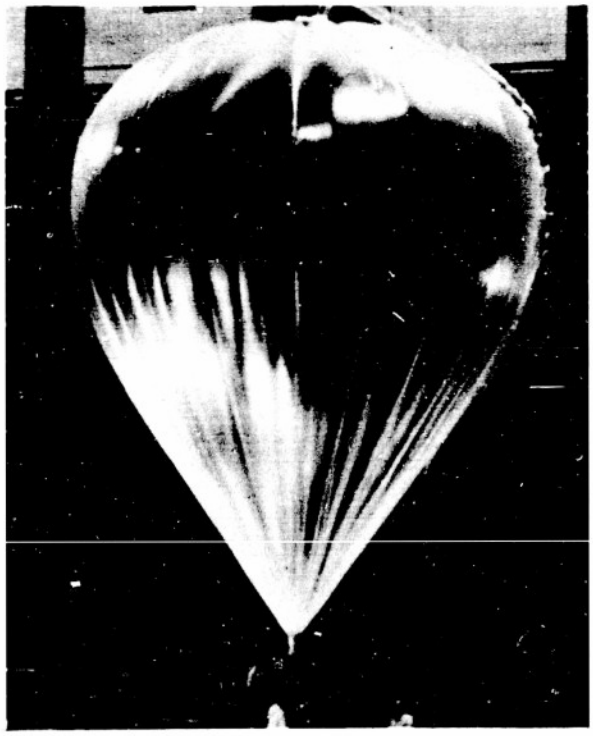

C. Gross load equals 471 pounds.

D. Top view or fully inflated cylinder. Gross load equals 471 pounds.

Sec III-C Fig 3 A 25' diameter by 45' gore length polyethylene cylinder at various stages of inflation with pure helium. The gross load lifted is indicated in each photograph. Because of the slack material near the bottom the true cone angle of the natural shape balloon is not necessarily the observed cone angle in the photograph.

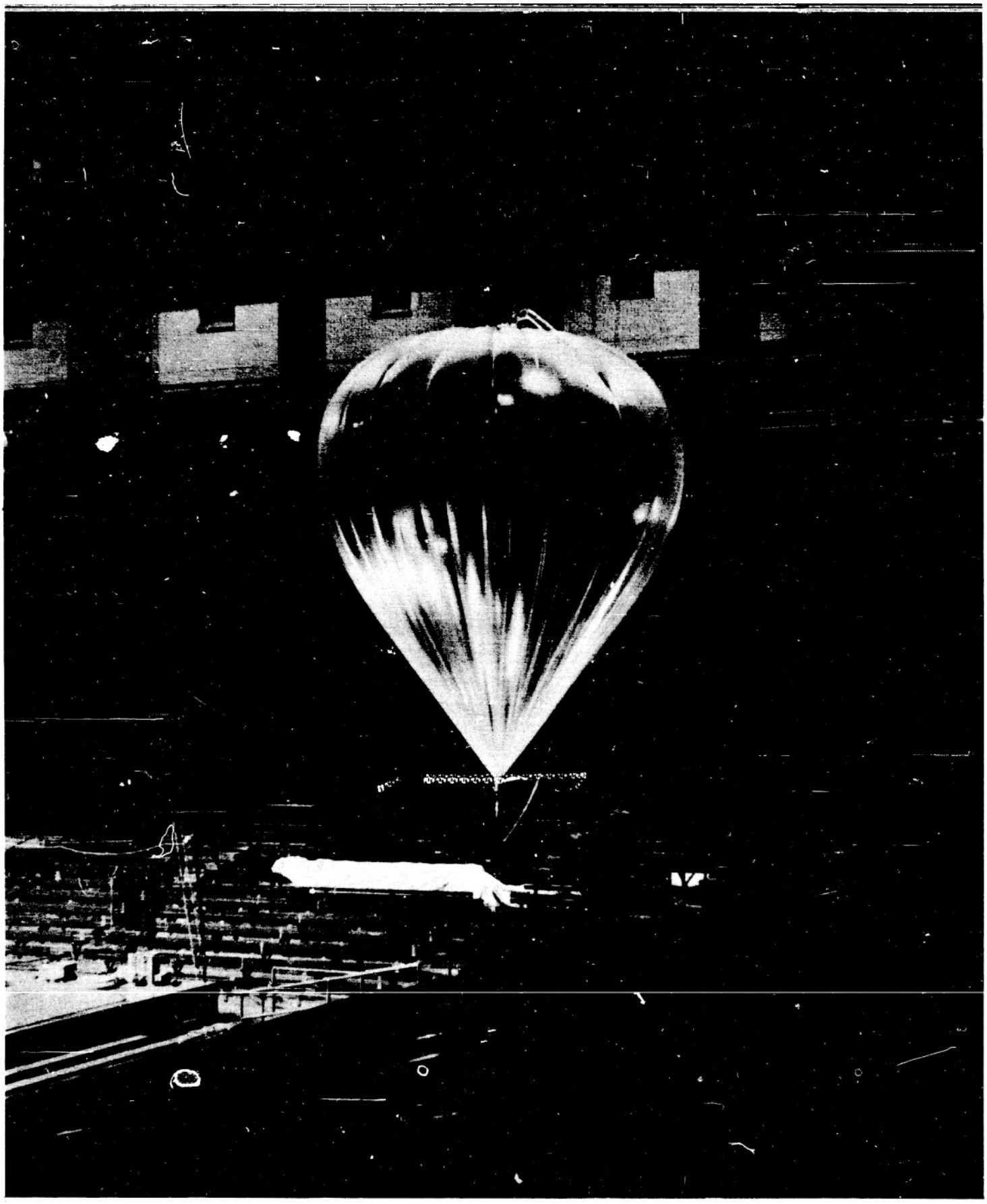

Sec III-C Fig 4 25' X 45' polyethylene cylinder completely inflated and lifting 490 pounds.

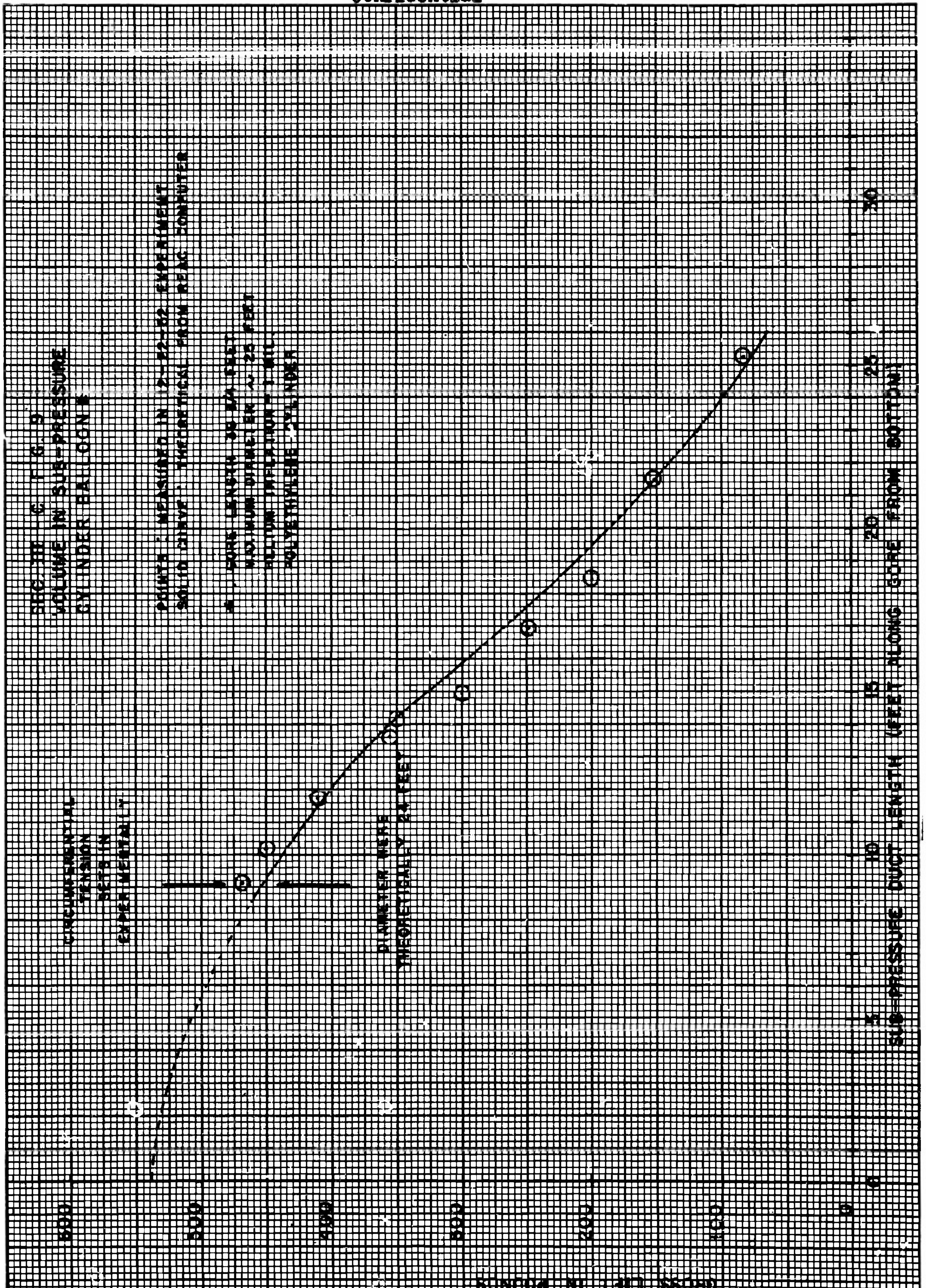
SEC. III C FIG. 9
VOLUME IN SUB-PRESSURE
CYLINDER BALLOON *
POINTS : MEASURED IN 12-22-52 EXPERIMENT
SOLID CURVE : THEORETICAL FROM REAC COMPUTER
POLYETHYLENE CYLINDER
CIRCUMFERENTIAL TENSION SETS IN EXPERIMENTALLY
DIAMETER HERE THEORETICALLY 24 FEET
0
5
10
15
20
25
30
SUB-PRESSURE DUCT LENGTH (FEET ALONG GORE FROM BOTTOM)
600
500
400
300
200
100
0
GROSS LIFT IN POUNDS

developed by DuPont, which has an ultimate tensile of 26,000 pounds per square inch. This factor of ten improvement in ultimate tensile, of course, means that a balloon of approximately 1/10 the weight can lift the same load. A 25' by 45' Mylar cylinder was constructed and inflated in Williams Arena with pure helium.* The balloon itself weighed approximately 6 pounds, was made of $\frac{1}{4}$-mil material and when the inflation was complete and the balloon had taken on the natural shape for its maximum diameter the gross load was 574 pounds. Even with this load, which represented the maximum volume of the balloon, one was far from the ultimate tensile in the Mylar material but it was felt that the general idea and the possibility of using Mylar in such a balloon had been adequately tested.

Figures III-C5 to III-C8 show a series of shots of the Mylar balloon which are strikingly different from the polyethylene in its marked transparency to visible radiation. It is clear that one can see the stands of Williams Arena through the balloon and when the inflation was being carried on, one had the impression that the balloon was much like a soap bubble. During this test one of the nylon lines securing the balloon to the Arena snapped and the balloon had to rise approximately 2 feet before being stopped by a second line. The balloon took a marked shock at this time and vibrated like a bowl of jelly but no harm to the balloon was done and it was felt that the natural shape balloon without tapes could stand appreciable shocks. It is well known that Mylar has extremely good low temperature properties and therefore a hangar inflation on a Mylar balloon is essentially the equivalent of a flight test except for the effect of ultra-violet or ozone which has yet to be investigated.

In addition to the hangar tests, four flights of 25' diameter by 45' long Mylar cylinders have been carried out (flights #59, 60, 61 and 62). The first of these four flights was a Mylar cylinder which had been inflated in the Arena and in the process of deflating this balloon it was dropped. On launching this

*All of the Mylar cylinder balloons described here were manufactured by Herb Shelly, Inc., Farmington, Minnesota.

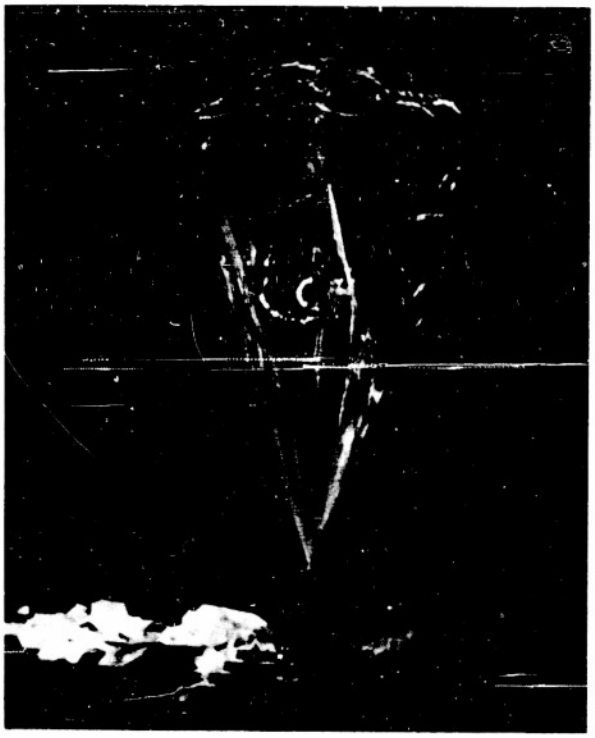

A. Gross load equals 274 pounds.

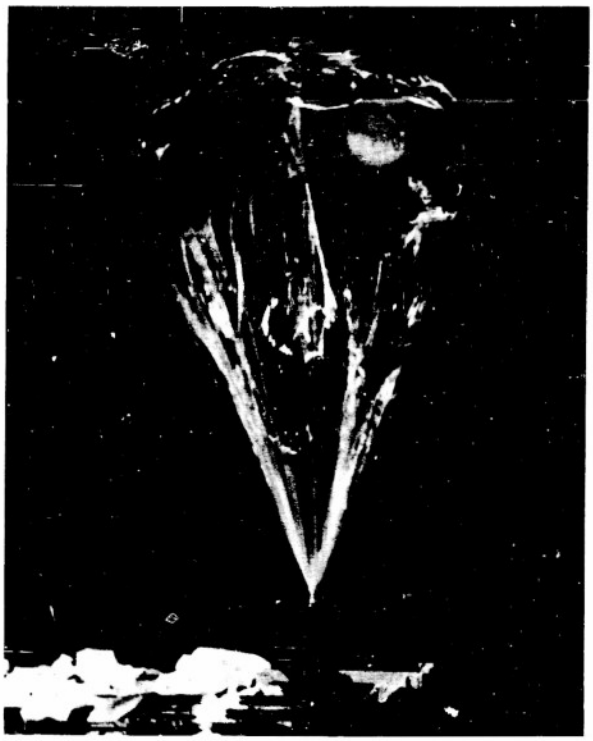

B. Gross load equals 329 pounds.

C. Gross load equals 379 pounds.

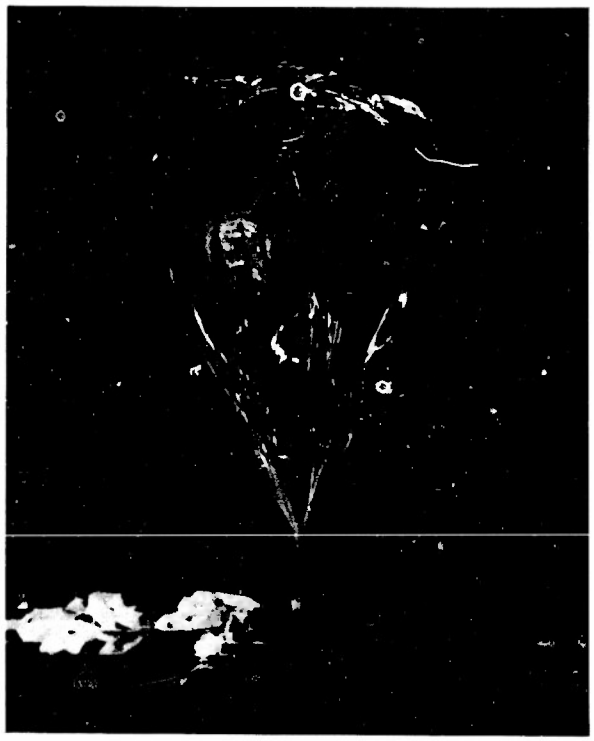

D. Gross load equals 429 pounds.

Sec III-C Figure 5

Sec III-C Figs 5&6. A 25' diameter by 45' gore length Mylar cylinder at various stages of inflation with pure helium. The gross load lifted is indicated on each photograph.

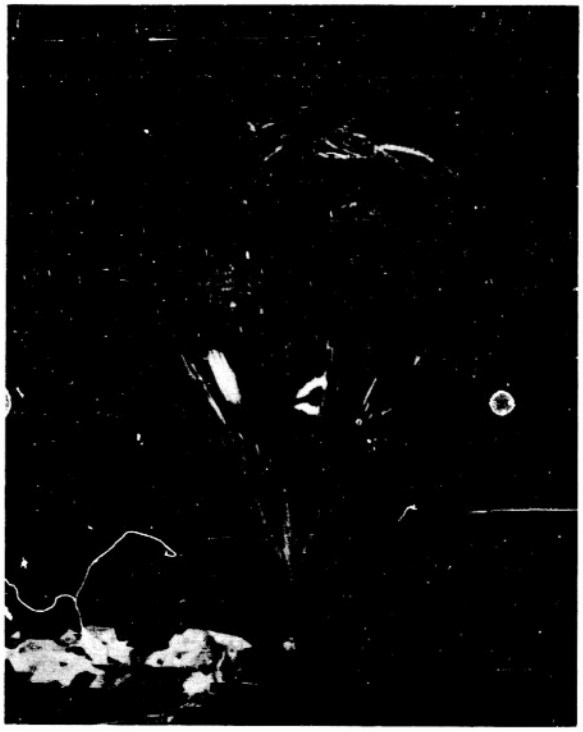

A. Gross load equals 479 pounds.

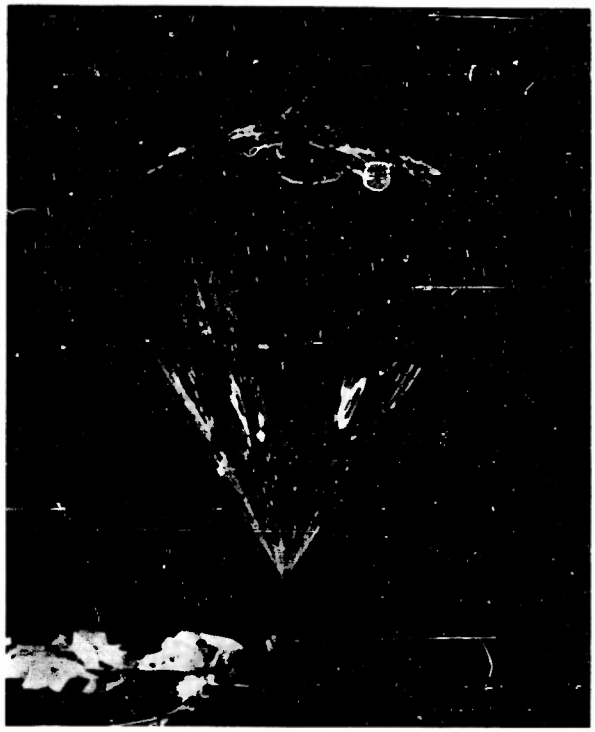

B. Gross load equals 529 pounds.

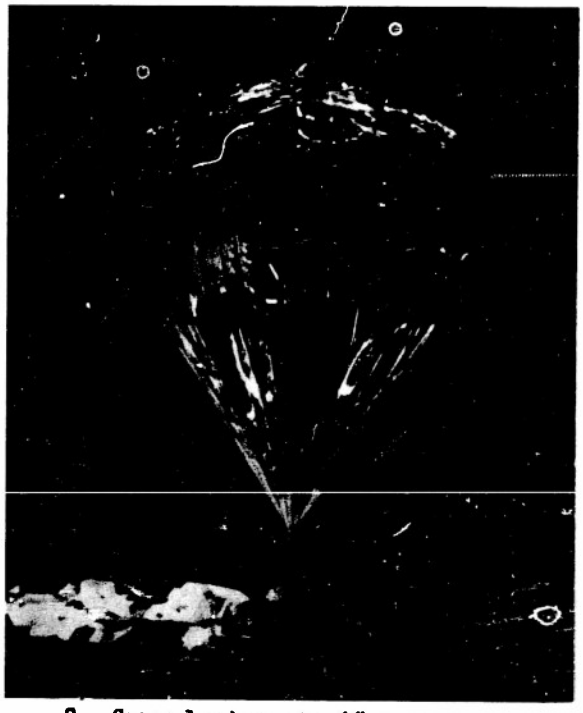

C. Gross load equals 554 pounds.

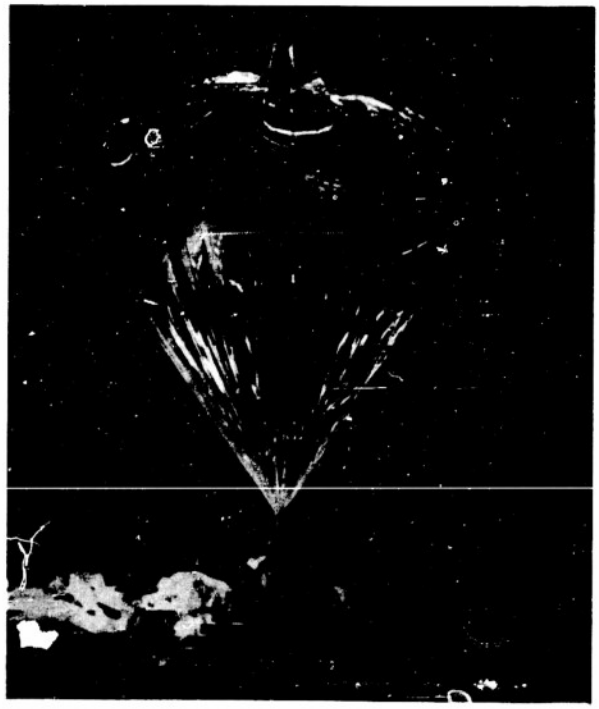

D. Gross load equals 574 pounds.

Sec III-C Fig 6

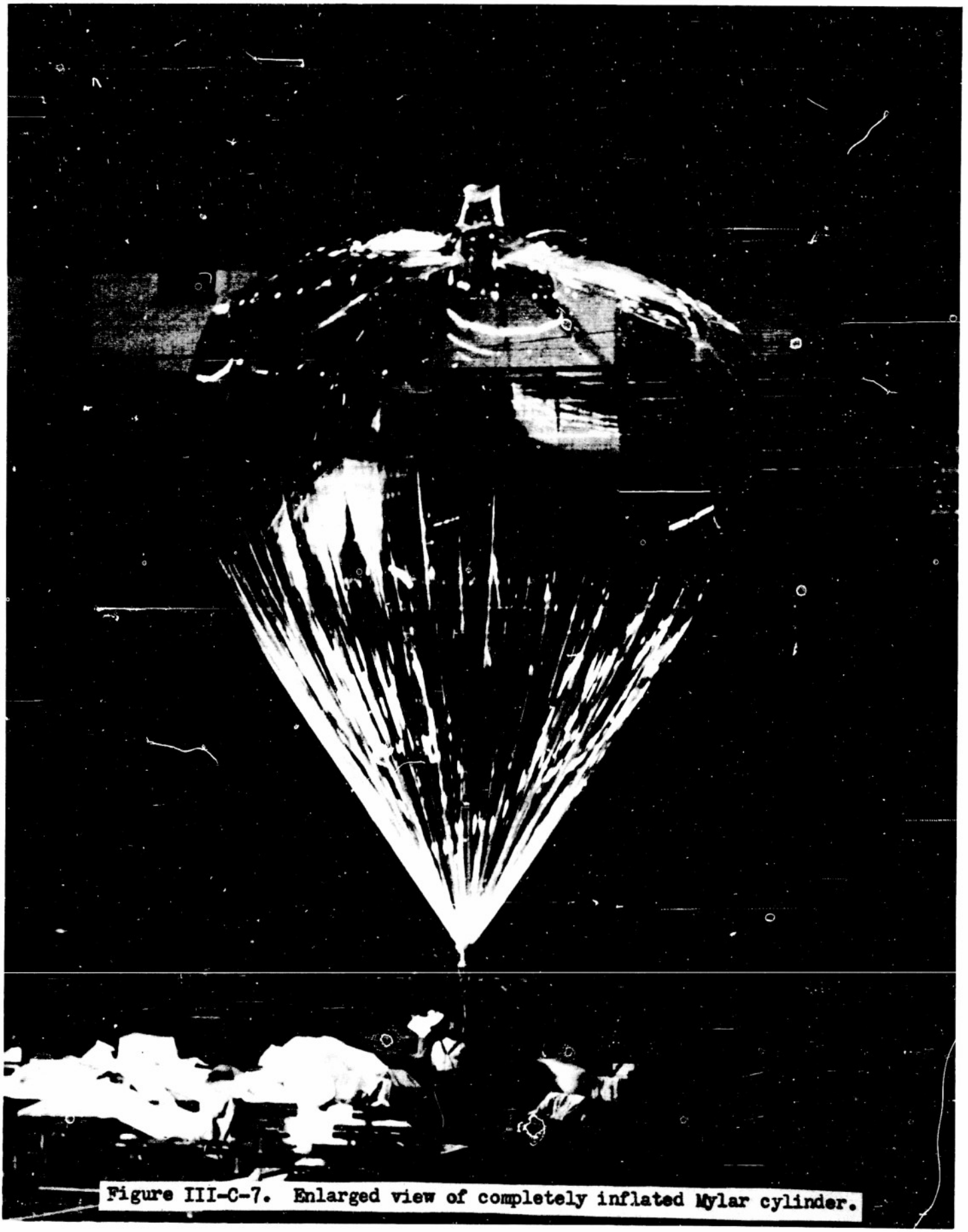

Figure III-C-7. Enlarged view of completely inflated Mylar cylinder.

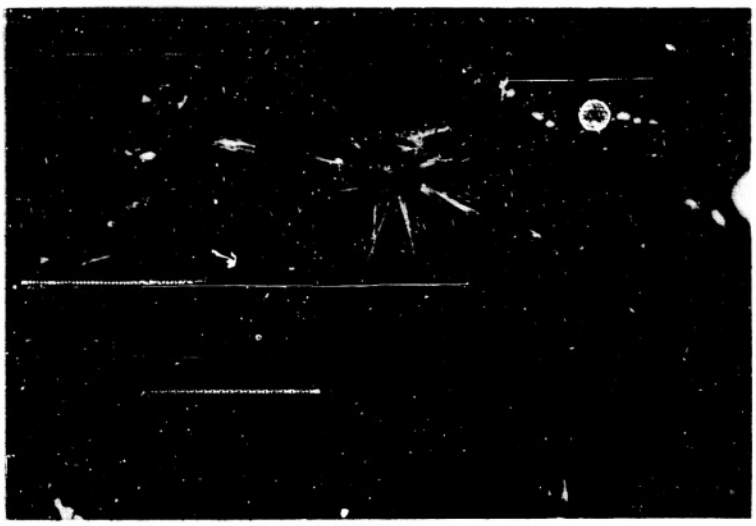

A. Shot looking up through the Mylar cylinder with the duct visible through the balloon.

B. View of the bottom of the cylinder showing the concentration of material carrying the load.

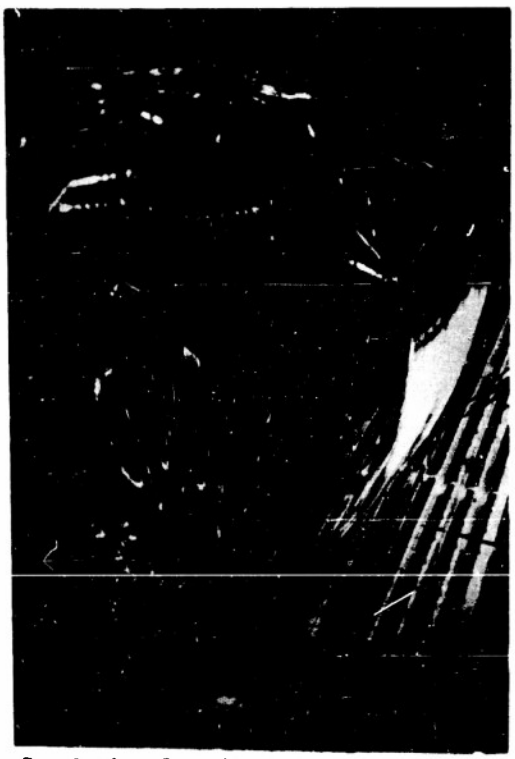

C. A view from the balcony looking down at the completely inflated Mylar cylinder.

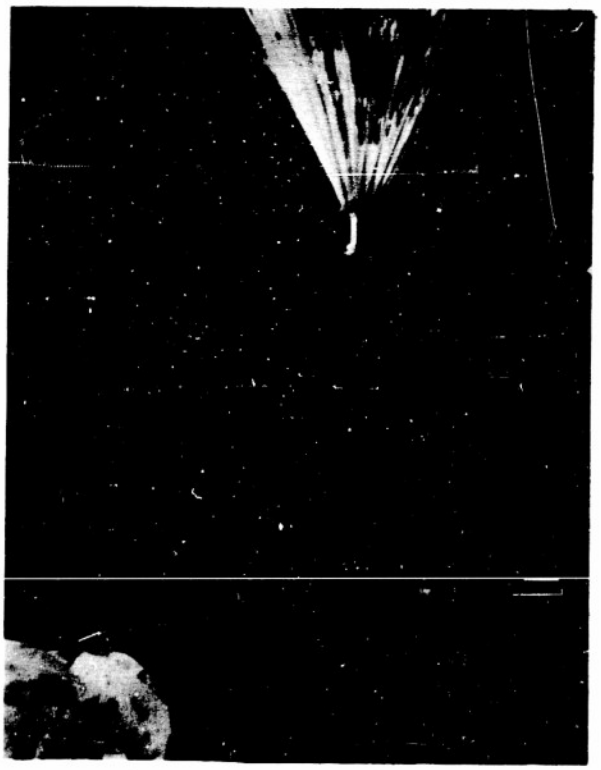

D. View of the bottom of the cylinder supporting a man plus additional tension in the line.

Sec III-C Fig 8

balloon rose only approximately 200 feet in the air and came back down immediately. This was either because of under-inflation or because of damage in the Arena. The three flights following this first one were all extremely successful. They behaved as one might have anticipated and showed no evidence of deterioration at ceiling, at least in the period of 24 hours. There was also no evidence in any of these balloons of measurable leakage. The sunset effect on these balloons corresponds to 3% of the displaced air rather than 6% to 9% of the displaced air in polyethylene balloons equipped with tapes. This reduction in sunset effect would be reflected in a direct reduction of ballast consumption in the same ratio, that is, the ratio of 3/9. Since essentially only sub-pressure cylinders have been tested, one of the future objectives of the program will be to investigate the zero pressure at the bottom and super-pressure balloons since these balloons should inherently be more stable and not show over-valving characteristics as do the slack sub-pressure natural shape balloons. These over-valving characteristics will be described in more detail in the next report in which the flights represented by the Mylar balloons are described in detail.

A rather simple sequence can be set up for the design of a zero circumferential stress, natural shape, cylinder balloon. It is to be stressed, however, that in order to obtain the proper performance from such a balloon, the procedure indicated below must be followed carefully. First, one must decide whether the balloon is to be sub-pressure, super-pressure, or zero pressure at the bottom. When this decision has been made, the ratio of the height of the balloon to the diameter of the balloon, or in a similar way, the ratio of the gore length to the diameter is determined. This means that the initial choice of how the balloon is to be operated, i.e. as super-or sub-pressure determines the ratio of the diameter to the height of the balloon as well as the cone angle at the bottom. The

way the ratio of diameter to height or gore length to diameter is a function of the sub-pressure height is shown in detail in connection with the REAC calculations on the natural shape balloon in Section III-B of this report. It is possible to operate a balloon whose gore length is 1.3 times its diameter as a sub-pressure or super-pressure balloon. A balloon made froma cylinder of these dimensions will always have enough material to take on the natural shape regardless of the super-pressure. Our original choice of a cylinder 45' long by 25' diameter can be replaced by a balloon 45' long by 35' in diameter and the latter balloon can be operated as a super-pressure or sub-pressure balloon depending on the choice of duct length. Current designs are based on this result.

It should be emphasized that the results of the theory must necessarily be used if the proper behavior is to be obtained from cylinder balloons in which it is possible by means of the duct to place the position of the zero pressure level.

SECTION III-D

COMPUTED "NATURAL" BALLOON SHAPE FOR A SPECIFIC REQUIREMENT OF THE MOBY DICK PROJECT

The tailored shape of a balloon is not necessarily the shape that the balloon will assume when it is floating at its ceiling altitude. If the tailored shape is chosen arbitrarily (sphere-on-cone, etc.) there will be regions on the balloon in which the fabric develops (circumferential) tensions perpendicular to the gore seals, and other regions in which there will be excess fabric lying in folds. Both kinds of regions can be avoided by proper choice of the tailored shape. This shape is sometimes called a "natural shape" and is uniquely determined as a solution of certain differential equations once the quantities that enter the equations as parameters have been specified. These parameters depend on the following conditions: volume of the balloon (or gore length), weight and number of load bearing tapes, weight per unit area of the fabric, weight of the load, and pressure difference across the fabric at the bottom apex (i.e., appendix length). A "natural shape" balloon will assume its tailored shape at ceiling altitude without developing circumferential tension or having excess fabric.

The "natural shape" given below was calculated using a specific requirement of the MOBY DICK project. The shape is applicable only to the conditions given. The calculations were made the the aid of a Reeve's analogue computer (REAC).

Given Conditions

Volume: 49,100 cu. ft.

Pay load: 285 pounds

Fabric weight: 0.0127 lbs/sq. ft. (2.5 mil polyethylene)

Tape weight: 0.00515 lbs/linear ft. (#890 glass filament)

Approximate number of gores; 35 (54 inch fabric width)

Circumferential stress: zero, throughout.

Pressure difference across fabric at bottom apex: zero.

Coordinates

r is the radial distance from the axis of the balloon.

z is the vertical distance along the axis, measured up from the bottom of the balloon.

Both measurements are in feet.

Values

z	r	z	r
0	0	29.83	24.63
1.54	2.25	30.38	24.58
3.70	5.32	31.05	24.48
4.33	6.22	32.18	24.12
6.17	8.79	33.95	23.75
6.99	9.98	35.15	23.27
8.38	11.75	35.31	23.18
9.21	12.82	37.35	22.00
10.32	14.12	37.42	21.95
12.44	16.55	38.52	21.12
15.48	19.26	40.50	18.92
16.95	20.39	41.62	17.13
18.08	21.17	43.02	14.02
20.56	22.59	43.05	13.92
22.23	23.39	43.78	11.17
24.52	24.12	44.12	9.51
27.69	24.65	44.26	7.55
28.23	24.67	44.36	5.45
28.60	24.69	44.38	5.00
29.29	24.66	44.39	0

SECTION III-E

APPENDIX DESIGN

The performance of the flights with open or standard appendices in the bottom of the balloon indicated that a definite mechanism to exclude air was essential in pursuing the study of balloon behavior. The flights prior to flight #36 showed that air intake through the appendix could be responsible for altering the flight characteristics so greatly as to make detailed analysis of the flights almost impossible. There was little possibility of determining the quantity of air in the balloons at any particular time and consequently its contribution to the static equilibrium of the system.

The "Howell" effect, the characteristic of the balloon floating after valving at ceiling altitude for approximately one hour and then descending, was felt possibly due to the intake of air and the loss of helium by diffusion and turbulence at the appendix. Another possible explanation was that as the balloon valved the free lift and the warming gas, it had a slightly larger volume due to the pressure required for valving. The balloon would assume a change of shape after valving and be different in volume. It was felt that an experiment which prevented overvalving and the intake of air would aid the analysis of the "Howell" effect as well as other portions of the flight.

The appendix designed to perform in this manner was the horsetail appendix. (Figure 1). In principle this was an inverted standpipe which controlled the pressure in the inflated balloon by the length below the base of the balloon. By placing the lower end below the base a slight super-pressure could be maintained in an effort to keep the balloon from relaxing after valving. The base of the balloon was tied off so no air could enter at this point. In the inflated position, air could not flow up the horsetail because of the lighter density gas at the top and higher relative pressure. Diffusion of air and helium in the

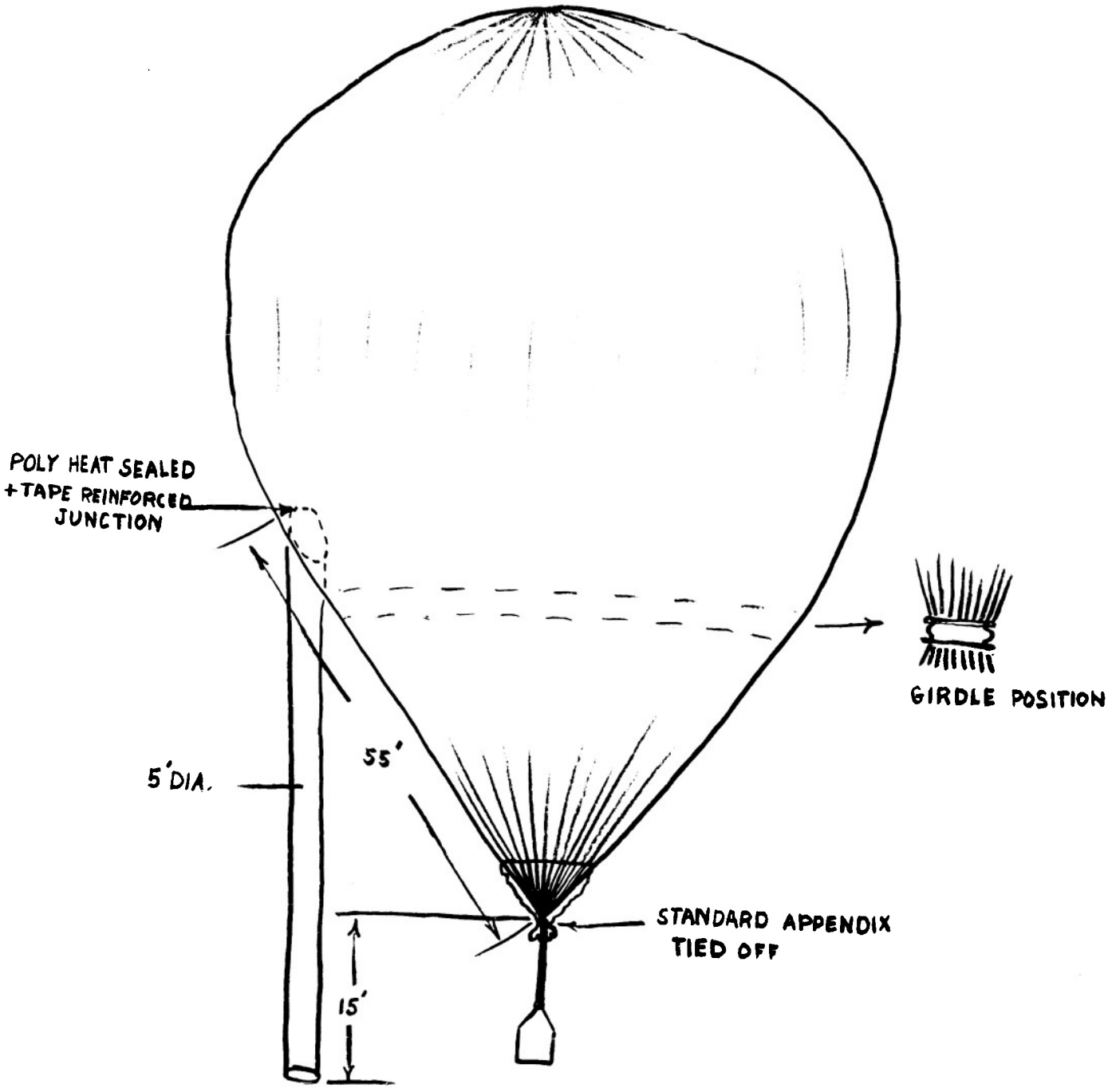

HORSETAIL APPENDIX
73' BALLOON

Section III-E
FIG NO. 1

pipe would be minimized by the small cross-sectional area and volume of helium in the appendix.

The horsetail appendix used in flight #36 was attached to the balloon above the girdle. The free end was rolled up to the attachment point and was expected to unroll after the balloon extended to its full length. This unrolling did not take place, however, and the balloon rose to ceiling altitude and burst from the free lift super-pressure.

The experiment was repeated on flight #37 with the horsetail unrolled prior to launching. After reaching altitude the balloon descended at once at 1000 ft/min to 4000 feet below its ceiling. From this point it descended at a constant rate of 130 ft/min. What appeared at first to be overvalving and a descent to establish static equilibrium by adiabatic compression was finally determined to be a structural failure at the appendix attachment point. Pictures from the up-camera showed a loose tape at this point, and also the illumination of part of the balloon by sunlight as though it were shining through a hole. Air was taken in through this hole during descent. The comparison of pictures of the balloon descending with those of the ascending balloon showed much more volume at each altitude. The air taken in was also being adiabatically compressed and contributed to the lift in the descent. It was decided to attempt a flight constants flight with the horsetail appendix in the hopes that the horsetail appendix would exclude more air than the standard appendix. Failure of this flight (flight #38) at ceiling altitude and the intake of air of flight #37 led to further changes in the appendix design and installation. The reason for the design change was because it was then realized at certain periods of the flight, the top of the horsetail appendix reached into a part of the balloon that was under negative pressure. At these times there would be a tendency for air to be drawn into the balloon. An attachment point which would be under positive pressure at all times was one near the top of the balloon. This means that as the balloon ascends or descends, the positive pressure difference which

exists would keep the air from flowing into the balloon at all times.

Examination of the calculated balloon shapes for sub-pressure balloons indicated that the 73' balloon could be flown with the duct cut to a sub-pressure length, about 45 feet above the base of the balloon, without introducing a significant volume defect (Figure 2). One inherent advantage in flying the balloon sub-pressure is that below the bottom of the duct there is no leakage of gas from the balloon. The tendency is for air to leak in. Because of its density compared to the lifting gas this is negligible. The first duct flight, flight #39, showed that a more positive method of reinforcing the attachment point was needed. The tape reinforced heat sealed structure became inadequate in the temperatures encountered in the stratosphere.

The first satisfactory installation incorporated an aluminum clamping ring which clamped the balloon and duct in position (Figure 3). The duct itself is simply a tube of the polyethylene material as it comes from the polyethylene converter. The 54" flat width tube opens up to form a 31" diameter duct. At the attachment point to the balloon this tube is gathered in on one side so as to form a 90° elbow, turning the duct tangent to the balloon surface. Sufficient tucks are taken in along this same side of the tube so the duct will conform to the inflated balloon shape.

This installation was flown very successfully on flight #40 and subsequent flights. In flight #40 after the balloon ascended to ceiling and valved through the duct, there was evidence of a very slight volume deficiency for the duct length used. The balloon oscillated with simple harmonic motion for seven cycles. The period of this motion was found to be five minutes which corresponds to the restoring force due to adiabatic expansion and compression of the balloon gas in the stratosphere. This oscillation continued for approximately 40 minutes, the time in which the balloon gas was coming up to equilibrium temperature. After this time the flight continued level at ceiling until affected by sunset.

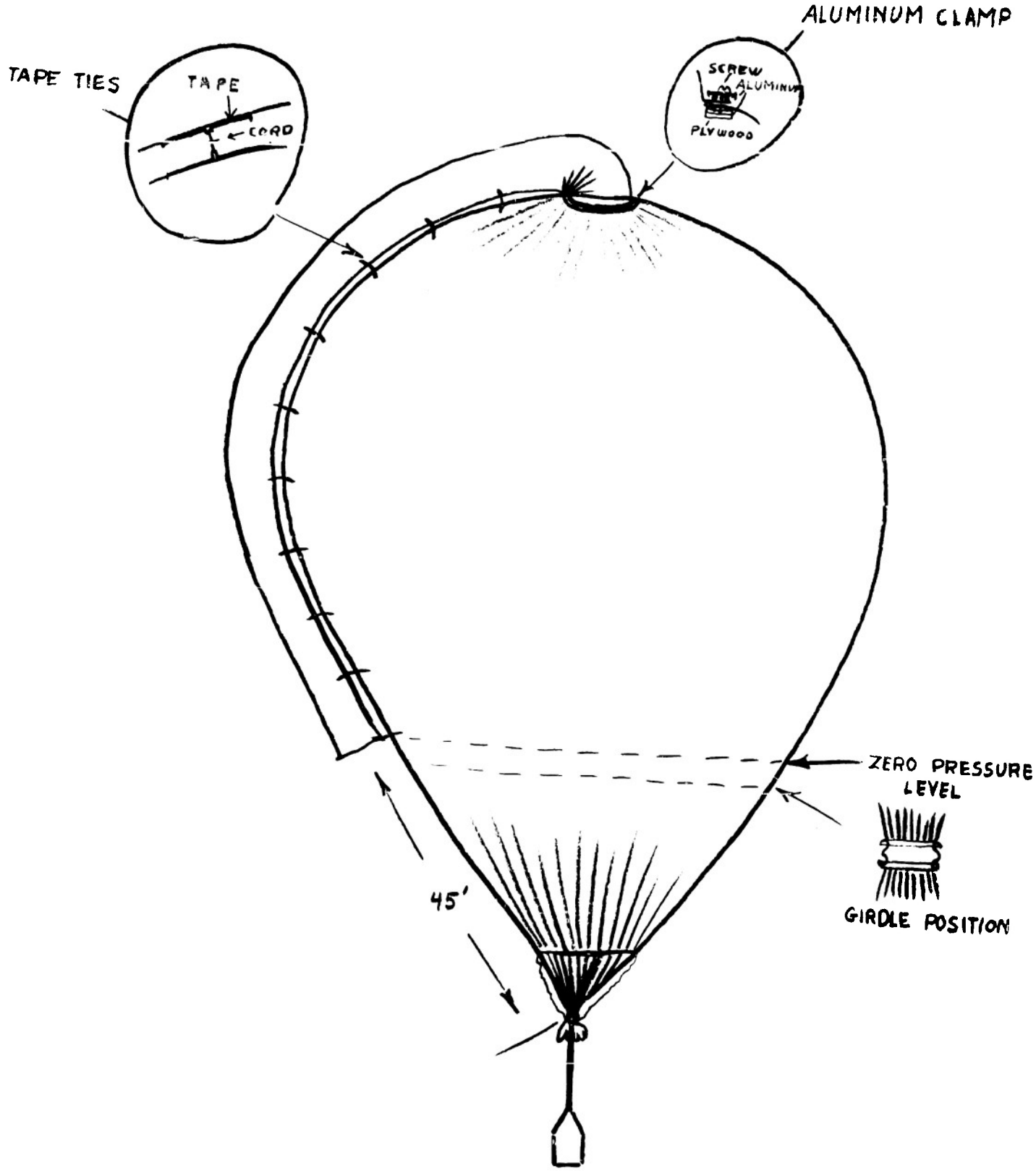

DUCT APPENDIX
73' BALLOON

Section III-E
FIG NO. 2

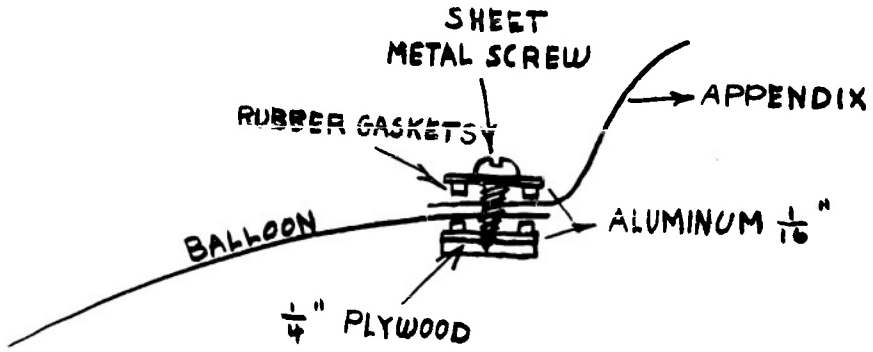

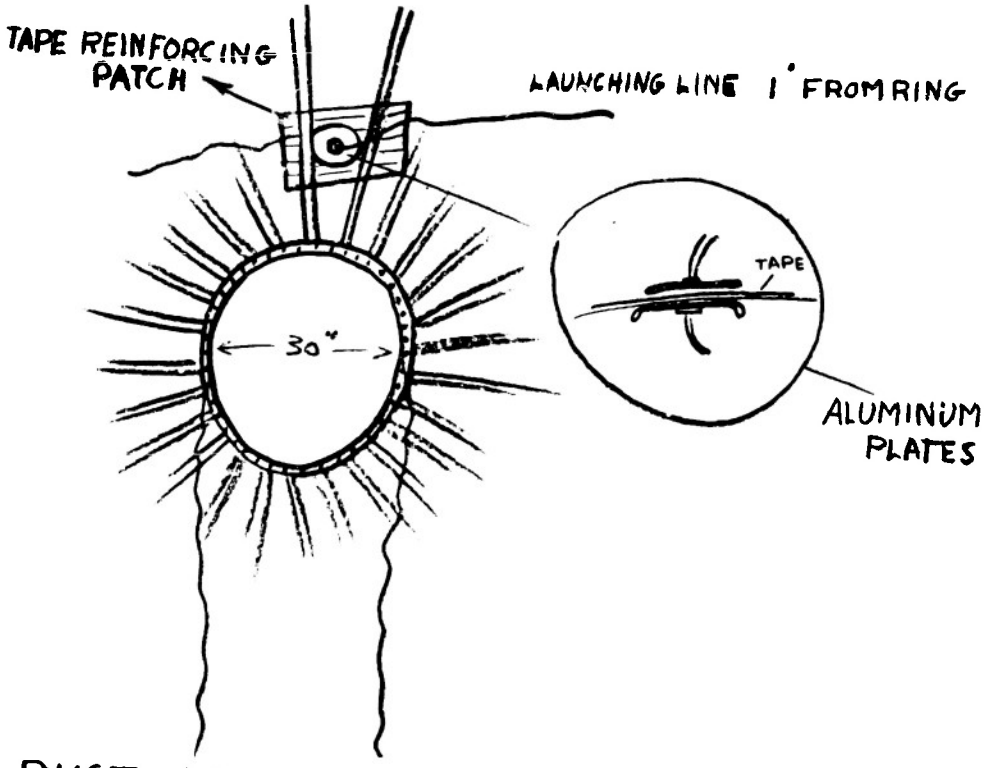

DUCT ATTACHMENT

FIG NO. 3

Section III-E

Examination of the balloon photographs recovered after flight showed that during the time it could be observed, it contracted in descent in the same manner that it had expanded during ascent, proof that the duct appendix was successful in elminating the intake of air at ceiling and during descent.

Some of these photographs taken from a camera in the gondola are included to show the appearance of the balloon and duct appendix during flight. The numbers correspond to flight numbers and to exposure numbers after launching, the interval between exposures being approximately one minute.

The expansion of the gas bubble can be followed from shortly after launching (40-42) up to ceiling altitude (40-137). The duct appendix can be clearly seen in most of the frames. The inflated portion of the appendix is noted to extend down a little below the widest portion of the bubble. The remainder of the appendix hangs limp alongside the balloon fabric. The expanding gas forces the balloon girdle down and finally off the balloon and into the catcher (40-130, 40-131) indicating the balloon is nearly inflated. In 40-137 the gas level approaches the bottom of the duct. Actual valving is taking place in 40-140 and 40-143 as can be seen by the opening in the duct. The duct appears to close after this (40-148) as the balloon maintains nearly constant altitude. Towards sunset (40-290) the folds in the balloon deepen as the volume and altitude decrease. It should be pointed out that in flight #45 a duct installation with the aluminum clamp rings was made on a 1-mil balloon. The attachment point was 14 feet from the top of the balloon, in a similar position that was used successfully in previous flights of heavier balloons. Failure in the thin material in the vicinity of the duct showed that local stresses were not taken up properly in the general area of the duct. At this time a switch was made to the top center installation where the balloon is much more reinforced. Consequently no further attempts to strengthen the structure away from the center of the balloon were made.

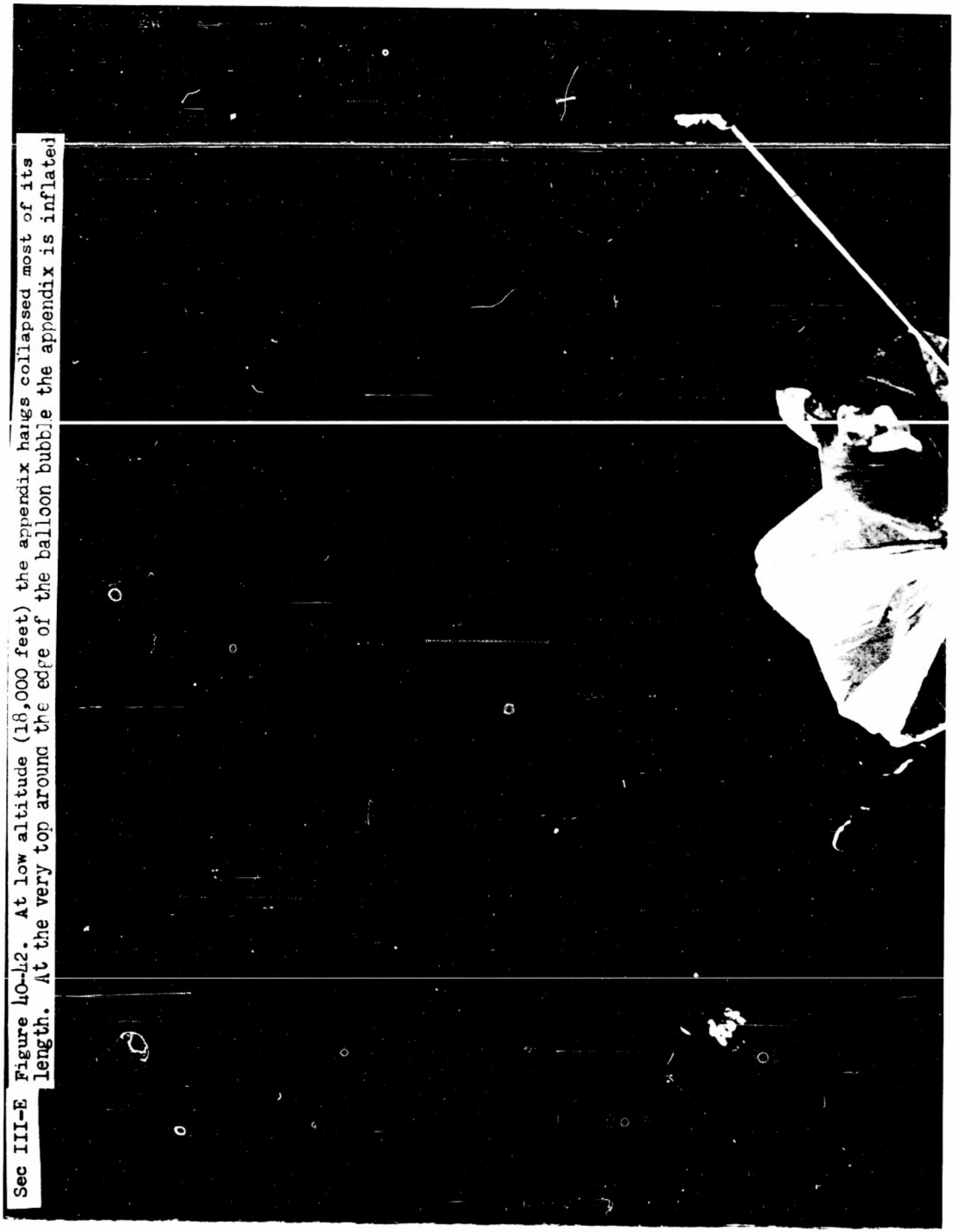

Sec III-E Figure 40-42. At low altitude (18,000 feet) the appendix hangs collapsed most of its length. At the very top around the edge of the balloon bubble the appendix is inflated

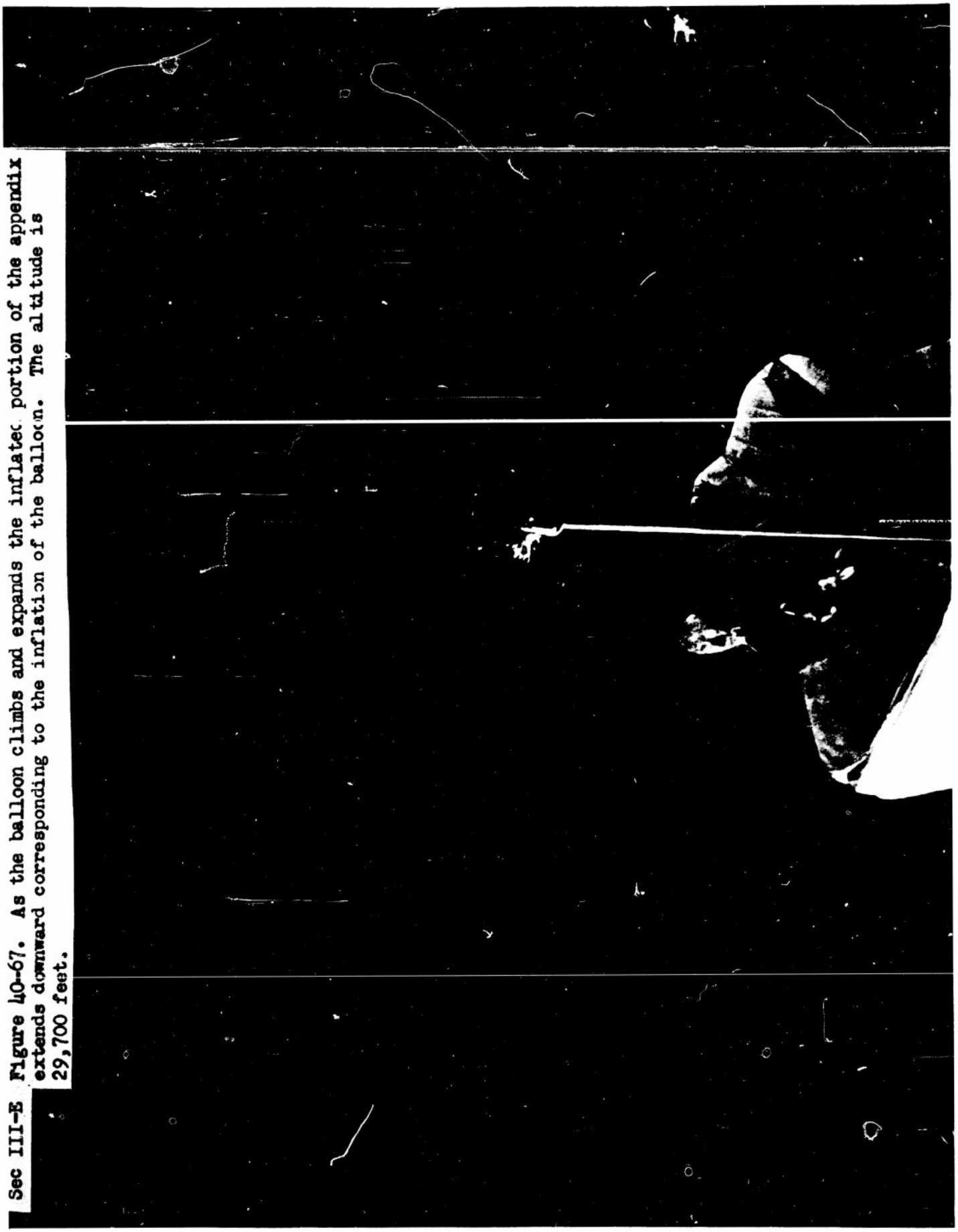

Sec III-E Figure 40-67. As the balloon climbs and expands the inflated portion of the appendix extends downward corresponding to the inflation of the balloon. The altitude is 29,700 feet.

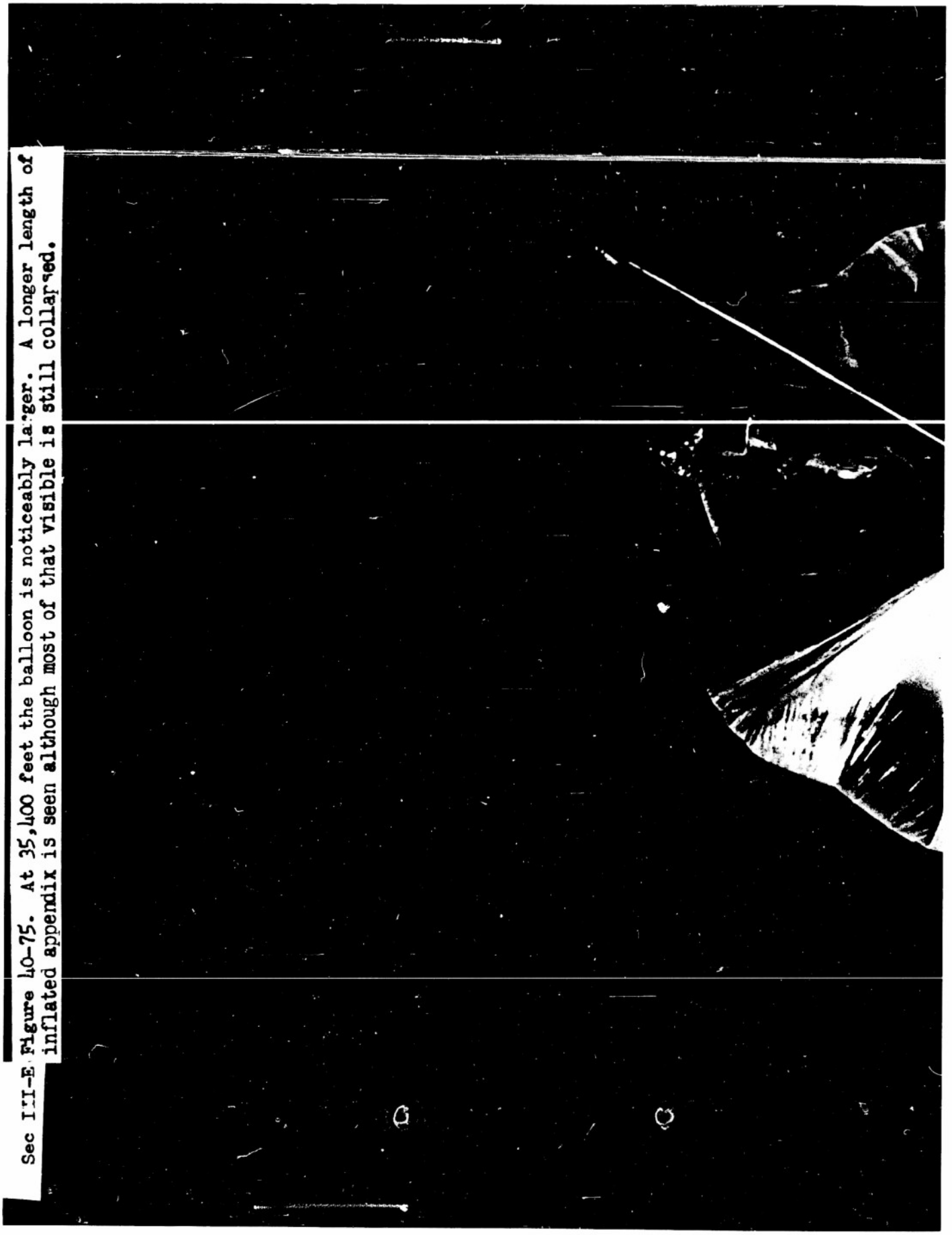

Sec III-E Figure 40-75. At 35,400 feet the balloon is noticeably larger. A longer length of inflated appendix is seen although most of that visible is still collapsed.

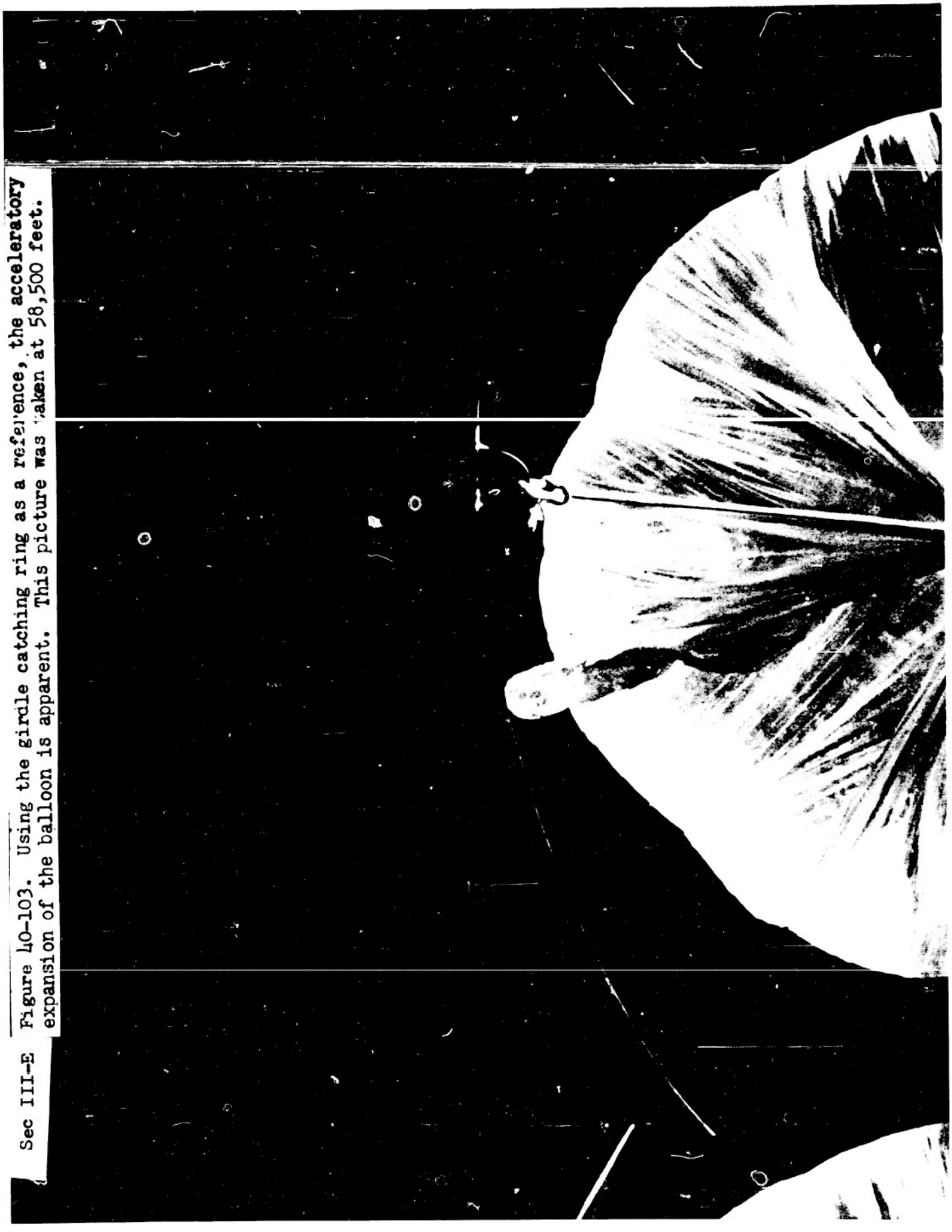

Sec III-E Figure 40-103. Using the girdle catching ring as a reference, the accelerator expansion of the balloon is apparent. This picture was taken at 58,500 feet.

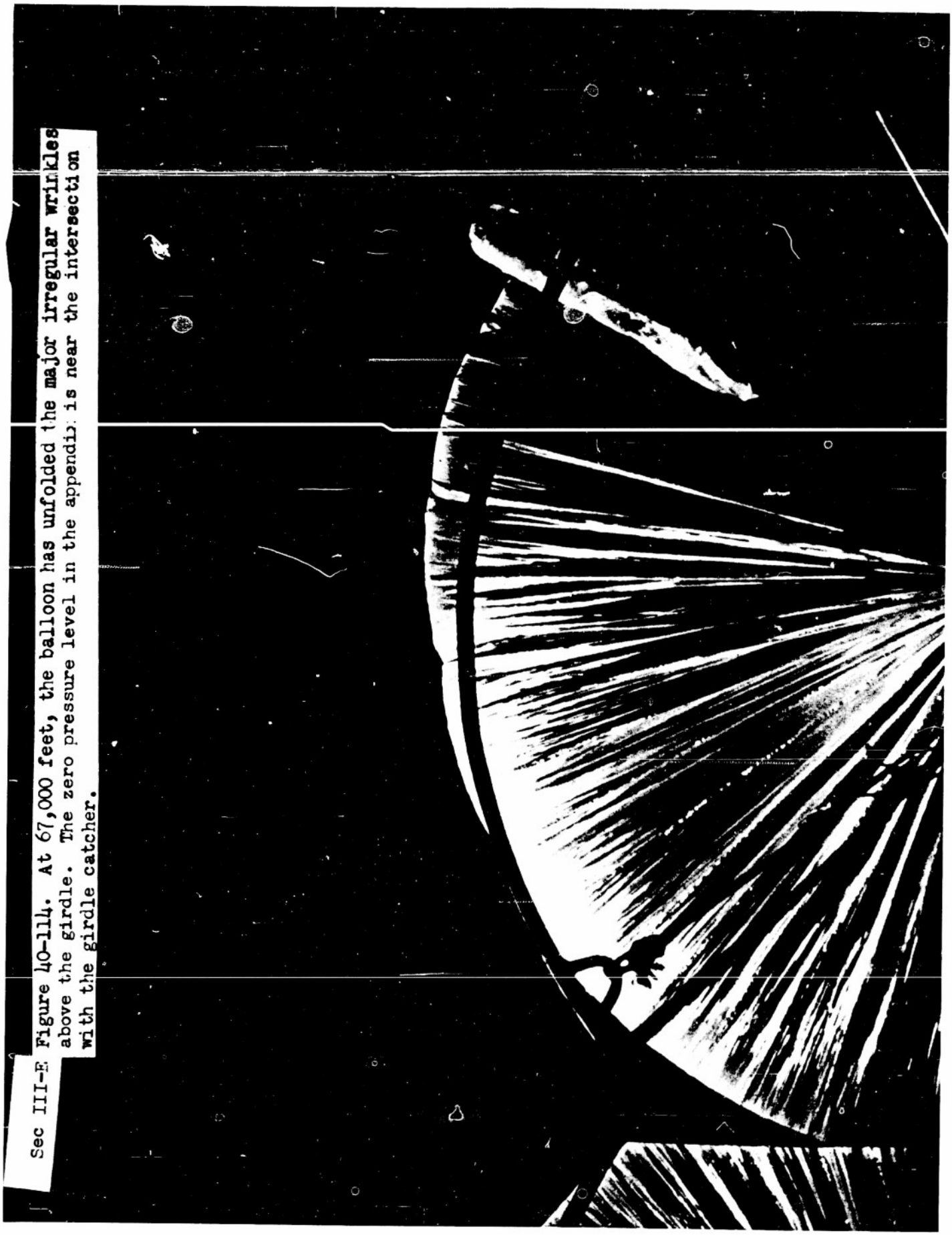

Sec III-E Figure 40-114. At 67,000 feet, the balloon has unfolded the major irregular wrinkles above the girdle. The zero pressure level in the appendix is near the intersection with the girdle catcher.

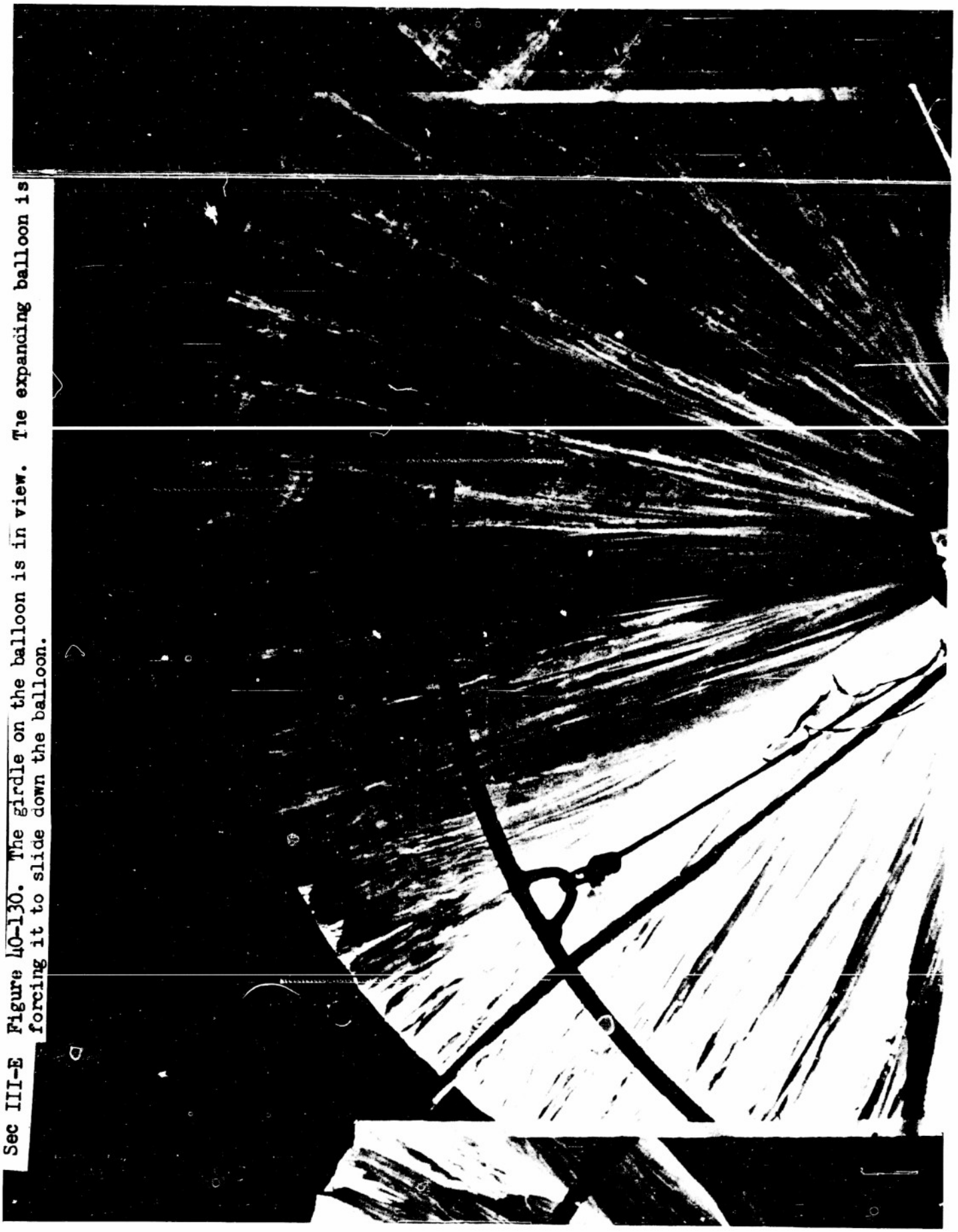

Sec III-E Figure 40-130. The girdle on the balloon is in view. The expanding balloon is forcing it to slide down the balloon.

Sec III-E Figure 40-131. One minute later at 79,300 feet the girdle has slipped into the catcher. The balloon is reshaped into major folds of material under less stress. The bottom of the appendix is still collapsed.

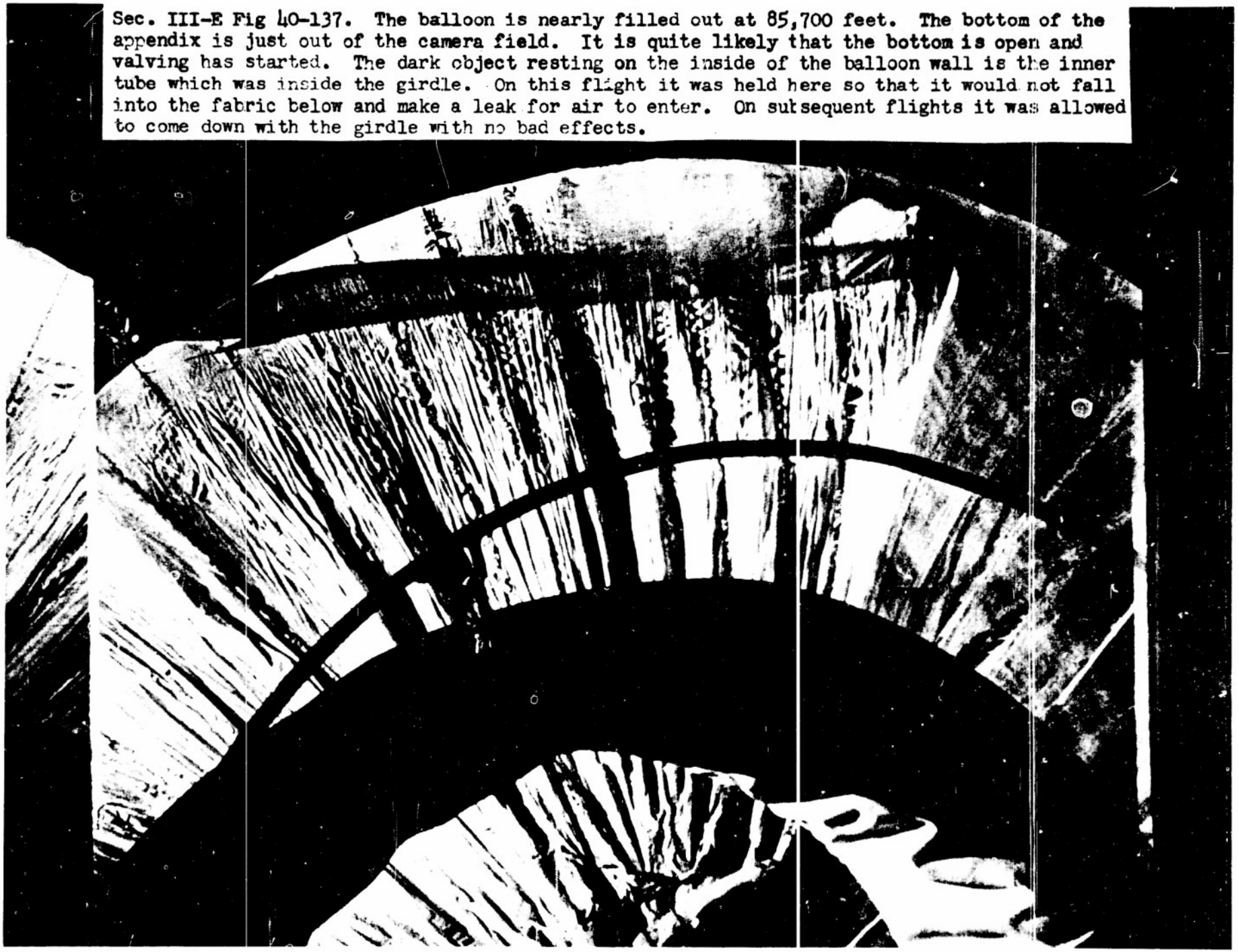

Sec. III-E Fig 40-137. The balloon is nearly filled out at 85,700 feet. The bottom of the appendix is just out of the camera field. It is quite likely that the bottom is open and valving has started. The dark object resting on the inside of the balloon wall is the inner tube which was inside the girdle. On this flight it was held here so that it would not fall into the fabric below and make a leak for air to enter. On subsequent flights it was allowed to come down with the girdle with no bad effects.

Sec III-E Fig 40-140. The appendix is clearly seen to be valving through the bottom opening at the highest altitude of 86,700 feet. Low valving pressure and low rate of flow is indicated by the narrow aperture at the bottom of the duct.

Sec III-E Figure 40-143. Continued valving is evidenced by the open duct. The balloon oscillated after reaching ceiling and valved as the gas warmed.

Figure 40-148. The base of the duct is closed at 86,200 feet altitude. The slight folds in the balloon are indicative of a very slight volume deficiency. This is very sensitive to the position of the bottom of the duct. A slight increase in duct length would have filled the balloon more nearly full but under essentially the same sub-pressure condition.

Sec III-E Figure 40-160. Vertical oscillations of the balloon have damped considerably. At the time of this picture the balloon was at 86,000 feet.

Sec III-E Figure 40-182. The bottom of the duct is closed as the five minute period oscillations have damped out.

Sec III-E Figure 40-205. All the fabric below the duct forms the sub-pressure part of the balloon. That is, there is more pressure outside the balloon than inside. The fabric does not collapse because of its longitudinal tension from the weight of the load and the lift of the gas.

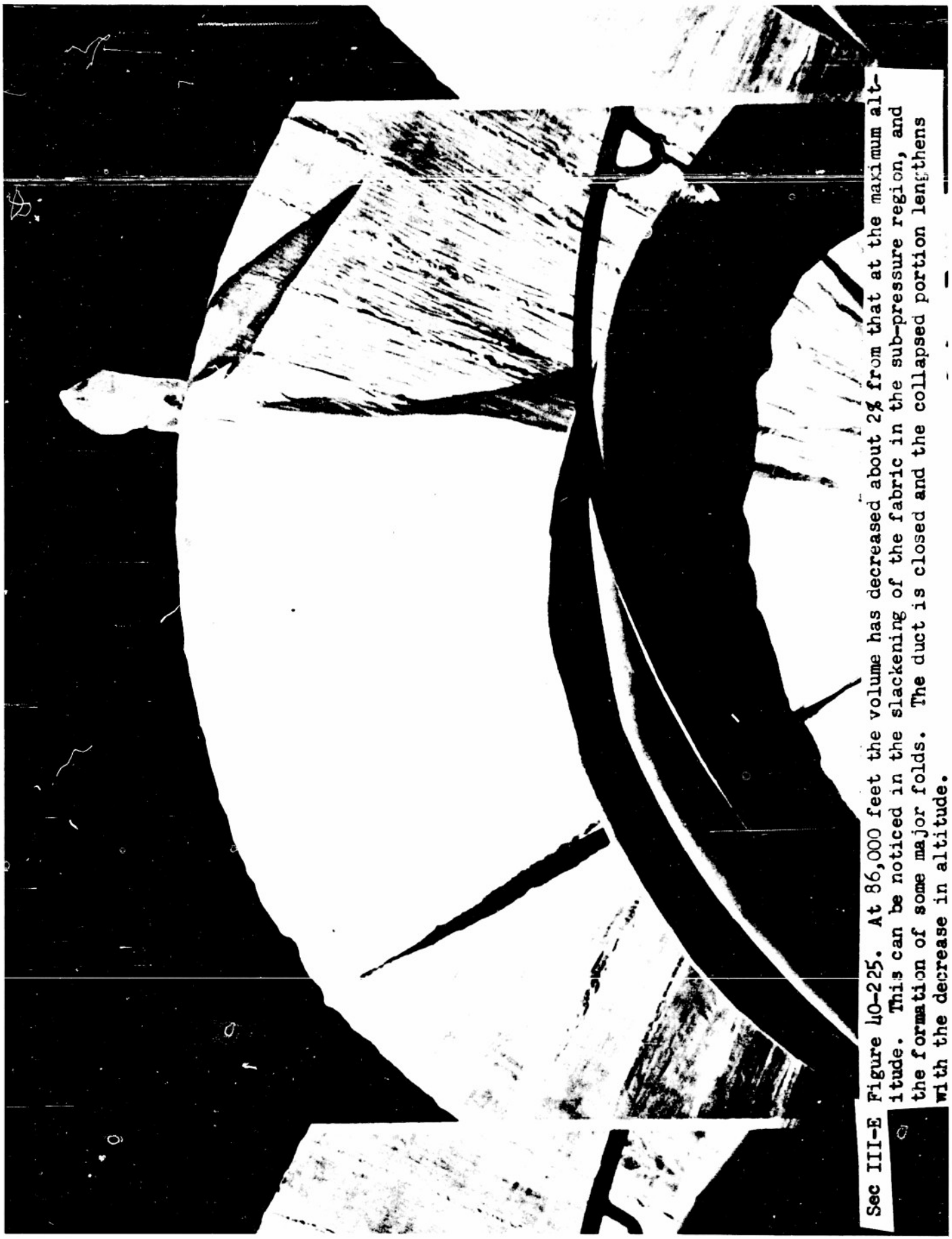

Sec III-E Figure 40-225. At 86,000 feet the volume has decreased about 2% from that at the maximum altitude. This can be noticed in the slackening of the fabric in the sub-pressure region, and the formation of some major folds. The duct is closed and the collapsed portion lengthens with the decrease in altitude.

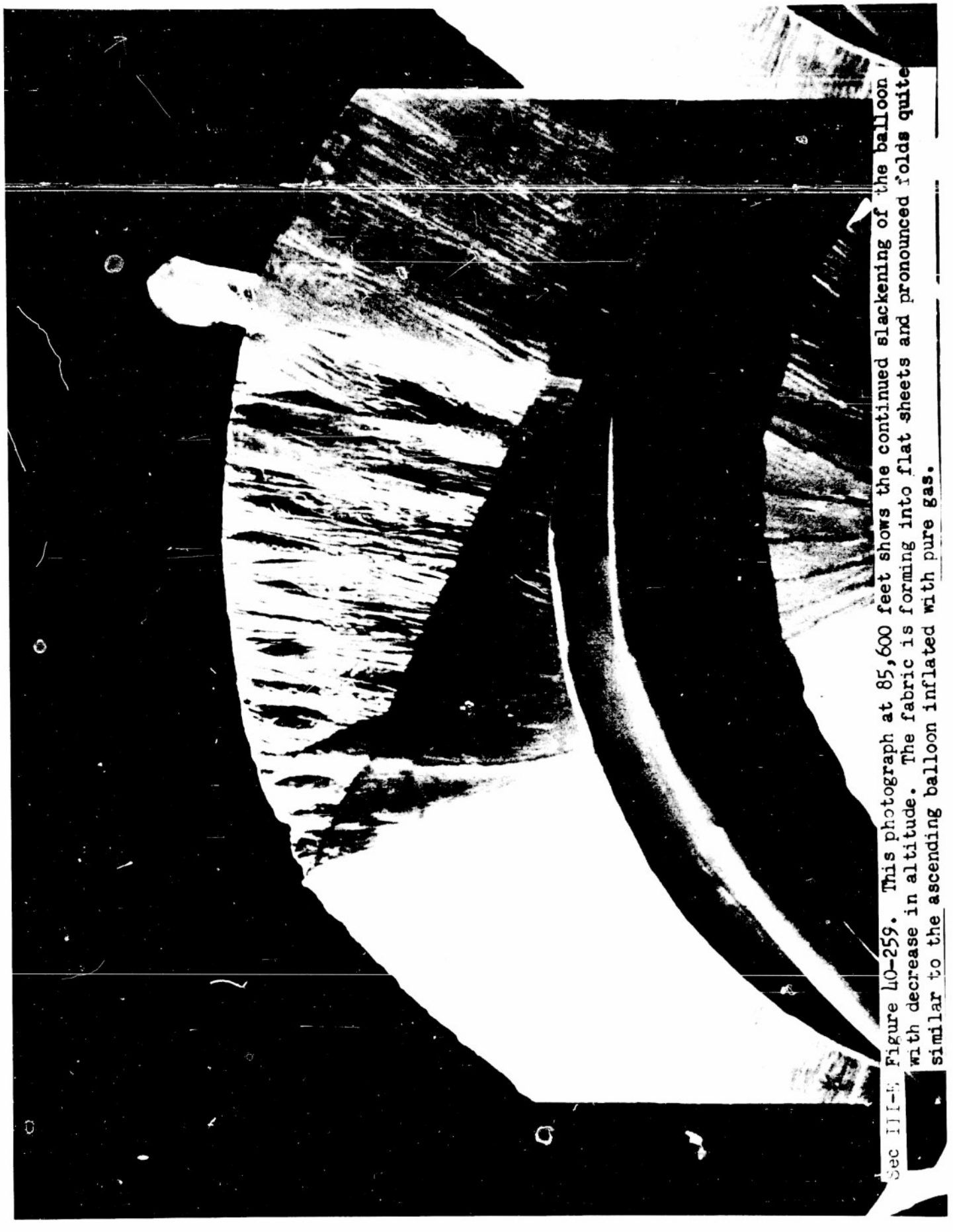

Sec III-E Figure 40-259. This photograph at 85,600 feet shows the continued slackening of the balloon with decrease in altitude. The fabric is forming into flat sheets and pronounced folds quite similar to the ascending balloon inflated with pure gas.

Sec III-E Figure 40-274. The arrangement of sheets and folds from a concave surface on the lower sub-pressure section. Had the appendix normally at the base of the balloon been open, air would have entered to allow tension in the fabric to straighten it into a conical section.

Sec III-E Figure 40-277. The lowering sun casts more pronounced shadows of the balloon folds. The altitude of 85,500 feet represents a volume change of 6% from the maximum volume.

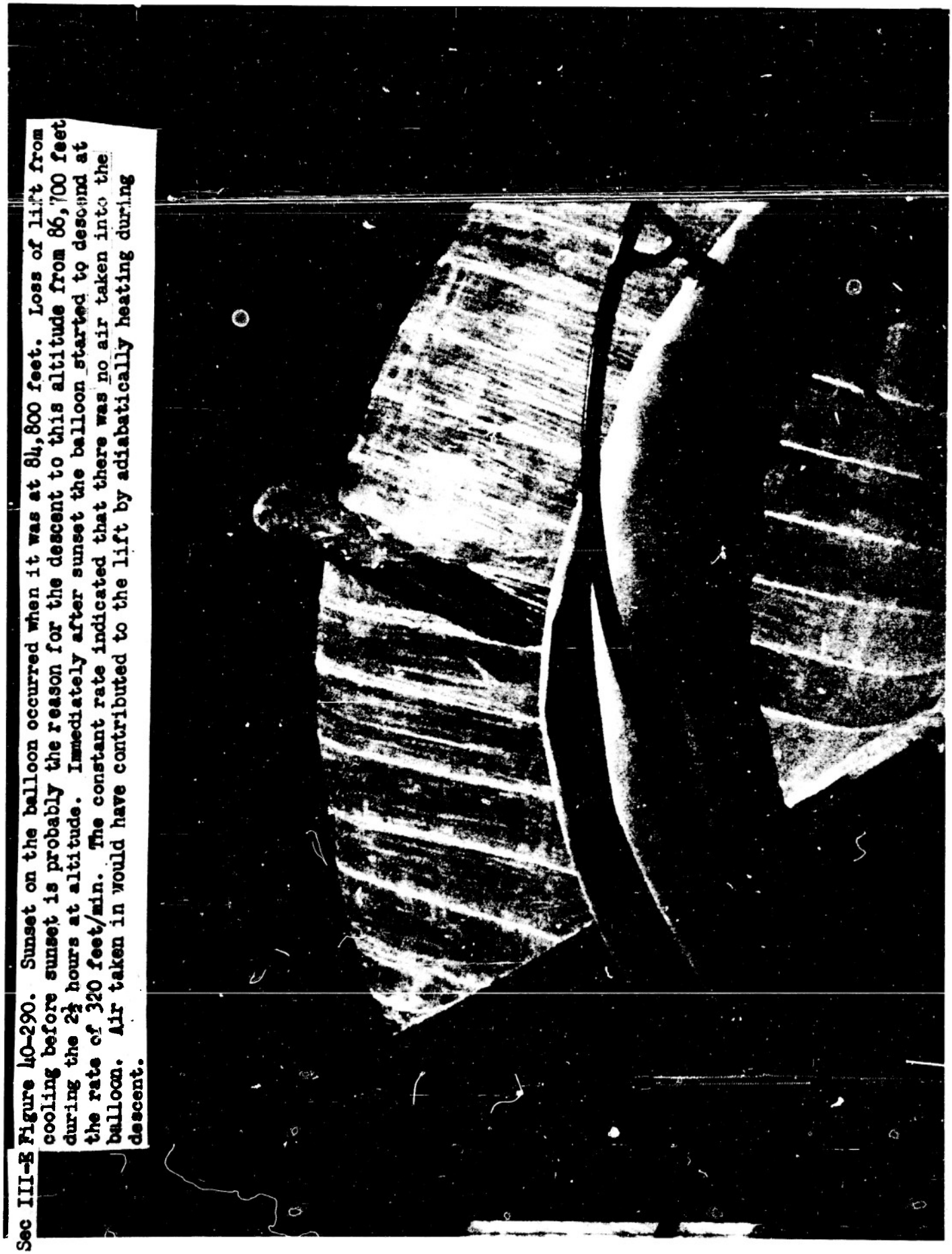

Sec III-E Figure 40-290. Sunset on the balloon occurred when it was at 84,800 feet. Loss of lift from cooling before sunset is probably the reason for the descent to this altitude from 86,700 feet during the 2½ hours at altitude. Immediately after sunset the balloon started to descend at the rate of 320 feet/min. The constant rate indicated that there was no air taken into the balloon. Air taken in would have contributed to the lift by adiabatically heating during descent.

Other methods have been used to install the duct appendix in the balloon. In Figure 4 the method designed and used by Winzen Research is shown. It consists basically of an aluminum ring structure at which the balloon tapes are terminated. The duct tube is taped over the hole thus formed and taped down one seam of the balloon.

A duct five feet in diameter was made and flown on a General Mills type 1161 balloon. The details are shown in drawings BA-490B. A 3000 pound pre-stressed nylon line was passed through the loop tie-ins to maintain the structure in the top of the balloon. This was flown in flight #66 which failed at 67,000 feet. The cause of failure has not been ascertained. The duct appendix attachments to the balloon have had no adverse effect on, nor have they complicated the balloon rigging and launching method developed by the University of Minnesota described in the last report. The appendix is handled similar to the rest of the balloon fabric in packing. It remains uninflated in the horizontal weigh-off position during launching. Only after the balloon is erected and the diaphragm cord is pulled does the appendix, along with the top of the balloon, become inflated. The gas zero pressure levels in the balloon and the appendix coincide, and this level can be seen quite distinctly in the appendix. One additional step in the launching procedure involves the tie-off of the bottom to form an air tight barrier. This is done by collapsing the former skirt appendix and binding it tightly about the balloon load ring with a piece of scrap polyethylene.

The pressure required to force the gas through the duct can be compared theoretically with the pressure required to valve through a simple orifice type appendix and also with the pressure of the head of gas already in the balloon. A typical case may help to illustrate these relative pressures. The 73' diameter balloon (225,000 cubic feet) has a ceiling altitude of 87,000 feet (20 mb) with a gross load of 400 pounds when helium inflated.

DUCT APPENDIX MODIFICATION TO GMI 1161 BALLOON

(1)

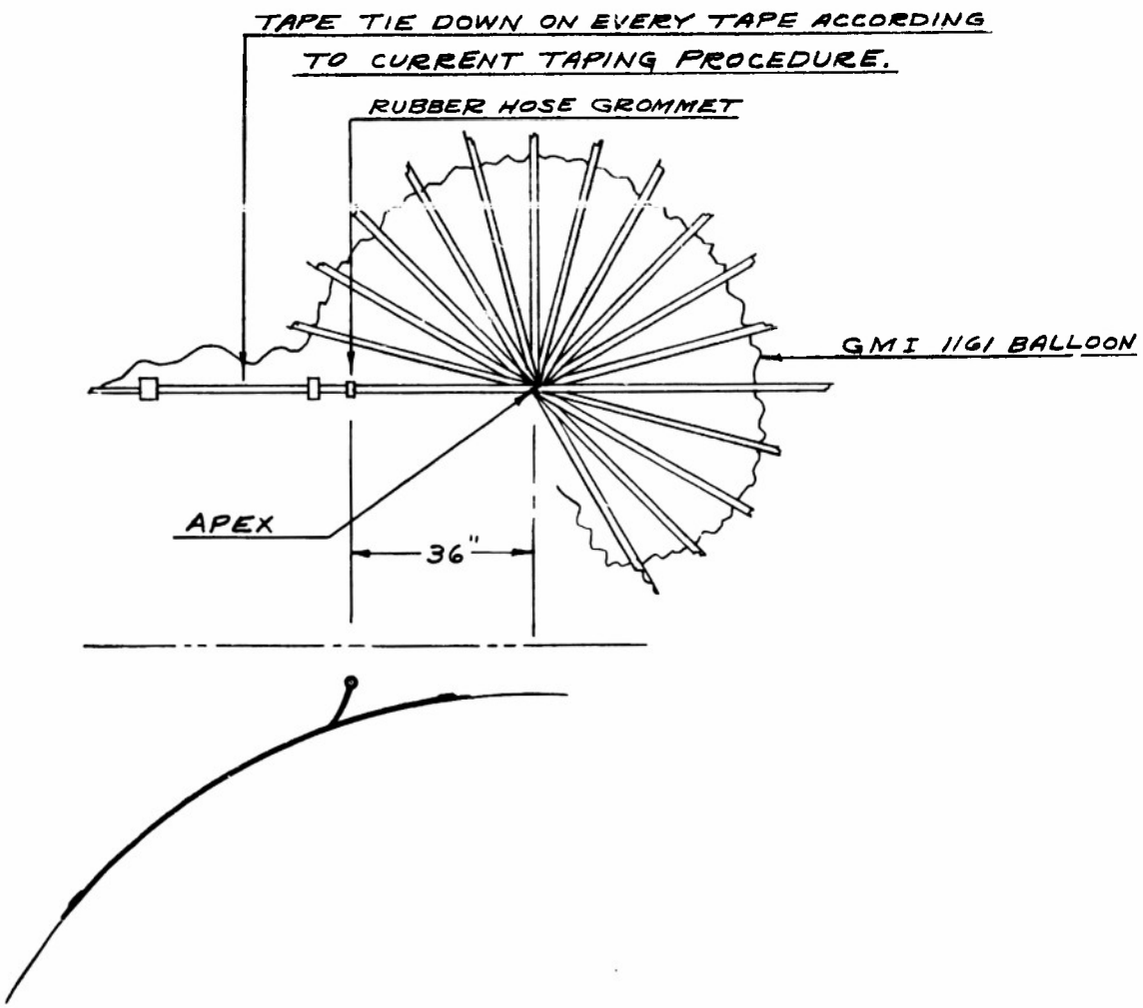

TITLE ABOVE	
SCALE	DEPARTMENT OF PHYSICS
DO NOT SCALE THIS DRAWING	UNIVERSITY OF MINNESOTA MINNEAPOLIS
DRAWN BY A. J. W.	DATE 12-2-52
CHECKED BY	APPR. BY
BA-490B	

DUCT APPENDIX MODIFICATION TO GMI 1161 BALLOON (CONT.)

②

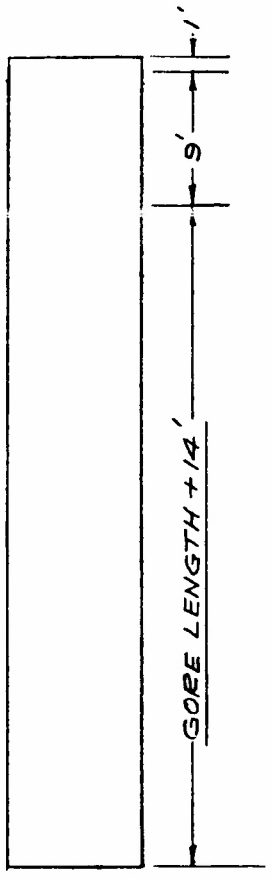

SPLIT AND HEAT SEAL TWO-2 MIL-54" TUBES TO MAKE TUBE 108" FLAT WIDTH, AND LENGTH EQUAL TO FULL BALLOON GORE LENGTH PLUS 24 FEET.

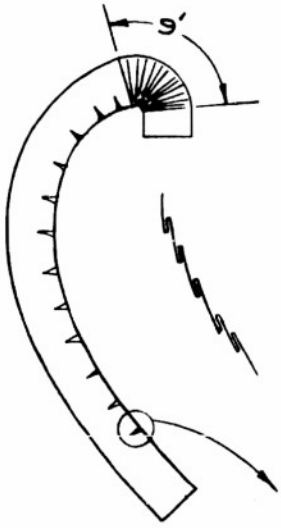

ON ONE SIDE OF TUBE, GATHER OR PLEAT 9' SECTION COMPLETELY, AND MAKE 3" PLEATS FOR EVERY 5° CHANGE OF BALLOON CONTOUR (TOTAL OF 14' IN PLEATS, OR 7' PLEAT LENGTH) ALSO PLEAT 1/2 MATERIAL AT SIDES OF TUBE IN 9' SECTIONS.

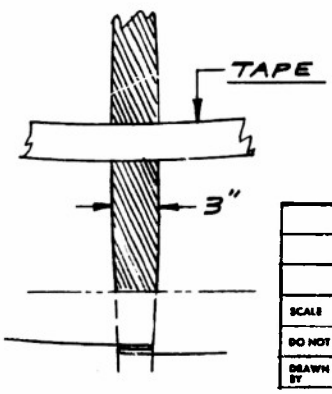

TITLE ABOVE	
SCALE DO NOT SCALE THIS DRAWING	DEPARTMENT OF PHYSICS UNIVERSITY OF MINNESOTA MINNEAPOLIS
DRAWN BY A. J. W.	DATE 12-2-52 BA-490B-1

Confidential

DUCT APPENDIX MODIFICATION TO GMI 1161 BALLOON (CONT.)

(3) ON APPROXIMATELY 34" RADIUS FROM APEX, LAP SEAL EXPOSED GORES TO FLANGED END OF DUCT, SKIPPING TAPES. TRIM EDGE AND TAPE WITH 2" POLY. TAPE.

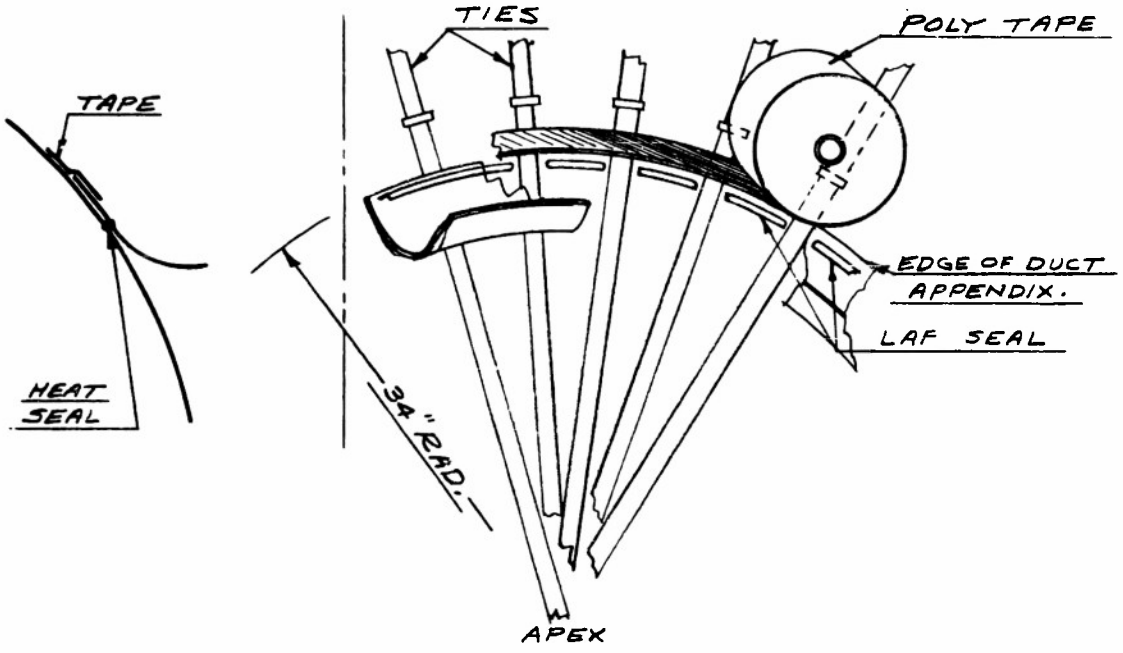

(4) TAPE PLEATED SIDE OF DUCT ALONG BALLOON TAPE FROM APEX TO BOTTOM

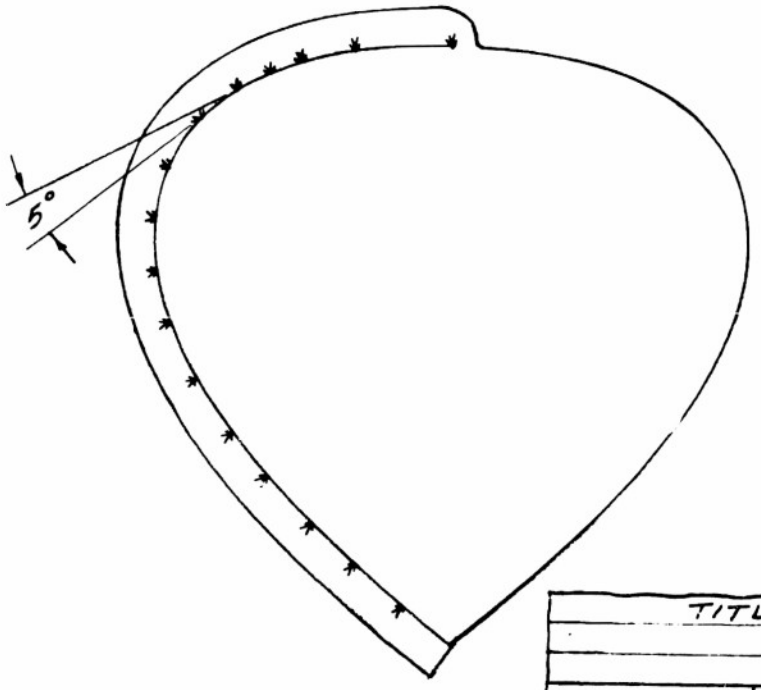

Confidential
SECURITY INFORMATION

TITLE ABOVE	
SCALE / DO NOT SCALE THIS DRAWING	DEPARTMENT OF PHYSICS, UNIVERSITY OF MINNESOTA, MINNEAPOLIS
DRAWN BY A.J.W.	DATE 12-2-52
CHECKED BY	APPD. BY
	BA-490B-2

Assuming the zero pressure level to be at the base of the balloon, the head is 102 feet. At 20 mb this is equivalent to 0.1 mb of air or 0.086 mb differential pressure of air and helium.

The valving pressure through an orifice is given by the equation:

$$\Delta P = \frac{.014 V^2 \mu^2 P M}{A^2}$$

where P = pressure, (millibars)

V = volume, (million cubic feet)

μ = rate of rise (1000 ft/min)

M = molecular weight of gas (gms/mol)

A = orifice area (square feet)

With a rate of rise of 800 feet per minute and an effective appendix diameter of $2\frac{1}{2}$ feet, ΔP turns out to be 0.0015 mb. If this orifice were in the base of the balloon where it could take in and later valve air, the valving pressure would be more than seven times this amount while air was being valved.

Poiselles law* for the flow of gas through a tube can be written:

$$\Delta p = V \frac{\pi}{8} \mu \frac{l}{a^4}$$

where ΔP = pressure (degree/cm^2)

V = volume flow (cm^3/sec)

μ = viscosity (poises)

l = length of tube (cm)

a = radius of tube (cm)

For a 130 foot tube of $2\frac{1}{2}$ foot diameter, Δp is equal to .0025 mb. It can be seen in this case that the valving pressures are at the limit of negligibility compared to the head pressure.

Principally because the 73' diameter cone-on-sphere balloon is more nearly shaped like a natural sub-pressure balloon, most of the duct appendix flights have been flown sub-pressure, or with the base of the duct higher than the base of the balloons. In comparison with former appendices at the base of the balloon; the sub-pressure

* Transition effects ignored.

duct has the following characteristics:

(a) Diffusive or turbulent mixing of gas and air through the appendix is eliminated.

(b) Decrease in valving pressure by earlier valving and valving only the lighter molecular weight lifting gas.

(c) Decrease in balloon stress because of decrease in head pressure.

(d) Decrease in loss of gas from pressure leaks because of decrease in head pressure.

(e) Termination of the flight at sunset because of decreased stability of a slack balloon with no air intake.

With the exception of (a) above, the opposite effects may be expected with a super-pressure balloon, one with the duct below the base of the balloon. The most interesting is the converse of (e), the possibility of greater stability with a balloon held full by super-pressure. This is discussed in Section III-D of this report.

SECTION IV

HANGAR INFLATION TESTS OF PLASTIC BALLOONS

Arrangements were made through the Office of Naval Research to use a part of Dock 2 at the US Naval Air Facility, Weeksville, North Carolina, to inflate plastic balloons for the purpose of obtaining first hand information on the appearance of these balloons when fully inflated and for obtaining measurements of stress, balloon shape and for the detailed study of the various defects that might be observed in the hangar but which are very difficult to observe during the flight of the balloon. The balloons chosen for the measurements were those that were available at the end of July 1952 and consisted of the following:

General Mills, Inc., type 733J-135, 2-mil balloon #478

Winzen double-wall, 1-mil, #2-100V-104 made on Air Force contract No. AF 33(600)-15182

Winzen 1.5-mil #150V-147

Winzen 1-mil, type 733, #157 packed by Minnesota method

General Mills, Inc., type 734-EH, 2-mil, double-taped balloon #192

General Mills 39' "natural shape," type and number unknown, intended for Mastenbrook Project.

The various things that were investigated are as follows:

I. Inflation and Gas Sampling. The balloons were inflated with a mixture of helium and air which, when the balloon was full, would give the desired lift. This was accomplished with a centrifugal blower and a carbureting device through which the helium was injected and well mixed. The gas proportions in the balloon were measured from top to bottom by carrying up a sampling hose and using a thermal conductivity gas measuring instrument.

II. Shape Measurements. Balloon shape measurements were made by a number of different methods, namely by the use of two surveying transits which were set up in the hangar and sighted on lights which had been strung along one of the balloon tapes around the side down towards the bottom. Plumb bob lines were hung also from known places on the lower portion of the balloon and from the length of the lines and the distances out the underneath profile was measured. Also peripherial measurements were made from gore to gore before the balloon was inflated. Due to fabric stretch these measurements have not been considered reliable. Many photographs were taken from various angles but in particular an 8 X 10 camera was set up in a measured position and the camera carefully adjusted to take a photograph of the balloon suitable for later analysis on a comparator. The top portions of the balloon were photographed from a catwalk above the balloon itself.

III. Stress Measurements. Stress measurements were first attempted by means of attached strain gages with spring balances but this proved unsuccessful and a vibrating bob type stress gage was developed and will be described later in another report.

IV. Hangar Launch. A University of Minnesota packed balloon was inflated in the hangar and the gas allowed to transfer just as in flight. The balloon, however, was kept secured to the floor. The inflation was continued using air so that the girdle was forced down in a manner resembling flight conditions and the slippage was investigated. The balloon was inflated until it burst and the bursting super pressure measured.

V. Heavy-load Inflation. A 2-mil thick balloon was inflated with a mixture which enabled it to lift about one ton when fully inflated. The balloon was examined carefully and the effect of the large stresses was observed.

VI. Rate of Rise Measurements. A series of rate of rise vs. free lift measurements were made on 7' balloons inside the hangar. It was found that large temperature variations existed in the hangar and these measurements have so far not been analyzed.

DETAILED PROCEDURES AND RESULTS OF TESTS

I. The balloons were inflated with a mixture of air and helium which was supplied to the balloons by a centrifugal blower. It was necessary first to insure that the helium and air were well mixed as experience and calculation shows that at atmospheric pressure the diffusion is so slow that any unmixed volume of air would remain settled out in the bottom of the balloon. This would produce a distorted hydro-static pressure head and change the balloon's shape. This is strikingly shown in Section IV, the Hangar Launch Tests. It was also necessary to control the relative fraction of helium in the air so that the fully inflated balloon would have the proper lift corresponding to normal loads carried at ceiling altitude. A diagram of the inflation set-up is shown in Figure 1. A 1000 cubic foot per minute centrifugal blower with a 1 hp motor was used and a carburetor was attached inside the intake tube. The carburetor consists of a small tube with many fine holes around its exterior. The helium fed in with measured pressure was sprayed out through these fine holes into the intake side of the blower. The vacuum on the intake side was also measured with a water manometer. A photograph of the blower and a partially inflated balloon is given in Figure 2. The blower was calibrated before leaving for Weeksville by inflating a 20' diameter balloon of known volume and measuring its lift. The calibration curve for this blower is given in Figure 3.

Most of the inflations fell into the 3-4% range and were well suited to analysis by a thermal conductivity type meter. Accordingly a gasalyser was obtained for this purpose. Absolute calibration of the gasalyzer was obtained from mass spectograph analysis of gas samples made on the Physics Department routine analysis spectograph. Because the balloon did not become buoyant until nearly one-half full it was hung from the top ring to a block and tackle sus-

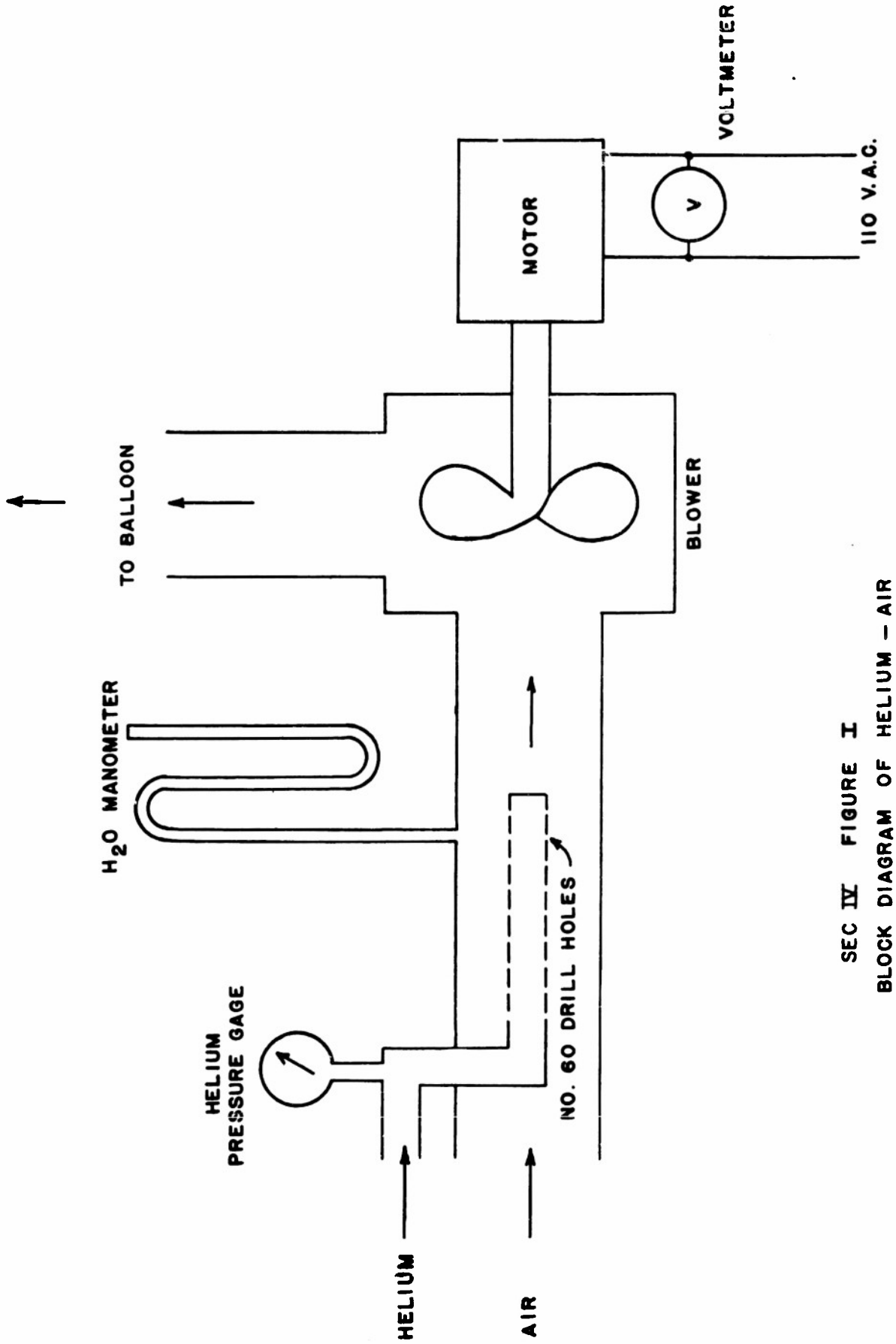

SEC IV FIGURE I

BLOCK DIAGRAM OF HELIUM – AIR CARBURATOR AND BLOWER

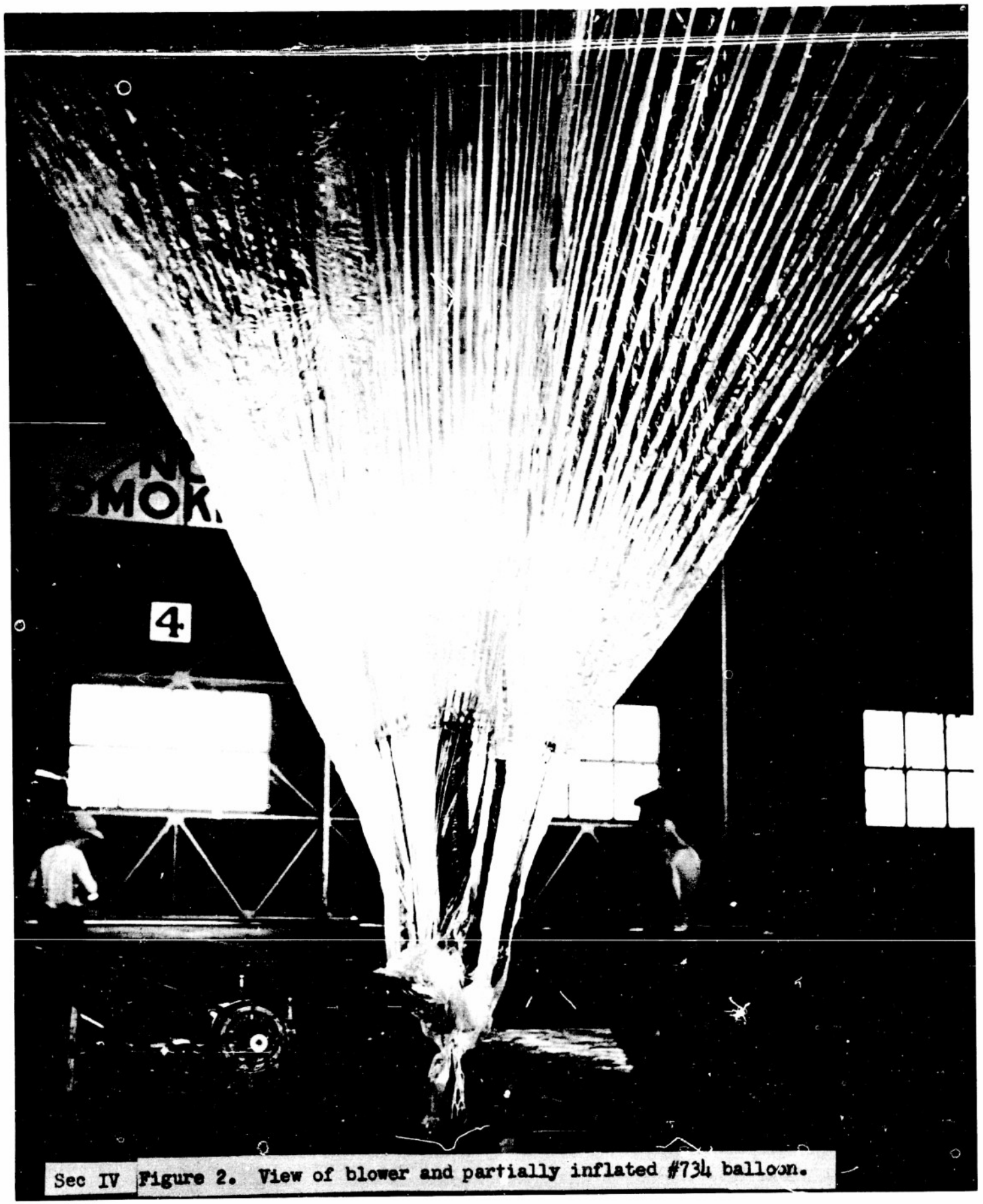

Sec IV Figure 2. View of blower and partially inflated #734 balloon.

pended from the roof of the hangar. Then as the inflation proceeded and the balloon became buoyant the top rope was removed from the pulley and the balloon was placed over the tie-down point in the center of the hangar where the inflation was completed. The inflation required 4 hours and 40 minutes for a 225,000 cubic foot balloon. Gas samples were made by suspending a rubber tube from a string which passed through a ring inside the top of the balloon. A vacuum pump was used to extract the samples. The mixture was pumped through the gasalyser and was also admitted to evacuated sample bottles for mass spectograph analysis. Figure 4 is a general view of the gas sampling procedure.

Figures 5 and 6 give the calibration curves for the gasalyser under the conditions of standardization given on the figure. The vertical concentration profile for the various balloons sampled is given in Figures 7A and 7B and the corresponding gross lift is also listed. It will be noted that the concentration is quite uniform down to a point about 15 feet above the appendix opening at which point the helium percentage drops off to zero at the bottom. This is a relatively small fraction of the total volume and possibly represents the settling out of the unmixed portion of the air. The results of the transit and plumb bob measurements are given in Figures 8 through 11. The first three of these refer to the cone-on-sphere type balloon and the last one to a balloon whose upper portion approximates the natural shape balloon with zero circumferential tension. It is notable on the first three balloons that they tend to depart from the sphere profile for which they were designed towards the natural shape balloon by bulging out on top and contracting in the upper conical section. It is not certain how much of this is due to stretching of the material while inflated compared to the error in manufacture although it seemed evident that there was a deficiency of material in the conical portion

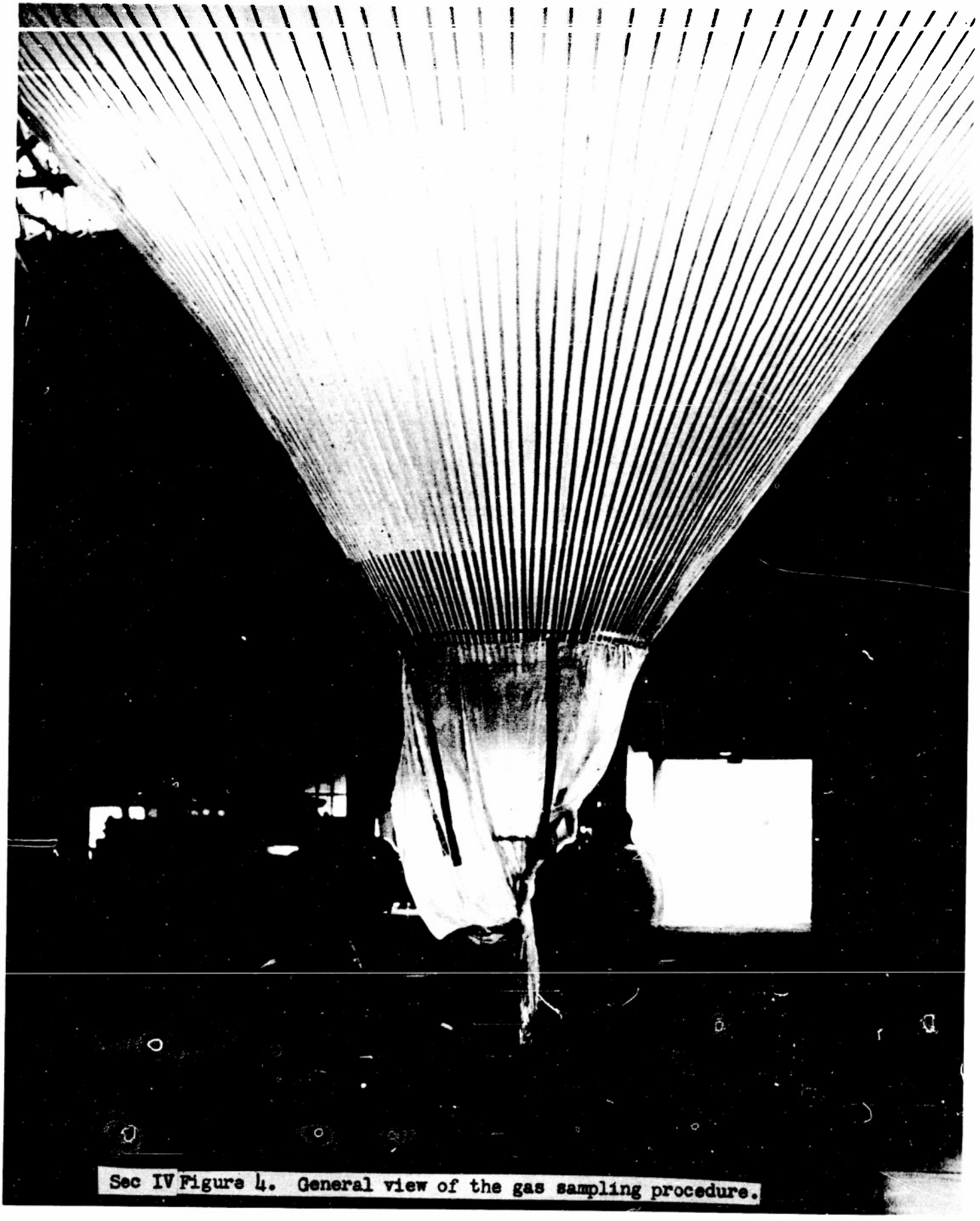

Sec IV Figure 4. General view of the gas sampling procedure.

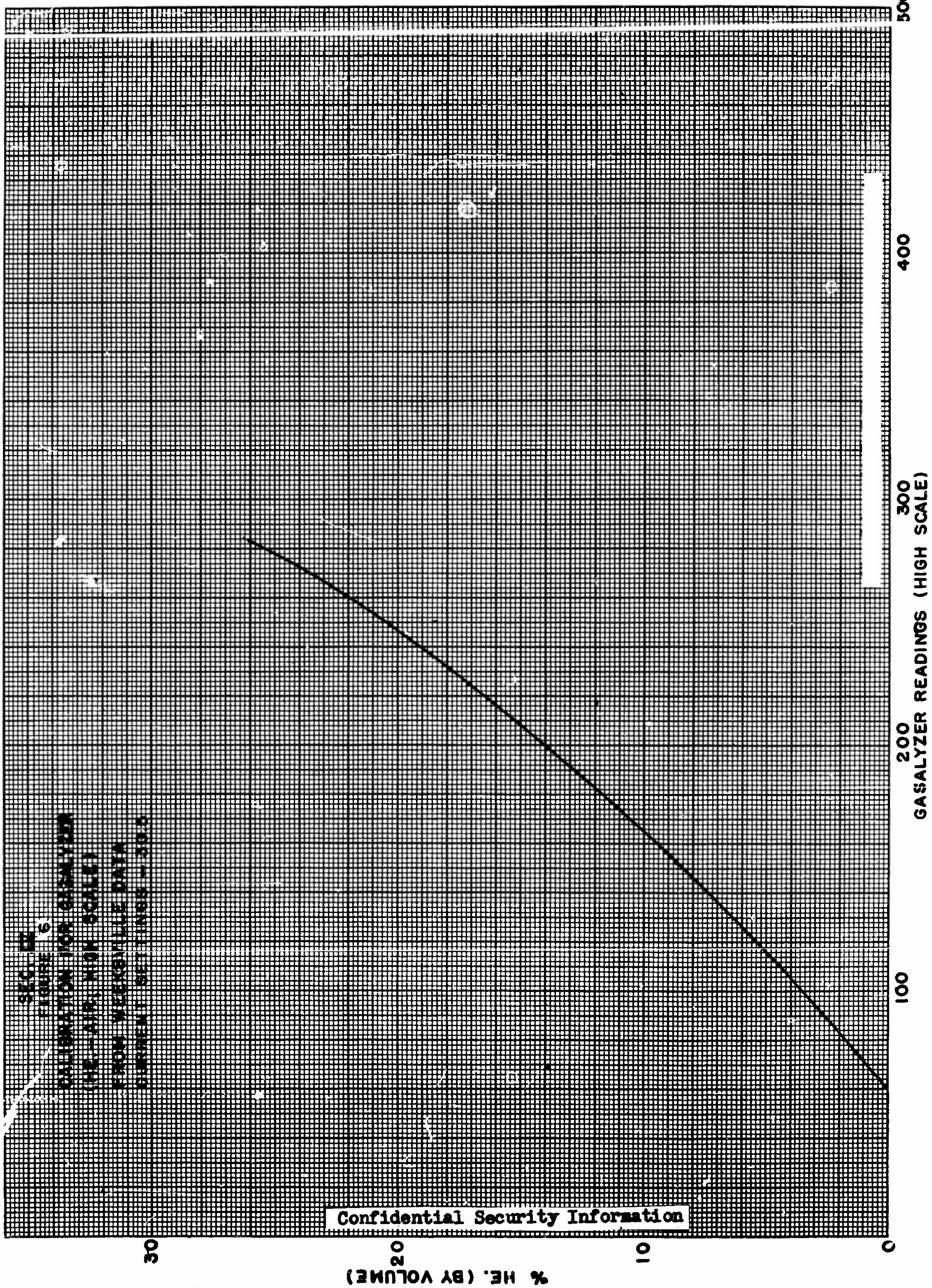
SEC. IV
FIGURE 6
CALIBRATION FOR GASALYZER
(HE.-AIR; HIGH SCALE)
FROM WEEKSVILLE DATA
GASALYZER READINGS (HIGH SCALE)
100
200
300
400
500
% HE. (BY VOLUME)
0
10
20
30

SEC. IV FIGURE 7-A, VERTICAL CONCENTRATION PROFILES FOR VARIOUS BALLOONS Confidential

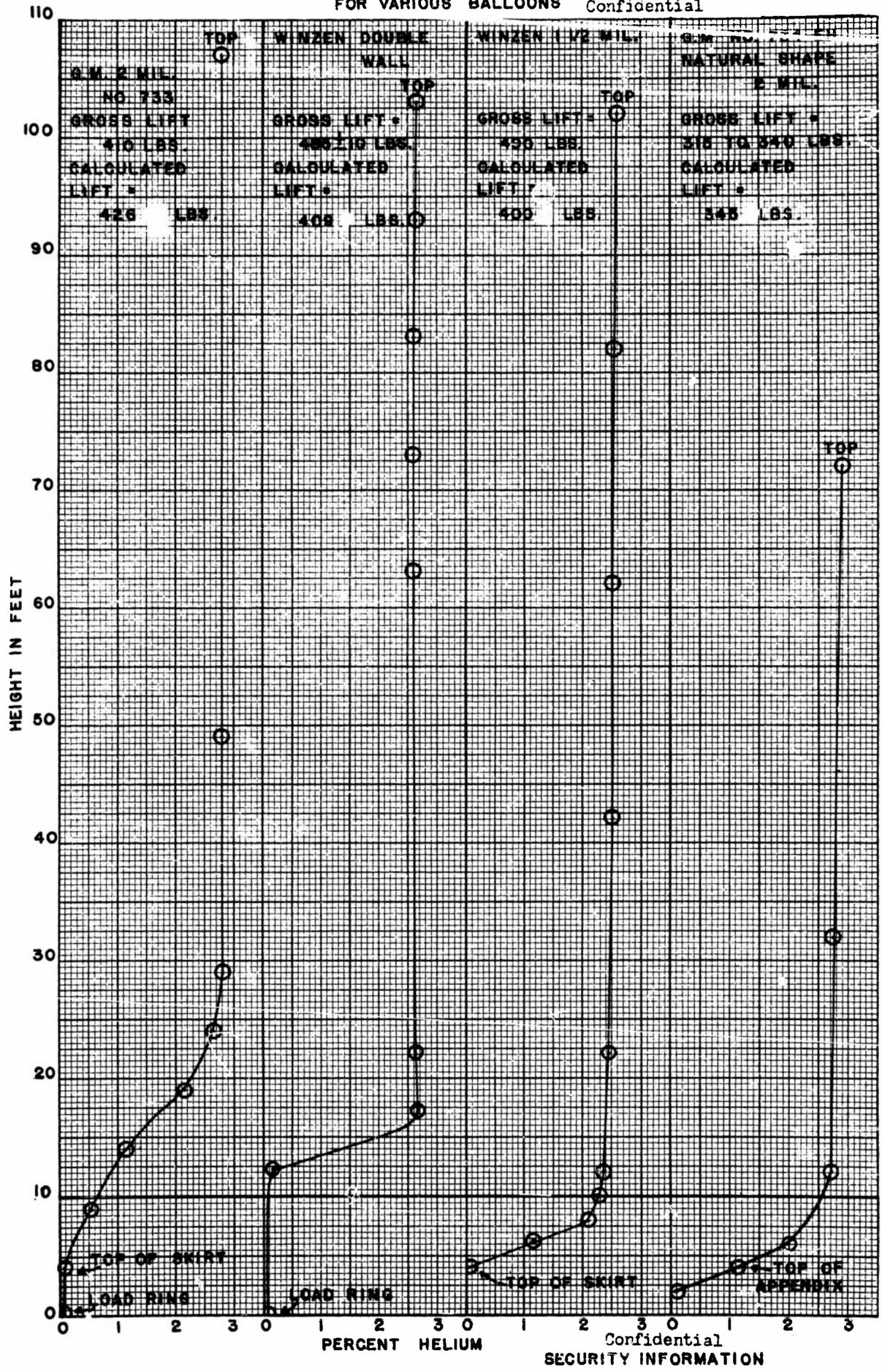

Confidential
SECURITY INFORMATION

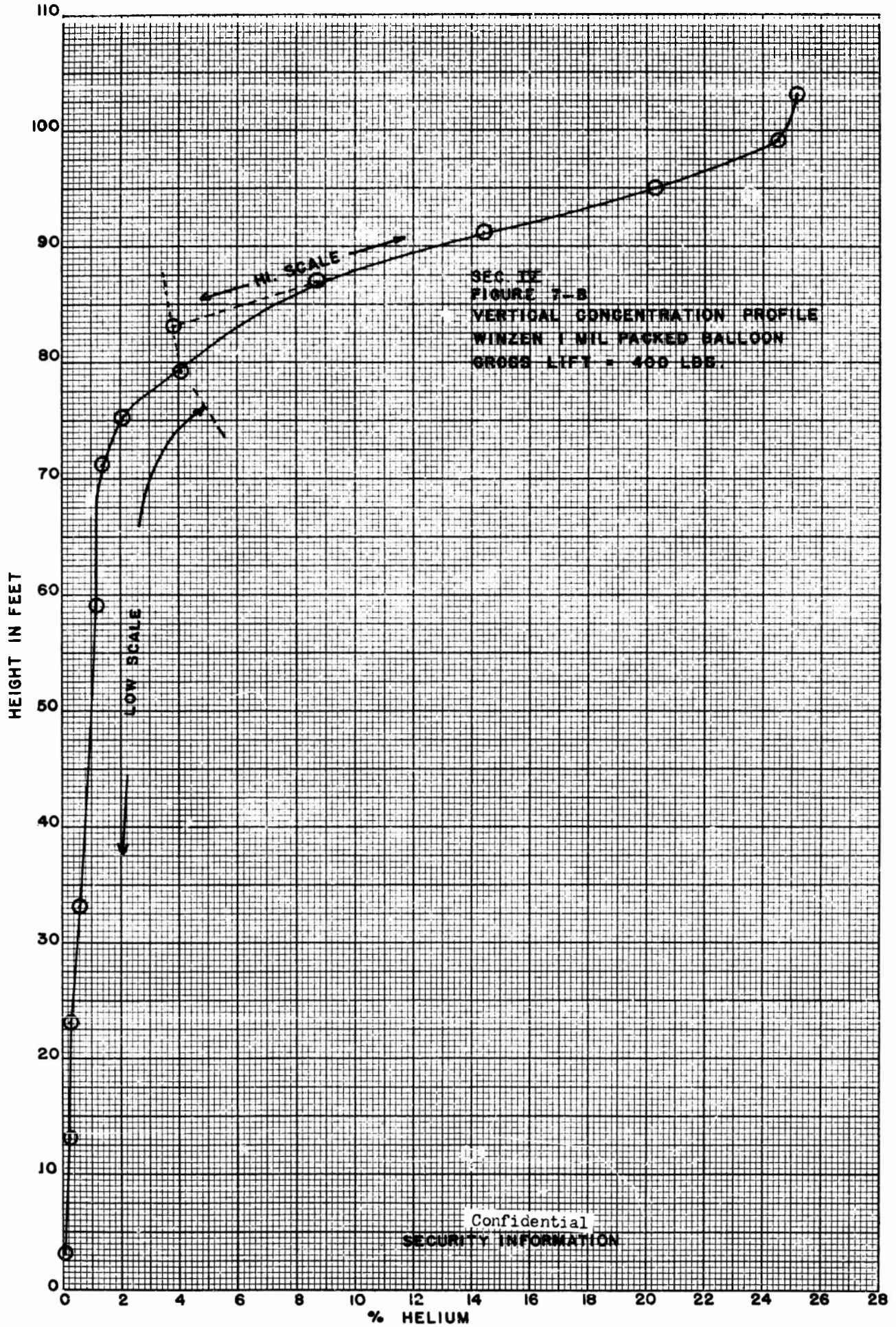
HEIGHT IN FEET
% HELIUM
HI. SCALE
LOW SCALE
SEC. IIE
FIGURE 7-8
VERTICAL CONCENTRATION PROFILE
WINZEN 1 MIL PACKED BALLOON
GROSS LIFT = 400 LBS.
Confidential
SECURITY INFORMATION

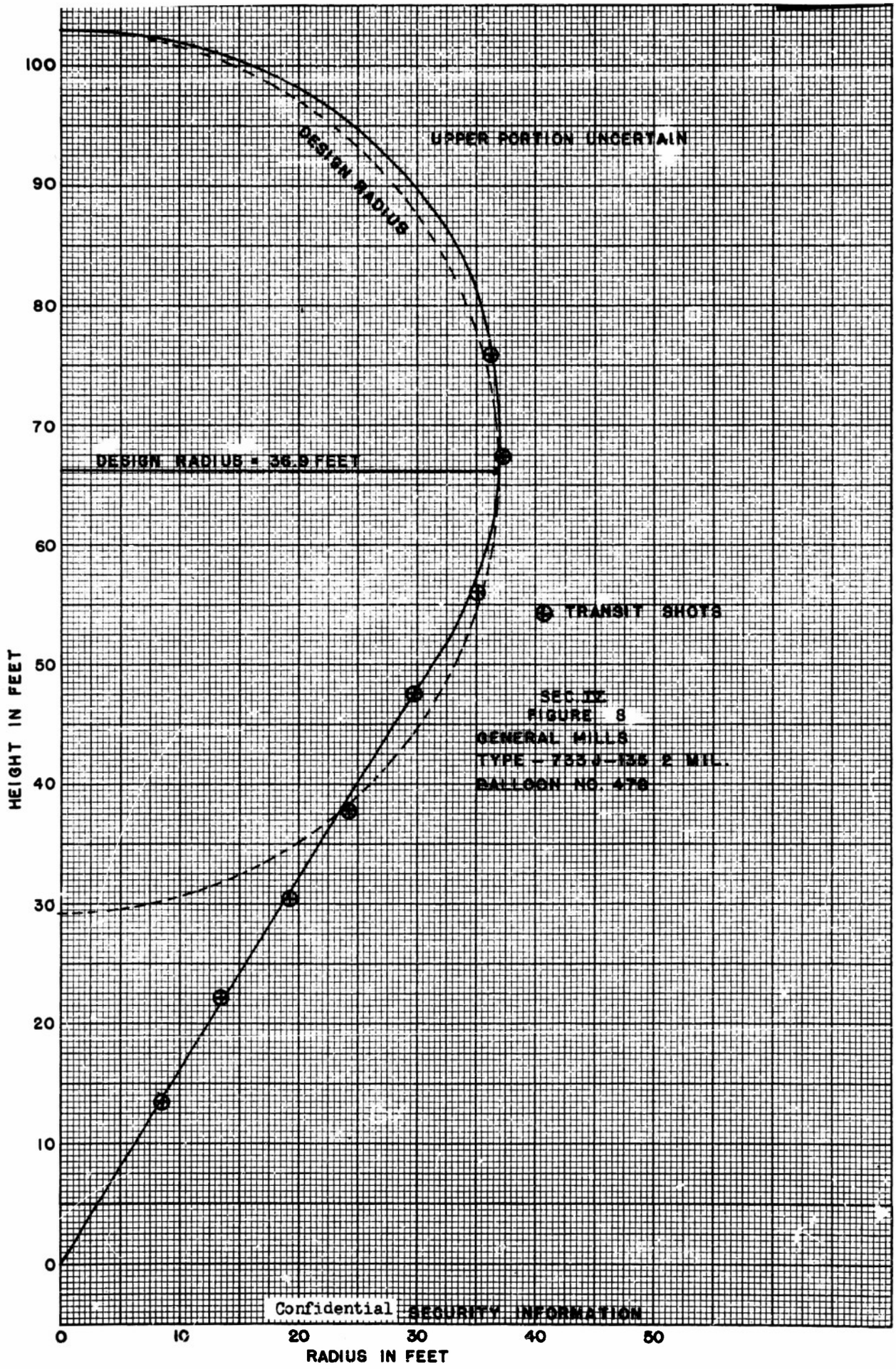
UPPER PORTION UNCERTAIN
DESIGN RADIUS
DESIGN RADIUS = 36.9 FEET
TRANSIT SHOTS
SEC. IX
FIGURE 8
GENERAL MILLS
TYPE - 7554-135 2 MIL.
BALLOON NO. 478
HEIGHT IN FEET
RADIUS IN FEET
0
10
20
30
40
50
60
70
80
90
100
Confidential SECURITY INFORMATION

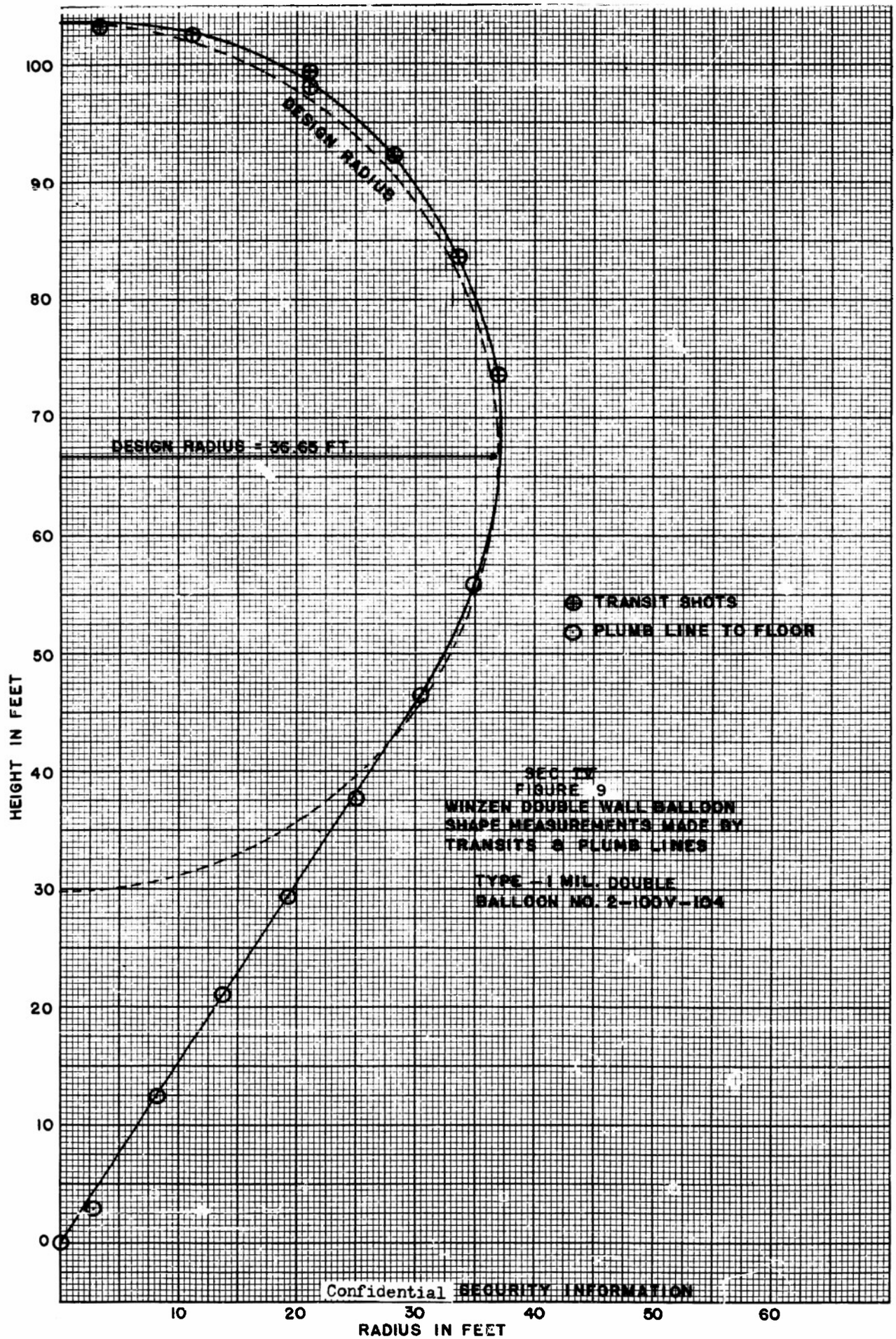
DESIGN RADIUS
DESIGN RADIUS = 36.65 FT.
TRANSIT SHOTS
PLUMB LINE TO FLOOR
SEC. IV
FIGURE 9
WINZEN DOUBLE WALL BALLOON
SHAPE MEASUREMENTS MADE BY
TRANSITS & PLUMB LINES
TYPE - 1 MIL. DOUBLE
BALLOON NO. 2-100V-104
HEIGHT IN FEET
0
10
20
30
40
50
60
70
80
90
100
RADIUS IN FEET
10
20
30
40
50
60

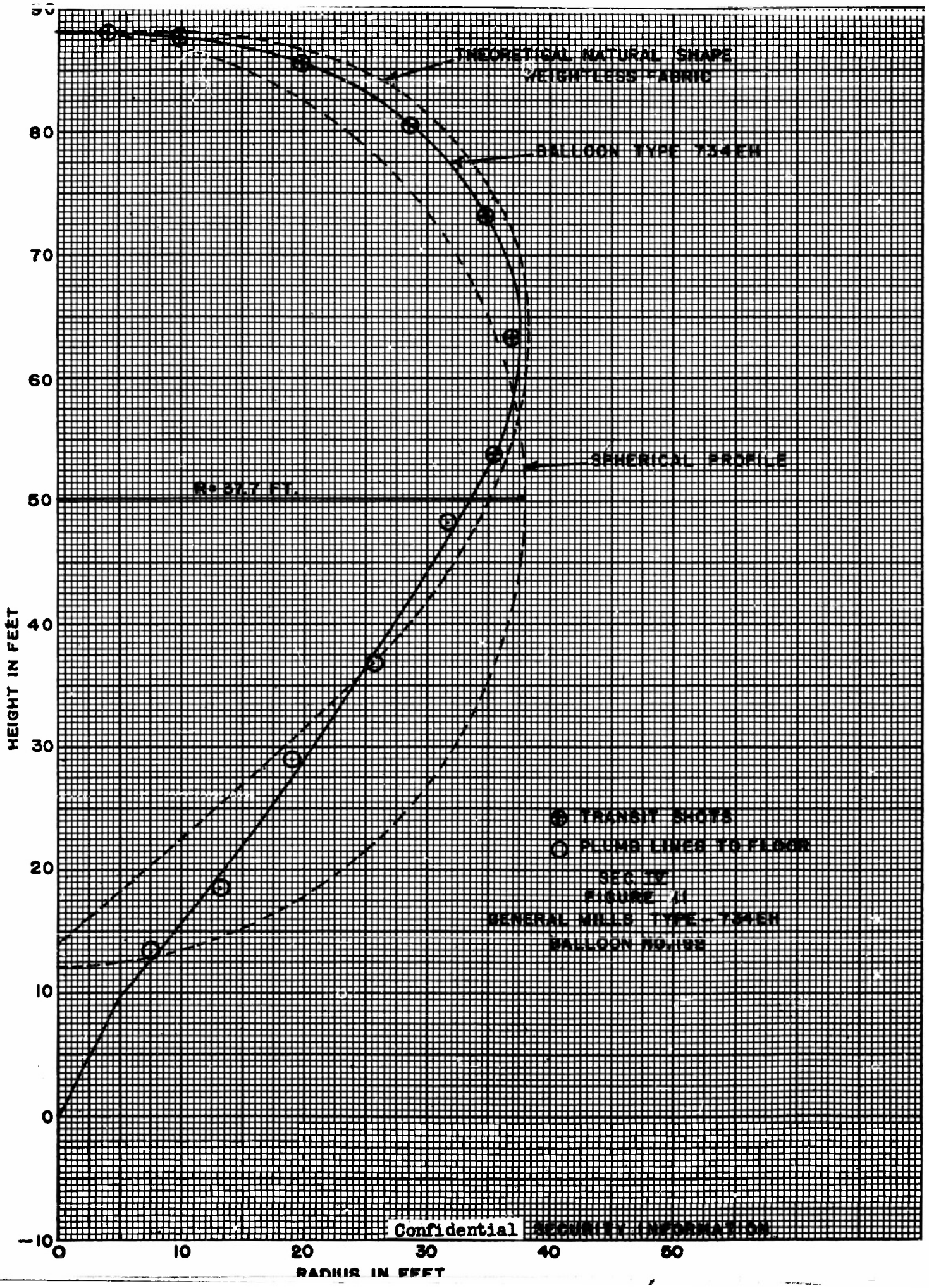
THEORETICAL NATURAL SHAPE WEIGHTLESS FABRIC
BALLOON TYPE 734 EH
SPHERICAL PROFILE
R = 37.7 FT.
HEIGHT IN FEET
RADIUS IN FEET
90
80
70
60
50
40
30
20
10
0
-10
0
10
20
30
40
50
TRANSIT SHOTS
PLUMB LINES TO FLOOR
SEC. IV
FIGURE 11
GENERAL MILLS TYPE - 734 EH
BALLOON NO. 1122
Confidential SECURITY INFORMATION

so that the balloons were concave at that point.

Figures 12 and 13 are views of a General Mills and Winzen cone-on-sphere type balloon made with an 8 X 10 view camera placed 350' from the balloon. Figures 14 and 15 show the upper portion of these balloons taken from a point one-half way up the hangar with a 4 X 5 camera. Careful measurement of these negatives were made on a microscopic comparator using the hangar door as a comparison grid and the meridional profile was calculated considering the geometry of the situation and assuming that the balloon was axially symmetric. The crown photographs were used to fill in the upper portion of the balloon as this was not visible to the floor camera. The composite result of these two photographs is given in Figures 12A and 13A. It will be noted that the tape length measured from the figure checks the actual measured tape length very closely. It should also be noted that the balloon departs from the theoretical cone-on-sphere profile in every case by contracting in the conical portion and near the equator, and by bulging out on top.

II. Shape Measurements. Prior to the beginning of inflation each balloon was laid out on the floor and one of the balloon tapes was marked every 10 feet starting at the top with a cross. The balloons starting with the second one tested were equipped with small flashlight bulbs which were wired along one of the gores every 10 feet down from the top and around the equator. It was found that the black crosses were not visable to the transits when sighting through the plastic from the other side of the balloon. It was determined that this was the best way to measure the profile by transits and that the lights gave something to focus on. From the lower portion of the balloon below the equator, fish lines were attached every 10 feet and the length of the fish lines was carefully measured. The fish lines were terminated in plumb bobs which, after the balloon was inflated, could be adjusted until they

Sec IV Figure 12. GMI type 733 J-135, 2-mil balloon, #478. 73' diameter.

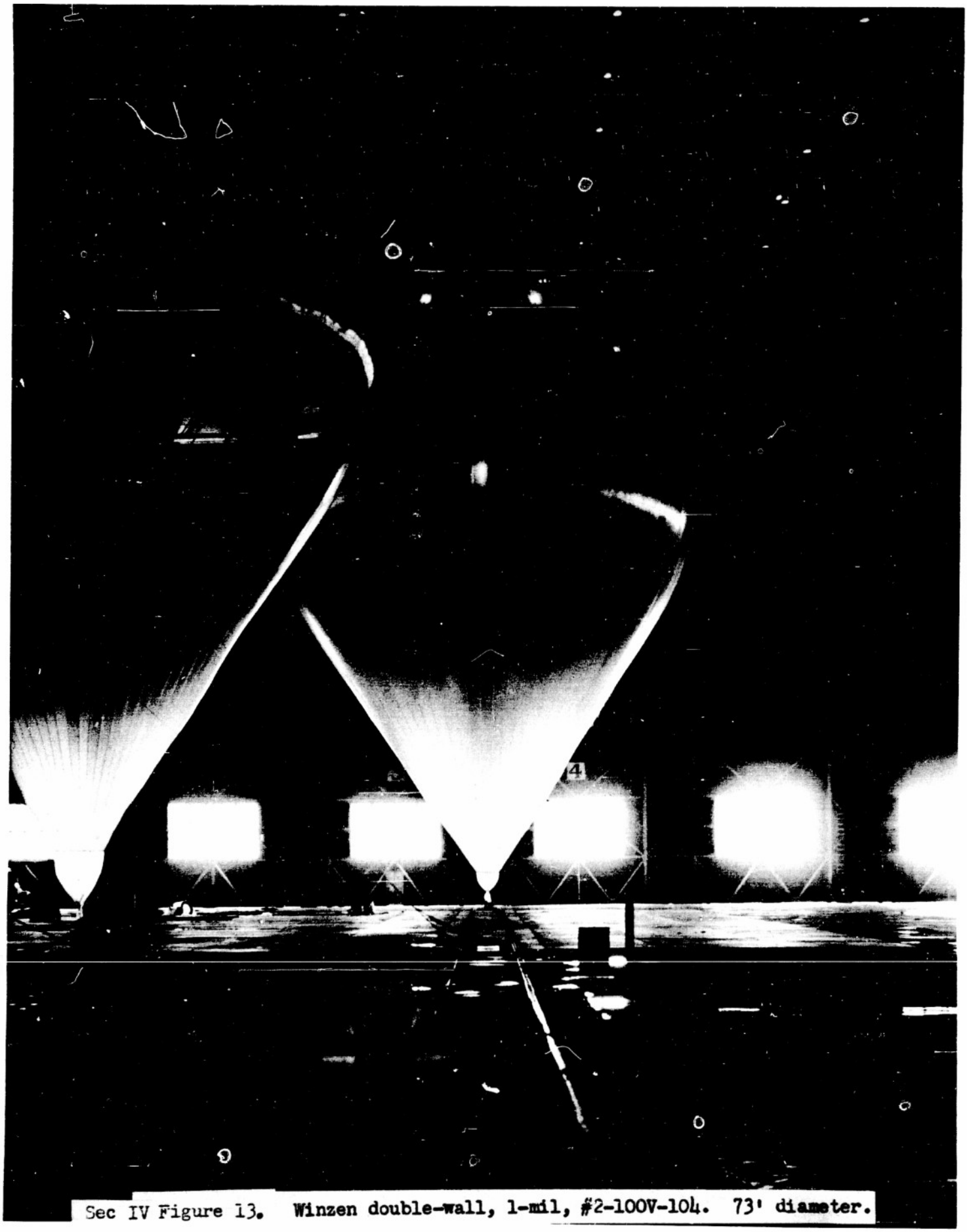

Sec IV Figure 13. Winzen double-wall, 1-mil, #2-100V-104. 73' diameter.

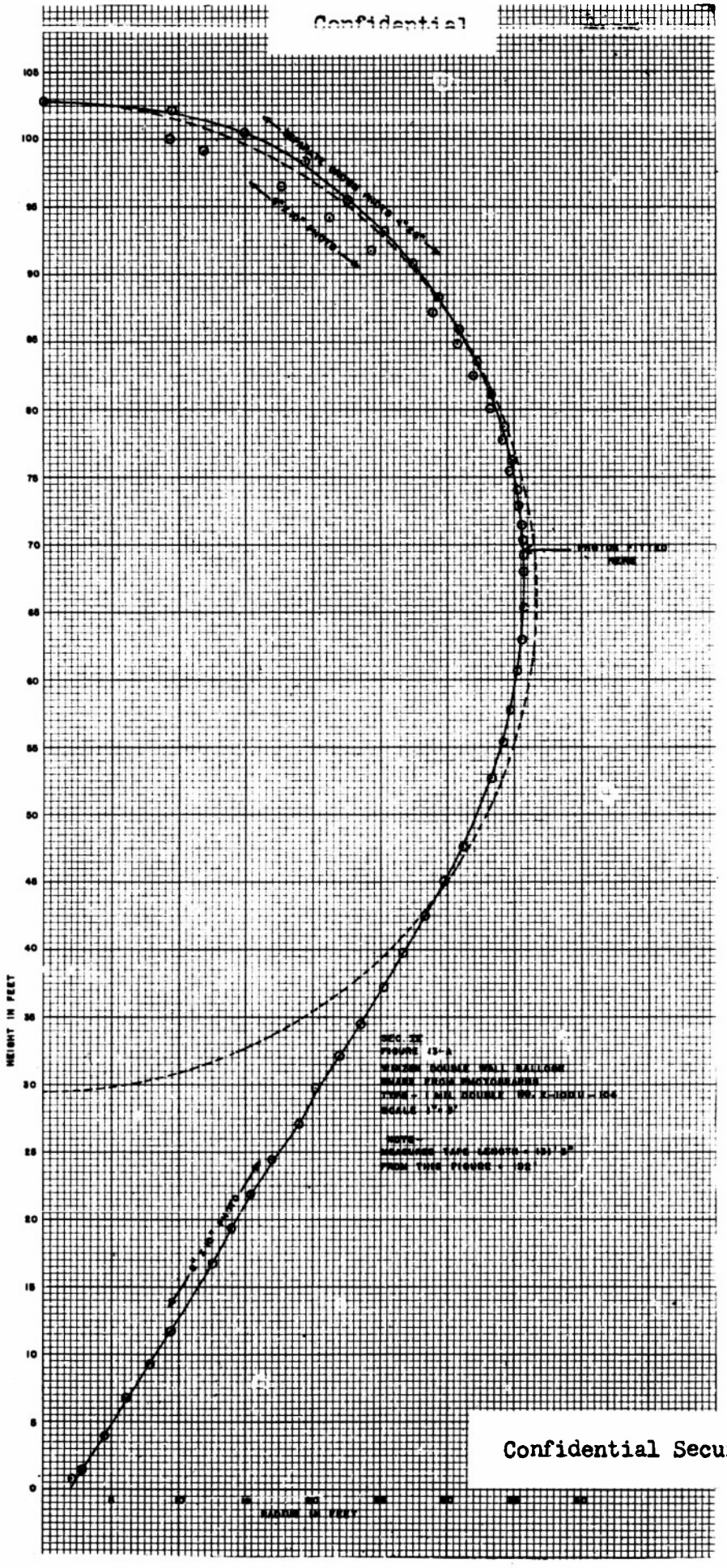

Confidential Security Information

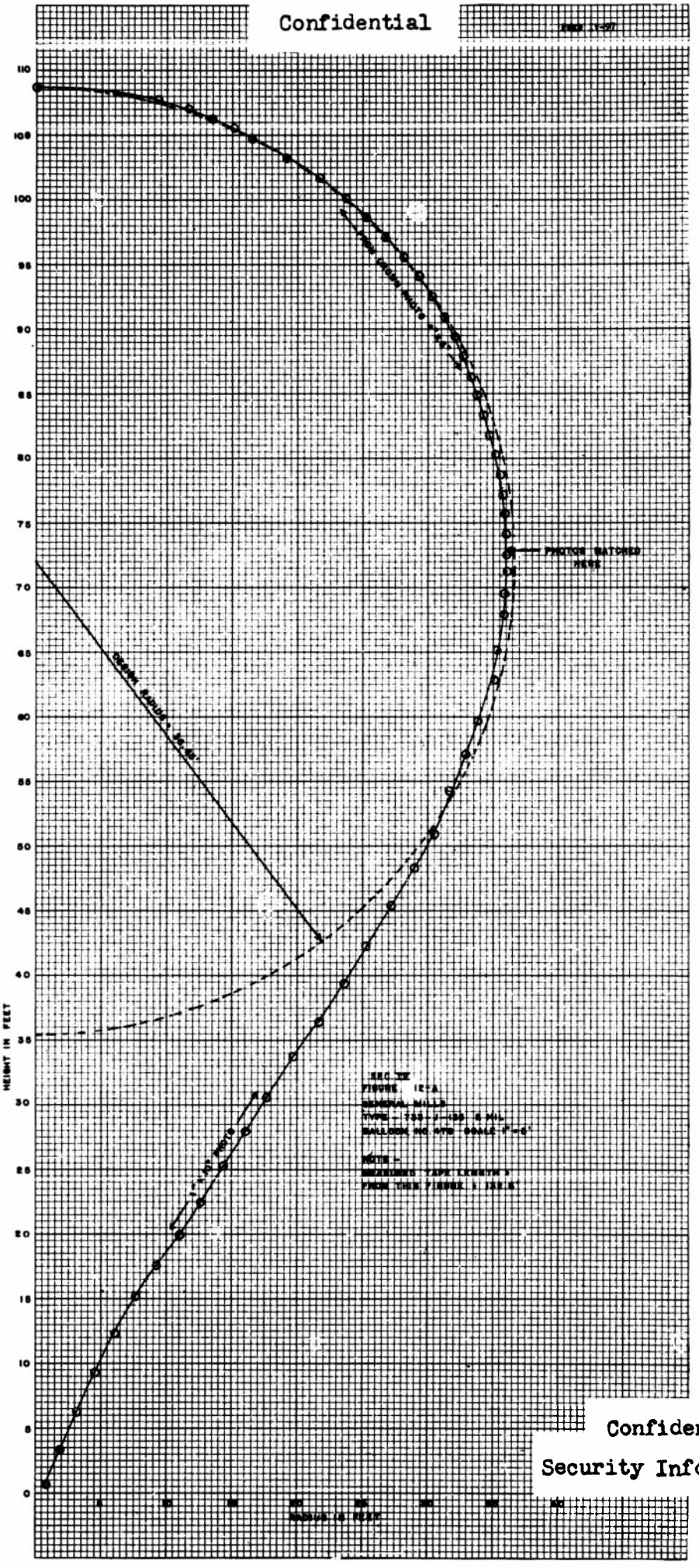
HEIGHT IN FEET
RADIUS IN FEET
FRICTION MATCHED HERE

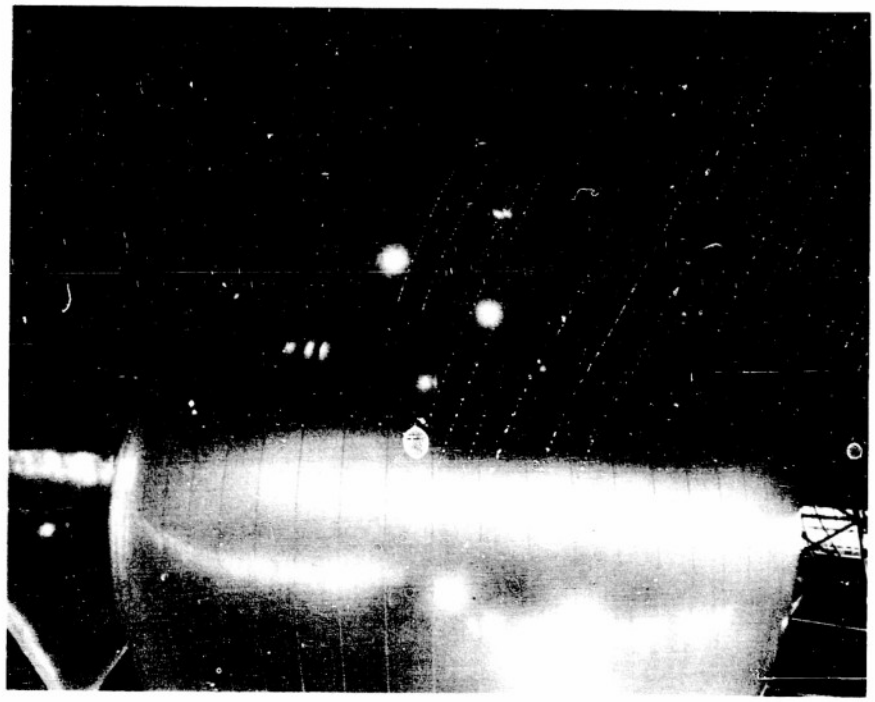

Sec IV Figure 14. Top view of GMI 73' balloon with a gross lift of about 450 pounds. Note the bulge about 10' down from the top with a flat section above.

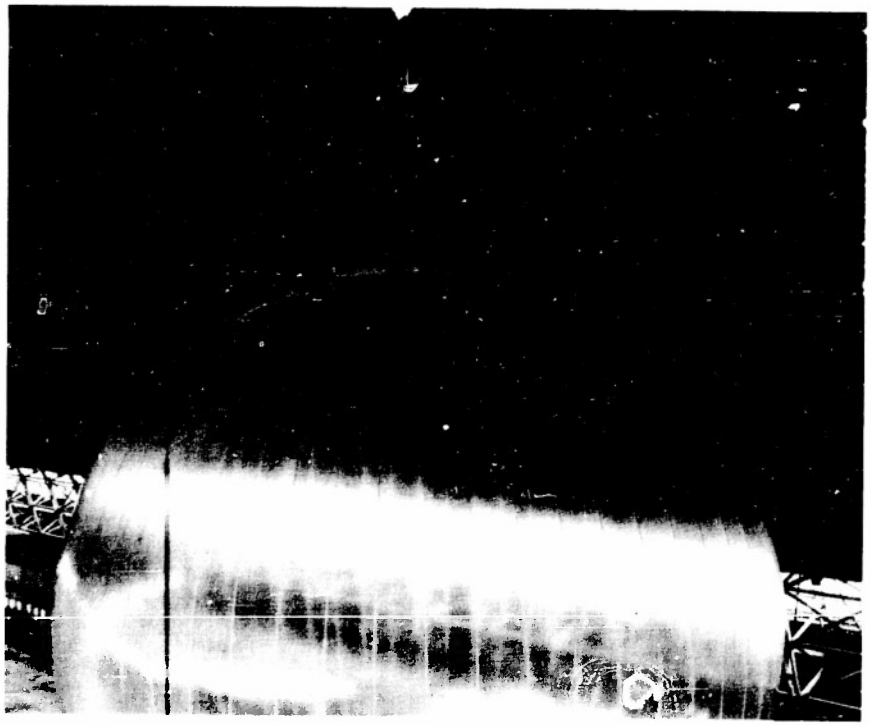

Sec IV Figure 15. Winzen 73' balloon inflated to about 450 pounds gross. This balloon also had a flattened top as can be seen from this photograph taken about half way up the hangar.

just touched the floor. By measuring the distance out from the balloon tie-down point to the plumb bob and knowing the length of the string up to the balloon the coordinates of the balloon could be determined. The periphery of the balloon was also measured at four places: 1. At the equator, 57.5 feet from the top on the 1/4 million cubic feet cone-on-sphere type balloons. 2. At a point half-way down the equator, 28.5 feet from the top. 3. At 77.4 feet from the top which was expected to be the point where the stress is large due to the change from spherical to conical profile. 4. At a point 100 feet from the top.

The width of each gore was measured with a hand ruler all the way around the balloon to get the periphery. It was found that this type of measurement was not very good because the plastic was stretched a little bit in an attempt to remove the wrinkles and the additive errors being all in one direction gave a sizable error in the result.

The balloon was also equipped with an internal line passing through a ring at the top which could be used to raise a sampling hose for the gas sampling. Photographs were taken of each balloon with an 8 X 10 camera placed about 350' away from the balloon down the hangar. This camera also photographed the grid work on the hangar door behind the balloon. This grid work was then surveyed carefully and the exact dimensions of the steel girders, height from the floor, etc., were determined so that the photographs could be standardized by measurements against this grid. Unfortunately only two balloons were successfully photographed with this equipment due to difficulties encountered in the US Naval Air Facility Photographic Laboratory, but these two photographs have been measured out and the results are given. This latter consitutes the most accurate way to determine the balloon shape. The transit measurements were evaluated by geometry knowing the position of the two transits on the hangar floor, the position of the tie-down point of the balloon and the various angles involved in

the transit measurements. Difficulty was encountered in making the transit measurements because the balloons were never quiet and even at night, due the convection currents in the hangar, would slowly move about. Accordingly, the two observers would follow the lamp on the balloon and when one of the plumb bobs hanging below the balloon passed over a fixed mark on the floor, a signal was given and the two observers would read together. The plumb bob measurements were also troubled by the motion of the balloon and accordingly, the outer plumb bob was used as reference and measurements taken on all the others when the outer plumb bob passed over the fiducial mark.

III. Stress Measurements. These will be treated in a later report.

IV. Hangar Launch Tests. It was felt desirable to inspect the University of Minnesota launching process at close range and accordingly a packed balloon was inflated in the hangar and the launching operations carried out so that the gas transferred and the balloon erected to its full height, but was at all times kept secured to the floor of the hangar. Still photographs, of which representative pictures are included here, and movies were taken of this. To simulate the continuing rise of a balloon in normal flight and the accompanying expansion and forcing down of the girdle, air was blown into the balloon and the slipping of the girdle as the top filled out was observed.

The hydrostatic head of the air being zero with respect to the outside, the shape of the balloon was quite different from that of a helium filled balloon, as can be seen from the photographs. This did not affect the characteristic slipping of the girdle which depends only on the angle of the fabric above it, the coefficient of friction and the weight of the girdle. A discussion of the girdle slipping problem is given in the first progress report. The vertical concentration profile of helium in this balloon when

completely full of helium and air is shown in Figure 7B. The helium remains at the top of the balloon completely but even there it is considerably diluted by air. An attempt was made to mix the air by blowing it in at the top through an inflation tube carried up inside on a small balloon, but this was relatively ineffective. Following the girdle slip test the air inflation was continued until the balloon ruptured from super pressure. The super pressure was estimated by connecting an aircraft altimeter to the interior of the balloon and a value of 8' of normal atmosphere was obtained. The balloon failed near the junction of the sphere-on-cone sections as would be expected from the theoretical stress considerations for this balloon shape. (In this connection see the first progress report, Page 3-7, Figure 1). The hangar-launch test gave no evidence of damage to the balloon which confirms the experience with numerous launchings using this technique.

Figures 29 - 34 illustrate various phases of this test, with self-explantory captions.

V. Heavy-load Inflations. The Winzen double-wall balloon #2-100-V-104, 73.3' in diameter, was re-inflated with a mixture of about 17% helium which would give a lift of approximately 2000 pounds when the balloon was full. The stresses in the balloon top, according to theory, would still be less than the ultimate tensile strength of the polyethylene and it was therefore a good test of the heat seals and general strength of this type of balloon. The balloon, of course, was not designed or guaranteed by the manufacturer to carry a load of this magnitude. This balloon was made with No. 880 nylon filament tapes. The results of the test are given in the series of photographs followed with a discussion in the caption of the photograph.

The correspondence between such an inflation and a balloon in flight is that the conditions represent this balloon at about 50,000 feet of altitude at all times but with a load and accordingly a volume which increases until the balloon is full.

Figures 16 - 38 are various aspects of the heavy load inflation. The figure captions are self-explantory.

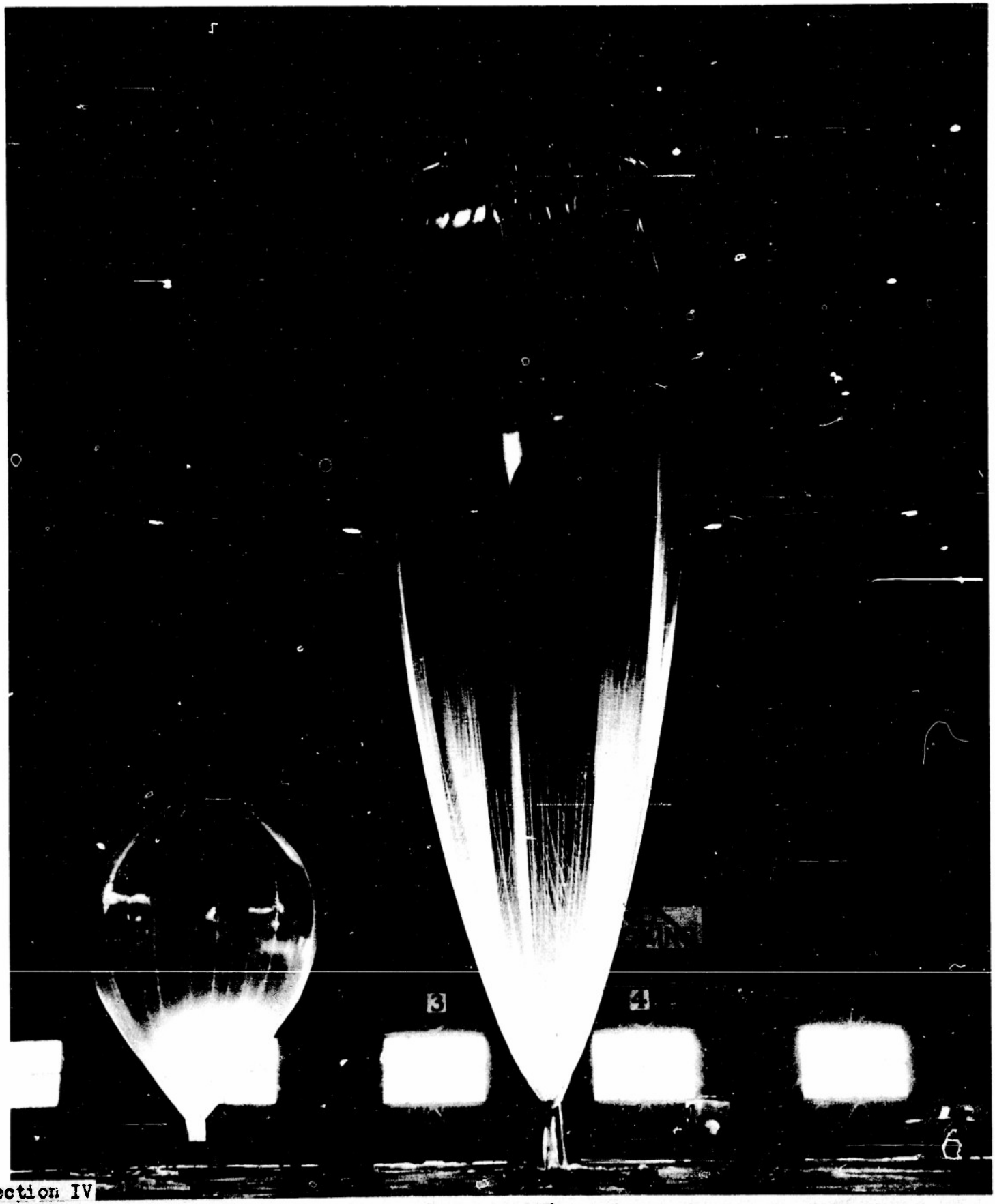

Section IV

Figure 16. Balloon just lifting its own weight, 235 pounds gross, near beginning of inflation. The small balloon to the left was a 39' balloon of special design.

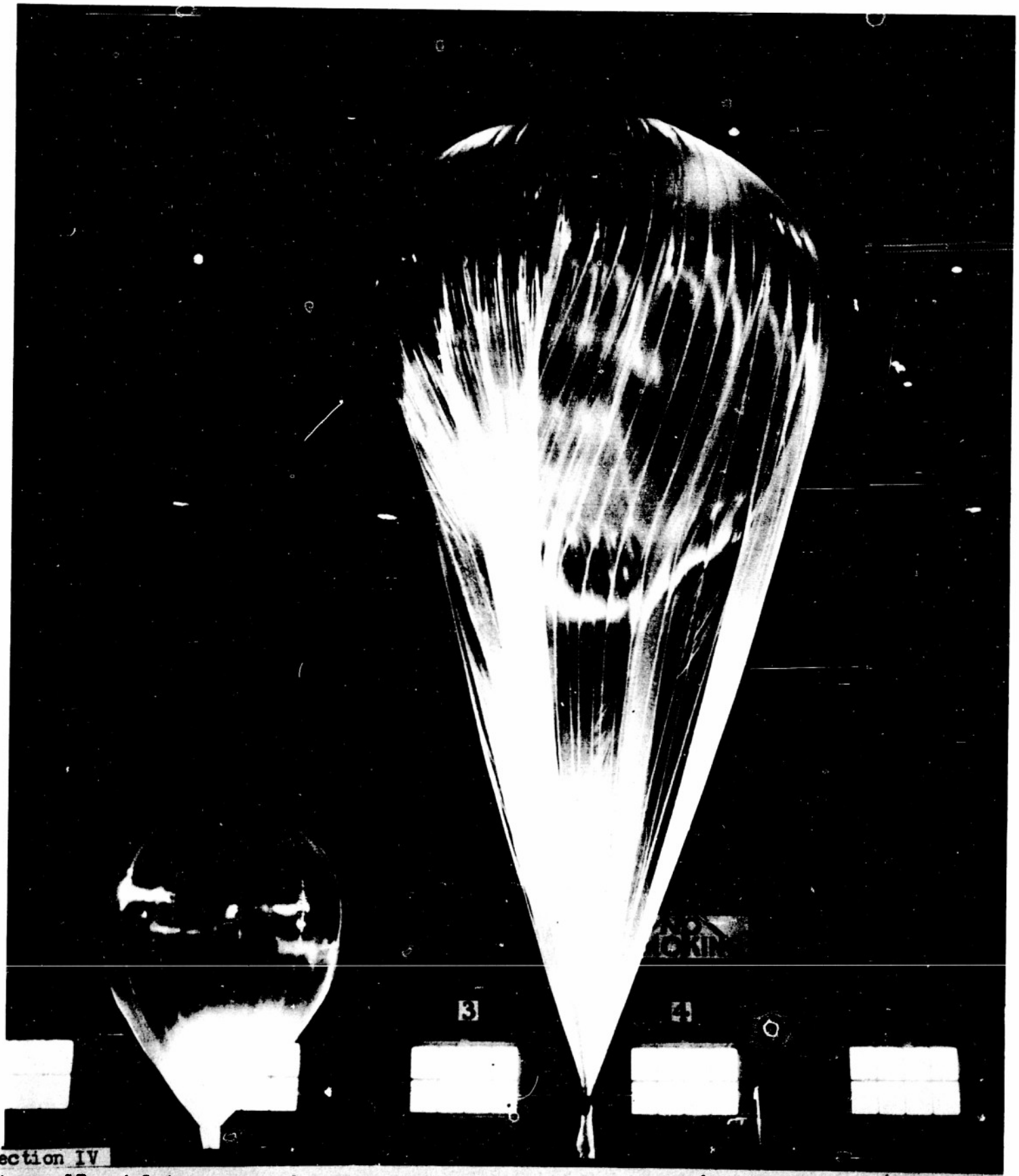

Section IV

Figure 17. A later stage of inflation. Lift about 450 pounds. Note the regions of negative pressure where the fabric bends inward. The top of the balloon is tight but there is excess fabric everywhere else. In the regions where there is excess fabric the balloon assumes the natural shape, at least between the large folds which extend down to the tie point.

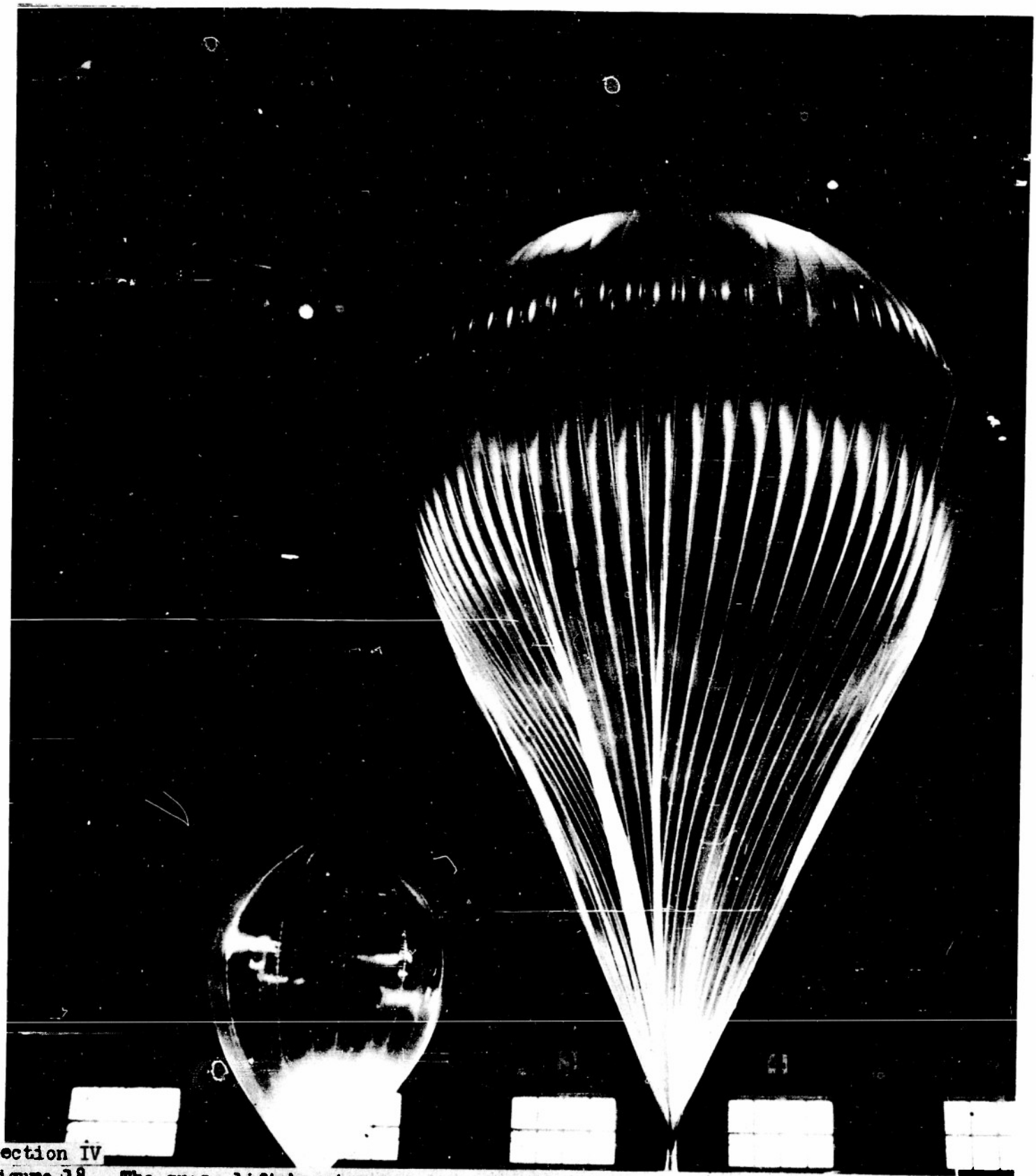

Section IV

Figure 18. The gross lift has increased to about 1000 pounds. The negative pressure regions can be seen at the bottom. The fabric scallops inward between the tapes below the equator and outward between the tapes above the equator. This balloon is now open all the way to the bottom. If the appendix is not closed during flight, at this stage the balloon will rapidly take air and fill out until the negative pressure regions disappear.

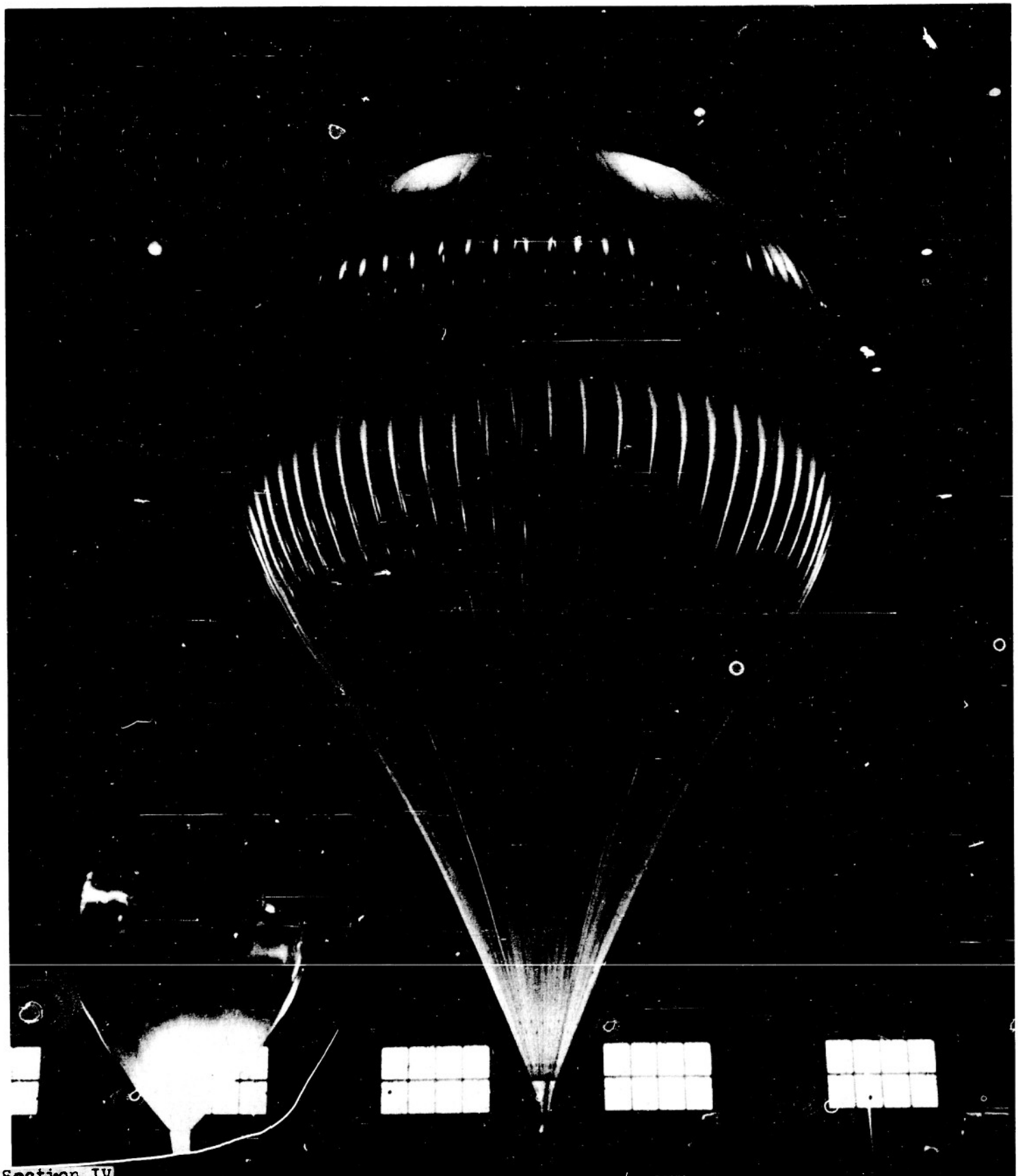

Section IV

Figure 19. Gross lift about 1500 pounds. The scalloping is more pronounced and the balloon is quite open at the bottom.

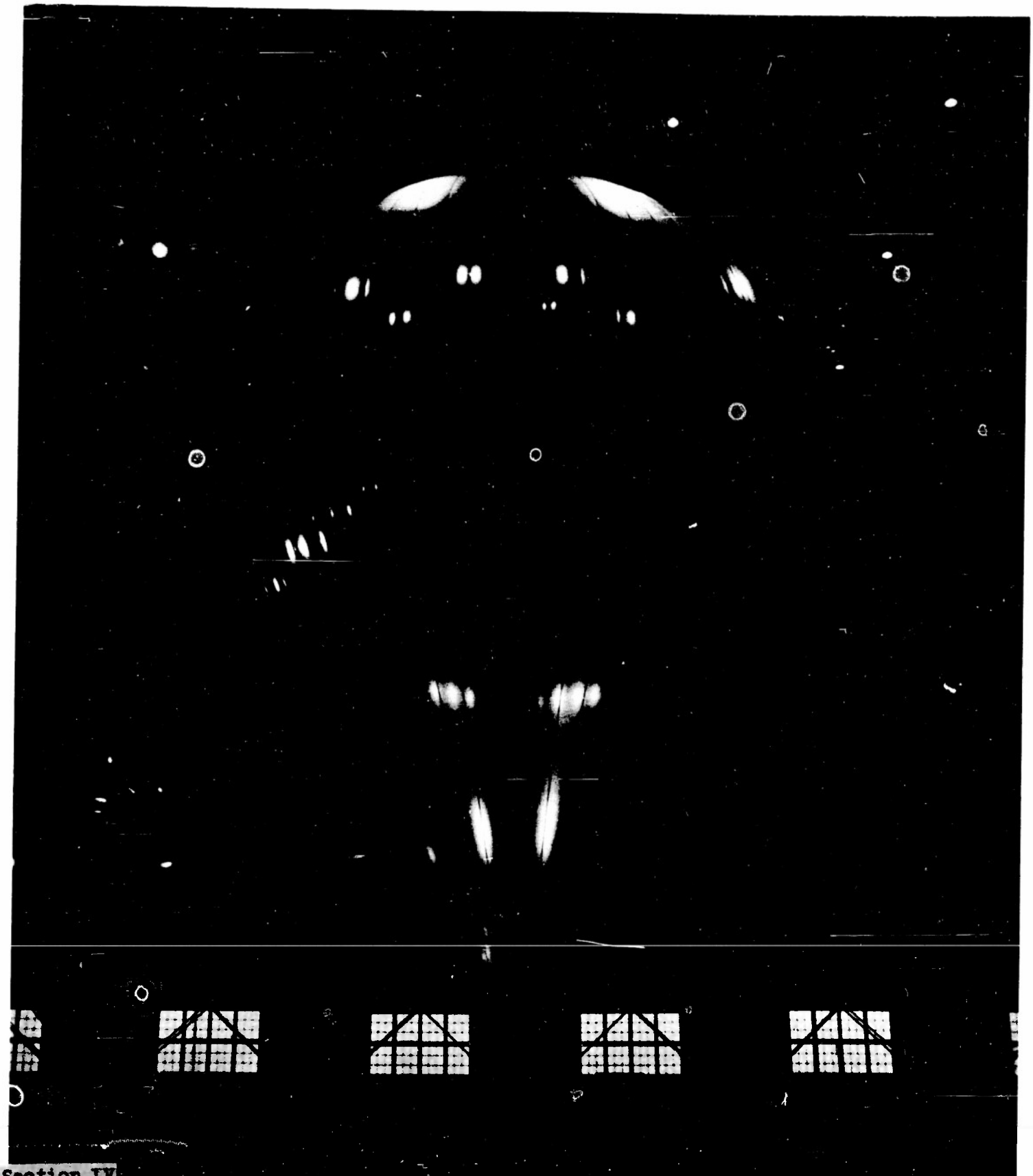

Section IV

Figure 20. Balloon completely inflated. Gross lift 2035 pounds. The plastic has a moderate bulging between the lines over the [illegible] upper portion but the appearance is generally good.

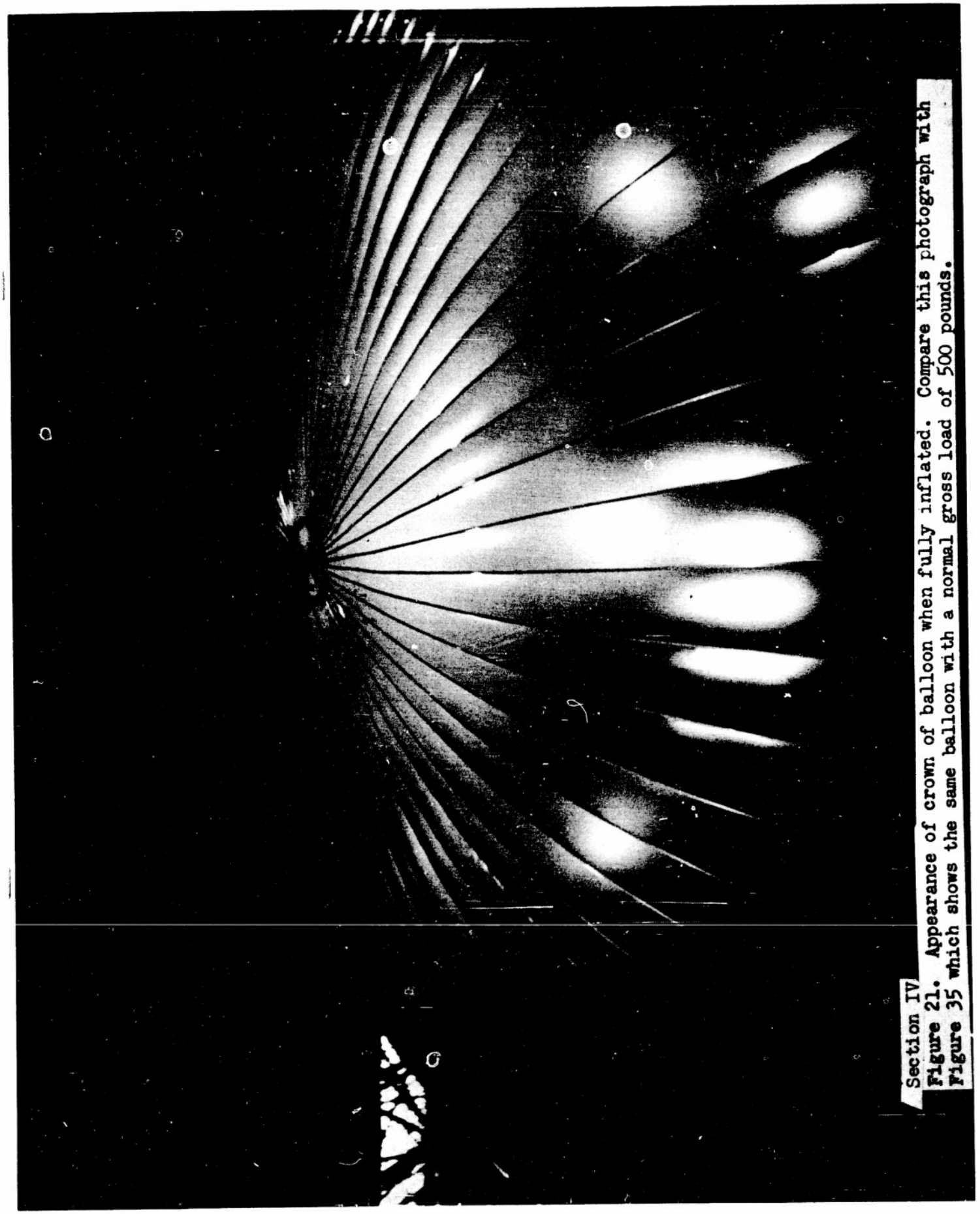

Section IV
Figure 21. Appearance of crown of balloon when fully inflated. Compare this photograph with Figure 35 which shows the same balloon with a normal gross load of 500 pounds.

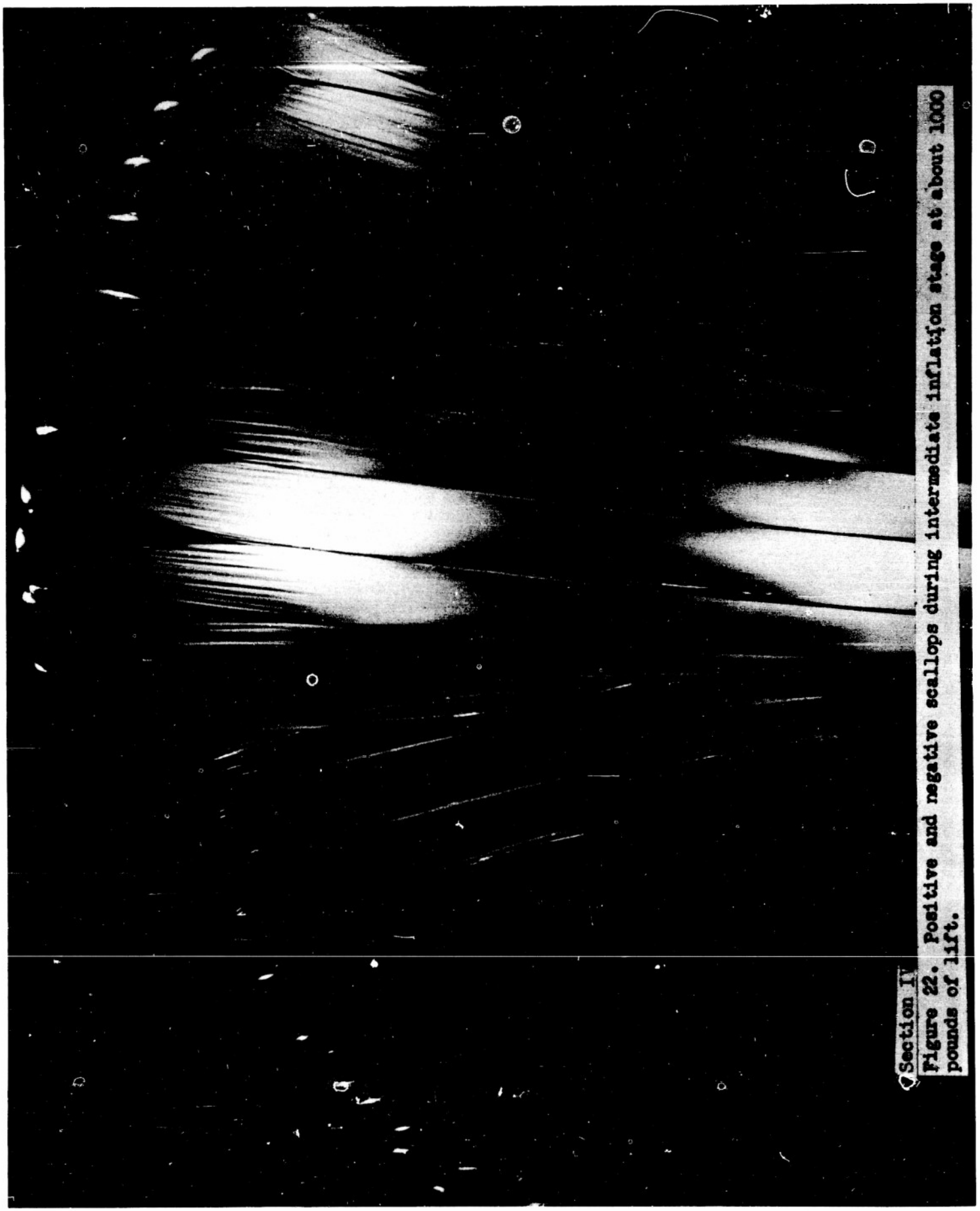

Section IV
Figure 22. Positive and negative scallops during intermediate inflation stage at about 1000 pounds of lift.

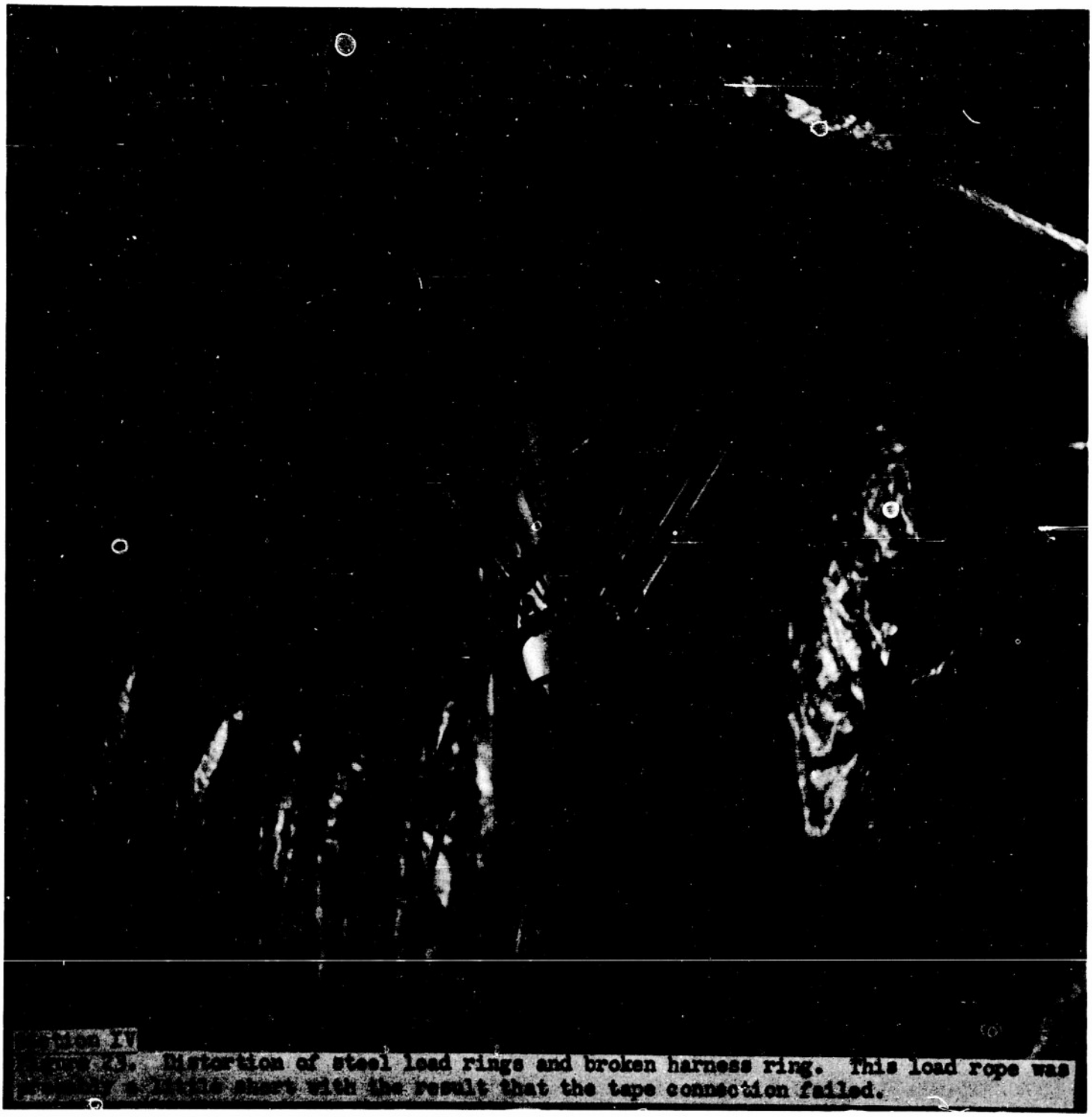

Distortion of steel lead rings and broken harness ring. This load rope was [illegible] with the result that the tape connection failed.

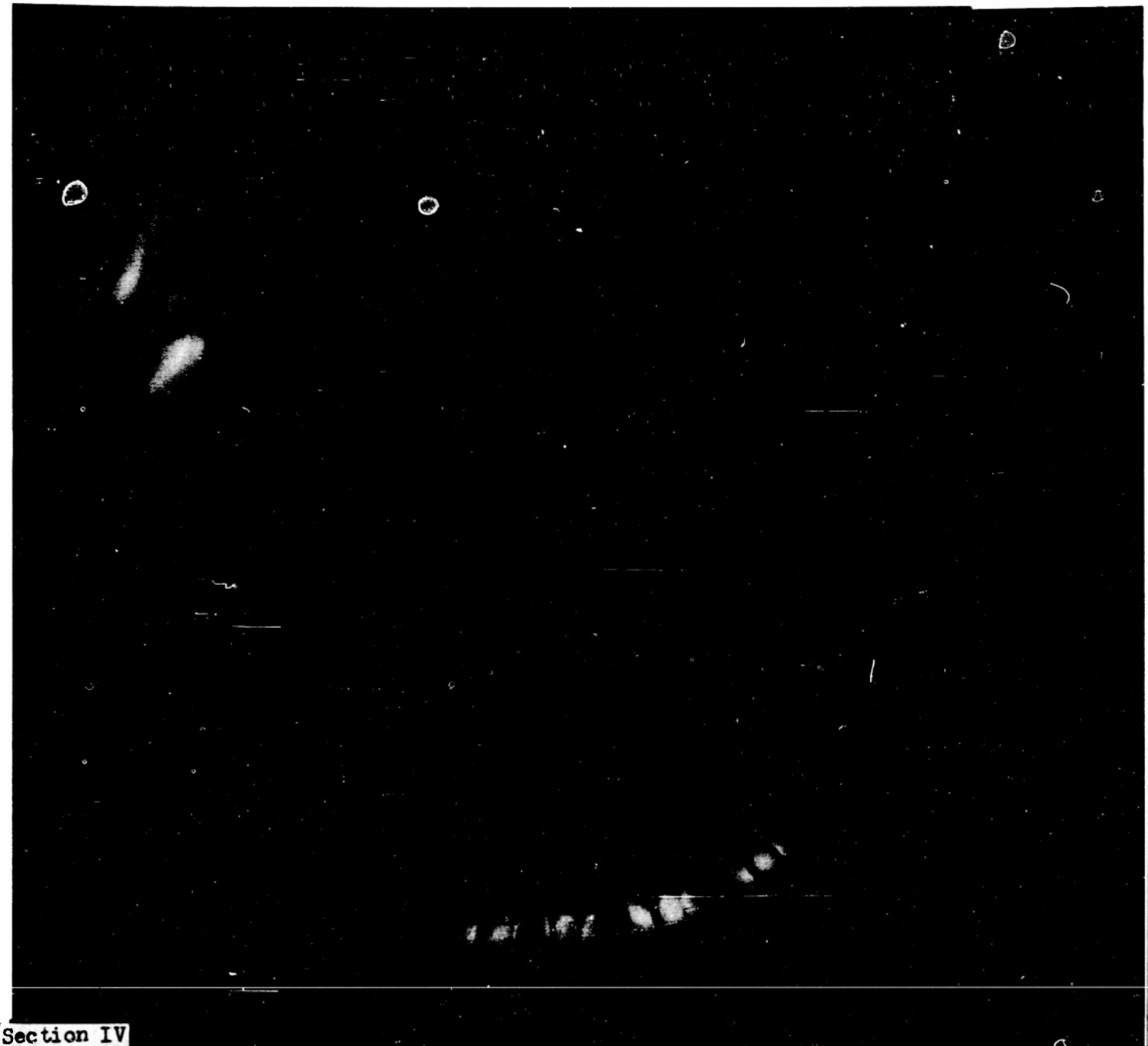

Section IV

Figure 24. View of top of balloon taken through the appendix opening at the bottom. The closed patched region is a section which was ripped out to deflate the balloon on a previous inflation. A tie rope for gas sampling hangs down the center.

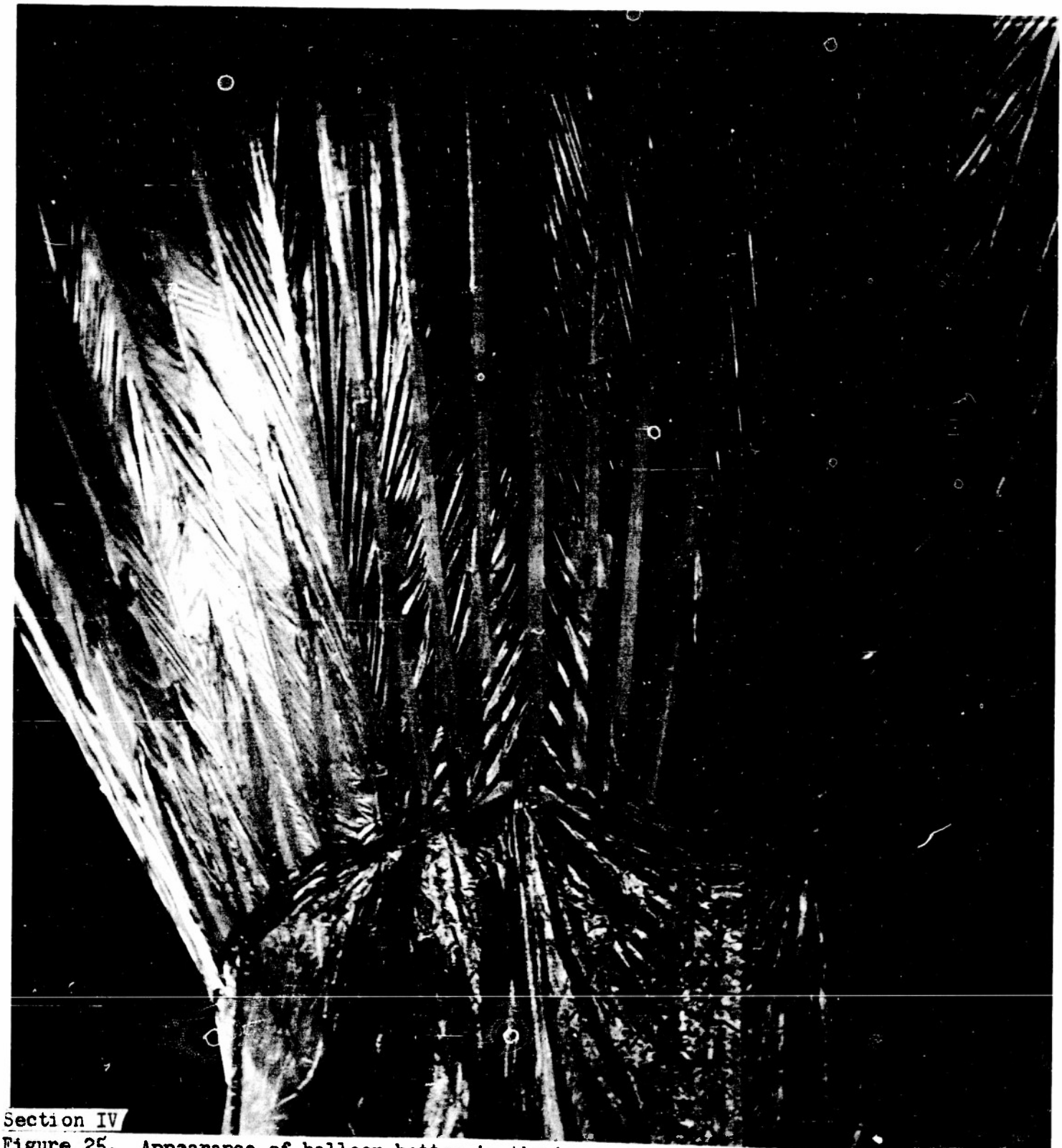

Section IV

Figure 25. Appearance of balloon bottom in the heavy load test. One or two of the load ropes have failed with the result that the adjacent areas take up the strain which is transferred through the plastic as can be seen by the numerous diagonal wrinkles.

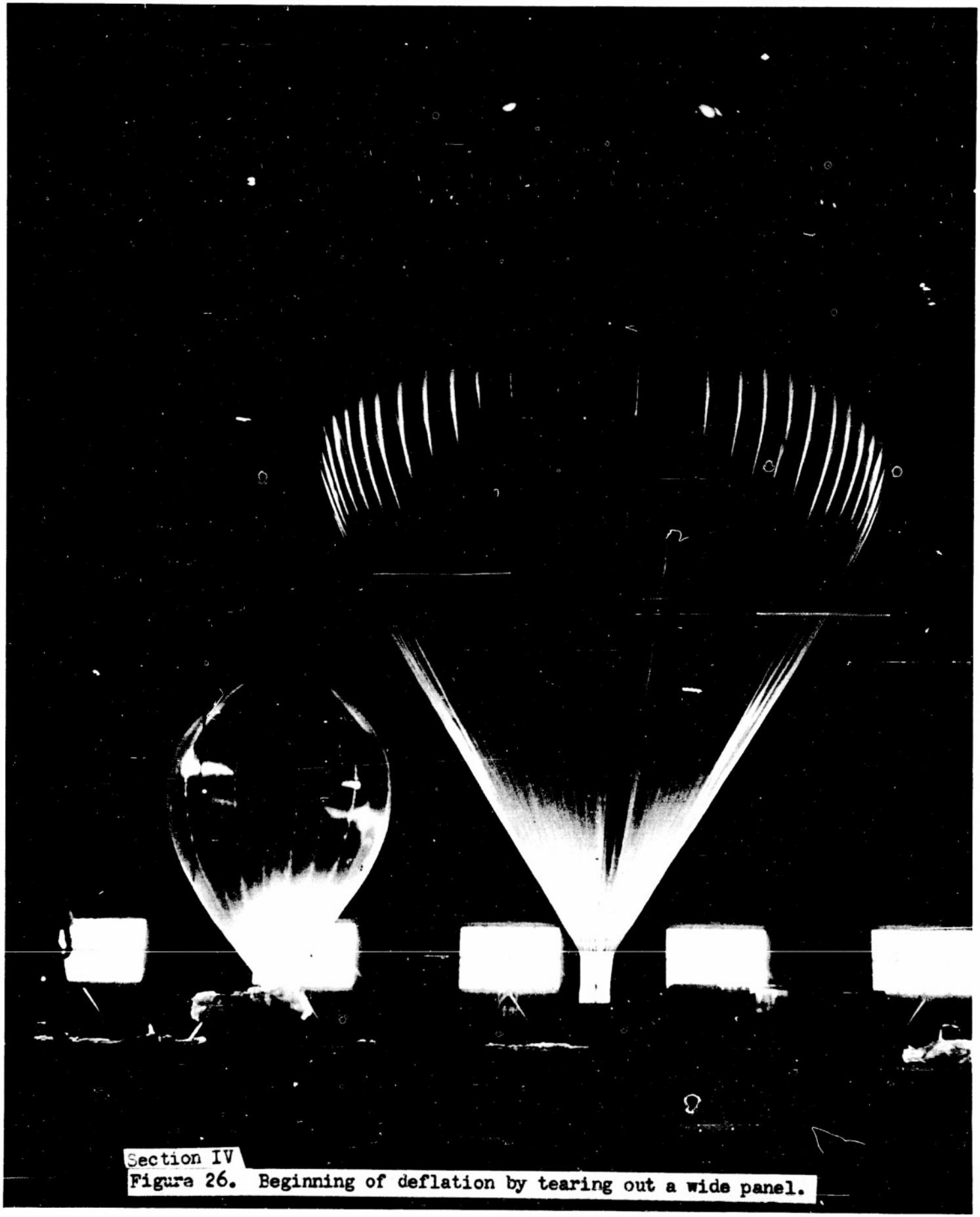

Section IV
Figura 26. Beginning of deflation by tearing out a wide panel.

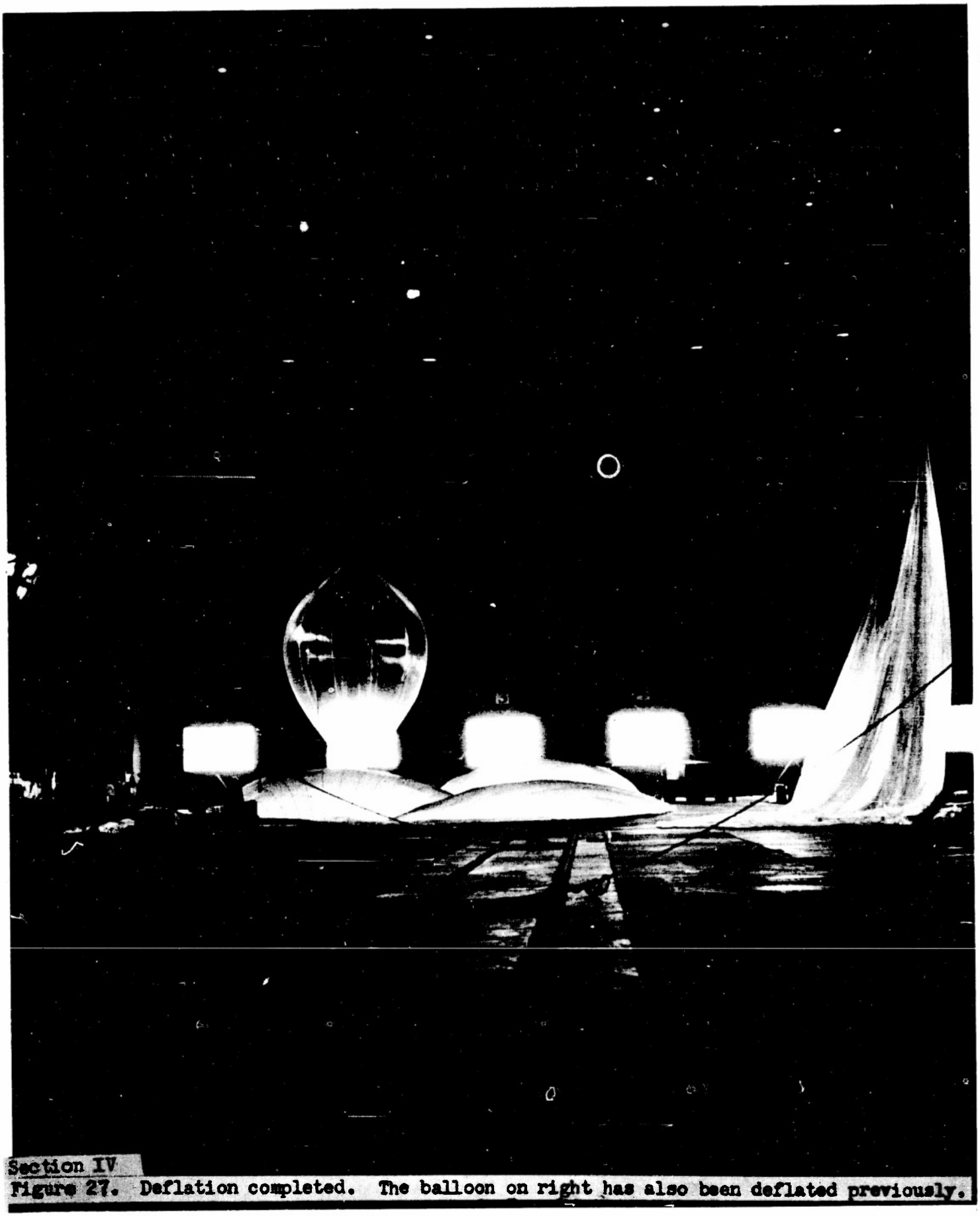

Section IV
Figure 27. Deflation completed. The balloon on right has also been deflated previously.

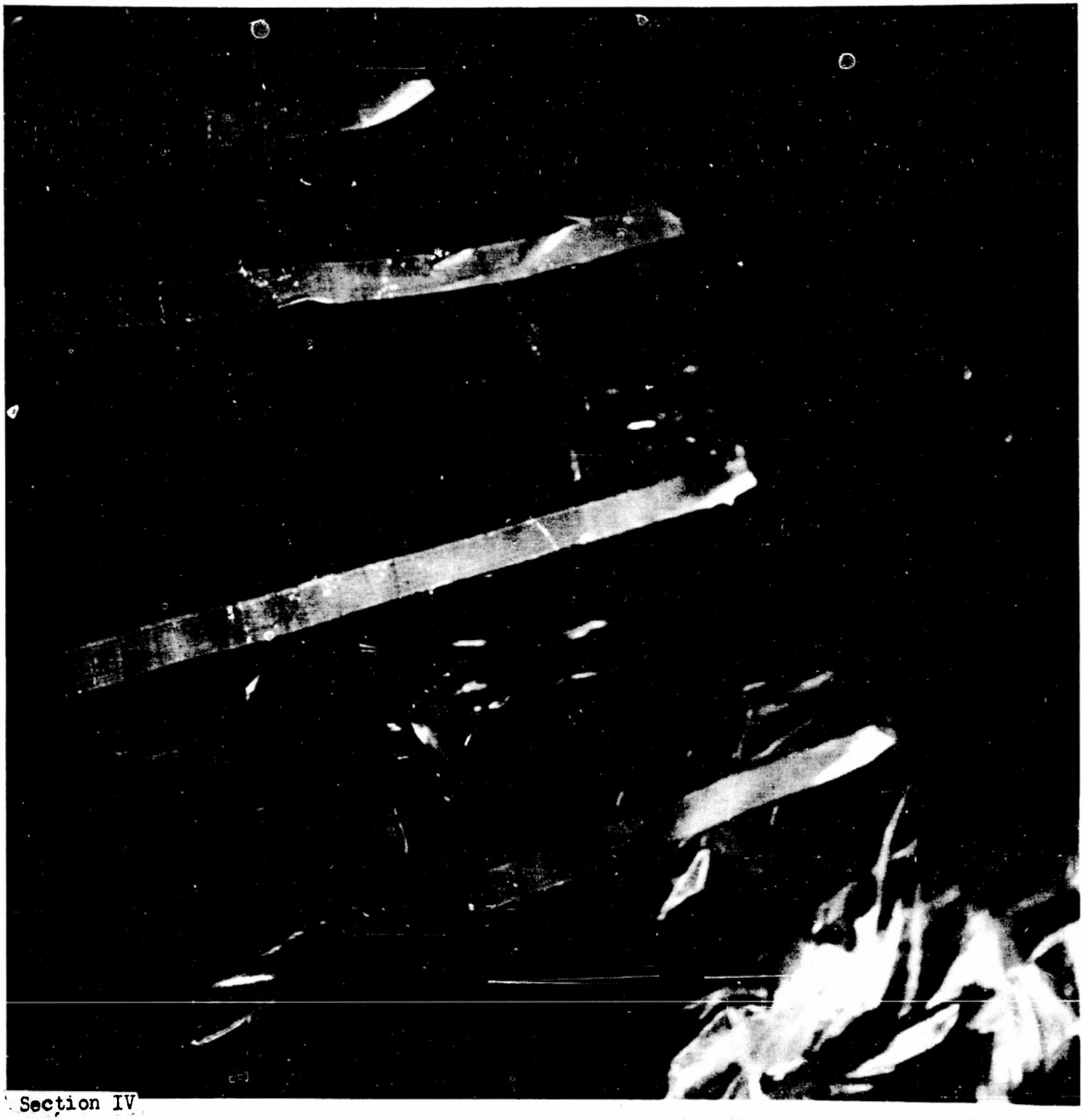

Section IV

Figure 28. Showing the failure of the rip panel patch which occurred during the night as the balloon remained under full inflation. This shows the importance of heat sealing every part of a balloon which is under tension as the tapes creep and slide under constant force. The panel was ripped out to deflate the balloon following the first light load inflation and was patched entirely with tapes as shown before the heavy load inflation was begun.

Section IV
Figure 29. Girdie part way down balloon with air inflation above.

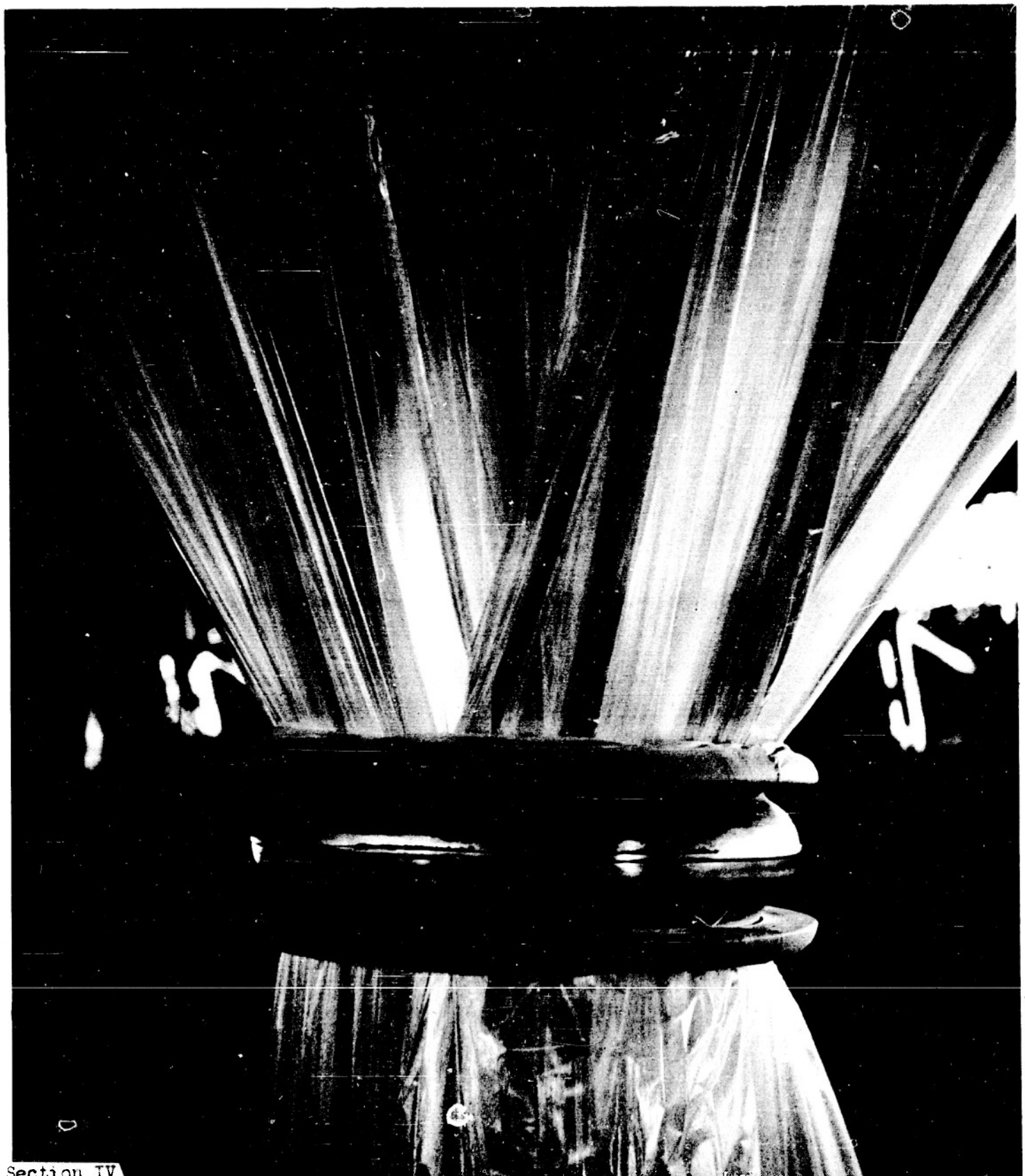

Section IV

Figure 30. Close-up of plastic feeding through the girdle. The girdle slipped very smoothly not by sudden jumps as might be expected. As far as could be seen no stretching or abrasion of the plastic resulted from the slipping. The cone angle of the plastic is approximately 60° as would be expected from theory.

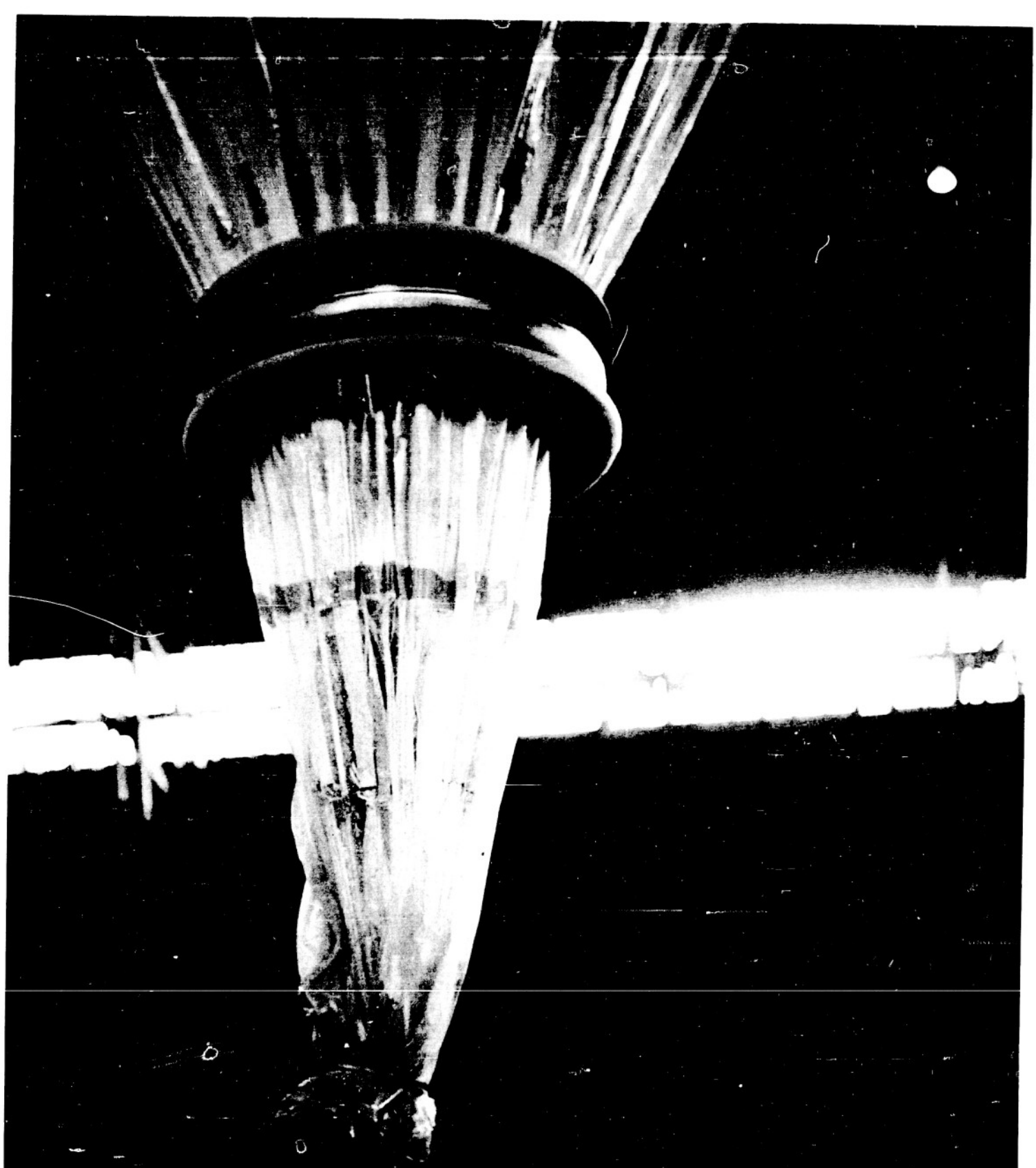

Section IV

Figure 30A. Girdle close to bottom of balloon ready to slip off. In normal flight a catcher ring is hung from the balloon load ring to prevent damage to the equipment by the falling girdle.

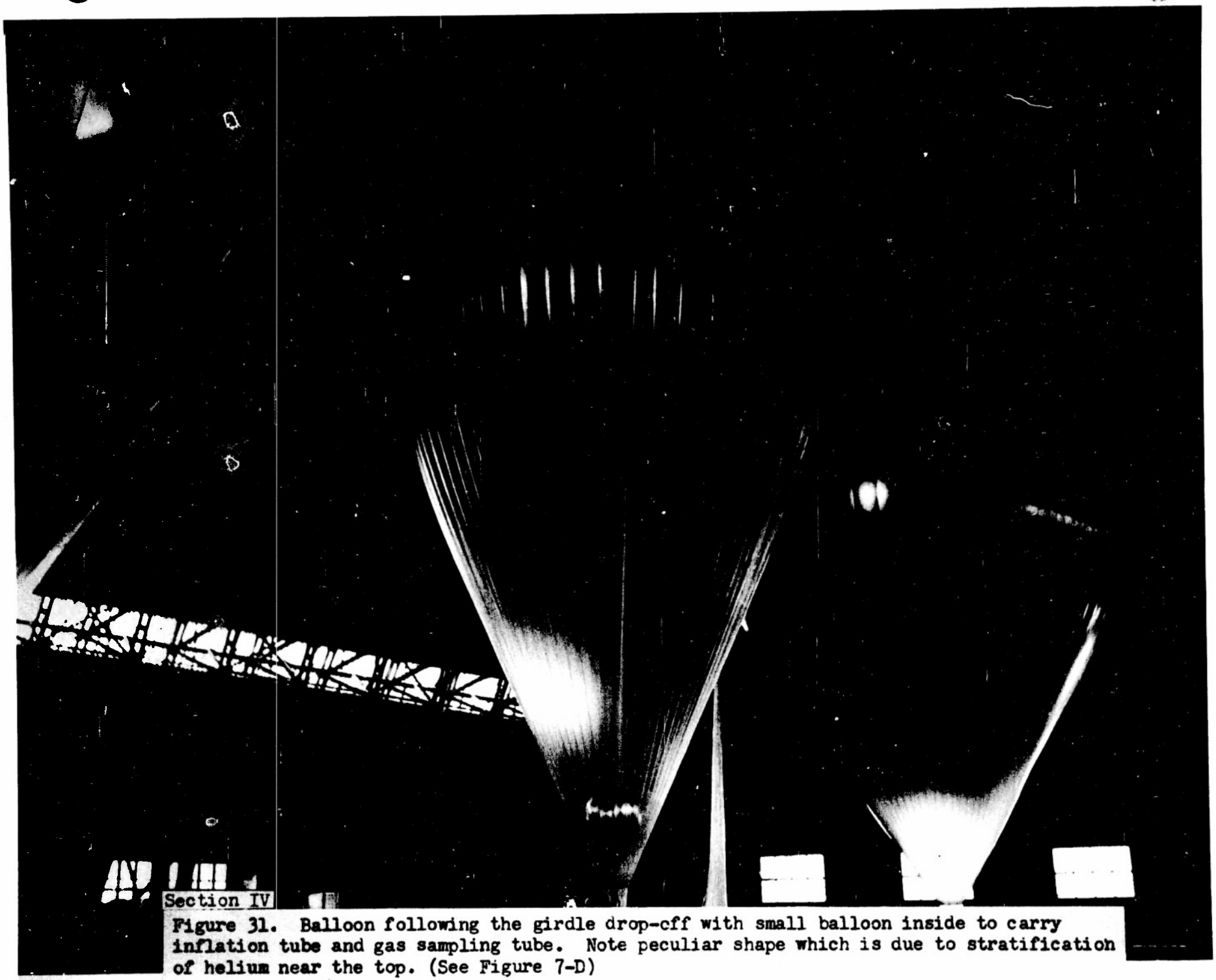

Section IV

Figure 31. Balloon following the girdle drop-cff with small balloon inside to carry inflation tube and gas sampling tube. Note peculiar shape which is due to stratification of helium near the top. (See Figure 7-D)

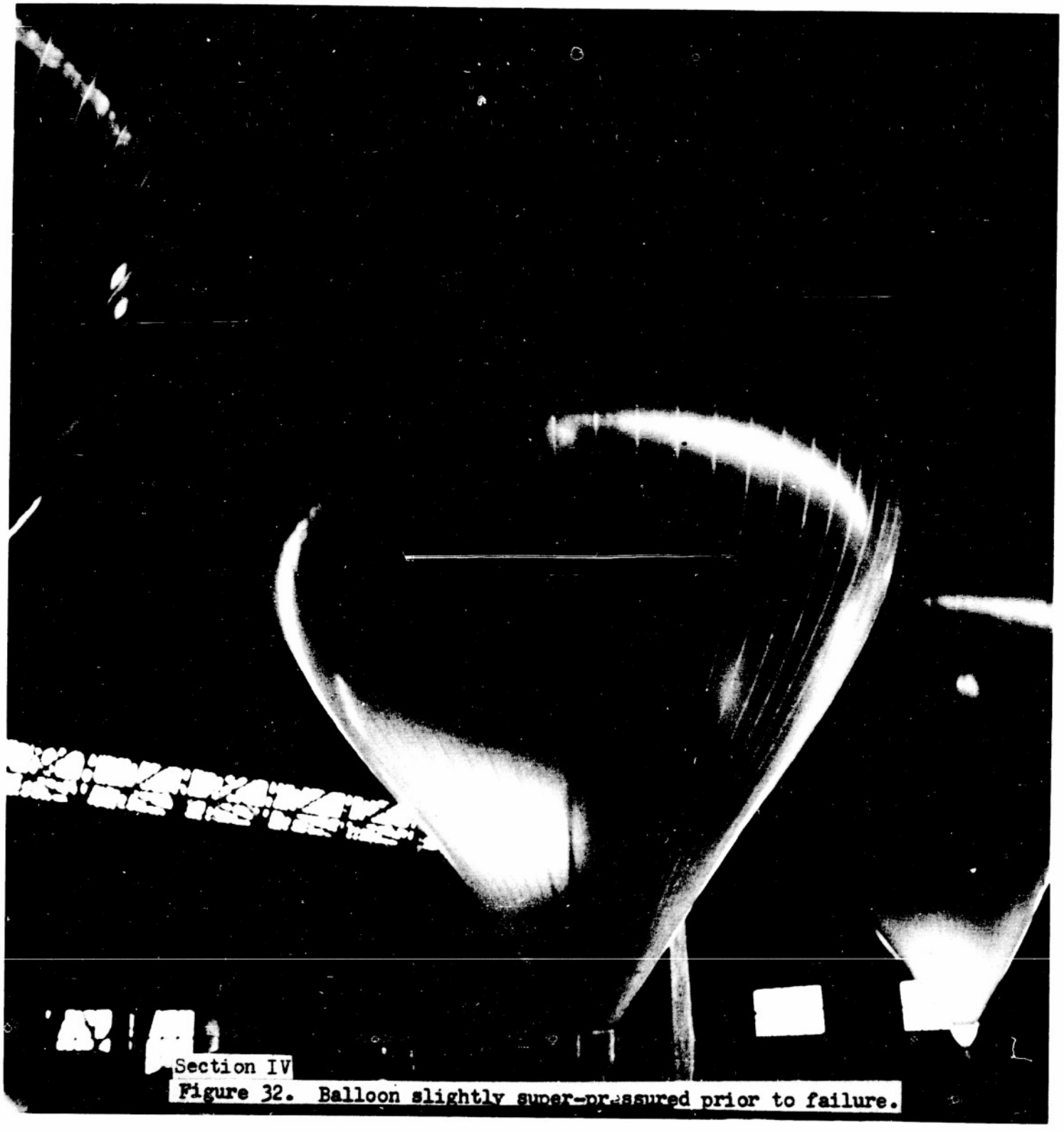

Section IV
Figure 32. Balloon slightly super-pressured prior to failure.

Section IV

Figure 33. Rupture occurring near point where cone joins sphere. Note large hole and two small holes. As the inflation was continuing the balloon ripped open all the way along the gore containing the large hole.

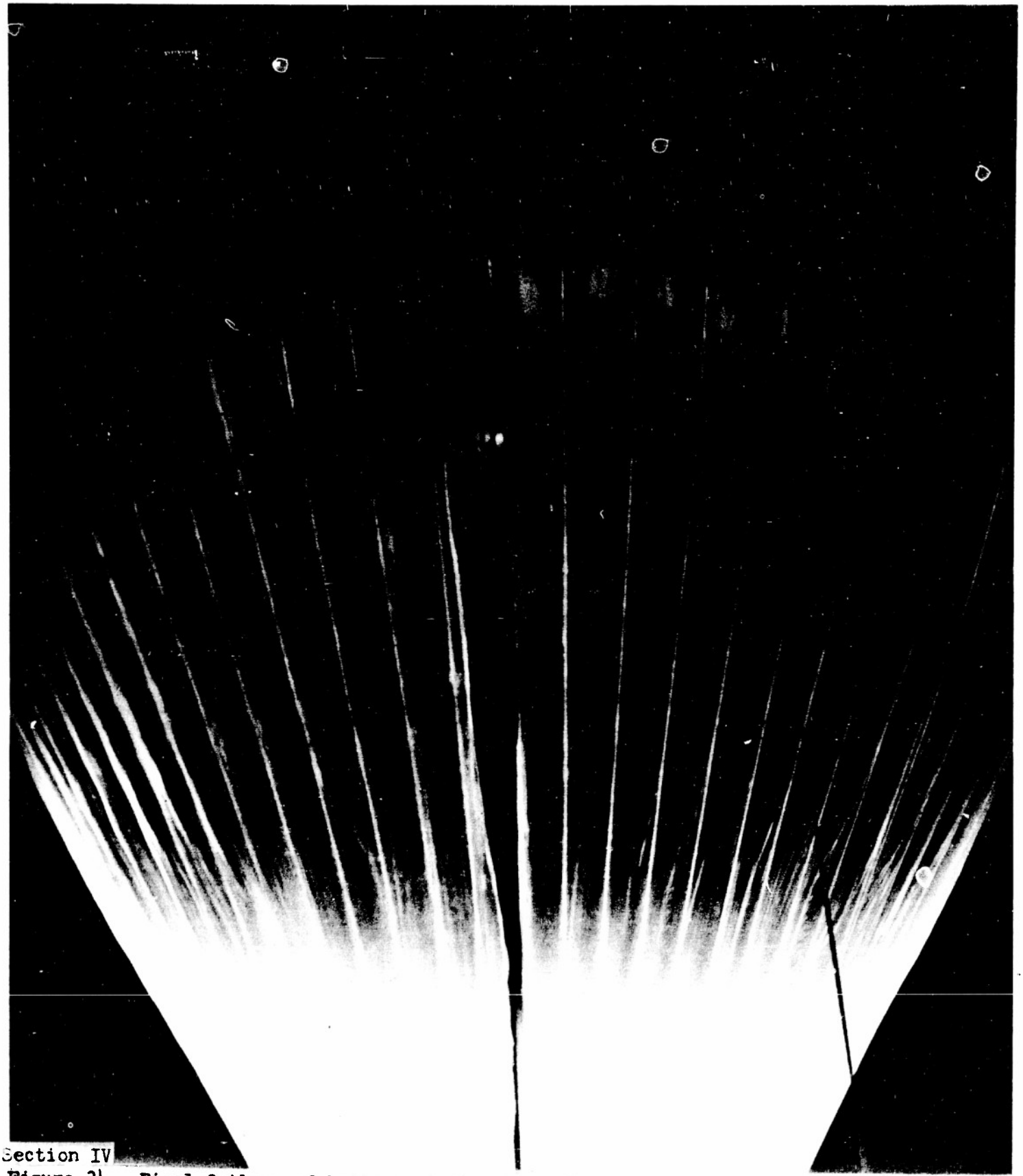

Section IV

Figure 34. Final failure of balloon which released super-pressure. It is evident that balloons which are not able to valve sufficiently fast upon reaching ceiling become super-pressured and fail in a manner similar to this with the difference that the plastic is cold and may fracture in an irregular manner.

Section IV

Figure 35. Top of Winzen double-wall 73' balloon inflated to a normal lift of about 500 pounds when full. This should be compared with Figure 21 which shows this balloon inflated to a gross lift of four times this amount.

Section IV

Figure 36. Showing the folds in the plastic as the balloon fills out. At bottom left center and middle left center can be seen regions where sticky tapes cause adherence of plastic. Note stress concentrations in many regions along the tapes. This is a Winzen double-wall.

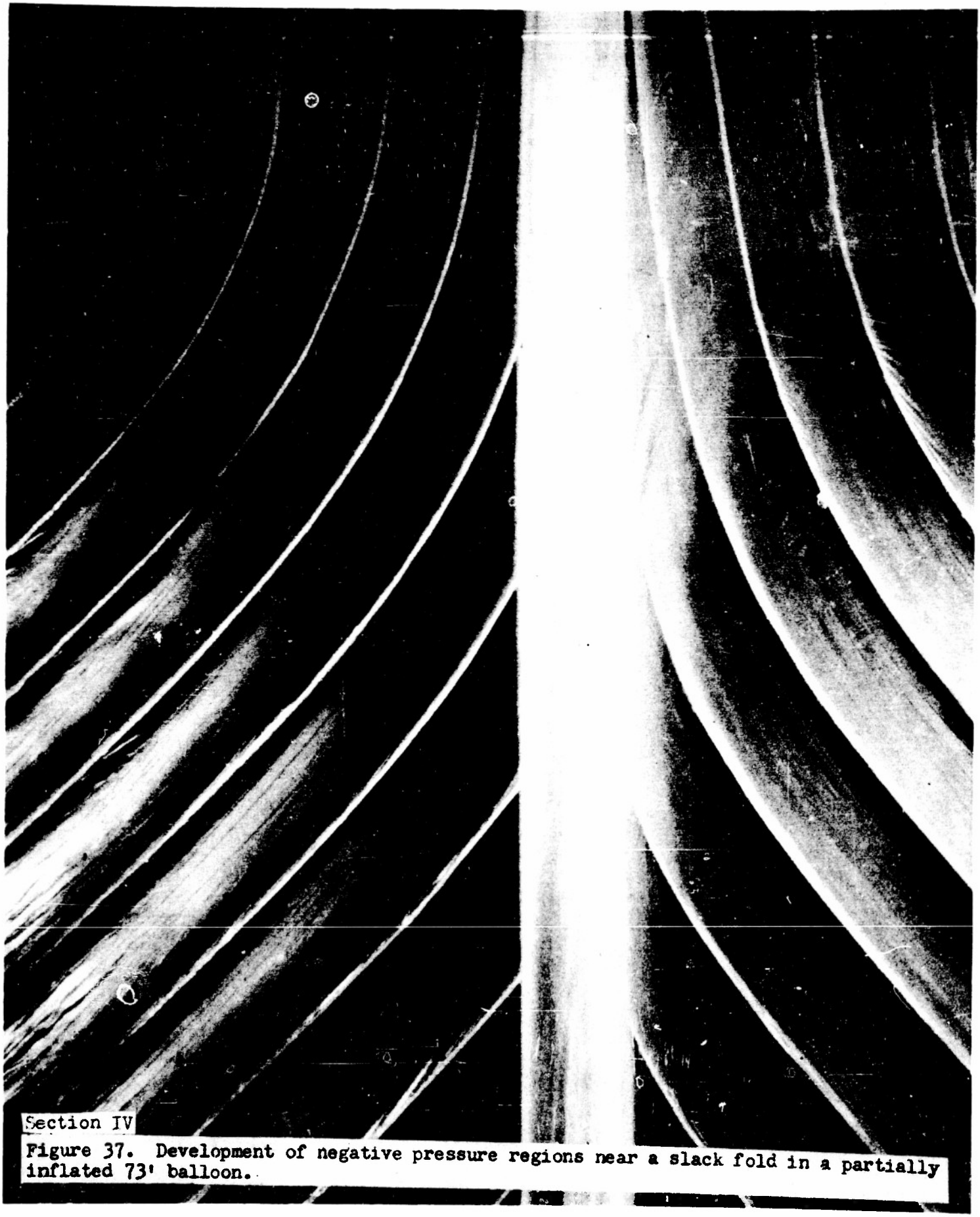

Section IV

Figure 37. Development of negative pressure regions near a slack fold in a partially inflated 73' balloon.

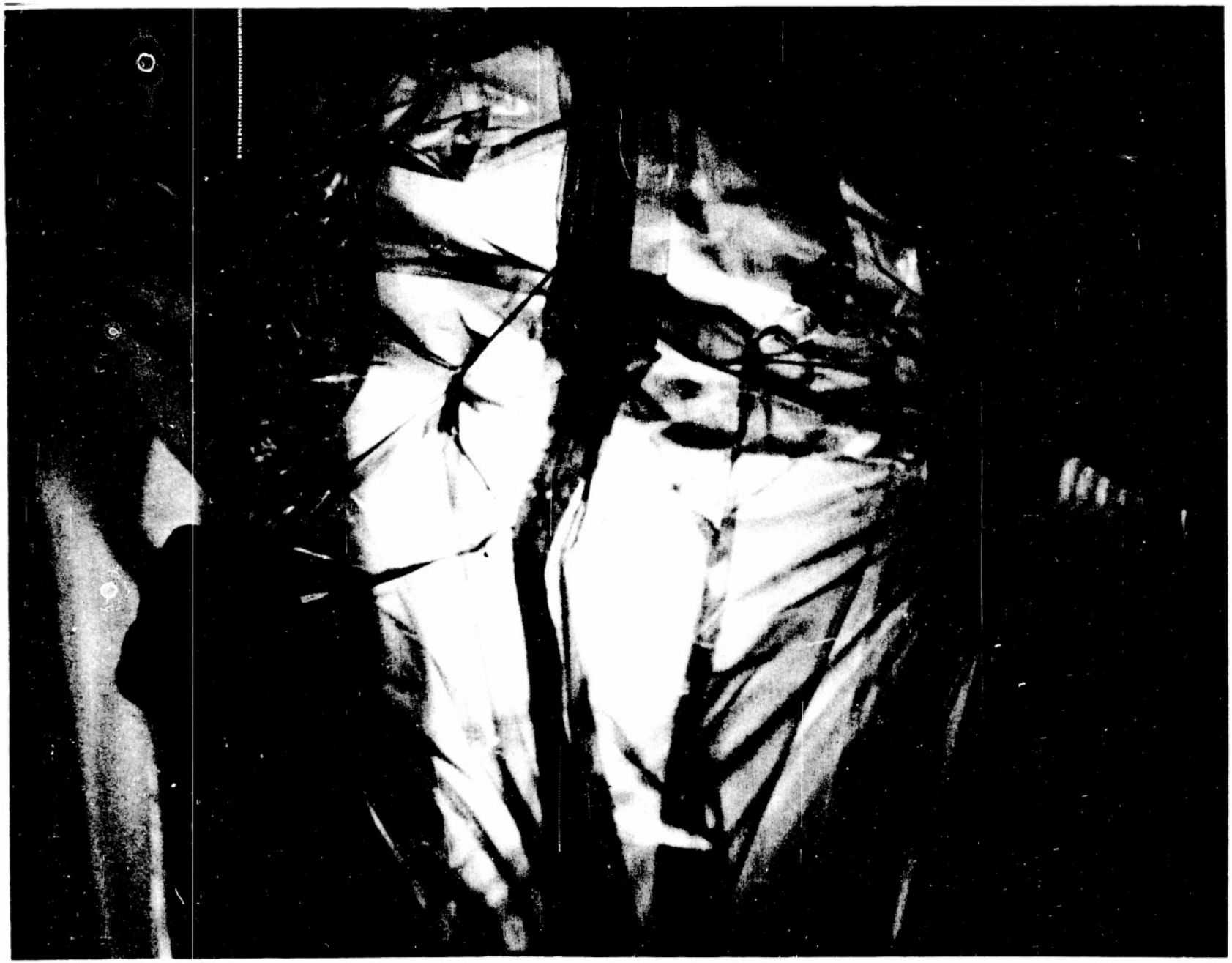

Section IV

Figure 38. Serious adhesion due to sticky tapes found on Winzen double-wall balloon. A piece of the tape has ripped off and adheres to the plastic adjacent, just to left of tape in center.

VI - Miscellaneous

The following series of photographs are miscellaneous details of balloon inflations which are of interest for specific reasons. The details of interest in each photograph are listed in the caption:

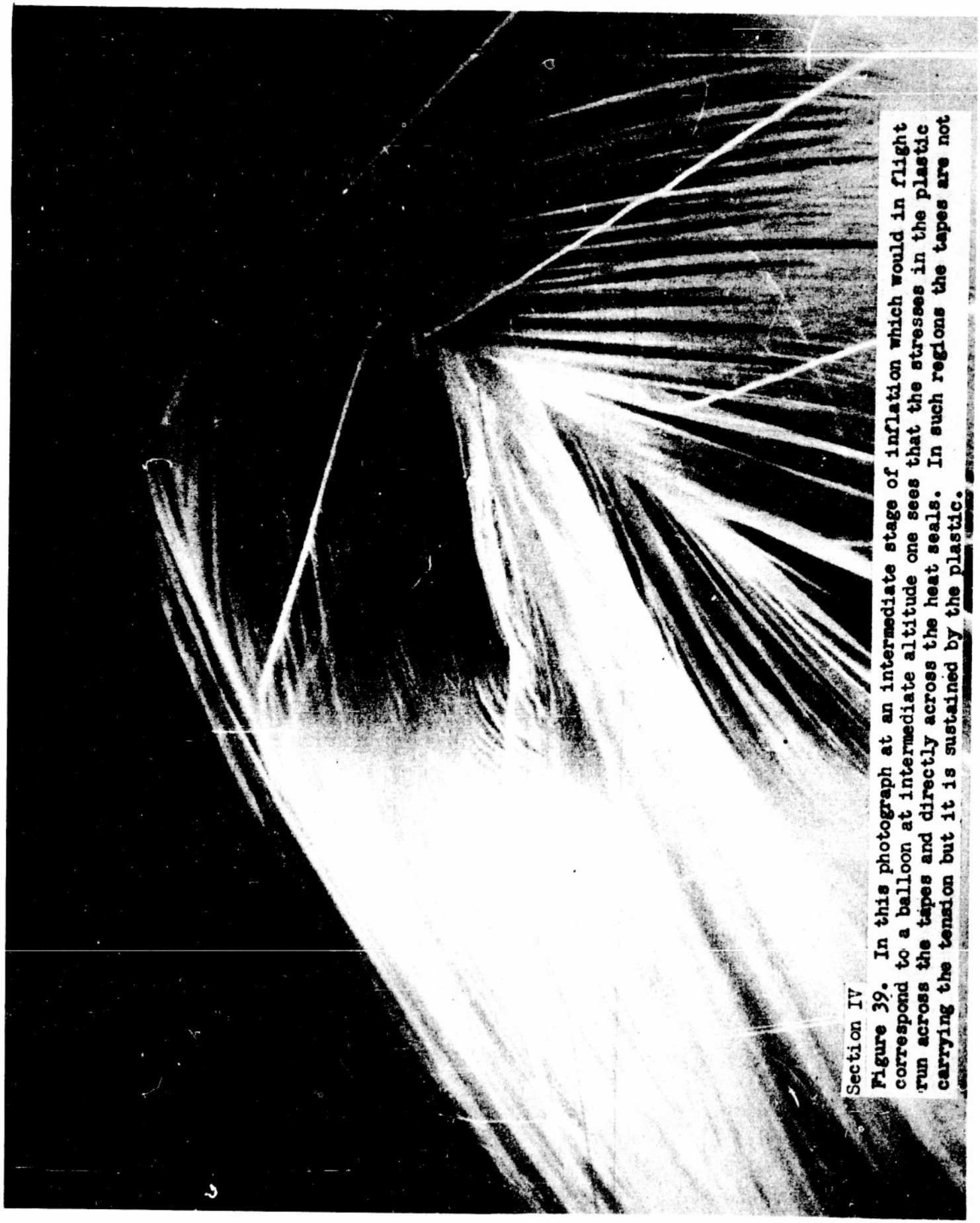

Section IV

Figure 39. In this photograph at an intermediate stage of inflation which would in flight correspond to a balloon at intermediate altitude one sees that the stresses in the plastic run across the tapes and directly across the heat seals. In such regions the tapes are not carrying the tension but it is sustained by the plastic.

Section IV
Figure 40. Change from negative center to positive top pressure in a partially inflated balloon showing the fabric bulging at top.

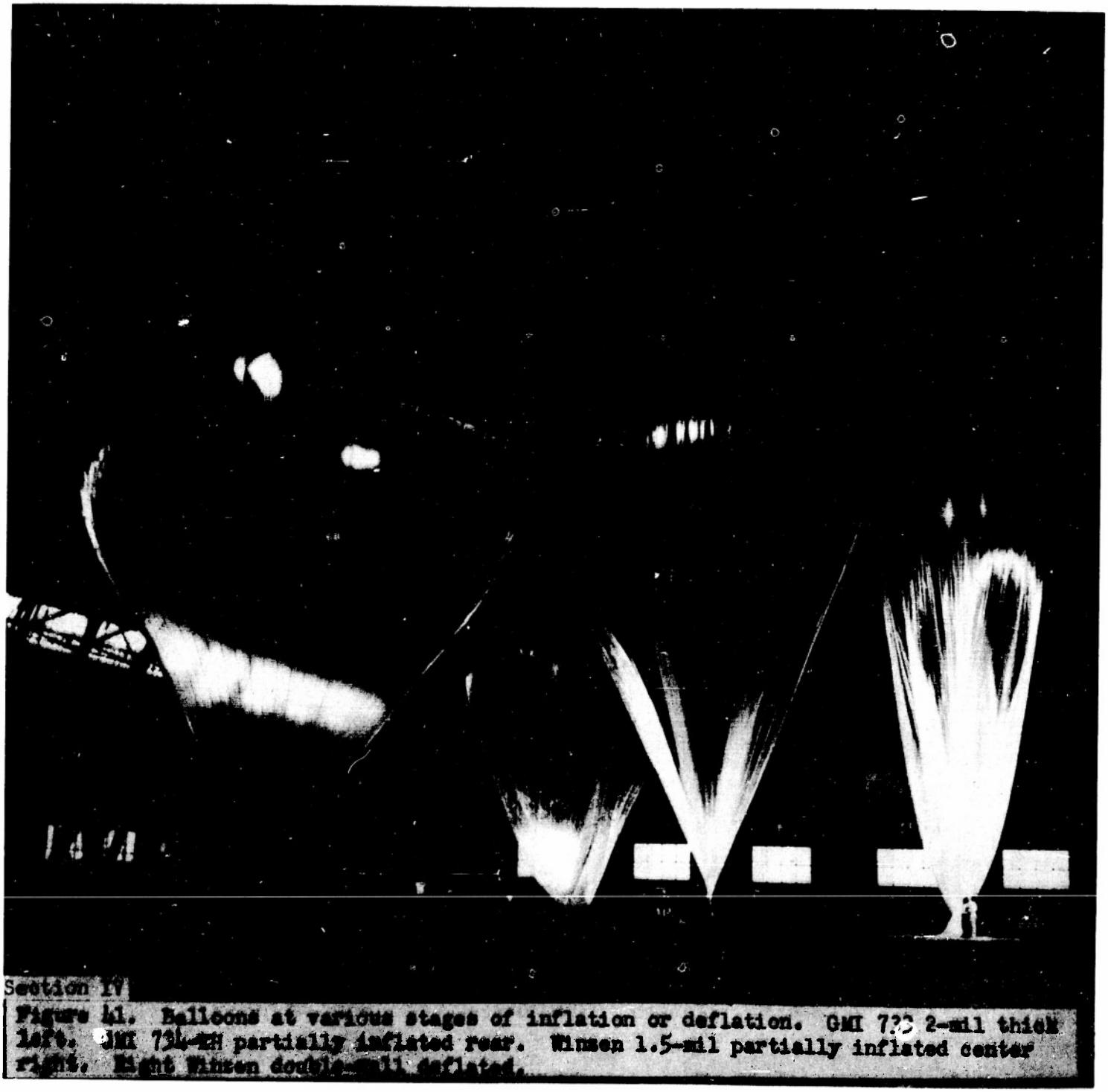

Section IV

Figure 41. Balloons at various stages of inflation or deflation. GMI 7[illegible] 2-mil thick left. GMI 7[illegible] partially inflated rear. Winsen 1.5-mil partially inflated center right. Right Winsen double-mil deflated.

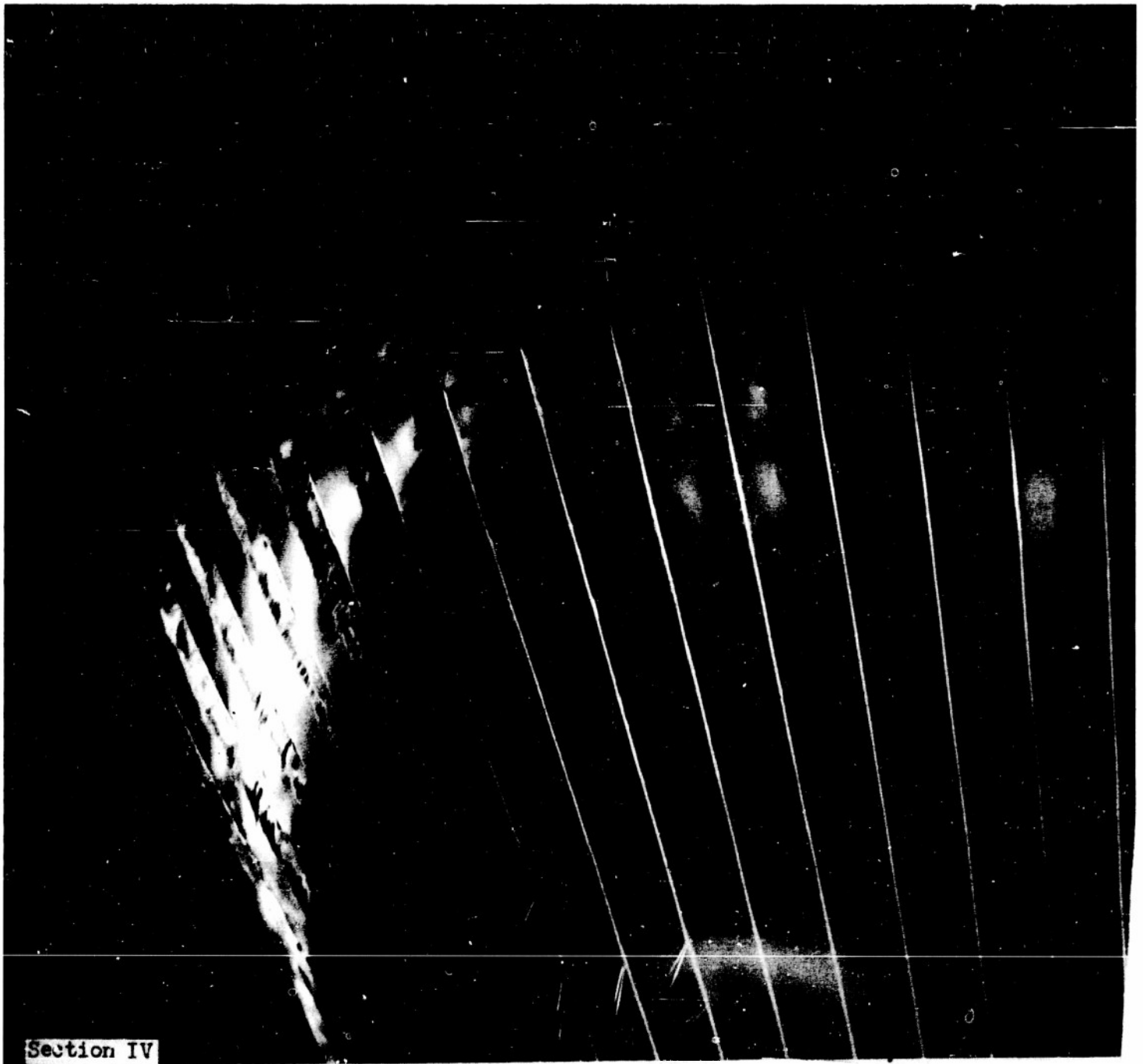

Section IV

Figure 42. Wrinkles observed in fabric of GMI 2-mil balloon probably because of the fact that gores are normally made of flat material. There are no serious stress concentrations showing here.

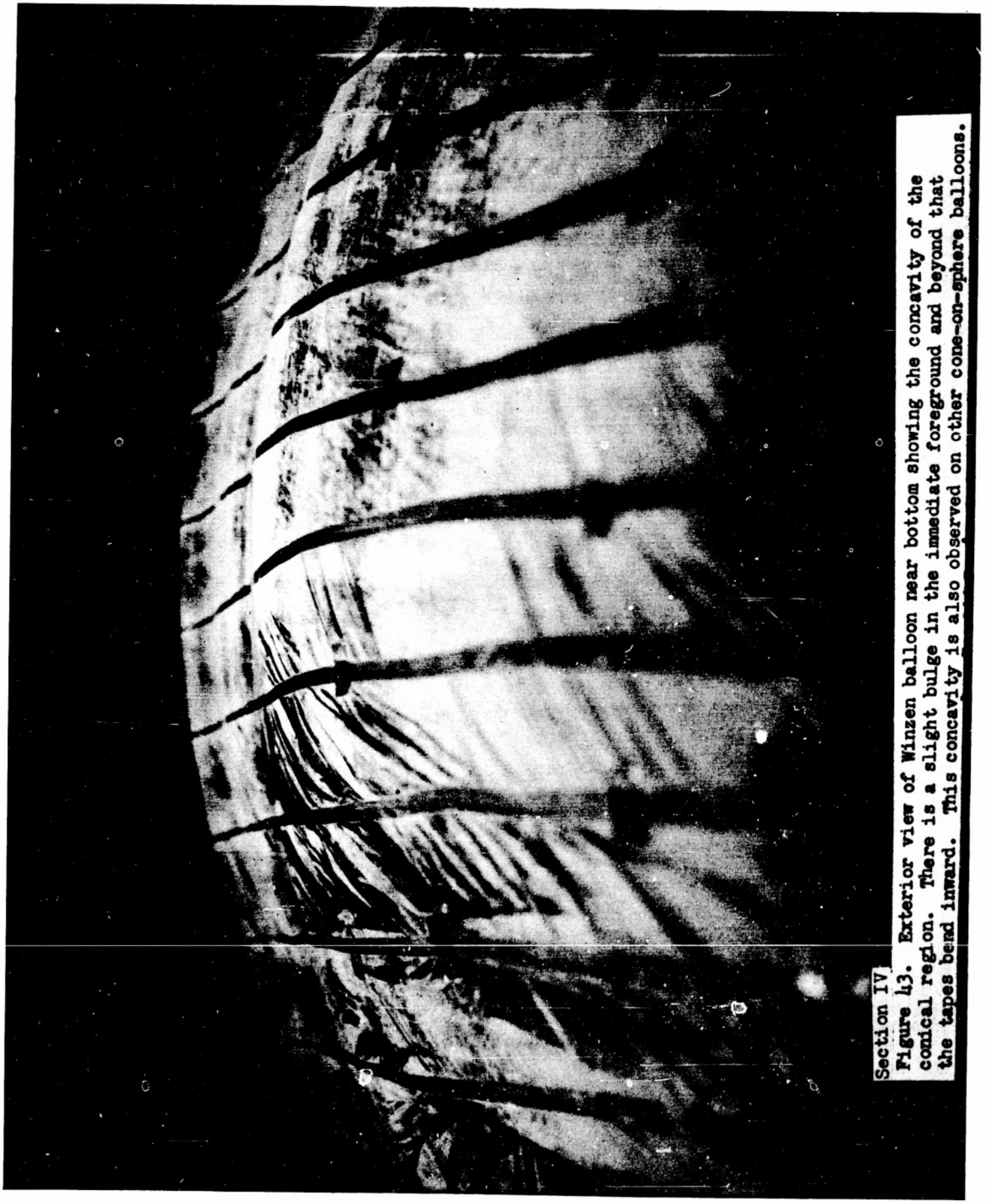

Section IV
Figure 43. Exterior view of Winzen balloon near bottom showing the concavity of the conical region. There is a slight bulge in the immediate foreground and beyond that the tapes bend inward. This concavity is also observed on other cone-on-sphere balloons.

Section IV

Figure 44. GMI 2-mil balloon left. Double-wall Winzen balloon right. The concavity near bottom can be seen on both of these.

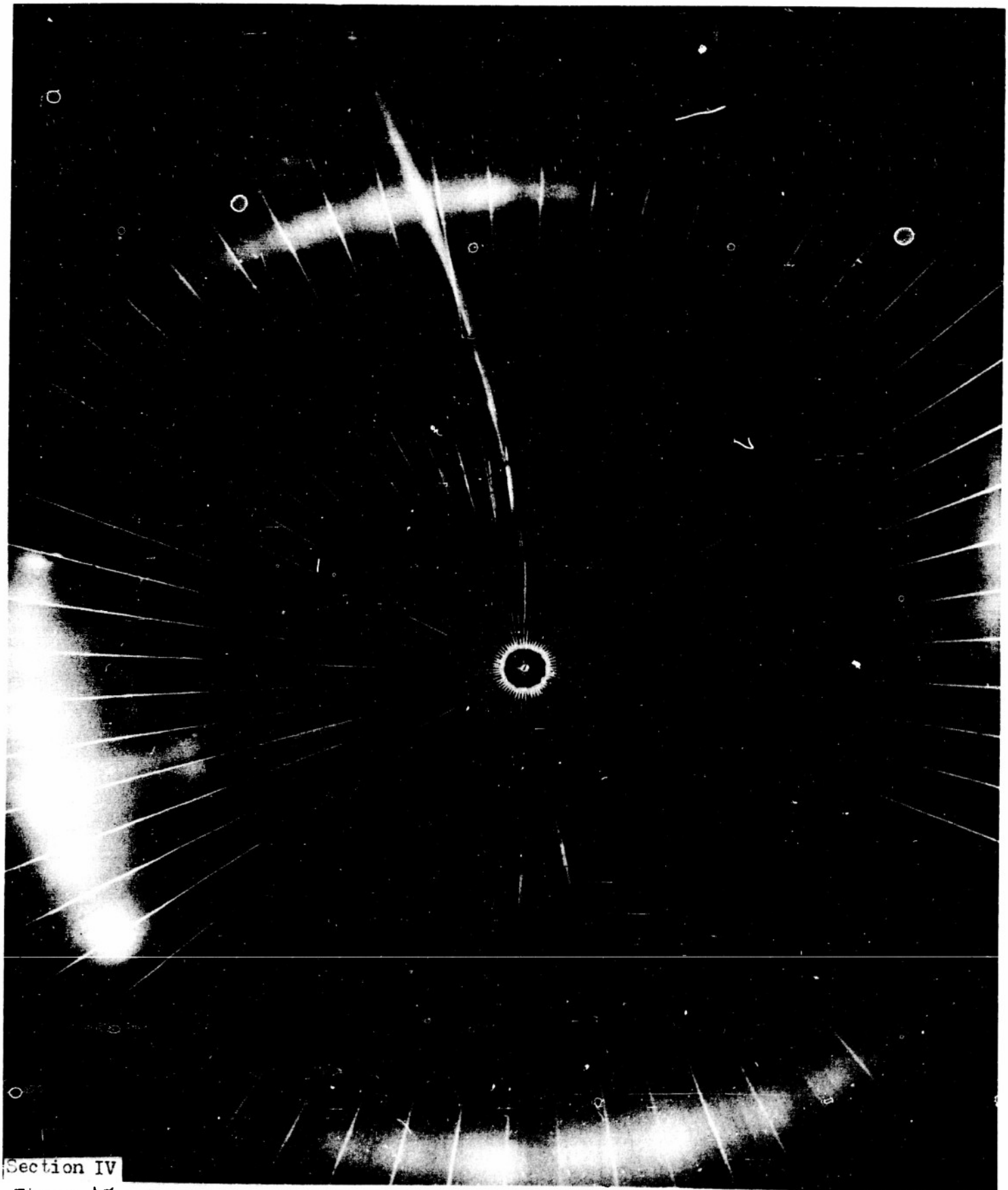

Section IV

Figure 45. Top interior view of inflated double-wall balloon. Rip panel has just been pulled out and deflation has begun.

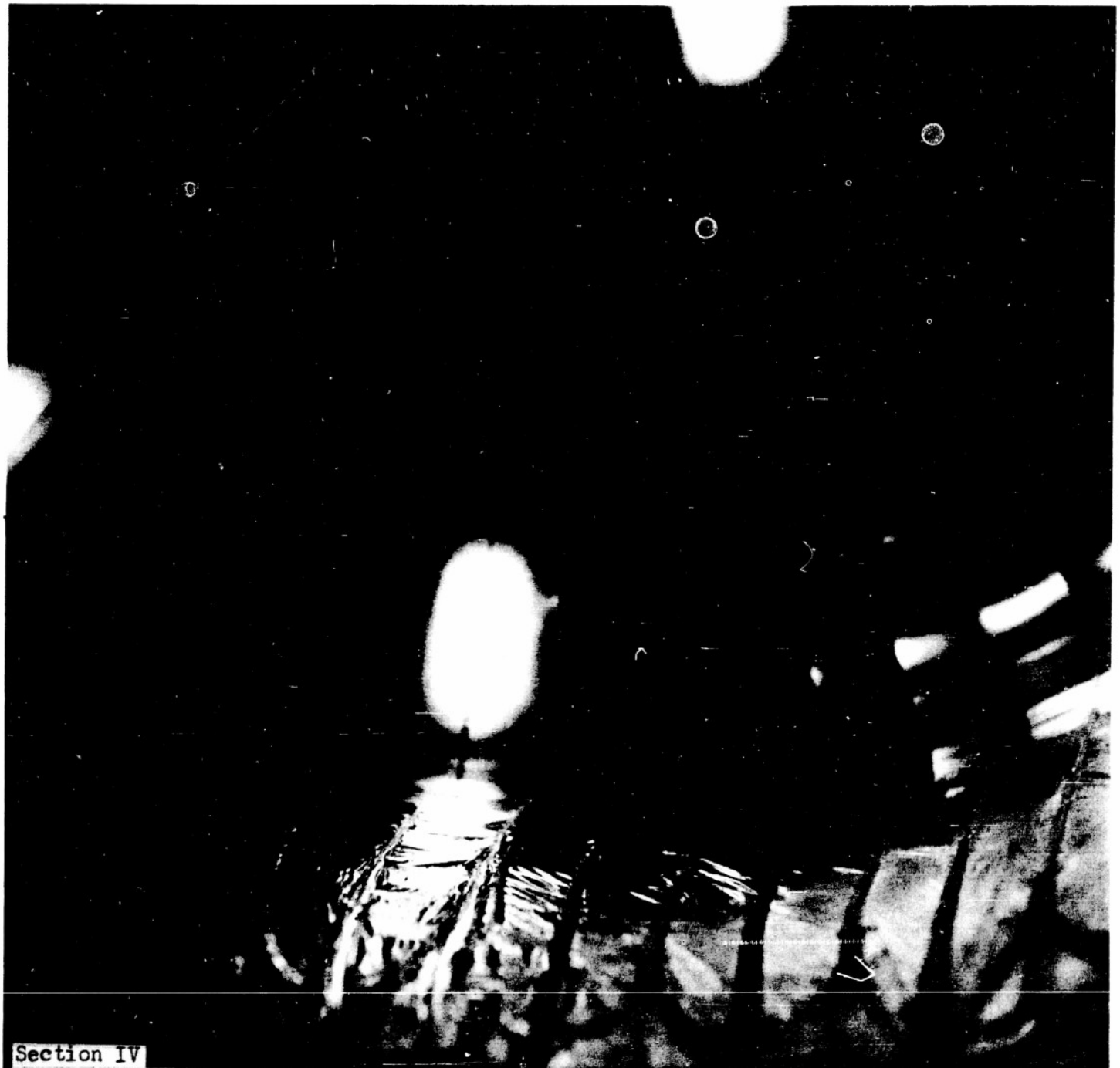

Section IV

Figure 46. Interior of inflated Winzen balloon. As can be seen the conical part is somewhat concave as pointed out on previous photographs.

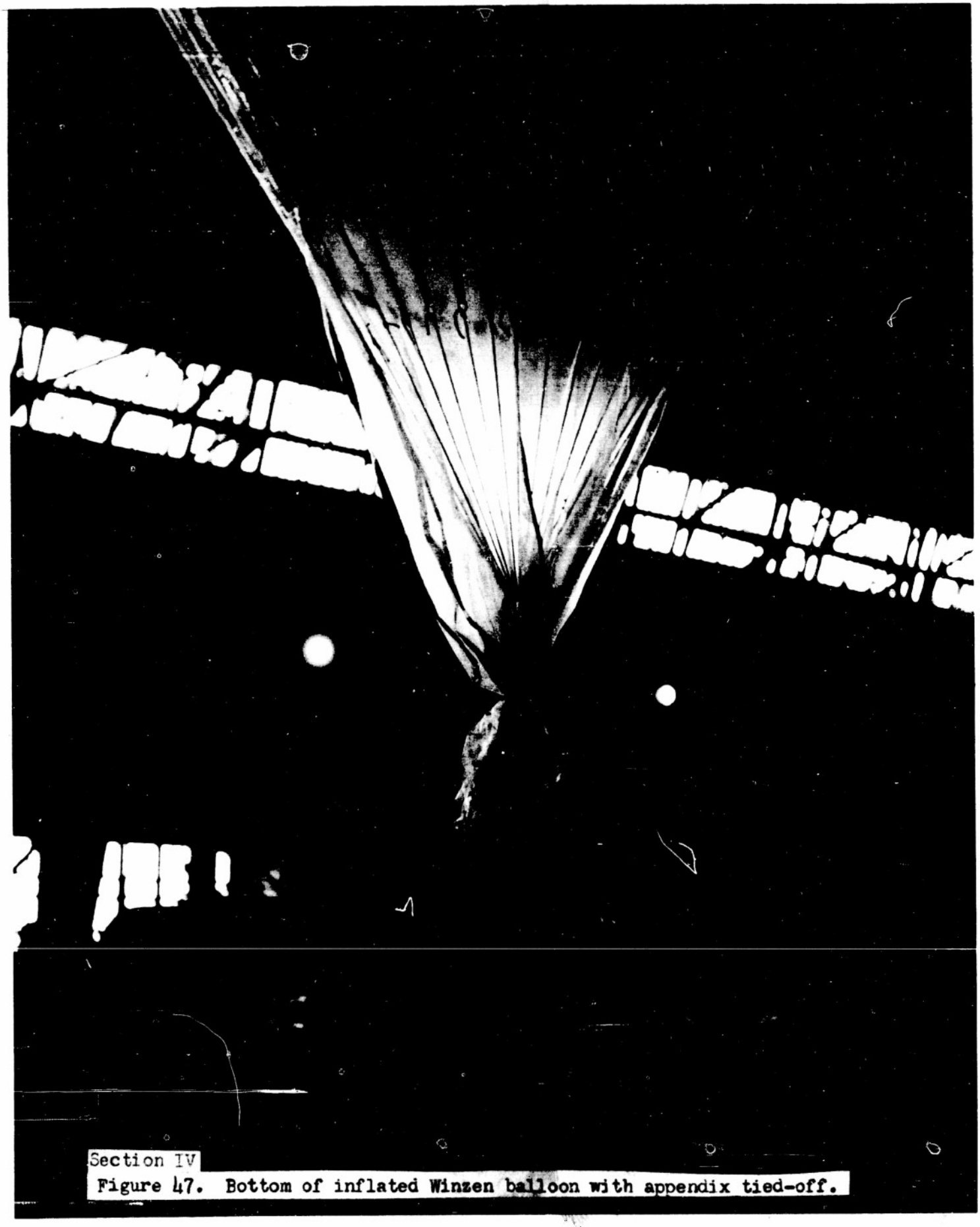

Section IV
Figure 47. Bottom of inflated Winzen balloon with appendix tied-off.

Section IV

Figure 48. Bottom of Winzen 1.5-mil balloon with wrinkles showing transfer of tension from tape to fabric and on to other tapes.

Section IV
Figure 49. Attaching strain gages to GMI 2-mil balloon from bos'n's chair.

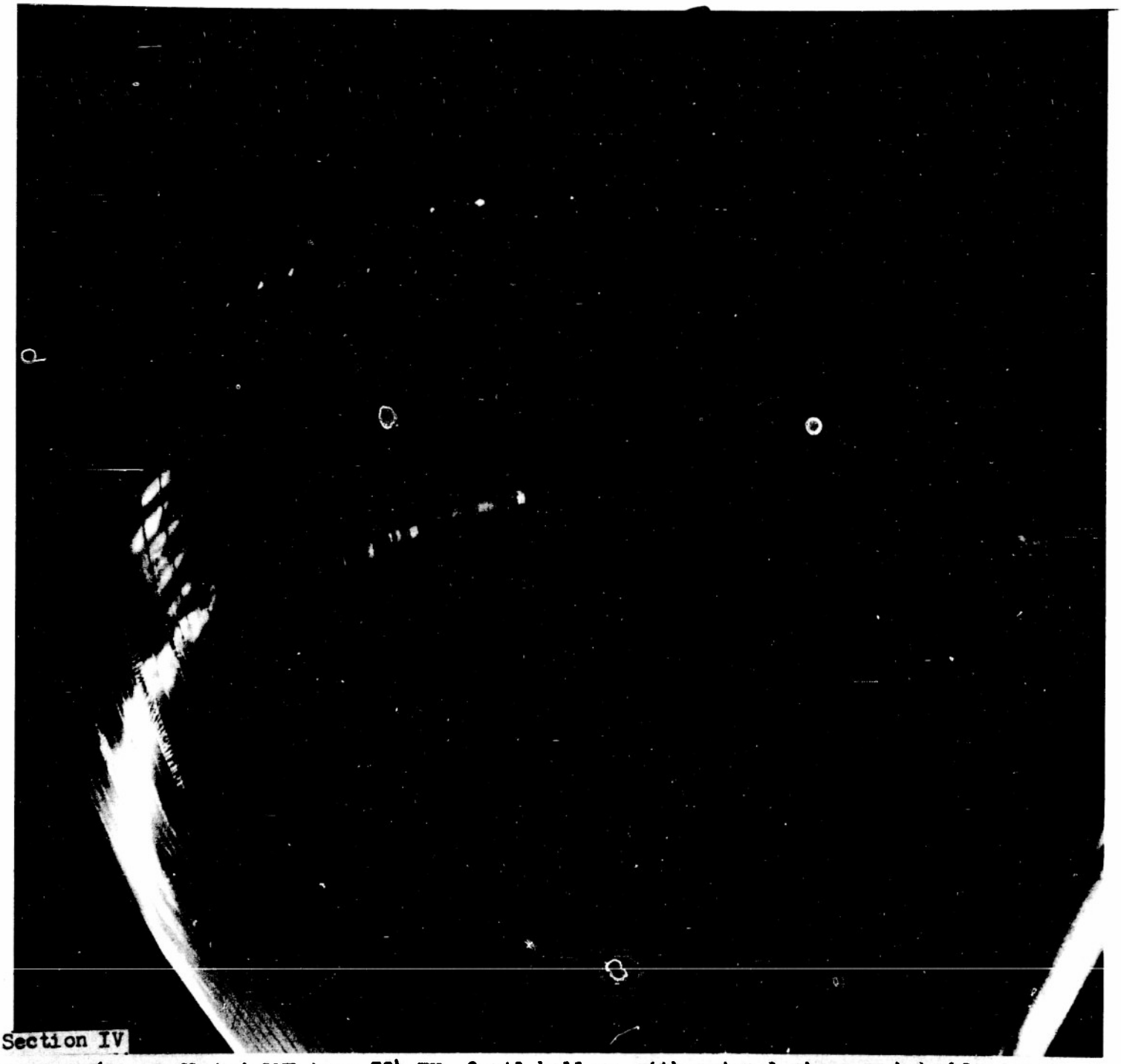

Section IV

Figure 50. Inflated GMI type 734-EH, 2-mil balloon with natural shape and double tapes. This balloon was lifting about 150 pounds which is much below the design value. Alternate tapes appear to be shorter and carry most of the tension. The others are wrinkled and slack. The tight tapes are those over the heat seals.

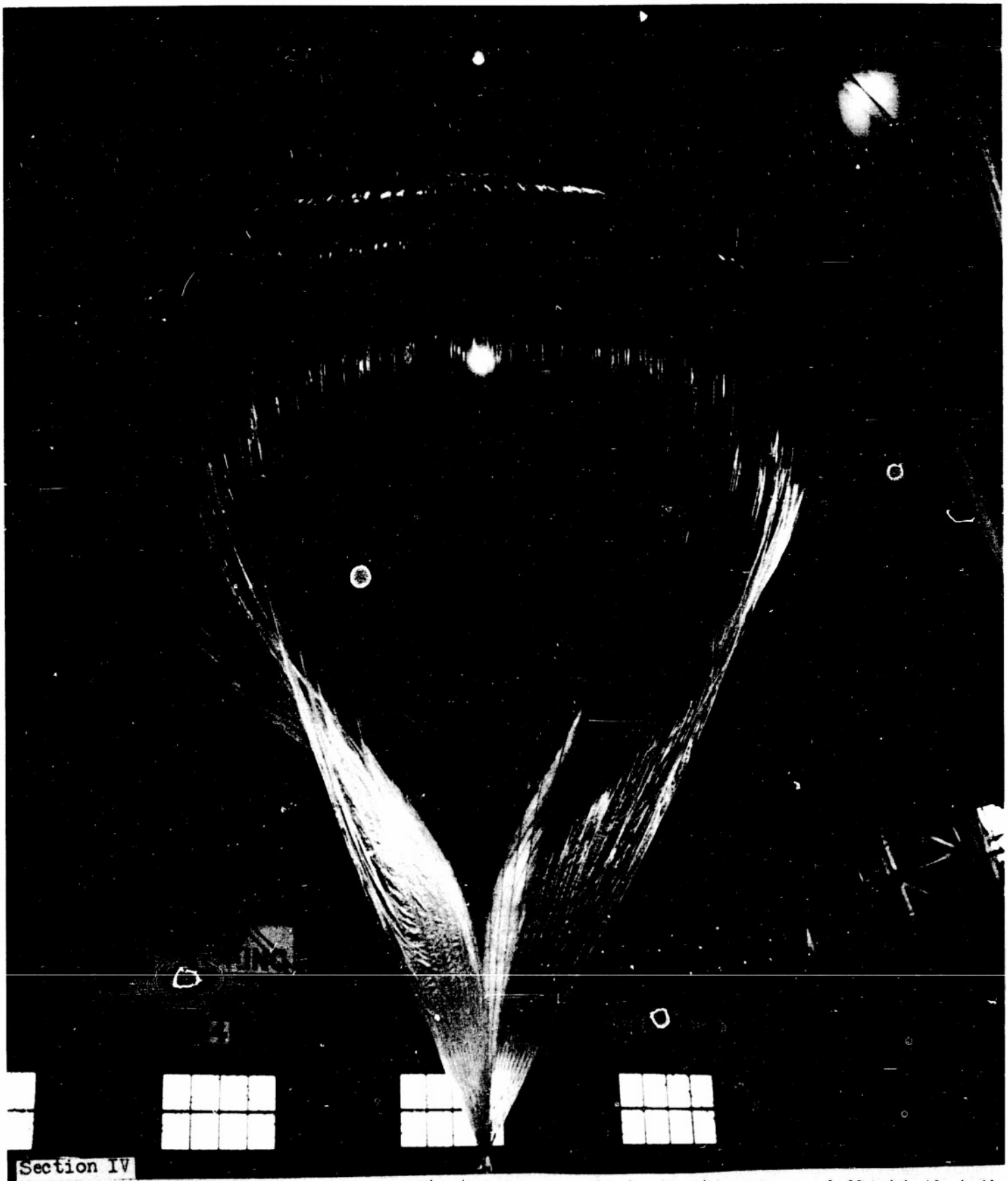

Section IV

Figure 51. Partially inflated GMI 734-EH balloon. It is at this stage of flight that the excess fabric in the top provided by the natural shape is especially important as the tension in the plastic is higher as the load is hung from a smaller area.

Section IV

Figure 52. Comparison of GMI natural shape type 734-EH on left and cone-on-sphere design type 733 on right. The volume of the natural shape balloon is 190,000 cubic feet and that of the cone-on-sphere is 225,000 cubic feet.

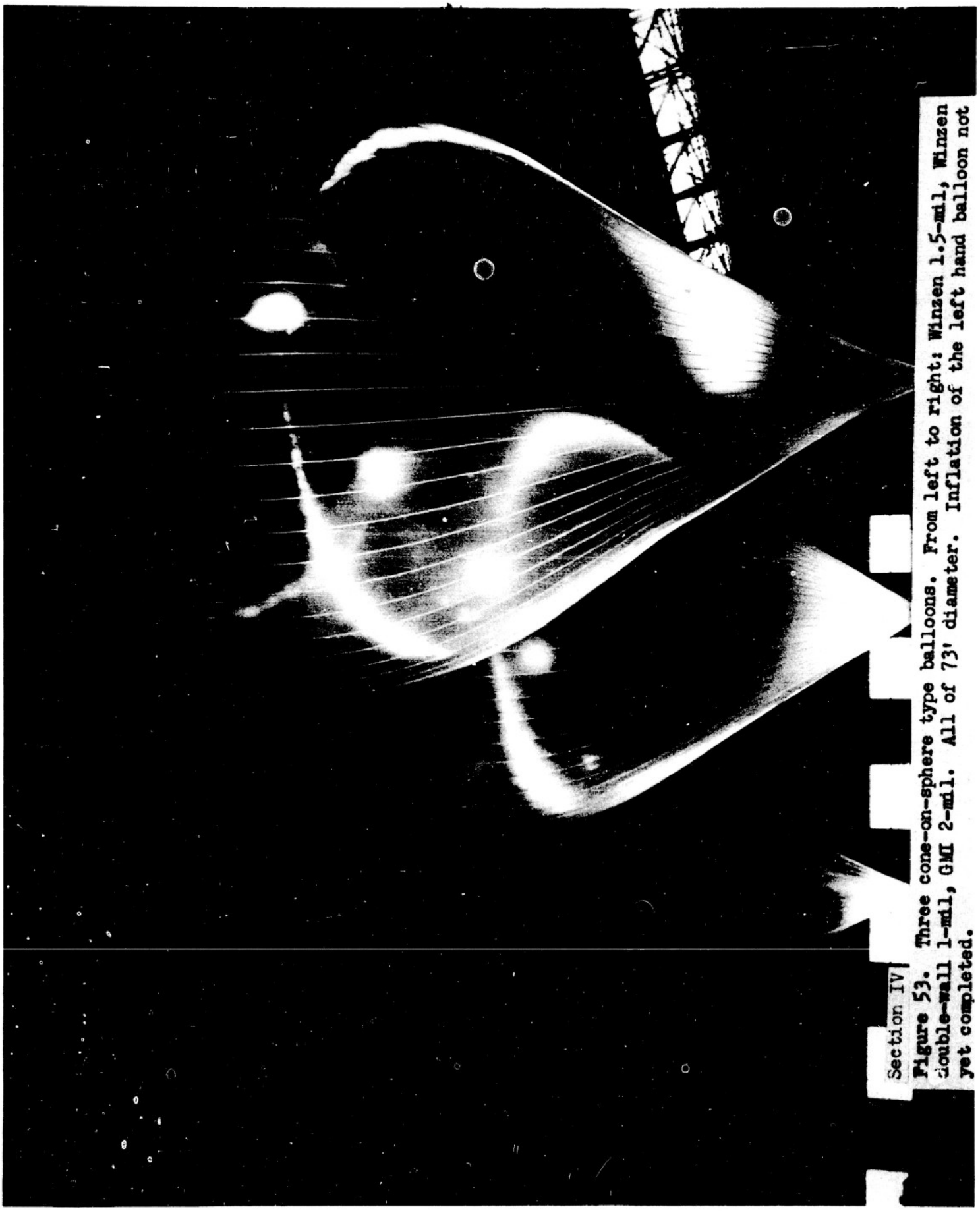

Section IV

Figure 53. Three cone-on-sphere type balloons. From left to right: Winzen 1.5-mil, Winzen double-wall 1-mil, GMI 2-mil. All of 73' diameter. Inflation of the left hand balloon not yet completed.

SECTION V

DIFFUSION AND MIXING OF GAS IN BALLOONS

A. General Discussion

It is common airship experience that it is difficult at atmospheric pressure to mix gases in balloons. That is, if one should inject air into a large balloon and then blow helium into it, it is found that the helium layers out on top. The reason for this can be seen from a simple diffusion calculation which will be presented below. It is of some interest to make diffusion calculations because of the effect of air on the behavior of constant volume balloons. Several of our flights are of special interest in this regard.

Flight #12 had an open appendix. It climbed initially to 90,000 feet (3000 feet below theoretical) During the ascent it was observed in the up- pictures that the balloon took in a large quantity of air, of the order of three times the volume of helium. However, only a small fraction of this air remained after valving as evidenced by the altitude being only 3000 feet below theoretical. The altitude indicates that after valving, only 10% of the balloon volume was filled with air. In other words, the air that was taken in layered out at the bottom of the balloon and was valved when the balloon reached ceiling. After flight #12 reached ceiling it floated level during the day and descended at night to 40,000 feet. During the next day it climbed back to an altitude of 78,000 feet. When the balloon was observed in the morning at 40,000 feet it was completely full showing that air had been taken in. In spite of this the balloon valved most of this air back out again indicating layering of the gas. At 40,000 feet the balloon mixture was 92% air and 8% helium. After leveling at

78,000 feet the mixture was approximately 50% air and 50% helium. If the air and helium had mixed at 40,000 feet the balloon could only have risen a few thousand feet at sunrise. The new altitude during the day indicated the extent to which mixing had taken place. This balloon repeated the descent and rise at least one more night. The table below shows the results already stated:

Flight #12

Condition	Time	Altitude	Pressure-mb	Mixture
Ascent	May 12	60,000	72.0	70% air 30% helium
After valving	May 12	90,000	17.5	10% air 90% helium
After descending	May 13-0630	40,000	188.0	92% air 8% helium
After ascent during day	May 13-1200	78,000	31.0	50% air 50% helium

The data show that some mixing takes place but that if the time is short most of the air is valved, provided the balloon is at low altitude, (high pressure), where the diffusion is slow. The data also show the increase in concentration of mixed air as time goes on. This will make the balloon reach lower ceiling altitude on successive days.

In contrast to this behavior, a balloon which is floating at low pressure with unmixed air and helium can mix them quite rapidly. Flight #32 was a good example of this. The balloon showed a Howell effect - it began descending 55 minutes after reaching ceiling. After the balloon had been descending for four hours at approximately 50 feet per minute, 10 pounds of ballast were dropped by radio. The ballast was sufficient to stop the descent. After thirty minutes more of level flight, 20 pounds more ballast was dropped. This did not cause a measurable change in altitude nor did the balloon rise subsequently. The pressure altitude remained 50 mb for five more hours at which time 30 pounds

of ballast were dropped. The balloon rose rapidly from 54 to 51 mb and leveled off. Since the ballast represented the same fraction of the air displaced that the change in pressure was of the total pressure, the conclusion is that complete mixing of the air and helium had taken place.

To summarize the experiments, the indication is that the air-helium mixing time at 40 mb is of the order of three to five hours and that the reason complete mixing does not take place on flights that descend to 200 mb or so is that the mixing time is correspondingly slower at the higher pressure.

Rather careful calculations of the diffusion of helium and air are presented in this section but the following argument gives the essential physics of the problem. Consider first the case of a balloon which is half air and half helium. The time constant for mixing, τ, is related to the diffusion constant D and the mixing length by the following equation:

$$\tau = \frac{L^2}{D}$$

The diffusion constant depends on the pressure in the following way:

$$D_p = \frac{DoPo}{P}$$ where D_p is the

diffusion constant at pressure p and D_0 is its value at pressure p_0. It can be seen that the lower the pressure the faster the diffusion. Combining the two equations and inserting a value for the diffusion constant gives τ(hours) = $4.2 \times 10^{-4} L^2 p$ where L is the mixing length in feet and the pressure is in mb. For a 73' diameter balloon, the mixing length would be approximately 36' and the mixing time:

$$\tau_{\text{(hours for 73' balloon)}} = .56\, P_{mb}$$

this would predict a mixing time of about 20 hours at 40 mb but the mixing would take place faster with some turbulent convection in the balloon. At sea level (1000 mb) the mixing time would be of the order of 500 hours in qualitative

agreement with the Weeksville tests. (See this report Section IV)

It is clear that the mixing is faster for smaller balloons at the same pressure and also faster at lower pressure for the same balloon.

It is also of some interest to consider the problem of diffusion through a standard appendix. A simple calculation shows that in this case the mixing time is:

$$\tau \cong \frac{LV}{AD}$$

where L is the appendix length, V, the balloon volume, A, the appendix area and D, the diffusion constant characteristic of the pressure considered. A small end correction must be applied to L. For appendices which have lengths twice their diameter, the following expression holds:

$$\tau = \frac{1.4\ LV}{A\ D}$$

If the appendix is long compared to its diameter the 1.41 should be replaced by 1. Since τ is the time constant, $\frac{1}{\tau}$ is the fractional loss of lift per unit time. The equation then becomes:

$$P = \frac{d^2}{LVp} \quad (3.32 \times 10^6)$$

where P is the percent loss of lift per day, L is the length of the appendix in feet, d the appendix diameter in feet, V the balloon volume in cubic feet and p the pressure in millibars.

To consider an example, take a 73' diameter balloon; appendix length eight feet; diameter four feet and a pressure of 20 mb. The value of P is 1.4% per day. Thus a standard skirt appendix can lose as much lift by diffusion through it as 1 to 2% per day.

There are a number of important consequences of the understanding of the diffusion of air and helium in balloons in the theory of ballooning. The first of these that will be discussed will be the effect of air on the initial rise of

the balloon to ceiling. Prior to the beginning of the Minnesota project, with the exception of a few appendix attempts on project GOPHER, all SKYHOOK balloons had been flown with more or less standard skirt appendices which hung straight down from the bottom of the balloon and through which the free lift gas was valved. These standard appendices were normally open unless they were closed by the Bernoulli forces due to the large flow of gas through them. Examination of a large number of up-pictures from our balloon flights with standard appendices and with open holes in the bottom of the balloons led us to the conclusion that a balloon which is rising normally reaches a point at which the balloon would like to intake air through the bottom because of the fact that the pressure at the bottom of the balloon is always less than the pressure at the bottom of the gas bubble and less than the atmospheric pressure. Finally the weight of the load hanging on the balloon opens the bottom up and at this instant the balloon begins to intake air very violently. A typical example of this was our flight #8 which first took in air at 80 mb and became completely full by the time the balloon had reached 41 mb. When the balloon finally reached ceiling, this ceiling was 26½ mb as opposed to 18½ theoretical ceiling. Obviously the balloon had intaken air violently and because of the low pressure had partially mixed that air. A very noticeable effect was observed in the time altitude curve and the fact that the balloon did not reach theoretical ceiling is proof of the partial mixing of the intaken air and helium. Fortunately the rate of rise was 940 feet per minute; it is believed that if the rate of rise were less than this the air would have had a longer time to mix and consequently the balloon would have reached a ceiling even further below its theoretical ceiling. Many SKYHOOK flights have shown this property, namely that a balloon which rises too slowly misses its theoretical ceiling by an appreciable amount and a number of cases showed that a balloon with a very small free lift which rose extremely slowly would not get even close to theoretical ceiling. The standard skirt appendix

on high rates of rise does a fair job of keeping out air and by controlling the factors one can reach a ceiling several thousand feet below theoretical. The danger, always present however, is that if the free lift is too low and the balloon rises slowly, it will reach a low and poorly predictable ceiling.

The other effect of great importance to ballooning is the behavior of a balloon with an open skirt appendix which descends for some reason or other. Such a balloon will freely take in air, since it descends slowly, mix the air and stay full. Since it now has an air-helium mixture in it, its ceiling is not as high as it was previously and in fact, the more air it takes in and mixes the lower will be its theoretical ceiling. An additional effect of the intake of air as the balloon descends is to greatly increase the drag because of the thermodynamic drag introduced by the very large mass of air, thereby slowing the descent rate a great deal. Upon dropping ballast one will find with such a balloon that it is impossible to drive it back to its original ceiling again and the gain in altitude upon dropping ballast will be the same fraction of the pressure that the ballast is of the air displaced Pre-mixing of air and helium in a balloon which can intake air is then capable of completely annulling the possibility of very extended flights if the balloon is allowed to descend at any time.

B. Mathematical Study of Diffusion Mixing

1. Introduction. We shall consider two different diffusion situations in this report. In the first a balloon is floating at a fixed level, taut with the appendix open. Initially the balloon is to be filled with some gas H. We then wish to calculate the average concentration of the given gas in the balloon at future times.

The second situation arises as follows. At sunset the balloon descends and during the descent, air is taken into the balloon in large quantities.

We suppose that at the finish of the descent the balloon is, by volume, half air and half H completely separated. The air is to be in the lower part of the balloon, H in the upper part. At sunrise the balloon will rise again and some of the mixture of air and H will be forced out. Were the balloon to reach the altitude it was at originally, half of the mixture would be ejected. If we calculate then the average concentration of H in the upper half of the balloon at sunrise we can determine the loss of lift brought about by the diffusion of air and H overnight.

During this process we assume that the appendix is closed. Were it open, the result would be substantially the same since we find that there is comparatively little diffusion in the situation discussed in the first paragraphs.

Actually the balloon will not reach its former ceiling at sunrise. From loss of lift calculated above a tentative new ceiling can be found. Then a more accurate value for the fraction of the mixture forced out can be calculated. From this a new average concentration of H is obtained, and a new loss of lift determined. The procedure may be repeated as long as desired. In this report we only calculate the first value for the average concentration of H.

The theory of the diffusion equation is the same as that of the equation of heat conduction. This is adequately treated in (1) and (2)*, the latter being more thorough. The material on Bessel functions needed in (4) is conveniently available in (5), particularly the list of formulas at the end of the text. As much as we need of Legendre polynomials is in (4). A more complete treatment of Legendre polynomials may be found in (6). The mathematics necessary to this report are all contained in the above works to which we shall refer as needed.

2. <u>General Assumptions</u>. We consider the balloon fabric as a surface rather than a solid. The concentration of some appropriate gas is then defined after diffusion starts everywhere except on the surface of theballoon. Initially,

*Numbers in brackets refer to references listed at the end of the report.

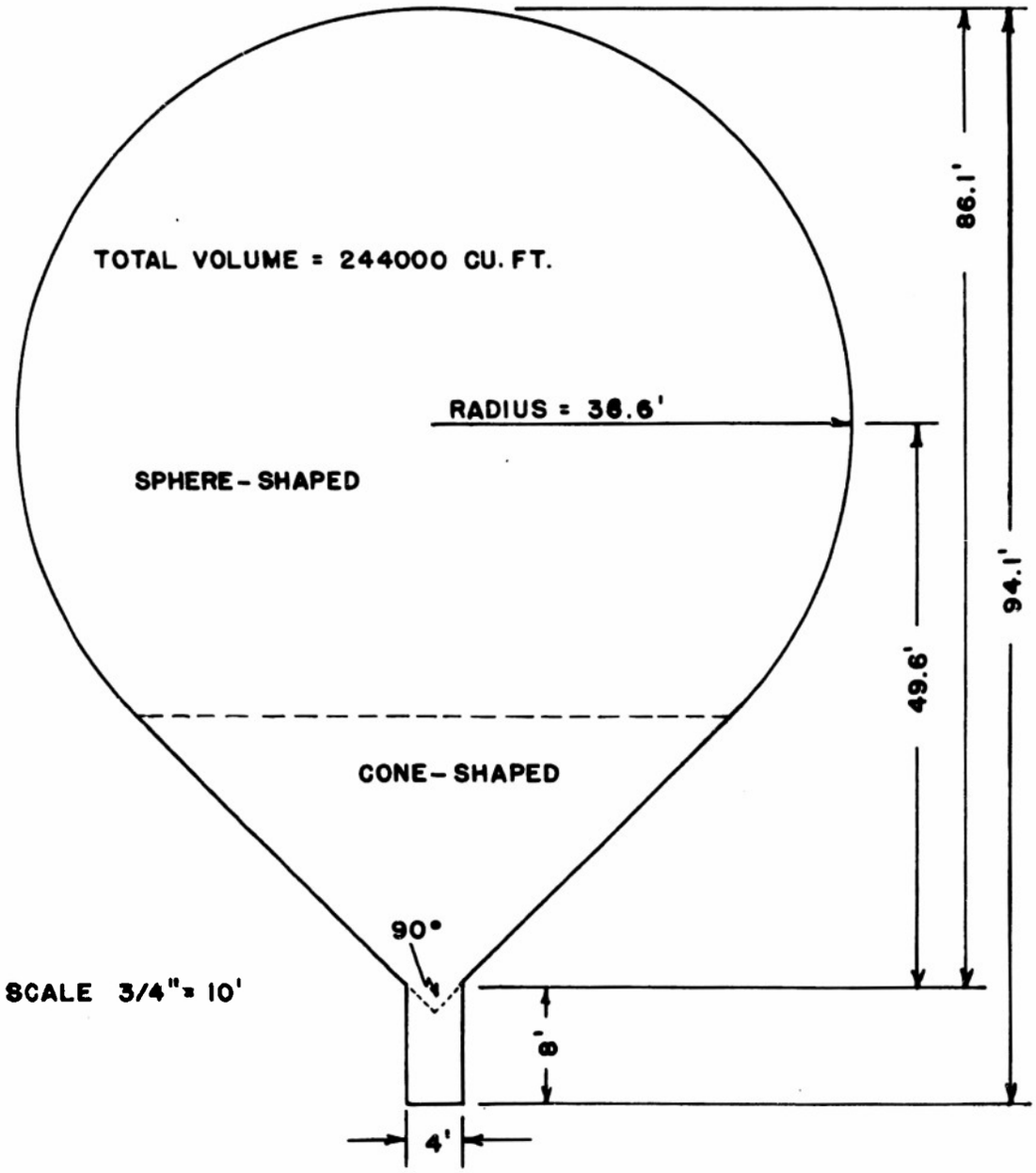

SEC. V FIGURE 1. CROSS-SECTION OF BALLOON

the situation is the same except that there may be additional surfaces where the concentration is undefined.

While diffusion goes on we assume that the temperature and the total pressure of air and H is independent of position and time. We also take the diffusion coefficient D to be independent of the ratio of the concentrations of the two gases. Thus our diffusion equation is:

$$D\nabla^2 C - \frac{\partial c}{\partial t} = 0 \qquad (1)$$

where c is the concentration of the appropriate gas, and t is the time.

This equation is to be satisfied for t greater than zero and everywhere except on the surface of the balloon, We assume that there is no entry or escape of gases through the balloon fabric; so that on the surface of the balloon we have the boundary conditions:

$$\frac{\partial c}{\partial n_i} = \frac{\partial c}{\partial n_e} = 0 \qquad (1')$$

where n_i and n_e, respectively, are the directions of the interior and exterior normals to the balloon surface. Note that c is not in general continuous across the surface of the balloon. The value of $\frac{\partial c}{\partial n_i}$ is obtained by first defining c on the surface of the balloon as the limiting value of c from the interior and then by differentiating. The treatment of $\frac{\partial c}{\partial n_e}$ is similar.

We take the shape of the balloon as in Figure 1. The irregular shape of the balloon makes the solution of the diffusion problem difficult even when the appendix is closed. Thus more regular shapes were taken as approximations to the actual one. When the appendix is open the problem is difficult no matter what the shape and then additional boundary conditions are imposed to yield soluble problems.

Thus, the true shape of the balloon plays little part in the discussion. However, the dimensions are used to give reasonable values for the parameters in the approximate solutions.

For numerical calculations we take H as helium, a pressure of 40 mb and a

temperature of 218°A. The value D_o for D under standard conditions is 0.63 cm^2/sec. Converting this to our conditions by means of

$$D = D_o \left(\frac{Po}{P}\right) \left(\frac{T}{To}\right)^{1.75}$$

we have D = 10.8 cm^2/sec or 43.2 ft^2/ hour.

3. No Air in Balloon Initially. At the upper end of the appendix the concentration c of H is never more than K, the fixed total concentration of air and H. At the lower end of the appendix c is never less than o. If we knew the values of c at the two ends of the appendix, we could solve the diffusion problem for the appendix, and calculate the amount of H lost into the atmosphere from the gradient of c at the lower end of the appendix. Unfortunately we do not know these values; but if we used K and zero, it seems reasonable that we would lose more H than in the actual case. (This argument is especially plausible if the problem is considered as one of heat flow. A rigorous proof would be desirable.) For the approximate problem the solution depends only on T and the distance Z above the lower end of the appendix. The equation is:

$$\begin{aligned} &D\frac{\partial^2 c}{\partial Z^2} - \frac{\partial c}{\partial t} = o \\ &c(Z,o) = K \\ &c(o,t) = 0 \\ &c(l,t) = K \end{aligned} \qquad (2)$$

where l is the length of the appendix.

The steady state solution of (2) is KZ/l, and the remainder of the solution is obtained by separation of variables (2: pp 76-77). Thus:

$$c(Z,t) = \frac{KZ}{l} + \frac{2K}{\pi} \sum_{n=1}^{\infty} \frac{e^{\frac{-Dn^2\pi^2 t}{l^2}}}{n} \sin \frac{n\pi Z}{l} \qquad (3)$$

The loss of mass of H is $\int_o^t DA \frac{\partial c(o,t)dt}{\partial Z}$, where A is the cross-sectional area of the appendix. If V is the volume of the balloon, and L is the loss of average concentration of H in the balloon: Then

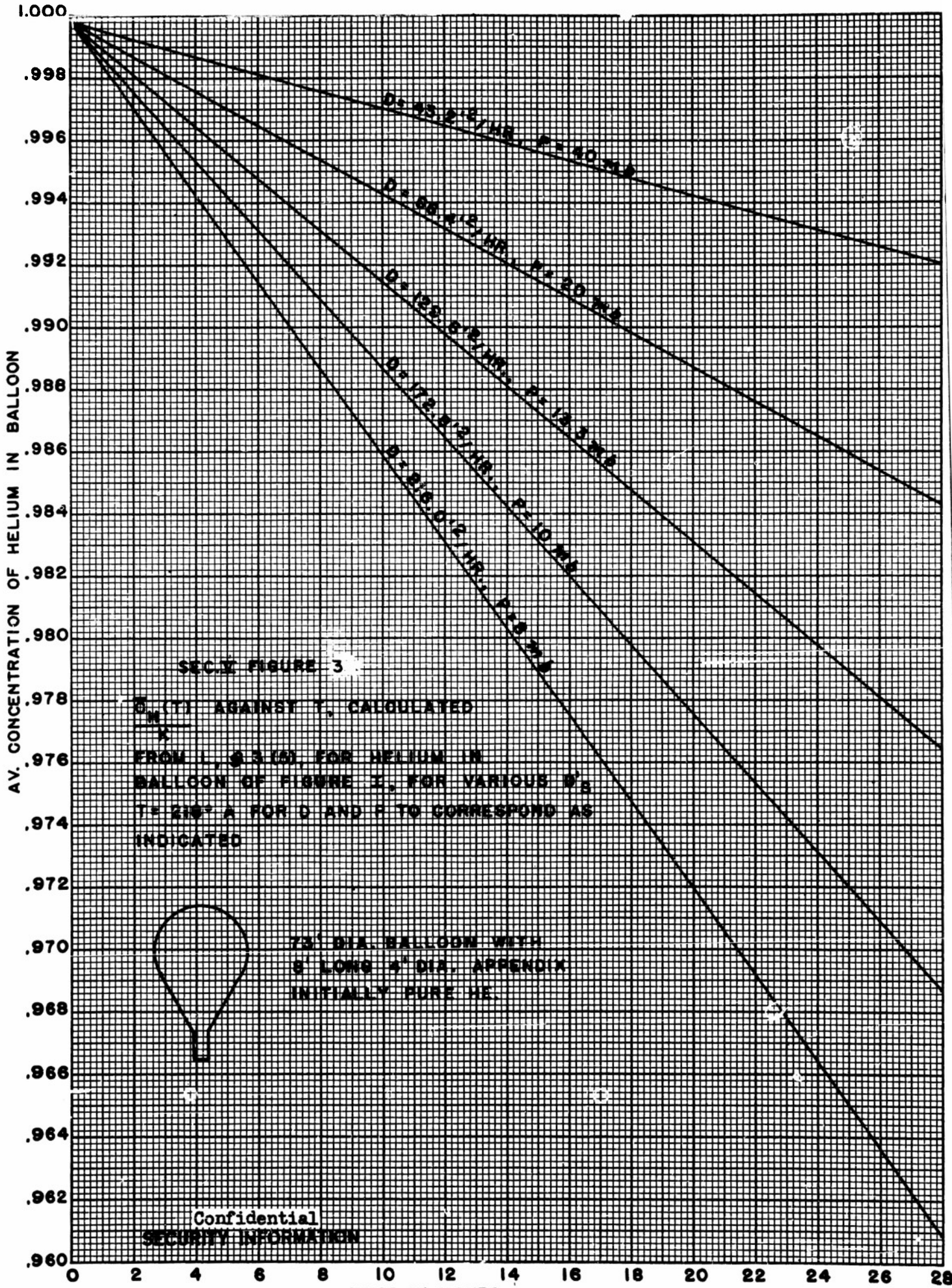
1.000
.998
.996
.994
.992
.990
.988
.986
.984
.982
.980
.978
.976
.974
.972
.970
.968
.966
.964
.962
.960
AV. CONCENTRATION OF HELIUM IN BALLOON
0 2 4 6 8 10 12 14 16 18 20 22 24 26 28
TIME IN HOURS
SEC. V FIGURE 3
$\frac{\bar{C}_{M_x}(T)}{X}$ AGAINST T, CALCULATED
FROM I, @ 3.(5), FOR HELIUM IN
BALLOON OF FIGURE 1, FOR VARIOUS θ'_s
T = 210° A FOR Q AND F TO CORRESPOND AS
INDICATED
73' DIA. BALLOON WITH
6' LONG 4' DIA. APPENDIX
INITIALLY PURE HE.
Confidential
SECURITY INFORMATION

$$L = \frac{1}{V}\int_0^t DA\,\frac{\partial c(0,t)dt}{\partial Z} = \frac{DAK}{V}\int_0^t \left[\frac{1}{l} + \frac{2}{\pi}\cdot\sum_{n=1}^{\infty} \frac{e^{\frac{-Dn^2\pi^2 t}{l^2}}}{n}\right.$$

$$\left.\left[\frac{n\pi}{l}\cos\frac{n\pi Z}{l}\right]_{Z=0}\right.$$

$$= \frac{DAK}{Vl}\left[T + 2\sum_{n=1}^{\infty}\left[-\frac{l^2}{Dn^2\pi^2}\, e^{\frac{-Dn^2\pi^2 t}{l^2}}\right]_0^t\right.$$

$$= \frac{DAK}{Vl}\left[T + \frac{2l^2}{D\pi^2}\sum_{n=1}^{\infty}\frac{1}{n^2} - \frac{2l^2}{D\pi^2}\sum_{n=1}^{\infty}\frac{e^{\frac{-Dn^2\pi^2 t}{l^2}}}{n^2}\right] \qquad (4)$$

$$L = \frac{DAK}{Vl}\left[T + \frac{l^2}{30} - \frac{2l^2}{D\pi^2}\sum_{n=1}^{\infty}\frac{c^{\frac{-Dn^2\pi^2 t}{l^2}}}{n^2}\right]$$

where we have used $\sum_{n=1}^{\infty}\frac{1}{n^2} = \pi^2/6$ to simplify the second term. With an error of at most $1AKe^{-(D\pi^2 t)/l^2}/3V$ we can write:

$$L \simeq \frac{DAK}{Vl}\left(T + \frac{l^2}{3D}\right) \qquad (5)$$

Note that the error is not that in comparing (5) with the actual problem but in comparing (5) with the complete solution (4) of the approximate problem (2). This also applies to errors that are given later.

For H as helium and the balloon as specified, D is 43.2 ft^2/hour, A is 12.57 sq ft, V is 24000 cu ft and L is 8 ft. Then for t in hours:

$$L \simeq .000278\,(t + .494)K$$

For T equal to 16 hours, about sunrise to sunset: $L \simeq .0046K$.

Note that the error introduced by using (5) instead of (4) is about $1.4 \times 10^{-50}K$.

This equation is shown graphically in Figure III.

Thus the average concentration of helium in the balloon at the end of 16 hours is at least 99.54% of the original value K.

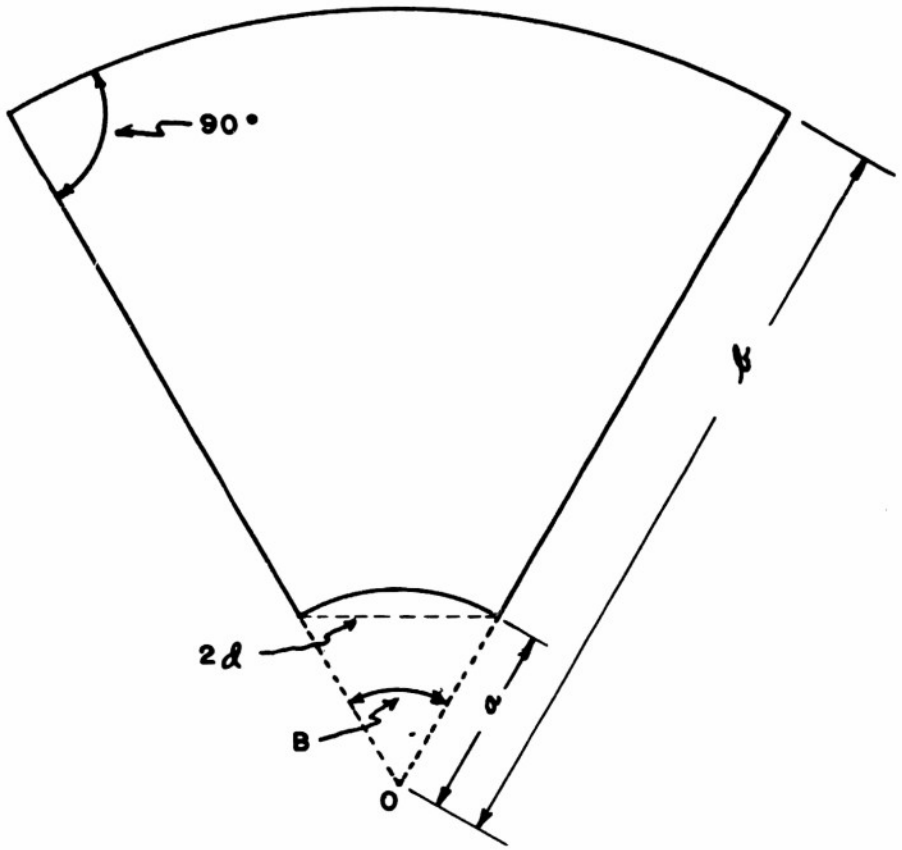

SEC. V FIGURE 2 CROSS-SECTION OF BALLOON APPROXIMATION

For T sufficiently large the formula for L is clearly wrong as compared with the real problem, since the concentration of H can not be reduced by more than K. However, in the numerical problem above it takes about 3400 hours for L to reach K, so this probably is of little consequence.

Another approximation to the actual loss of average concentration of H in the balloon which is very likely an upper bound and does not have the defect of becoming greater than K may be made. Moreover, this solution will give some idea of the concentration of H as a function of position which the previous solution does not.

Consider, as in Figure 2, an inverted truncated cone capped by a segment of a sphere perpendicular to the cone. The spherical surface and the lateral surface of the cone are the balloon fabric and the surface of truncation is to be the opening of the appendix. The region between the appendix opening and a spherical surface of radius $\underline{a}$ about O is to be kept filled with air so that the concentration of air at the lower spherical surface is always K. In numerical work we ignore this pocket of air as its contribution to the average concentration of air in the balloon is less than $K \times 10^{-5}$.

We use spherical coordinates. The concentration C of air in the balloon is then only a function of ρ and T. Our equation is:

$$D\left(\frac{\partial^2 c}{\partial r^2} + \frac{2}{\rho}\frac{\partial c}{\partial \rho}\right) - \frac{\partial c}{\partial t} = 0$$

$$\begin{aligned} c(\rho,0) &= 0 \\ c(a,t) &= K \\ \frac{\partial c}{\partial \rho}(b,t) &= 0 \end{aligned} \qquad (6)$$

The steady state solution is K. Letting v/r be the remainder of the solution and setting $\rho = s + a$, we have:

$$D\frac{\partial^2 v}{\partial s^2} - \frac{\partial v}{\partial t} = 0$$
$$v(s,o) = -K(s \neq a)$$
$$v(o,t) = 0 \qquad (7)$$
$$\frac{\partial v}{\partial s}(b-a,t) = \frac{v(b-a,t)}{b}$$

Separation of variables yields:

$$v = \sum_q A_q e^{-D\alpha_q^2 t} \sin \alpha_q s$$

where $\alpha_q > o$, $\tan (b-a)\alpha_q = b\alpha_q$, and $A_q = 2Ka/\alpha_q [a - b \sin^2 (b-a)\alpha_q]$

The equation for α_q has been used to simplify A_q.

Thus: $$c(n,t) = K\left[1 + \frac{2a}{n}\sum_{\alpha_q} \frac{e^{-D\alpha_q^2 t} \sin \alpha_q (n-a)}{\alpha_q [a-b \sin^2 (b-a)\alpha_q]}\right] \qquad (8)$$

$$\tan (b-a)\alpha_q = b\alpha_q, \quad \alpha_q > o$$

The amount of air in the balloon is $\int_o^t DA\left[-\frac{\partial c(a,t)}{\partial n}\right] dt$ where A is the area of the spherical surface at radius a. If we let γ be the spherical angle subtended by the cone, the average concentration, $\bar{C}$, of air above the surface at radius a is given by:

$$\bar{C}(t) = \frac{1}{\frac{\gamma}{3}(b^3-a^3)} \int_o^t D\gamma a^2 K \left[\frac{2a}{n^2}\sum_{\alpha_q} \frac{e^{-D\alpha_q^2 t} \sin \alpha_q (n-a)}{\alpha_q [a-b \sin^2 (b-a)\alpha_q]} - \frac{2a}{n}\sum_{\alpha_q}\right.$$

$$= \frac{3DKa^2}{b^3-a^3} \int_o^t (-2)\sum_{\alpha_q} \frac{e^{-D\alpha_q^2 t}}{a-b \sin^2 (b-a)\alpha_q} dt \left.\frac{e^{-D\alpha_q^2 t} \cos \alpha_q (n-a)}{[a-b \sin^2 (b-a)\alpha_q]}\right]_{n=a} dt$$

Since $\bar{C}(o) = o$, $\bar{C}(\infty) = K$, and the total concentration of air and H is K; we can write: $\bar{C}_H(t) = \frac{-6DKa^2}{b^3-a^3} \sum_{\alpha_q} \int_t^\infty \frac{e^{-D\alpha_q^2 t}}{a-b \sin^2 (b-a)\alpha_q} dt$

where $\bar{C}_H$ is the average concentration of H above the surface of radius a.

Thus: $$\bar{C}_H(t) = \frac{-6DKa^2}{b^3-a^3} \sum_{\alpha_q} -\frac{e^{-D\alpha_q^2 t}}{D\alpha_q^2 [a-b \sin^2 (b-a)\alpha_q]}\Bigg|_t^\infty$$

$$\bar{C}_H(t) = \frac{6Ka^2}{b^3-a^3} \sum_{\alpha} \frac{e^{-D\alpha^2 t}}{\alpha^2[b\sin^2(b-a)\alpha - a]} \qquad (9)$$

Setting $X = (b-a)\alpha$ we have finally for purposes of computation:

$$\bar{C}_H(t) = \frac{6Ka^2(b-a)}{b(b^2+ab+a^2)} \sum_{\chi} \frac{e^{\frac{-D\chi^2 t}{(b-a)^2}}}{\chi^2[\sin^2\chi - \frac{a}{b}]} \qquad (10)$$

$$\tan\chi = \frac{b\gamma}{b-a} \quad \text{and} \quad \gamma > 0$$

The N^{th} positive root χ_n of $\tan X = bX/(b-a)$ is between $(n-1)\pi$ and $(n-\frac{1}{2})\pi$, and $(n-\frac{1}{2})\pi - \chi_n$ decreases to 0 as n increases. By changing to the equation $(b-a)\sin\chi = b\chi\cos\chi$ and working with the Maclaurin series for the functions it may be shown that the first root χ is larger than $\sqrt{5a/2b}$. Then $\sin^2\chi$ is greater than $4\chi_1^2/\pi^2$ which in turn is greater than $20a/12\pi^2 b$. As π^2 is less than 10, $\sin^2\chi$ is greater than a/b. Since $\sin^2\chi_n$ is greater than $\sin^2\chi$ all the terms in the series in the right of (10) are positive. As $\bar{C}_H(0) = K$ we have:

$$\frac{6a^2(b-a)}{b(b^2+ab+a^2)} \sum_{\chi} \frac{1}{\chi^2(\sin^2\chi - \frac{a}{b})} = 1$$

Thus the error introduced in $\bar{C}_H(t)$ by dropping all but the first term of the series is at most:

$$\left[1 - \frac{6a^2(b-a)}{b(b^2+ab+a^2)\chi_1^2(\sin^2\chi_1 - \frac{a}{b})}\right] e^{\frac{-D\chi_1^2 t}{(b-a)^2}}$$

Since χ_2 is greater than $\chi_1 + \pi$, the error is at most:

$$\left[1 - \frac{6a^2(b-a)}{b(b^2+ab+a^2)\chi_1^2(\sin^2\chi_1 - \frac{a}{b})}\right] e^{\frac{-D(\pi+\chi_1)^2 t}{(b-a)^2}}$$

This formula for the error involves only χ_1. If the approximation is not satisfactory χ_2 is calculated and a similar error formula may be used.

In calculating the roots it is better to change the equation to the arctan form or the sine-cosine form.

In choosing numerical values for a, b, and β we preserve the height and volume of the balloon and the area of the appendix opening. This also preserves the average cross sectional area of the balloon for horizontal cross-sections. We take a as 3.994 ft., b as 97.56 ft. and β = 1.0488 radians.

The values of a, b, and β may be rounded off as much as one wishes before starting calculations, but from that point on it is best to treat them as exact numbers. To have accuracy of about .005% in the average concentration of helium, it is best to carry about six significant figures. For example, one calculation rounding off the value of b - a from 93.566 to 93.57 led to an appreciable error in the average concentration of helium. The error in the reported loss of helium would have been about twice the reported loss itself. The term $(\sin^2\chi - a/b)$ is sensitive, especially so for $\chi = \chi_1$, so the values of χ should be taken to the fourth decimal place.

In our computation we will need only χ_1 and χ_2. However, as they may be useful to someone else we list the first four values for χ. They are: 0.3490, 4.5025, 7.7306 and 10,9079.

We find that for t in hours:

$$\bar{C}_H(t) = K\left[.9993e^{-.000601t} + .0005e^{-.1000t}\right] \qquad (11)$$

with an error of less than $.0002\,e^{-.294}$ due to omitted terms. Finally $\bar{C}_H(16) = .9898K$ with an error of less than $2 \times 10^{-6}K$ due to omitted terms. If we compare the loss of helium by (11) and by the first method, it is seen that the loss of helium by (11) is greater for the first 3000 hours. The solution (11) thus yields an upper bound for the loss of helium for 3000 hours and very likely will do so for all time. Another plausible conjecture is that the solution obtained by adjusting (5) to an exponential form would yield an upper bound to the loss of helium concentration: i.e.

$$L' \simeq K\left[1 - e^{-\frac{DA}{Vl}\left(t + \frac{l^2}{3D}\right)}\right]$$

The last paragraph is mainly for satisfaction of personal curiosity, as we are not much interested in time periods longer than 24 hours. However, it does indicate the role the appendix plays in cutting down diffusion of air into the balloon. Various methods were used to calculate approximations to the loss of helium, most of which ignored the exact shape of the appendix. The best result obtained by any of these methods is that of (11). However, even for this solution the loss of helium in 16 hours is still twice as great as that obtained by our first solution; and despite the considerable difference between the actual concentration of helium at the upper end of the appendix and K for large values of t, the original solution is the better for at least 3000 hours.

So far we have been concerned with upper bounds to the loss of H. A likely lower bound for the loss of H may be obtained as follows. Suppose a cylindrical column based on the appendix were run up to the top of the balloon, closing off the inside of this column from the rest of the balloon. The amount of air normally diffusing into the balloon would be more than that diffusing into the closed-off column. If we assume a fixed concentration of air, K^1, at the lower end of the column and no escape of air at the upper end of the column, we must solve, where c is the concentration of air:

$$\begin{cases} D\dfrac{\partial^2 c}{\partial z^2} - \dfrac{\partial c}{\partial t} = 0 \\ c(z,0) = 0 \\ c(0,t) = K' \\ \dfrac{\partial c}{\partial z}(l,t) = 0 \end{cases} \qquad (12)$$

The solution to this (2: Page 84, with $\chi = z - l$) is:

$$c(z,t) = K' - \frac{4K'}{\pi}\sum_{n=0}^{\infty} \frac{e^{-\frac{D(2n+1)^2\pi^2 t}{4l^2}}}{2n+1} \sin\frac{(2n+1)\pi z}{2l} \qquad (13)$$

The average concentration of air in the column is:

$$\bar{c}(t) = K' - \frac{8K'}{\pi^2} \sum_{n=0}^{\infty} \frac{e^{\frac{-D(2n+1)^2\pi^2 t}{4\ell^2}}}{(2n+1)^2} \qquad (14)$$

If ℓ is 94.1 ft. and t is 16 hours, than $\bar{c}$ is $.3153K^1$. If this air were spread over the entire balloon, the average concentration would be $.0015K^1$.

If K^1 is K/2, the smallest it could be, the loss of helium concentration would be .0008K, a definite lower bound for the loss. If K^1 is K, probably closer to the truth, the loss would be .0015K.

4. Balloon Initially Half Air, Half H. In this situation the balloon is closed, the air and H each fill half of the volume of the balloon. Essentially, the air is in the lower part of the balloon at the start of diffusion, but for some shapes it is convenient to take a curved surface rather than a plane as the surface of separation.

In all cases the volume of the approximating body is kept equal to the volume of the balloon. When this is not sufficient to determine the dimensions of the body, other reasonable conditions are added.

In an effort to reduce the problem to one involving but a single space variable, the balloon was approximated by a cylinder of altitude 86.1 feet, the altitude of the balloon without appendix. The separation surface was taken as a horizontal plane. After 8 hours the average concentration of helium in the upper part of the balloon was .756K.

Again the balloon was approximated by a shape similar to that in Figure 2, except that the vertical angle of the cone was taken as 90°, other dimensions were changed to preserve volume, and no truncation was made. The surface of the separation was spherical with center at the vertex of the cone. After eight hours the average concentration of helium in the upper part of the balloon was .571K.

The serious discrepancy between the results for these two different shapes forces us to attempt a shape closer to that of the actual balloon. There seems to be no better shape that can be used and still keep the problem of diffusion to one space variable. Hence we try to approximate by means of a sphere.

We are thus led to the following problem. A sphere of radius a initially has its lower hemisphere filled with air at concentration K and its upper hemisphere filled with H at concentration K. We wish to know the average concentration of H in the upper hemisphere at future times.

We use spherical coordinates r, θ and φ (θ is the colatitude). The solution is independent of φ and our equation, where c is the concentration of H, is:

$$\begin{cases} D\left[\frac{\partial^2 c}{\partial r^2} + \frac{2}{r}\frac{\partial c}{\partial r} + \frac{1}{r^2 \sin\theta}\frac{\partial}{\partial \theta}\left(\sin\theta \frac{\partial c}{\partial \theta}\right)\right] - \frac{\partial c}{\partial t} = 0 \\ c(r,\theta,0) = \begin{matrix} K & 0 < \theta < \frac{\pi}{2} \\ 0 & \frac{\pi}{2} < \theta < \pi \end{matrix} \\ \frac{\partial c}{\partial r}(a,\theta,t) = 0 \end{cases} \tag{15}$$

It saves a little inconvenience in getting a complete set of functions to obtain the steady state solution first, even though the boundary conditions do not demand this. As the normal derivative on the boundary is zero, the steady state solution is a constant and must be $\frac{K}{2}$ to keep the same amount of H present as at the start. Thus $c = \frac{K}{2} + v$ where after setting $\mu = \cos\theta$

$$\begin{cases} D\left[\frac{\partial^2 v}{\partial r^2} + \frac{2}{r}\frac{\partial v}{\partial r} + \frac{1}{r^2}\frac{\partial}{\partial \mu}\left((1-\mu^2)\frac{\partial v}{\partial \mu}\right)\right] - \frac{\partial v}{\partial t} = 0 \\ v(r,\theta,0) = \begin{matrix} K/2 & 0 < \theta < \frac{\pi}{2} \\ -K/2 & \frac{\pi}{2} < \theta < \pi \end{matrix} \\ \frac{\partial v(a,\theta,t)}{\partial r} = 0 \end{cases} \tag{16}$$

Then:

$$v = \sum_{q,n} A_{q,n} (qr)^{-\frac{1}{2}} J_{n+\frac{1}{2}}(qr) P_n(\mu) e^{-Dq^2 t} \tag{17}$$

where J is a Bessel function of the first kind, P_n is the n^{th} Legendre polynomial, n is a non-negative integer, and α is a non-zero root of $2\alpha a J_{n+\frac{1}{2}}(\alpha a) - J_{n+\frac{1}{2}}(\alpha a) = 0$ (2; pp 210-212).

It is shown in the usual way (compare 2; pp 172-173), (4; pp 129-130) that the functions involved are orthogonal when a weighting factor of $\sqrt{r}$ is attached to each $J_{n+\frac{1}{2}}$. The coefficient $A_{\alpha,n}$ is evaluated as usual (compare 2; Page 173, (4)) and we have, after using the equation for α and the even-odd characteristics of $P_n(\mu)$

$$A_{\alpha,n} = \frac{4(2n+1)\alpha^{5/2} K \left(\int_0^1 P_n(\mu)\,d\mu \begin{matrix} n \text{ even} \\ n \text{ odd} \end{matrix}\right)}{\left[4a^2\alpha^2 - 4\left(n+\tfrac{1}{2}\right)^2 + 1\right] J_{n+\frac{1}{2}}(a\alpha)} \int_0^a r^{3/2} J_{n+\frac{1}{2}}(\alpha r)\,dr$$

Thus the average concentration of H in the upper hemisphere is given by:

$$\bar{C}(t) = \frac{K}{2} + \frac{2\pi}{\frac{2\pi a^3}{3}} \sum_{\alpha,n\,\text{odd}} A_{\alpha,n}\,\alpha^{-\frac{1}{2}} e^{-D\alpha^2 t} \int_0^a \int_0^{\frac{\pi}{2}} r^{-\frac{1}{2}} J_{n+\frac{1}{2}}(\alpha r) P_n(\mu)\, r^2 \sin\theta\, d\theta\, dr$$

$$= \frac{K}{2} + \frac{3}{a^3} \sum_{\alpha,n\,\text{odd}} A_{\alpha,n}\,\alpha^{-\frac{1}{2}} e^{-D\alpha^2 t} \int_0^a r^{3/2} J_{n+\frac{1}{2}}(\alpha r)\,dr \int_0^1 P_n(\mu)\,d\mu$$

$$= \frac{K}{2} + \frac{3K}{a^3} \sum_{\alpha,n\,\text{odd}} \frac{4(2n+1)\alpha^2 e^{-D\alpha^2 t}}{\left[4a^2\alpha^2 - 4\left(n+\tfrac{1}{2}\right)^2 + 1\right] J_{n+\frac{1}{2}}^2(a\alpha)} \left[\int_0^a r^{3/2} J_{n+\frac{1}{2}}(\alpha r)\,dr\right]^2 \left[\int_0^1 P_n(\mu)\,d\mu\right]^2$$

$$= \frac{K}{2} + \frac{3K}{a^3} \sum_{\alpha,n\,\text{odd}} \frac{4(2n+1)\alpha^2 e^{-D\alpha^2 t}}{\left[4a^2\alpha^2 - 4\left(n+\tfrac{1}{2}\right)^2 + 1\right] J_{n+\frac{1}{2}}(a\alpha)} \left[\alpha^{-5/2} \int_0^a r^{3/2} J_{n+\frac{1}{2}}(r)\,dr\right]^2 \left[\int_0^1 P_n(\mu)\,d\mu\right]^2$$

Using the value for $\int_0^1 P_n(\mu)\,d\mu$ (4; Page 133, Ex. 10) and setting $\chi = a\alpha$ this becomes:

$$\begin{cases} \bar{C}(t) = \frac{K}{2} + 12K \sum_{\chi,n\,\text{odd}} \frac{(2n+1) e^{-\frac{D\chi^2 t}{a^2}}}{\chi^3 \left[4\chi^2 - (2n+1)^2 + 1\right] J_{n+\frac{1}{2}}^2(\chi)} \frac{1}{n^2} \frac{n^2(n-2)^2 \cdots 1^2}{(n+1)^2(n-1)^2 \cdots 2^2} \left[\int_0^\chi r^{3/2} J_{\text{or } \frac{1}{2}}(r)\,dr\right]^2 \\ 2\chi J'_{n+\frac{1}{2}}(\chi) - J_{n+\frac{1}{2}}(\chi) = 0, \quad \chi \neq 0 \end{cases} \tag{18}$$

Finally using (5; Page 158, #22) and repeated integration by parts we reduce $\int n^{3/2} J_{n+\frac{1}{2}}(n)dn$ to a form to which (5; Page 158, #20) may be applied, obtaining

$$\int n^{3/2} J_{n+\frac{1}{2}}(n)dn = -\left[n^{3/2} J_{n-\frac{1}{2}}(n) + (n+1) n^{\frac{1}{2}} J_{n-\frac{3}{2}}(n) + (n+1)(n-1) n^{-\frac{1}{2}} J_{n-\frac{5}{2}}(n) + \ldots + (n+1)(n-1)\ldots 2\, n^{1-\frac{n}{2}} J_{\frac{n}{2}-1}(n)\right]$$

As $n \to 0$ all terms approach 0 except the last, since $J_n(n)$ is of order n^n near $n = 0$. The limit of the last term as $n \to 0$ is readily evaluated by means of the well-known recursion formula for the Gamma function and the value of $\Gamma(\frac{1}{2})$. Thus:

$$\int_0^x n^{3/2} J_{n+\frac{1}{2}}(n)dn = -\left[x^{3/2} J_{n-\frac{1}{2}}(x) + (n+1) x^{\frac{1}{2}} J_{n-\frac{3}{2}}(x) + (n+1)(n-1) x^{-\frac{1}{2}} J_{n-\frac{5}{2}}(x) + \ldots + (n+1)(n-1)\ldots 2 \cdot x^{1-\frac{n}{2}} J_{\frac{n}{2}-1}(x)\right] + (n+1)(n-1)\ldots 2 \frac{n}{n(n-2)(n-4)\ldots 1}\sqrt{\frac{2}{\pi}} \tag{19}$$

To solve the equation $2x J'_{n+\frac{1}{2}}(x) - J_{n+\frac{1}{2}}(x) = 0$ we use (5; Page 158, #16) to find the equation is equivalent to $(n+1) J_{n+\frac{1}{2}}(x) = x J_{n-\frac{1}{2}}(x)$. We now apply the recursion formula (5; Page 158, #18) for the J's to reduce this to an equation involving $J_{\frac{1}{2}}(x)$ and $J_{-\frac{1}{2}}(x)$. Expressing these in terms of $\sin x$ and $\cos x$ (5; Page 159, #32, #33) we have a trigonometric equation of the type:

$$\tan x = R_n(x)$$

where $R_n(x)$ is rational and $\lim_{x \to \infty} R_n(x)$ is zero. To get the first few roots of this equation it is best to use the form $P_n(x) \sin x - Q_n(x) \cos x = 0$ where $P_n(x)$ and $Q_n(x)$ are polynomials. For x sufficiently large the roots are close to multiples of π, and then it is easy to use the tangent form of the equation.

For $n = 1$ the equation is:

$$\tan x = \frac{2x}{2 - x^2}$$

and the first four positive roots are 2.082, 5.898, 9.206, and 12.404. For $n = 3$ the equation is:

$$\tan x = \frac{7x^3 - 60x}{-60 + 27x^2 - x^4}$$

and the first three positive roots are 4.514, 8.584, and 11.973. We do not use the negative roots of the equations which lead to complex values for the Bessel functions of half-integral order.

From the study of the equations $\tan\chi = R_n(\chi)$ that has been made, the following conjectures are plausible but have not been proved. For χ large $R_n(\chi)$ is negative and the degree of the numerator is one less than the degree of the denominator being n and $n+1$ respectively. The function $R_n(\chi)$ is odd. These statements should be relatively easy to verify; but the following seem more difficult. The graph of $y = R_n(\chi)$ has $(n+1)$ vertical asymptotes. In any finite region for χ these asymptotes approach those of $y = \tan\chi$ as n increases. The graph as a whole approaches that of $y = \tan\chi$ as n increases. If $\chi_{n,1}$ is the first positive root of $\tan\chi = R_n(\chi)$, then $\frac{\pi n}{2} - \chi_{n,1}$ decreases to 0 as n increases.

Since $4\left(\frac{\pi n}{2}\right)^2 - (2n+1)^2 + 1 = ((\pi-2)n+1)(\pi n+2n+1) + 1$, it is thus probable that $4\chi^2 - (2n+1)^2+1$ is positive for our values of χ. This is verified for $n=1$ and $n=3$. Thus the error incurred by dropping various terms of the double expansion can be calculated as in §3.

For purposes of calculation we reduce all the Bessel functions to $J_{1/2}(\chi)$ $J_{-1/2}(\chi)$ and then to trigonometric functions (5; pp. 158-159, #18, #32, #33). The terms for $n=1$ and $n=3$, respectively are:

$$9\sum_{\chi} \frac{e^{\frac{-D\chi^2 t}{a^2}}(2-\chi^2-2\cos\chi)^2}{(\chi^2-2)\chi^6\cos^2\chi}$$

and

$$21\sum_{\chi} \frac{e^{\frac{-D\chi^2 t}{a^2}}\left[\chi^4-27\chi^2+60-(3\chi^2+60)\cos\chi\right]^2}{(\chi^2-12)\chi^{10}\cos^2\chi}$$

where we have used $\tan\chi = R_n(\chi)$ to remove the $\sin\chi$ terms. For $n = 1, 3$ the denominator has simplified exceedingly, but the reason is not evident.

If we ignore all terms but the one corresponding to the first root for $n=1$ we have:

$$\bar{C}(t) \simeq K\left[\frac{1}{2} + .3638\, e^{\frac{-4.335\,Dt}{a^2}}\right] \qquad (20)$$

with an error of at most $.1362 e^{\frac{-20.39Dt}{a^2}} K$. This equation is graphed in Figure IV. If we ignore all terms but those corresponding to the first roots for $n = 1$ and 3, we have:

$$\bar{c}(t) \simeq K\left[\tfrac{1}{3} + .3638\, e^{\frac{-4.335Dt}{a^2}} + .0480\, e^{\frac{-20.39Dt}{a^2}}\right] \qquad (21)$$

with an error of at most $.0882\, e^{\frac{-34.79Dt}{a^2}} K$. The error is calculated on the assumption that the first roots for n greater than 3 are at least $4.514 + \pi$, so that the numerically smallest exponent we have in the omitted terms is the one arising from the second root for $n = 1$.

For numerical work we take a as 38.77 feet to yield the volume of the actual balloon. We take t as 8 hours, about from sunset to sunrise. D is as before, 43.2 feet^2/hour. The only terms which will contribute an appreciable amount are the first terms for $n = 1$ and 3.

Then for t in hours:

$$\bar{c}(t) = K\left[.5 + .3638\, e^{-.1246t} + .0480\, e^{-.5857t}\right] \qquad (22)$$

with an error of at most $.0882\, e^{-t} K$. Finally for t equal to 8 hours:

$$\bar{c}(8) = K\left[.5 + .1343 + .0004\right] = .6347K$$

with an error of at most 3×10^{-5} due to omitted terms.

E. <u>Agreement with Observed Data</u>. As regards the case that there is no air in the balloon initially, it is known that the loss of helium from the balloon is small which agrees in general with our results.

For the case that the balloon is filled half-and-half with air and helium, some observations on a balloon flight afford an opportunity to check our results roughly. Example from flight #8.

At one point in the flight the balloon was filled half-and-half with air and helium. Seventy-six minutes later the proportions were 70% helium and 30% air. In the meantime the balloon was rising, the appendix was open so some of

the mixture escaped. The pressure change was from 40 mb to 27 mb.

The original entry of the air in the balloon was rather violent so that it is not likely that the air and helium were separated then. Again some of the mixture was ejected before there was much opportunity for diffusion. These two effects cannot be treated numerically; and as they tend to offset each other we shall ignore them.

With the pressure increasing by a factor of 40/27 the gas originally in the upper hemisphere will at the end occupy 20/27 of the volume. Let X be the per cent by volume of helium in this region. The per cent by volume of helium in the remainder of the balloon is at most 50%.

Thus: $\frac{20}{27} X + \frac{7}{27} 50 \geq 70$

and: $X \geq 77\%$

As the balloon is slowing down, it spends more time at lower pressures; so the average pressure is not more than the average of the extreme values 40 and 27. Tentative calculations based on an exponential approach to ceiling give average pressure of 32 mb but this is probably too high. However we will use this value.

The formula for $\bar{c}(t)$ from (21) is then:

$$\bar{c}(t) = K\left[.5 + .364 e^{-.1558t} + .048 e^{-.7321t}\right]$$

For $t = 7\frac{1}{2}$ hours, we have $\bar{c} = 82\%$. This is in fair agreement with the value 77%.

SEC. V FIGURE IV

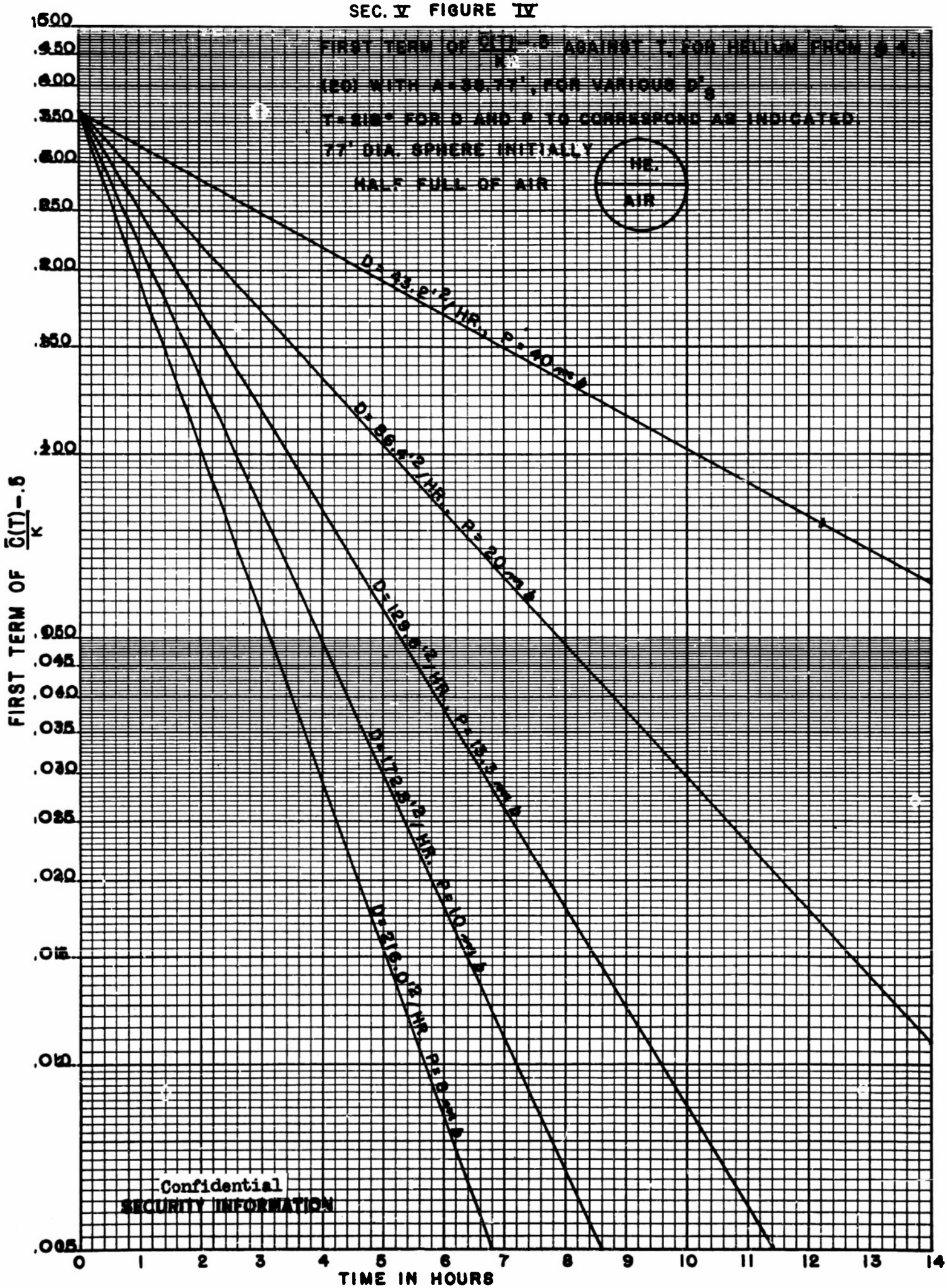

References

1. H.S. Carslaw, Introduction to the Mathematical Theory of the Conduction of Heat in Solids, first American edition, Dover Publications, 1945.

2. H.S. Carslaw and K.C. Jaeger, Conduction of Heat in Solids, Clarendon Press, 1947.

3. Sir James Jeans, An Introduction to the Kinetic Theory of Gases, Cambridge University Press, 1940.

4. O.D. Kellogg, Foundations of Potential Theory, Frederick Ungar Publishing Company.

5. N.W. McLachlan, Bessel Functions for Engineers, Clarendon Press, 1934.

6. E.T. Whittaker and G.N. Watson, A Course in Modern Analysis, fourth edition Cambridge University Press, 1927.

SECTION VI

VERTICAL FLIGHT

A. Ascent Behavior. Some knowledge about the fundamentals of balloon behavior can be obtained from the study of the balloon's motion as it ascends and descends. This type of balloon motion is called vertical flight. A great body of information concerning vertical flights of balloons is now available. Prior to the University of Minnesota Balloon Project a large number of balloon flights had been made for project SKYHOOK mostly by the General Mills, Inc. and some by Winzen Research. In addition to this, a number of time-altitude curves have been made available from the General Mills' Project GOPHER sponsored by the Air Force and some very good detailed information has been available through project MOBY DICK. All of these sources of information have been used in helping to formulate our ideas about the relation of vertical flight to the physics of the balloon problem. As this data was studied it became evident that all of the flights could not be explained on a simple basis since the behavior of balloons varied quite widely. In all of the sources of data, with the exception of MOBY DICK and of project GOPHER, the accuracy of the telemetered altitude data was perhaps insufficient to really decide about the true behavior of balloons. In addition to the sources of data quoted at the time of writing this report, 55 flights made on our project are available for study.

The present status of the study of the vertical flight of the balloon is that all of the properties of this motion are not understood in quantitative enough terms to write a complete equation of motion which covers all cases, but it is true that the basic physics of vertical flight is well enough understood so that experiments which have been formulated and are now in progress should allow the complete solution of this problem in the near future. In all the flights that we have studied from the sources quoted and from our own flight series prior to #40, with the exception of perhaps a few flights in which the

appendix was either fouled or tied off, the behavior of the balloon during ascent was completely obscured by the intake of air at unknown altitudes and usually in unknown quantity. Once this fact is understood and realized one can look back at previous flights and explain many of the flights which showed queer behavior simply in terms of intake of air. The problem of intake of air and of mixing this air with the helium is quite completely discussed in the section of this report on air mixing and diffusion. It will be mentioned here only where the mixing of air has a marked effect on the characteristics of the flight. Most balloon flights are launched with an amount of free lift which is from 5% to 20% of the air displaced by the balloon on the ground. In all of our work free lift will be expressed as a percentage of air displaced since this determines the size of the balloon and is a quantity of interest in trying to relate observation with theory. In a very general way it has always been observed that with a given free lift in the range indicated a balloon will take off and acquire a rate of ascent and maintain approximately this rate of ascent all the way to its theoretical ceiling or to a ceiling below this if air intake has been important. One of the outstanding puzzles of balloon performance has been this fact that balloons show essentially a constant rate of rise. The factors that determine the rate of rise of a balloon at any altitude are the buoyancy of the balloon and the total drag which it is subject to. As the balloon ascends it is possible for it to acquire a temperature which is relatively different from the air temperature as compared with that temperature difference which existed at take-off. This will be reflected, of course, in a changed free lift as a function of altitude. Let us first consider this part of the problem alone.

In order to decide what the free lift of a balloon at any altitude is, it would be necessary to bring the balloon in equilibrium, measure its free lift at that altitude and compare this with the free lift that the balloon had when

it left the ground. So far this experiment has not been conducted but experiments have shown that the balloon as it rises, since it is subject to different quantities of infra-red flux as well as solar radiation very probably does acquire a temperature which is very different from the air temperature at each altitude. GOPHER flight #759 is an example of this. In this flight the balloon was weighed off 5 per cent heavy on the ground so that it would not have risen had it not been carried up with a tow. At the time the tow was cut it was found that the balloon was essentially in equilibrium and one can interpret this to mean that the balloon has acquired a super heat relative to the outside air greater than that which existed on the ground. The magnitude of this super heat corresponds approximately to 5% of the air displaced in the flight and indicates that relative to the outside air a balloon in the stratosphere runs as much as 5% warmer than the air as compared with the approximately zero on the ground. Our flight constants flight #56 is a further example of this. In this flight two ballast drops were made which correspond to the lift of the tow balloon which carried this system to the altitude at which the tow was cut. After completing these two ballast drops if the balloon had not acquired super heat in the stratosphere it would have been in equilibrium. It was observed, however, that the balloon in the stratosphere had a rate of rise of 150 to 200 feet per minute and this rate than indicates the relative warming of the balloon at this altitude. It is quite clear that it is important in describing the ascent behavior of a balloon to understand just what temperature field the balloon at rest would be subject to at different positions in the atmosphere. This effect should be quantitatively measured at night and in the daytime probably for typical summer-winter conditions. If one assumes that one knows this temperature field that the balloon is subject to, it is then possible to decide what its rate of rise will be, given an initial free lift on the ground and given this temperature

field the balloon is immersed in. The rate of rise would be determined by equating the free lift to the total drag and solving for the velocity. However, as soon as the balloon begins to move the buoyancy which it has at rest will be altered by the fact that the gas inside the balloon is expanding if the balloon is rising or compressing if the balloon is descending. This expansion or compression of the balloon gas will be reflected by a change in balloon temperature and therefore a change in the balloon's buoyancy as it moves. Since this change in buoyancy is not present for a floating balloon it then appears as an effective drag on the balloon since, as the balloon rises it cools, losing buoyancy and thereby has a smaller driving force to be compensated by aerodynamic drag. The amount of this loss of buoyancy of the rising balloon or gain in buoyancy of the descending balloon will be determined by the rate at which the balloon is rising or descending and by the efficiency of the heat transfer from the surroundings of the balloon into the balloon gas. If there were no heat transfer from its surroundings at all it would be clear that the balloon with a small amount of free lift would rise, the gas inside would expand adiabatically, cooling 4° per 1000 feet of ascent. It would take only a few thousand feet of ascent of this sort to cool the balloon sufficiently so that its free lift would be gone and the balloon would come to rest. Since this does not happen it is clear that the flow of heat into the balloon is adequate to allow a temperature difference to exist and therefore a buoyancy loss over the situation at rest. This loss of buoyancy is spoken of as thermodynamic drag. The previous discussion of the effect was included to show that the thermodynamic drag is not a drag term in the same sense as the aerodynamic drag is and in fact the so-called thermodynamic drag may be different for balloons of the same size which have different absorption properties since it depends upon the heat transfer from the outside air into the balloon system and this heat transfer may be quite vitally dependent

upon the actual temperature of the balloon film. One application of the use of the idea of thermodynamic drag in the balloon system is the discussion of the sunset rate of descent in the balloons which is included in VolumeVI, Section VI of this report.

A final factor in describing the ascent or descent of balloons is the aerodynamic drag which will be responsible for the velocity acquired once one knows the net buoyancy of the balloon and as was just indicated this net buoyancy in turn will be determined by the thermodynamic loss of lift or the thermodynamic drag and by the actual free lift which the balloon would have, if it were brought to rest at the position in the atmosphere which is being considered. The quantitative measurement of the thermodynamic drag, the aerodynamic drag and the temperature field that the balloon is subject to is not merely of academic interest. In order to realistically design ballast systems or to be able to control a balloon in its vertical flight it is necessary to understand in detail these three factors and to be able to put them in equations in a quantitative way. The first major contribution to understanding vertical flight on our project came at flight #40, with the introduction of the duct appendix. The very misleading effects of air intake have so complicated the analysis that in many of the previous flights the most predominant effect determining the rate of rise or descent of the balloon was the thermodynamic drag introduced by the very large quantities of intaken air. Our flight #8 is a good example of the effect on the ascent time-altitude curve of intake of air and is included in this section as figure 1. In contrast to the ascent behavior of flight #8 a portion of thetime altitude of flight #40 is also included in figure 2 to show the difference in the time-altitude curve as the balloon neared ceiling. The notations on Figure 1 refer to the appearance of the balloon as determined by up-pictures taken during flight. Figure 2 is a diagramatic sketch of the balloon appearance in three flights that intook air.

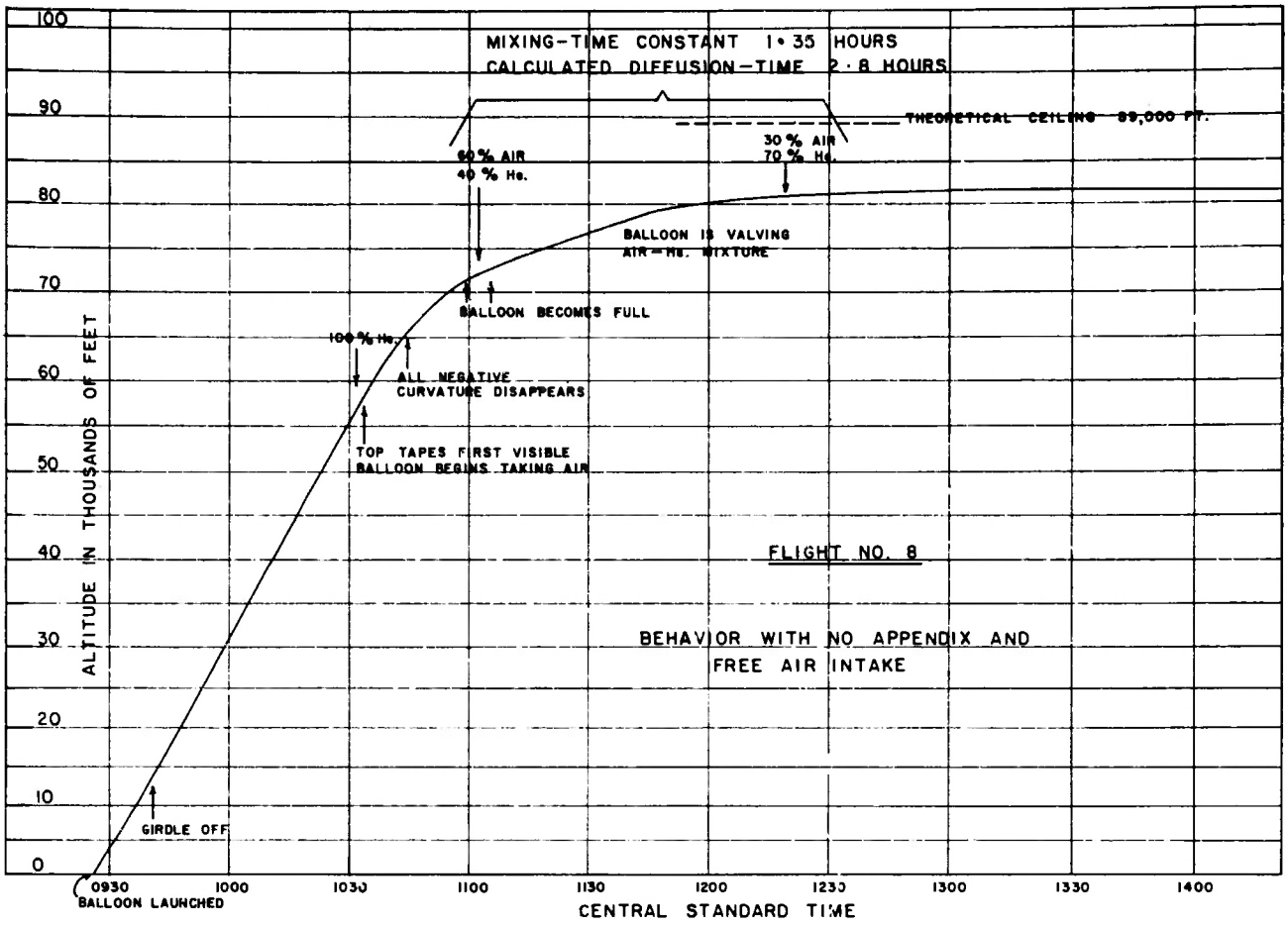
MIXING-TIME CONSTANT 1·35 HOURS
CALCULATED DIFFUSION-TIME 2·8 HOURS
THEORETICAL CEILING 89,000 FT.
60 % AIR
40 % He.
30 % AIR
70 % He.
BALLOON IS VALVING AIR-He. MIXTURE
BALLOON BECOMES FULL
100 % He.
ALL NEGATIVE CURVATURE DISAPPEARS
TOP TAPES FIRST VISIBLE
BALLOON BEGINS TAKING AIR
GIRDLE OFF
FLIGHT NO. 8
BEHAVIOR WITH NO APPENDIX AND FREE AIR INTAKE
ALTITUDE IN THOUSANDS OF FEET
100
90
80
70
60
50
40
30
20
10
0
0930
BALLOON LAUNCHED
1000
1030
1100
1130
1200
1230
1300
1330
1400
CENTRAL STANDARD TIME

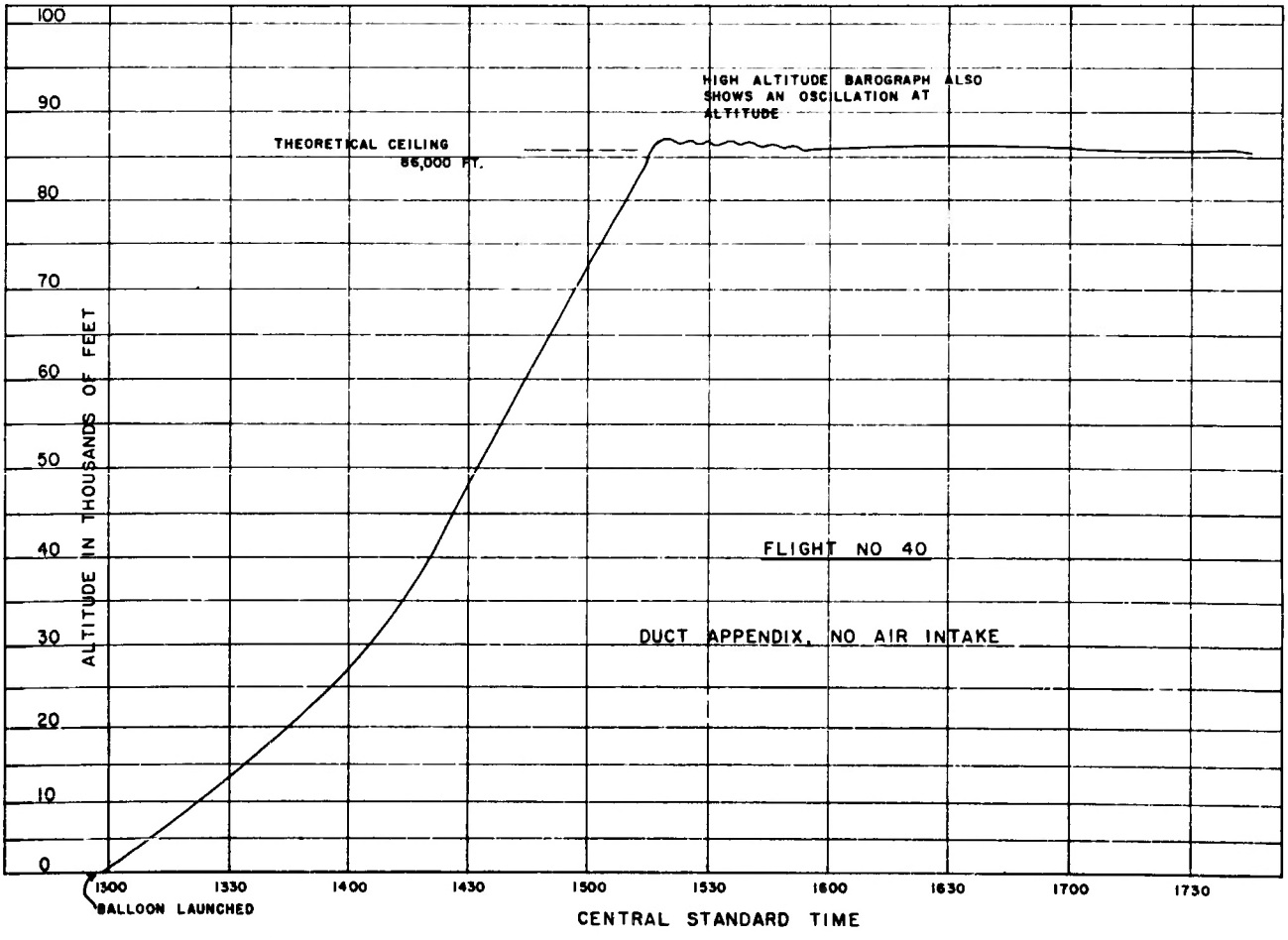
HIGH ALTITUDE BAROGRAPH ALSO SHOWS AN OSCILLATION AT ALTITUDE
THEORETICAL CEILING
86,000 FT.
FLIGHT NO 40
DUCT APPENDIX, NO AIR INTAKE
ALTITUDE IN THOUSANDS OF FEET
100
90
80
70
60
50
40
30
20
10
0
1300
BALLOON LAUNCHED
1330
1400
1430
1500
1530
1600
1630
1700
1730
CENTRAL STANDARD TIME

SEC. VI FIG. 1

MIXING - TIME CONSTANTS SEC. VI. FIG. 2

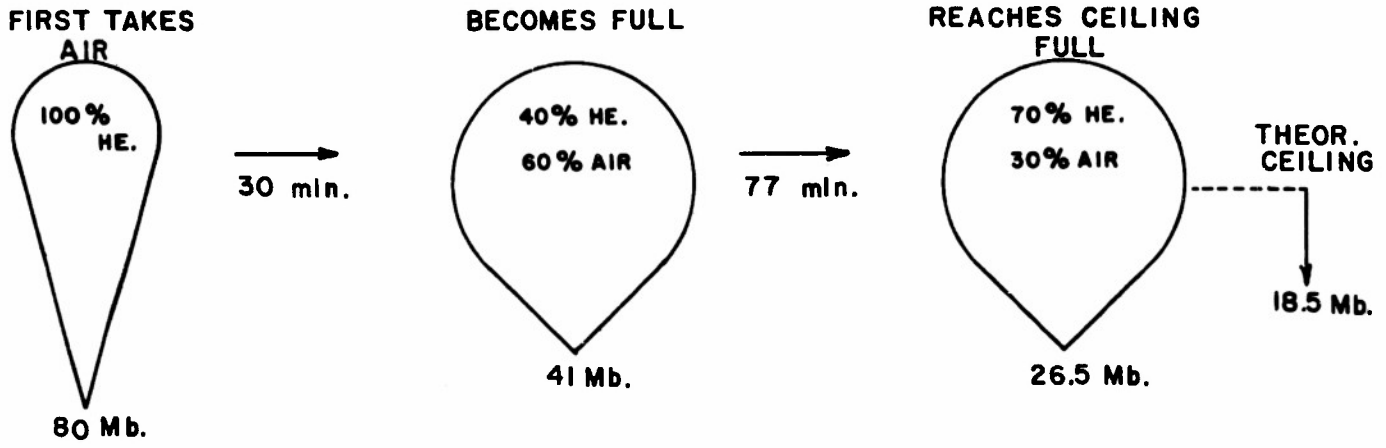

GROSS LIFT = 413 LBS.
INITIAL RATE OF RISE = 940 ft/min.

FLIGHT NO. 8

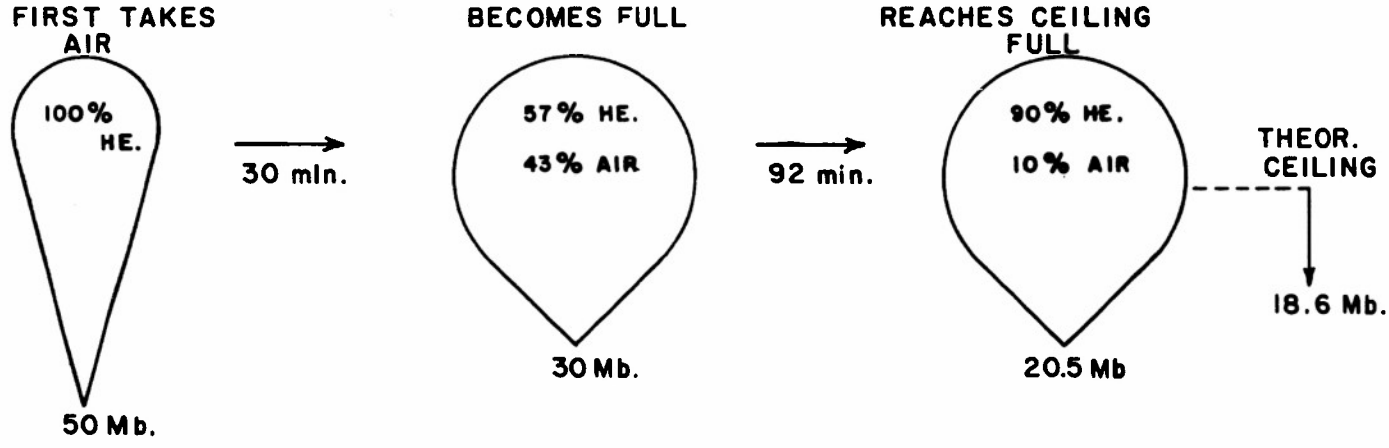

GROSS LIFT = 436 LBS.
INITIAL RATE OF RISE = 830 ft/min.

FLIGHT NO. 9

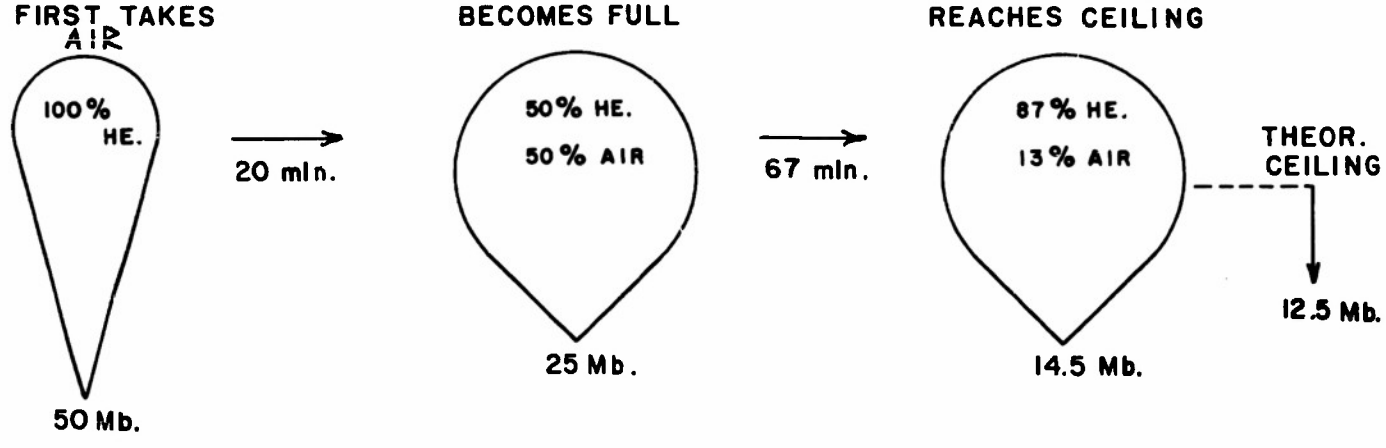

GROSS LIFT = 292 LBS.
INITIAL RATE OF RISE = 850 ft/min.

FLIGHT NO. 10

The data were obtained from up-pictures. The effect of the intake of air even at relatively high rates is that at pressures approximately 4 to 5 times the ceiling pressure of the balloon, the bottom of the balloon becomes open, air rushes in and fills out the balloon greatly increasing its drag since a quantity of air equal to approximately four to five times the air displaced originally by the flight can be taken in. This air acts as an insulator thermally and must be warmed as the balloon rises and the effect of this is to greatly slow down the ascent of the balloon at the instant of air intake. The balloon never reaches its theroetical ceiling because as the air is mixing inside the balloon, the balloon finally reaches ceiling with an impure mixture after valving out only a portion of the air. The fact that the thermodynamic drag that the air introduces slows down the rate of ascent of the balloon means that the balloon spends more time at altitudes at which the air can mix and thereby makes the problem even worse allowing the air to appreciably contaminate the helium. Slow rising balloons which are subject to this effect with open appendices or straight skirt appendices may miss their theoretical ceiling by a very large amount due to the air mixing. The introduction of the duct appendix has eliminated this unsavory feature of balloon flights and has in a sense helped understand the behavior of balloons in vertical flight. Flight #40 which was given as an example of the use of the duct was the first successful application of the duct appendix in ballooning and it is clear that if there is no intake of air the rate of rise of the balloon is maintained near its ceiling altitude and the balloon reaches this theoretical ceiling altitude with a square corner on the time altitude curve. Numerous flights since flight #40 have shown that the balloon floating at ceiling can begin to descend with the duct appendix and will, while it descends, not intake any air. As it descends it will acquire the shape and size corresponding to the balloon during its ascent, whereas balloons which

freely intake air through the bottom as they descend slowly, always remain completely full.

We will now discuss some characteristics of the ascent curves of balloons which do not have the contributing effect of air intake to cloud the analysis. Figure 3 shows a plot of the initial rate of rise, that is, the rate of rise between the ground and 30,000 feet for a number of flights in which the free lift was measured by weighing the balloon off. Although there is considerable scatter of the points it is clear that there is relationship between initial free lift and initial rate of rise. The indications are that an initial rate of rise in the range of 400 to 1000 feet per minute can be obtained by launching balloons with from 4 to 18% of air displaced as free lift. Figure 4 shows a similar plot of this data between the altitudes 30,000 and 52,000 feet. This figure shows a plot of the rate of rise between 30,000 and 50,000 feet as a function of the initial free lift. The effect of the temperature field of the balloon is beginning to be evident in this plot which shows essentially no dependence of the rate between these altitudes upon the initial free lift, as long as the free lift is in the range of 5% to 20% of the air displaced. This is interpreted as meaning that the balloon at these levels has its free lift more determined by the radiation balance falling upon it than upon the free lift it had when it left the ground. The general behavior of the balloon during ascent can be characterized in the following way. It takes off with a rate of rise determined by the initial free lift as indicated by Figure 3. If the initial rate of rise is relatively low, say 300 to 400 feet a minute, the balloon will change its rate quite appreciably as it rises through the troposphere and will acquire essentially a constant rate by the time it enters the stratosphere. The rate of rise in the stratosphere will then either stay constant, rise, or decrease, depending upon a variation in the stratospheric lapse rate and depending upon whether the balloon was launched in the summer time or the winter and whether or not it was launched over an overcast. In

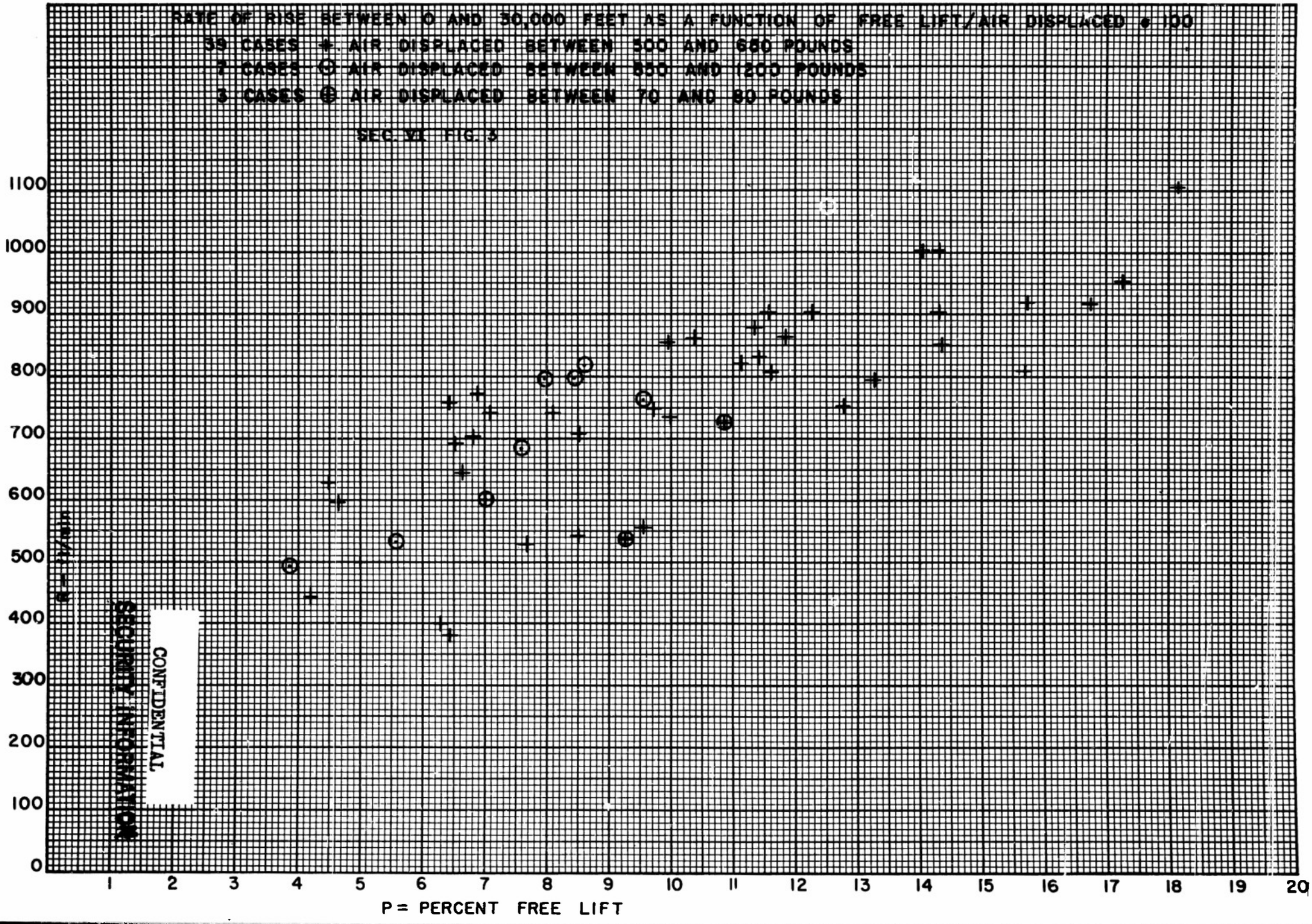
RATE OF RISE BETWEEN 0 AND 30,000 FEET AS A FUNCTION OF FREE LIFT/AIR DISPLACED * 100
39 CASES + AIR DISPLACED BETWEEN 500 AND 650 POUNDS
2 CASES ⊙ AIR DISPLACED BETWEEN 850 AND 1200 POUNDS
3 CASES ⊕ AIR DISPLACED BETWEEN 70 AND 80 POUNDS
SEC. VI FIG. 5
1100
1000
900
800
700
600
500
400
300
200
100
0
1
2
3
4
5
6
7
8
9
10
11
12
13
14
15
16
17
18
19
20
P = PERCENT FREE LIFT
CONFIDENTIAL
SECURITY INFORMATION

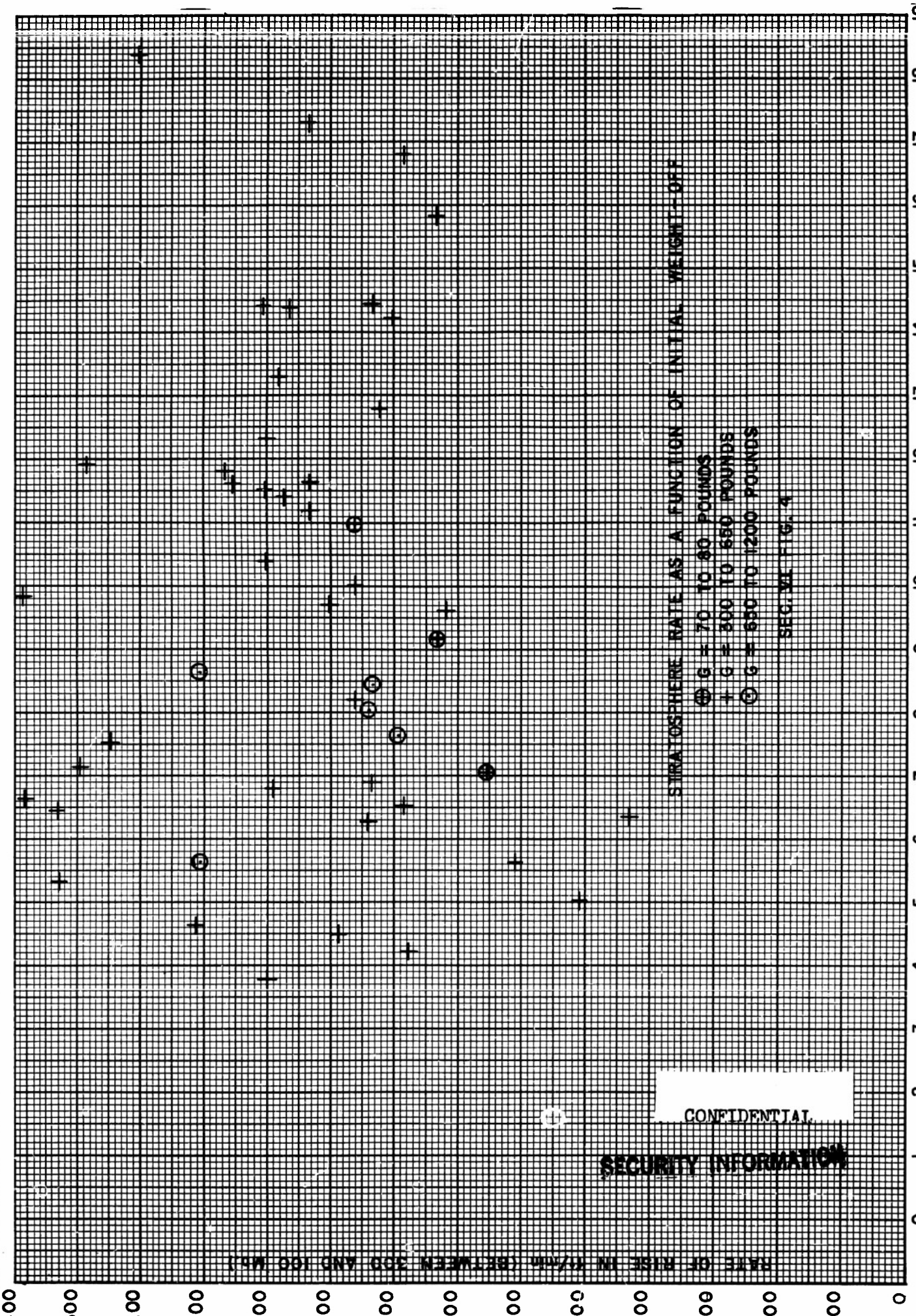
RATE OF RISE IN ft/min (BETWEEN 300 AND 100 Mc)
P= PERCENT FREE LIFT OF AIR DISPLACED
STRATOSPHERE RATE AS A FUNCTION OF INITIAL WEIGHT--OFF
⊕ G = 70 TO 80 POUNDS
+ ⊙ G = 300 TO 650 POUNDS
G = 650 TO 1200 POUNDS
SEC. VI, FIG. 24
CONFIDENTIAL
SECURITY INFORMATION

a general way it is observed that the rate of rise in the stratosphere will be relatively high, say 800 to 1000 feet a minute if the conditions represent a large amount of infra-red flux falling on the balloon, that is, if the balloon were launched in the summer time on a clear day. The stratosphere rate of rise, on the other hand, will be lower if the balloon is over an overcast or if the ground is covered with snow as it is in the wintertime and in any case, strong changes in the lapse rate of the outside air since they affect the transfer of power into the balloon will be reflected in rate changes through the medium of the thermodynamic drag which the balloon has. If the drag of the balloon were entirely thermodynamic, that is, if the aerodynamic drag were small in comparison and if the temperature field did not correspond to increased free lift as the balloon passes into the stratosphere, then the tropopause should be reflected in a marked decrease in rate of rise in balloon. This is generally not true in helium filled flights. It can be shown, however, that the atmospheric lapse rate and the thermodynamic drag are extremely important factors by putting into the balloon a quantity of air. Our flight #53 is a good example of this fact. Flight #53 was a quarter of a million cubic foot balloon launched with a mixture which was half air and half helium. It showed an increase in troposphere rise rate finally reaching a value of approximately 500 feet per minute. On entering the stratosphere the lapse rate changed, the balloon immediately slowed its rate of rise to approximately 200 feet per minute and this rise rate slowly increased to about 300 by the time the balloon reached ceiling. It is now believed that normal balloon flights have the rate of rise determined at different altitudes by quite a changing balance of buoyancy, thermodynamic, and aerodynamic drag. The indications are quite clear that a quarter of a million cubic foot balloon floating at ceiling altitude will be subjected to essentially pure thermodynamic drag when it changes this altitude slowly. A rate of descent

from ceiling of 400 to 500 feet a minute will correspond to pure thermodynamic drag. On the ground, on the other hand, the rate of rise is more limited by aerodynamic drag than by the thermodynamic although even near the ground at low rates of rise the effect of temperature inversions are evident on the balloon behavior and are a demonstration of its thermodynamic drag. For a given constant rate of rise the aerodynamic drag of the balloon decreases as the balloon approaches ceiling. The thermodynamic drag, however, will be constant throughout the stratosphere and in general becomes a bigger and bigger effect as the aerodynamic drag drops off. Many people have tried to describe the ascent behavior of balloons in terms of pure aerodynamic drag and of the free lift given to the balloon on the ground. Since the aerodynamic drag depends upon the pressure linearly and on the area of the balloon it can be shown that this drag decreases for the same velocity as the pressure drops. Pure aerodynamic drag and a fixed free lift then correspond to a rate of rise in the balloon increasing steadily as the pressure drops and with the rate of rise essentially dependent upon the sixth root of the atmospheric pressure. This pure aerodynamic drag behavior is not observed and because of the complexity of theproblem it is not expected that one can describe the behavior in terms of aerodynamic drag alone. A factor which complicates the calculation of the aerodynamic drag for the rising balloon is the fact that for most flights the Reynolds number of the balloon as it reaches ceiling corresponds to laminar flow whereas at take off the flow is turbulent. This means that somewhere in between the transition between turbulent and laminar flow has taken place with a corresponding complicated change in the coefficient of drag in the balloon. In addition to this the balloon shape is changing. It starts out quite long and slim and reaches ceiling almost spherical. It is now realized that it is not possible to calculate the aerodynamic drag during the rising part of the curve and experiments are being designed to measure this aerodynamic drag directly as a function of altitude and velocity.

Since the aerodynamic drag does go, however, as a square of the velocity, it does set an upper limit to the velocity which the balloon can acquire at any altitude and the following discussion is pertinent to this effect.

The longitudinally stressed natural shape balloon, with zero circumferential stress, has the property whereby the shape of the balloon responds to, and is solely a function of the forces on the fabric. In the static and low velocity regions the shape is well defined by the force of the lifting gas alone. At higher balloon velocities the aerodynamic forces become greater. In some cases of ascending balloons, they approach the static forces in magnitude and consequently are too large to be neglected.

According to Bernoulli, the dynamic pressure is expressed as:

$$\Delta p = \tfrac{1}{2}\rho v^2$$

where Δp = dynamic pressure (lbs/sq ft)

ρ = mass, density of fluid, air (slugs)

v = velocity (ft/sec)

This pressure acts at the stagnation point in the air flow at the top center of the balloon where the relative velocity is reduced to zero and no kinetic energy remains (Figure 5). The relative velocity of air along the balloon surface increases from zero at this point to a maximum near the equator of the balloon and then diminishes again below the equator. If the total energy of the air remains constant the pressure decreases as the velocity of air increases to a maximum near the equator. The velocity diminishes from its maximum as the flow continues around the underside of the balloon. In an ideal fluid, the pressure builds up with the decreasing velocity on the underside of the balloon similar to the pattern on top. In air, this complete build-up is not realized because of the viscous losses of energy resulting from the flow around an object.

The described dynamic pressure loading on the balloon is such as to make the balloon more oblate than its original natural shape. A different drag

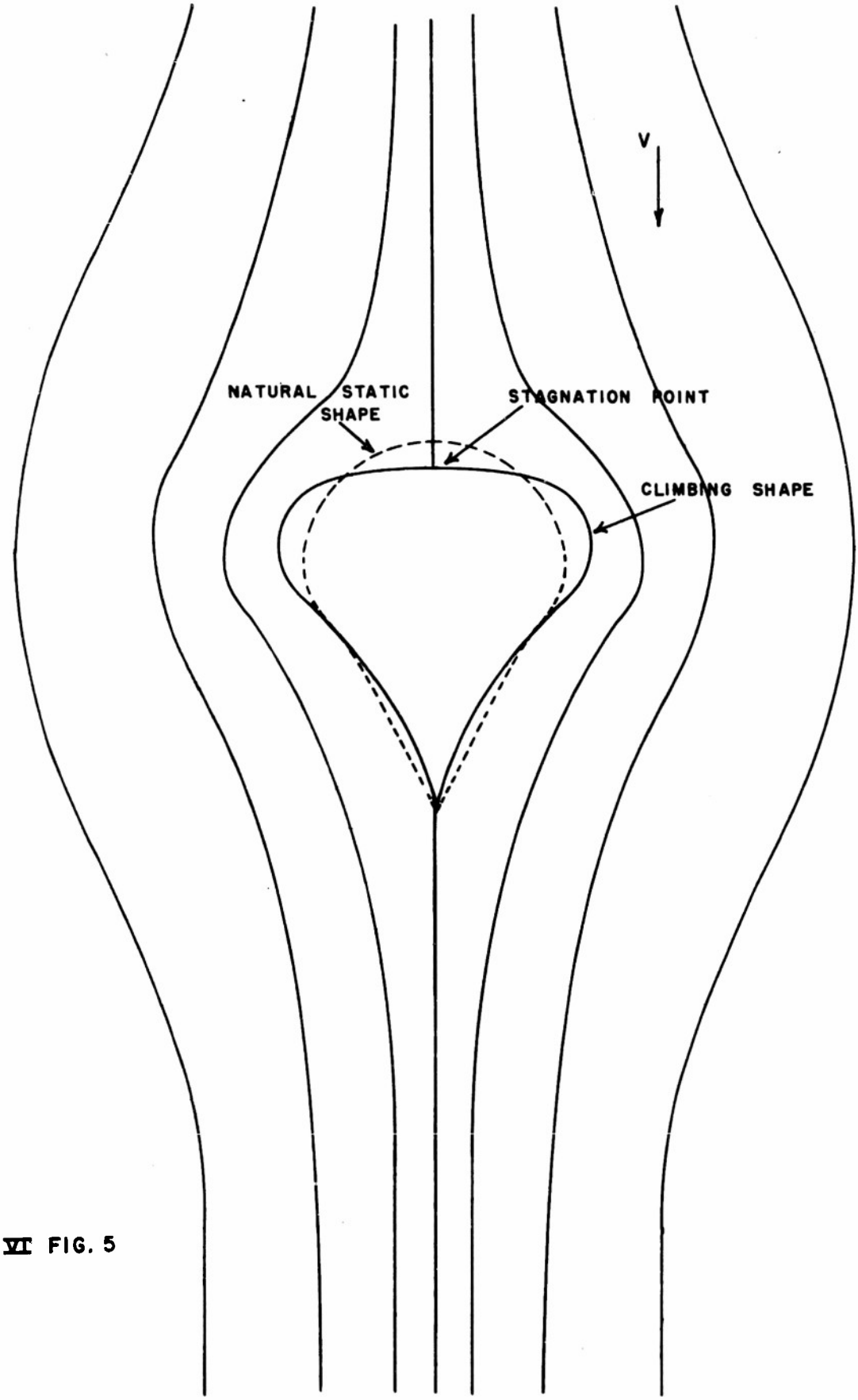

SEC. VI FIG. 5

SKETCH SHOWING IDEAL FLUID FLOW ABOUT A NATURAL SHAPED BALLOON

coefficient for the new shape will result and will affect the final equilibrium velocity.

The static pressure at the top of the balloon is expressed as follows:

$$P = (\rho_{air} - \rho_{gas}) q z$$

where P = static head pressure (lbs/sq ft)

q = acceleration of gravity

z = pressure head measured from the zero pressure level (ft)

The condition of dimpling the top of the balloon is expressed by equating the inside and outside pressures at this point:

$$\frac{1}{2}\rho_{AIR} v^2 = (\rho_{AIR} - \rho_{GAS}) q z$$

$$v = \sqrt{2qz(1-\frac{1}{T})}$$

where $T = \frac{\rho_{air}}{\rho_{GAS}}$

OR $v = \sqrt{\frac{2qz}{K}}$

where $K = \frac{T}{T-1}$

The dimpling velocities for helium and ammonia inflated balloons are plotted in Figure 6.

It is not difficult to imagine that a balloon free to change shape with dynamic forces will have done so appreciably before the velocity of dimpling has been reached. As well as changing the shape and drag coefficient, dynamic forces will change the center of gravity of the lifting gas with respect to the load and also might affect the static pressure head in the balloon. This could contribute to a more or less governing action on the rates of rise at lower altitudes. Natural shaped balloons in motion in an ideal fluid will be investigated in detail with the aid of the REAC computer.

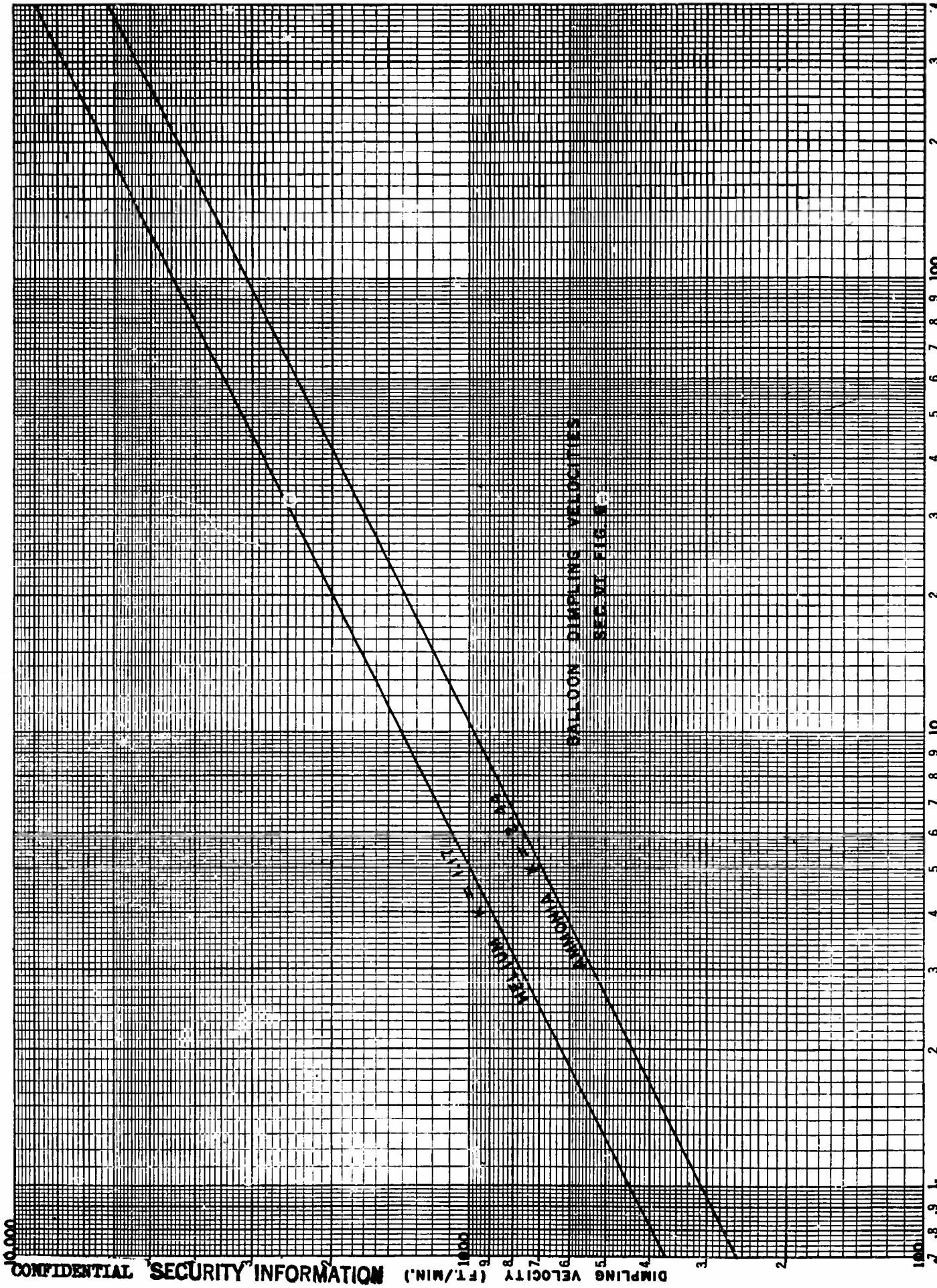
BALLOON DIMPLING VELOCITIES
SEE DT FIG 18
MEAN
RANDOM
MEDIAN
DIMPLING VELOCITY (FT/MIN.)
PRESSURE HEAD (FT)
1000
100
10
1

B. Behavior at Altitude. The behavior of the balloon after it has reached ceiling altitude can be discussed in terms of various categories of flights. A number of our flights before the introduction of the duct appendix were analyzed in this way. The analysis is included in Figures 7 and 8. Flights are analyzed in four categories, A, B, C and D. Category A corresponds to balloons which took in air, were inflated with pure helium and had no appendix at all so that one did not have the air limiting effect of a standard skirt appendix. The characteristic behavior of these flights is that they approached ceiling very slowly with a round corner and floated level at ceiling after reaching this altitude. Their ceiling altitude is always below the theroetical ceiling of the balloon and this fact is indicated by the arrows with the dotted lines which correspond to the theoretical ceiling of these balloons. Category B corresponds to balloons with skirt appendices. The balloons have a high rate of rise, the skirt appendices are fairly effective in keeping air out during the ascent part of the flight. In category B are balloons with ammonia plus helium and good appendices and one flight with pure helium and 22 pounds of dry ice which was allowed to evaporate freely. It was later found that the evaporation rate of dry ice is quite low, a 25 pound chunk of dry ice will only evaporate approximately 8 pounds of dry ice in a six hour flight. The characteristics of the flight, however, in category B, are such that they reach ceiling with a square corner, float level for an appreciable length of time after reaching ceiling. It is believed that the dry ice and the ammonia are stabilizing factors which keep the balloon from descending. It should be noted that the ammonia was inserted in the balloon with the helium and may have acted as a cork in the bottom of the balloon to prohibit the diffusion of air into it. The dry ice, however, was used as an automatic ballast dropper.

Category C corresponds to flight curves with good appendices and pure helium. In other words the flights in category C are similar to those in

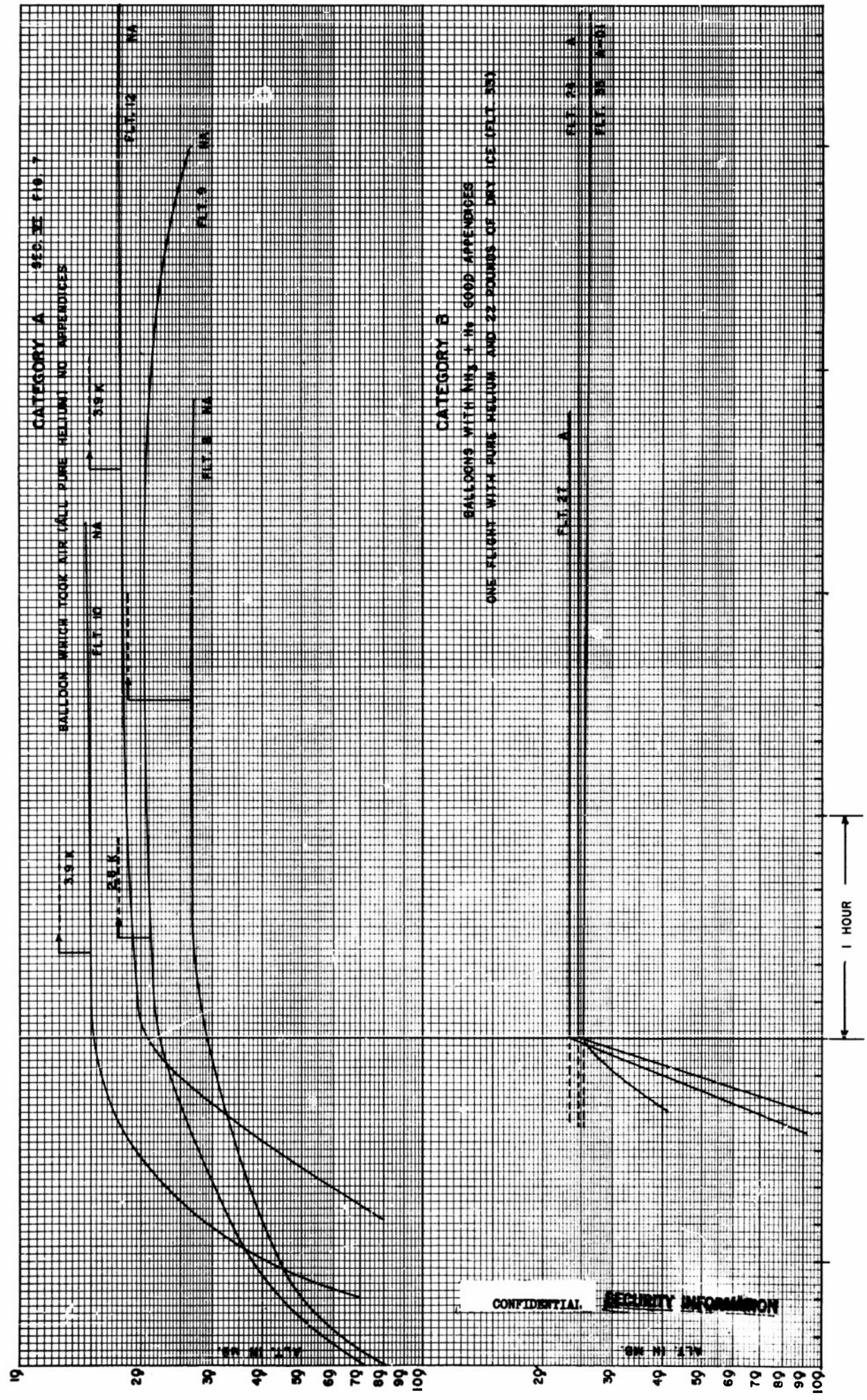
CATEGORY A
SEE FIG 7
BALLOON WHICH TOOK AIR (ALL PURE HELIUM NO APPENDICES
FLT. 12
NA
FLT. 9
NA
FLT. 8
NA
3.9 K
FLT. 10
NA
3.9 K
29.5
CATEGORY B
BALLOONS WITH NH3 + He GOOD APPENDICES
ONE FLIGHT WITH PURE HELIUM AND 22 POUNDS OF DRY ICE (FLT 33)
FLT. 24
A
FLT. 33
A
FLT. 27
A
1 HOUR
ALT. IN MB.
10
20
30
40
50
60
70
80
90
100
CONFIDENTIAL
SECURITY INFORMATION

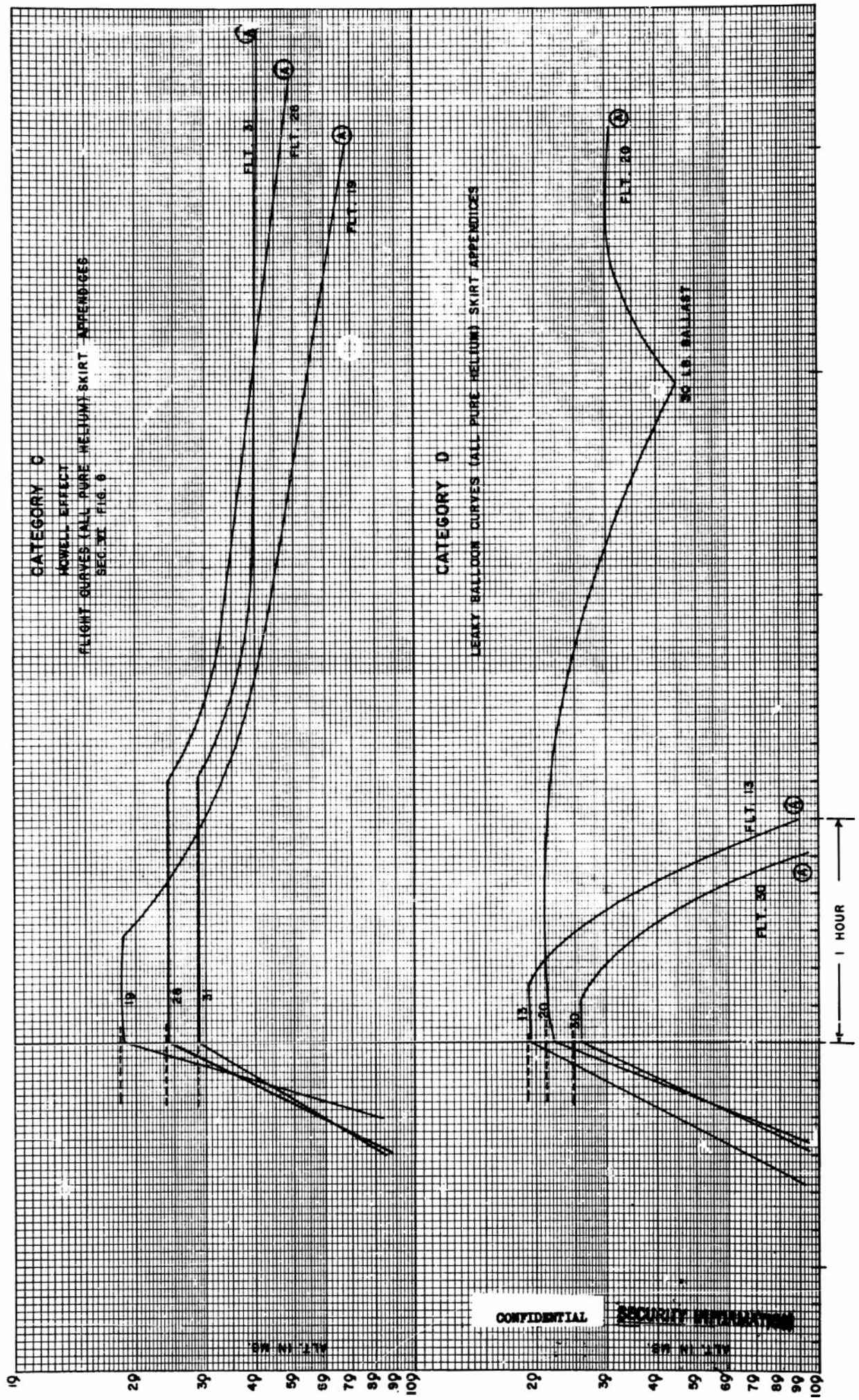
CATEGORY C
HOWELL EFFECT
FLIGHT CURVES (ALL PURE HELIUM) SKIRT APPENDIGES
SEE ALSO FIG. 6
FLT. 31
FLT. 26
FLT. 19
19
26
31
CATEGORY D
LEAKY BALLOON CURVES (ALL PURE HELIUM) SKIRT APPENDICES
FLT. 20
30 LB. BALLAST
FLT. 13
FLT. 30
13
20
30
1 HOUR
ALT. IN MS
10
20
30
40
50
60
70
80
90
100
CONFIDENTIAL

category B except for the absence of ammonia and the absence of any stabilizing ballast drop. Characteristic of these flights is that they reach ceiling with a square corner as do flights of category B but they float at ceiling level only for a limited length of time. Any flight upon reaching ceiling must overvalve a small amount of gas. In general this is not responsible for the balloon's descent immediately because the gas in the balloon is cold due to its expansion as the balloon was rising so after reaching ceiling the balloon can then warm up and make up for any overvalving which occurs. It has been observed, however, that balloons with good appendices, pure helium and no ballast drops will reach a ceiling, float level for one hour and then began descending. Since these flights could take in air the rate of descent is rather low due to the thermodynamic drag of the air. There is, however, a pronounced loss of lift after floating at ceiling for about an hour which is responsible for the descent of the balloon. It has been shown by temperature measurements that a warming of the gas upon reaching ceiling takes place in a time of the order of 10 minutes. Therefore this level period of flight is not the period in which the balloon gas warms up but is a longer period. The descent of these balloons is believed to be the result of one of two possible causes. The first of these may be a change in shape of the balloon after it has been floating full for some time resulting in a valving of gas after a period of time and a corresponding loss of lift. The other possibility is that the diffusion through the appendix, which can be shown to correspond to something like 2% of loss of lift per day, is responsible for replacing some of the helium in the balloon with air thereby causing a net loss of lift. The affect of descent after level flight for approximately an hour is called the "Howell " effect as it was first clearly delineated in MOBY DICK flights and pointed out to us by Professor Howell of Tufts College. Numerous discussions with people at General Mills, Inc. and

on other balloon projects have indicated that this effect had been previously observed. MOBY DICK flights, however, were the first to point this up as a clearly defined effect not associated with leakage.

Category D corresponds to balloons which had leaks. The difference between the ceiling behavior in category D and category C is that the leaky balloon shows a descent curve which is concave downwards in contrast to category C which is concave upwards. The flights for category D did remain level at ceiling for a short period of time and this period of time is in quite good agreement with the measured time constant for the warming of the gas after reaching ceiling. It is fairly clear in these flights that the balloon reaches ceiling with a hole. As long as the gas is warming up the balloon can continue to valve and maintain a ceiling. However, as soon as the warming ceases the leakage takes over and the balloon begins descending with an ever increasing rate. One of the original reasons for introducing the duct appendix was to understand the "Howell" effect as evidenced by the curves of category C. It was believed that the duct would eliminate the possibility of diffusion of air into the helium mixture. As soon as the duct was introduced the "Howell" effect was eliminated. As soon as the balloon reached ceiling with the duct prohibiting intake of air, the flight would level off and float level until some definite loss of lift occurred such as the loss of lift at sunset. The duct was therefore responsible for the elimination of the "Howell" effect but did not establish which of the two causes was responsible for it. The balloons flown with ducts were flown as sub-pressure balloons and could take on a natural shape in the lower regions of the balloon. It is, however, unlikely that a change in shape has been responsible for the "Howell" effect. It is more probable that the introduction of the duct did cut down diffusion of air into the balloon and that this was responsible for its success in eliminating the "Howell" effect.

Another interesting characteristic of the balloon at ceiling which occurs as soon as the duct is used is that the balloon oscillates about at ceiling altitude. This is shown in Figures 1 and 9. Figure 1 has already been quoted and is the time-altitude curve for flight #40. It is quite easy to see the oscillation at ceiling altitude which has a period of approximately five minutes. This value for the period is in very good agreement with calculations which show that the period of oscillation depends only upon the absolute temperature of the atmosphere and the atmospheric lapse rate. The balloon bobs about its ceiling altitude cooling adiabatically as it overshoots its altitude and warming adiabatically as it is descending below the altitude. The period of oscillation should be approximately 5 minutes in the stratosphere and approximately 7 minutes in the troposphere. Figure 9 is a photograph of the barograph trace from flight #40 and clearly shows the oscillation of the balloon at ceiling. The duct allows this oscillation since the balloon can rise and descend without taking in air which would immediately stop this bouncing. The effect of bouncing at ceiling will also show whether or not the balloon has slack volume which will allow it to rise above its ceiling altitude. This was true in the first duct flights in which the duct was cut short enough so that the cone-on-sphere balloon took on approximately natural shape near the bottom of the balloon and therefore had some slack volume to fill out. Up-pictures show clearly that the balloon was not tight in the lower portion of the conical region. In fact it was quite clear that a change in curvature occurred at the bottom of the duct. In these flights the duct was cut approximately a third of the distance up from the bottom along the gore since this is the position of the zero pressure level which had been calculated to give approximately a 60° cone angle for a natural shape balloon. 60° cone-on-sphere balloons were the ones which were being flown at the time of flight #40. It perhaps should be pointed out here that a ninety degree cone-on-sphere balloon would require a duct cut

Sec VI Fig 9. Photograph of barograph trace showing oscillation at ceiling in flight #40.

much nearer the bottom, almost to the apex of the balloon, in order to make it acquire approximately natural shape in the lower regions. The equation for the period of the bouncing of the balloon at ceiling is as follows:

$$T = .117\sqrt{\frac{t}{L'+L}}$$

where T = the period in minutes

t = the atmospheric temperature

L' = the lapse rate of the filling gas in °C/1000 feet (+4 for Helium)

L = the atmospheric lapse rate (normally -2 in the trosphere, 0 in the stratosphere)

The fact that flight #40 oscillated for approximately 6 or 7 full periods is evidence that the aerodynamic drag at ceiling is really quite small since it does not damp out this oscillation in this period of time. In fact the aerodynamic drag of the balloon can be calculated at ceiling since the balloon is nearly spherical. It is clearly in the laminar region of flow. Such a calculation leads to the result that of a rate of rise of 700 ft/min the aerodynamic drag can only correspond to 6 pounds for a full balloon at ceiling. A free lift of more than 60 pounds, however, is required to produce a stratosphere rate of 700 ft/min. This is further support to the fact that large balloons in the stratosphere have their rates determined principally by radiation balance and thermodynamic drag.

C. Descent Behavior. As was previously noted flights prior to our flight #40 on descending with skirt appendices could take in air and thereby remain full. The effect of the intake of air in a descending balloon was to greatly slow down its descent rate since the great mass of intaken air needs to be compressed as the balloon descends and represents an extremely large drag. To give an example of the magnitude of this effect, one observes that a balloon which allows the intake of air through the bottom at sunset may descend at a rate of approximately 50 ft/min whereas a duct appendix on the same balloon would allow the balloon losing the same amount of lift to descend at 250 to 500 ft/min, almost 10 times faster than the air balloon.

To summarize all flights which were allowed to descend before our flight #40 one can say that the descent rates of these flights were determined by the thermodynamic drag of the intaken air and by the possibility of the warming of this intaken air in case the balloon descended into a region where the static condition would allow super heating of the intaken gas. It is quite possible for a balloon which intakes air to become stable if the balloon can run slightly warmer than the outside air since the intaken air can be warmed and can contribute buoyancy. As soon as intaking of air was eliminated the behavior of descending balloons became much easier to understand than in the case of balloons which had a large and unknown quantity of air flowing into them. It is observed that when a definite amount of lift is lost at sunset the balloon descends and maintains approximately a constant rate throughout the stratosphere. This rate will, however, reflect changes in the lapse rate and if it is relatively small (200 to 500 f/min) these changes in lapse rate produce pronounced changes in the rate of descent. On entering the troposphere the rate of descent increases very greatly since the average condition corresponds to the change from zero lapse rate in the stratosphere to -2° per thousand feet in the troposphere. It can be shown that if the drag is all thermodynamic (a good approx-

imation at these rates and altitudes) that the rate of descent should be proportional to L ÷ 4. The ratio of L÷4 in a normal stratosphere to its value in a normal troposphere is 2 to 1 and one would expect then for pure thermodynamic drag to have an increase in rate upon entering the troposphere a factor of 2. The changes in rate that accompany the descent of a balloon which cannot intake air have been consistent with this picture. It is therefore believed that a 73 foot balloon descending from ceiling at sunset is subject to pure thermodynamic drag. One can carry this picture a little further. Consider a balloon which is floating at ceiling during the day and which is warmed relative to the outside air by 20°. The sun sets on this balloon and it immediately begins to descend. If it is subject to thermodynamic drag alone its rate of descent represents an equilibrium condition since it is an equilibrium condition just as surely as the balloon is in equilibrium at ceiling. One then comes to the conclusion that the balloon descends at such a rate that it compresses the gas and produces a net temperature of the gas above the outside air of 20° or in other words the same as the temperature superheat above the outside air that existed during the day. Attempts are being made to measure the mean temperature of the gas as the balloon descends after sunset but the prediction is that this average temperature will not change. To say it another way as soon as the balloon is subject to another temperature changing effect which would take away its super heat it will begin descending at just such a rate that it maintains its super heat the same. It would, in principle, then be possible to make balloons descend more slowly at sunset if one could somehow make the transfer of heat into the balloon less effective since the rate of transfer of heat into the balloon is what must be responsible for the resultant temperature difference between the balloon and the outside air. The amounts of power involved are quite large. A balloon with a double

1-mil polyethylene construction and a single set of tapes will descend at sunset at approximately 350 ft/min, if it has a gross load of about 500 pounds of air displaced. The power input will be of the order of 3 to 4 kilowatts and this power must be transferred from the gas in the balloon to the outside air. On might believe that the convection between the inside gas and the outside air is similar for the descending balloon to the convection at ceiling except for the fact that at ceiling the inside gas is essentially at constant temperature and at the temperature of the film whereas the descending balloon has its inside gas warmer than the film which in turn is warmer than the outside air. The assumption is, however, that the loss of heat from the inside gas to the outside air is similar for the descending balloon to the situation at ceiling has been quite a successful one as is indicated by the section on Sunset Effects. All of our sunset descent data can be correlated in a simple formula which assumes that the drag is all thermodynamic during descent and that the convection of the balloon during descent is similar to convection while floating at ceiling. The data on ten balloon flights have been used for this analysis and the data are fitted by a single constant to within probable error of 9%. In this simple picture the descent rate of the balloon is determined by its absorption of solar energy per pound of material and therefore the simple relation relating the rate of descent to the weight of displaced air and the balloon weight can be solved for the absorption of the material. For polyethylene balloons the value of the absorption turns out to be 18 watts per pound of material. The analysis leading to the equation for the descent and the complete discussion of this problem is included in the section on sunset effects. It is included here merely as evidence for almost purely thermodynamic drag at the rates of descent encountered by a balloon descending at sunset.

D. Thermodynamic Effects. It has been previously pointed out here that rising balloons are cooler than balloons at equilibrium and descending balloons are warmer than the corresponding balloon at equilibrium. This fact leads to rather interesting thermodynamic effects when the state of the balloon's motion is suddenly changed by the dropping of an increment of ballast. Figures 10, 11 and 12 are included to show these effects. Figure 10 shows a balloon which is descending at 370 ft/min (flight #42). 15 pounds of ballast have dropped and immediately after the ballast drop the balloon rises a small distance and then acquires a new downward rate of 120 ft/min. The explanation of this effect is that as soon as the ballast is dropped the balloon found itself suddenly warm because of its previous descent rate but lighter than it had previously been and therefore it climbed until it cooled somewhat by adiabatic expansion and convection and finally acquired the temperature that it needed to have at equilibrium at its new descent rate of 120 ft/min. Figure 11 shows the same flight later in the flight descending at the rate of 160 ft/min. Twenty five pounds of ballast are dropped and the balloon rises extremely rapidly for 4.3 minutes while it is cooling adiabatically to acquire the temperature which it will have at equilibrium at its final rate which turns out to be 140 ft/min upwards. The height of the bounce of the balloon after the drop of ballast allows one to determine the change in temperature between the initial condition of descending at 160 ft/min and the final condition of rising at 140 ft/min. In this case the change in temperature corresponds to 9.2°. These effects in flight #43 indicated to us that the balloon could be used as its own thermometer and it was decided to attempt to drop exactly the right sunset ballast after the balloon had begun descending at night and to observe the net temperature change by the height of the bounce before the balloon acquired equilibrium. The cases of flight #42 were unfortunate from the

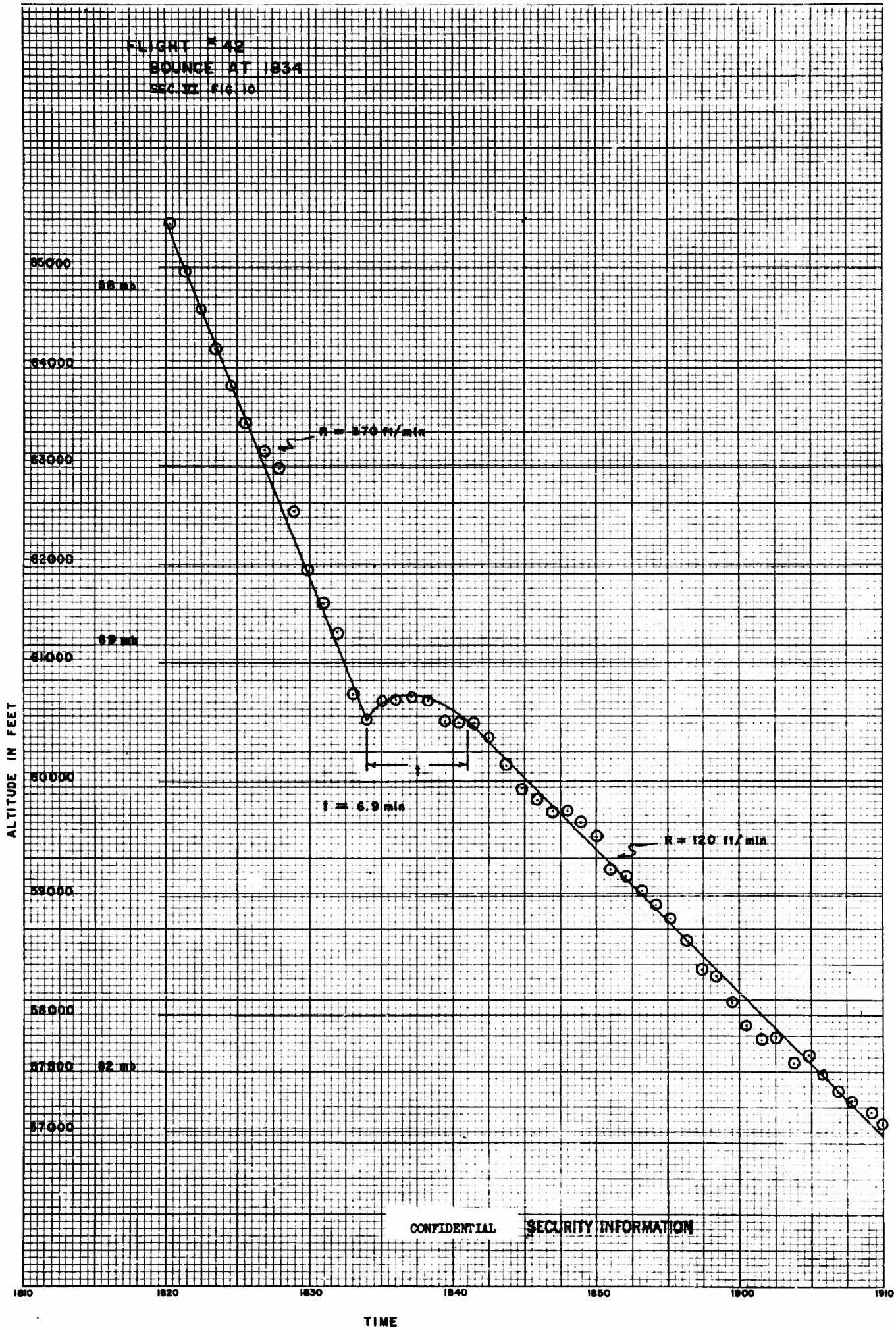
FLIGHT # 42
BOUNCE AT 1834
SEC. VII FIG. 10
65000
64000
63000
62000
61000
60000
59000
58000
57000
56 mb
69 mb
62 mb
R = 570 ft/min
t = 6.9 min
R = 120 ft/min
ALTITUDE IN FEET
1810
1820
1830
1840
1850
1900
1910
TIME
CONFIDENTIAL SECURITY INFORMATION

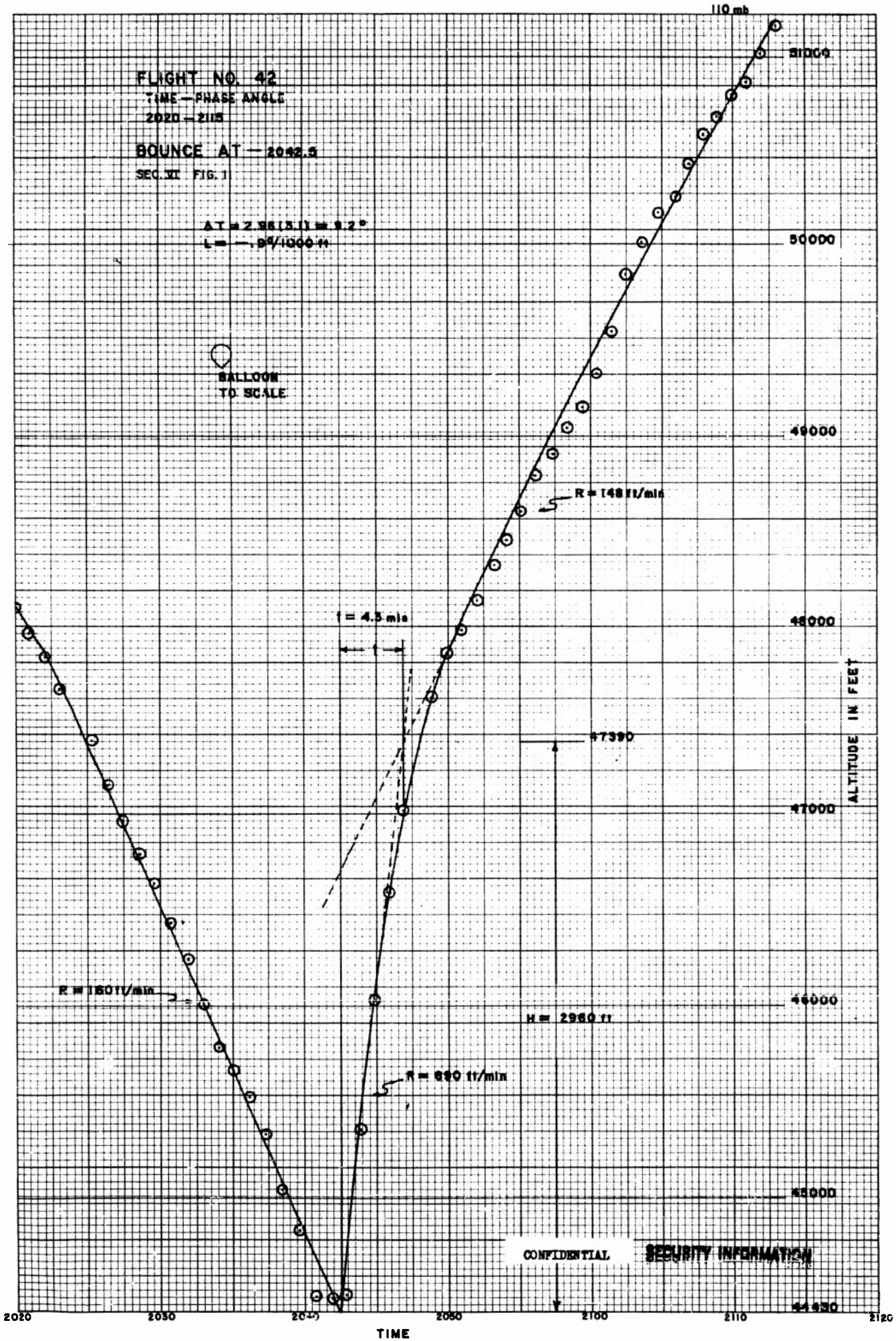
FLIGHT NO. 42
TIME—PHASE ANGLE
2020—2115
BOUNCE AT — 2042.5
SEC. XII FIG. 1
ΔT = 2.96 (3.1) = 9.2°
L = —, 9°/1000 ft
BALLOON
TO SCALE
110 mb
51000
50000
49000
48000
47000
46000
45000
44430
R = 148 ft/min
t = 4.3 min
t
47390
R = 1501 ft/min
H = 2960 ft
R = 690 ft/min
ALTITUDE IN FEET
2020
2030
2040
2050
2100
2110
2120
TIME
CONFIDENTIAL
SECURITY INFORMATION

standpoint that neither ballast drop had a final condition which corresponded to the balloon floating level. Figure 12, however, shows flight #53 in which exactly the right amount of ballast was dropped to compensate for the sunset effect. Before the ballast drop the balloon was descending at 485 feet a minute. After the ballast drop of 45 pounds the balloon rose extremely rapidly for 4.3 minutes meanwhile cooling its gas as it expanded adiabatically. It then leveled off at an altitude far below its ceiling altitude and floated essentially level for the remainder of the night. The ballast drop was 45 pounds with 540 pounds of air displaced. Since the ballast was just adequate to make the balloon float level at night this percentage represents the sunset effect and is 8.4%. The actual temperature change between floating level at night and floating level during the daytime therefore corresponds to 8.4% of the absolute temperature. Now if aerodynamic drag can be neglected the temperature change obtained from the height of the bounce should be the same fraction of the absolute temperature that the ballast is of the air displaced. It turns out that the temperature change calculated from the bounce height is 17.5°C and this is 8.1% of the absolute temperature in striking agreement with the 8.4% which the ballast is of the air displaced. It should be pointed out that this behavior, rapidly rising to change the temperature, could only occur in a balloon which did not have air in it and for this reason these effects have not been observed prior to the introduction of the duct appendix.

Analysis of the thermodynamic bounce to determine relative temperature change has proved and will prove to be an effective tool in studying balloon performance since it essentially uses the balloon as a thermometer.

In connection with the thermodynamic effects, particularly bounces, one is led to ask the question of whether or not a balloon which is launched should not undergo a bounce before establishing its final rate. In this connection

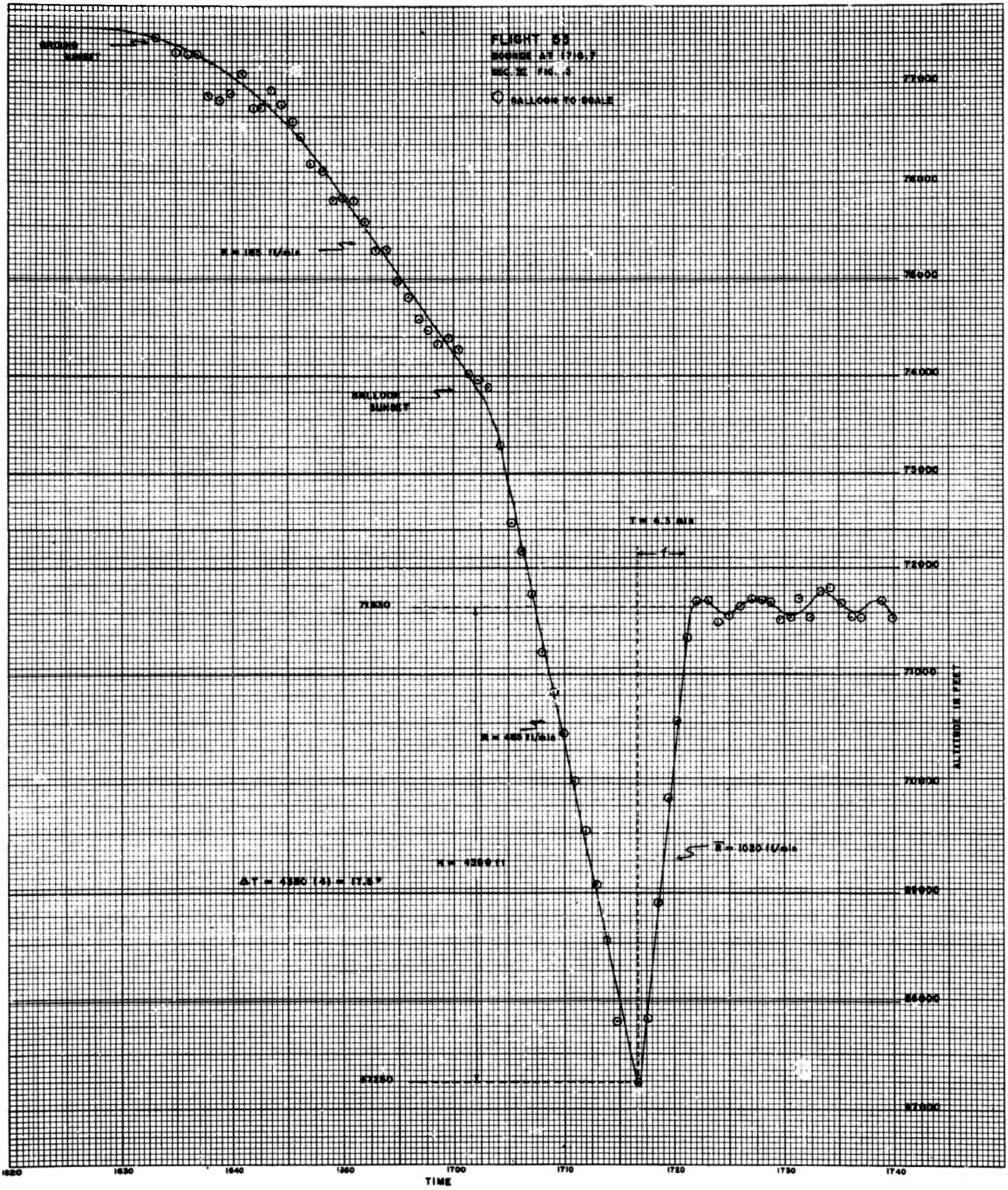
FLIGHT 53
BALLOON TO SCALE
BALLOON SUNSET
BALLOON SUNSET
T = 4.3 min
ALTITUDE IN FEET
TIME
1620
1630
1640
1650
1700
1710
1720
1730
1740

one should point out that the aerodynamic drag is a much bigger factor on the ground and in fact it would tend to obscure thermodynamic bounce. However, careful examination of several flights have shown that bounces do indeed exist and to demonstrate this the take-off bounce on flight #47 is included here as Figure 13. The height of the bounce was 2830 feet indicating a temperature change of 5.7° acquired before the balloon established its final rate. Its initial rate on take-off was 1000 feet/min and after the bounce had taken place the rate slowed down to 660 feet per minute. It is somewhat more difficult to get data on the take-off bounce than it is to get data on the bounces at altitude in our flights because of the fact that we do not drop our telemetering antenna in general until the balloon has reached an altitude of 5,000 or 6,000 feet. In more recent flights we have been recording the Olland Cycle data on the camera. With this system it is possible to go back and determine the time-altitude curve from the moment of take-off.

E. Aerodynamic and Thermodynamic Drag. The aerodynamic and thermodynamic drag have been discussed briefly in various parts of this report as well as in our first Progress Report. Unfortunately we have still not determined the temperature field in which the balloon works and consequently it has not been possible yet to obtain a completely reliable equation of motion. However, we have a number of pieces of data which have been put together to indicate the way in which the rate of rise depends upon the free lift. The basis of the combination of aerodynamic and thermodynamic drag into a free lift equation was outlined in our first Progress Report but at that time no figures were available to put in. In brief the convection theory indicates that the thermodynamic part of the drag should depend upon the velocity to the 3/4 power whereas the aerodynamic drag depends upon the velocity squared. A dimensional argument allows one to determine the dependence of the aerodynamic and of the thermodynamic drag on such quantities as the gross load, lapse rate, etc.

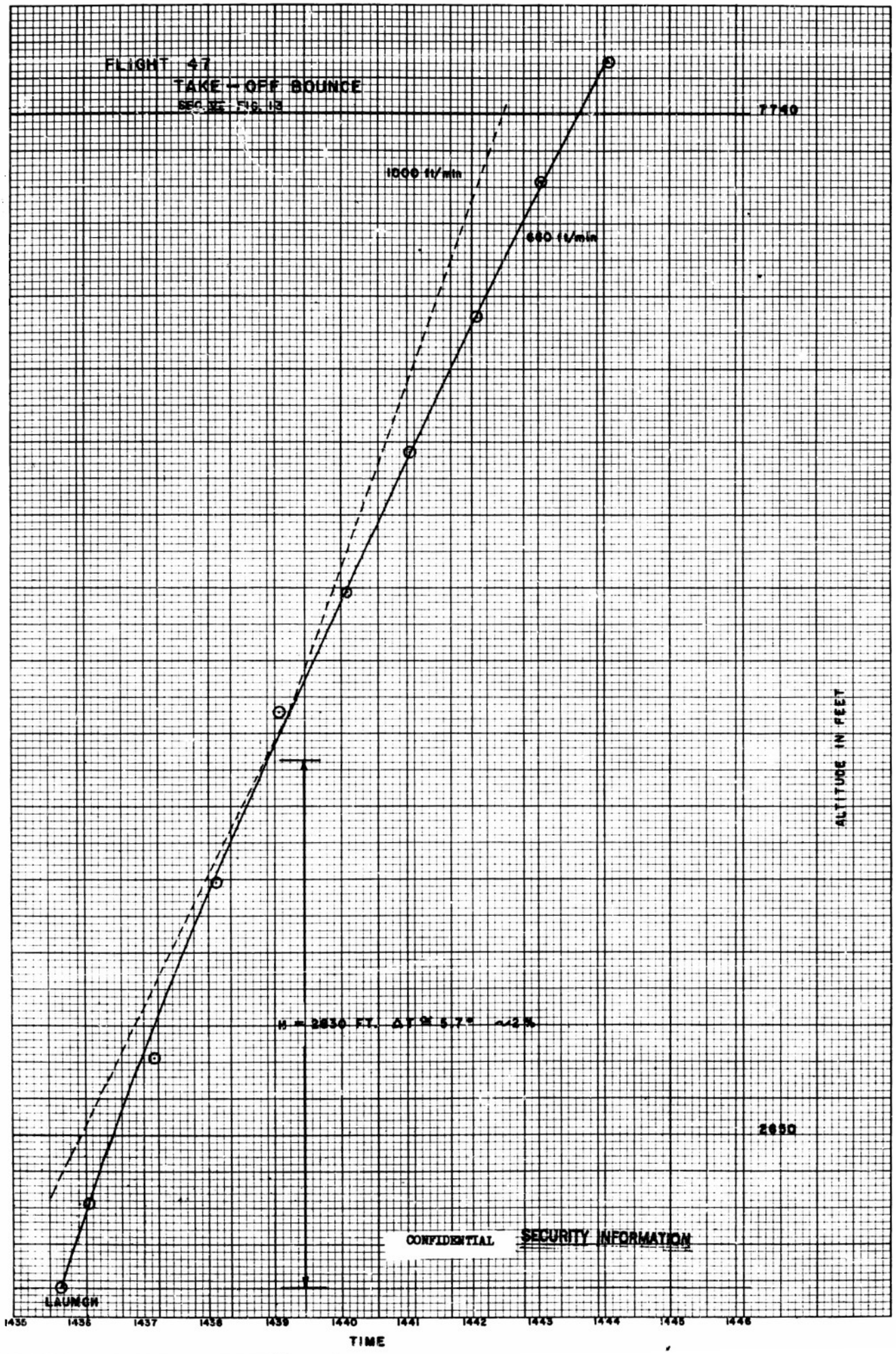
FLIGHT 47
TAKE-OFF BOUNCE
SEC XE, Fig. 13
7740
1000 ft/min
660 ft/min
h = 2830 FT. Δγ ≅ 5.7° ~2 %
2830
ALTITUDE IN FEET
CONFIDENTIAL SECURITY INFORMATION
LAUNCH
1435
1436
1437
1438
1439
1440
1441
1442
1443
1444
1445
1446
TIME

If one then assumes that the free lift is given at any altitude it is possible to calculate from an equation including both the thermodynamic and aerodynamic drag what velocity will result. The equation which has had some success in explaining our results is:

$$\underbrace{P = C_1 (L+4)^{3/4} \frac{G^{1/4}}{T^{1/2}} v^{3/4}}_{\text{Thermodynamic drag}} + \underbrace{C_2 \frac{\rho^{1/3}}{T^{1/3}} G^{-1/3} v^2}_{\text{Aerodynamic drag}}$$

where P = per cent free lift of air displaced

L = atmospheric lapse rate in °C/1000 ft

G = air displaced in pounds

T = air temperature in °K

v = rate of rise in ft/min

ρ = atmospheric pressure in mb

$C_1 = 7.4 \times 10^{-4}$

$C_2 = 6.5 \times 10^{-7}$

The constants in this equation were determined from the free lifts and rates in flight #42 and from the average rate of rise for a balloon at take-off with known free lift. It should be emphasized that the equation which is presented here is considered to be a good approximation at the present time but it has not been possible yet to determine whether the equation needs to be modified depending upon whether the balloon is rising or falling and whether the equation can be used without regard to whether the balloon is rising or descending in day vs. night. The equation should therefore be used with some caution until it is possible for the project to answer a number of questions concerning restrictions on the use of such equations. Figure 14 is a graph which can be used in place of numerically solving the equation and is useful because it allows one to see what the relative contributions of aerodynamic and thermodynamic are at different altitudes and in the stratosphere and in the troposphere. The

PERCENT FREE LIFT OF AIR DISPLACED AS A FUNCTION OF VELOCITY, FOR THERMODYNAMIC AND AERODYNAMIC DRAG
SEC. VI FIG. 14

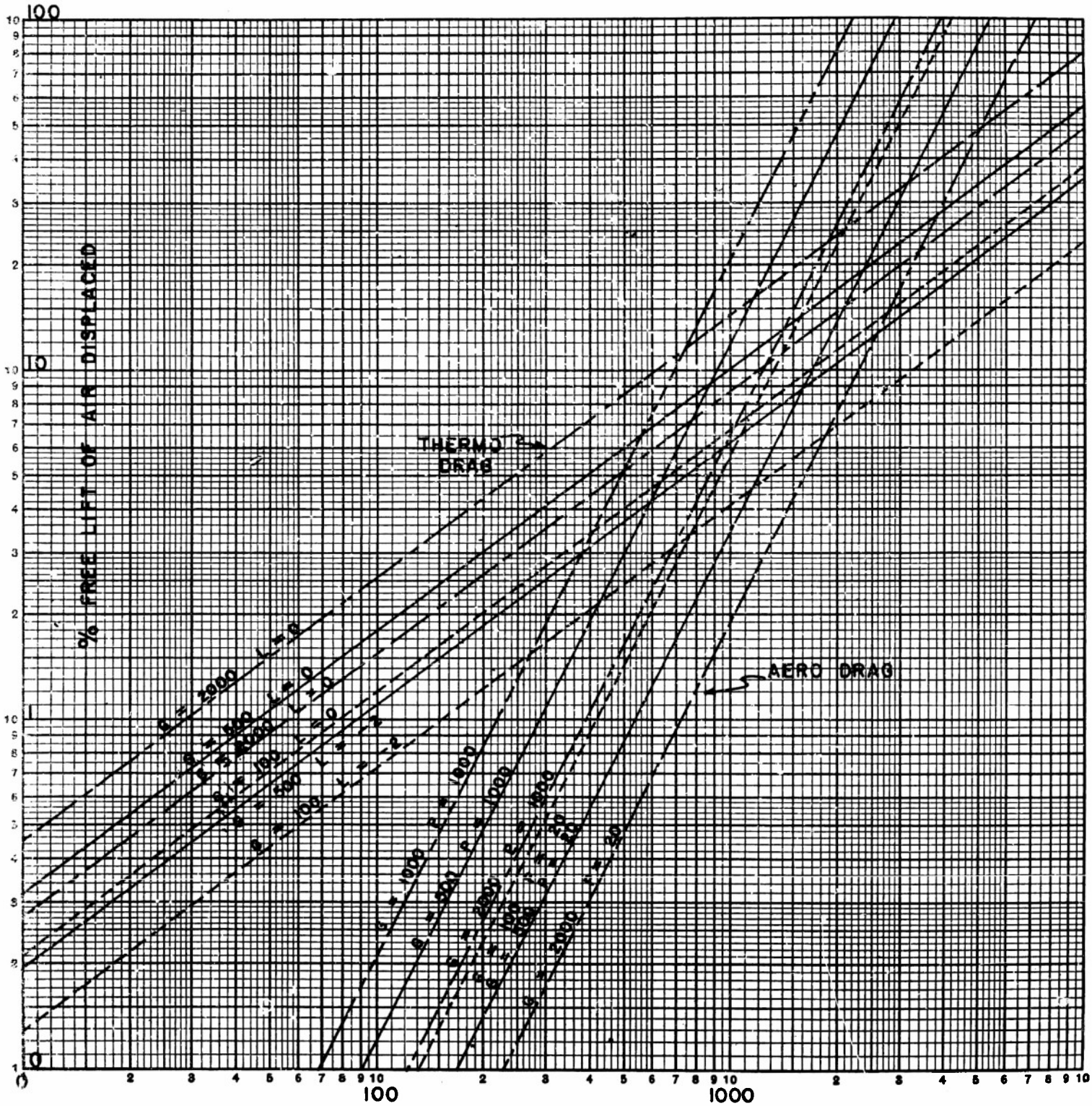

per cent free lift is plotted against the rate of rise on a series of curves. Each curve corresponds to a certain condition of gross load and lapse rate and pressure. Since the theory indicates that thermodynamic drag should be independent of pressure the quantities which are varied from curve to curve on the thermodynamic curves are lapse rate and gross load. The two values of lapse rate considered are -2° per thousand feet (troposphere) and 0° per thousand feet (the average stratosphere). The gross load is taken as 100, 500 and 2000 pounds. The aerodynamic drag curves are shown at pressures of 1000 mb and at 20 mb and at gross loads of 150, 500 and 2000 pounds. Since the aerodynamic drag does not depend upon the lapse rate this is not indicated on the aerodynamic drag curves. In order to use these curves one looks for example at the rate of rise and finds a corresponding percentage free lift represented as aerodynamic drag and the corresponding percentage free lift represented as thermodynamic drag. The sum of these two terms then is the total per cent free lift required to produce this rate of rise. To take a numerical example, suppose the rate of rise is 700 feet a minute, the pressure is 20 mb, the lapse rate is 0 and the gross load is 500 pounds. This is a common stratospheric condition. One reads from 700 feet a minute up to the proper aerodynamic drag curve and obtains a per cent free lift of 1.7%. The corresponding thermodynamic drag curve gives a value of 7.7% free lift in thermodynamic drag. Total drag is therefore 9.4%.

Experiments are in progress to improve the knowledge of the equation of motion of the balloon and it is hoped that more detailed information will be available in the next report.

SECTION VII

INSTRUMENTATION

The instrumentation section during the period of flights #21 to #55 has been concerned approximately equally with the development of new apparatus and improvement of apparatus used previously. Since this development and improvement was a continuous process few successive flight gondolas contained identical components and no components remained unchanged during this period. The method of construction of gondola equipment used in this project is a multi-unit method in which each unit completely serves one purpose and is separate from the other units except for keying and power. This method allows assembly of different purpose gondolas from standardized units with a minimum of time necessary for design and construction between flights and allows quick replacement of equipment found faulty at check-out or after recovery. This technique necessitates heavy construction in that connectors, wire, mounting plates and covers are duplicated.

The largest proportion of developmental effort during this period was spent on the flight constants gondolas flown on flights #31, #32, #35, #42, #51 and #54 (see Figure 1). These flights required a balloon valve and a packaged ballast dropper operated by radio command. In order to be assured of proper radio control and to allow for proper tuning of the ground transmitter during flight it was desired that a signal be sent by the gondola to indicate operation of the equipment. A continuously generated Morse code signal which keyed the radio transmitter when the command equipment was operated was developed to do this. Since the receiver to be used contained only two command channels, a limitation imposed by the resonant relay filters used to control operations, and there were three command operations desired (valving, ballasting and flight termination) the ballast dropper was used to furnish the flight termination impulse. Because of the complexity of the inter-relations between the various units the inclusion of a distribution box became necessary. It allowed multiple

interconnections to be made with both ease and speed and with a degree of standardization between flights not obtainable when each gondola was wired for a particular flight.

Another important development in this period was that of a small gondola for light weight flights. These gondolas were less than a quarter of the volume of our standard gondolas and therefore could be used only for the basic minimum of flight control and telemetering equipment. No experimental or developmental apparatus could be contained in them. The weight of these gondolas complete is roughly 1/3 of a similar large gondola.

A third development worthy of mention was that of a pressure operated sequence ballast dropper. Three different techniques of electrically keying ballast drops from the mechanical motion of a bellows were used before a reliable, easily set, and accurate mechanism was found. Another new development was that of a recording device to keep a record in the gondola of the telemetered signal in case the radio signal was lost during the flight. This signal was recorded on the camera films.

A. Flight Control Equipment

1. Safety devices. On all of the flights indicated in column 2 in Figure 1 blinker beacons were flown. The remainder of the flights which have no blinker beacon indicated were shorter than one day and were both launched and brought down in daylight. The type of blinker beacon used for the most part during this period was a commercially made flashing truck flare made by the Dayco Company of Dayton, Ohio. This company unfortunately has gone out of business and while we were able to obtain eight of their flares, over a period of time these eight flares were lost or destroyed in flight and we were not able to replace them. These flares are based on a mechanically oscillating mechanism driven by an electromagnet lighting three incandescent bulbs. The current drain on the self contained battery was very low and this flasher has been checked out in

Summary of Equipment Contained in Gondolas
Flights 21 - 55

Flight No.	(1) Gondola	(2) Blinker Beacon	(3) Blow-Down Box	(4) Cameras	(5) Telemeter Film Recorder	(6) Barothermograph	(7) Ballast Dropper	(8) Ballast Tank, Level Recorder & Xmitter	(9) Balloon Valve	(10) Signal Coder	(11) Distribution Box	(12) Strobe Flasher	(13) Xmitter Cycler	(14) Photo Recording Ammeter	(15) Thermister Photo Recorder	(16) Cosmic Ray Plates
21	L	I	A,T	U,D		S										X
22	L	I	A,T,C	U,D		S		X								X
23	L	I	A,T,C	U,D,H		S	C									X
24	L	I	A,T,C	U,D,H		S	C				X					X
25	L	I	A,T,C	U,D,B		S		X								X
26	L	I	A,V,C	U,D,H		S	C				X					X
27	L	I	A,V,C	U,D,H		S	C				X					X
28	L	I	A,V,C	U,D,H		S	C				X					X
29	L	I	A,T,"	U,D		S		X	X		X		X			
30	S		A,T			S										
31	L	I	A,T,V	U,D,H		S	C		X		X					
32	L	I	A,V,C	U,D		D	C		X	X	X					
33	S		A,T			S										X
34	S		A,T			D										X
35	L	I	A,V,C	U,D		D	C		X	X	X	X				
36	L	I	A,V	U,D		D										
37	L	I	A,V	U,D		D										X
38	L	I	A,V,C	U,D		D	C		X	X	X					
39	L	I	A,V	U,D		D	C				X					X
40	L	I	A,V	U,D		D	C				X					X
41	L	I	A,V,C	U,D		D	C		X	X	X					
42	L	I	A,V	U,D	D	D	P									X
43	L	I	A,V	U,D		D										X
44	L	I	A,V	U,D	D	D	P									X
45	L	I	A,V	U,D	D	D	P									X
46	L	G	A,V	U,D	U,D		P								X	X
47	L	I	A,V	U,D	U,D		P									X
48	L		A,V	U,D	UD,R		P							X		
49	L	G	A,V	U,D	U,D		P					X				X
50	L	I	A,V	U,D	U,D		P									X
51	L	G	A,V,C	U,D	U,D		C		X	X	X					X
52	S	G	A,V	U,D	U,D		P									X
53	S	G	A,V	U,D	U,D		P									X
54	L	G	A,V,C	U,D	U,D		C		X	X	X					
55	S	I	A,V,F	U,D	U,D		P									

Note: All flights contained in addition to the above, Olland Cycles, Antenna droppers, and Radio gear.

Column	1	L = Large S = Small
"	2	I = Incandescent G = Gaseous
"	3	A = Low Altitude Release T = Timers V = Low Voltage Release C = Radio Command F = Film Blowdown
"	4	U = Uo D = Down H = Horizontal B = Balloon Crown
"	5	U = Up camera D = Down camera R = Photo Recording Ammeter
"	6	S = Single Bellows D = Double Bellows
"	7	C = Radio Command P = Pressure operated
"	8-16	X = Presence of indicated apparatus

laboratory to operate for more than one week at temperatures below those encountered in flight. A number of thermally operated flashers were tested in the laboratory but none of them would operate at low temperatures. The inclusion of three bulbs in this particular model was found to be desirable because on several flights after recovery it was found that one or in extreme cases two bulbs had been burned out or broken during flight. On the latter flights shown in the table in Figure 1, column 2 a simple RC circuit operating a gaseous discharge tube at 300V was built in the laboratory and used as a blinker beacon. This flasher had a number of disadvantages in that the cost was approximately $14.00 per flasher not including the labor to construct it, their light intensity was not as great as that of the incandescent type, and changing of the battery was extremely difficult, because the mechanism was potted in order to avoid arc over at high altitudes. Since the period covered by this report a mechanism similar to that used in the Dayco flasher has been constructed in the shop.

2. Blow down box. The blow down box used in these gondolas is shown in Figure 2 and the wiring diagram is given in Figure 3. This blowdown box is a multi-purpose unit which contains six different methods for accomplishing flight termination. The first and most important method is the low-altitude release which has been described in the first Progress Report, (Section V, p 1,3, Appendix 2 p 7-9, Appendix 11, BA 410-D). No changes in this mechanism have been made during this time. A new method of blow down has been included in this box which will release the flight when the main 6V batteries in the gondola have reached the break in their discharge curve. Since it is not advisable to keep a gondola in the air after the equipment in it no longer can function properly this circuit was included. The basic element in this circuit was a surplus ultra-sensitive relay found

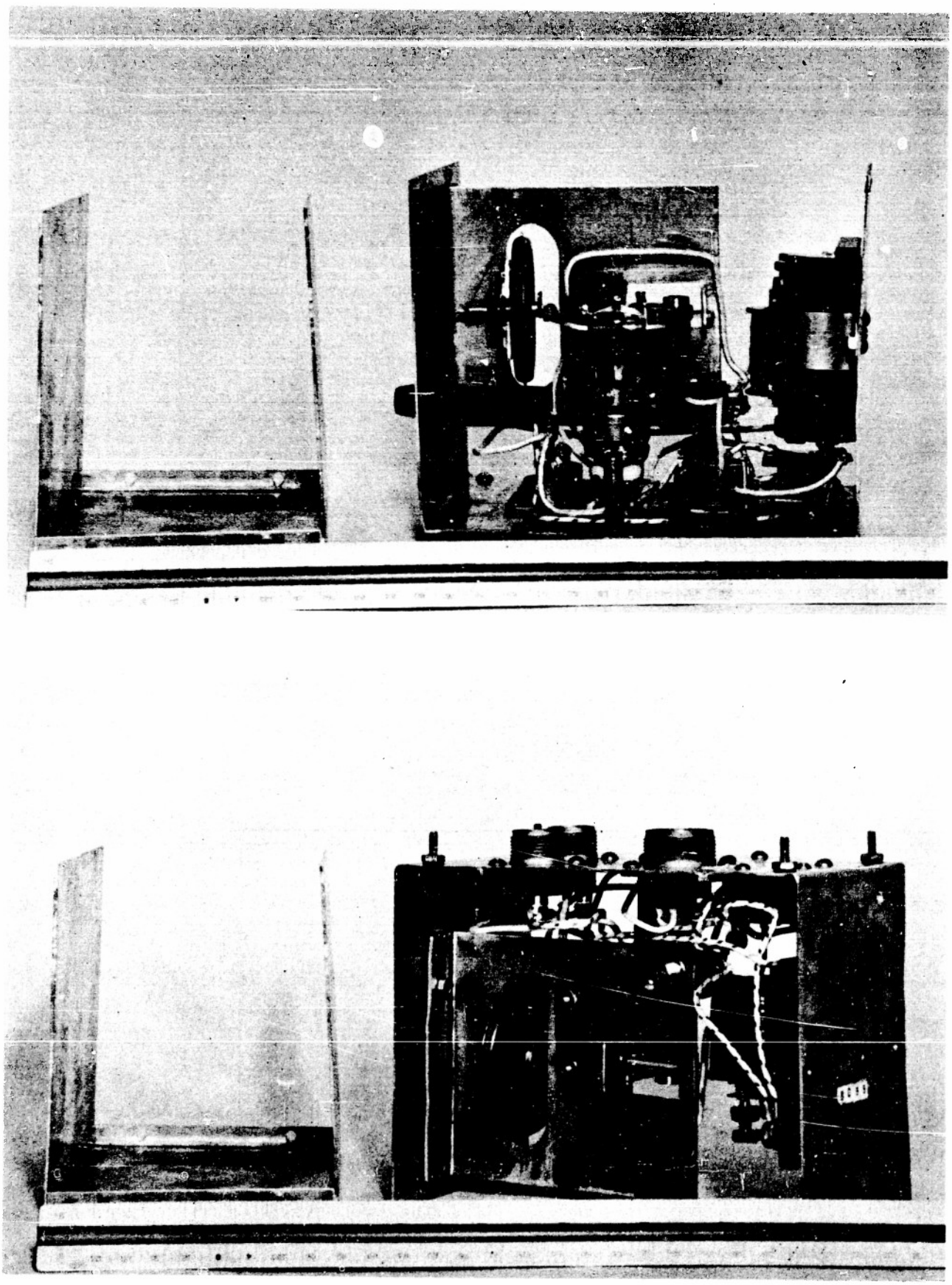

Sec VII Figure 2. Blow-down box, right and left views

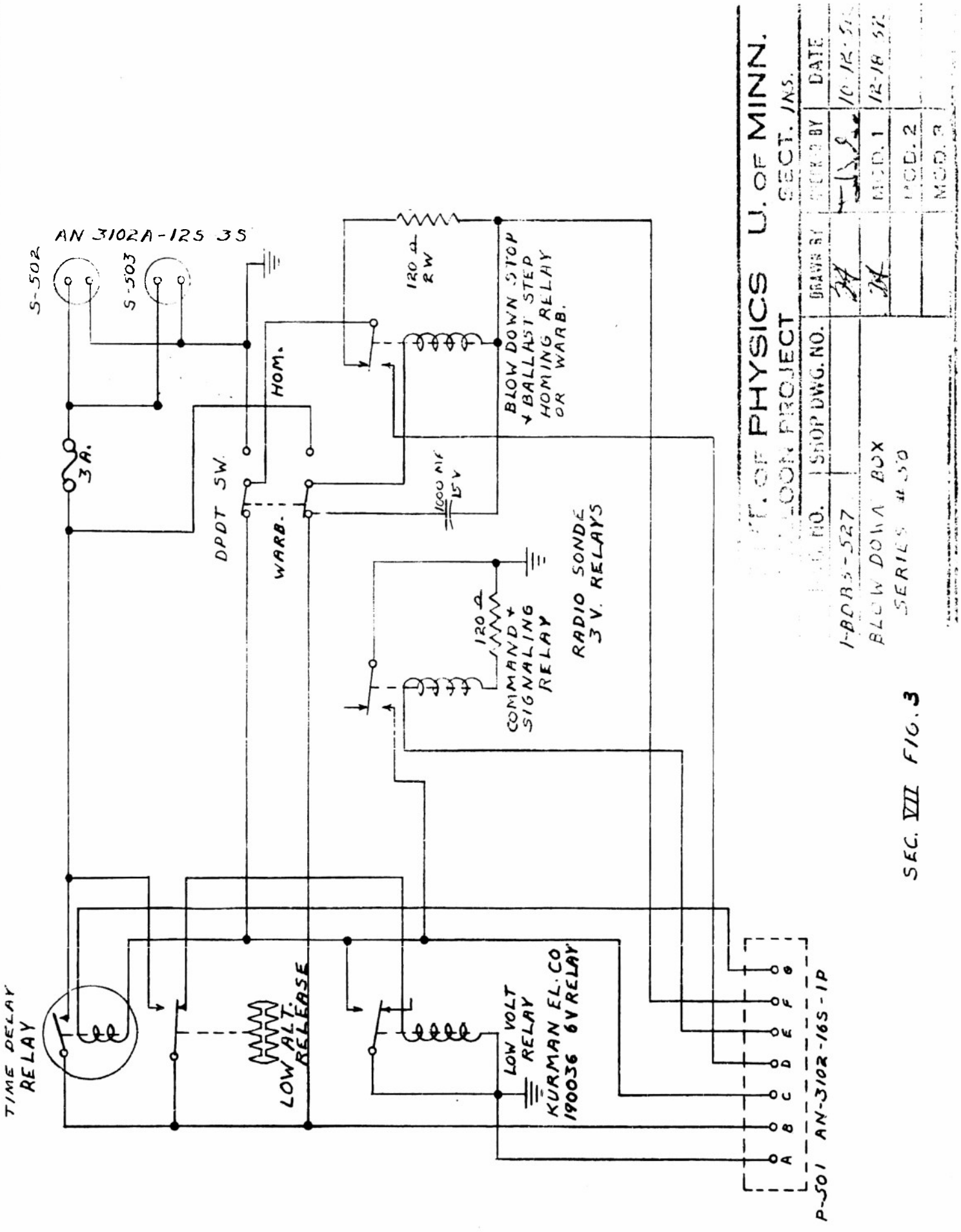
AN 3102A-12S 3S
S-502
S-503
3A.
DPDT SW.
HOM.
WARB.
120 Ω 2W
BLOW DOWN STOP
BALLAST STEP
HOMING RELAY
OR WARB.
1600 MF 15V
120 Ω
COMMAND
SIGNALING
RELAY
RADIO SONDE
3 V. RELAYS
TIME DELAY
RELAY
LOW ALT.
RELEASE
LOW VOLT
RELAY
KURMAN EL. CO
190036 6V RELAY
P-501 AN-3102-16S-1P
A B C D E F G
U. OF MINN.
DEPT. OF PHYSICS
SECT. INS.
LOOK PROJECT
SHOP DWG. NO.
1-BOR3-527
BLOW DOWN BOX
SERIES 4 50
DRAWN BY
CHECKED BY
DATE
MOD. 1
MOD. 2
MOD. 3

SEC. VII FIG. 3

in the stockroom of the Physics Department and which bore no markings as to manufacturer or origin. It seems that this relay may be the same as the Kurman Electric Co. of New York, model 190036, but as yet we have not had an opportunity to check with this manufacturer. On several flights in the series this relay was used as a timing device (column 3, Figure 1) by the inclusion of a resistor in the 6V circuit which would time the discharge of the battery so that the flight could be terminated by the low voltage relay at a calculated time.

Another input to this box allowed blowdown of the flight by three different techniques. A negative key from radio command, timers similar to the clock timers described in the first Progress Report, or the film blowdown could be fed directly into this terminal for termination. The sixth method of blowdown input was used only with the sequence ballast dropper flown in the flight constants flights. Without undue complication the circuitry in the ballast dropper could only furnish a positive key.

Another feature of this blow down box which has been mentioned in the first Progress Report (Section V, p 6) was a blowdown warning transmitted for one minute before the flight was terminated. This delay which was not wired into the low altitude blowdown was originated by a temperature compensated thermal time delay relay and the warning signal was generated by a 3V Radiosonde relay made by Price Electric Company in an RC circuit. This pulsing relay, when the blowdown box is used with the sequence ballast dropper in a flight constant flight, motors the sequence ballast stepper to the blowdown position.

3. Ballast droppers. The sequence ballast dropper flown in the flight constants flights is shown in Figure 4 and the wiring diagram is given in Figure 5. The basic element of this ballast dropper is a 2-bank 24 volt dc telephone stepping relay of the type made by Automatic Electric Company.

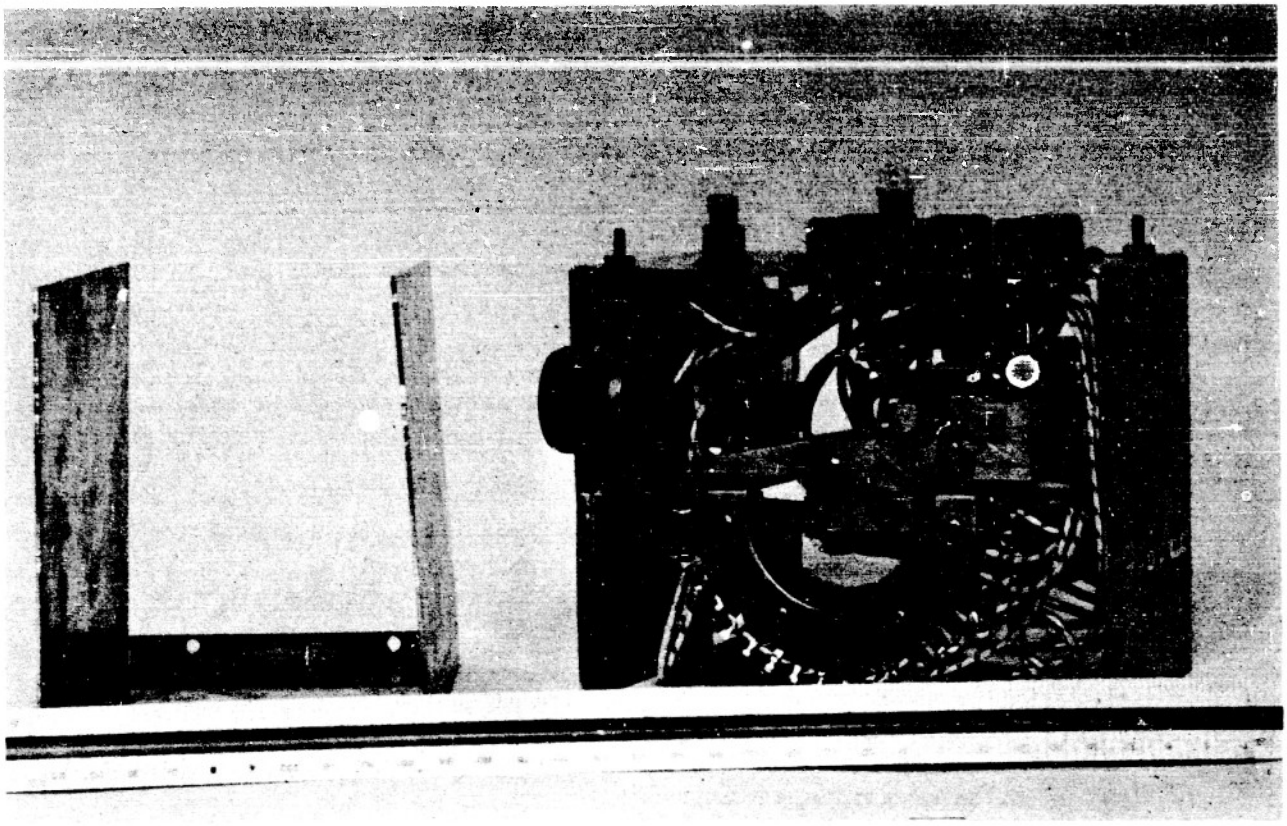

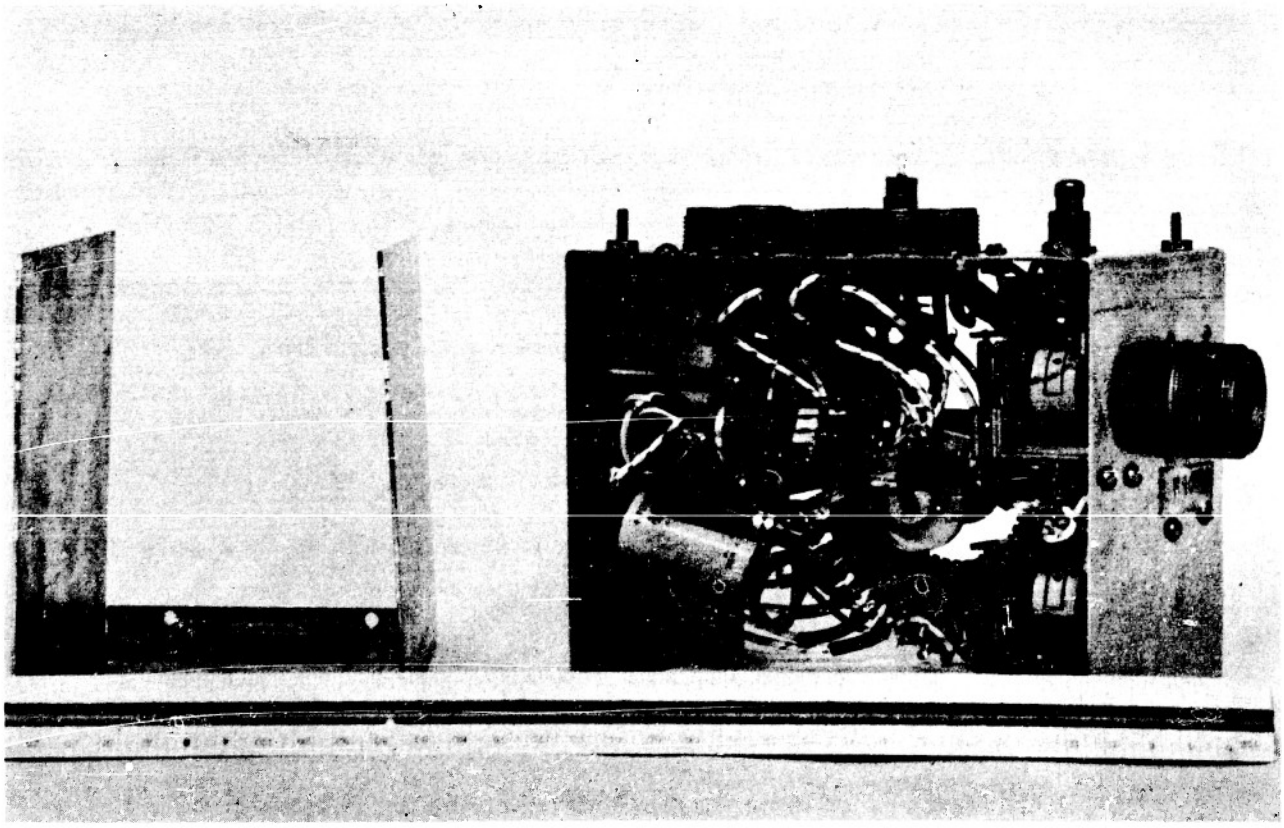

Sec VII Figure 4. Sequence ballast dropper command operated. Right and left views.

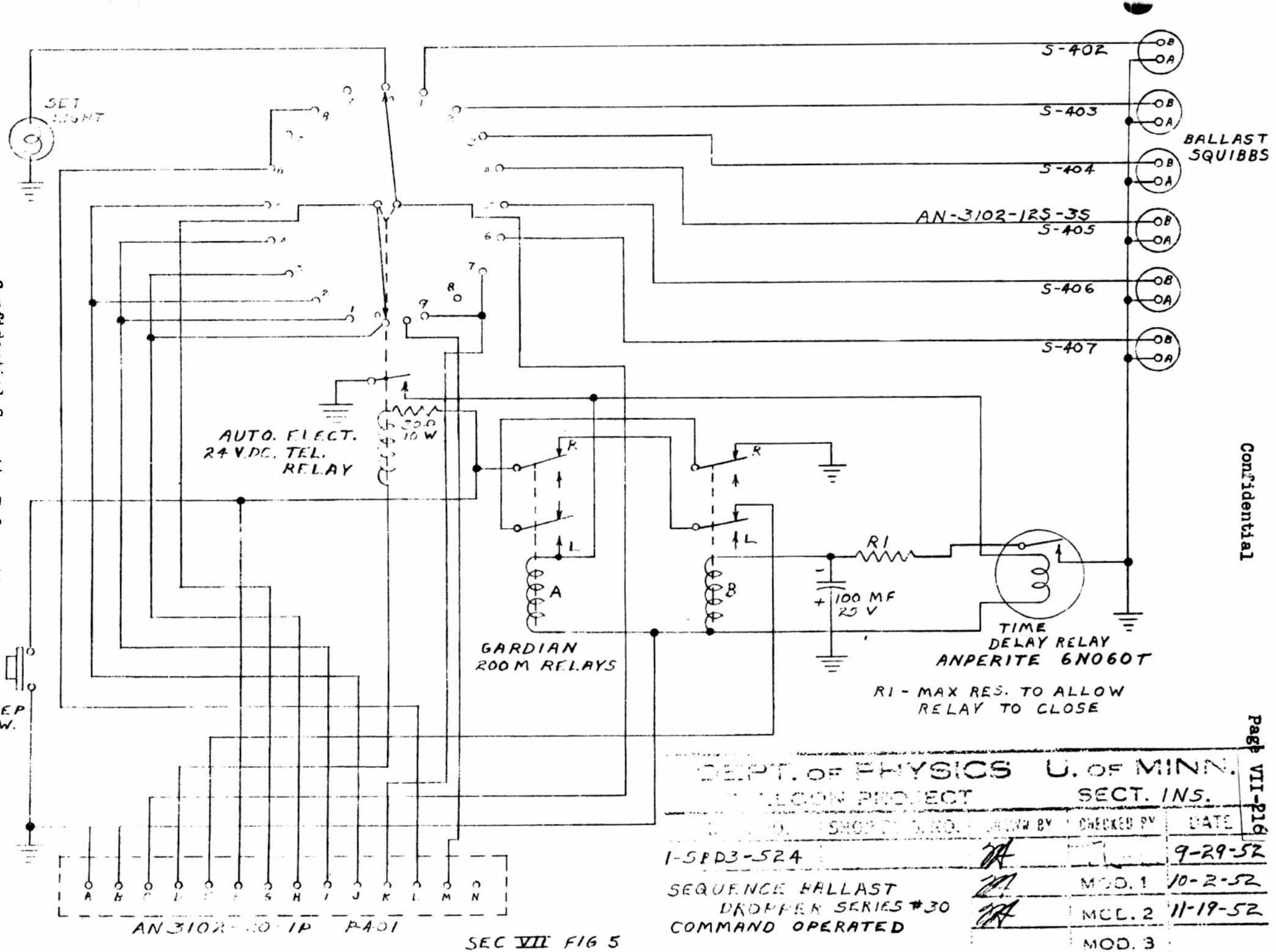

SEC VII FIG 5

DEPT. OF PHYSICS U. OF MINN.
SECT. INS.

	DRAWN BY	CHECKED BY	DATE
1-SRD3-524			9-29-52
SEQUENCE BALLAST DROPPER SERIES #30 COMMAND OPERATED		MOD. 1	10-2-52
		MOD. 2	11-19-52
		MOD. 3	

Each command impulse transmitted from the ground by the receiver control steps this relay one step and immediately pulses whatever is connected to that step. The second bank of contacts furnishes a negative key through the coder to the transmitter to signal which step the relay is on. This signal is only transmitted when the receiver picks up an impulse from the ground transmitter. Since it was found on flight #35 that an intermittant radio signal could key the ballast stepper several steps, an anti-chatter circuit was included thereafter, based on a time-delay relay of the thermally compensated type which would prevent the stepping relay from moving more than one step at a time. However, the time delay relay was found to arc on make and break, originating its own chatter, and therefore a second circuit was found necessary to prevent this. The final model has a 1 minute delay after the first momentary impulse and then a second delay of approximately 17 seconds while the time delay relay cools down and opens the circuit for further operation.

An early cutdown on flight #41 before all the ballast sacks were blown was found to have caused a ripped parachute, therefore in addition an unloader circuit was included to blow all of the ballast sacks when the flight termination squibs are fired. The blow down warning relay in the blowdown box was wired around the anti-chatter circuit and used as a motor to step the telephone relay around to blowdown position. Since voltage is left on the termination squibbs after blowdown the stepping relay must be stopped to prevent obscuring the altitude signal and this is accomplished by shorting out the step beyond blowdown. This unloading process takes less than one second and the ballast sacks are all blown before the parachute can open. This method of blowdown works for all techniques of flight termination including low-altitude release. The flight termination warning circuit in the blowdown box is not used on flight constants flights to send termination warning; instead this warning originates in the signal coder when it is keyed by the blowdown box.

A pressure operated sequence ballast dropper developed during this period is shown in Figure 6 and the wiring diagram and shop construction diagrams are shown in Figures 7 and 8. This type of ballast dropper uses a Friez Radiosonde Linear Bellows Movement type 515307-2 with a special lucite plate and contact assembly substituted for the printed scale. In action the bellows arm moves along a bar until it drops off the end at high altitude onto the lucite plate. On any subsequent loss of altitude the arm moves down the scale and touches the first contact firing a ballast squib. If descent continues the arm then touches the second ballast contact and that ballast package is fired also. Fuses were included in this circuit because two flights were recovered with the insulation melted from the squib leads due to a short circuit after the ballast package squibs had been fired. This ballast dropper is very similar to that used by General Mills, Inc. for balloon control.

The ballast used for packaged drops is magnetic steel shot, Amasteel #330. This was used mainly because of its weight and because of its pouring qualities. The shot was weighed and poured into canvas sacks 10" in diameter and 10" high which had a 1000 pound nylon drawstring top closure which could be tied directly to the gondola. A two grain squib was taped to the center of the bottom of the sack and when fired blew the bottom off. However, flight #51 was recovered with 2 pounds of ballast still in one corner of a bag and for this reason the shape of the bottom has been changed so that it now is a flattened cone shape with the squib inside at the apex of the cone. This allows a funnel shape at the bottom of the sack and assures us of complete emptying of all ballast. The bags have a capacity of 40 pounds of shot.

Flights #22, #25, and #29 contained a ballast tank similar to that described in the First Report of this project (Section V p 5). There were no changes in the construction of the tank during this period but an improved magnetic

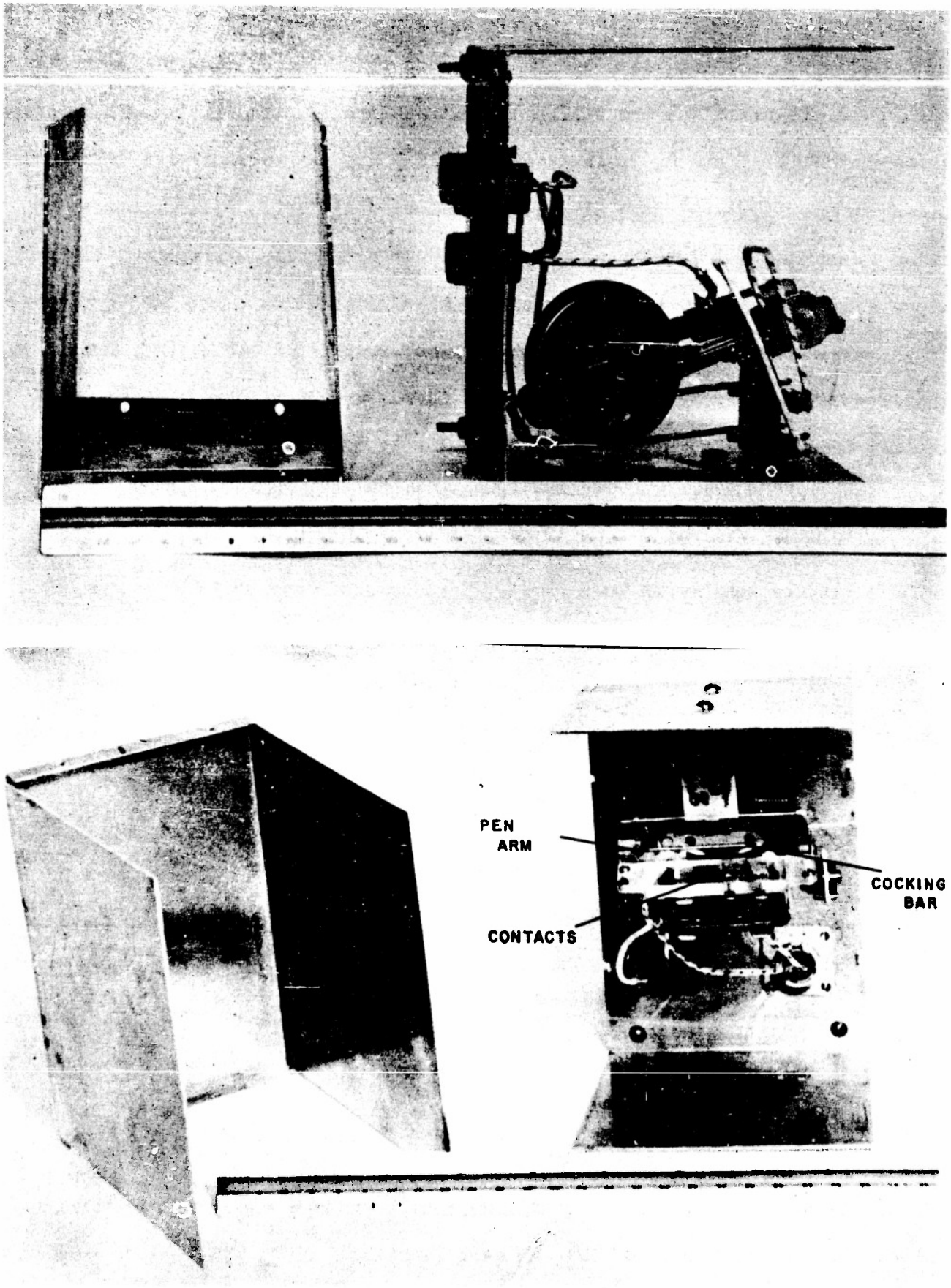

Sec VII Fig 6. Sequence ballast dropper, pressure operated.
Right side and bottom.

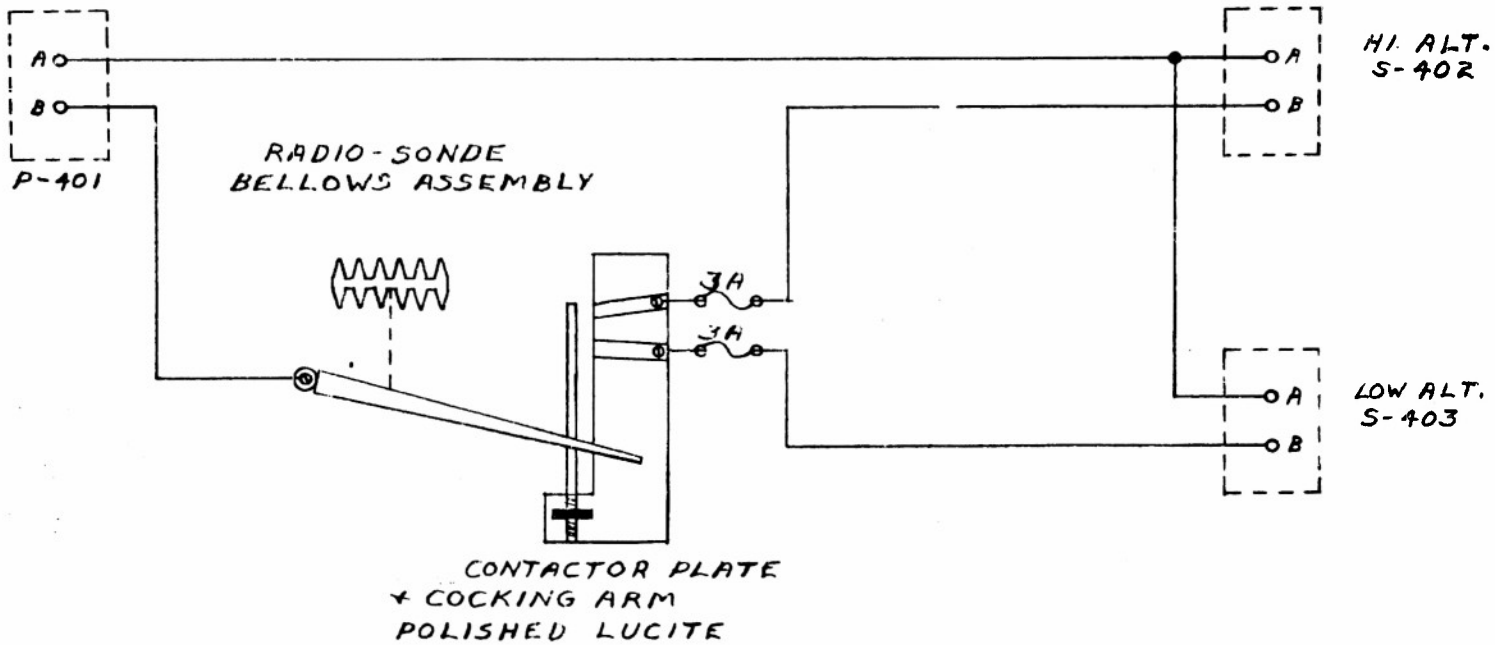

P-401 - AN-3102-12S-3P
S-402 & 3 - AN-3102-12S-3S

DEPT. OF PHYSICS U. OF MINN.
BALLOON PROJECT SECT. INS.

SHOP DWG. NO.	DRAWN BY	CHECKED BY	DATE
1-SBU 6-532	[illegible]	[illegible]	11-29-52
SEQUENCE BALLAST DROP SERIES # 60 (PRESSURE OPERATED)		MOD. 1	
		MOD. 2	
		MOD. 3	

SEC. VII FIG 7

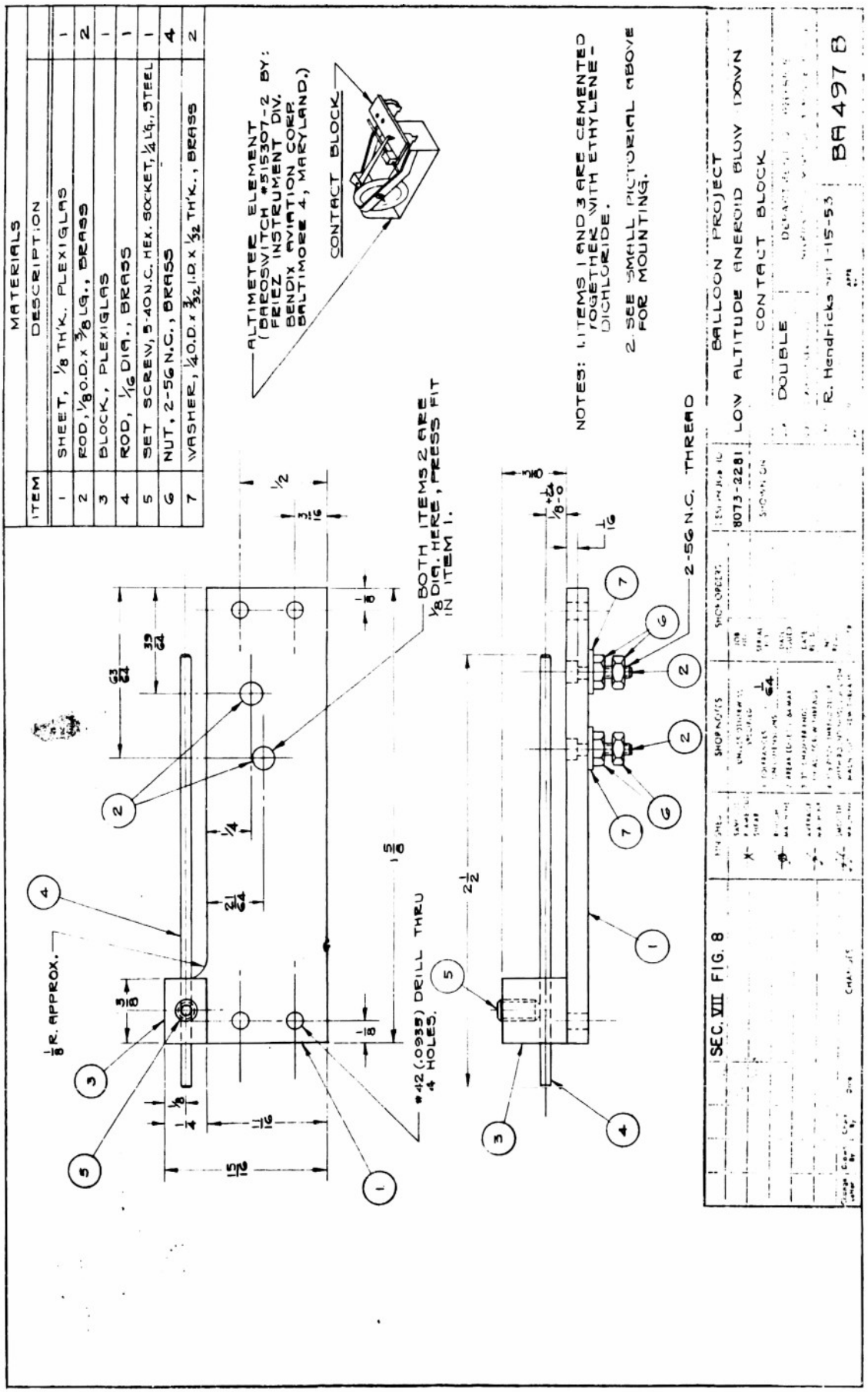
MATERIALS
ITEM
DESCRIPTION
1 SHEET, 1/8 TH'K. PLEXIGLAS 1
2 ROD, 1/8 O.D. x 3/8 LG., BRASS 2
3 BLOCK, PLEXIGLAS 1
4 ROD, 1/16 DIA., BRASS 1
5 SET SCREW, 5-40 N.C. HEX. SOCKET, 1/4 LG., STEEL 1
6 NUT, 2-56 N.C., BRASS 4
7 WASHER, 1/40 O.D. x 3/32 I.D. x 1/32 TH'K., BRASS 2
ALTIMETER ELEMENT (BAROSWITCH #515307-2 BY: FRIEZ INSTRUMENT DIV. BENDIX AVIATION CORP. BALTIMORE 4, MARYLAND.)
CONTACT BLOCK
NOTES: 1. ITEMS 1 AND 3 ARE CEMENTED TOGETHER WITH ETHYLENE-DICHLORIDE.
2. SEE SMALL PICTORIAL ABOVE FOR MOUNTING.
BOTH ITEMS 2 ARE 1/8 DIA. HERE, PRESS FIT IN ITEM 1.
2-56 N.C. THREAD
#42 (.0935) DRILL THRU 4 HOLES.
1/8 R. APPROX.
BALLOON PROJECT
LOW ALTITUDE ANEROID BLOW DOWN
CONTACT BLOCK
8073-2281
DOUBLE
R. Hendricks 11-15-53
BA 497 B
SEC. VII FIG. 8

valve (Figure 9) was designed for use with it. This valve uses the rotor magnet from a Brailsford motor to hold the steel shot in a magnetic gap in the tube. A coil is placed around the tube itself which, when energized, bucks the magnetic field of the permanent magnet and allows the shot to fall free. Average delivery rate is 1 kilogram per minute. The use of a magnetic valve with steel shot was suggested by the MOBY DICK Project.

4. Balloon valve. The balloon valve used in these flights was a plate valve operated by a reversible 27V dc motor andpowered by three wires taped along one of the balloon gores from the gondola. This motor is relatively slow, rotating at 270 rpm and it opens the plate to a distance of 1 diameter. The outside of the valve is covered with foam rubber to protect the balloon and through this foam rubber portholes are cut to equal the cross-sectional area of the valve. This valve was first developed in a 4" size which was flown in flights #29, #31, and #32. However, this size was found to valve too slowly for the desired results and a larger valve was built with a 9" opening which was flown on flights #35, #38, #41, #51 and #54.

During flight #35 it was discovered that the valve oscillated but did not open when radio command was attempted. This was traced to RF noise from the motor present in the control wires, paralleling the receiver antenna up the side of the balloon, blocking the receiver. Therefore the motor circuit was carefully grounded in the gondola, a special pi filter was installed across the motor and the valve circuit was altered so that once the valve was commanded it opened to its fullest extent and unless command was continued at that time, it closed automatically. This relieved the command receiver of the necessity of overriding any RF noise. On later flights this was discontinued because the grounding and filtering removed the noise completely. A bellows operated pressure switch was also installed which automatically opened the valve at a preset altitude in case radio command failed, but after the development of the duct appendix, the practice of tying off the balloon

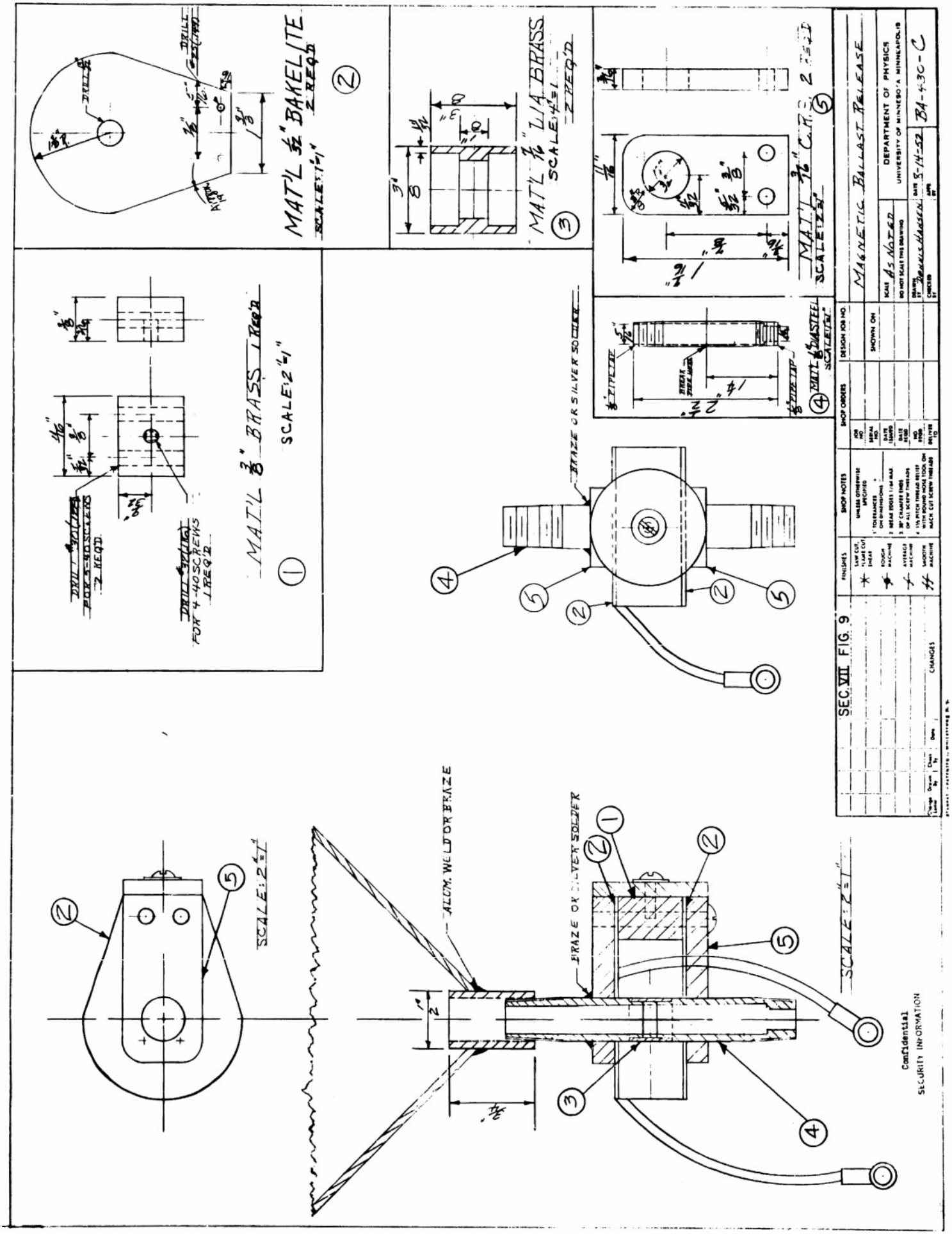
MAGNETIC BALLAST RELEASE
DEPARTMENT OF PHYSICS
UNIVERSITY OF MINNESOTA MINNEAPOLIS
BA-4-3C-C
SEC. VII FIG. 9
MATL 3/8" BRASS 1 REQ'D
SCALE 2"=1"
MATL 3/8" BAKELITE
2 REQ'D
SCALE 1"=1"
MATL 1/4" LUCITE
SCALE 1"=1"
MATL 1/16" CRES
SCALE 1"=1"
MATL 1/4" STEEL
SCALE 1"=1"
DRILL & TAP FOR 4-40 SCREWS 2 REQ'D
DRILL & TAP FOR 4-40 SCREWS 1 REQ'D
BRAZE OR SILVER SOLDER
ALUM. WELD OR BRAZE
BRAZE OR SILVER SOLDER
SCALE 2"=1"
SCALE 2"=1"
Confidential
SECURITY INFORMATION

no longer required this safety feature.

This large valve weighs seven pounds complete and the time to open it to its fullest extent is one minute. A picture of the large valve without its covers is shown in Figure 10 and the wiring diagram for the same valve is shown in Figure 11. Shop drawings are unavailable at this time.

5. Distribution box. The distribution box used in the flight constants flights is shown in Figure 12. The box wiring diagram is given in Figure 13. 157 terminals are connected to seven 5-pin connectors, one 7-pin connector, one 10-pin connector and three 14-pin connectors. Two special shorting plugs used to start the equipment before flight are included and one 18-pin test plug for checking battery conditions, operating equipment and testing keying circuits. Power input is through a permanently connected cable. Figure 14 is included to show a typical jumper circuit diagram for flight #51 and Figure 15 is the test unit used to check the circuits through the distribution box.

B. Flight Recording Equipment

1. Cameras. There have been very few major changes in the basic construction of the cameras since the last report. A minor change has been made in the design of the cam drive which triggers the shutter resulting in more positive action of this portion of the camera mechanism and all cameras now are driven by Brailsford motors, either 1 rpm or 1/5 rpm depending upon the length of flight. Because the film capacity of the camera is not more than 50 feet, a 1 rpm motor will allow ten hours of operation and a 1/5 rpm motor will allow 50 hours of operation. A picture of a down-camera open is shown in Figure 16 and a current wiring diagram for all cameras is shown in Figure 17.

A telemetering recorder has been developed and used on all recent flights. This recorder duplicates on film the signal sent over the radio transmitter thereby keeping a record of all the information which might be lost in case the

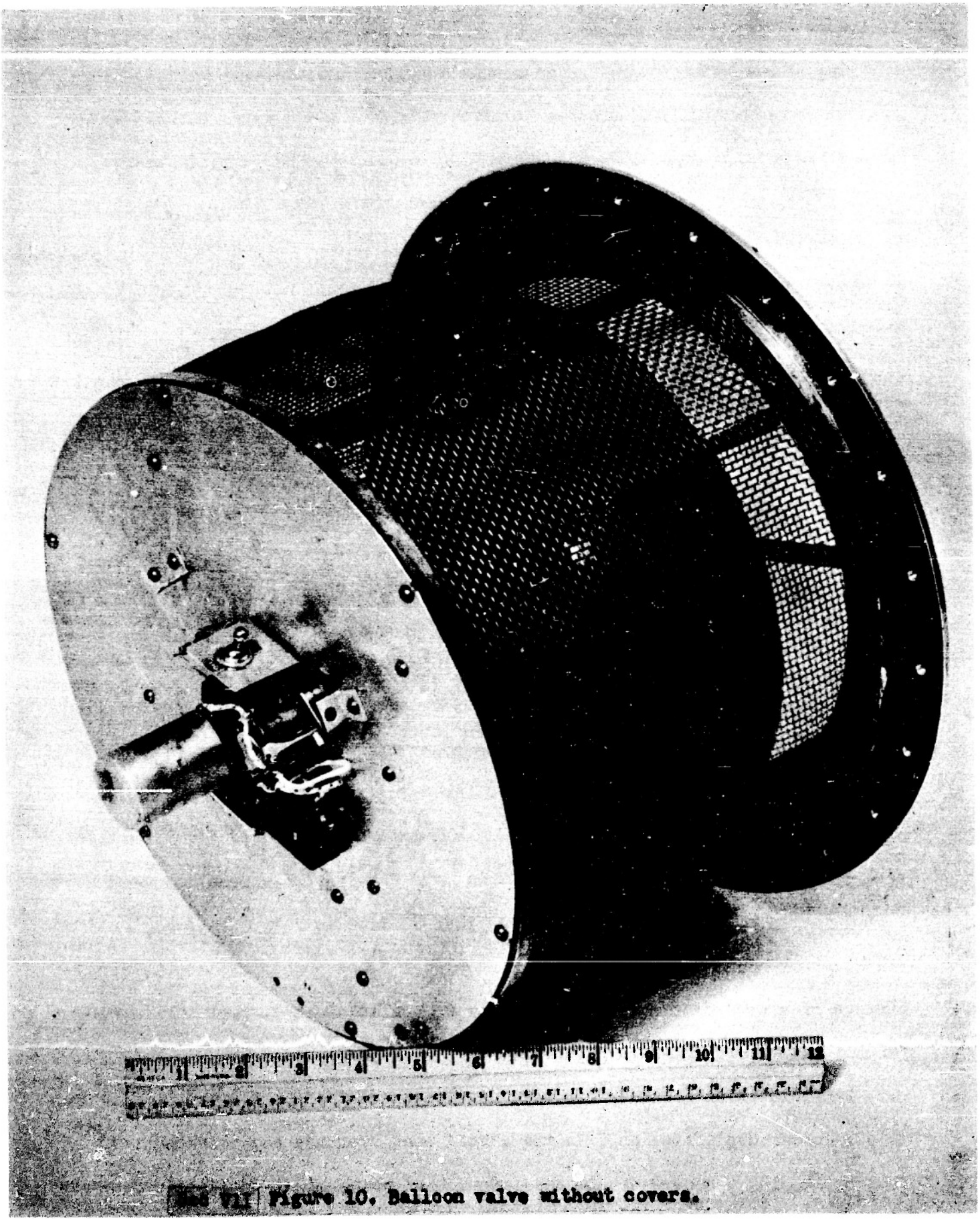

Figure 10. Balloon valve without covers.

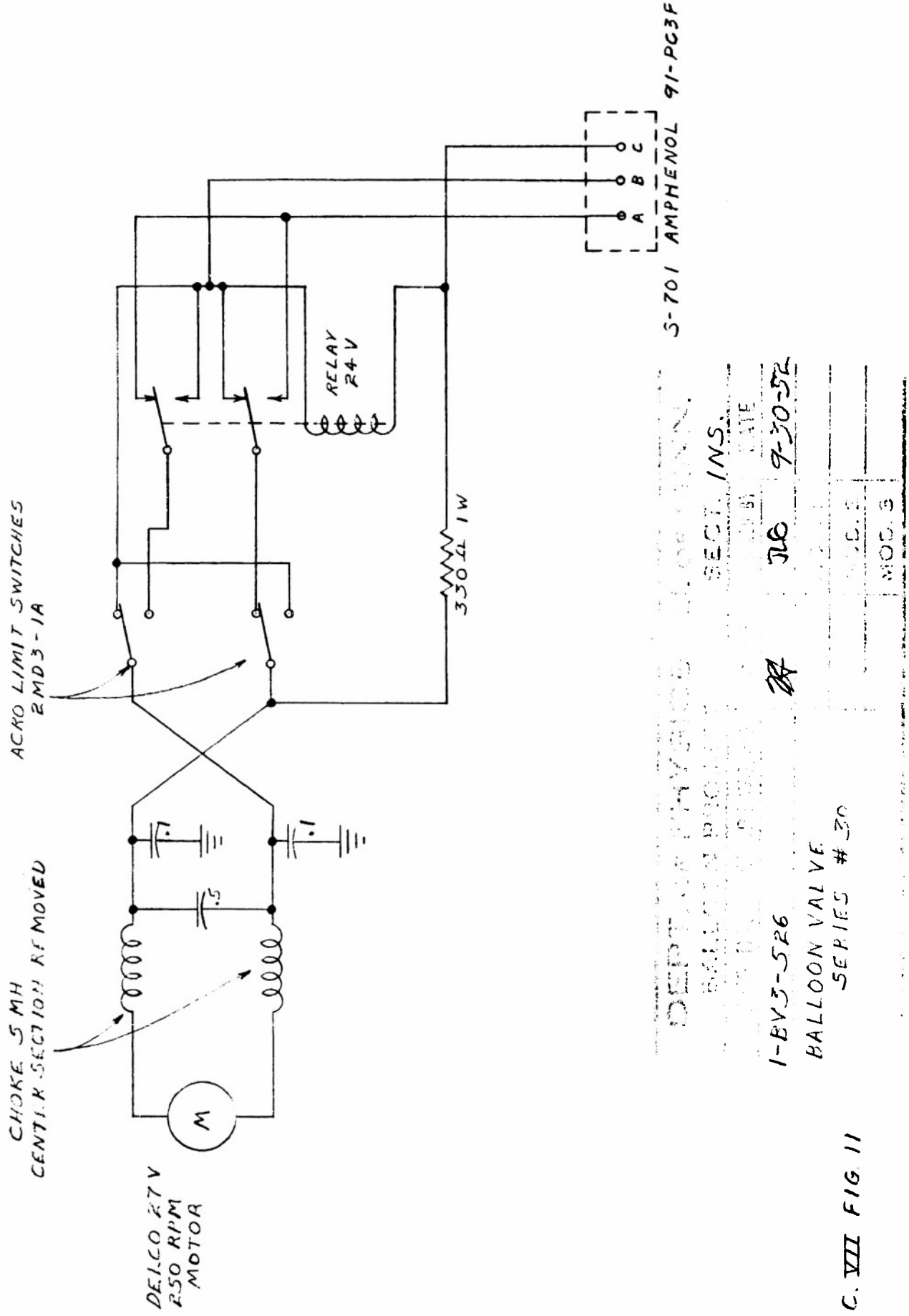

SEC. VII FIG 11

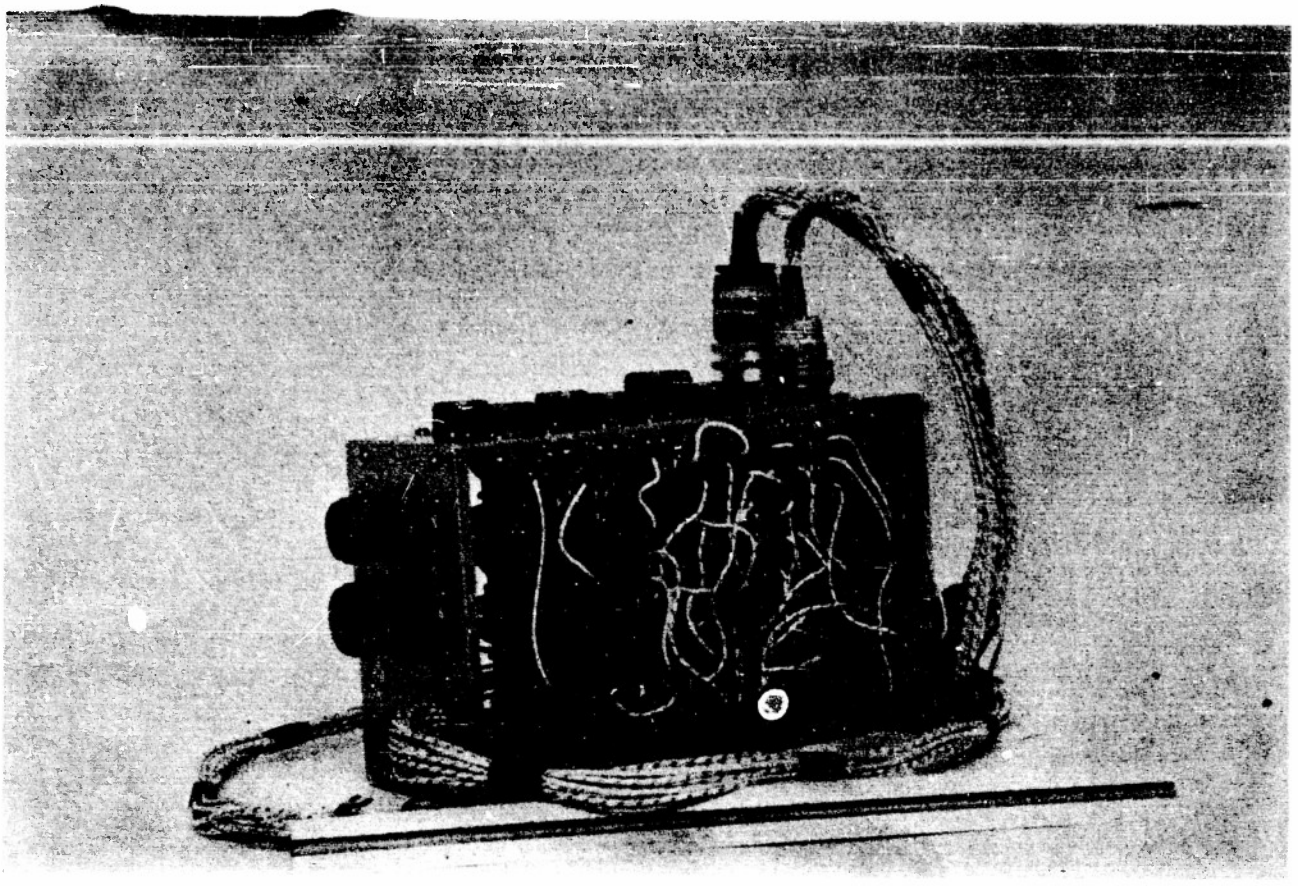

front

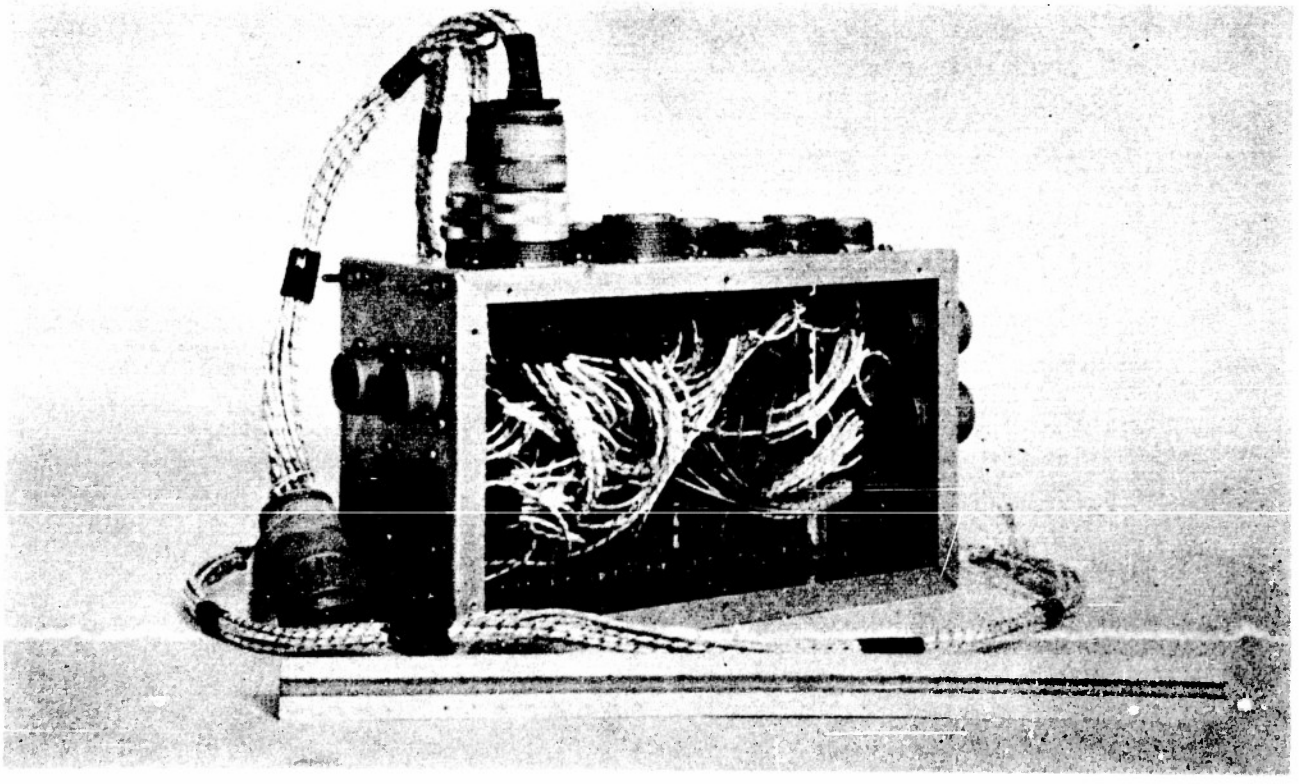

back

Sec VII Figure 12. Distribution box. Front and back view.

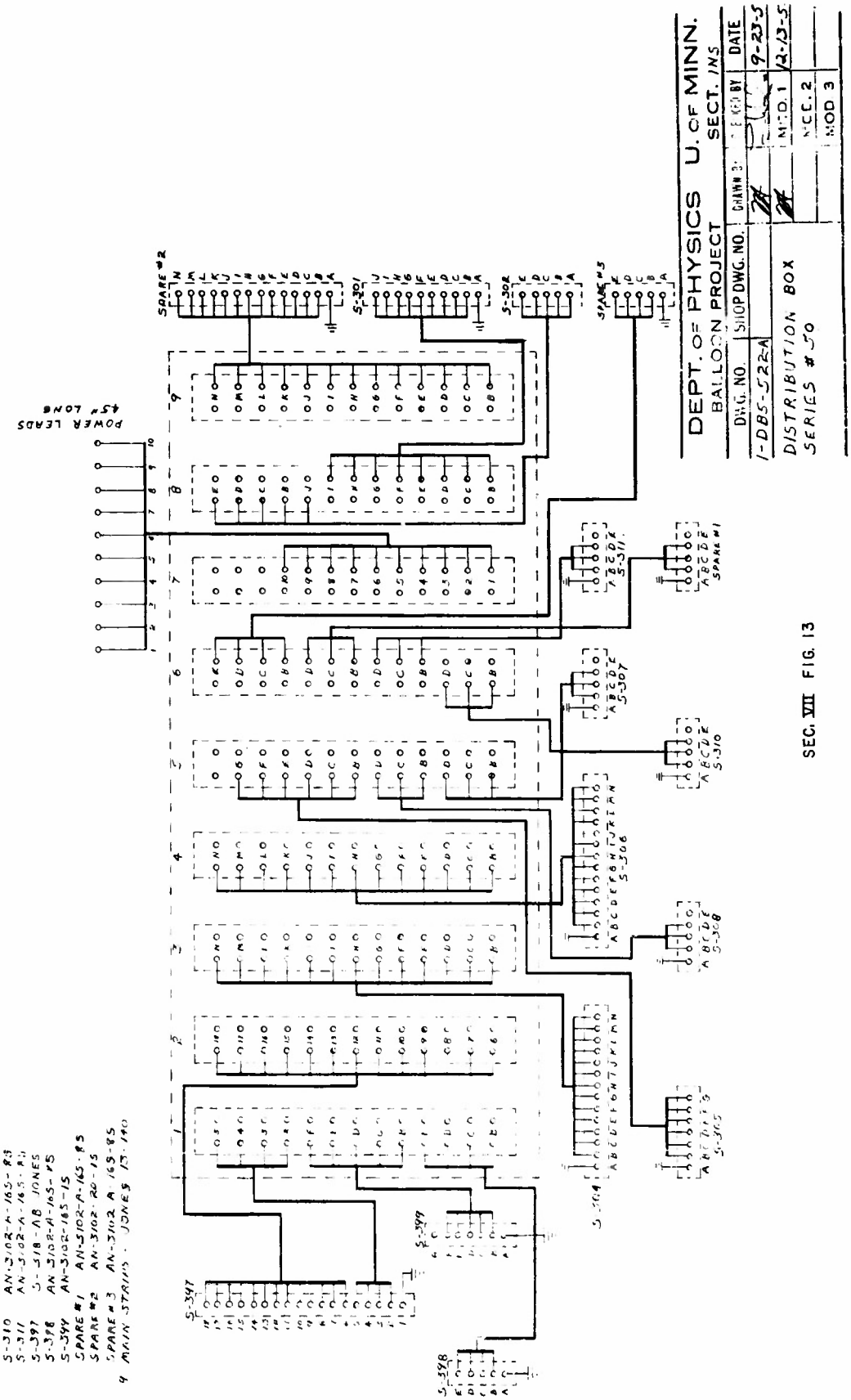

SEC. VIII FIG. 13

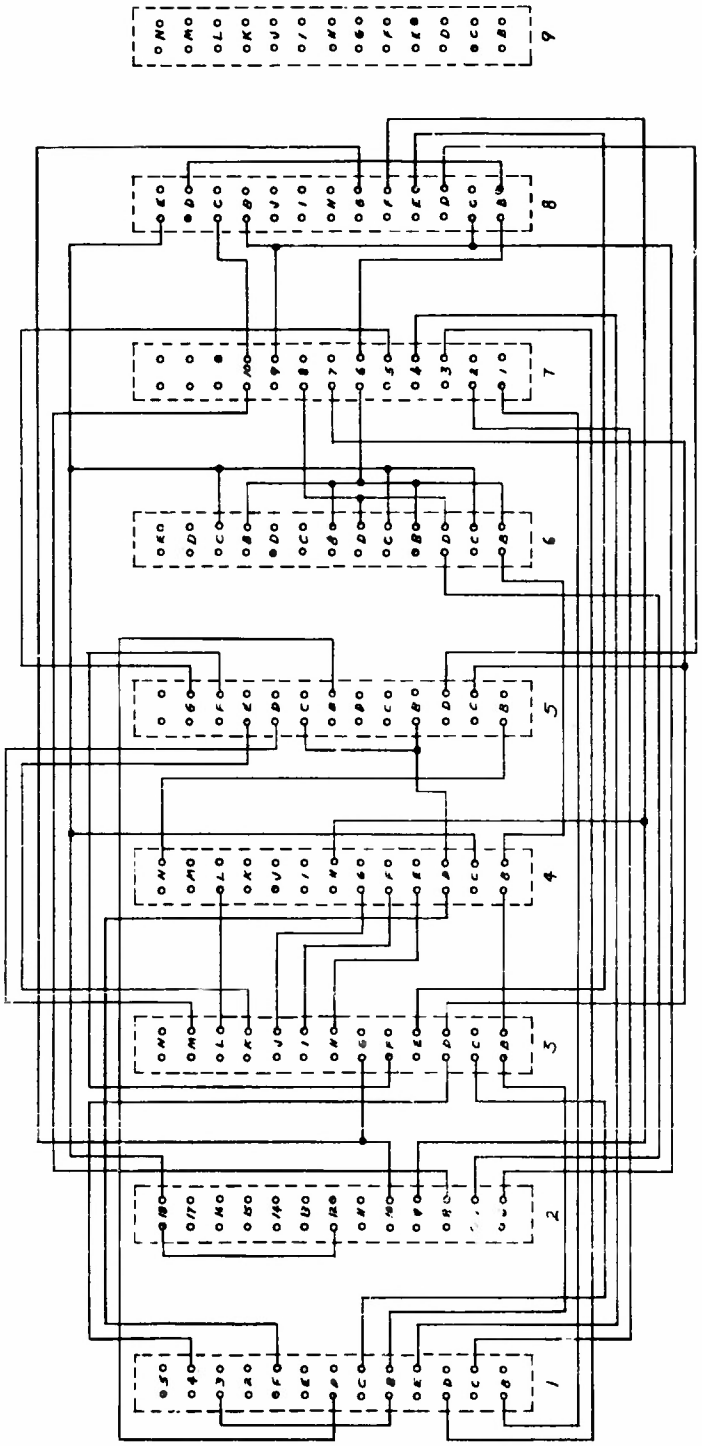

DEPT. OF PHYSICS U. OF MINN.
SECT. INST.
BALLOON PROJECT

DWG. NO.	SHOP DWG. NO.	DRAWN BY	CHECKED BY	DATE
1-DBS-522B				9-25-52

DIST. BOX SERIES #50
JUMPER CIRCUITS
FLIGHT # 51
GONDOLA # 30
DATE 11-24-52

MOD. 1	
MOD. 2	
MOD. 3	

SEC. VII FIG. 14

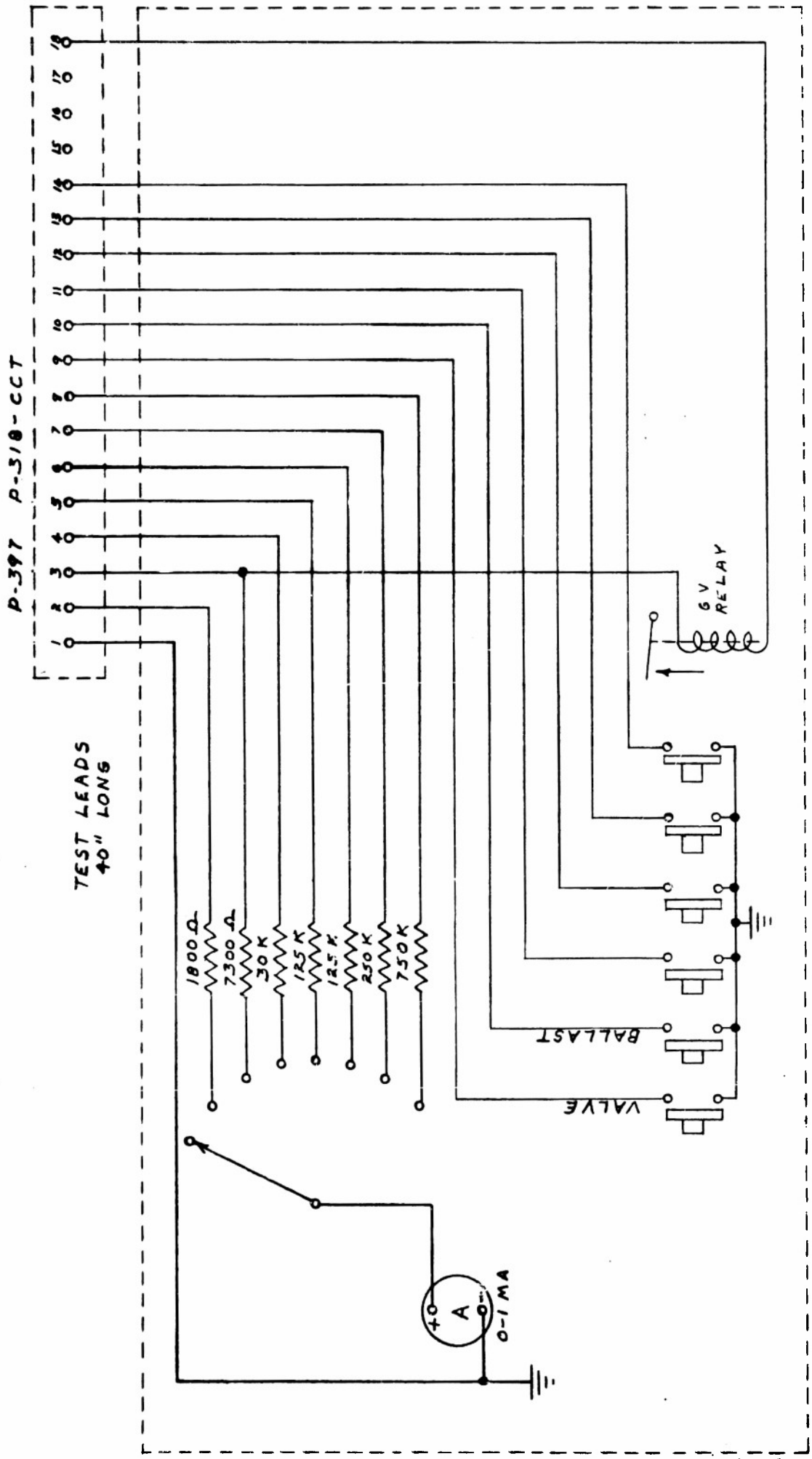

DEPT. OF PHYSICS U. OF MINN.
BALLOON PROJECT
SECT. INS.

DWG. NO.	SHOP DWG. NO.	DRAWN BY	CHECKED BY	DATE
4-TU2-523			JLG	9-24-52

PORTABLE TEST UNIT (GONDOLA)

MOD. 1
MOD. 2
MOD. 3

SEC. VII FIG. 15

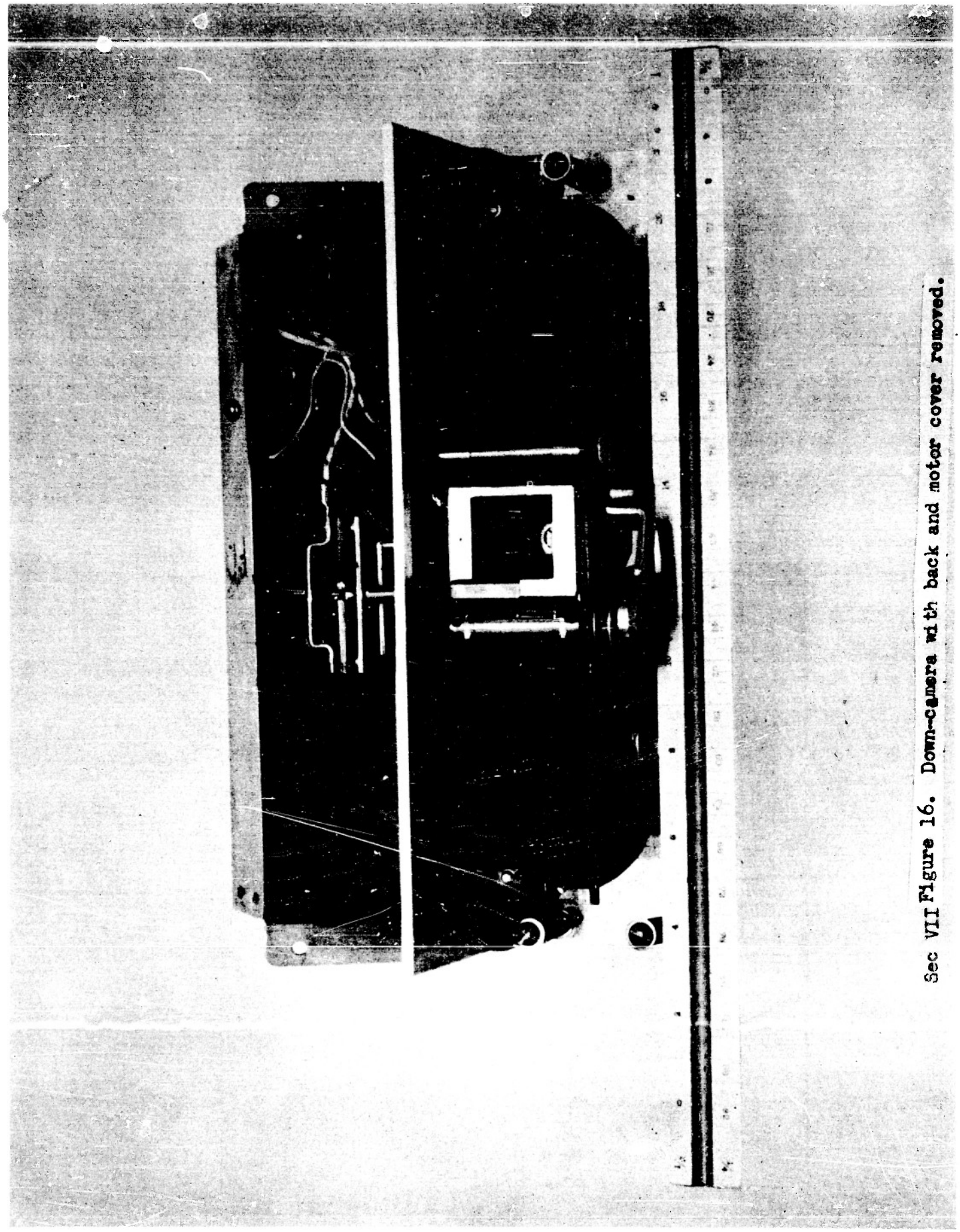

Sec VII Figure 16. Down-camera with back and motor cover removed.

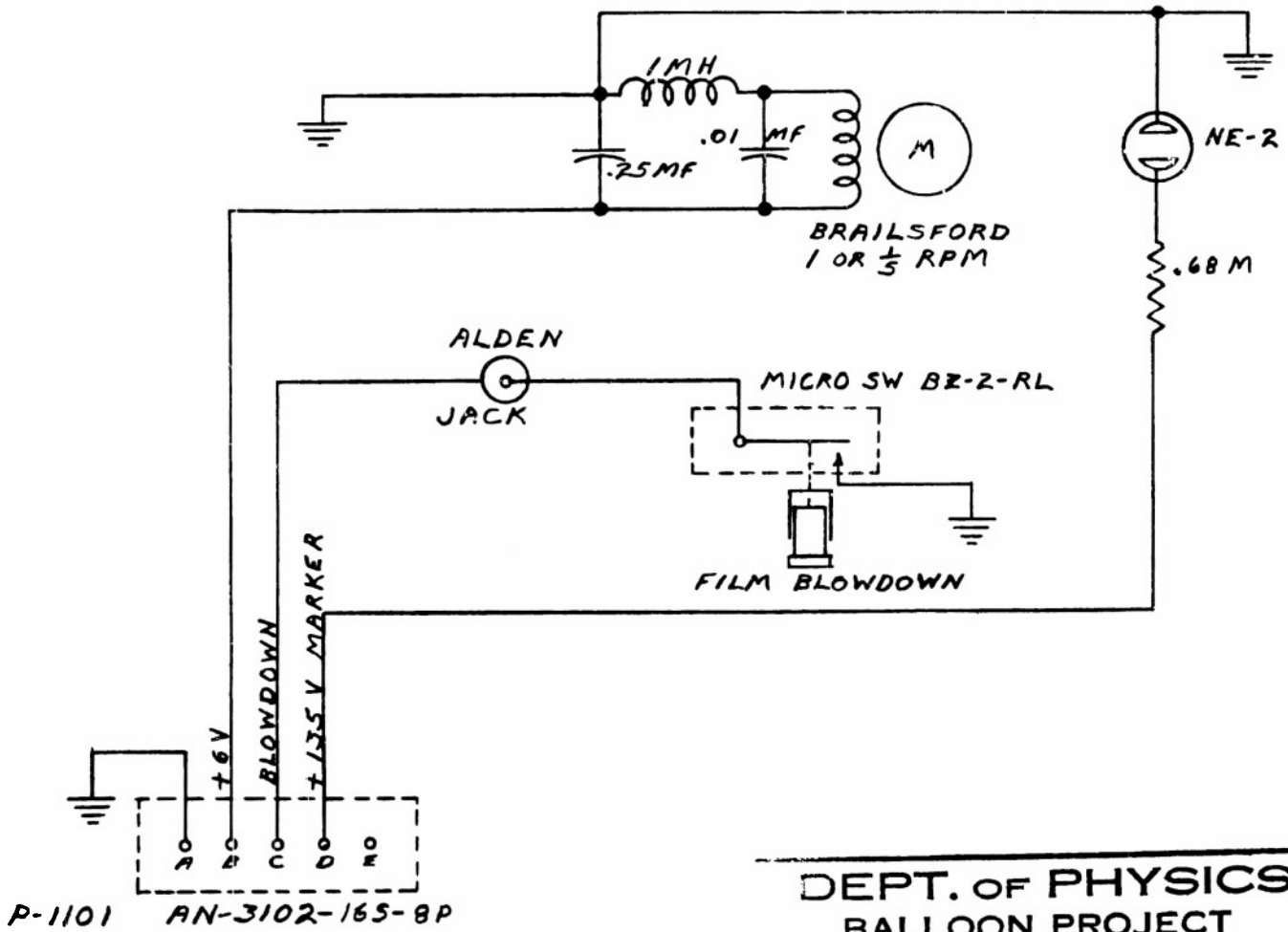

SEC. VII FIG. 17

DEPT. OF PHYSICS U. OF MINN. BALLOON PROJECT			SECT. INST	
DWG. NO.	SHOP DWG. NO.	DRAWN BY	CHECKED BY	DATE
2-TR3-535		[illegible]	[illegible]	2-11-54
TELEMETERING RECORDER + CAMERA CKT			MOD. 1	
			MOD. 2	
			MOD. 3	

radio signal was not readable. A master relay installed in the Olland Cycle keys 135V to a neon lamp installed in each camera in the gondola whenever the transmitter relay is keyed. Small NE-2 neon bulbs installed in each camera put a small dot of light on the film near the edge of the picture area through a hole approximately 1/1000 of an inch in diameter. In making the lamp shield it was found that the smallest hole that could be manufactured was desirable for the light aperture in order to prevent halation and light spread on the film itself. Even with a 1/1000 hole reading the trace from a film driven at 1/5 rpm is very difficult and a 1 rpm film drive proves much more desirable. Irregularities in film drive due to the film moving in small jerks instead of sliding freely are more and more apparent at a slow speed and the very close spacing of the light spots adds to the difficulties of reading.

Another innovation was completed for flight #55, a blow down timer relying upon the amount of film in the camera. A polished button riding on the back of the film releases a micro-switch mounted on the back of the camera when the end of the film passes through the film drive and this micro-switch terminates the flight through the blow down box. In order to prevent pressure sensitization of the film emulsion and scratching of the surface of the film, a highly polished button is necessary with extremely light pressure extending over as large an area as possible.

Two special cameras have been used during this period, one of them a camera mounted so as to take a picture of the horizon in order to find the amount of spin that the gondola has at altitude. This was an ordinary up-camera unit mounted in a horizontal position. The other special camera was a completely self-contained unit mounted in the top of the balloon intended to take pictures of the inside of the balloon. This crown mount contained separate batteries and a bellows actuated micro-switch to start the camera.

The switch was ordinarily set for 3000 feet altitude. This mount had to be carefully protected so that it would not damage the balloon material and also protected against the possibility of its freezing. Four of these cameras have been furnished during this period to the Naval Research Laboratory Transosonde Project, ONR 81200, in an attempt to trace balloon trajectories but they have not worked as well as down cameras as in their originally intended application. The failure seems to be in the insulation surrounding the cameras because there is evidence that the batteries dropped to such a low temperature that they no longer put out enough voltage to maintain the cameras in operation. Shop drawings of the Crown Mount are shown in Figures 18-a and 18-b.

2. Baro-thermograph. A barothermograph has been flown on a number of flights as indicated in column 6, Figure 1, but after the development of the film telemetering recorder it was thought no longer necessary to fly this duplicate recorder. The single bellows barograph was essentially the same as that included in the first Progress Report but the double-bellows barograph was an improvement containing a high altitude bellows made by the Kollsman Company (SK 901-901 which had the same scale deflection between 60 and 10 mb the Bendix-Friez Radiosonde Movement had from 1000 to 10 mb. These Kollsman bellows are, unfortunately, quite expensive and also in our experience unobtainable from the factory because of long delivery time and reluctance of the manufacturer to take orders. Just after the decision was made not to fly barothermographs a new design was completed by the shop and a picture of it is shown in Figure 19. This barothermograph has both barograph bellows and a thermograph element. It also has provision for a fourth smoked disc to record other information. This model has a built-in marker to put known pips on each smoked disc and the clockwork mechanism is completely enclosed with a layer of kerosene soaked felt inside the enclosure to preserve a lubricating atmosphere around the clockwork mechanism. The weight is $3\frac{1}{4}$ pounds.

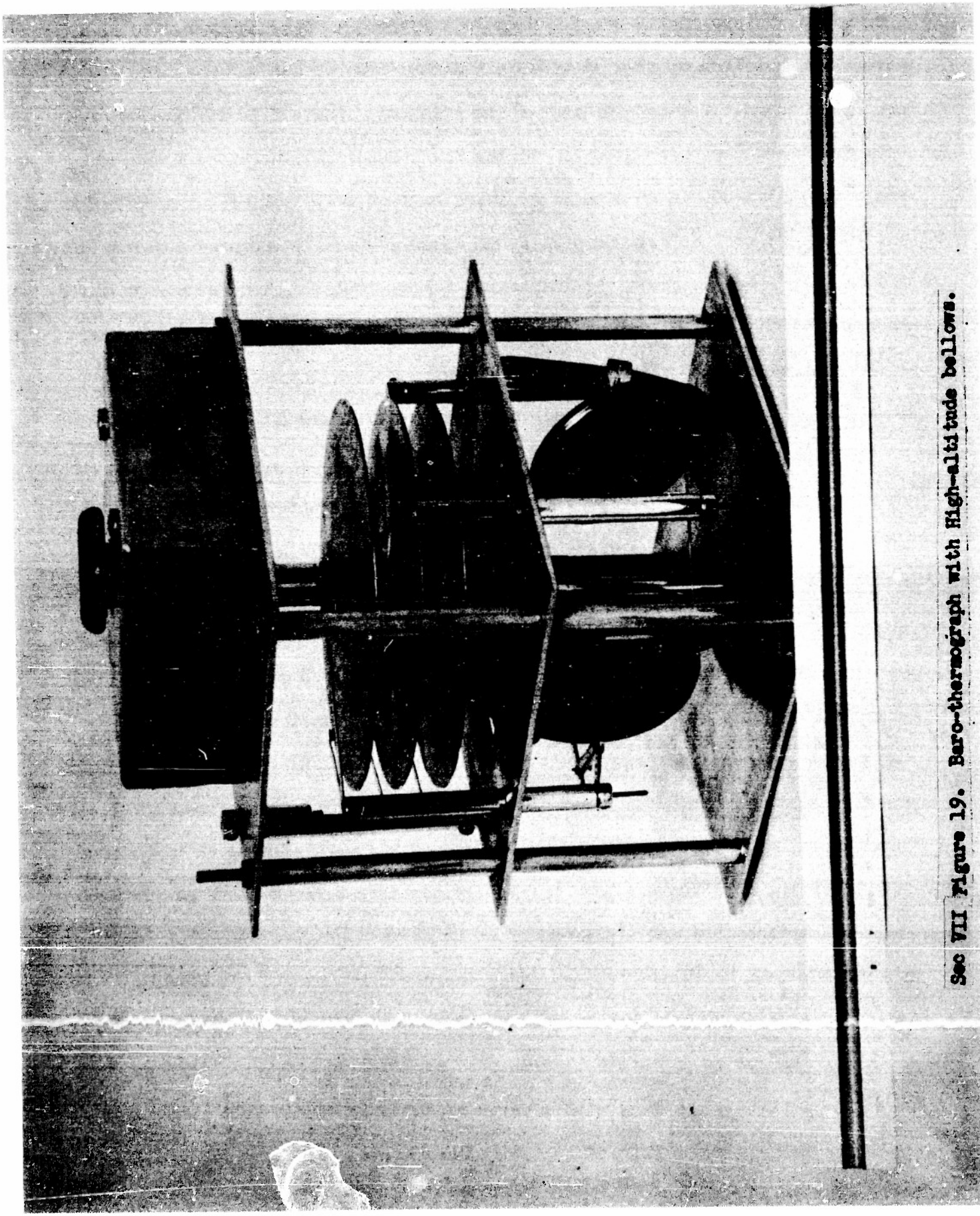

Sec VII Figure 19. Baro-thermograph with High-altitude bellows.

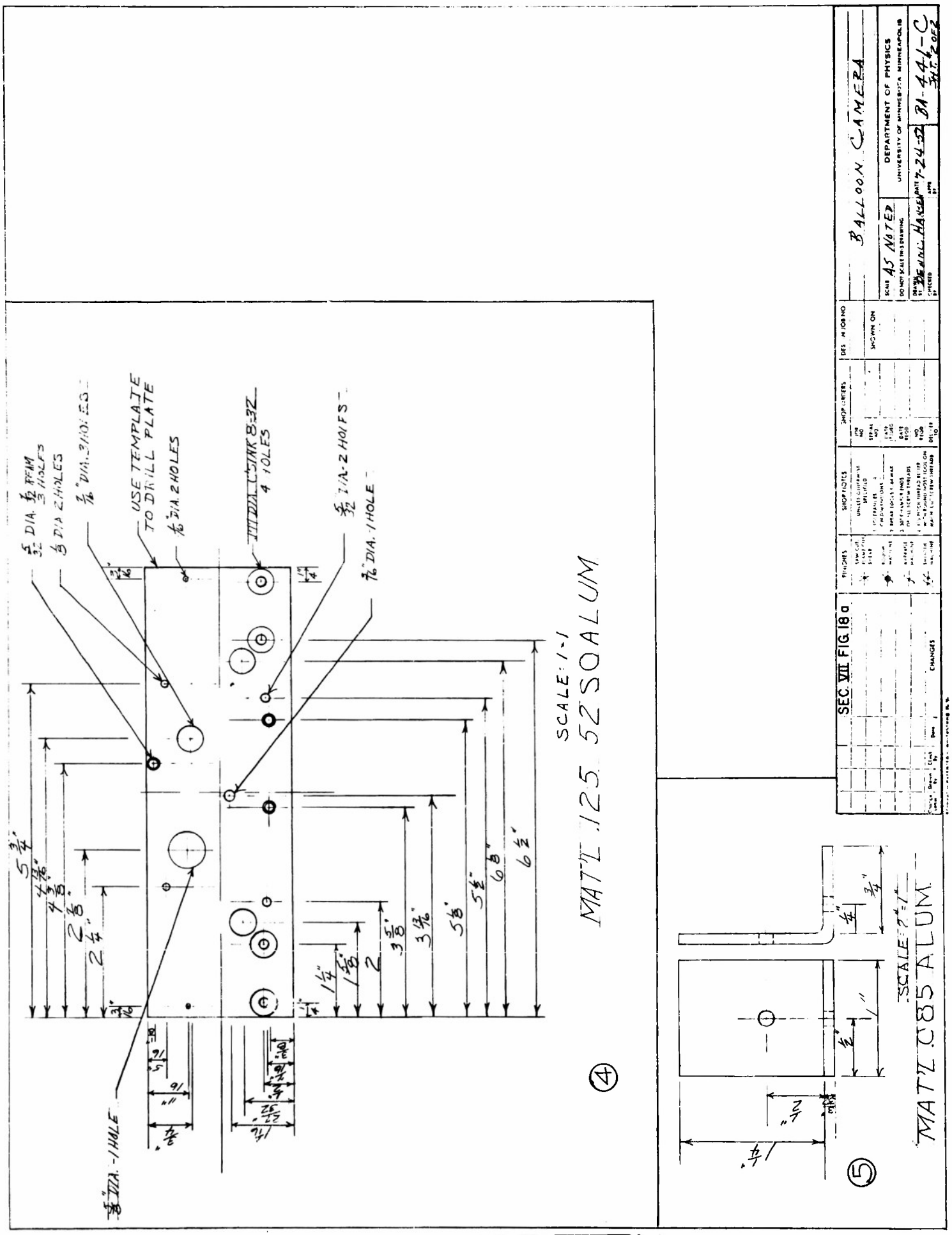
SEC VII FIG 18a
BALLOON CAMERA
DEPARTMENT OF PHYSICS
UNIVERSITY OF MINNESOTA MINNEAPOLIS
BM-441-C
SCALE: 1-1
MATL .125 52SOALUM
④
SCALE 2=1
MATL .085 ALUM
⑤

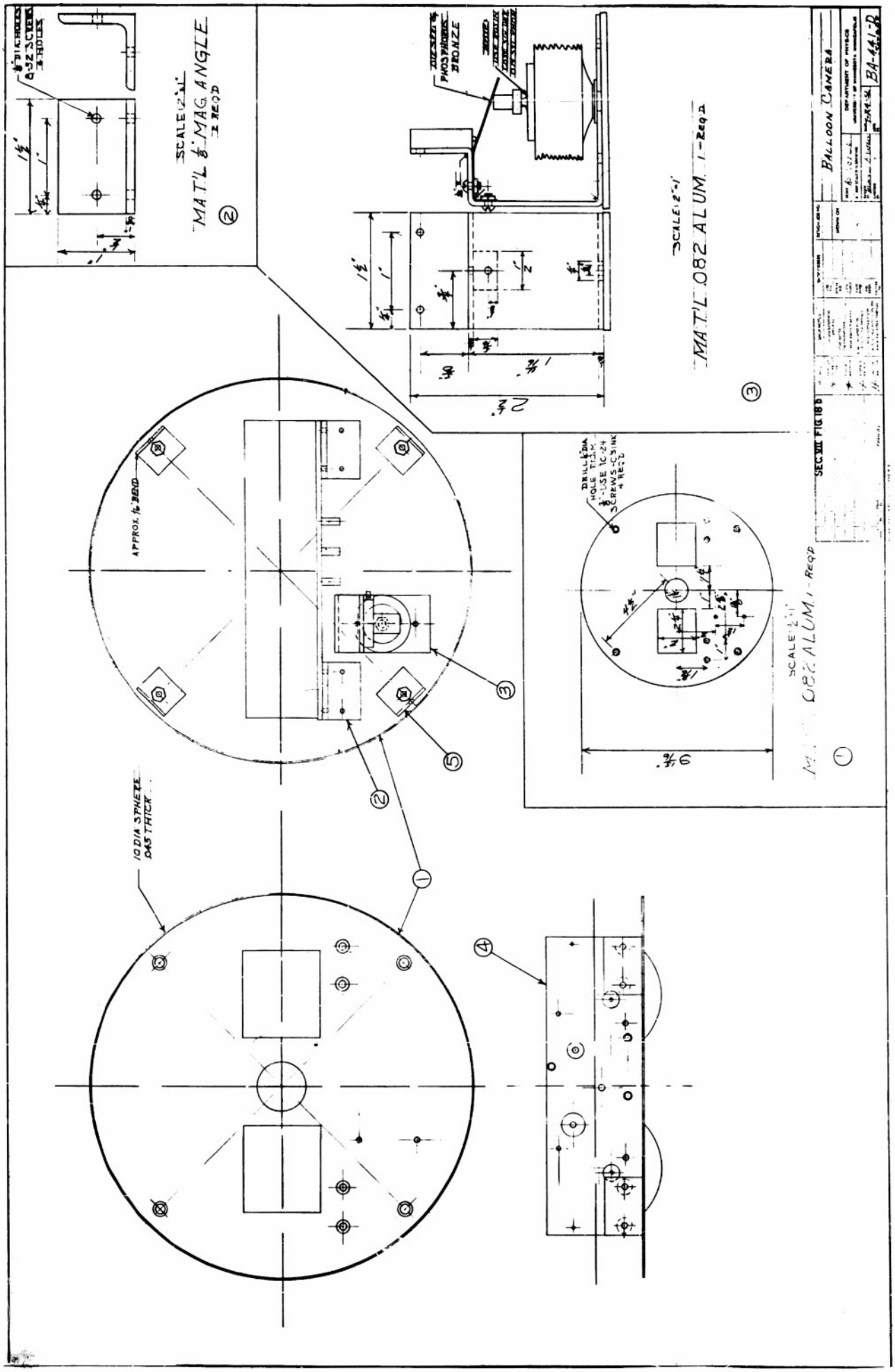
BALLOON CAMERA
SEC VIII FIG 18 D
BA-441-D
MATL .082 ALUM. 1-REQD
MATL 1/8 MAG ANGLE
2 REQD
MATL .082 ALUM. 1-REQD
MATL .082 ALUM. 1-REQD
APPROX. 1/8 BEND
10 DIA SPHERE .045 THICK
DRILL 4 DIA HOLE THRU 4-USE 10-24 SCREWS-CSINK 4 REQD
PHOSPHOR BRONZE
SCALE 2:1
SCALE 2:1
SCALE 2:1

2. Signal coder. The signal coder used in the flight constants flights is shown in Figure 20 and a wiring diagram for it is given in Figure 21. Unfortunately there is no shop drawing available at this time. The basic unit is a 1 rpm Brailsford motor driving an insulated rotor with brass pins pressed into the surface to contact a common sleeve within the insulation. Voltage applied by the unit originating a signal is coded by the spacing of the pins and the interrupted voltage on the common sleeve keys the transmitter relay. Filter chokes have been installed across all of the contact points for reduction of sparking and RF noise. There is also a choke on the Brailsford motor as there is on all motors installed in flight constants flights. The 3V DC relay shown is a special relay to allow differentiation of the valving signal so that both opening and closing of the valve can be coded separately.

3. Olland Cycle. The Olland Cycle is discussed in detail in another part of this section.

4. Ballast level transmitter and recorder. The ballast level transmitter shown in Figures 22, and 23-a and 23-b is a new model developed since the last ballast tank flight and as yet not flown. Basically it is an improvement on the previous type of transmitter mentioned in the first report (Section V p 5). The phase angle of a reference point and a point varying with the extension of a spring supporting the ballast tank is transmitted as an index of the amount of ballast left in the tank. This information is repeated once every minute by a Brailsford motor rotating the phase angle discs.

The ballast level recorder flown on these flights was the same as that used before flight #21. It was a simple lever linkage to record the amount of spring extension on a smoked disc driven by the barothermograph motor.

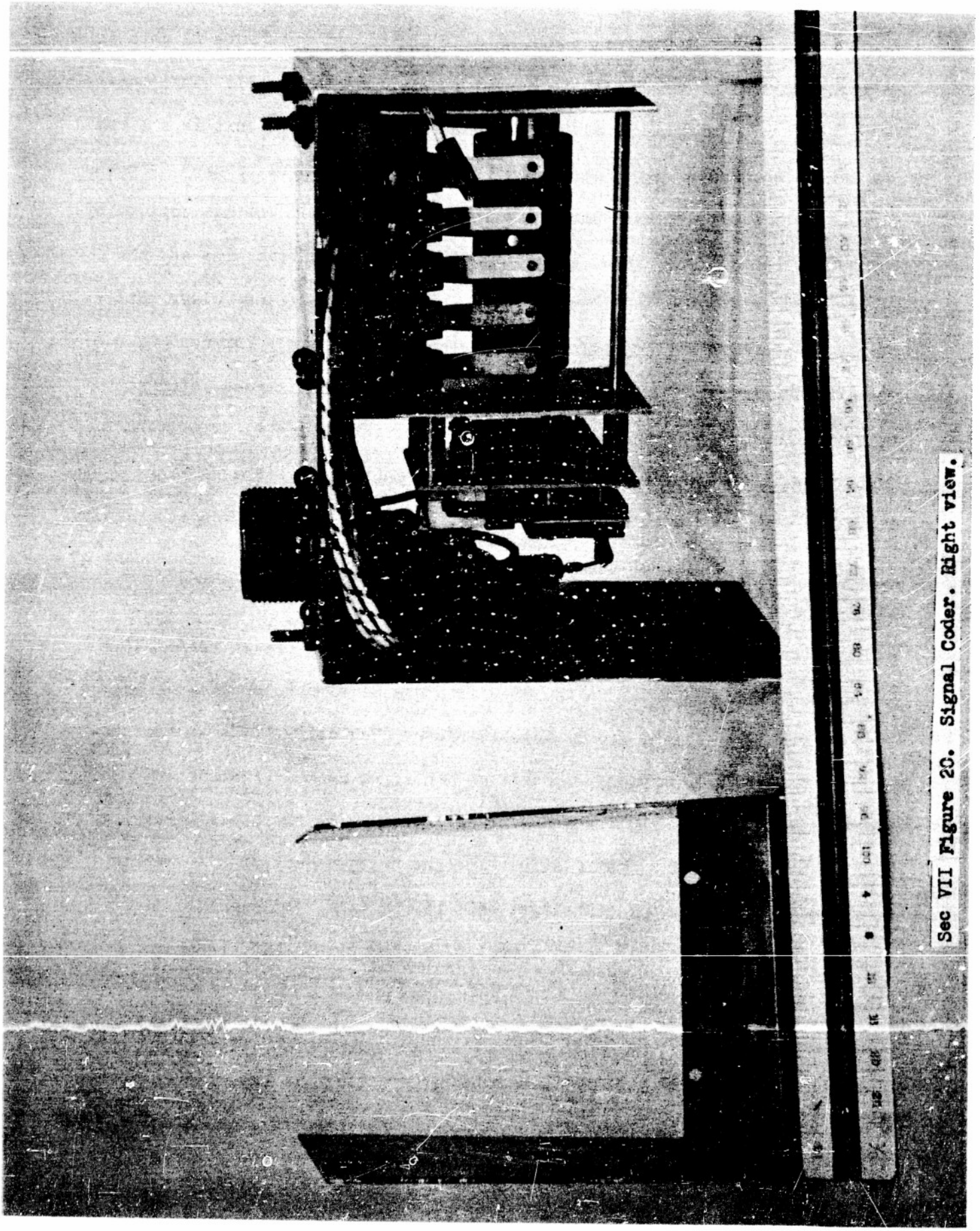

Sec VII Figure 20. Signal Coder. Right view.

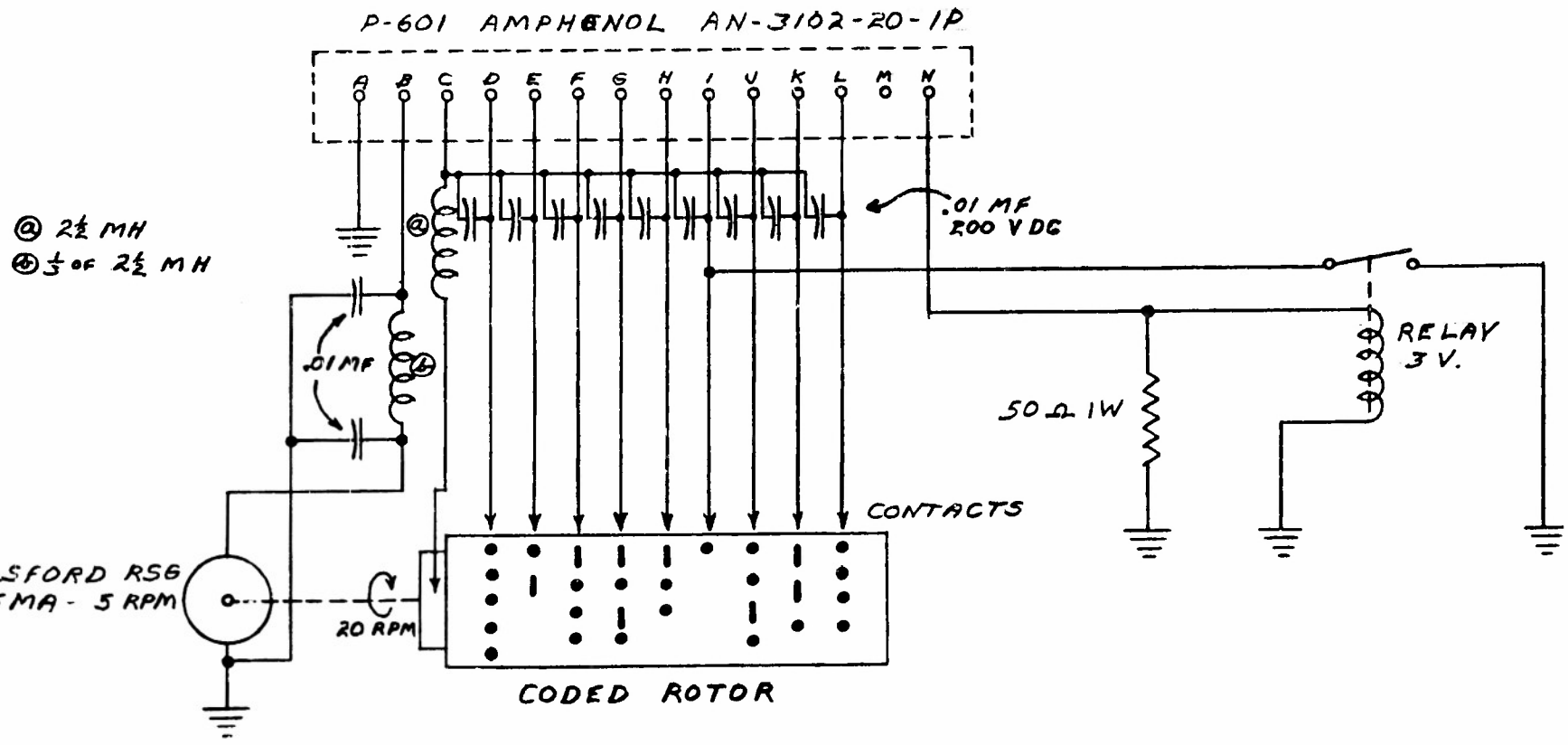

SEC. VII FIG. 21

DEPT. OF PHYSICS U. OF MINN.
[illegible] PROJECT SECT. INS.

[illegible] DWG. NO.	DRAWN BY	CHECKED BY	DATE
2-SC-3-529	[illegible]	RWA	11-11-52
SIGNAL CODER SERIES #30	[illegible]	MOD. 1	2-2-53
		MOD. 2	
		MOD. 3	

Confidential Security Information

Confidential

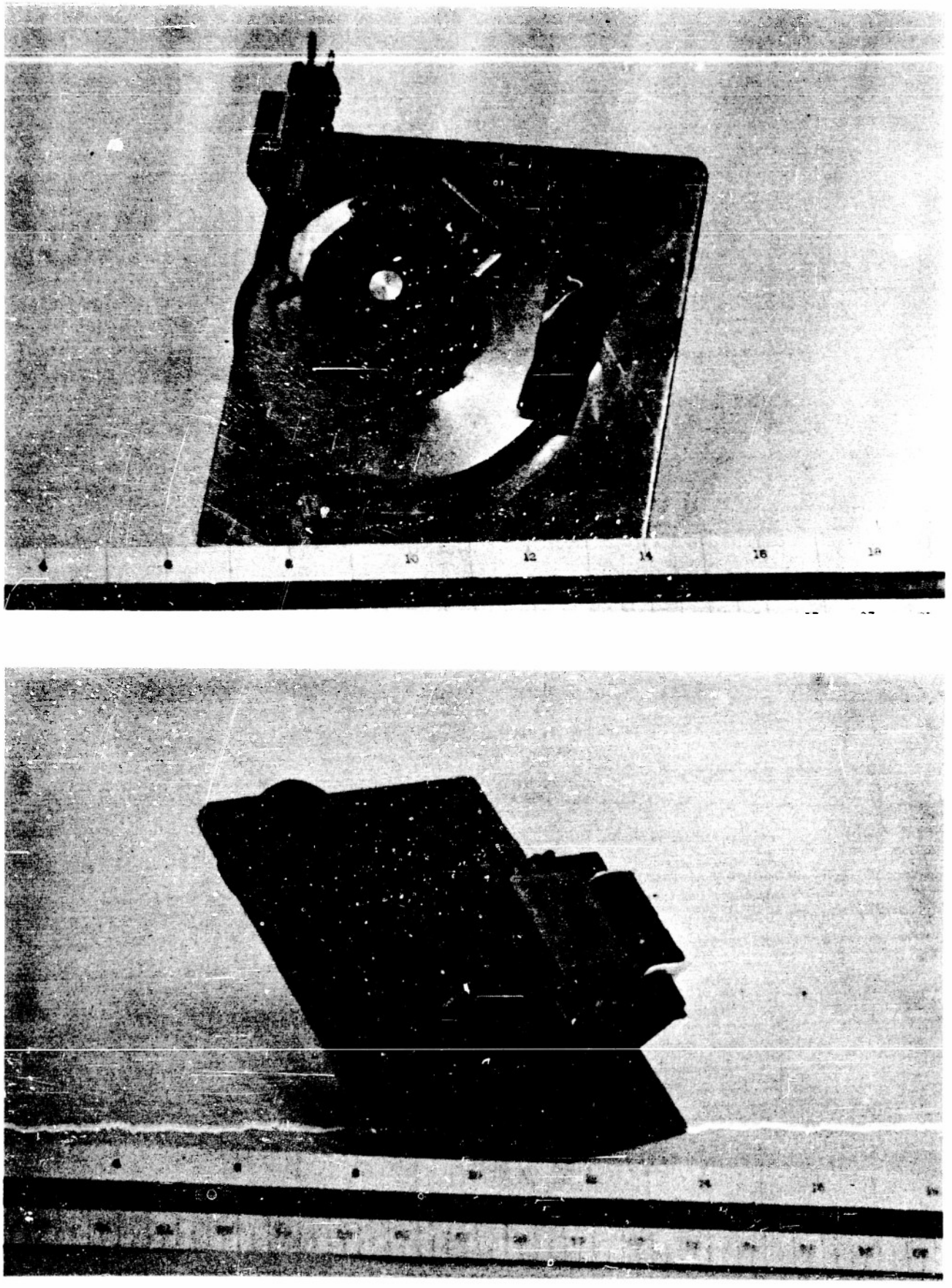

Sec VII Figure 22. Ballast level transmitter. Back and front views.

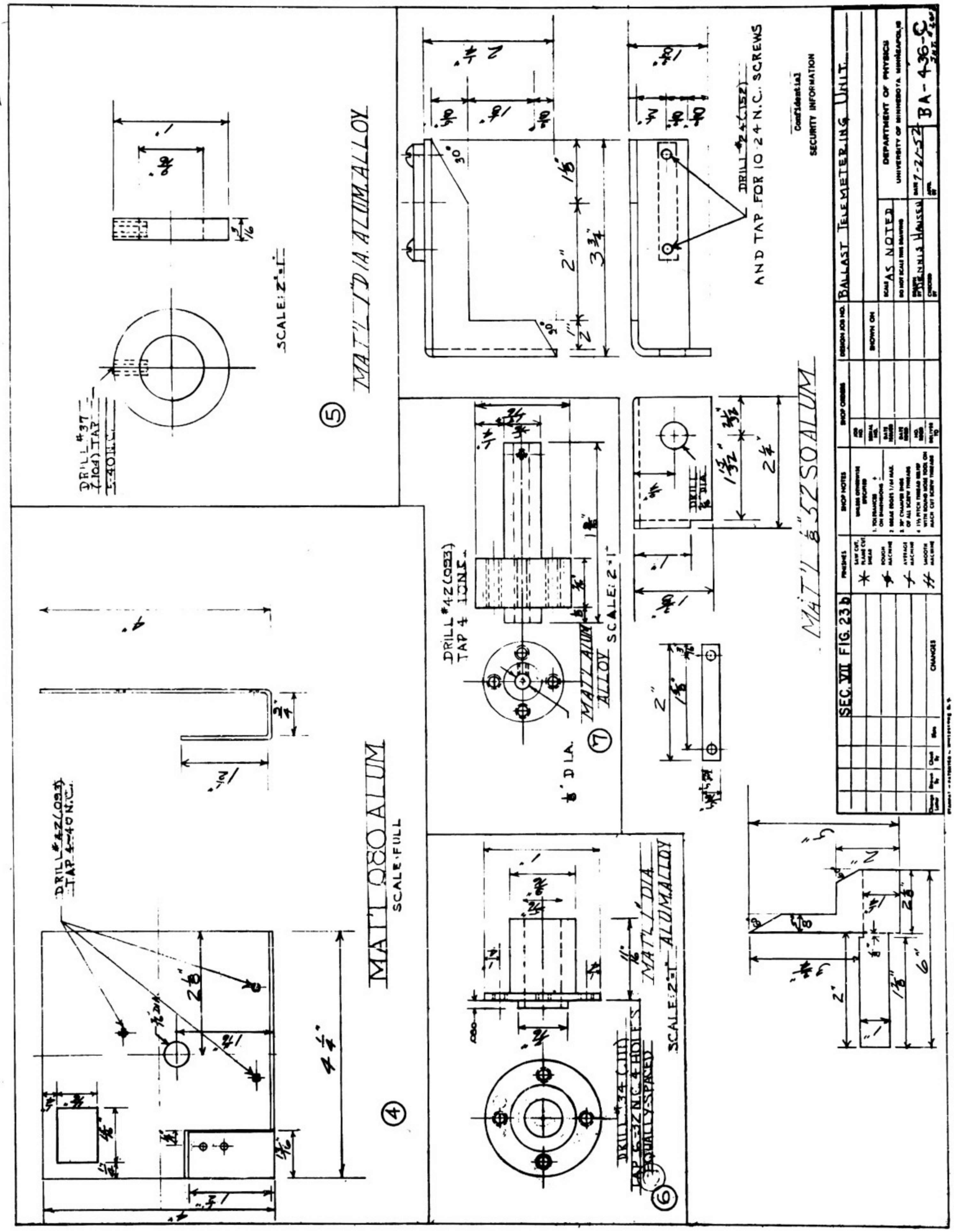
VII-242
BALLAST TELEMETERING UNIT
SEC. VII FIG. 23b
BA-436-C
DEPARTMENT OF PHYSICS
UNIVERSITY OF MINNESOTA MINNEAPOLIS
AS NOTED
Confidential
SECURITY INFORMATION
DRILL #24 (.152) AND TAP FOR 10-24 N.C. SCREWS
MAT'L 1/8" 52 SO ALUM
MAT'L 1" DIA. ALUM ALLOY
SCALE: 2"=1"
DRILL #37 (.104) TAP 5-40 N.C.
DRILL #42 (.093) TAP 4-40 N.C.
MAT'L .080 ALUM
SCALE: FULL
MAT'L ALUM ALLOY
DRILL #34 (.111) TAP 6-32 N.C. 4 HOLES EQUALLY SPACED
MAT'L 1" DIA ALUM ALLOY

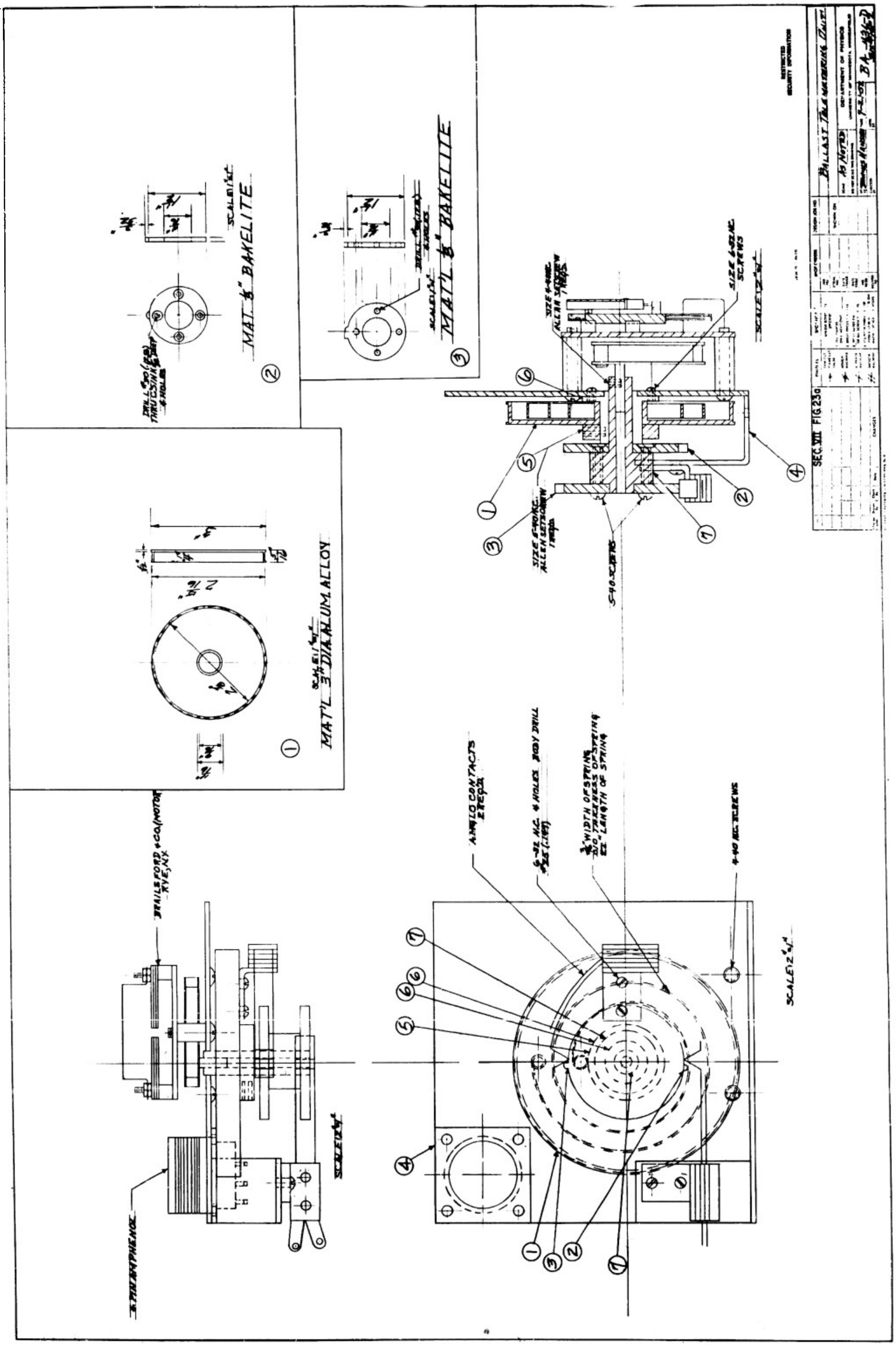
BALLAST TELEMETERING UNIT
SEC. VII FIG 23a
MAT'L 3" DIA ALUM ALLOY
MAT'L 1/8" BAKELITE
BRAILSFORD & CO (MOTOR) RYE, N.Y.
AMPHENOL CONTACTS
4-40 REC. SCREWS
SIZE 6-32 NC SCREWS
5-40 SCREWS

5. Antenna dropper. The antenna dropper is essentially the same design that was discussed in the first Progress Report (Section V p.7 and Appendix 2 p.2). There have been two minor changes during this period; one is the enclosure of the antenna dropper in a plywood box in order to cut down heat transfer through the aluminum can in which it was originally contained in order to maintain higher operating temperatures for batteries and equipment in the gondola. The other change has been a slight shortening in the length of the dropper itself to better contain it in the small gondola. Because of two dropper failures, it has been found necessary to specify that no acid flux be used to solder the brass sylphons since the acid crystalizes the brass in time causing the sylphon to leak. The present model of the antenna dropper is shown in Figure 24 and shop drawings are shown in Figures 25-a and 25-b.

C. Special Instrumentation

1. Transmitter-Cycler. The transmitter cycler shown in Figure 1 as having been flown on flight #29 was a Brailsford motor with a cam so cut as to turn the transmitter on and off in order to reduce the duty cycle of the transmitter. This cylcer has not been used since and was included in this flight to reduce the high battery drain of the transmitter.

2. Photo-recording ammeter. In an attempt to discover the ratio of interference to our own radio command signal in the vicinity of 6420 kc a recording ammeter was flown on flight #48 which recorded the amount of AVC control used in the command receiver. This instrument was a standard camera with its shutter fixed open and a lens tube extension of sufficient length to allow the lens to be focused on the face of a Simpson milliammeter. A mask containing a narrow slit was placed over the face of the meter and the needle was illuminated, showing through the mask as a small spot of light. Since the movement of the meter was perpindicular to the direction of film travel, the illuminated spot of light traced a plot of meter deflection vs. time. Sig-

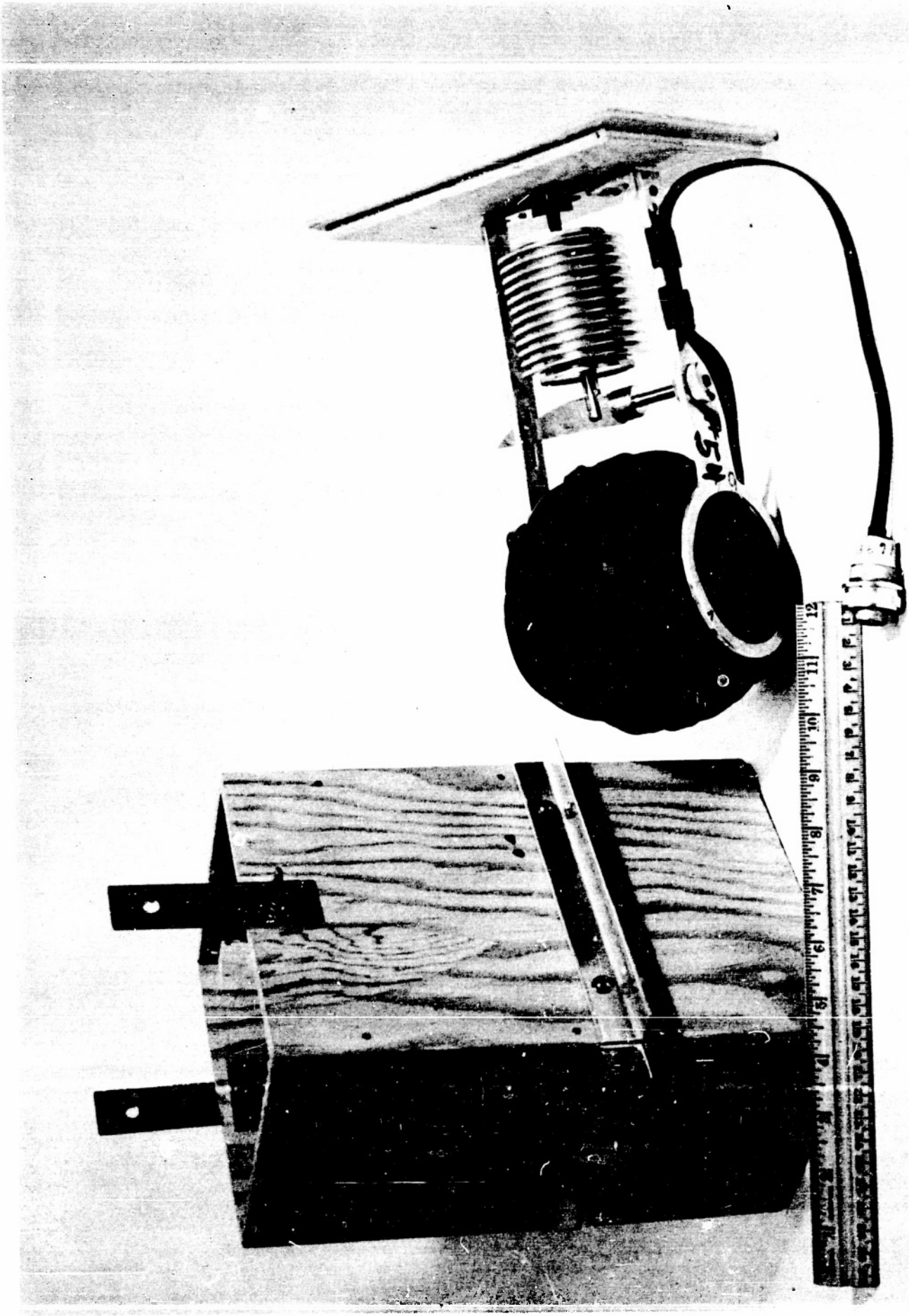

Sec VII Figure 24. Antenna dropper and box.

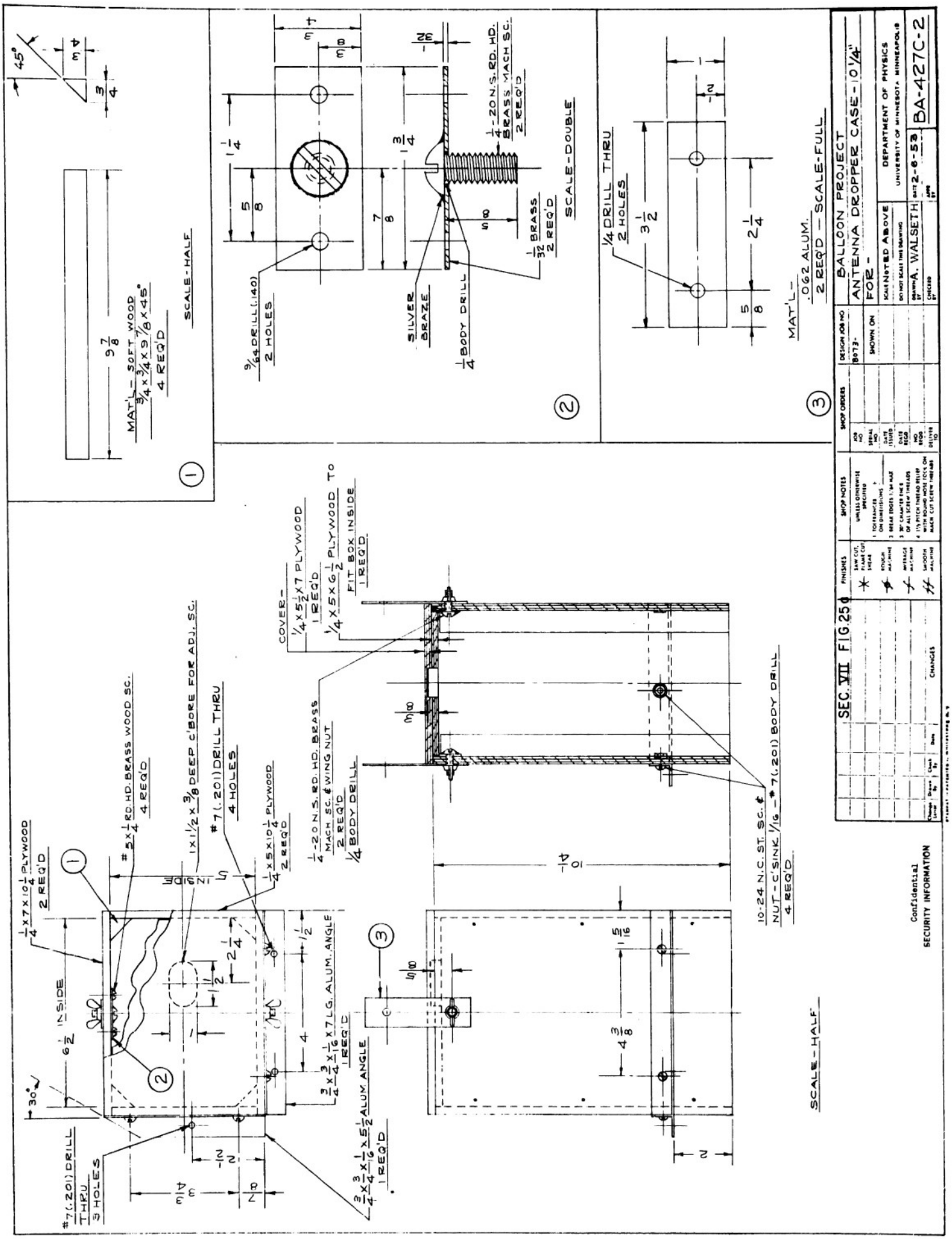
SEC. VII FIG. 25
BALLOON PROJECT
ANTENNA DROPPER CASE - 10 1/4"
FOR -
DEPARTMENT OF PHYSICS
UNIVERSITY OF MINNESOTA MINNEAPOLIS
BA-427C-2
DRAWN A. WALSETH
DATE 2-6-53
SCALE - HALF
SCALE - DOUBLE
SCALE - FULL
SCALE - HALF
MAT'L - SOFT WOOD
MAT'L - .062 ALUM.
2 REQ'D
4 REQ'D
1 REQ'D
2 REQ'D
4 HOLES
3 HOLES
#7 (.201) DRILL THRU
#7 (.201) BODY DRILL
1/4 DRILL THRU
2 HOLES
SILVER BRAZE
1/4 BODY DRILL
1/32 BRASS
2 REQ'D
1/4-20 N.S. RD. HD. BRASS MACH SC.
2 REQ'D
9/64 DRILL (.140)
2 HOLES
COVER - 1/4 X 5 1/2 X 7 PLYWOOD
1 REQ'D
1/4 X 5 X 6 1/2 PLYWOOD TO FIT BOX INSIDE
1 REQ'D
1/4-20 N.S. RD. HD. BRASS MACH SC. & WING NUT
2 REQ'D
1/4 BODY DRILL
10-24 N.C. ST. SC. & NUT - C'SINK 1/16 - #7 (.201) BODY DRILL
4 REQ'D
1 X 1 1/2 X 3/8 DEEP C'BORE FOR ADJ. SC.
#5 X 1/4 RD. HD. BRASS WOOD SC.
4 REQ'D
1/4 X 7 X 10 1/4 PLYWOOD
2 REQ'D
1/4 X 5 X 10 1/4 PLYWOOD
2 REQ'D
3/4 X 3/4 X 1/16 X 7 LG. ALUM. ANGLE
1 REQ'D
3/4 X 3/4 X 1/16 X 5 1/2 ALUM ANGLE
1 REQ'D
6 1/2 INSIDE
5 1/2 INSIDE
30°
45°
Confidential
SECURITY INFORMATION

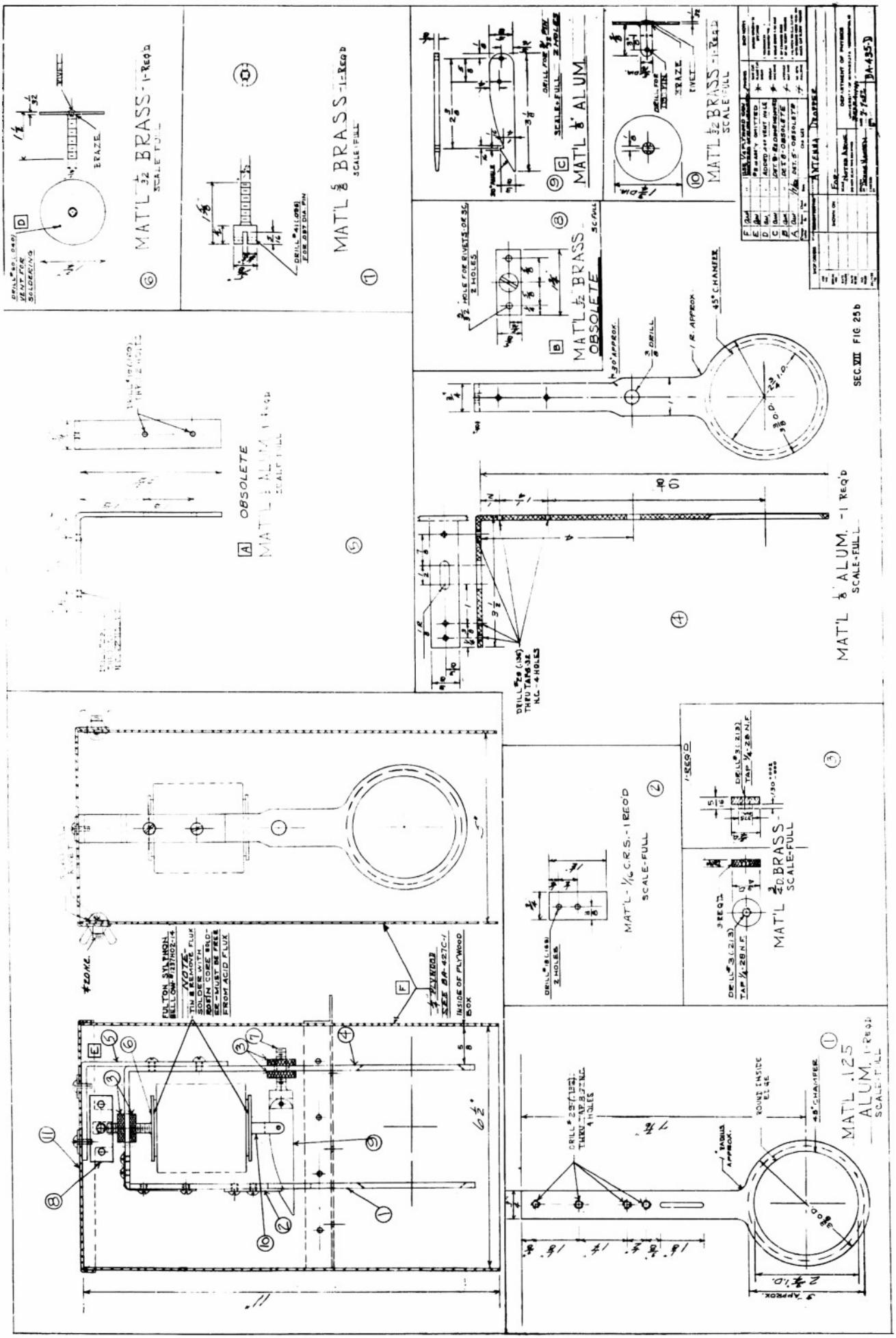

nificant results were unobtainable from this flight because of balloon failure and a similar attempt has not been made since. A picture of the unit is shown in Figure 26 and a wiring diagram is given in Figure 27.

3. Thermister photo recorder. Flight #46 was a test flight for an instrument being developed by the project to measure temperatures and radiation in the balloon and in the air outside of the gondola. This particular instrument shown in Figure 28 was only an attempt to test the basic design and was not intended for further flight. Since flight #46 a multi-channel instrument based on the same design has been completed and flights are now being made with it. It will be discussed at greater length in the next progress report when more complete results are available.

4. Strobe flasher. The flights #35 and #49 contained a special unit intended to illuminate the balloon after sunset in order to take pictures of descent. This was a standard photographic strobe flash unit (Figure 29) made and modified by the electronics section and was a modification of the flasher flown on flight #11. It had become apparent that the 450 volts used in the flasher were arcing over even at ground elevation in spite of high voltage insulation and a pressurized container which was designed to prevent this. The unit is now contained in a 1 foot diameter sphere with the discharge tube located at the top of the sphere and protected by a plastic cover. Unfortunately results with this instrument were inconclusive because of early flight termination on the single attempted flight using it.

5. Cosmic ray plates. As indicated in column 16 of Figure 1 a large number of gondolas contained cosmic ray plates. These plates were not a part of the equipment of this project but were for the most part hitch-hike loads of small weight flown for the convenience of the cosmic ray project at this university. In some cases the cosmic ray plates were contained in 30 pound lead or paraffin blocks which were used as ballast packages to be dropped on separate parachutes by command or pressure operated ballast droppers.

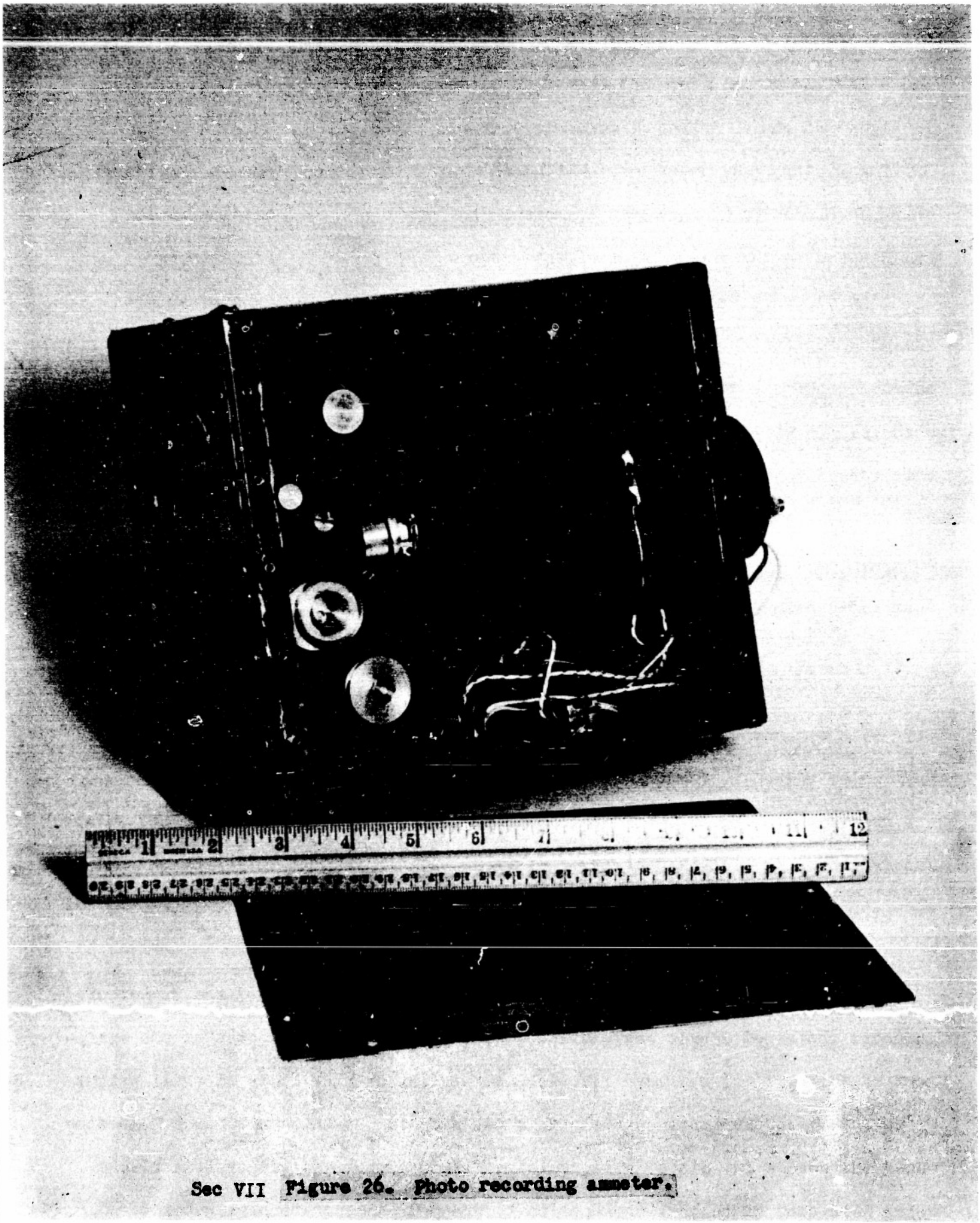

Sec VII Figure 26. Photo recording ammeter.

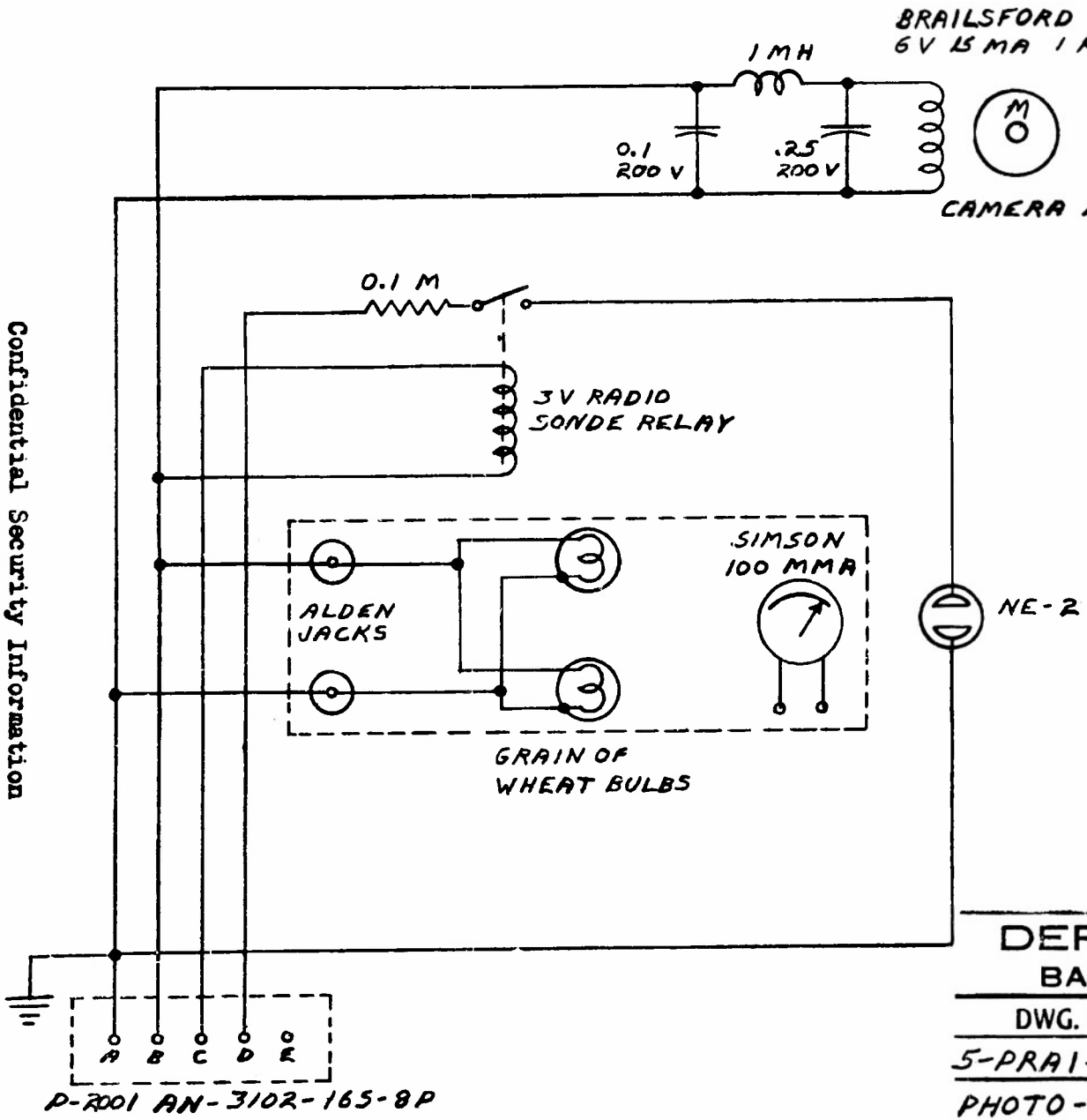

SEC VII FIG 27

DEPT. OF PHYSICS U. OF MINN.
BALLOON PROJECT SECT. INST.

DWG. NO.	SHOP DWG. NO.	DRAWN BY	CHECKED BY	DATE
5-PRA1-538		[illegible]	[illegible]	3-6-53
PHOTO-RECORDING AMMETER SERIES #1			MOD. 1	
			MOD. 2	
			MOD. 3	

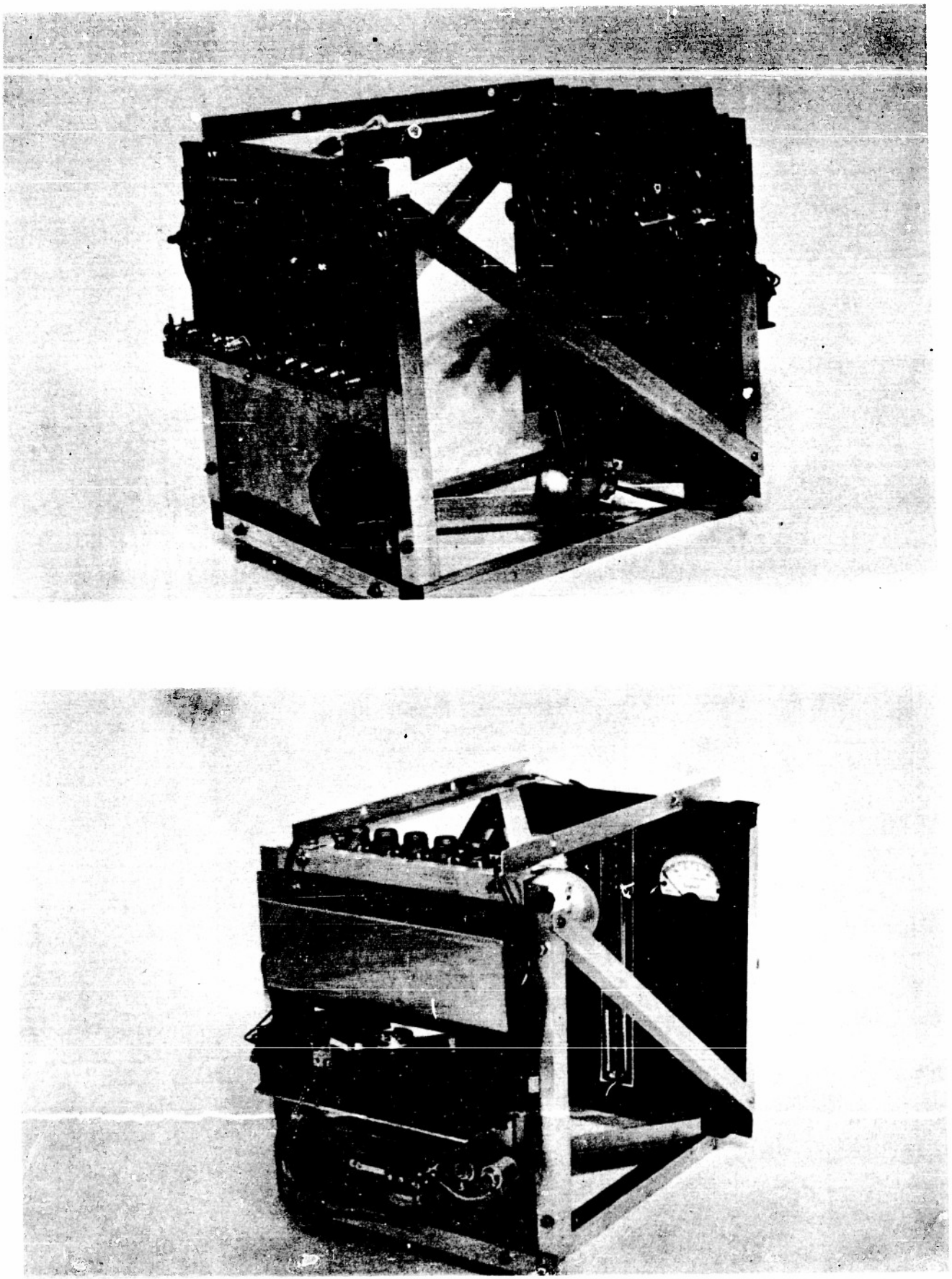

Sec VII Figure 28. Thermistor photo recorder

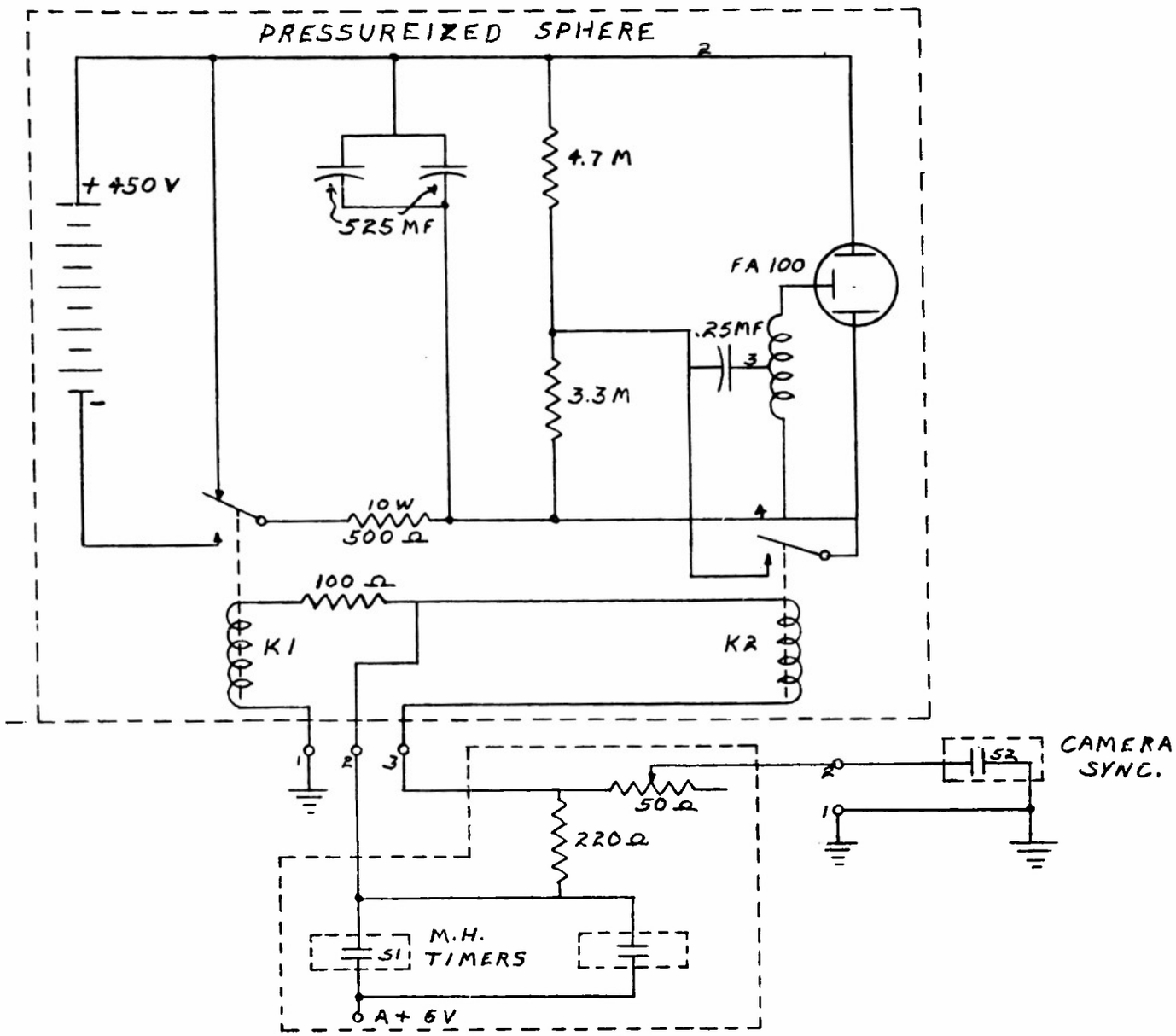

DEPT. OF PHYSICS U. OF MINN.				
BALLOON PROJECT			SECT. INS.	
DWG. NO.	SHOP DWG. NO.	DRAWN BY	CHECKED BY	DATE
2-SF-2-513				8-27-52
STROBE FLASHER SERIES*20			MOD. 1	
			MOD. 2	
			MOD. 3	

SEC. VII FIG. 29

D. Miscellaneous Apparatus

1. Gondolas. The standard gondola used during this period is identical with that reported in the first Project Report (Section V, p. 1). The small gondolas which have been developed during this period are shown in Figures 30-a and 30-b. These gondolas could contain only the standard equipment used on our flights if very closely packed with no special instrumentation. A 4" styrofoam box encloses these gondolas to insulate them and a bright red canvas case is used to cover the outside of the styrofoam box. Though of very light construction, these frames have been found to withstand landing impact proportionately better than the large frames. The only portion of the gondolas seriously damaged has been the load supporting U bolt at the top which in one or two cases has been badly bent by the parachute opening shock.

2. Motors. This project now uses only Brailsford motors in its equipment and we have had very few failures attributable to them. In two cases it was found that there was a weak gear in the train of these motors and now all motors are disassembled before installation and this gear, the next one to the output shaft, is soldered to prevent the spline from shifting on the wheel. It has also been found necessary to file a flat on the output shaft in order to properly connect the motor to mechanisms requiring any amount of torque. As long as the battery voltage is maintained properly during flight these motors have not failed. All motors flown in flight constants gondolas have pi filters to reduce radio interference.

3. Batteries. No change has been found necessary in the basic powering of our gondolas during this period. The main flight power source are Willard ER40 batteries or when the calculated expected battery drain is low Willard ER12 batteries have been used. It has been found that with proper cycling and charging wet cell batteries can be used several times reliably. Dry cells either Everyready or Burgess are used now exclusively for furnishing voltages

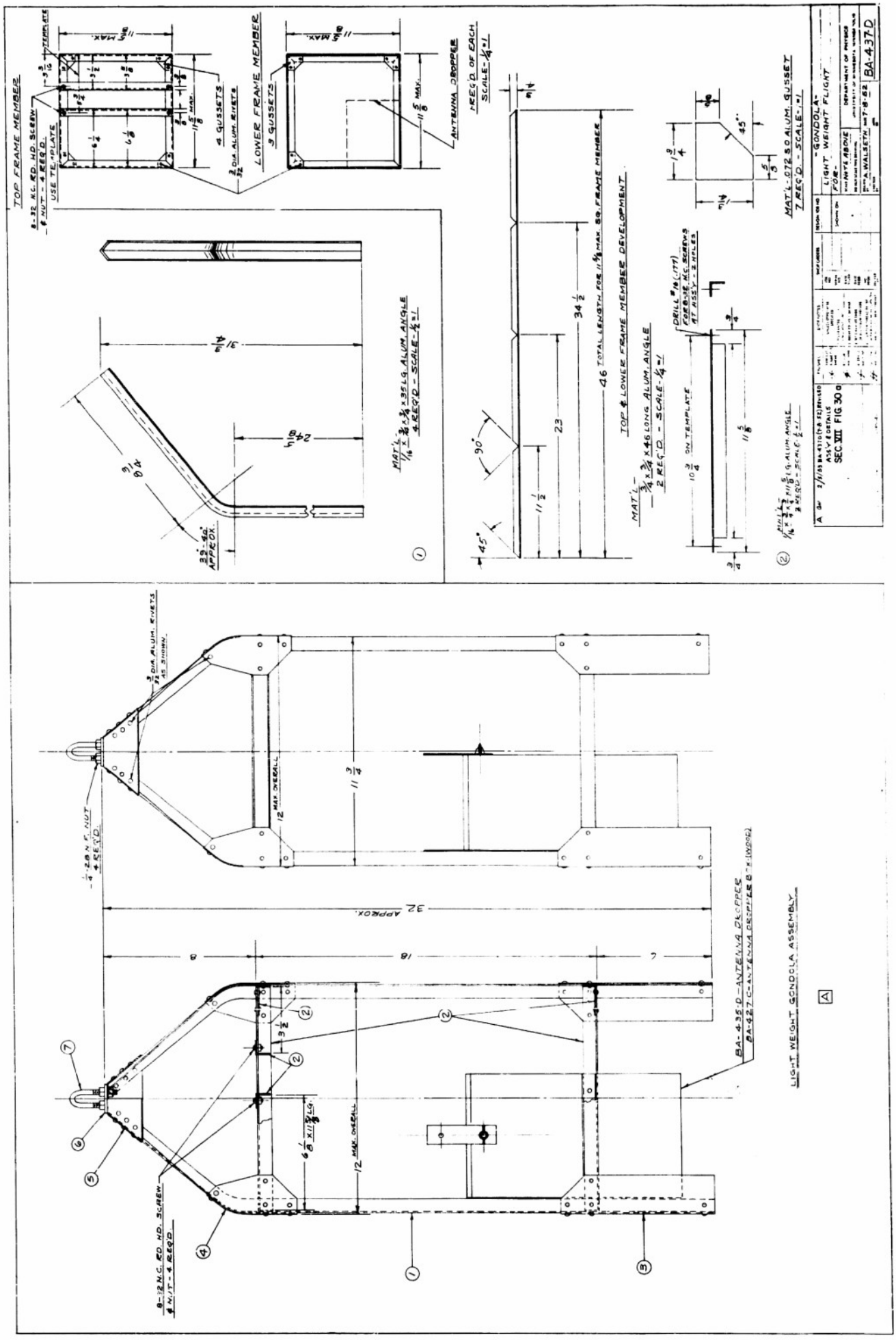
TOP FRAME MEMBER
LOWER FRAME MEMBER
4 GUSSETS
3 GUSSETS
ANTENNA DROPPER
REQ'D OF EACH
SCALE-1/4"=1'
MAT'L-1/16 X 3/4 X 3/4 X 39 LG. ALUM. ANGLE
4 REQ'D - SCALE-1/4"=1'
MAT'L-3/4 X 3/4 X 46 LONG ALUM. ANGLE
2 REQ'D - SCALE-1/4"=1'
TOP & LOWER FRAME MEMBER DEVELOPMENT
MAT'L-.072 S.O. ALUM. GUSSET
7 REQ'D. - SCALE-1"=1'
- GONDOLA -
LIGHT WEIGHT FLIGHT
FOR-
DEPARTMENT OF PHYSICS
APPD. A. WALSETH
BA-437-D
SEC XIII FIG 30
LIGHT WEIGHT GONDOLA ASSEMBLY
BA-435-D - ANTENNA DROPPER
BA-427-C - ANTENNA DROPPER
8-1/2 N.C. RD. HD. SCREW
4 NUT - 4 REQ'D.
USE TEMPLATE
3/32 DIA. ALUM. RIVETS
32 APPROX.
12 MAX. OVERALL
11 3/4
18
8
7

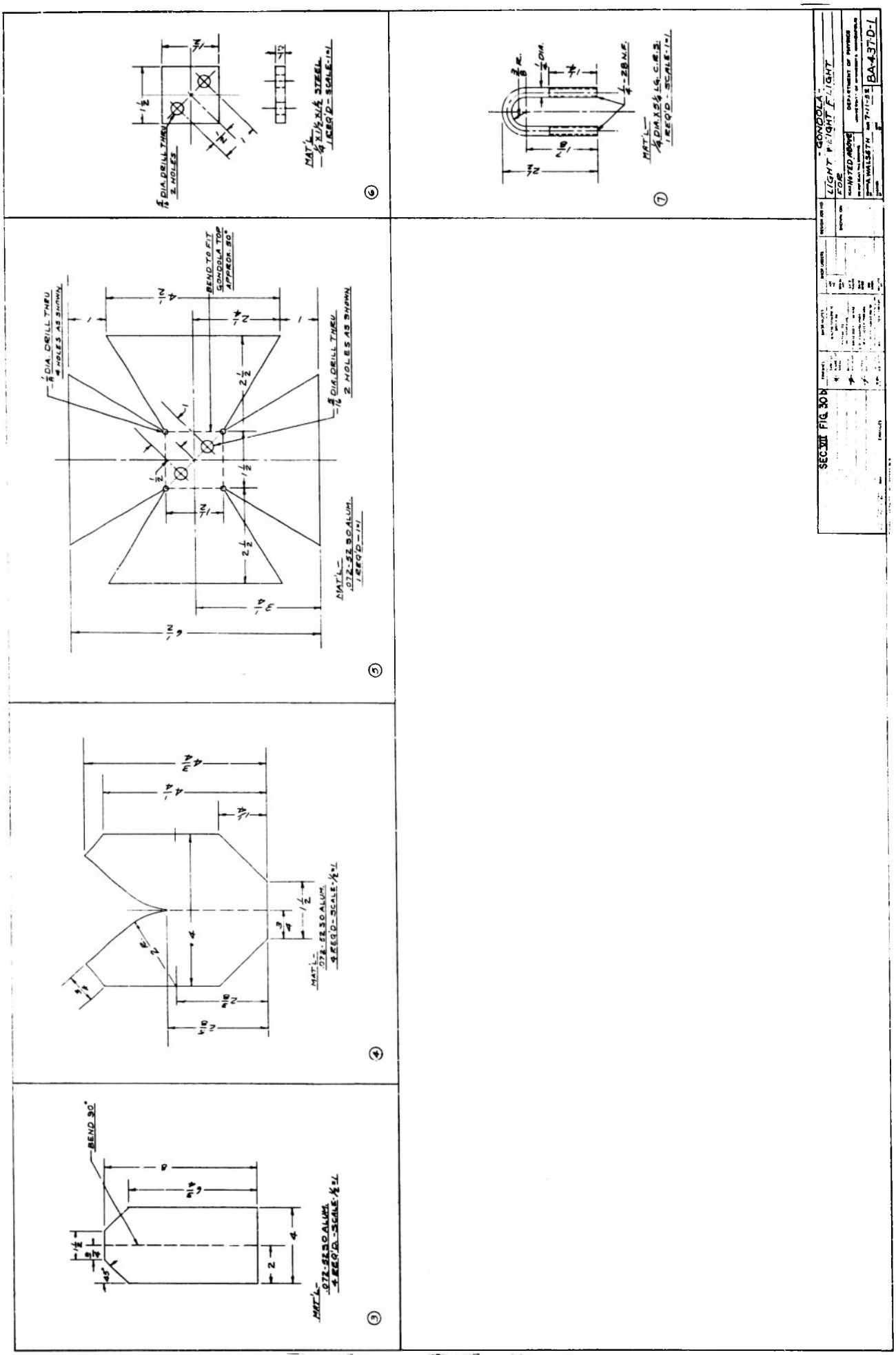
SECTION FIG. 30b
GONDOLA
LIGHT FLIGHT
FOR
BA-437-D-1
BEND TO FIT GONDOLA TOP APPROX. 90°
2 HOLES AS SHOWN
BEND 90°

higher than the 6V supplied by the wet cells. We have found that voltages higher than 270 V are very apt to arc and therefore this upper limit has been set on the voltage systems in the gondola unless pressurizing is used.

4. Wire. During the period covered by the first report Vinyl insulated wire was used throughout the gondola because of its cost, size, and good dielectric qualities. However, it has been discovered that the Vinyl insulation breaks down both mechanically and electrically at low temperatures and for that reason all wiring now is glass insulated made by Alpha Wire Corporation, New York. This wire has the added advantages of being easy to solder without burning the insulation, it has better dielectric properties and it also does not fray as cotton covered wire does.

E. Flight Operations

1. Checkout. The instrumentation section has found it advisable to have someone familar with the particular gondola being flown present at every launch. This is necessary because the complexities of each gondola are different and only a person familar with them can reliably check the operation of all the units at launching time. In cases of flight constants flights operation of the valve before the balloon is inflated as well as radio command keying of every operation in the gondola is necessary. It has been found that extreme care must be taken with circuits to which squibbs are connected since on several occasions squibbs have been fired at launch time when they were accidentally grounded while being connected or by such obscure causes as the heat of the sun firing an uncompensated thermal-delay relay within the gondola. In one case a bystander was hit by the metal cutter from a squibb cannon at launching time, and as a result the squibb cannonswere redesigned to prevent the cutters from escaping from the cannon. In addition, all squibbs are kept at ground potential and only compensated thermal delay relays are used. The only danger at present from the accidental

firing of a squibb is the possible blast burn, or in the case of a ballast package, the flying shot which might penetrate clothing.

2. Tracking. On days when it is possible to keep visual contact with the balloon the instrumentation section has been asked to furnish a theodolite operator to aid in the mapping of the balloon trajectory. A permanent installation at the University of Minnesota Airport and a series of portable theodolite stations are used and the theodolite crews have been thoroughly instructed in the process of zeroing in a theodolite for accurate position location. A great need for a theodolite operator has been fulfilled in the development of a battery operated portable WWV receiver to give correct time intervals for theodolite readings. The audio-tone of WWV with its one minute warning has been found to have great advantages over any other system of timing. On several flights double theodolite readings have been taken in order to check the various methods of flight tracking for accuracy, and if the stations are properly located, and accurate time is used this appears to be the most accurate method of position plotting yet attempted by the project.

F. Recovery

The percentage of flights recovered has dropped towards the end of the period covered by this report because, we believe, of the winter conditions which prevent people from discovering our equipment as it comes down. At the present writing flights #28, #43, #52, and #55 have been unrecovered. Only the gondola is missing from flight #28, the balloon having been reported in and the approximate location of the gondola from flight #43 is known but it has not been recovered.

The recovery system used by this project is, on special occasions, to have plane tracking but principle reliance is placed upon recovery by persons in the vicinity of the impact point. Metal reward tags attached to all of the apparatus flown by the project are depended upon to inspire the finder to

contact us. In order to have complete recovery we have found it necessary to have a special telephone system set up so that recovery calls can be received at any time of the day or night since a great number of recovery calls come in off-work hours. A reward consisting of between $5.00 and $15.00 is paid for recovery of apparatus. Complete recovery notes are taken at the impact point if possible by the recovery crews. This information has been found extremely valuable in telling what conditions the flights came down and often times has helped to determine whether there was a basic equipment failure or whether certain observed conditions were due to ground impact. A complete autopsy is done on every gondola returned to the laboratory with detailed notes being taken on the condition and, if possible, operation of every piece of gear. This has helped in a number of cases to prevent faulty equipment or equipment faulty in design from being flown again. We have had vandalism of our equipment on very few occasions.

THE OLLAND CYCLE METHOD OF PRESSURE RECORDING

A. Introduction and Principle of Operation

The Olland Cycle is basically a method of locating the position of a pen arm with a very high degree of accuracy by using a vernier principle. The instrument was suggested to this project by the New York University Constant Level Balloon Project where it was used in a more elementary way and apparently originated with Olland of Utrect, Holland, as a hydrographic device to record the flow of water associated with the dikes. The instrument when used for the measurement of atmospheric pressure utilizes a bellows and contact arm assembly usually of the type used in weather bureau instruments. The Olland Cycle drum is substituted for the commutator to measure the precise position of the contact arm. It consists of a spindle of insulating material with a spiral metal contact which is wound around the arm and is carefully made flush with the surface of the cylinder. This cylinder is rotated by a small motor at constant speed of about 1 rpm and as the contact arm from the bellows touches the spiral a relay is closed and a signal is transmitted over the telemetering system. Contact is also made by fixed contact at one end of the spiral so that the position of the movable contact arm can be determined by the phase angle between the time of contact of the fixed reference and the time of contact of the movable arm considering the time between two successive reference contacts as being equal to 360°. The instrument as originally used by the NYU Project had a single spiral of about 10 turns. This introduces an ambiguity in that from the phase angle one knows only how far between turns of the screw the pen is located and one does not know which turn of the spiral is referred to. A major improvement was made during the work of this contract by introducing a one turn helix which is placed right over the 10 turn helix. The movable arm therefore makes contact with both the one turn and the 10 turn helix and as it moves across the scale the phase angle of the one turn helix changes 360° and serves unambiguously to locate which of the 10 turns

the contact pen is located between. The instrument has been improved considerably by eliminating the second contact which normally serves as a reference and introducing instead one or two straight contact bars parallel to the axis of the cylinder and having a small width like that of the spiral itself. These provide a fixed reference contact which is made by the movable pen itself and so there can be no relative phase displacement between a movable pen and any fixed reference pen due to changes in the mounting of the instrument or perhaps shifting of the drum. Most of the flights have used a type of construction in which the contacts were made on the spiral which was a small metal bar wrapped around a brass core and projecting above its surface. The spaces in between were then coated with a plastic material which was then polymerized and the whole surface was ground off perfectly smooth so that the pen would ride smoothly over the contact spiral from the insulating material.

To simplify the construction of the instrument this process was reversed and grooves were cut into a brass cylinder using ordinary lathe techniques where the spirals were desired to be placed. The grooves were then filled with plastic which was polymerized and the whole cylinder was turned off and polished as smoothly as possible. This means that contact is normally made on the drum but is broken when the pen arm passes over the spiral and the relay is opened and makes contact keying the transmitter. The Olland Cycle as used on the first 20 flights was briefly discussed in the first Progress Report (Volume I, p. 5-4).

B. Method of Manufacture

The original method of manufacturing the rotor was to turn an 11 turn helix on a brass drum, then cut through this helix for the one turn helix and silver solder a wire of the proper diameter into the gaps cut in the 11 turn helix and to the surface of the drum. The whole drum was sent out of the Physics Department shops to the Wolkerstoffer Company, Minneapolis, to have a hard surface plastic, Heresite, sprayed and baked to the surface. The rotor then was ground at high speed to uncover the helices and to polish the surface. It was cleaned very carefully to remove any traces of grinding coolant and grease and then given a very light silver plate to improve the conducting surfaces. A drawing of the rotor surface unwrapped is shown in Figure 31.

A 1 rpm Brailsford motor was used to drive the rotor and a Bendix Freiz Radiosonde Bellows Movement, type 51537-2 was used as the pressure measuring element. The reference arm, taken from a radiosonde movement, was mounted so that it contacted only the end of the fast (one turn) helix. Shop drawings for this instrument are shown in the first Progress Report, Volume II, Appendix XI, Drawing BA421-D.

During the period covered by this report a new Olland Cycle has been designed, and though it was not flown on any of these flights, the improved features will be discussed here.

Silver soldering the fast helix onto the surface of the rotor was a process that was both difficult and also resulted in a number of rejects because of small accumulations of solder in the angles formed at the intersection of the helixes. In addition, the grinding process was found to result in rough edges along the helixes because of the tearing action of the wheel, and because the hot particles of metal torn out of the helixes

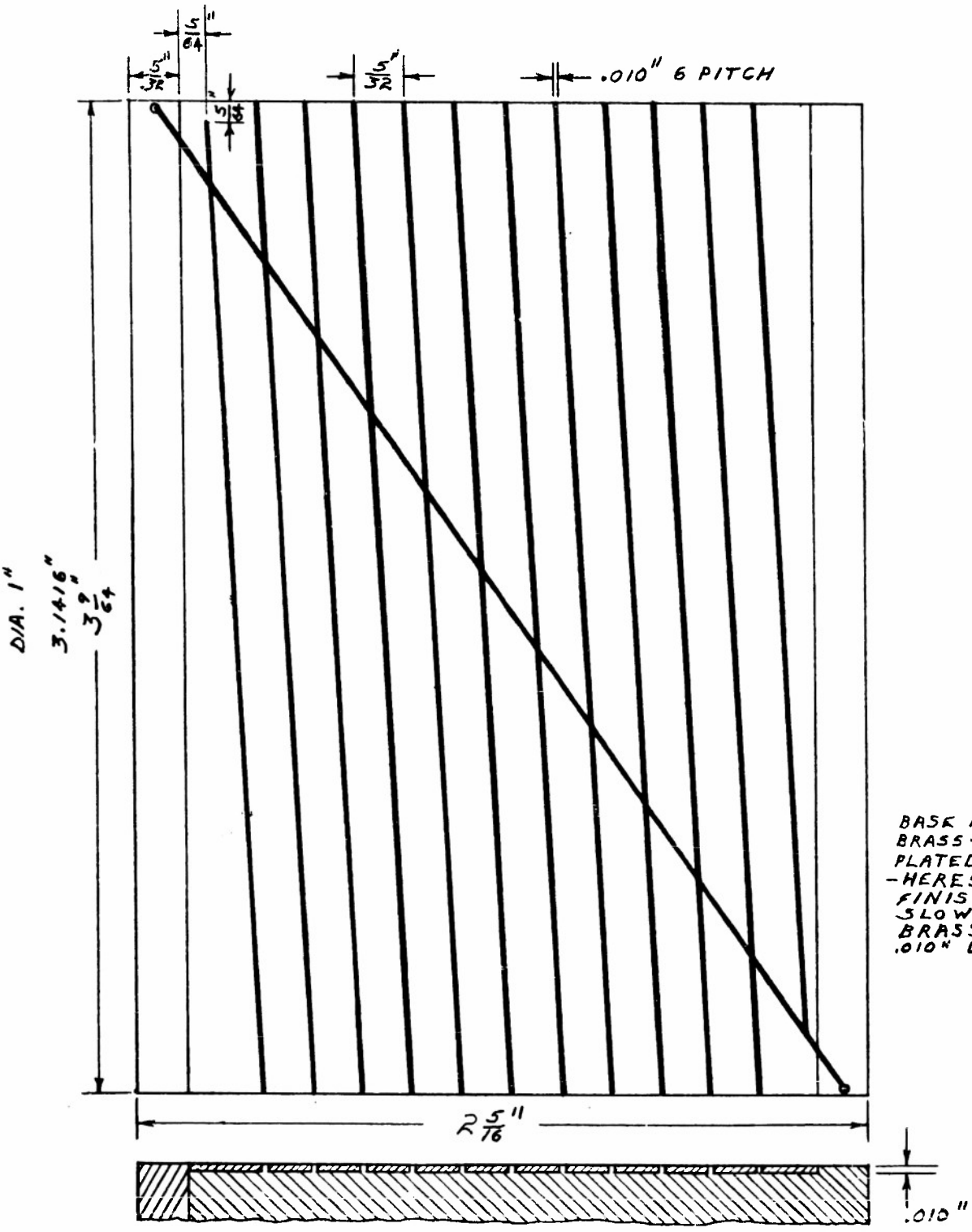

BASE MATERIAL - BRASS - SILVER PLATED, · INSULATION - HERESITE .010" FINISHED TO .005", SLOW HELIX - BRASS WIRE INLAY .010" DIA.

DEPT. OF PHYSICS U. OF MINN. BALLOON PROJECT			SECT. BYT	
DWG. NO.	SHOP DWG. NO.	DRAWN BY	CHECKED BY	DATE
6-PIF-186		[illegible]	[illegible]	10-16-52
SURFACE PLAN + DETAIL I + II TURN HELIX OLLAND CYCLE UNIT			MOD. 1	
			MOD. 2	
			MOD. 3	

SEC. VII FIG. 31

become imbedded in the plastic.

A new method of construction was decided upon where the helixes would be burned into the surface of the drum, a much simpler process, and the helix would then be filled by an insulating material. A plastic Araldite 101 and Hardener 951 which could be applied in the shop was obtained from the Ciba Company, New York thus reducing the necessity of sending the rotors out. Smoothing the surface consisted of removing the excess plastic with a very high turning speed and slow tool feed and a sharp tool. The metal was barely touched on the last cut, keeping to a minimum the amount of metal removed and the rough edges. The rotor was polished with rouge applied on wet fingers.

Since it had become apparent that frequent polishing and occasional replacement of the rotor or motor was necessary as a part of the between-flight servicing of the cycle, a mandrel mounting and a rigid bracket from which the rotor could be easily removed was designed with a gear link to the motor. This gear link also allowed one to change the speed of rotation easily by changing the gears. Pictures and shop drawings of this new cycle are shown in Figures 32 and 33-a, b, and c. A wiring diagram of this cycle is shown in Figure 34. The principle feature of this circuit is a differential relay which closes only when the two pen arms are at different potentials. This allows one to read through "cross-overs"; i.e. telescoping of the pips when the reference arm contacts at the same time as the bellows arm contacts a helix. Smoothing condensers are also included to reduce relay chatter when the arms make and break contact. The second relay furnishes the pulses to the neon lamps in the cameras to record the Olland Cycle data on film.

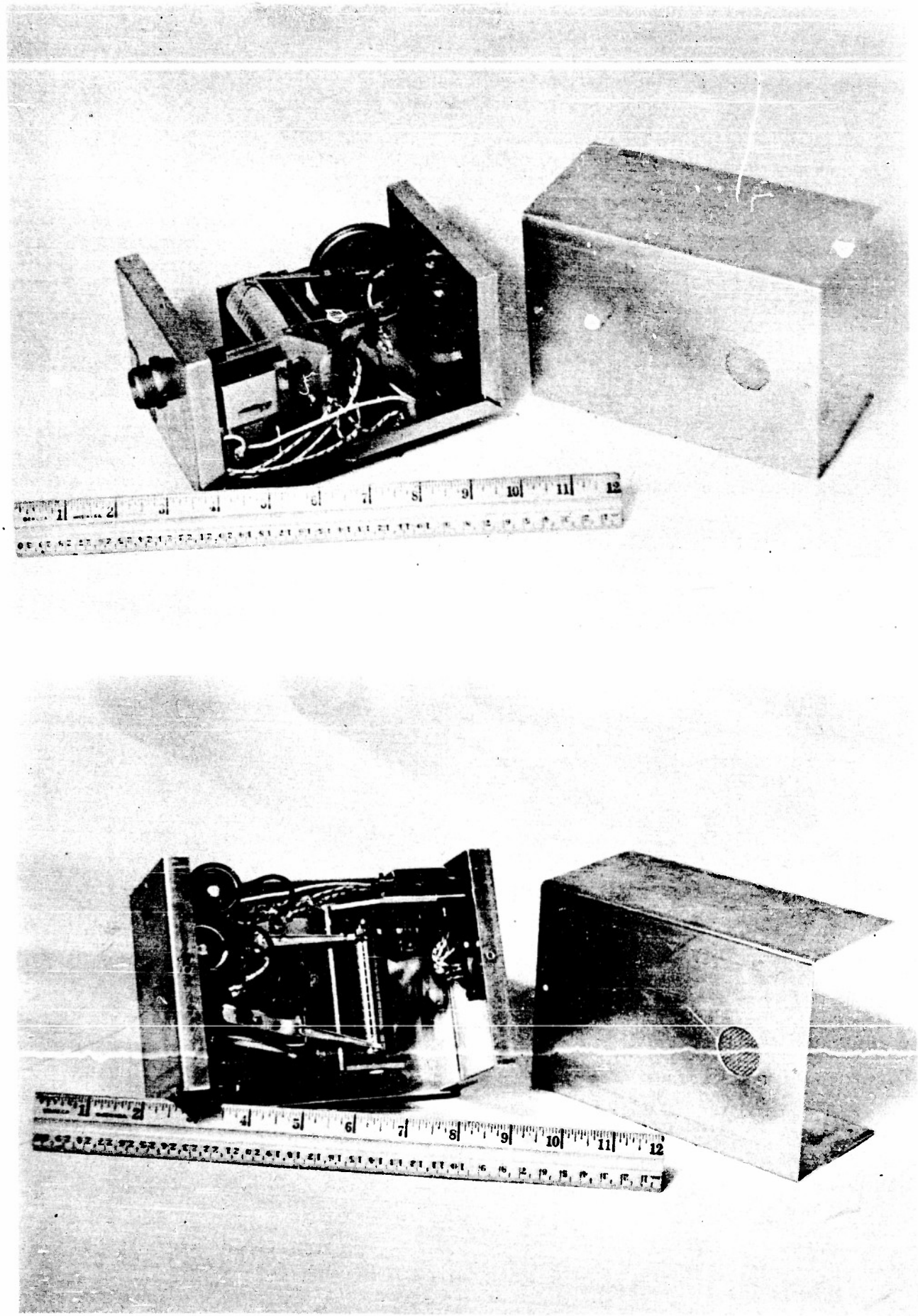

Sec VII Fig 32. Olland Cycle. Right and top views.

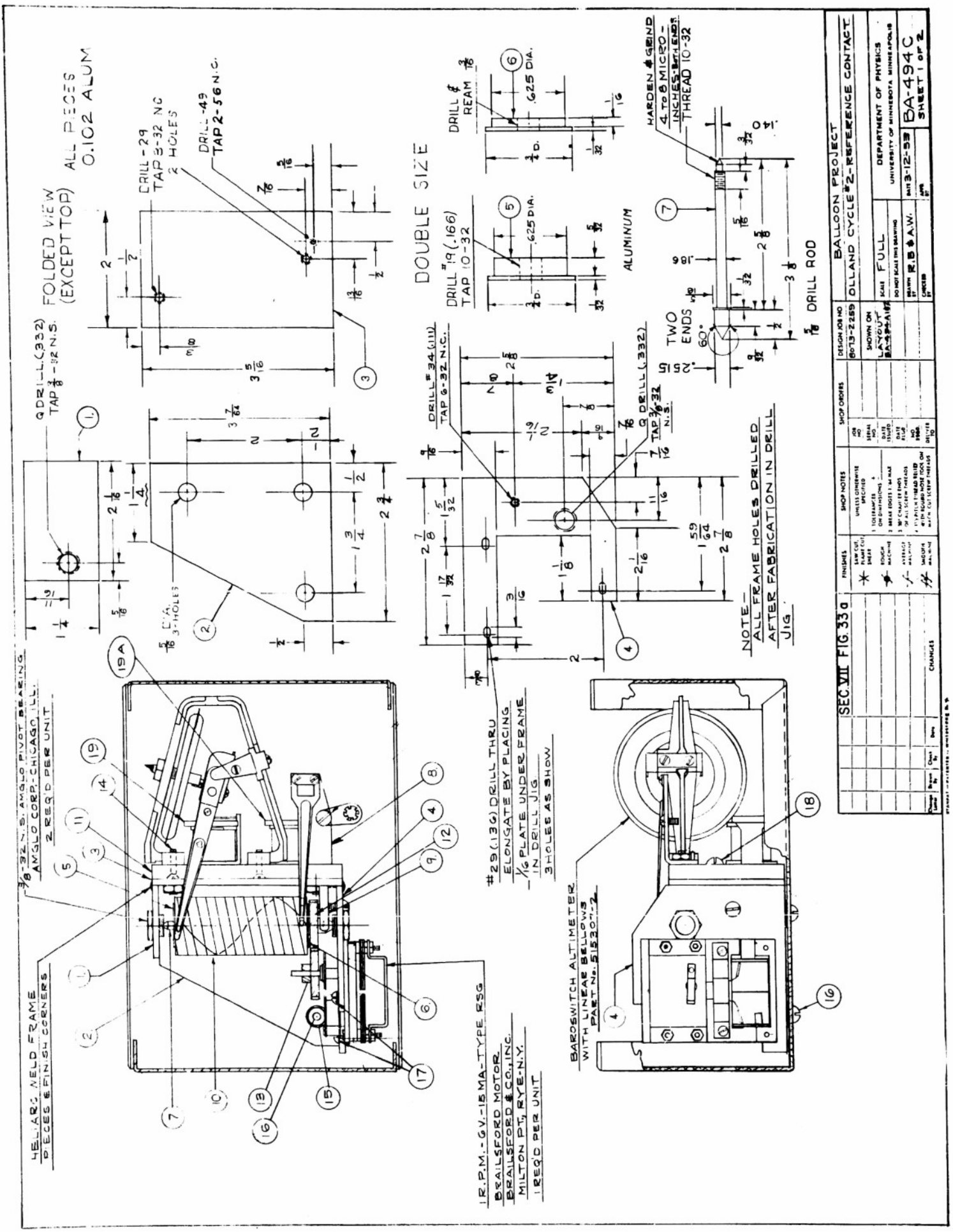
FOLDED VIEW (EXCEPT TOP) ALL PIECES 0.102 ALUM
DOUBLE SIZE
ALUMINUM
TWO ENDS
DRILL ROD
NOTE— ALL FRAME HOLES DRILLED AFTER FABRICATION IN DRILL JIG
#29 (.136) DRILL THRU ELONGATE BY PLACING 1/16 PLATE UNDER FRAME IN DRILL JIG 3 HOLES AS SHOW
BAROSWITCH ALTIMETER WITH LINEAR BELLOWS PART No. 5153-2
1 R.P.M.-GV.-15 MA-TYPE RSG BRAILSFORD MOTOR BRAILSFORD & CO., INC. MILTON PT., RYE, N.Y. 1 REQ'D PER UNIT
4 BLIND WELD FRAME PIECES & FINISH CORNERS
3/8-32 N.S. ANGLO PIVOT BEARING ANGLO CORP.-CHICAGO, ILL. 2 REQ'D PER UNIT
BALLOON PROJECT
OLLAND CYCLE #2-REFERENCE CONTACT
DEPARTMENT OF PHYSICS
UNIVERSITY OF MINNESOTA MINNEAPOLIS
BA-494C
SHEET 1 OF 2
SEC VII FIG 33a

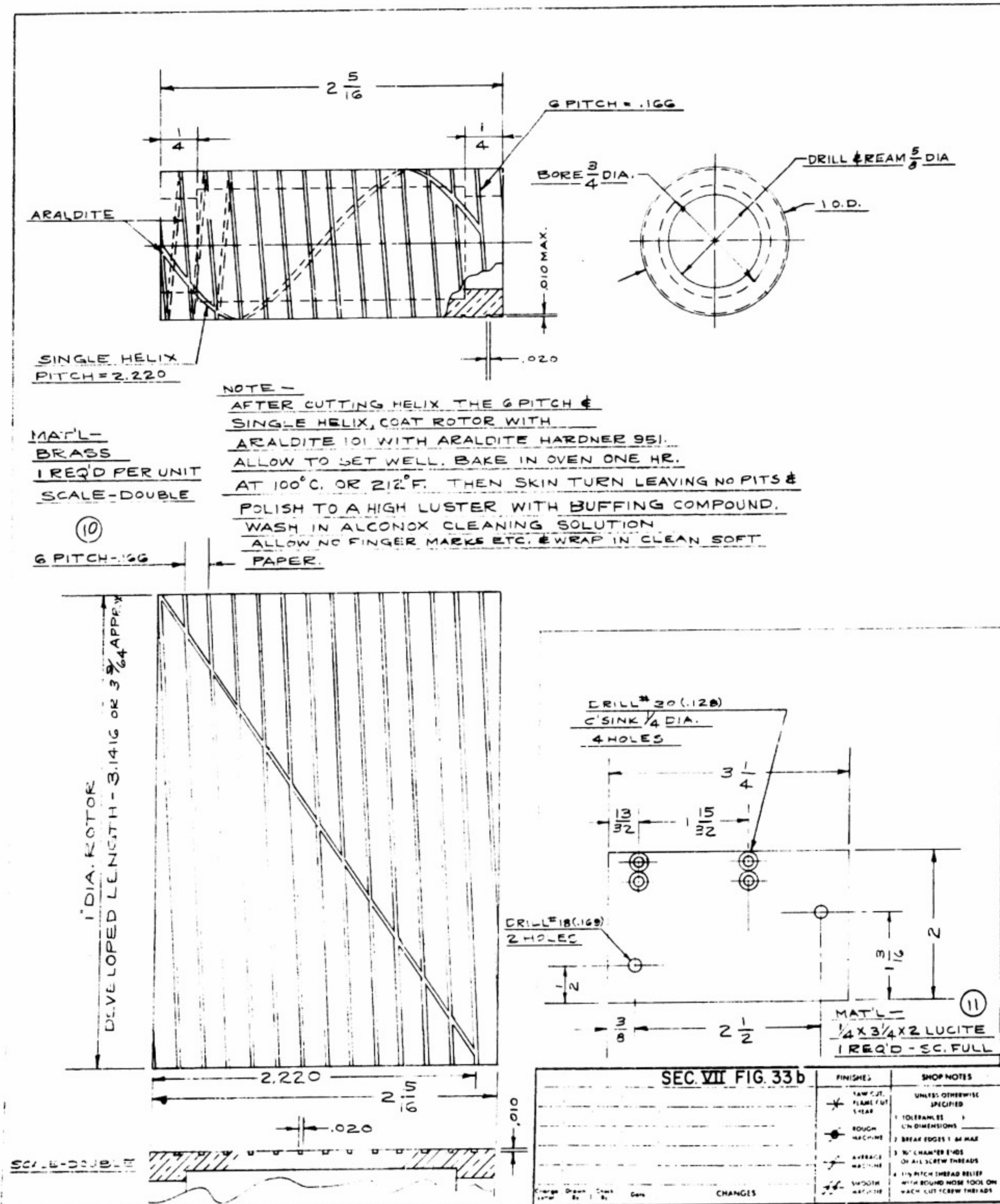

MATERIALS		
ITEM	DESCRIPTION	REQ'D
1	PLATE – .102 TH'K. – ALUM.	1
2	" " " "	1
3	" " " "	1
4	" " " "	1
5	ROTOR END FLANGE – 3/4 DIA. x 3/16	1
6	" " " 3/4 DIA. x 3/32	1
7	ROTOR PIVOT SPINDLE	1
8	REFERENCE POINTER ANGLE MOUNT	1
9	CONTACT – .012 PHOSPHOR BRONZE	1
10	ROTOR – 6 PITCH – 2.220 SINGLE HELIX	1
11	SHEET – 1/4 TH'K. PLEXIGLAS	1
12	BOSTON GEAR – 48 P. – 40 TEETH – 1/8 FACE – BRASS	1
13	" " " " " " BR. WITH HUB	1
14	MACH. SC. – 5-40 N.C. FLAT H'D. BRASS	4
15	GROMMET – 5/16	3
16	MACH. SC. 8-32 N.C. – R'D. H'D – 4 NUTS – BRASS	3
17	MACH. SC. – 5-40 N.C. – R'D. H'D – MOTOR M'T. – BRASS	3
18	MACH. SC. – 8-32 N.C. – R'D. H'D. – BRASS	2
19 & 19A	1001 SPDT 3 V. D.C. – 19A – 6 V. D.C. MIDGET RADIO-SONDE RELAY – PRICE ELECTRIC CO. FREDRICKS, MD.	1 EA.

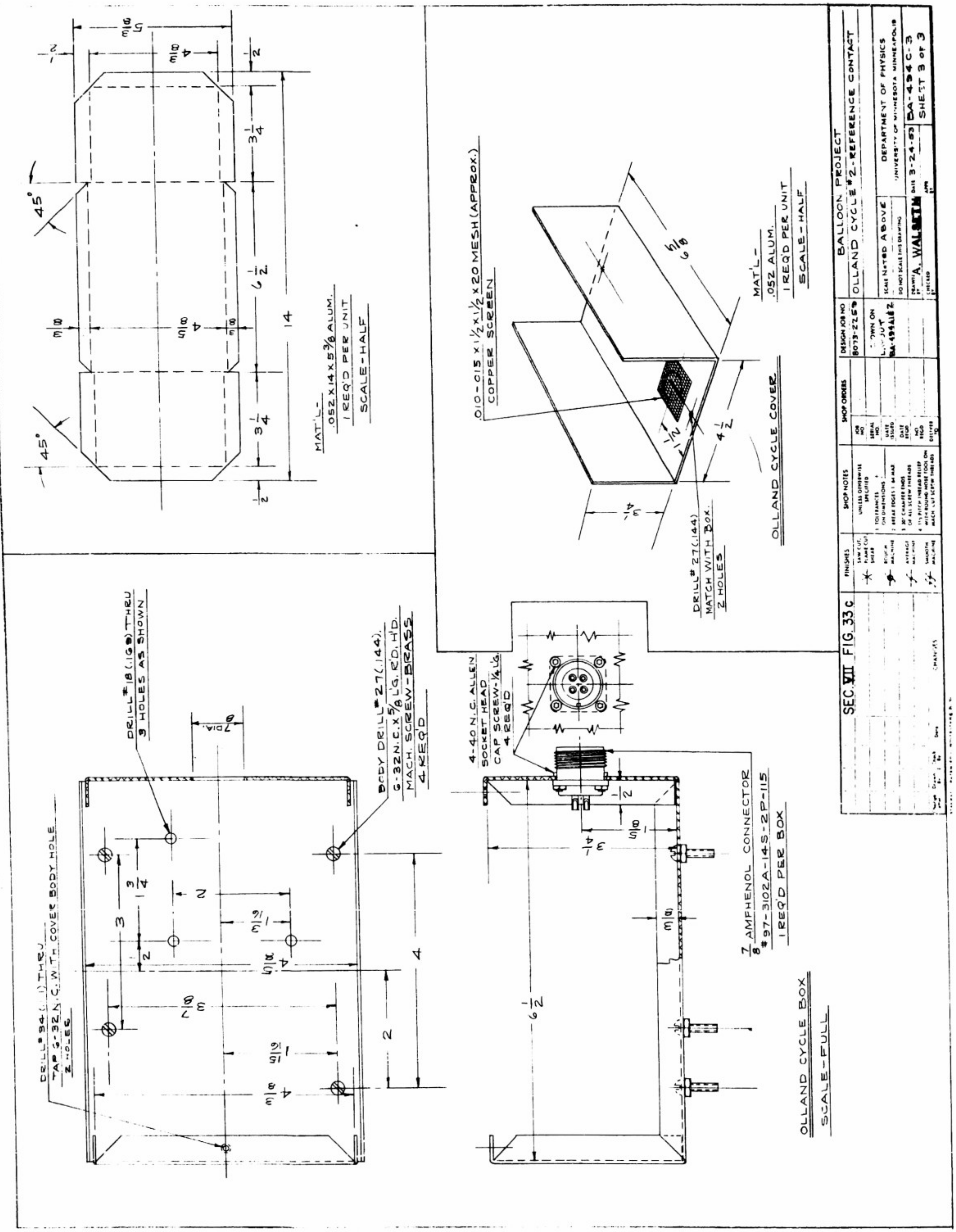
MAT'L - .052 X 14 X 5 3/8 ALUM.
1 REQ'D PER UNIT
SCALE - HALF
.010-.015 X 1 1/2 X 1 1/2 X 20 MESH (APPROX.)
COPPER SCREEN
MAT'L - .052 ALUM.
1 REQ'D PER UNIT
SCALE - HALF
OLLAND CYCLE COVER
DRILL #27 (.144)
MATCH WITH BOX.
2 HOLES
DRILL #18 (.169) THRU
9 HOLES AS SHOWN
BODY DRILL #27 (.144).
6-32 N.C. X 5/8 L'G. R'D. H'D.
MACH. SCREW - BRASS
4 REQ'D
4-40 N.C. ALLEN
SOCKET HEAD
CAP SCREW - 1/4 L'G.
4 REQ'D
7/8 AMPHENOL CONNECTOR
#97-3102A-14S-2P-115
1 REQ'D PER BOX
DRILL #34 (.111) THRU
TAP 6-32 N.C. WITH COVER BODY HOLE
2 HOLES
OLLAND CYCLE BOX
SCALE - FULL
BALLOON PROJECT
OLLAND CYCLE #2 - REFERENCE CONTACT
DEPARTMENT OF PHYSICS
UNIVERSITY OF MINNESOTA MINNEAPOLIS
SCALE NOTED ABOVE
DO NOT SCALE THIS DRAWING
DRAWN BY A. WALSTIN
DATE 3-24-53
BA-494C-3
SHEET 3 OF 3
DESIGN JOB NO 8073-2269
SEC. VII FIG. 33 c

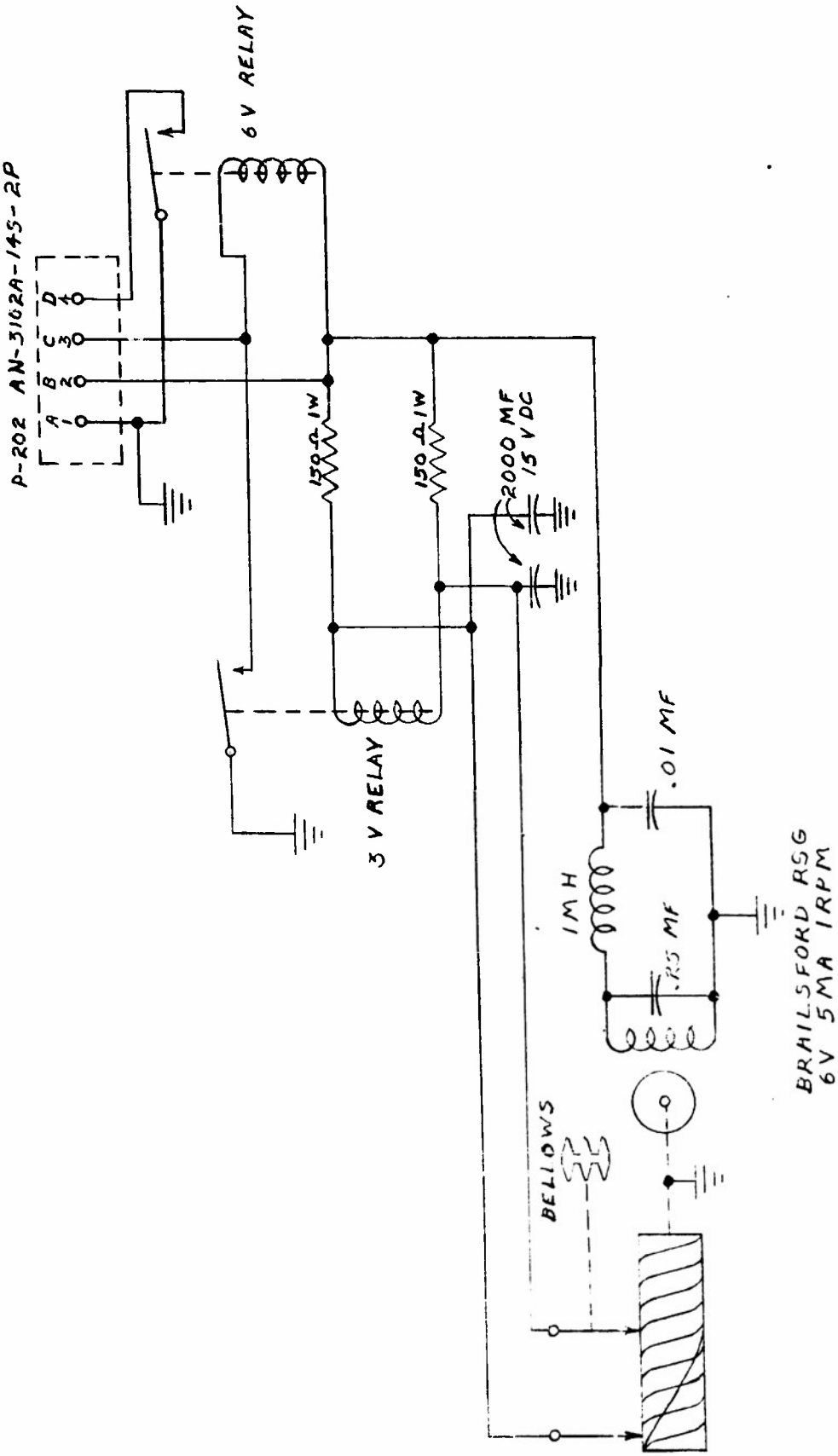

DEPT. OF PHYSICS U. OF MINN.
BALLOON PROJECT
SECT. INS.

DWG. NO.	SHOP DWG. NO.	DRAWN BY	CHK'D BY	DATE
2-OC2-SK1				9-18-52
			MOD. 1	11-18-52
			MOD. 2	12-3-52
			MOD. 3	2-2-53

OLLAND CYCLE UNIT

SEC. VII FIG. 34

C. Calibration Procedure and Accuracy

The Olland Cycle relay normally keys the telemetering transmitter on, and at the receiving station a beat frequency in the audio range is produced and is passed through filters and is used to deflect a Leeds-Northrup strip chart recorder. The type used is type G, model S-60,000 with a paper feed of 3" per minute. The Olland Cycle is calibrated in the laboratory by connecting it directly to the strip chart recorder with the Olland Cycle under a bell jar. Many of the flights were calibrated by pumping the bell jar down to a certain pressure and leaving this pressure on for a short period while the Olland Cycle recorded several cycles on the strip chart, at the same time the pressure was read accurately. Pressures are normally determined by a Wallace and Tiernan type FA-135 mercury manometer which is permanently mounted to the base plate of the bell jar. This manometer can be read precisely to 0.1 mb but it can be inaccurate because of a zero error due to slight displacement of the scale and to small amounts of gas above the mercury column. If the mercury column is run up and down over the full range of the scale very many times there is a possibility that air is liberated into the evacuated region above the column and so periodically the manometer must be re-zeroed in accordance with the instructions furnished by the manufacturer to remove this air. The zero error of the manometer is determined by comparing it with a Stokes-McLeod gage (Flosdorf modification 276-50). As a check on the McLeod a series of readings were taken with a 50 mm Wallace and Tiernan Bourdon gage. This Bourdon gage was checked for zero error in a system where the pressure was known to be less than 10 microns. The results of such a zero check are shown in Figure 35 where it can be seen that the Bourdon gage and the McLeod gage agree to within 01 - 0.2 mb, thus using this particular set of data one would correct the manometer readings by adding 0.8 mb. The calibration procedure was im-

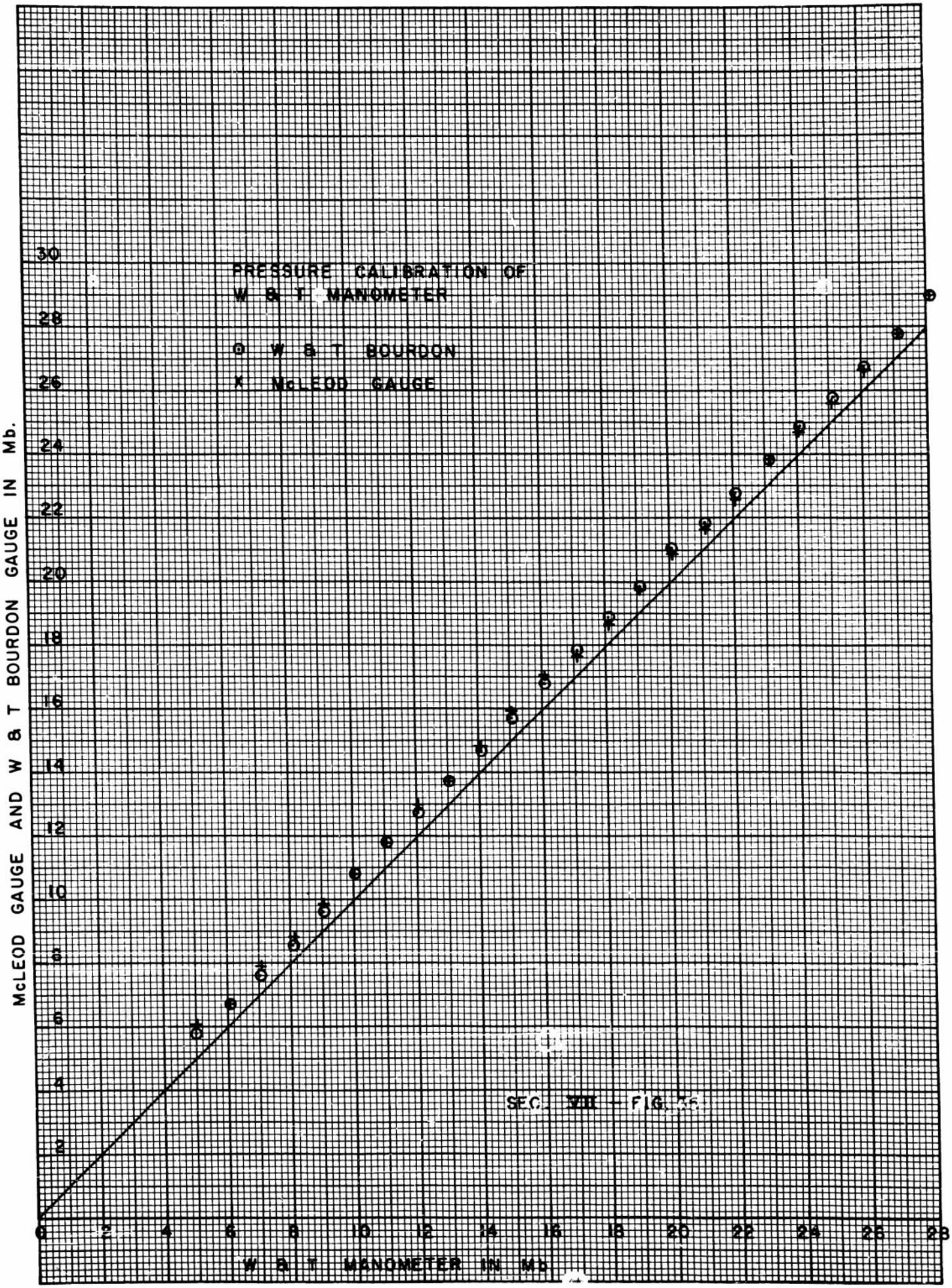

SEC. VIII - FIG. 36

proved considerably by establishing a steady pumping rate of the bell jar from atmospheric pressure down to the lowest pressure reached by the calibrations which is in the vicinity of 10 mb. This pump down takes about 90 minutes in emptying the 3.75 cubic foot bell jar. A pressure reading to the nearest 1/10 mb is taken exactly on the minute and written on the strip chart next to an accurate time mark made by a pen arm operated by a telechron synchronous motor and also recorded on the strip chart. All the pressure readings are then corrected for manometer error and the time of each pressure pip both one turn and 10 turn helices as marked by the Olland Cycle is recorded on the strip chart. This record looks exactly like a flight record, and the same method is used in reading the calibration record as in reading the telemetering recorder during an actual balloon flight. Several methods have been used for doing this, the simpliest being to use an accurately divided steel ruler graduated in hundredths of an inch. One measures the distance between the leading edges of two reference pips which mark one revolution of a cycle rotor and the distances from the leading edge of the first reference pip to both the 11 turn and one turn helix pip which are included between the two references. Then a slide rule is used to determine a phase angle and this is plotted as a function of the pressure. During flight the phase angle is then determined and the pressure read from the calibration chart. This process can be simplified by using a reader similar to the one shown in Figure 36. The inter-reference distance is first set up on the reader by lining up the leading edge of one reference under the edge of the plastic base line and swinging the pivoted arm out until it intersects the other reference on some arbitrarily selected line on the strip chart paper. The graduated scale is then moved up on its guide until it touches the pivoted arm and since the scale contains 360 divisions it automatically indicates 360° between references. Now the pivoted arm can be moved so that

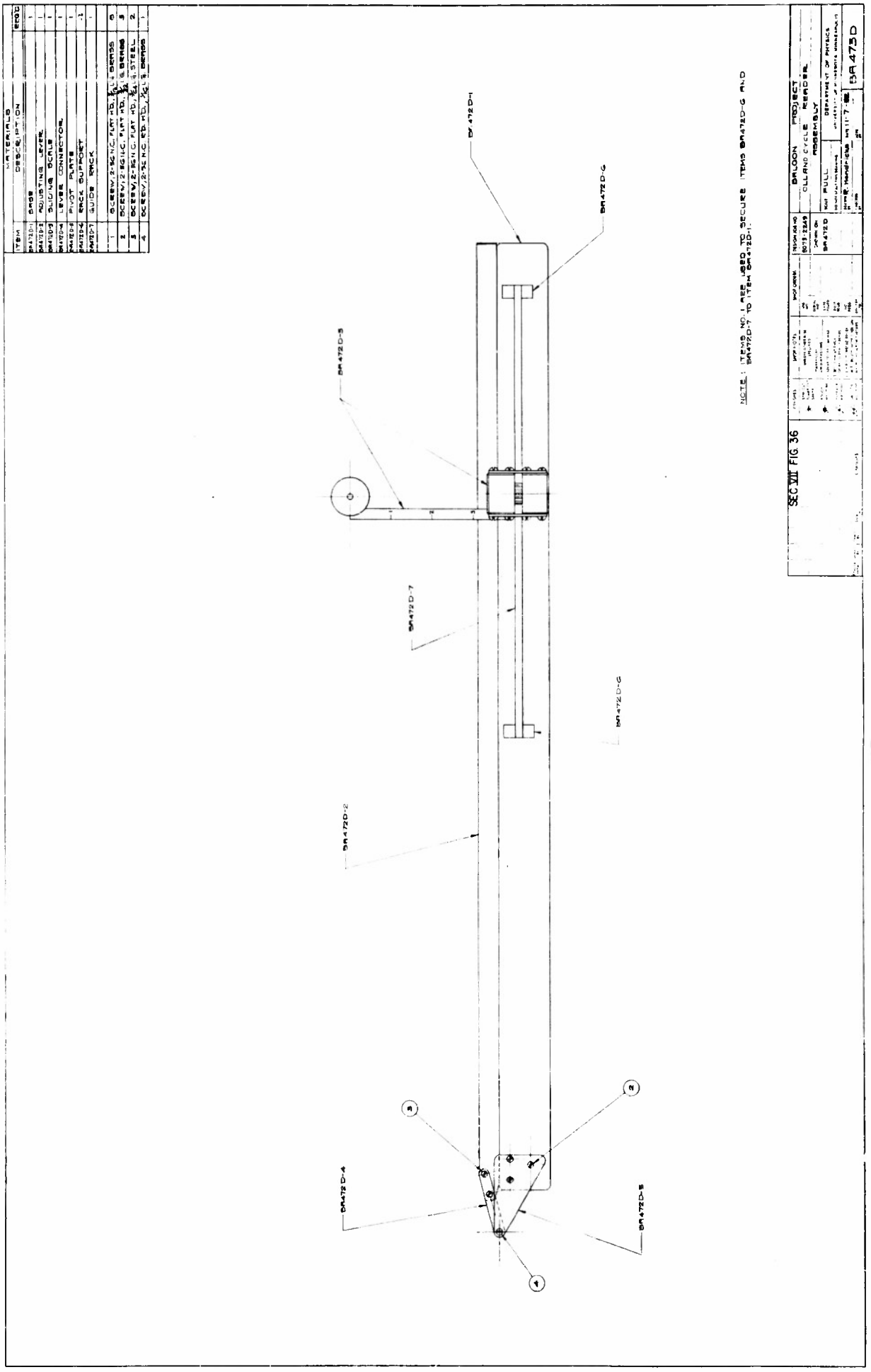
MATERIALS
ITEM
DESCRIPTION
QTY
BA472D
BRASS
ADJUSTING LEVER
SLIDING SCALE
LEVER CONNECTOR
PIVOT PLATE
RACK SUPPORT
GUIDE RACK
SCREW 2-56 N.C. FLAT HD. STEEL
SCREW 2-56 N.C. FLAT HD. BRASS
SCREW 2-56 N.C. FLAT HD. STEEL
SCREW 2-56 N.C. FLAT HD. BRASS
NOTE: ITEMS NO. 1 ARE USED TO SECURE ITEMS BA472D-6 AND BA472D-7 TO ITEM BA472D-1.
BA472D-1
BA472D-2
BA472D-3
BA472D-4
BA472D-5
BA472D-6
BA472D-7
BALOON
CLEVELAND CYCLE
ASSEMBLY
BA472D
BA475D
SEC VII FIG 36

it intersects the leading edge of a helix pip on the same arbitrary line as was used for the reference. The phase angle can then be measured directly on the graduated scale. Actually it is not necessary to use the phase angle at all but the chart can be mounted so that one reads pressure directly by setting the reading device on the strip chart record by a suitable alignment of the calibration curve the pressure in mb is read directly from an index line. This procedure has not been used during the first 55 flights covered by this report and will be described in more detail in a later report.

Figure 37 shows the results of a calibration in which the same Olland Cycle element was pumped down and read six times in succession. The plotting is a little different than that shown in the calibration record of Figure 38 In this figure the phase angle is plotted as the vertical axis and the pressure in mb in the horizontal axis. In Figure 37 the 11 cycles represented by the 11 turn helix are shown as the series of points which gradually change their slope and as can be seen at very low pressures the bellows becomes insensitive as the phase angle changes very little with the pressure, at least in a relative sense. The points seem to group around two lines of which the first three runs constitute one and the second three runs constitute the other as if the instrument suffered a slight shift in its standardization during the time that the runs were being made. The spread of the points falling on the curves on Figure 37 probably are a good representation of the absolute accuracy with which this instrument measures pressure and the error is of the order of $\mp$ 1 mb at the worst place on the scale. With special treatment the Olland Cycle's absolute accuracy can be improved but better accuracy than $\mp$ 1 mb for the flights of this series is not claimed. However, a much higher order of accuracy in a relative sense can be obtained. To exploit the ultimate possibilities of the Olland Cycle one plots the phase angle directly as measured by the instrument in a suitable way and gets the altitude dependence by an average figure representing the relation between phase angle

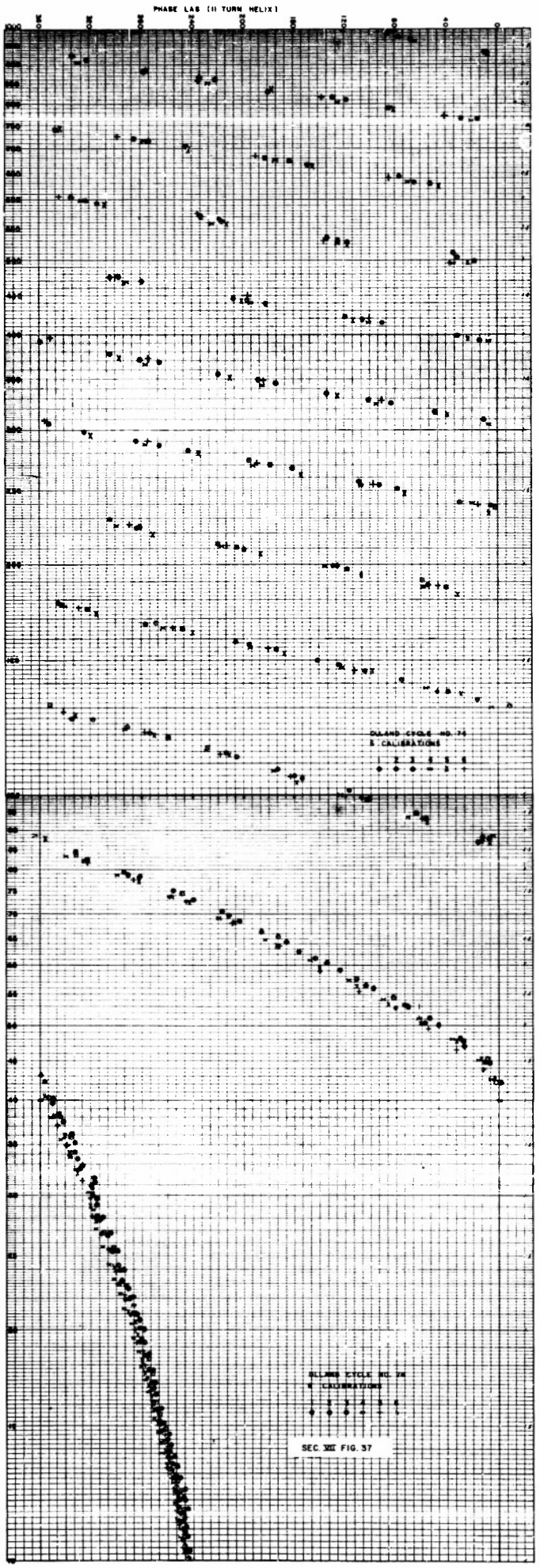
PHASE LAG (II TURN HELIX)
SEC XIII FIG. 37

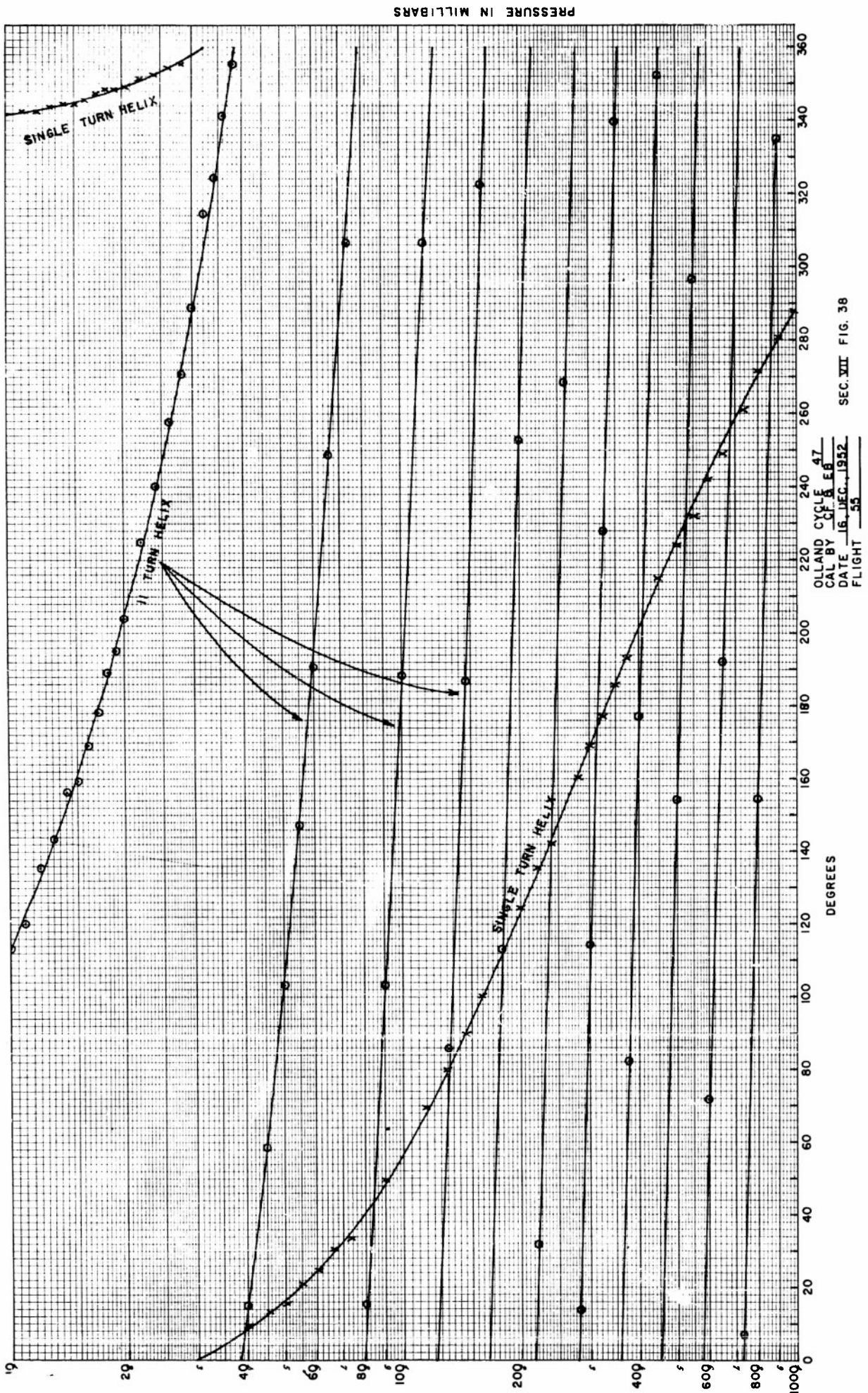
PRESSURE IN MILLIBARS
SINGLE TURN HELIX
II TURN HELIX
SINGLE TURN HELIX
DEGREES
OLLAND CYCLE 47
CAL BY C.F.A.E.B.
DATE 16 DEC. 1952
FLIGHT 55
SEC. VIII FIG. 38

and pressure for the altitude range in question. If this procedure is followed changes in altitudes of the balloon of the order of the height of the balloon which is about 100 feet can be detected at an altitude of 80,000 feet. Data obtained by this technique is extremely valuable for studying the vertical flight of balloons and examples of it are given in Section VI, Figures 10-13 which are phase angle plots on which the altitude is also indicated. On these figures the scale of the balloon is given by a sketch in actual size.

D. Characteristic Results in Flight

Figures 39 through 42 show portions of an actual flight record. Figure 38 is the calibration chart and refers to flight #55. This calibration chart is of the older type made by stopping the bell jar pumping at various fixed pressures and reading the pressure and the OllandCycle phase angle and then going on to the next point. As can be seen on the calibration record, both the 11 turn and one turn helixes show as a series of lines and by reading the phase angle of both of these one finds the pressure in mb unambiguously. Figure 39 shows a portion of flight #55 with a very good noise free signal three hours after launching with the balloon an estimated range of 100 miles. In this particular flight the reference pulse was made double to distinguish it from the single turn helix and from the time pips. A differential relay was also used so that when the 11 turn helix crossed over the reference, that is, when the phase angle was in a neighborhood of zero the differential relay would produce a reverse signal so that a narrow pulse could be read in the middle of a wide pulse. The values of time in central standard time and the pressure in mb are recorded in each cycle of the instrument. One would be able, by reference to the calibration chart given here, to read off these same values from the strip chart record.

Figure 40 is the same flight, #55, about 12 hours after launching with an approximate range of 500 to 600 miles. The record is completely readable but there is more noise on the base line. With a little practice all of the various Olland Cycle pips can be read out of the noise background. Figure 41 shows the record of flight #55 18 hours after launch with an approximate distance of 800 to 900 miles. The signal is still readable but the noise has increased. One should note that the rotation rate of the Olland Cycle helix is much slower which puts the reference pips much further apart, which is probably a temperature effect. Figure 42 shows the signal from #55 18½ hours after launching

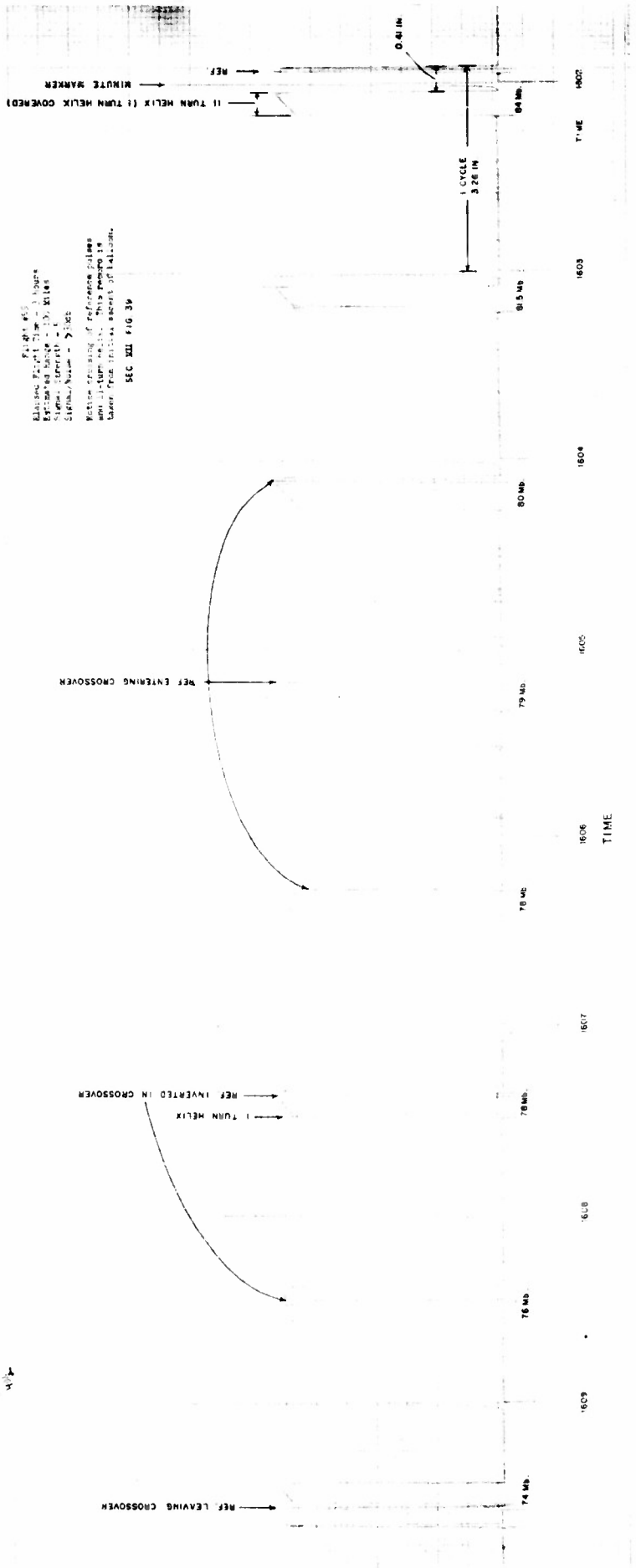
REF
MINUTE MARKER
11 TURN HELIX (1 TURN HELIX COVERED)
0.41 IN
1 CYCLE
3.26 IN
TIME
1602
1603
1604
1605
1606
1607
1608
1609
81.5 Mb
80 Mb
79 Mb
78 Mb
76 Mb
74 Mb
REF ENTERING CROSSOVER
REF INVERTED IN CROSSOVER
1 TURN HELIX
REF LEAVING CROSSOVER
TIME

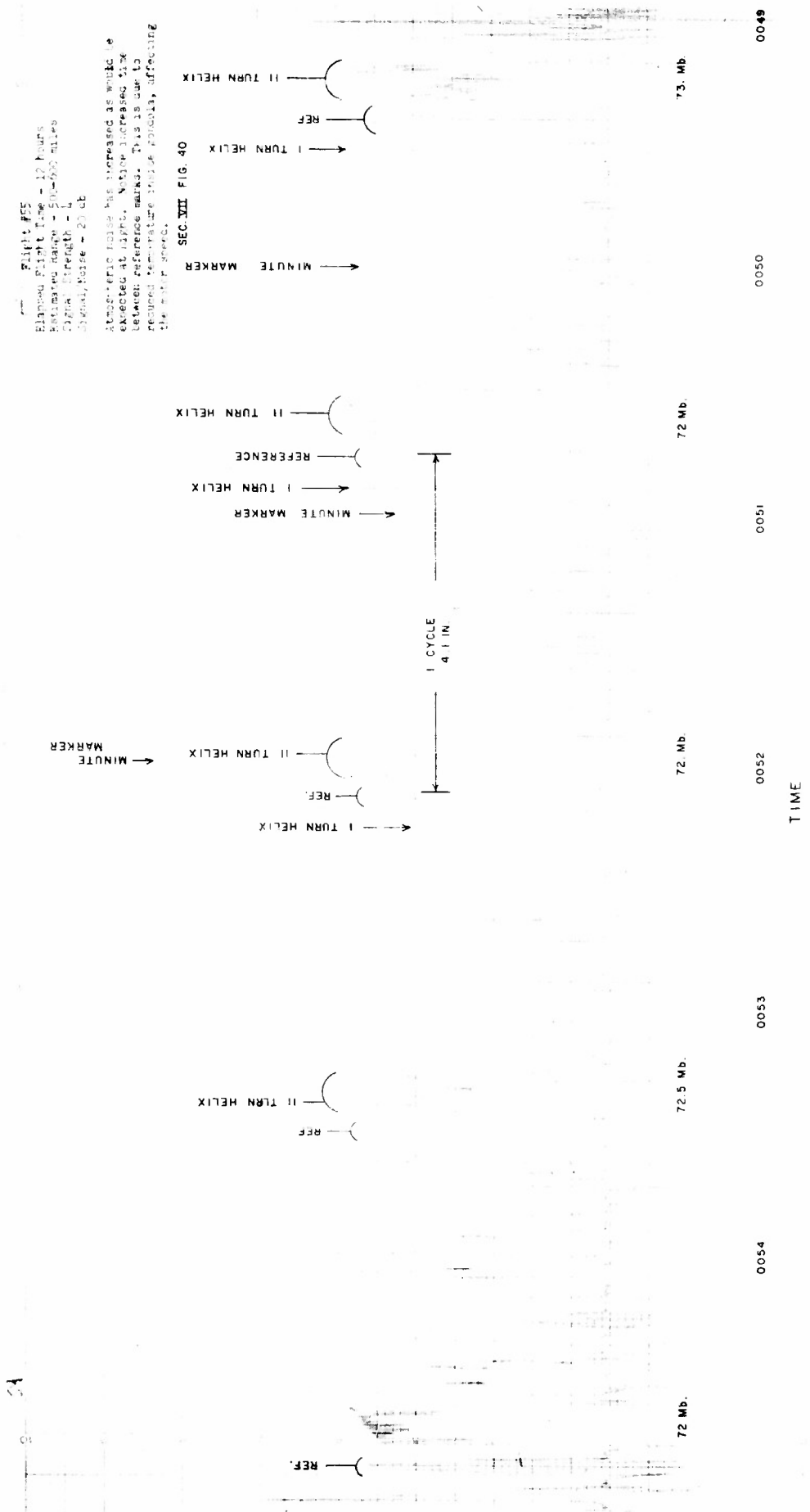
Flight #55
Elapsed Flight Time - 12 hours
Estimated Range - 5000-5500 miles
Data Strength - 4
Data, Noise - 20 db
SEC. VII FIG. 40
MINUTE MARKER
II TURN HELIX
I TURN HELIX
REF
73 Mb
0049
0050
REFERENCE
72 Mb
0051
1 CYCLE
4 1 IN.
72 Mb
0052
72.5 Mb
0053
72 Mb
0054
TIME

SEC. VII FIG 41

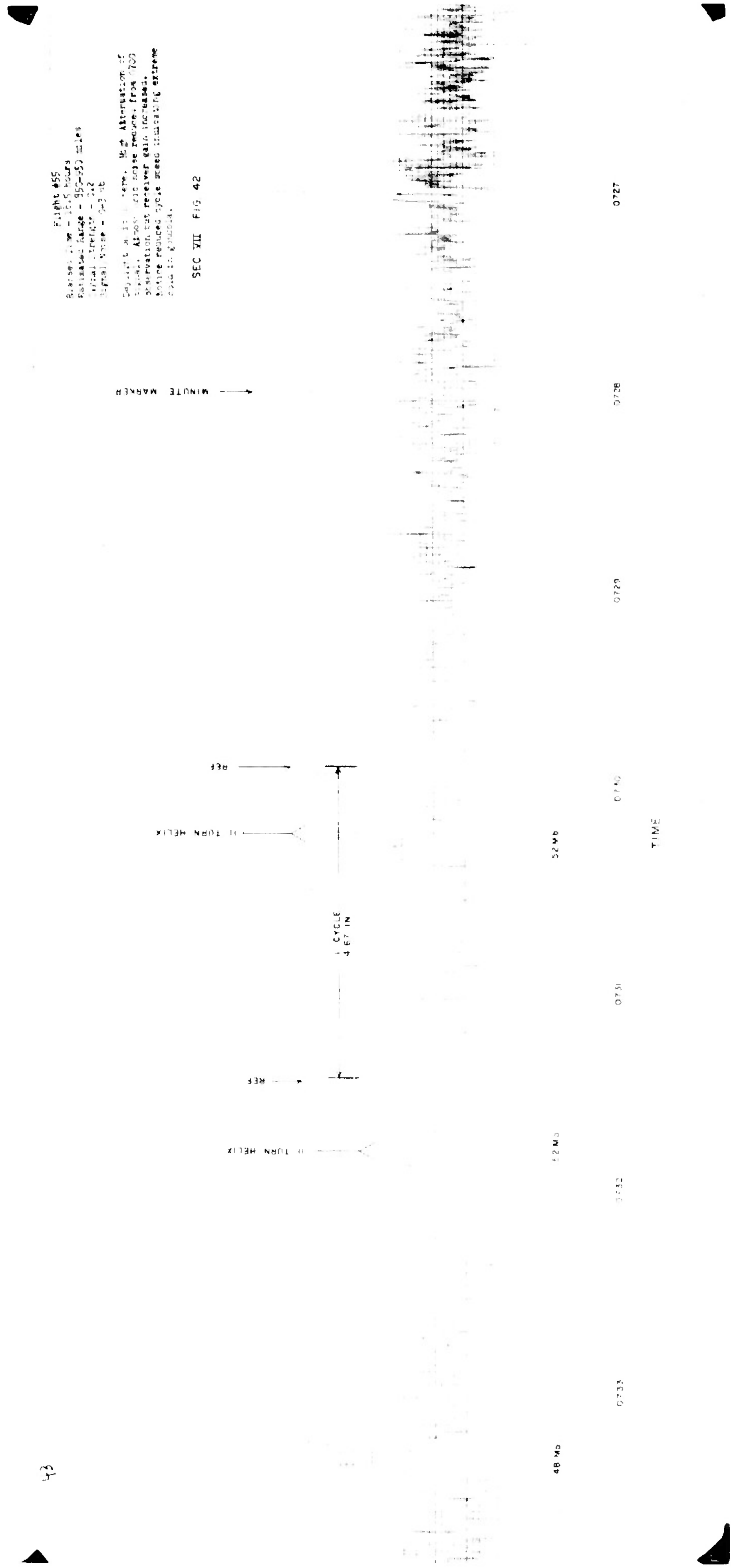
Flight #55
SEC VII FIG 42
MINUTE MARKER
REF
TURN HELIX
1 CYCLE
4.67 IN
0727
0728
0729
0731
0733
52 Mc
48 Mc
TIME

just before the signal was lost. In this portion of the record the signal faded in again and points were obtained and these points were indexed on the strip chart shown. The signal faded out as expected when sunrise occurred with the frequency in use which was 1638 kc and the range involved, approximately 950 miles. The relation between range, frequency and time of year, power, etc. is discussed in Section VIII of this report which deals with the radio propagation and telemetering problems. Although the Olland Cycle has customarily been recorded on a strip chart for the most accurate presentation for measurement the altitude can be determined by listening to the CW keyed signal transmitted from the balloon on any communications receiver equipped with a beat frequency oscillator and using an ordinary wrist watch with a sweep second hand. By making a list of the times the various pulses come on one can get an accuracy of measuring altitude which is very good and for many purposes is quite satisfactory. The signal from the Olland Cycle can also be easily recorded on tape for playback through the strip chart recording system at a later date. This process has been carried out on numerous occasions.

GONDOLA PHOTOGRAPHS AND BLOCK DIAGRAMS

The following pages contain for reference purposes photographs and block wiring diagrams of the various gondolas flown on flights #21 - #55. Most of the flights differ in their details but wherever possible have been constructed of standard components. The frequency of use of various items can be seen by reference to the table at the beginning of this section.

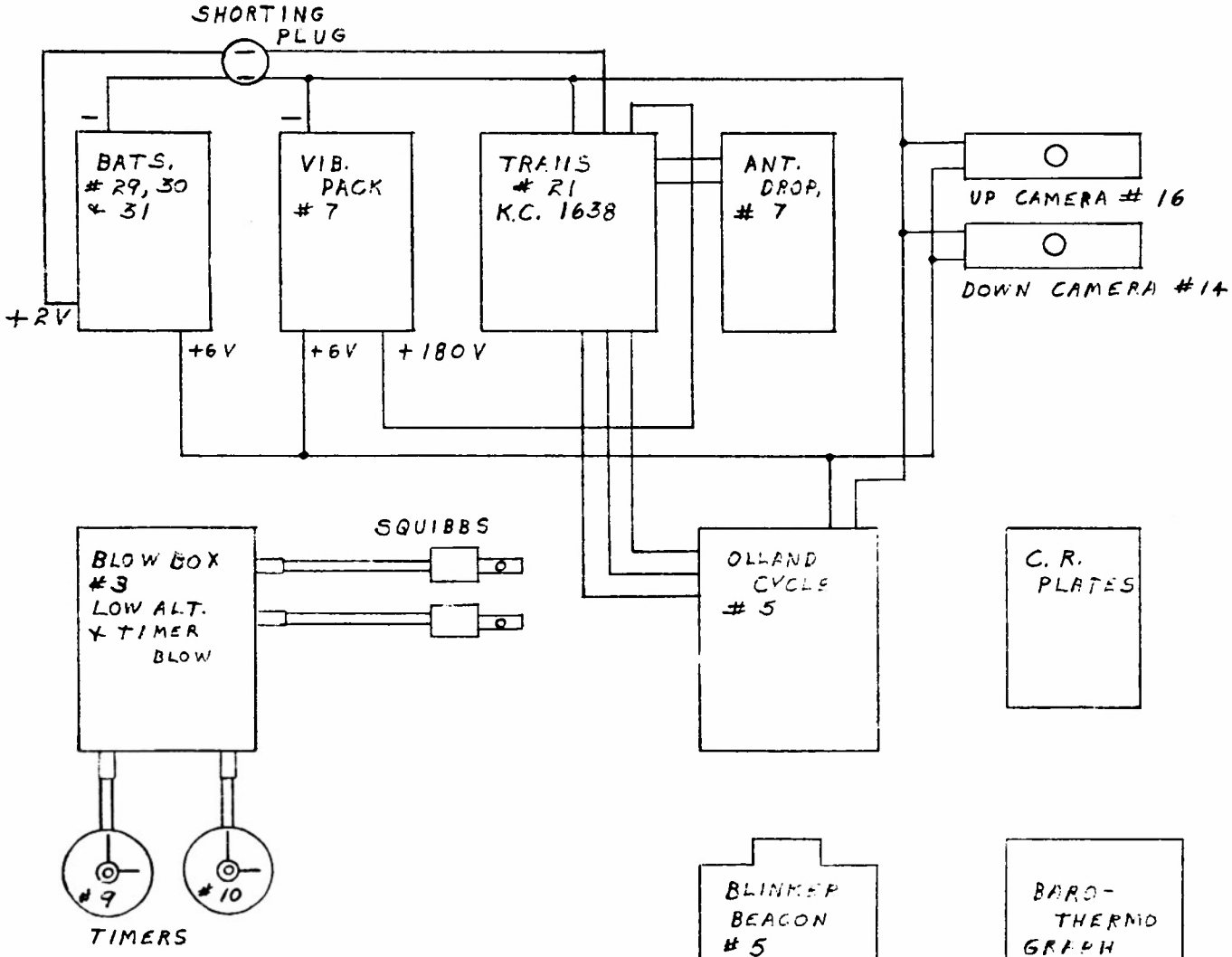

DEPT. OF PHYSICS U. OF MINN.

...DON PROJECT SECT.

...G. NO.	SHOP DWG. NO.	DRAWN BY	CHECKED BY	DATE
				6-25-52
FLIGHT # 21 GONDOLA # 5			MOD. 1	
			MOD. 2	
			MOD. 3	

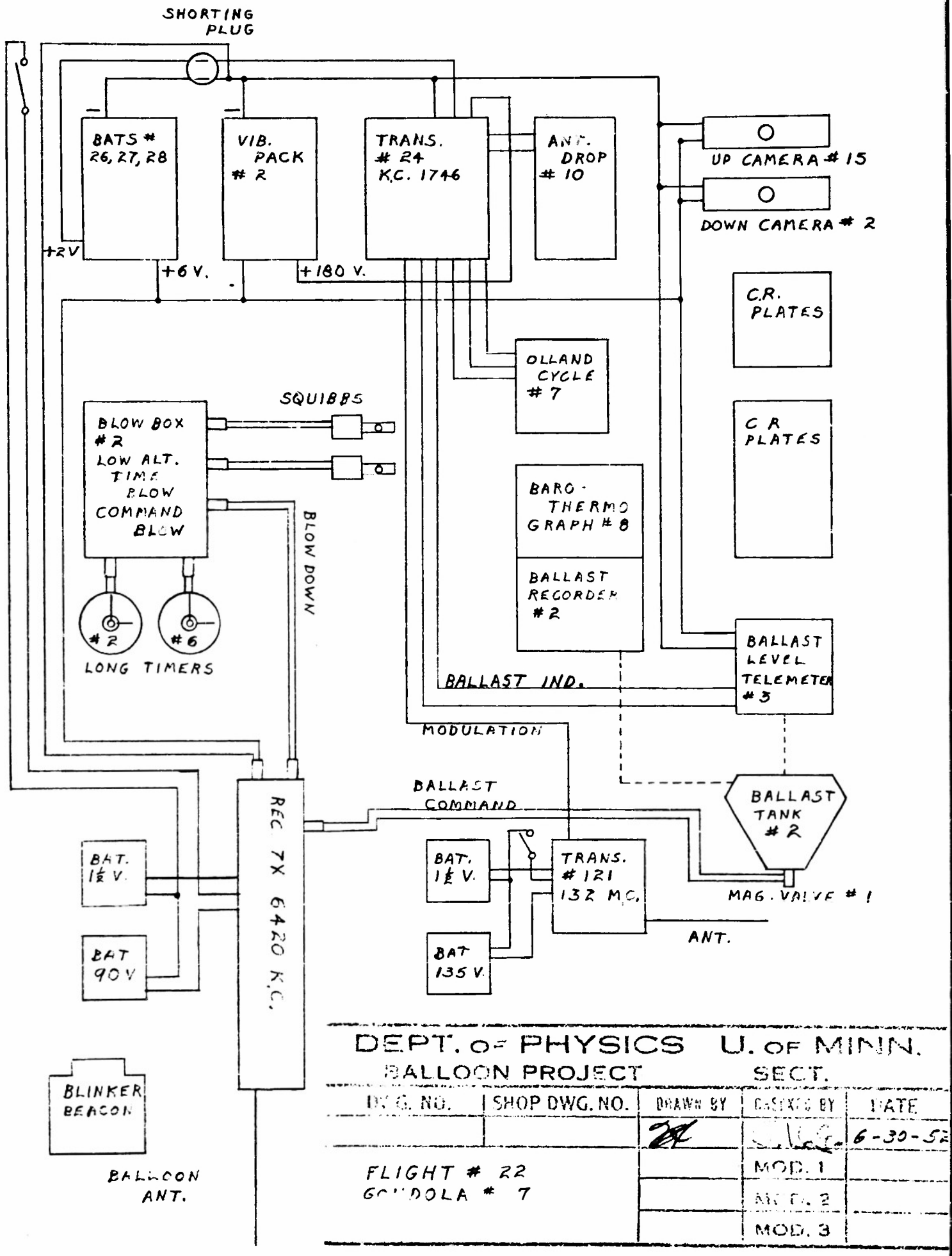
SHORTING PLUG
BATS # 26, 27, 28
VIB. PACK # 2
TRANS. # 24 K.C. 1746
ANT. DROP # 10
UP CAMERA # 15
DOWN CAMERA # 2
+2V
+6 V.
+180 V.
C.R. PLATES
OLLAND CYCLE # 7
SQUIBBS
BLOW BOX # 2
LOW ALT. TIME BLOW
COMMAND BLOW
BLOW DOWN
BARO-THERMO GRAPH # 8
BALLAST RECORDER # 2
C R PLATES
#2
#6
LONG TIMERS
BALLAST IND.
BALLAST LEVEL TELEMETER # 3
MODULATION
BALLAST COMMAND
BALLAST TANK # 2
REC. TX 6420 K.C.
BAT. 1½ V.
BAT 90 V
BAT. 1½ V.
TRANS. # 121 132 M.C.
MAG. VALVE # 1
ANT.
BAT 135 V.
BLINKER BEACON
BALLOON ANT.
DEPT. OF PHYSICS U. OF MINN.
BALLOON PROJECT
SECT.
DWG. NO.
SHOP DWG. NO.
DRAWN BY
CHECKED BY
DATE
6-30-52
FLIGHT # 22
GONDOLA # 7
MOD. 1
MOD. 2
MOD. 3

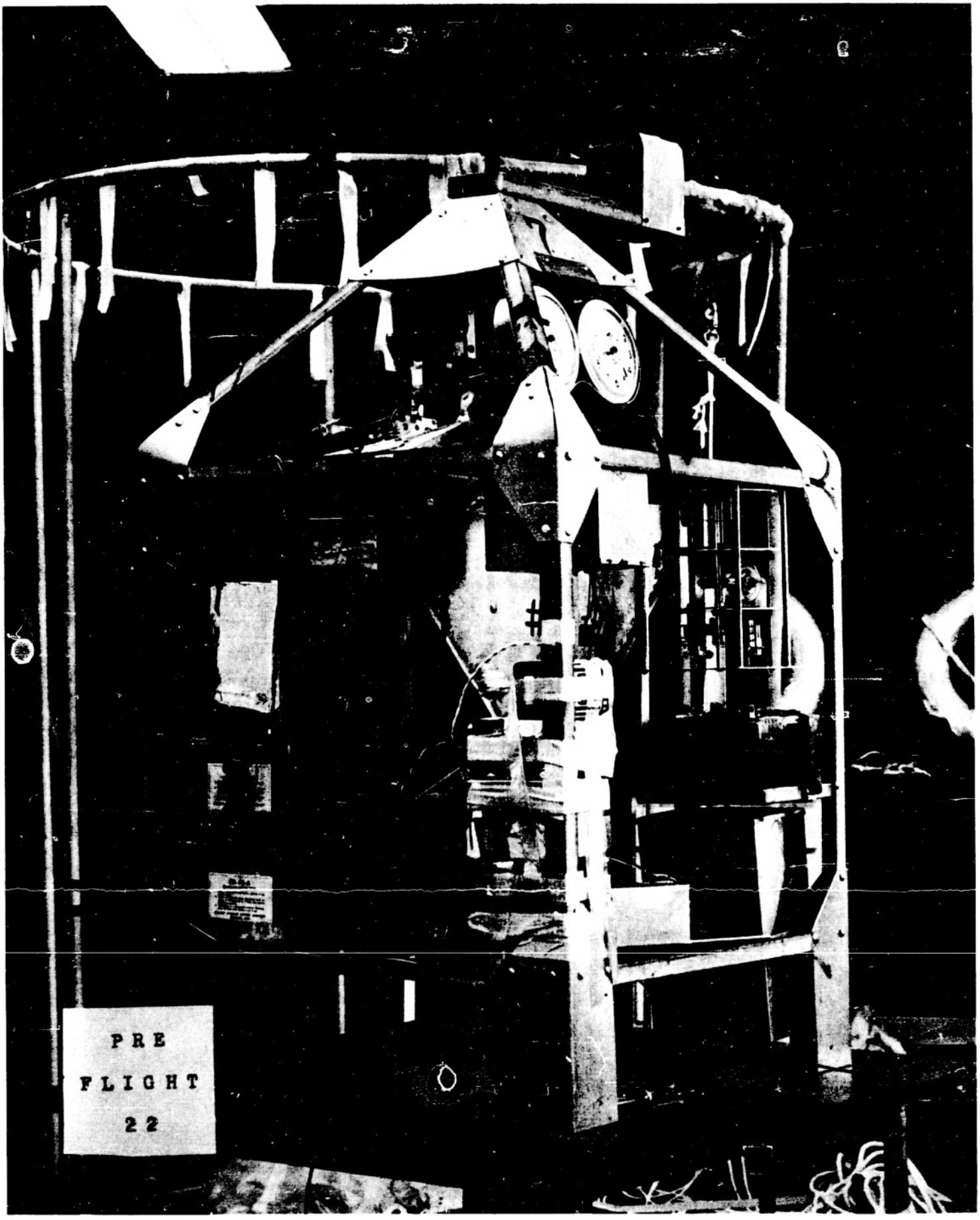
PRE
FLIGHT
22

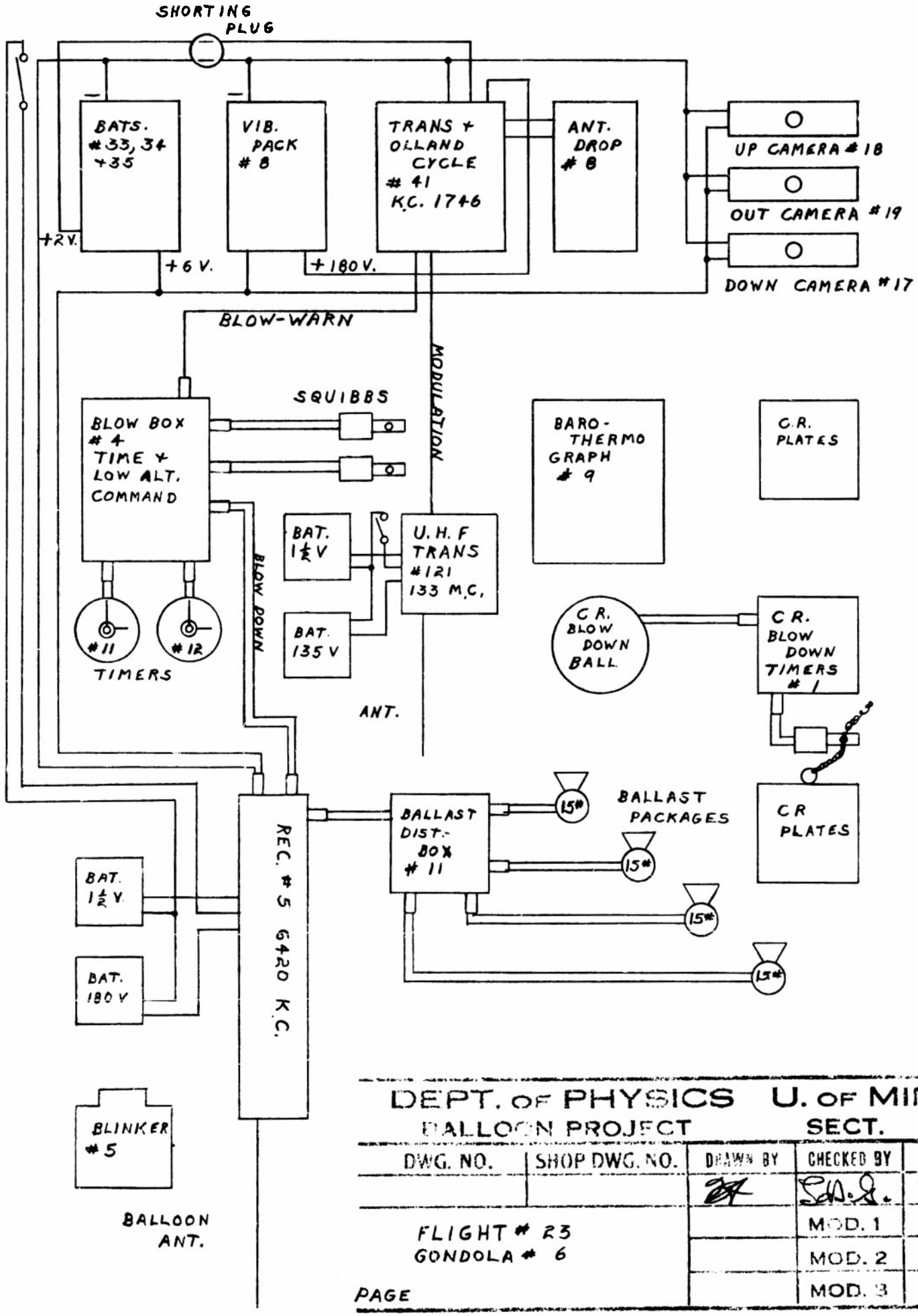

DEPT. OF PHYSICS U. OF MINN.
BALLOON PROJECT SECT.

DWG. NO.	SHOP DWG. NO.	DRAWN BY	CHECKED BY	DATE
				7-3-52
FLIGHT # 23 GONDOLA # 6			MOD. 1	
			MOD. 2	
PAGE			MOD. 3	

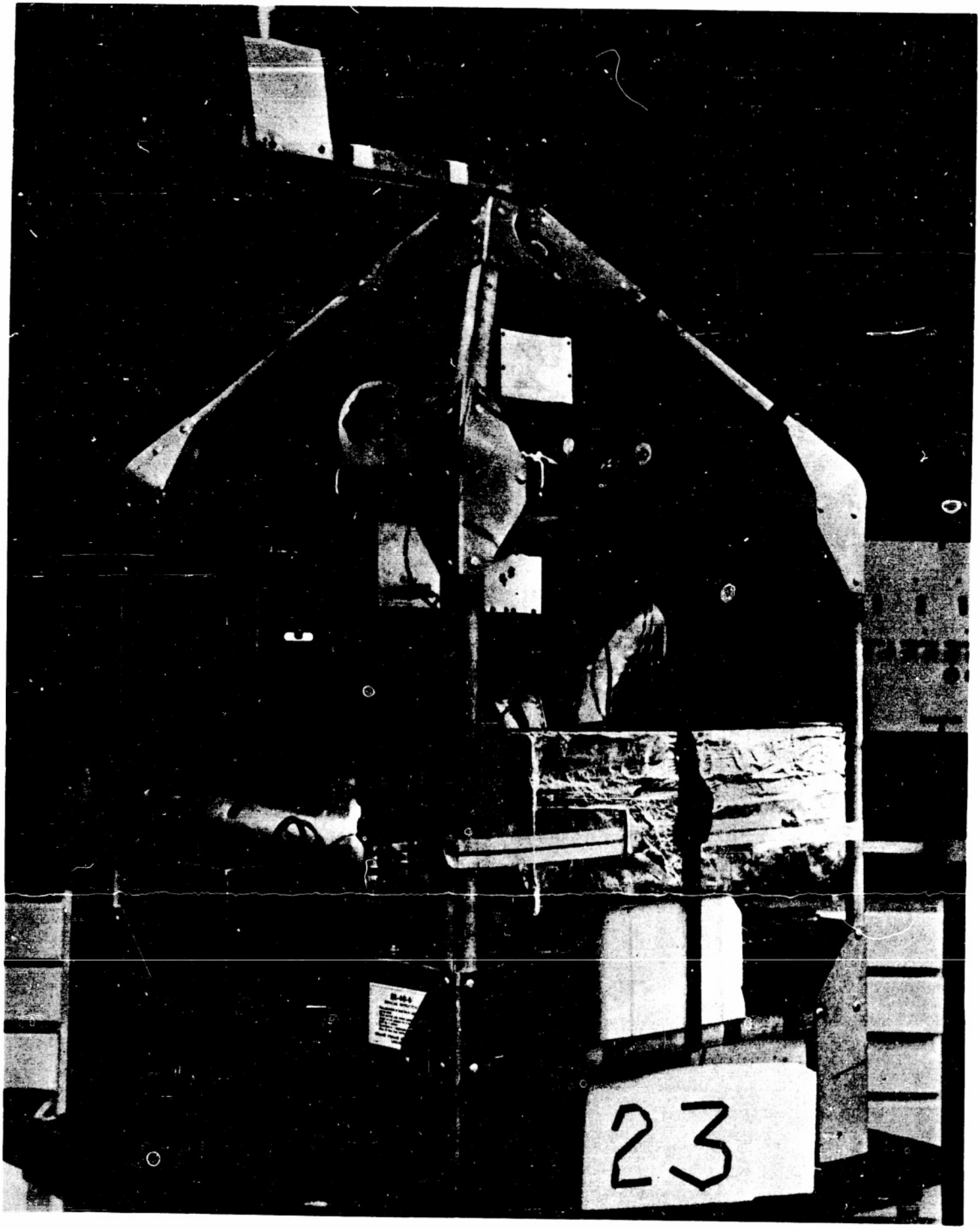
23

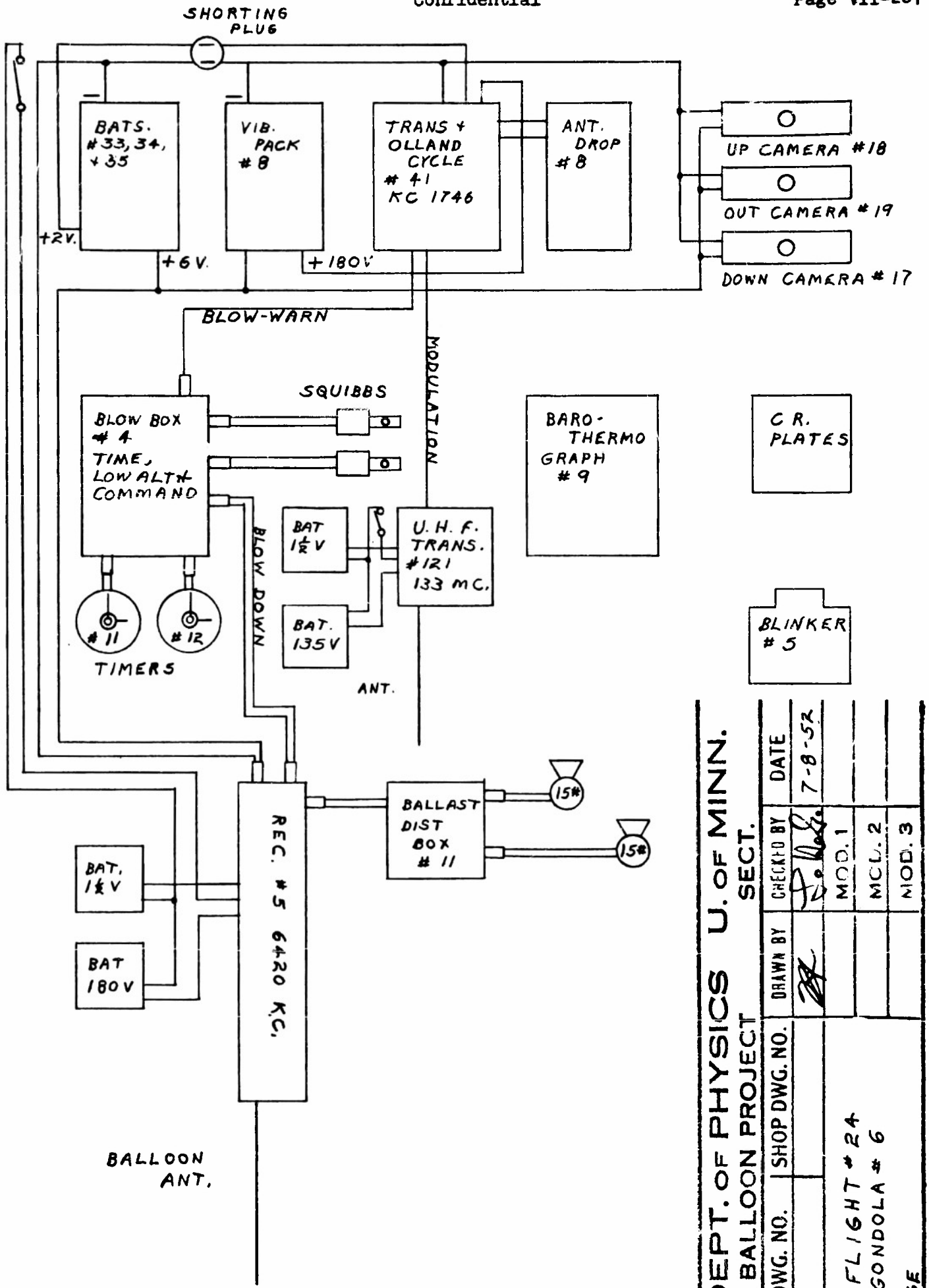

DEPT. OF PHYSICS U. OF MINN.
BALLOON PROJECT SECT.

DWG. NO.	SHOP DWG. NO.	DRAWN BY	CHECKED BY	DATE
				7-8-52
			MOD. 1	
			MOD. 2	
			MOD. 3	

FLIGHT #24
GONDOLA #6
PAGE

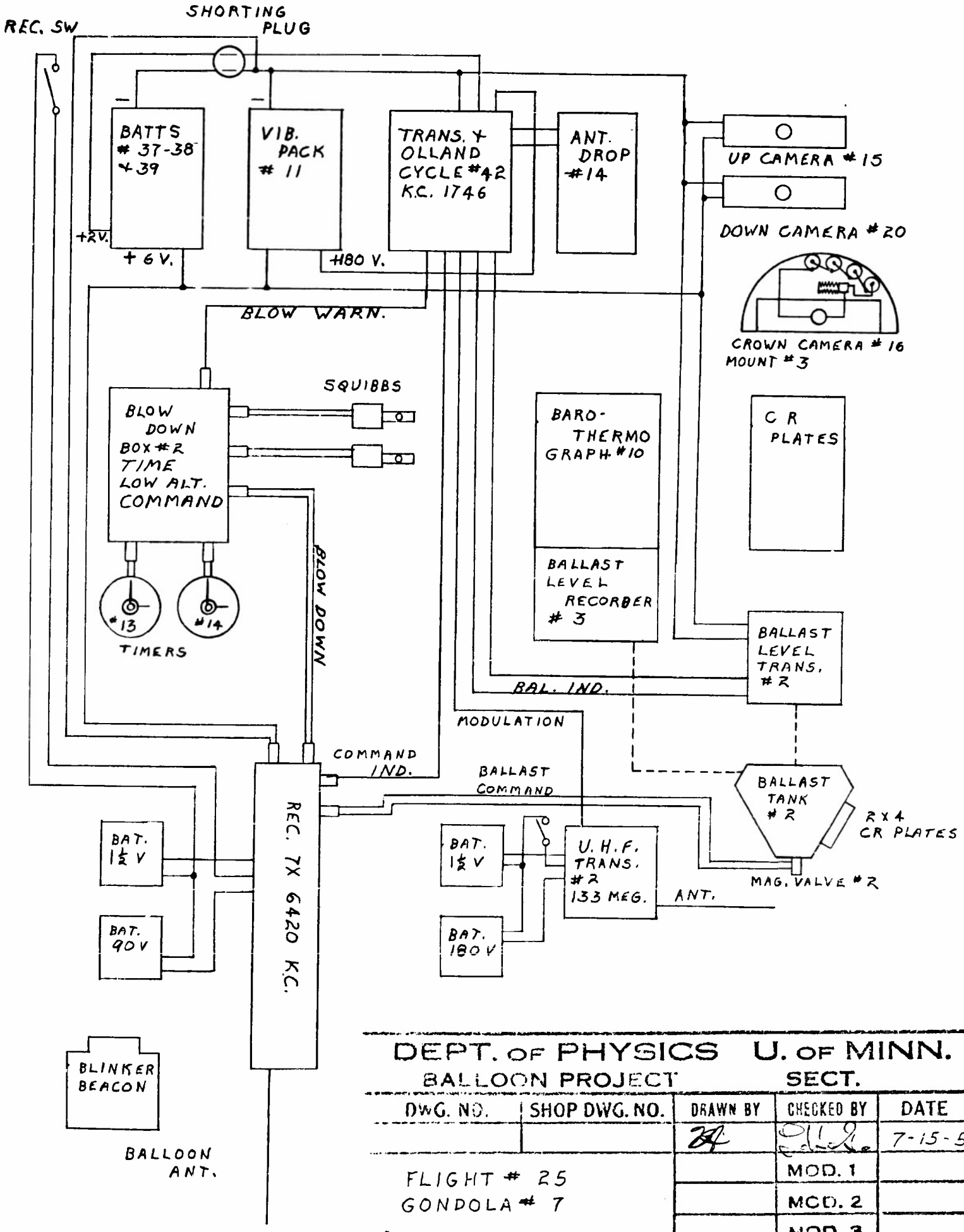

DEPT. OF PHYSICS U. OF MINN.				
BALLOON PROJECT			SECT.	
DWG. NO.	SHOP DWG. NO.	DRAWN BY	CHECKED BY	DATE
		ZA	[illegible]	7-15-52
FLIGHT # 25			MOD. 1	
GONDOLA # 7			MOD. 2	
PAGE			MOD. 3	


#2
FLIGHT
25

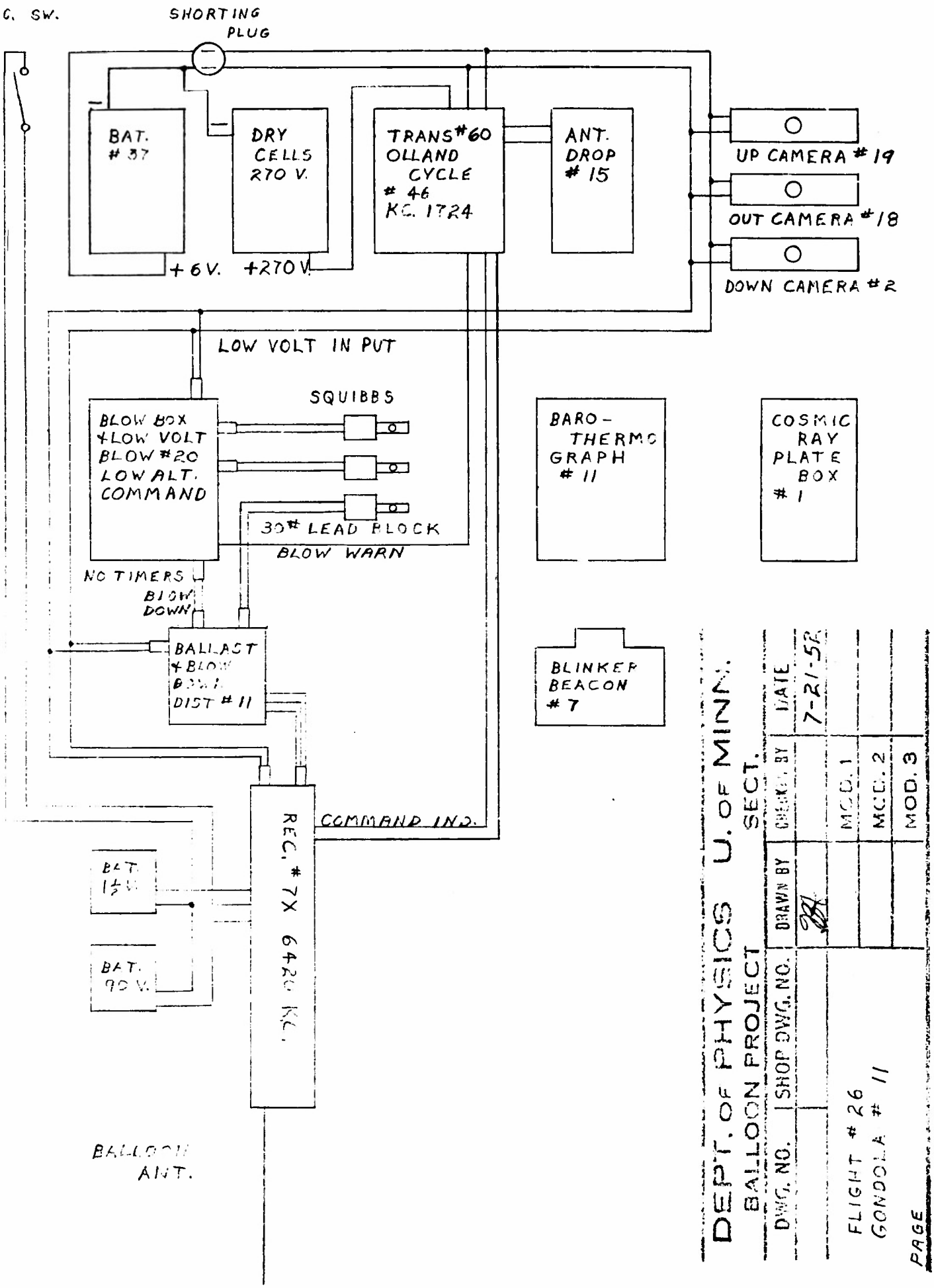
REC. SW.
SHORTING PLUG
BAT. # 37
DRY CELLS 270 V.
TRANS #60 OLLAND CYCLE # 46 KC. 1724
ANT. DROP # 15
UP CAMERA # 19
OUT CAMERA # 18
DOWN CAMERA # 2
+6 V.
+270 V.
LOW VOLT IN PUT
SQUIBBS
BLOW BOX & LOW VOLT BLOW #20 LOW ALT. COMMAND
30# LEAD BLOCK
BLOW WARN
BARO-THERMO GRAPH # 11
COSMIC RAY PLATE BOX # 1
NO TIMERS
BLOW DOWN
BALLAST & BLOW DIST # 11
BLINKER BEACON # 7
COMMAND IND.
REC. # 7X 6420 KC.
BAT. 12 V.
BAT. 90 V.
BALLOON ANT.
DEPT. OF PHYSICS U. OF MINN.
BALLOON PROJECT
SECT.
DWG. NO.
SHOP DWG. NO.
DRAWN BY
CHECKED BY
DATE
7-21-52
MOD. 1
MOD. 2
MOD. 3
FLIGHT # 26
GONDOLA # 11
PAGE

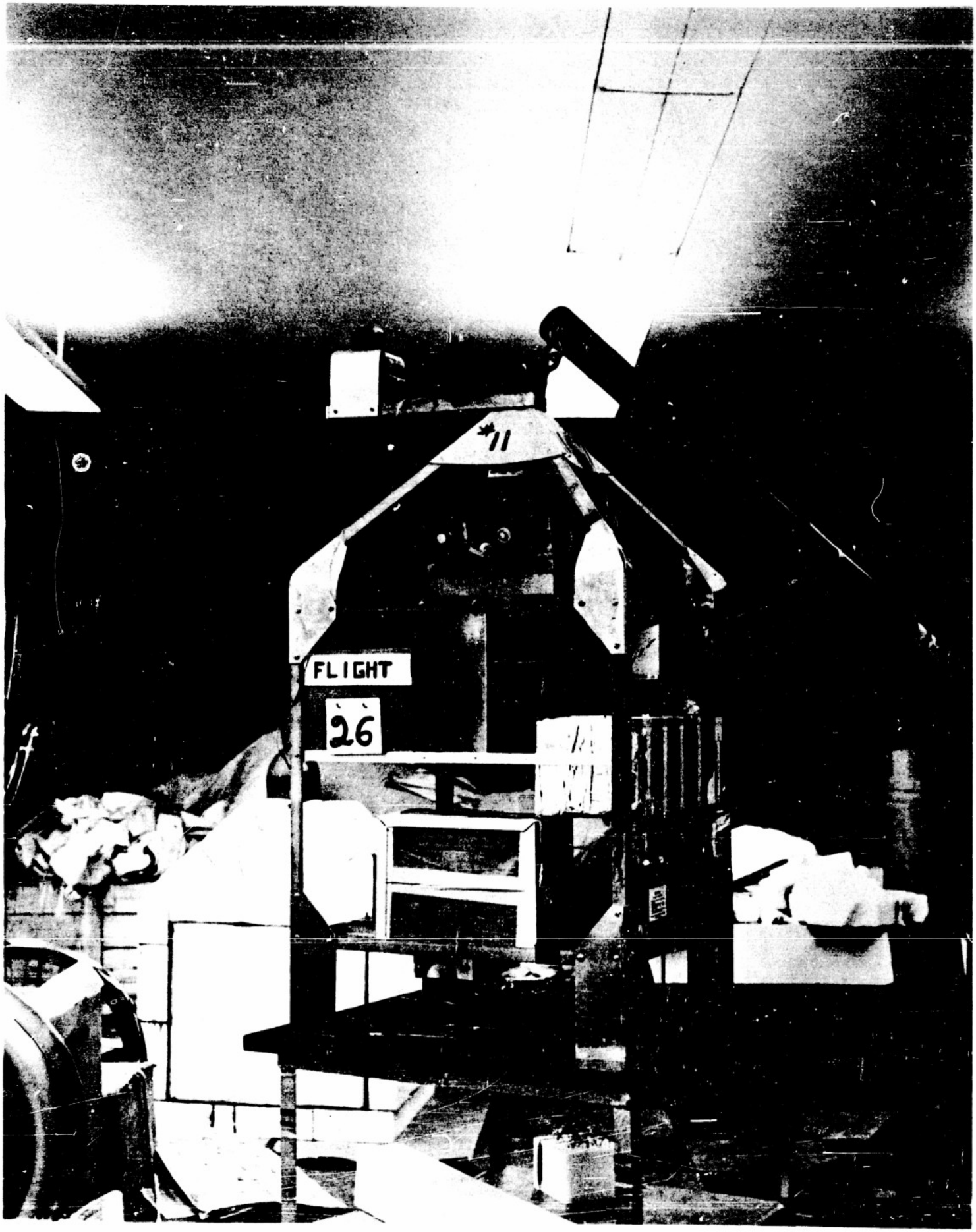
FLIGHT
26

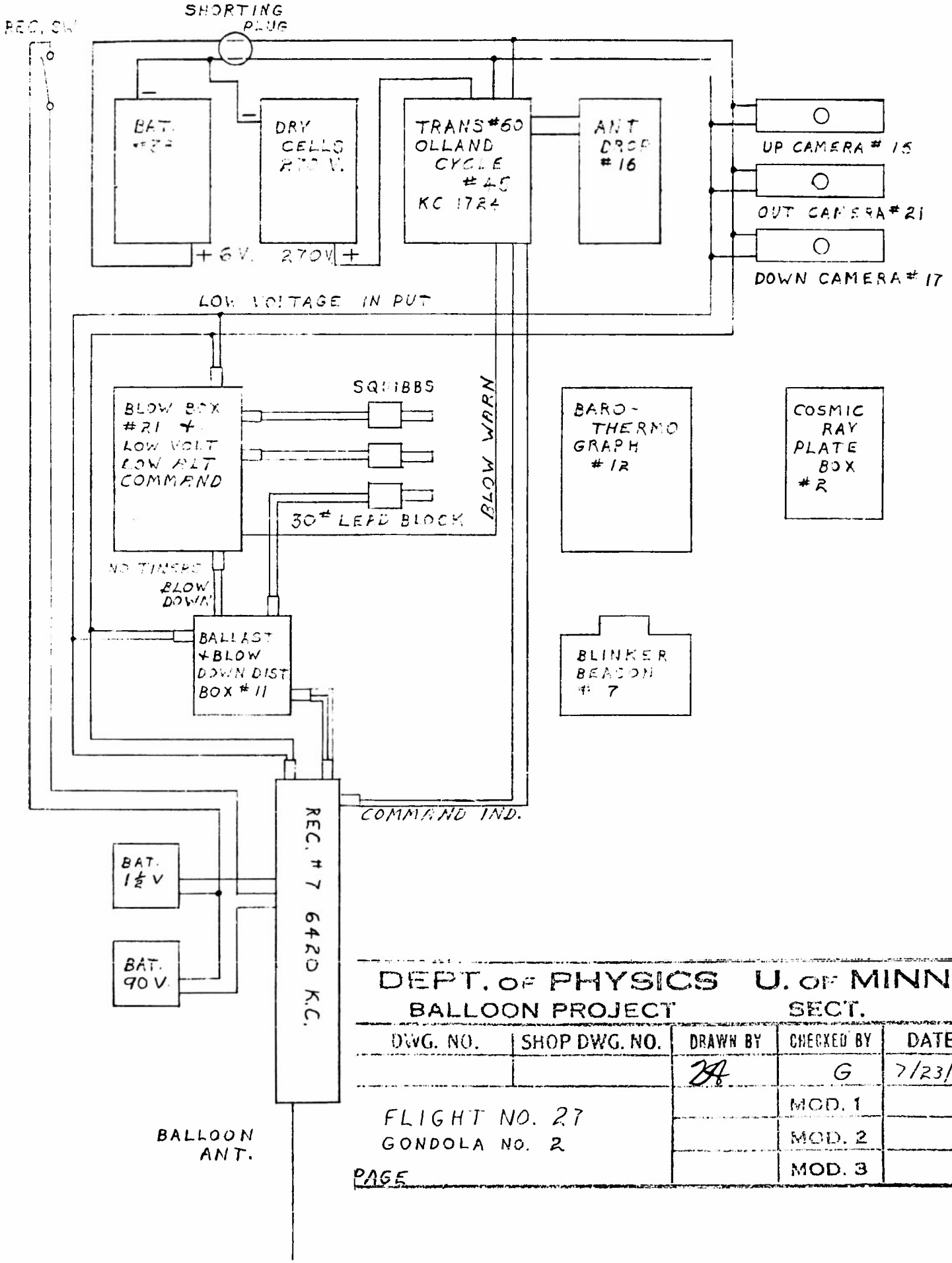

DEPT. of PHYSICS U. of MINN.
BALLOON PROJECT SECT.

DWG. NO.	SHOP DWG. NO.	DRAWN BY	CHECKED BY	DATE
		[illegible]	G	7/23/52
			MOD. 1	
FLIGHT NO. 27			MOD. 2	
GONDOLA NO. 2			MOD. 3	
PAGE				

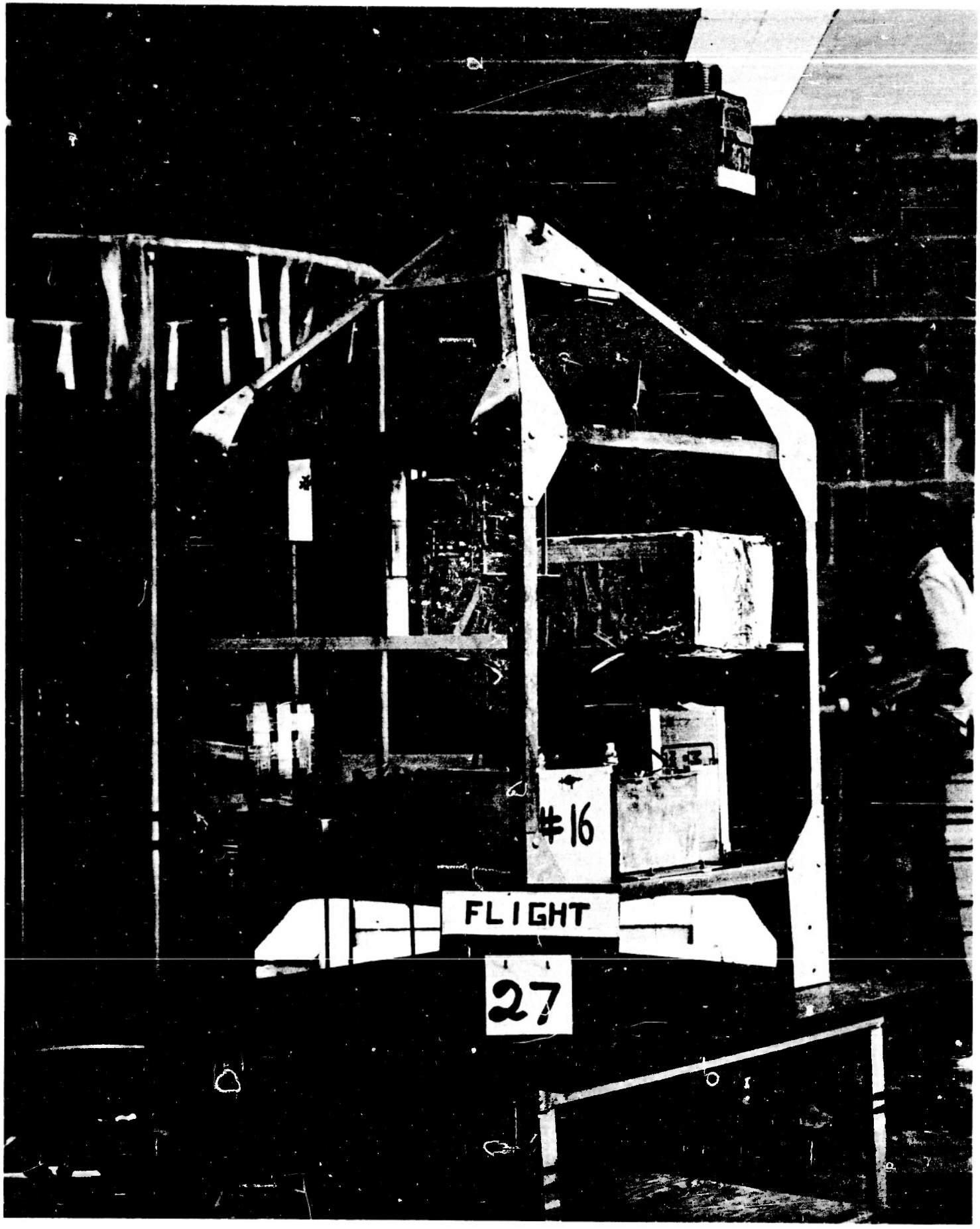
#16
FLIGHT
27

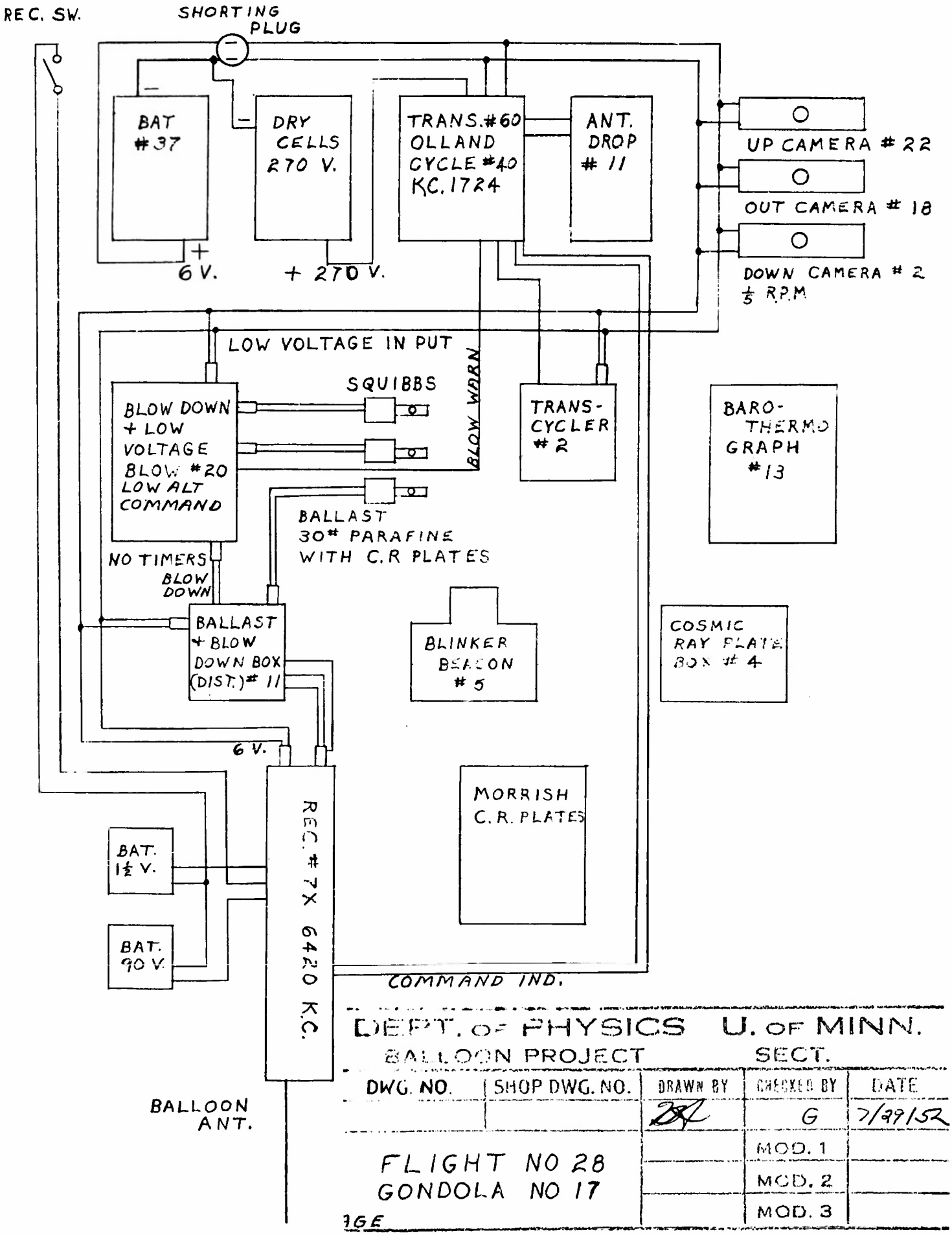

DEPT. OF PHYSICS U. OF MINN.
BALLOON PROJECT SECT.

DWG. NO.	SHOP DWG. NO.	DRAWN BY	CHECKED BY	DATE
			G	7/29/52
FLIGHT NO 28 GONDOLA NO 17			MOD. 1	
			MOD. 2	
IGE			MOD. 3	

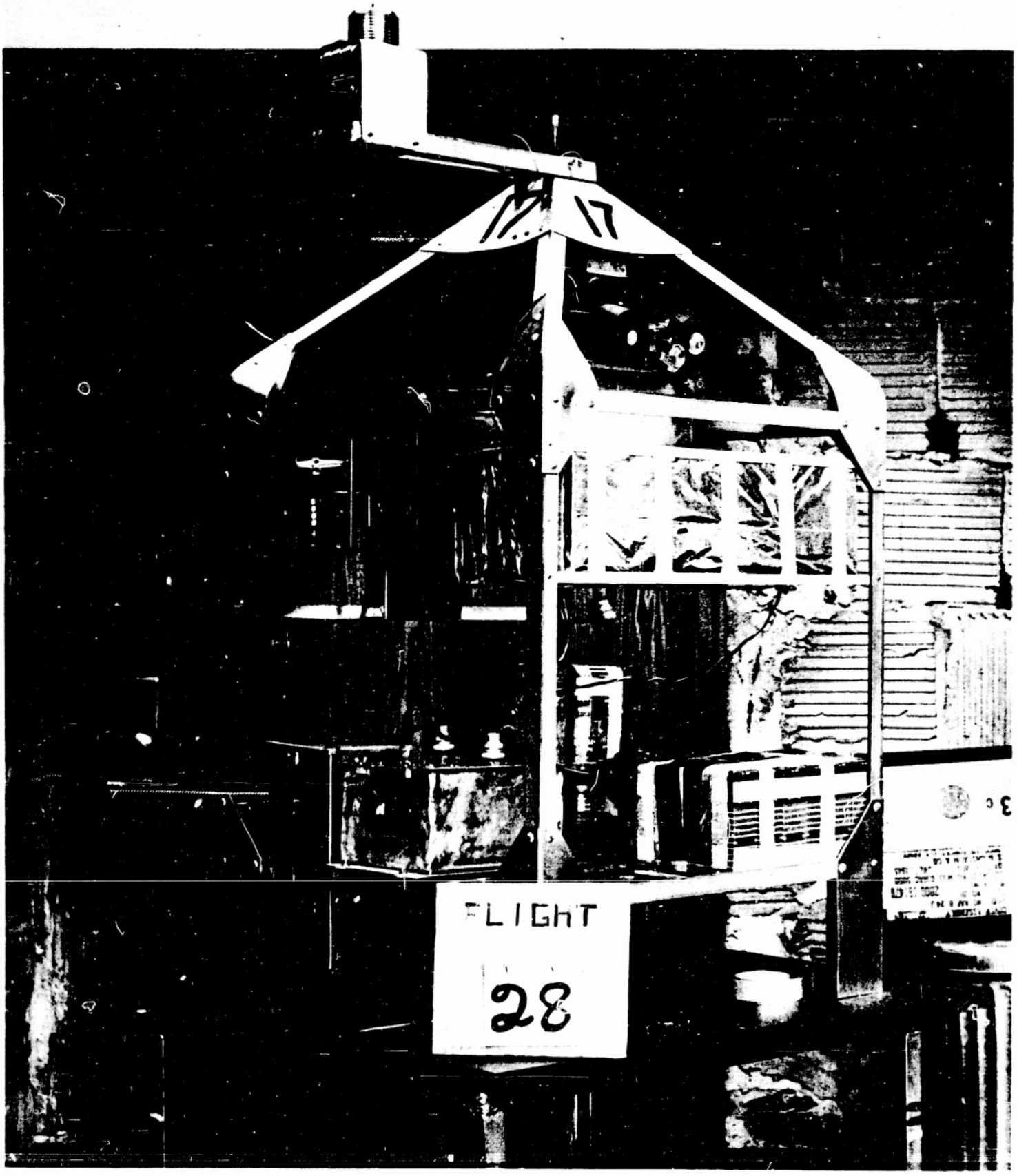
FLIGHT
28

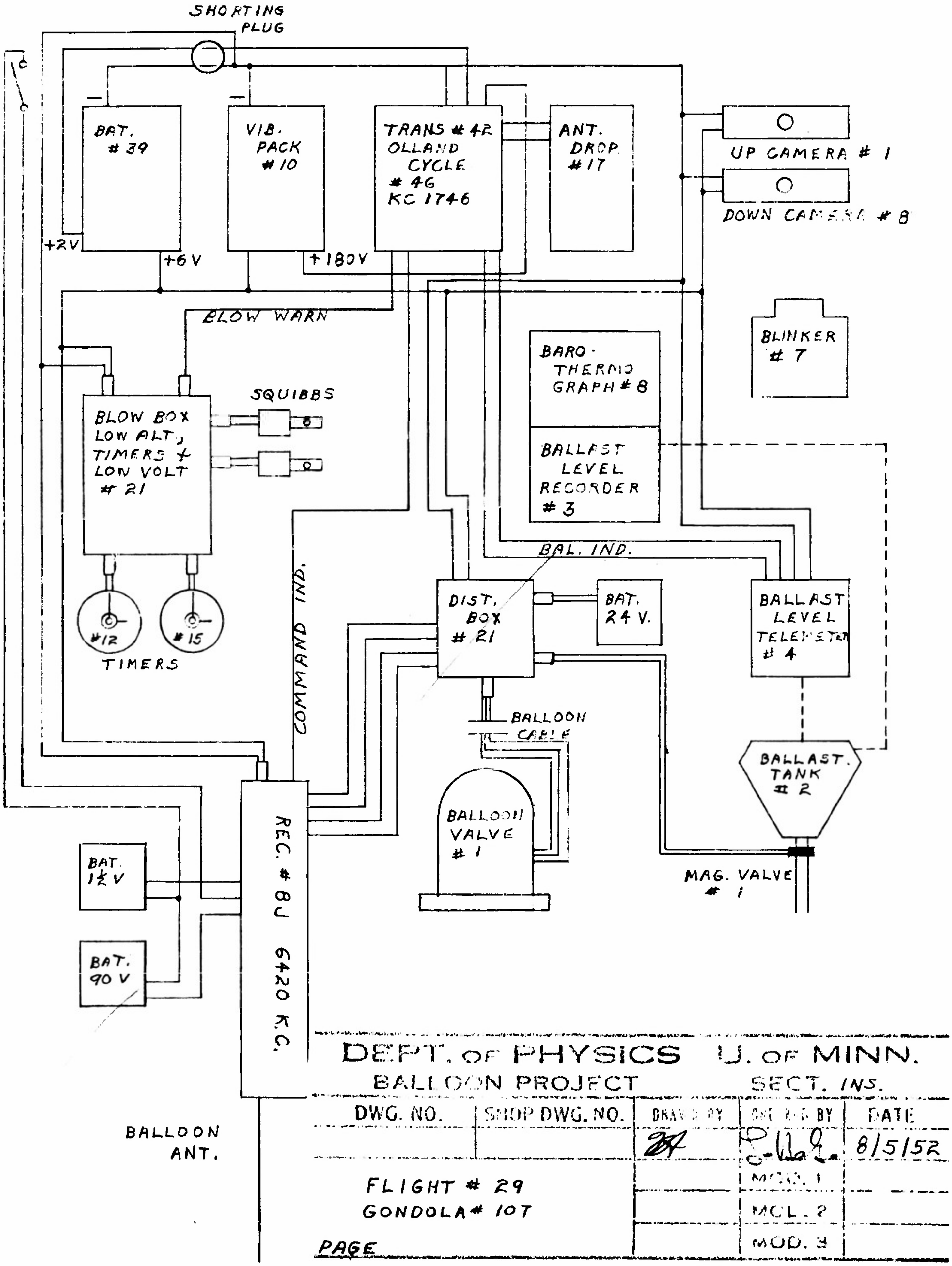
SHORTING PLUG
BAT. # 39
VIB. PACK # 10
TRANS # 42 OLLAND CYCLE # 46 KC 1746
ANT. DROP # 17
UP CAMERA # 1
DOWN CAMERA # 8
+2V
+6 V
+180V
BLOW WARN
BLINKER # 7
BARO-THERMO GRAPH # 8
BALLAST LEVEL RECORDER # 3
SQUIBBS
BLOW BOX LOW ALT, TIMERS + LOW VOLT # 21
#12
#15
TIMERS
COMMAND IND.
BAL. IND.
DIST. BOX # 21
BAT. 24 V.
BALLAST LEVEL TELEMETER # 4
BALLOON CABLE
BALLAST TANK # 2
BALLOON VALVE # 1
MAG. VALVE # 1
BAT. 1½ V
BAT. 90 V
REC. # 8J 6420 K.C.
BALLOON ANT.
DEPT. OF PHYSICS U. OF MINN.
BALLOON PROJECT SECT. INS.
DWG. NO.
SHOP DWG. NO.
DRAWN BY
DATE
8/5/52
MOD. 1
MOD. 2
MOD. 3
FLIGHT # 29
GONDOLA # 107
PAGE

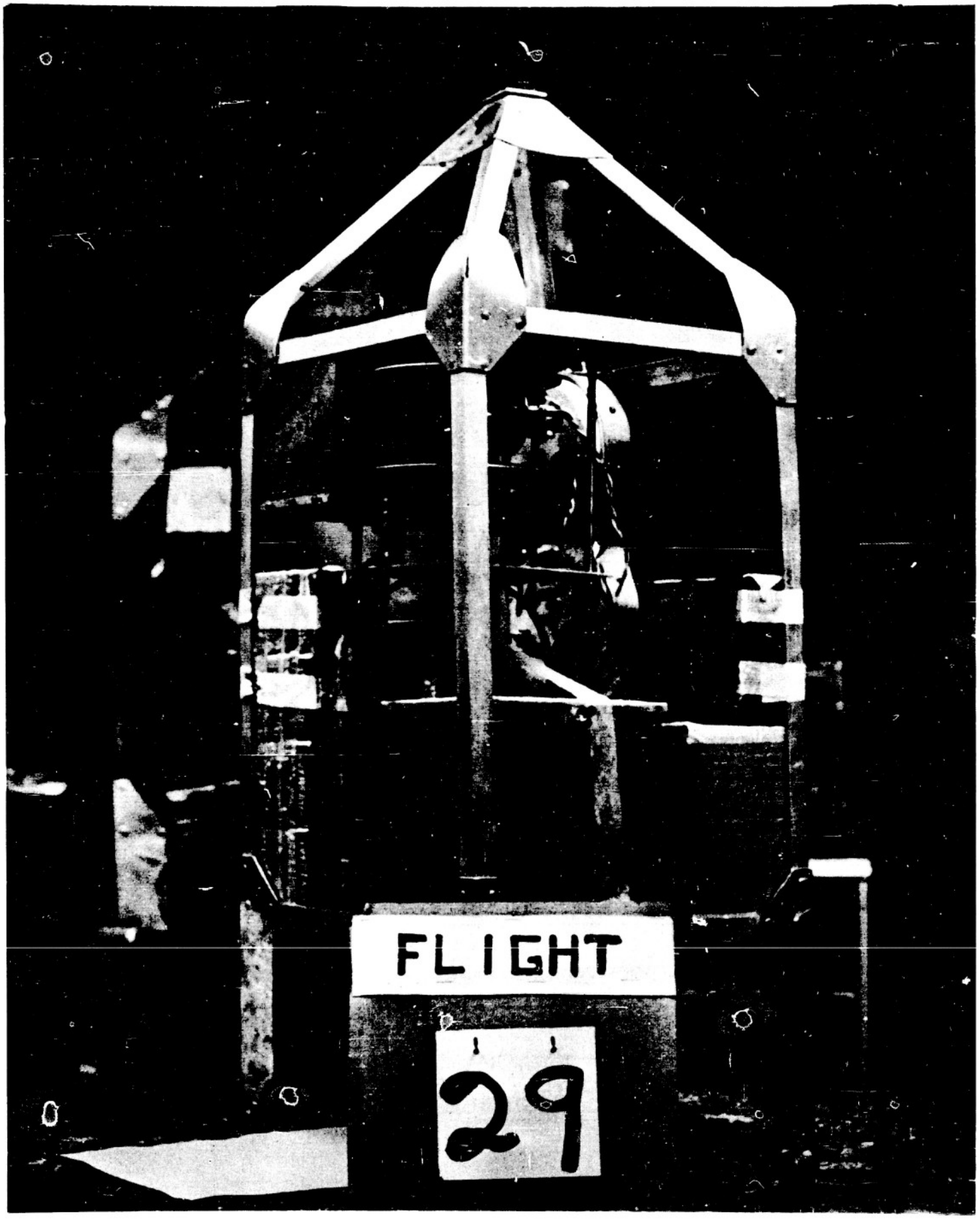
FLIGHT
29

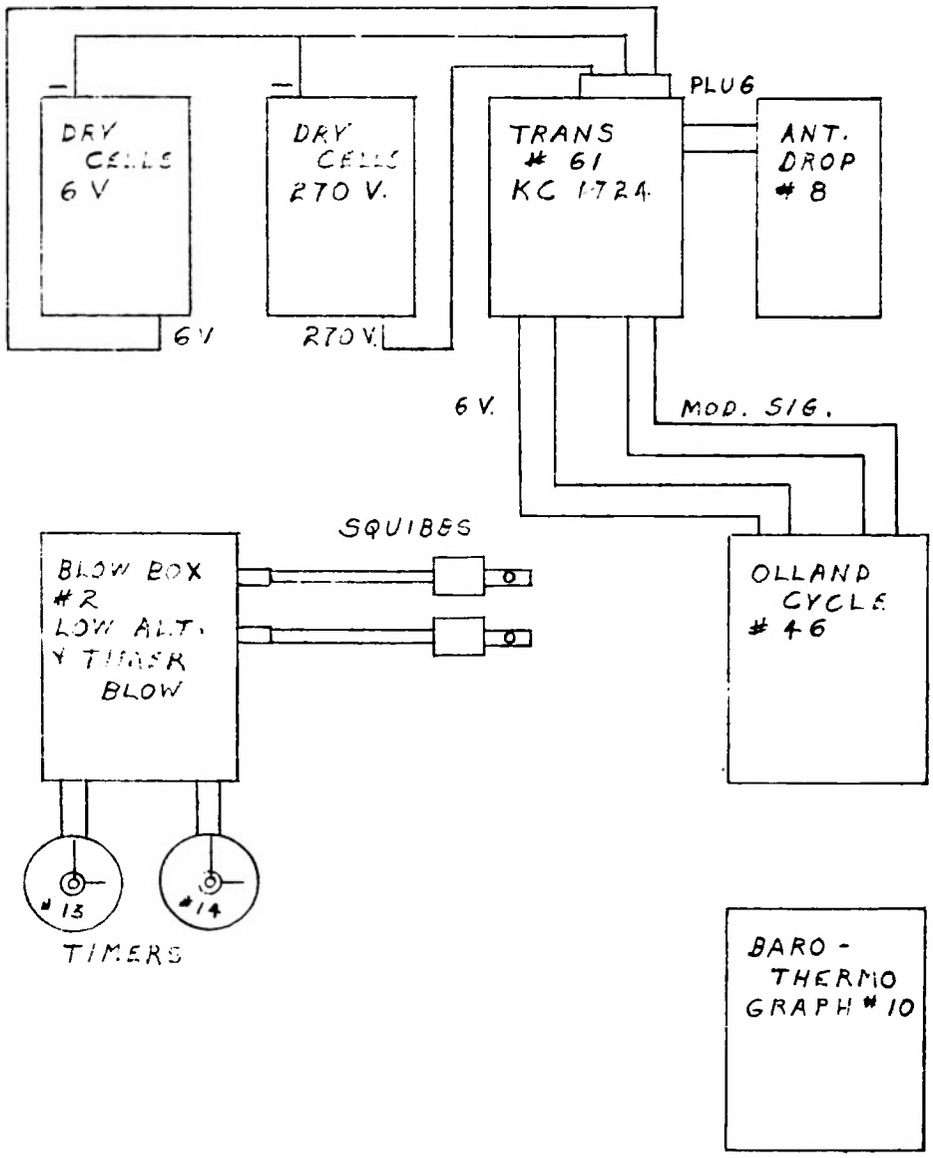

DEPT. OF PHYSICS U. OF MINN. BALLOON PROJECT			SECT. INST.	
DWG NO.	SHOP DWG. NO.	DRAWN BY	CHECKED BY	DATE
				8/6/52
FLIGHT # 30			MOD. 1	
GONDOLA # 51			MOD. 2	
PAGE			MOD. 3	

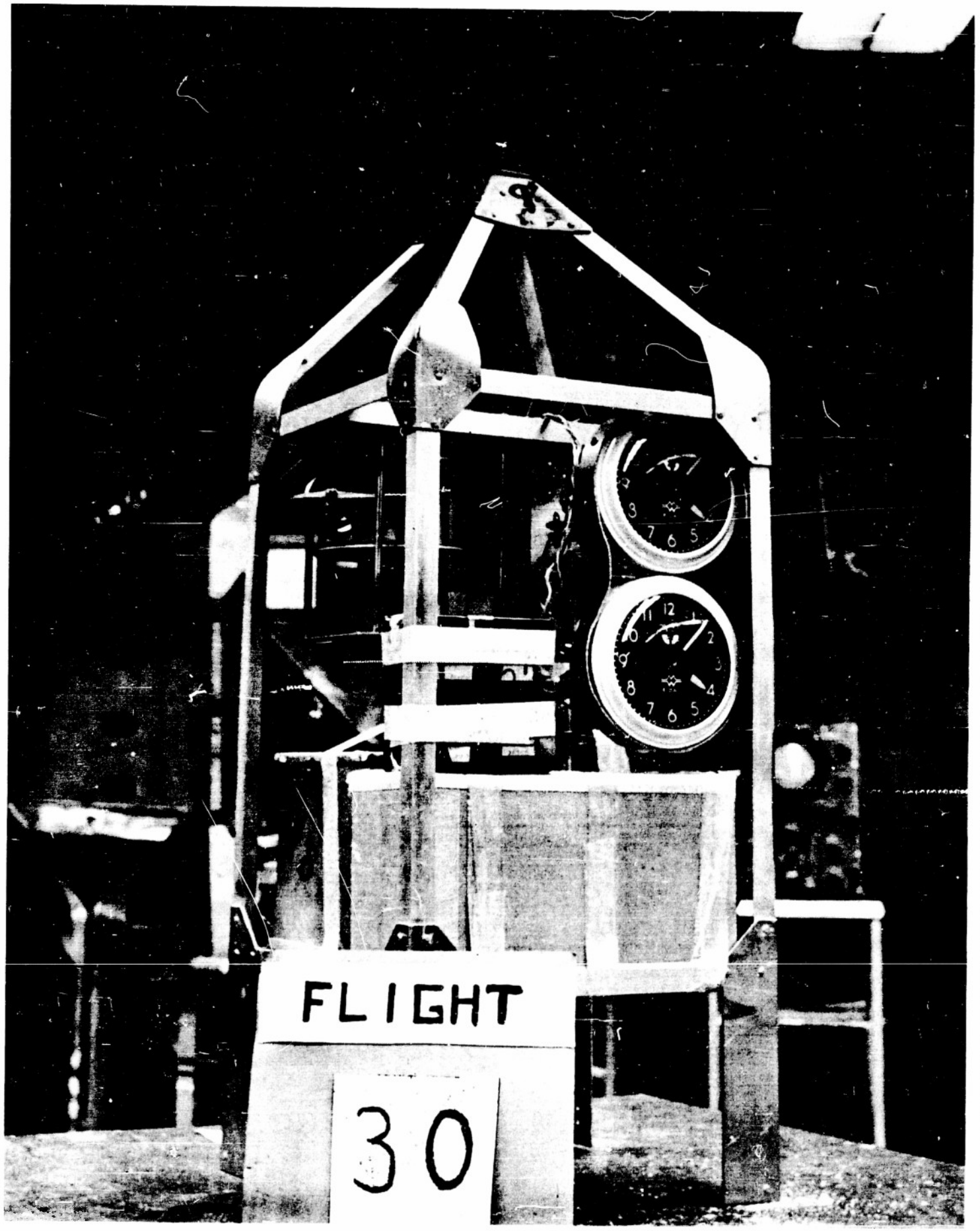
FLIGHT
30

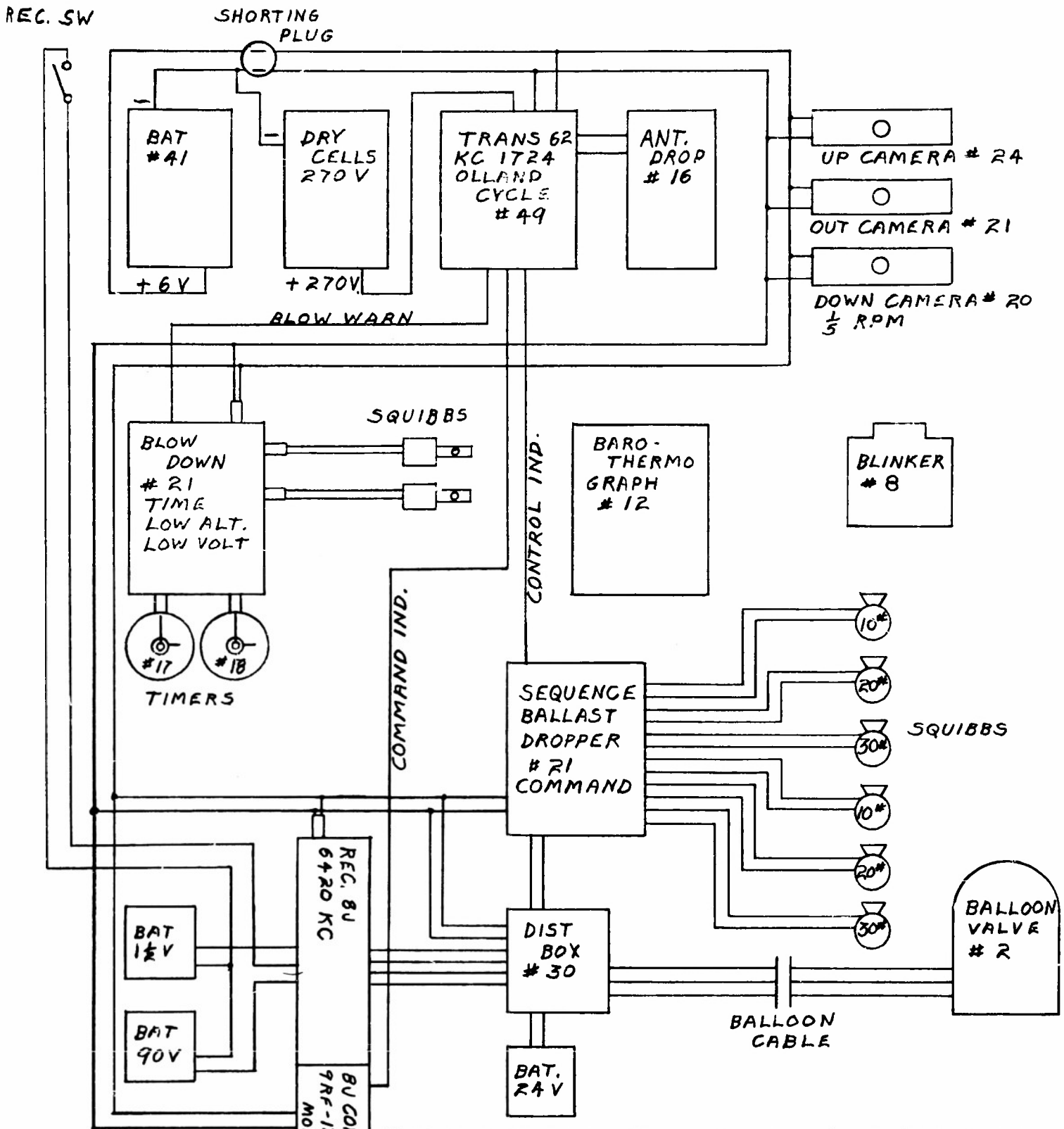

DEPT. OF PHYSICS U. OF MINN.

BALLOON PROJECT SECT. INST

DWG. NO.	SHOP DWG. NO.	DRAWN BY	CHECKED BY	DATE
				8-12-52
FLIGHT # 31			MOD. 1	
GONDOLA # 2			MOD. 2	
AGE			MOD. 3	

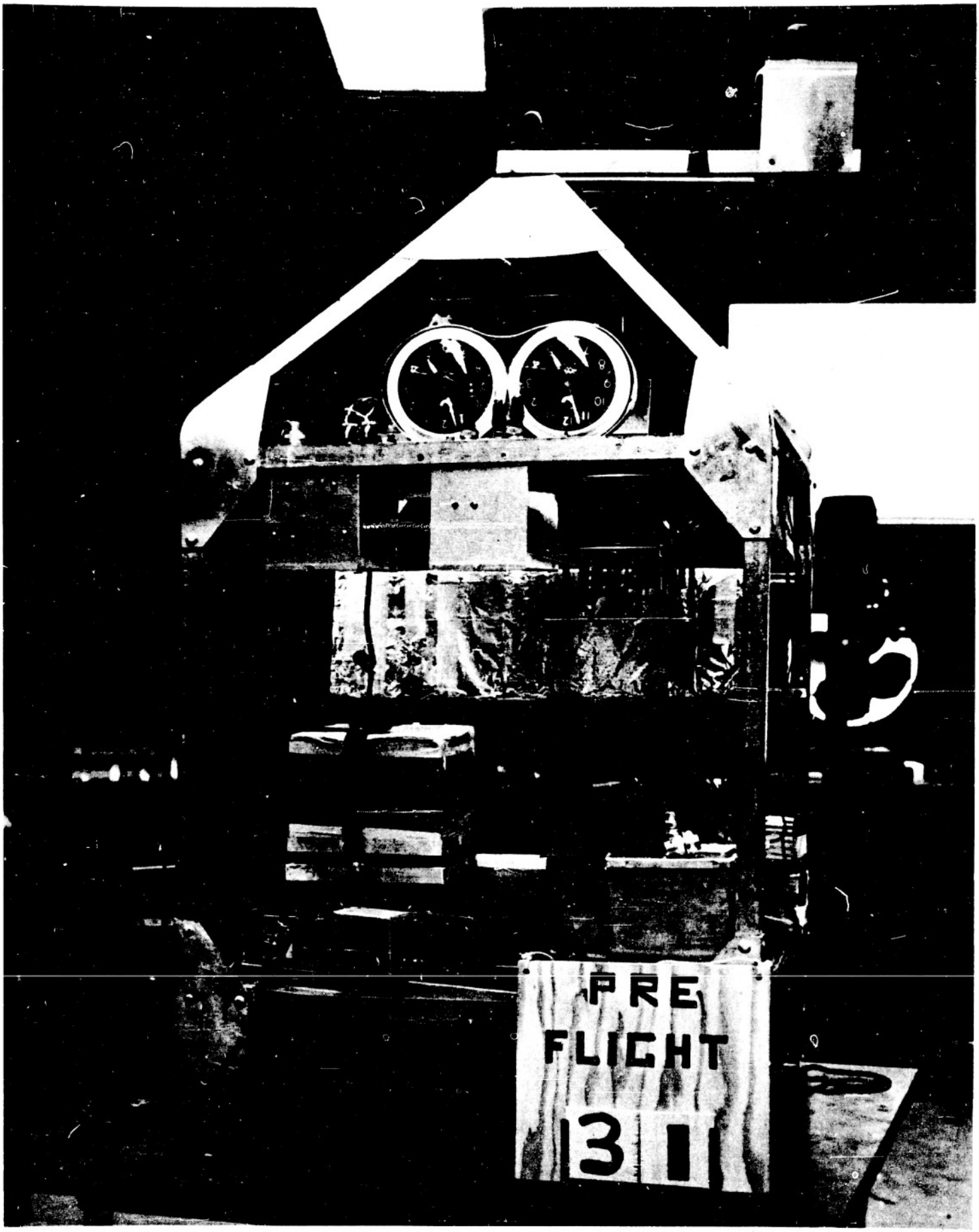
PRE
FLIGHT
13

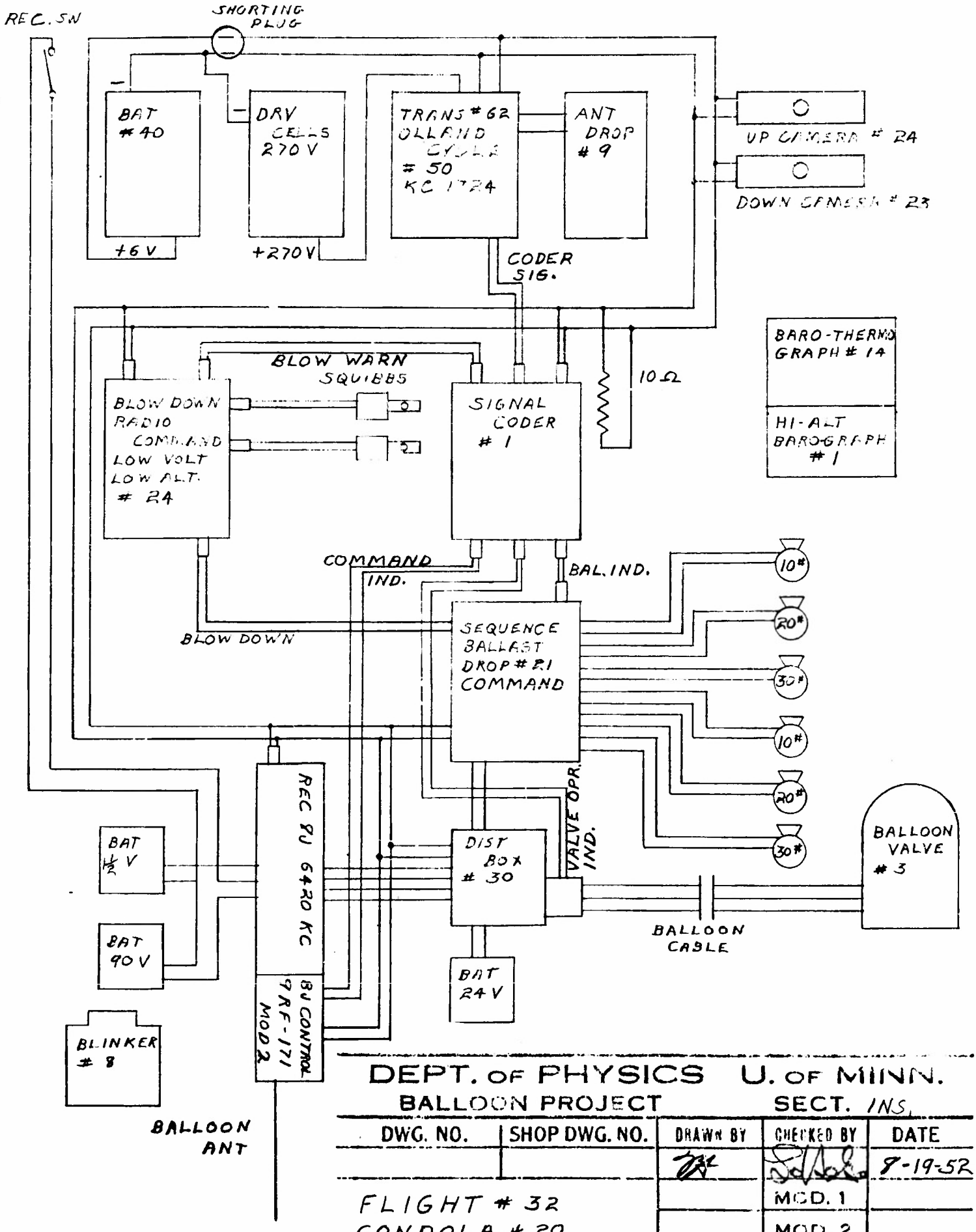

DEPT. OF PHYSICS U. OF MINN.

BALLOON PROJECT SECT. INS.

DWG. NO.	SHOP DWG. NO.	DRAWN BY	CHECKED BY	DATE
				8-19-52
FLIGHT # 32			MOD. 1	
GONDOLA # 20			MOD. 2	
PAGE			MOD. 3	

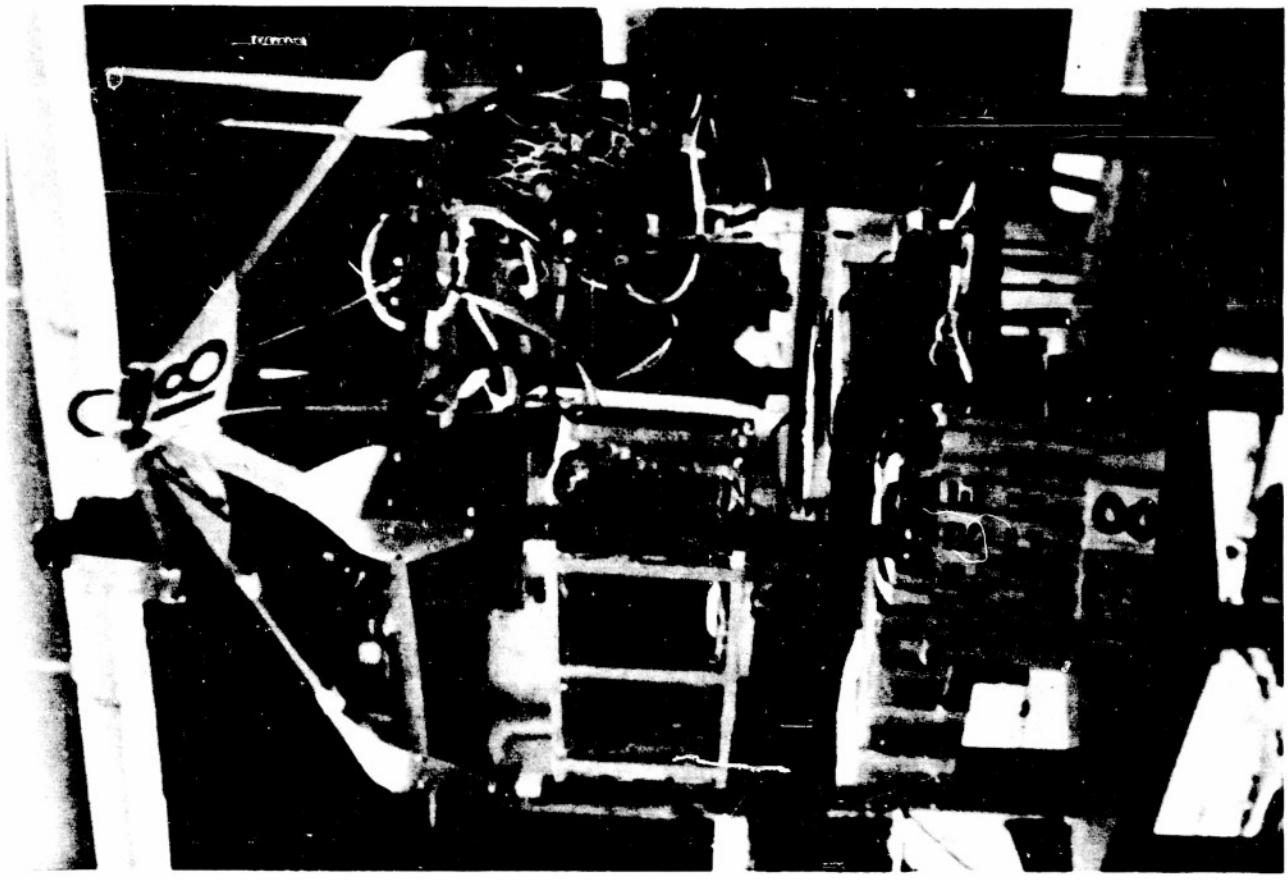

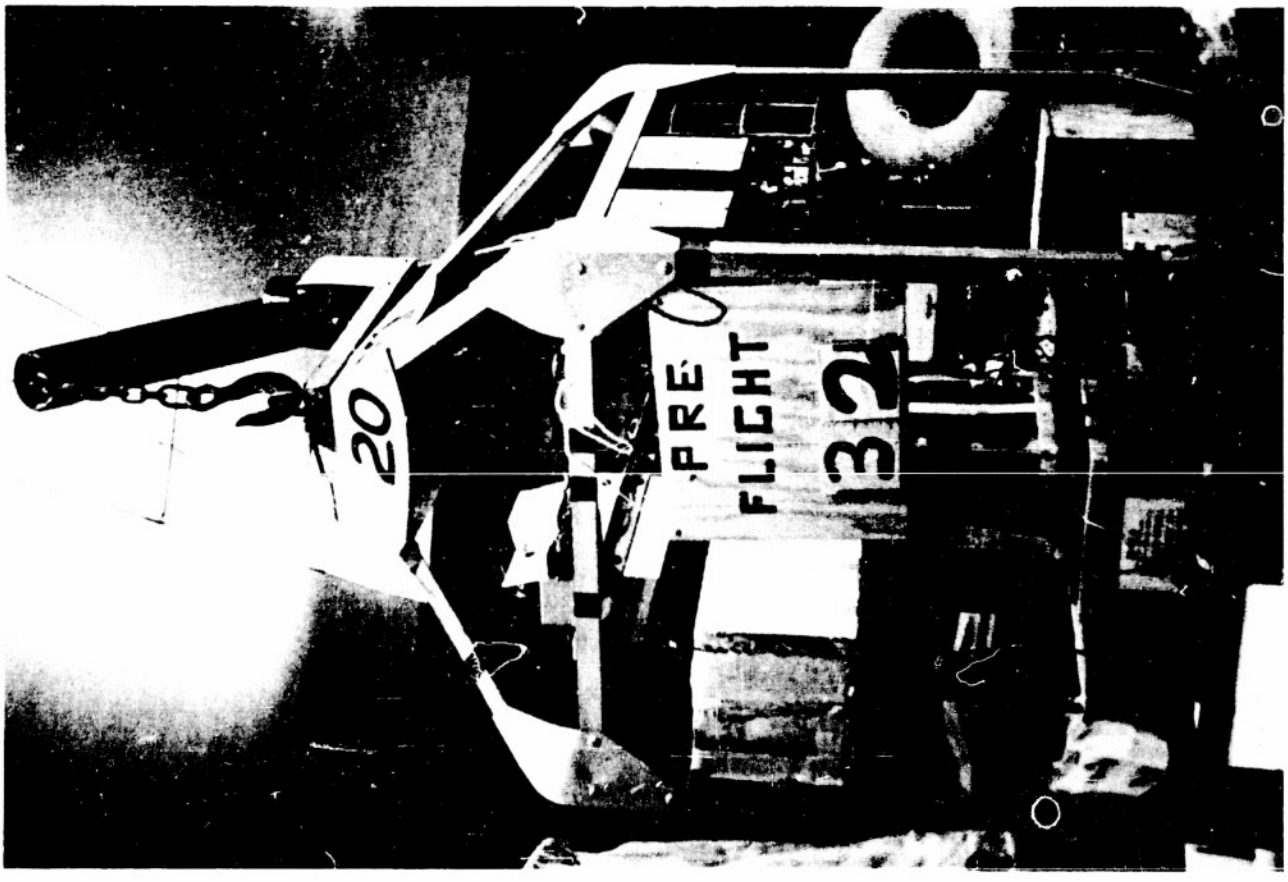
PRE
FLIGHT
20

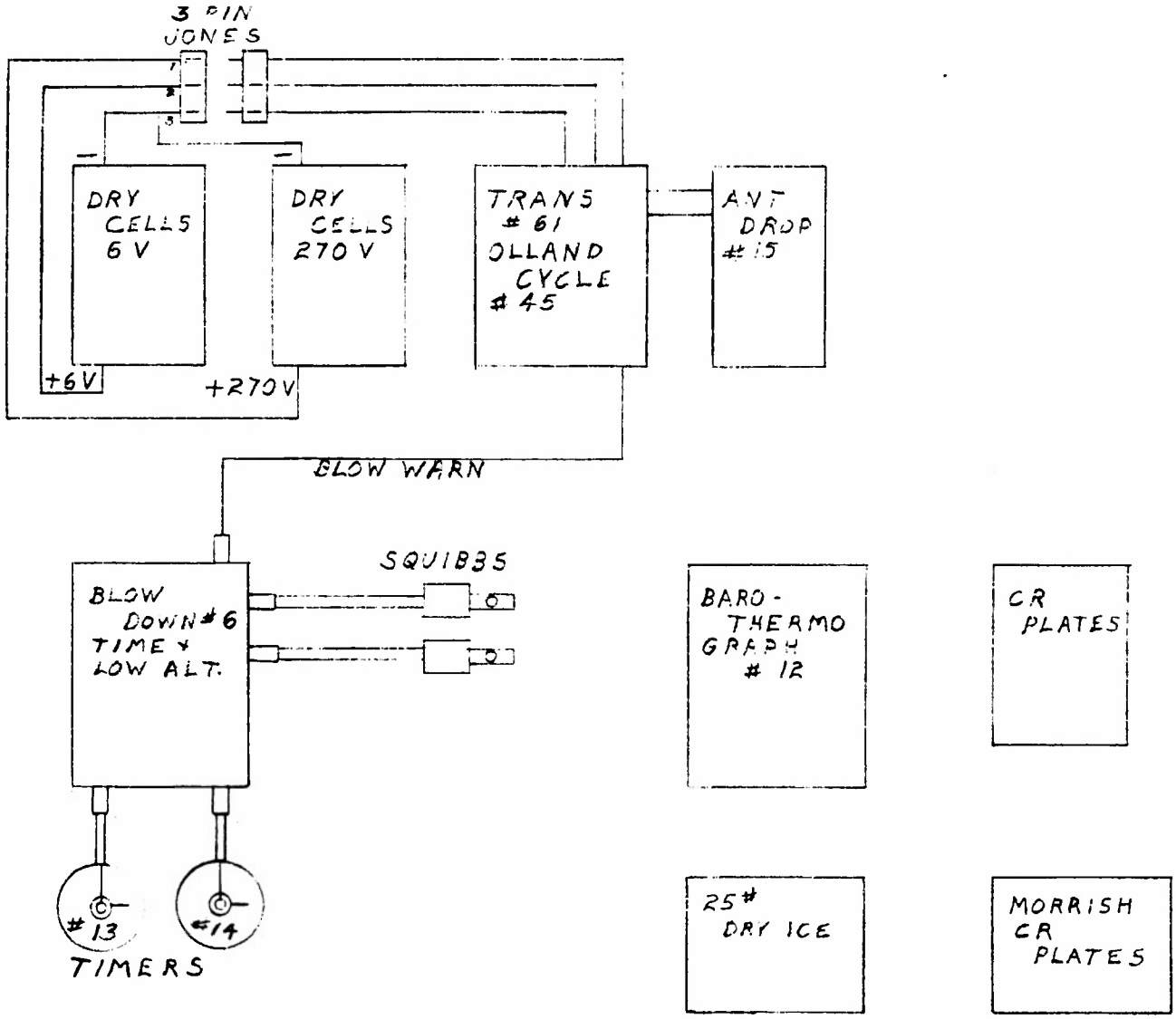

DEPT. OF PHYSICS U. OF MINN.
BALLOON PROJECT INS

DWG. NO.	SHOP DWG. NO.			DATE
				8-21-52
FLIGHT # 33			MOD. 1	
GONDOLA # 51			MOD. 2	
PAGE			MOD. 3	

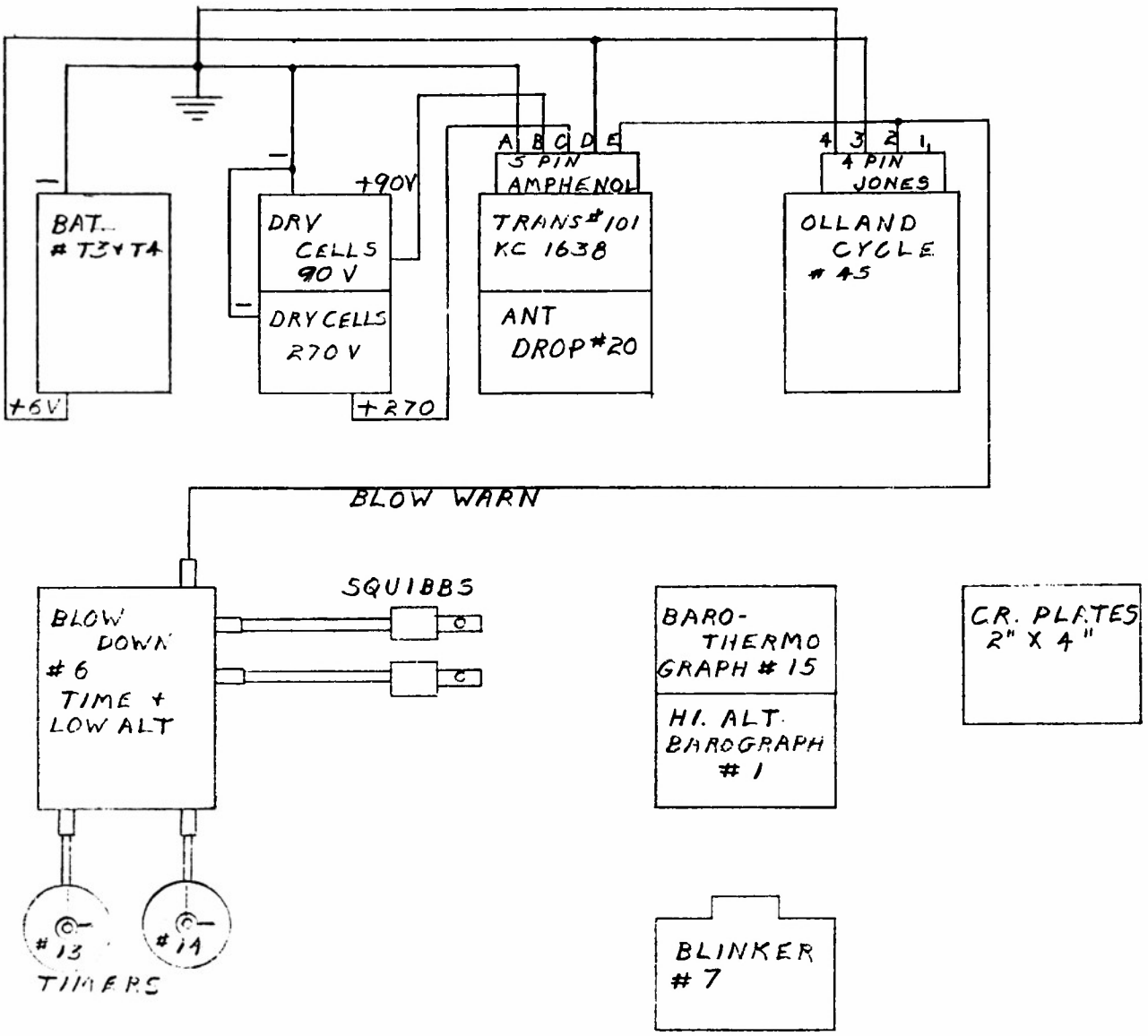

DEPT. OF PHYSICS U. OF MINN.
BALLOON PROJECT SECT. INS.

DWG. NO.	SHOP WORK ORD. NO.	DRAWN BY	CHECKED BY	DATE
		[illegible]	[illegible]	8-28-52

FLIGHT # 34
GONDOLA # 52

PAGE

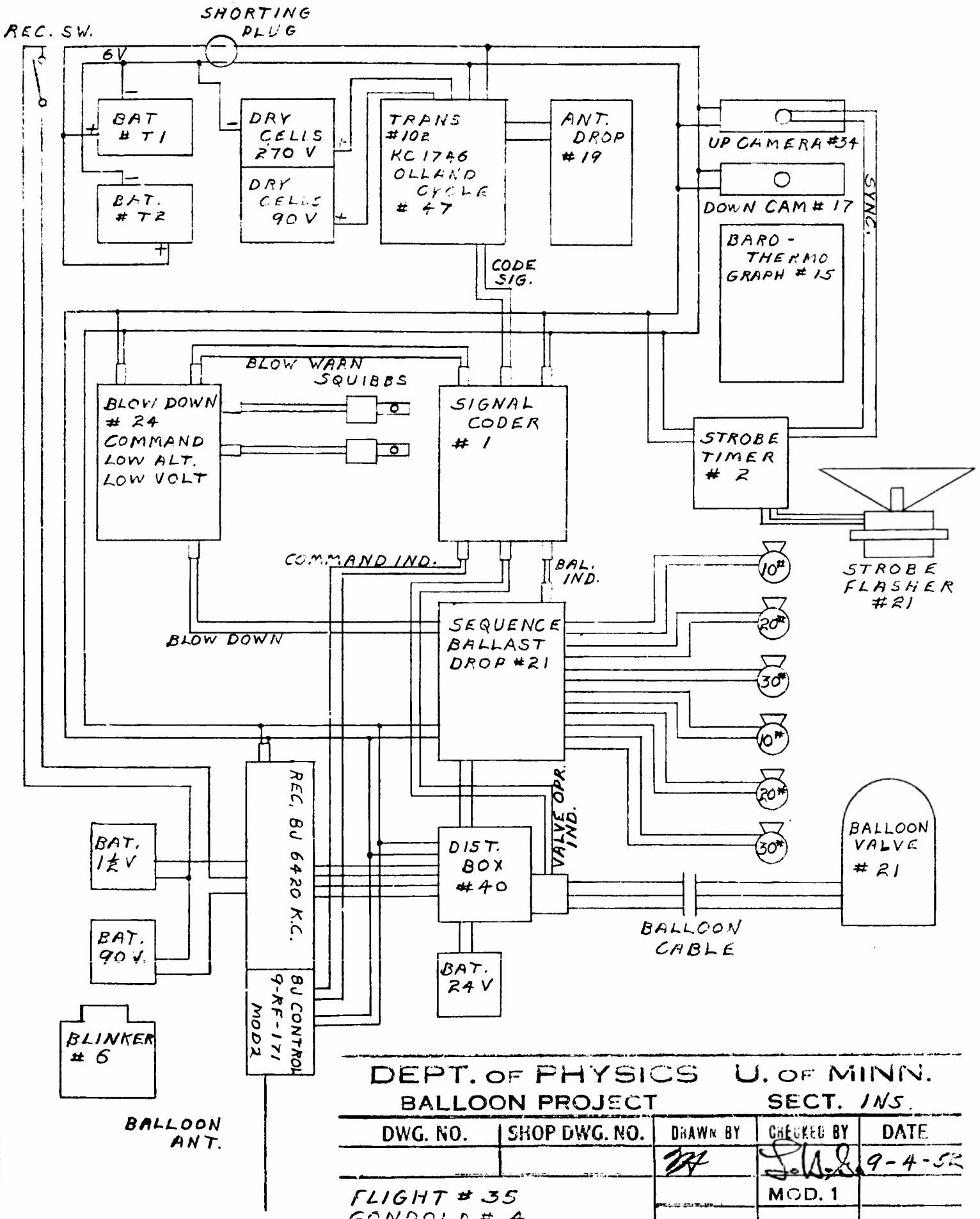

DEPT. OF PHYSICS U. OF MINN.

BALLOON PROJECT SECT. INS.

DWG. NO.	SHOP DWG. NO.	DRAWN BY	CHECKED BY	DATE
		ZH		9-4-52
			MOD. 1	
			MOD. 2	
			MOD. 3	

FLIGHT # 35
GONDOLA # 4

PAGE

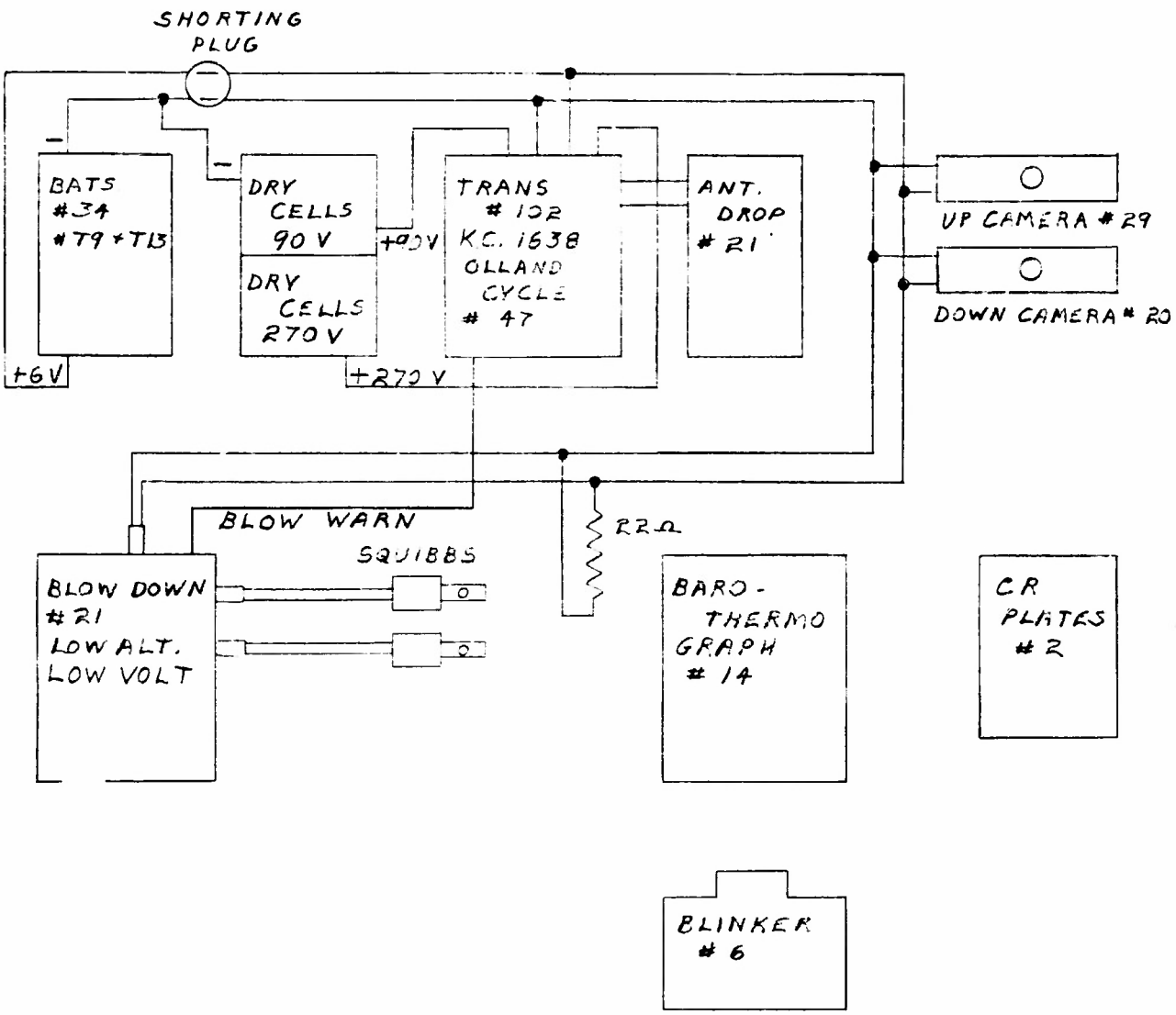

DEPT. OF PHYSICS U. OF MINN.				
BALLOON PROJECT			SECT. INS.	
DWG. NO.	SHOP DWG. NO.	DRAWN BY	CHECKED BY	DATE
				9-15-52
FLIGHT # 36			MOD. 1	
GONDOLA # 2			MOD. 2	
PAGE			MOD. 3	

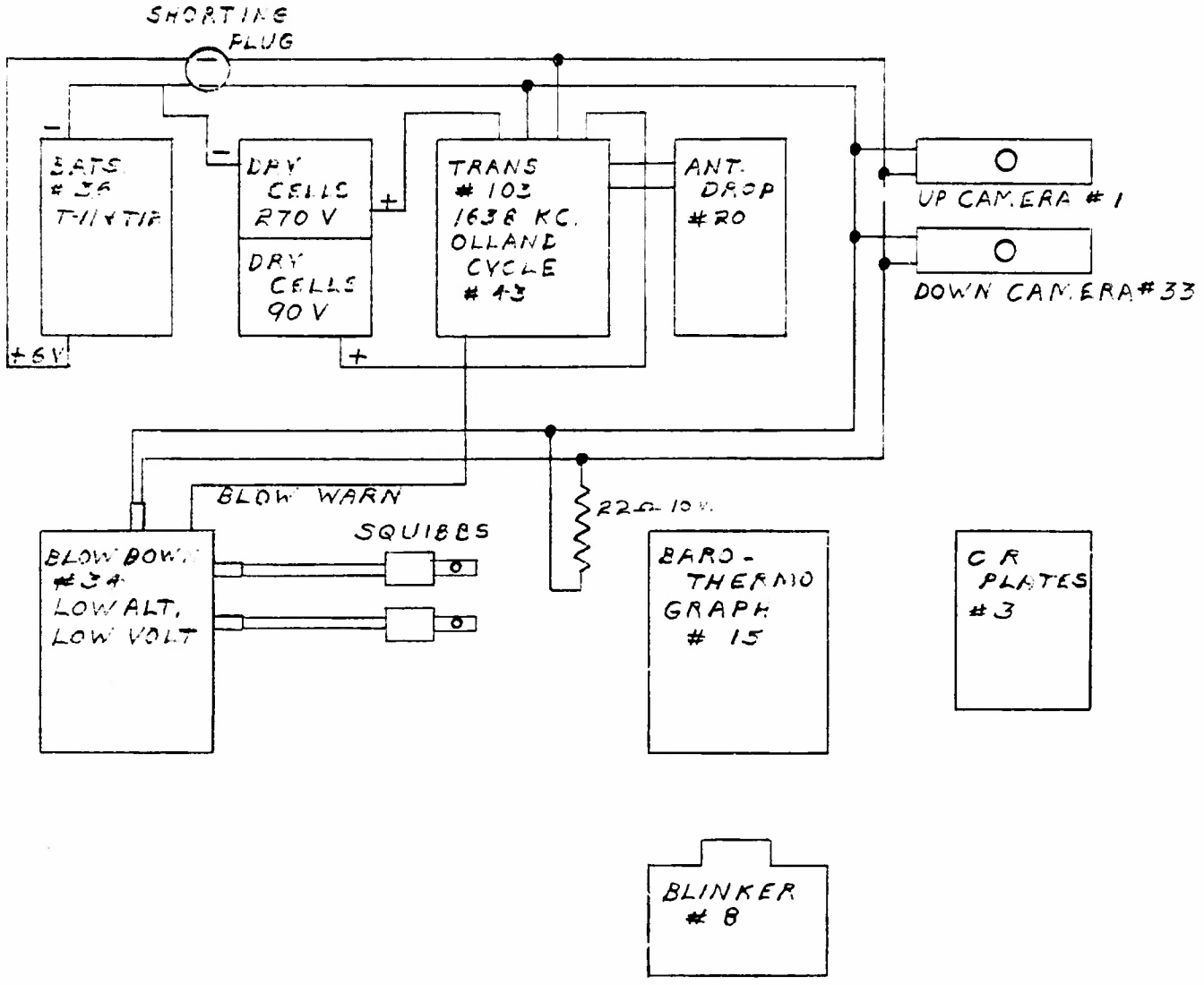

DEPT. OF PHYSICS U. OF MINN.				
BALLOON PROJECT			SECT. INS	
DWG. NO.	SHOP DWG. NO.	DRAWN BY	CHECKED BY	DATE
				9-17-52
FLIGHT #37			MOD. 1	
GONDOLA # 4			MOD. 2	
PAGE			MOD. 3	

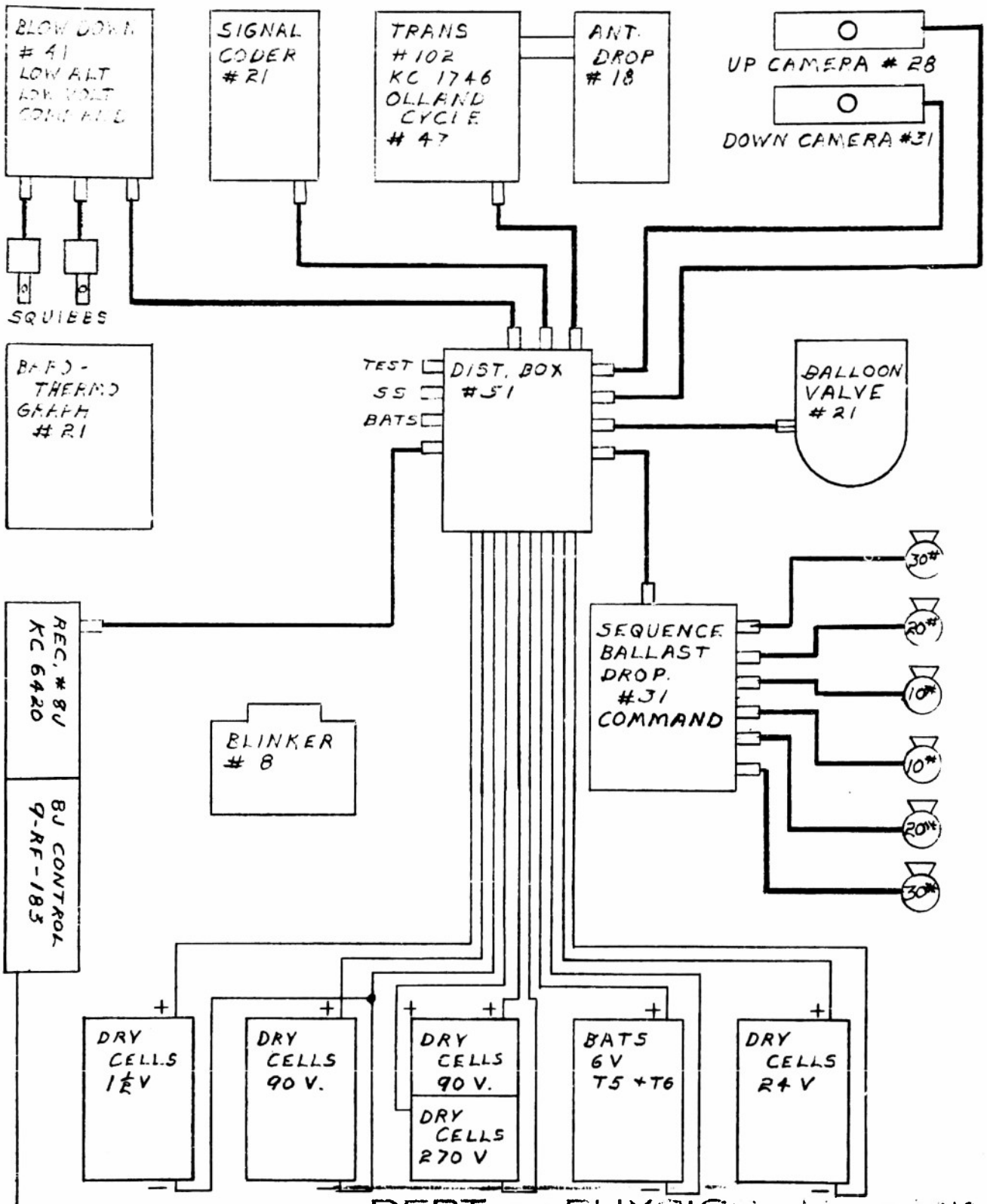

DEPT. OF PHYSICS U. OF MINN.

BALLOON PROJECT SECT. INS.

DWG. NO.	SHOWING NO.	DRAWN BY	CHECKED BY	DATE
				9-22-52
FLIGHT #38			MOD. 1	
GONDOLA # 18			MOD. 2	
PAGE			MOD. 3	

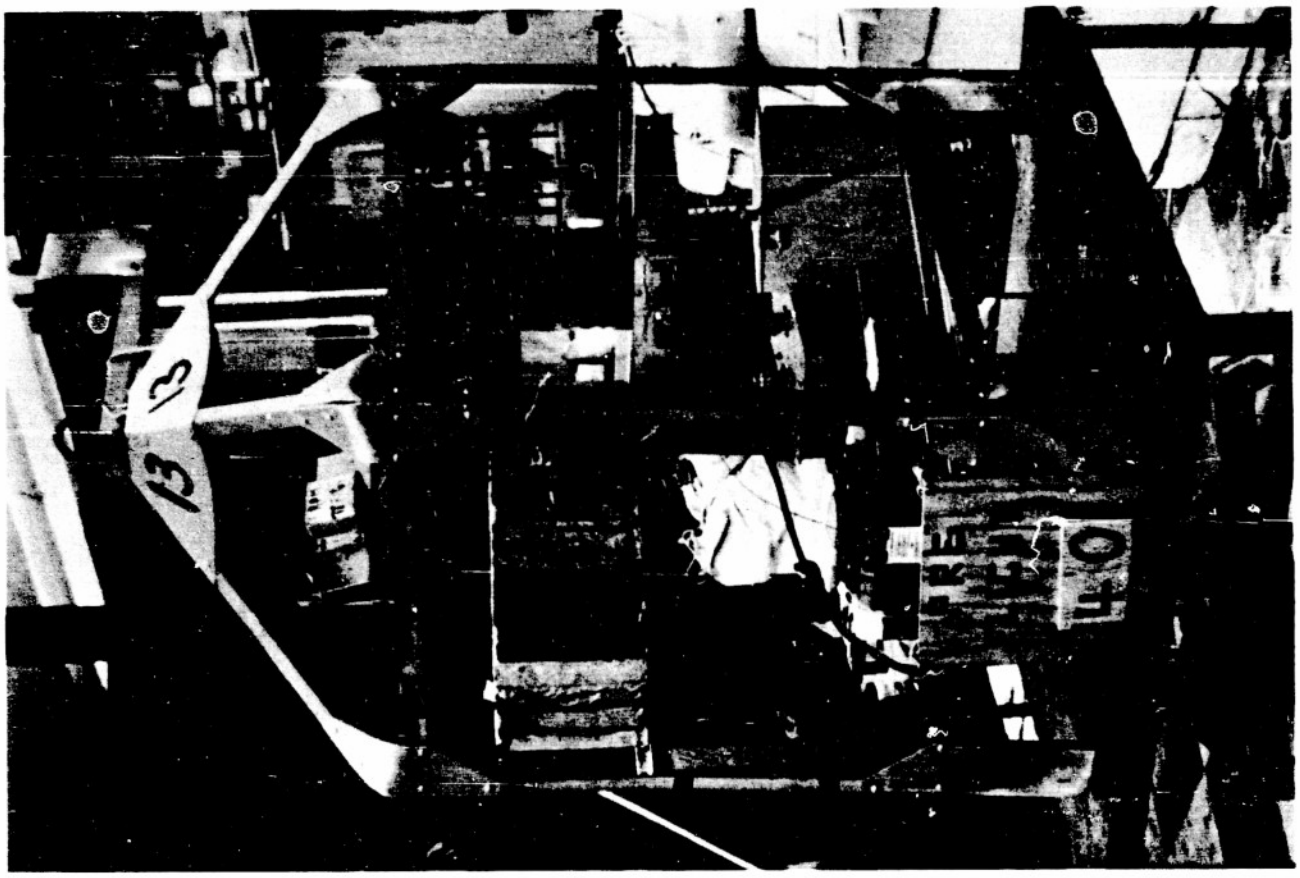

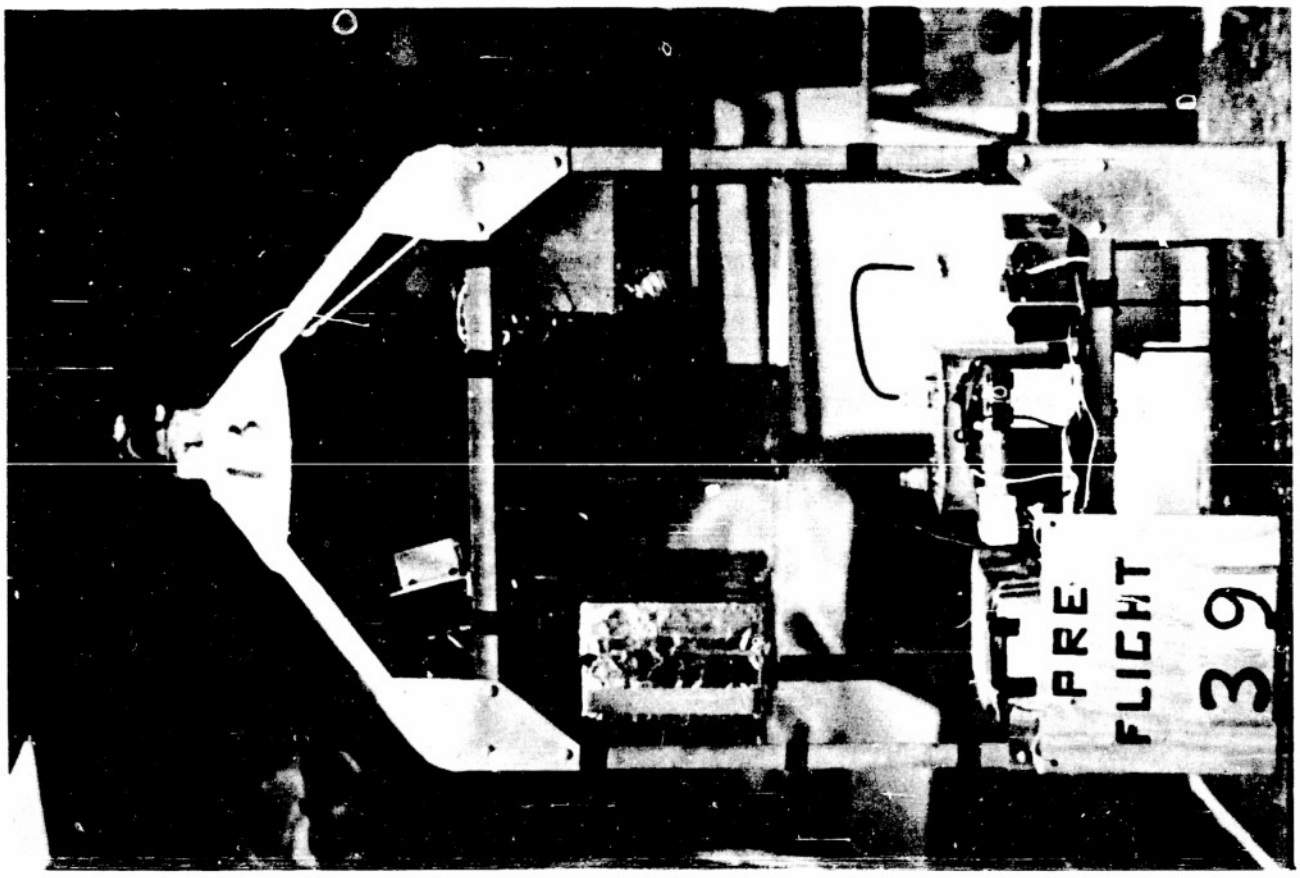
PRE
FLIGHT
39

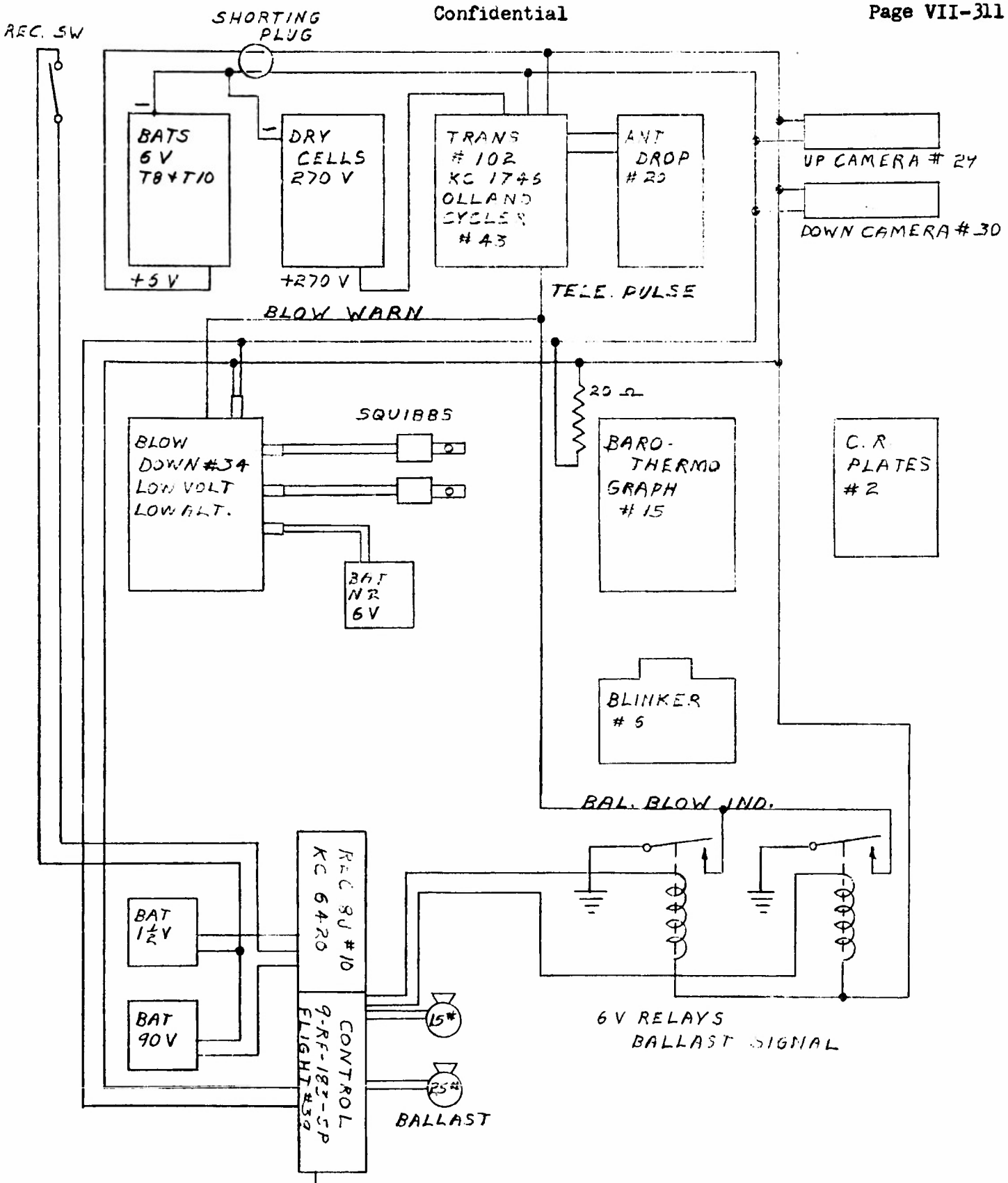

DEPT. OF PHYSICS U. OF MINN.
BALLOON PROJECT SECT INS.

DWG. NO.	SHOP DWG NO.	DRAWN BY	CHECKED BY	DATE
				9-24-52
FLIGHT # 39			MOD. 1	
GONDOLA # 13			MOD. 2	

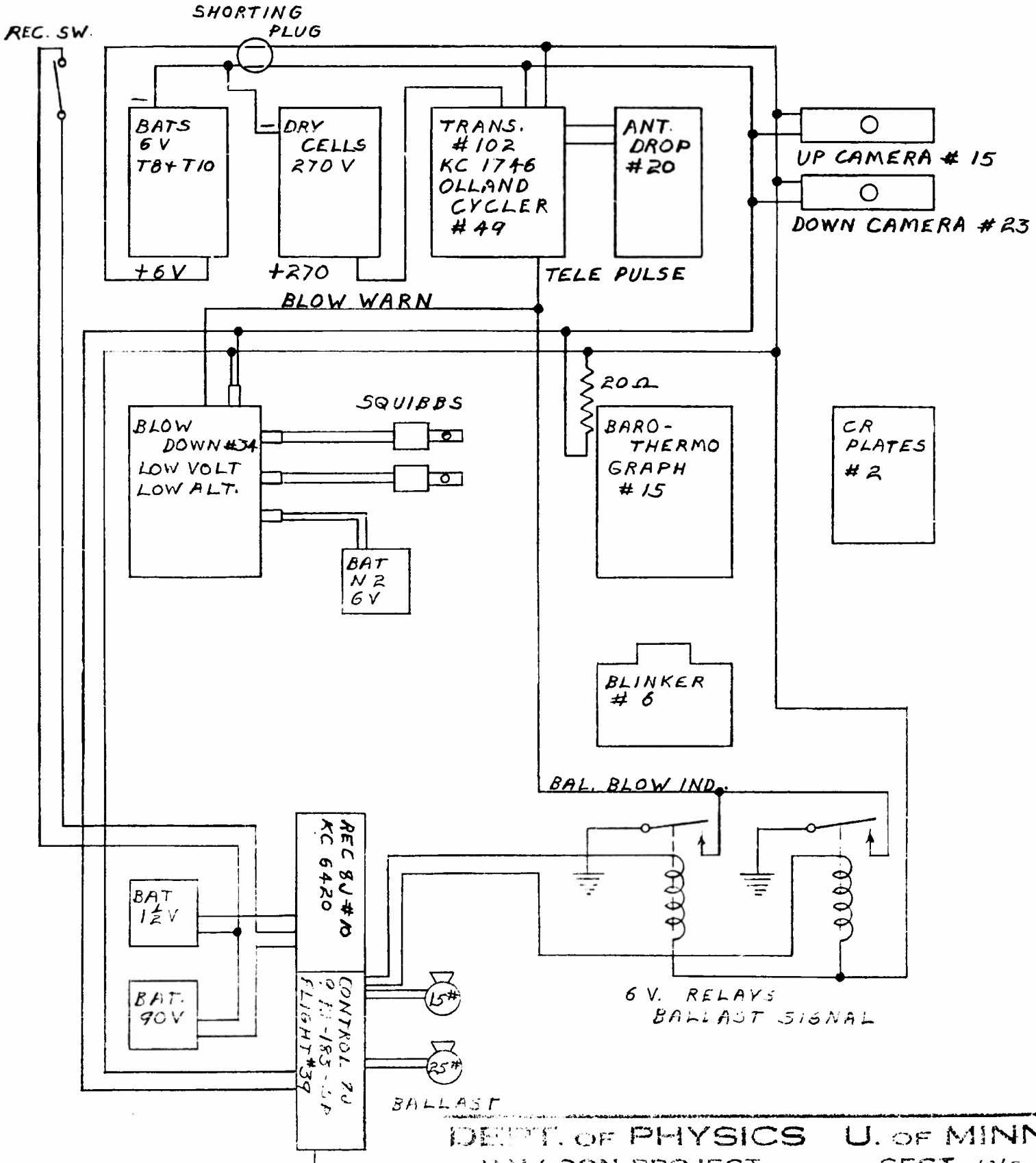

DEPT. OF PHYSICS U. OF MINN.
BALLOON PROJECT SECT. INS.

DWG. NO.	SHOP DWG. NO.	DRAWN BY	CHECKED BY	DATE
				9-26
FLIGHT # 40			MOD. 1	
GONDOLA # 13			MOD. 2	
			MOD. 3	

PAGE

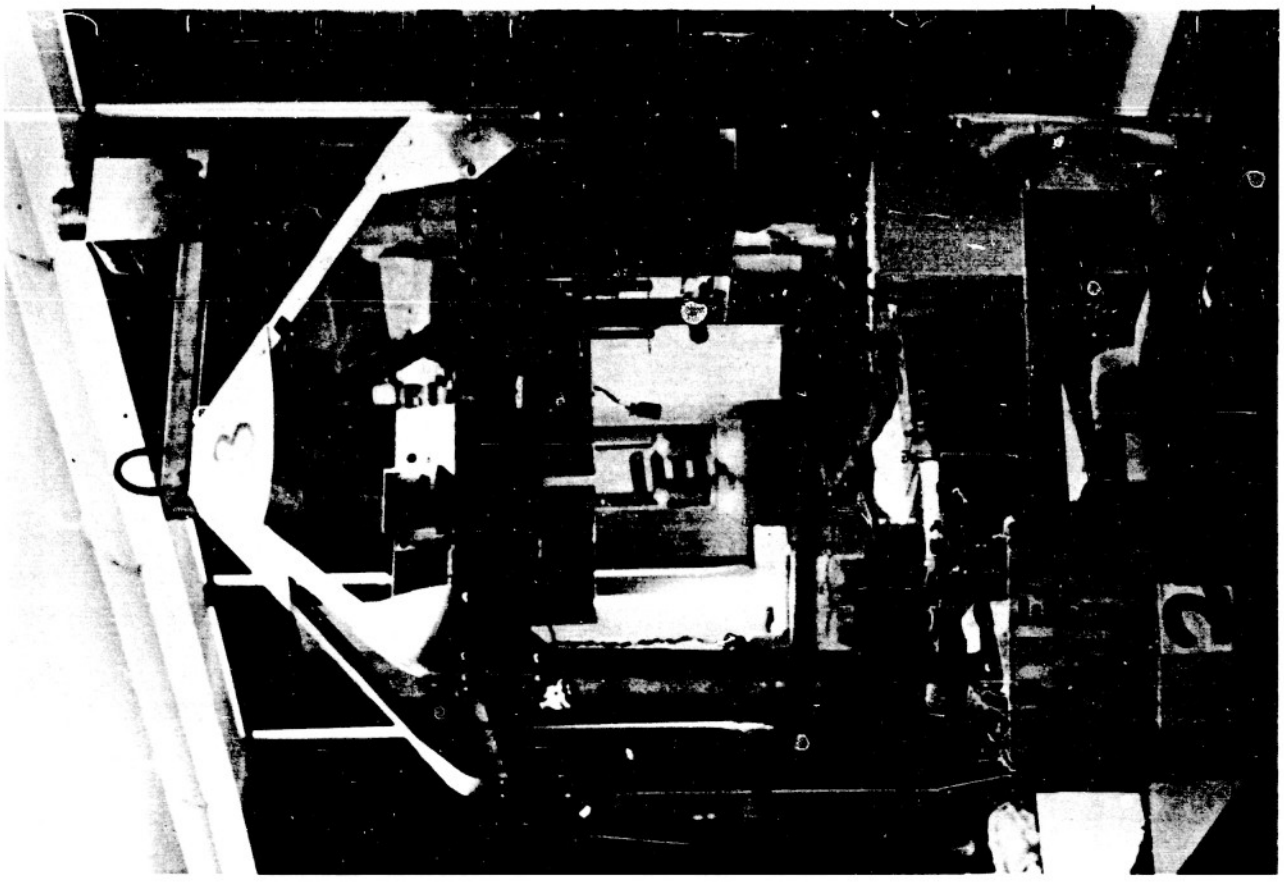

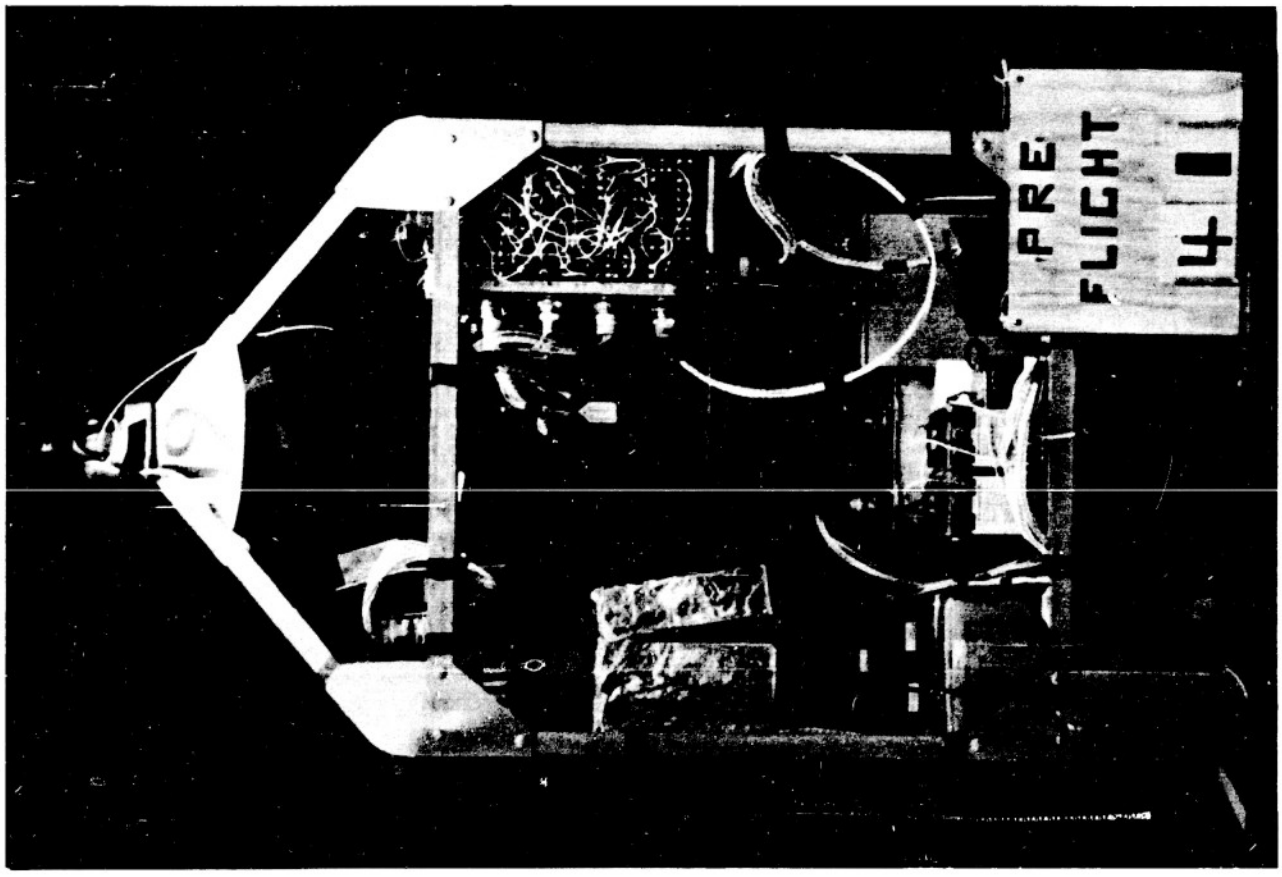
PRE
FLIGHT
14

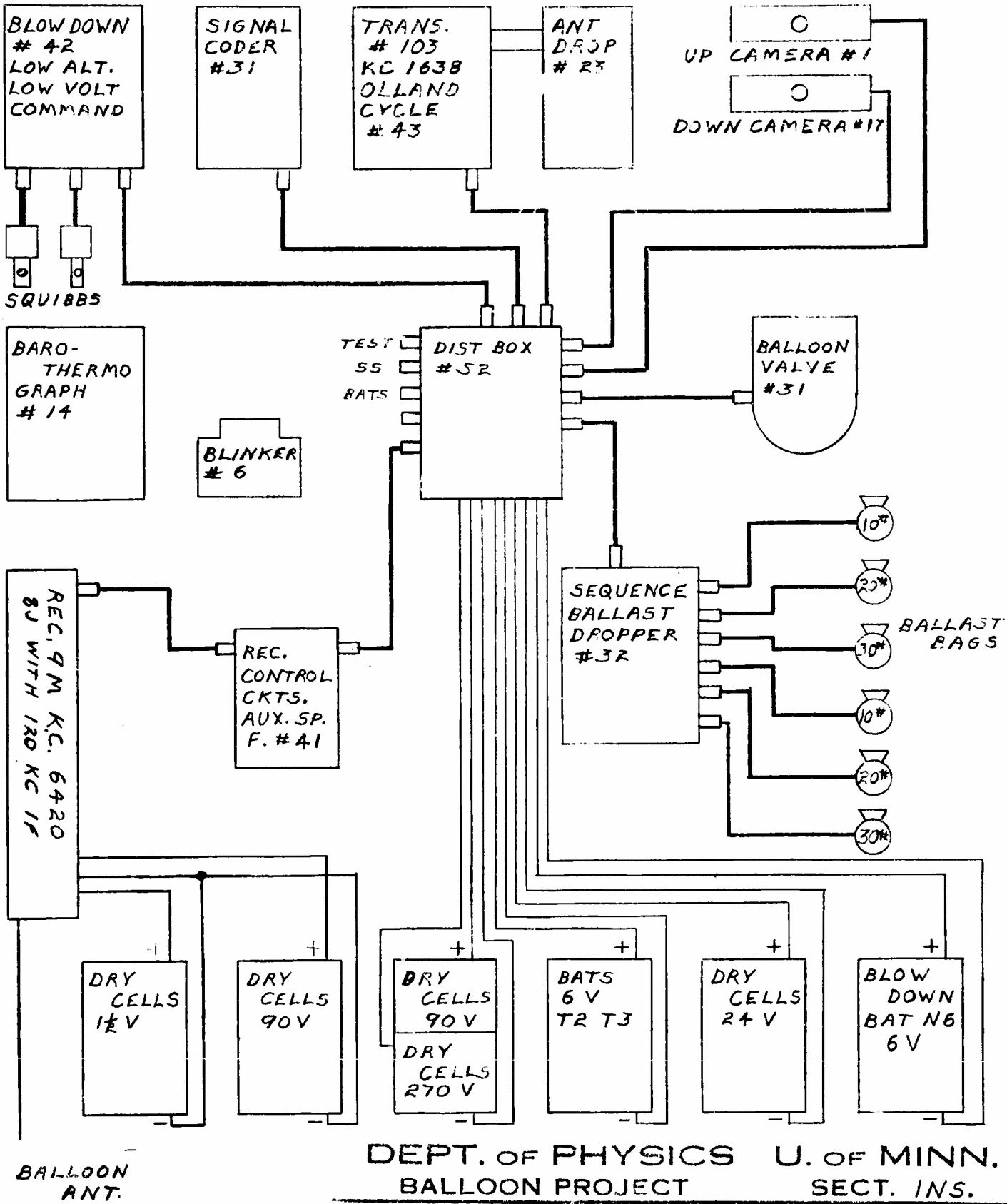

DEPT. OF PHYSICS U. OF MINN.

BALLOON PROJECT SECT. INS.

DWG. NO.	SHOP DWG. NO.	DRAWN BY	CHECKED BY	DATE
				10-2-52
FLIGHT # 41			MOD. 1	
GONDOLA # 19			MOD. 2	
PAGE			MOD. 3	

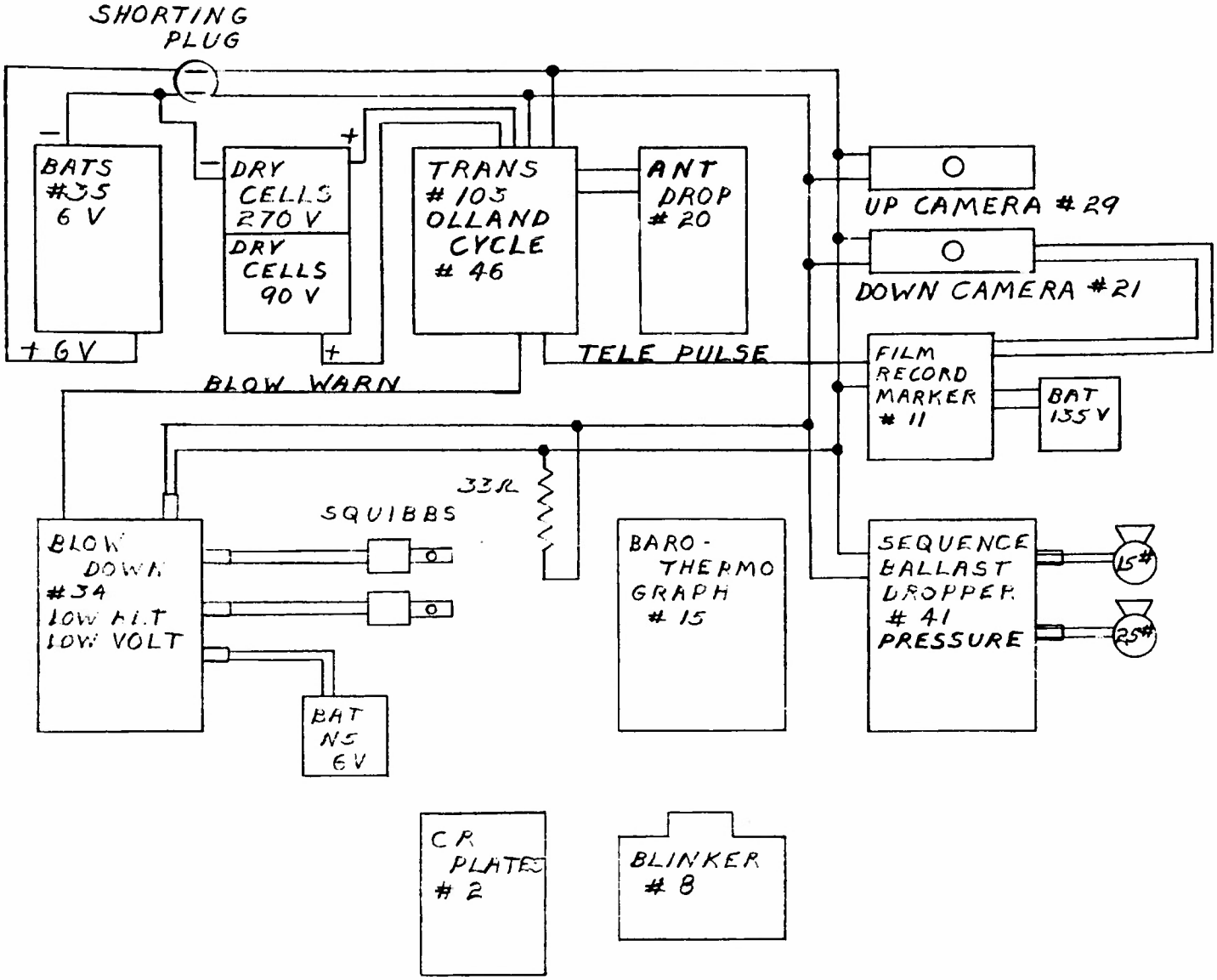

DEPT. OF PHYSICS U. OF MINN.				
BALLOON PROJECT			SECT. INS.	
DWG. NO.	DRAWN BY	CHECKED BY	DATE	
			10-9-52	
FLIGHT # 42		MOD. 1		
GONDOLA # 13		MOD. 2		
PAGE		MOD. 3		

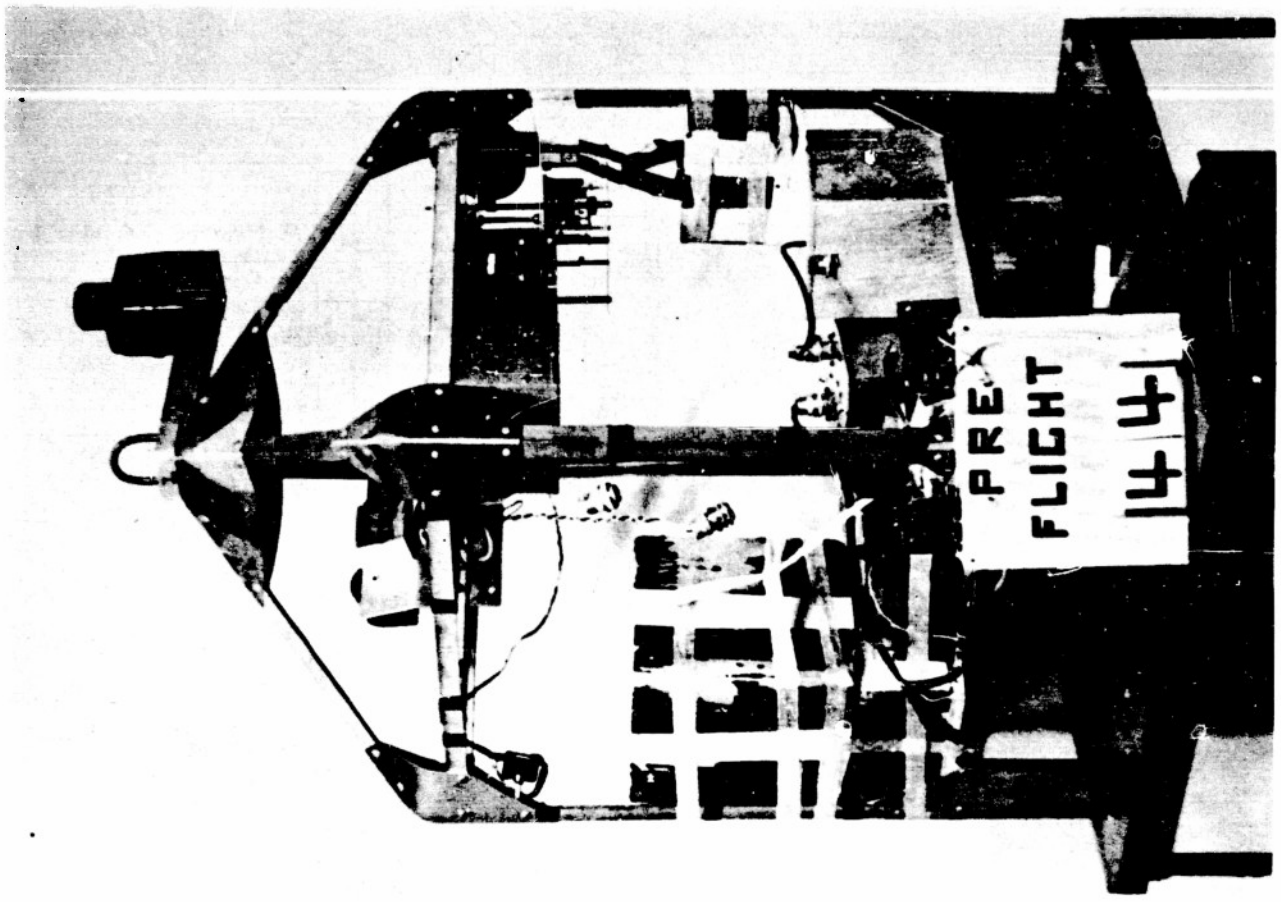
PRE
FLIGHT
144

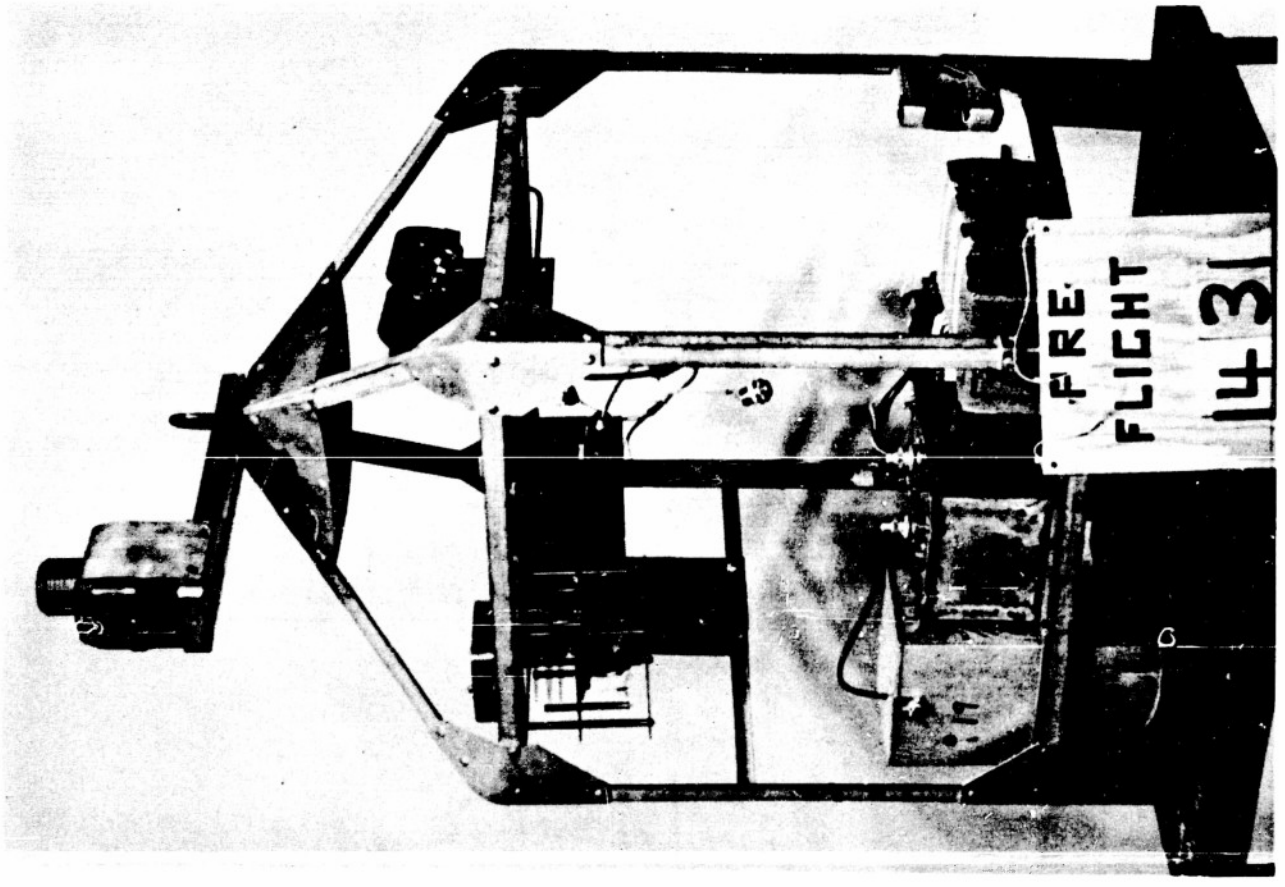
PRE
FLIGHT
143

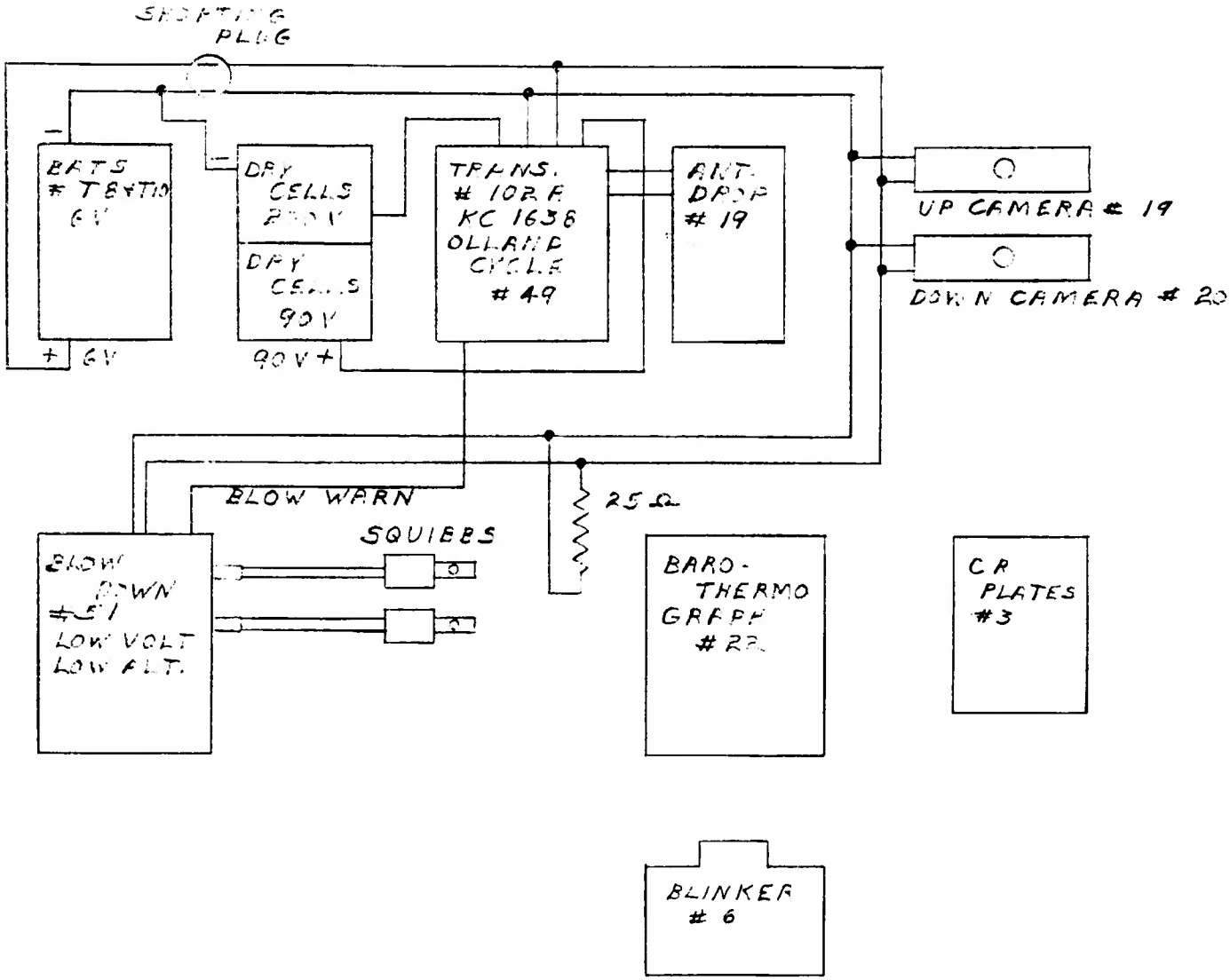

DEPT. OF PHYSICS U. OF MINN.				
BALLOON PROJECT			SECT. INS.	
DWG. NO.	SHOP DWG. NO.	DRAWN BY	CHECKED BY	DATE
		[illegible]	D.M.B.	10-14-52
FLIGHT # 43			MOD. 1	
GONDOLA # 4			MOD. 2	
			MOD. 3	

PAGE

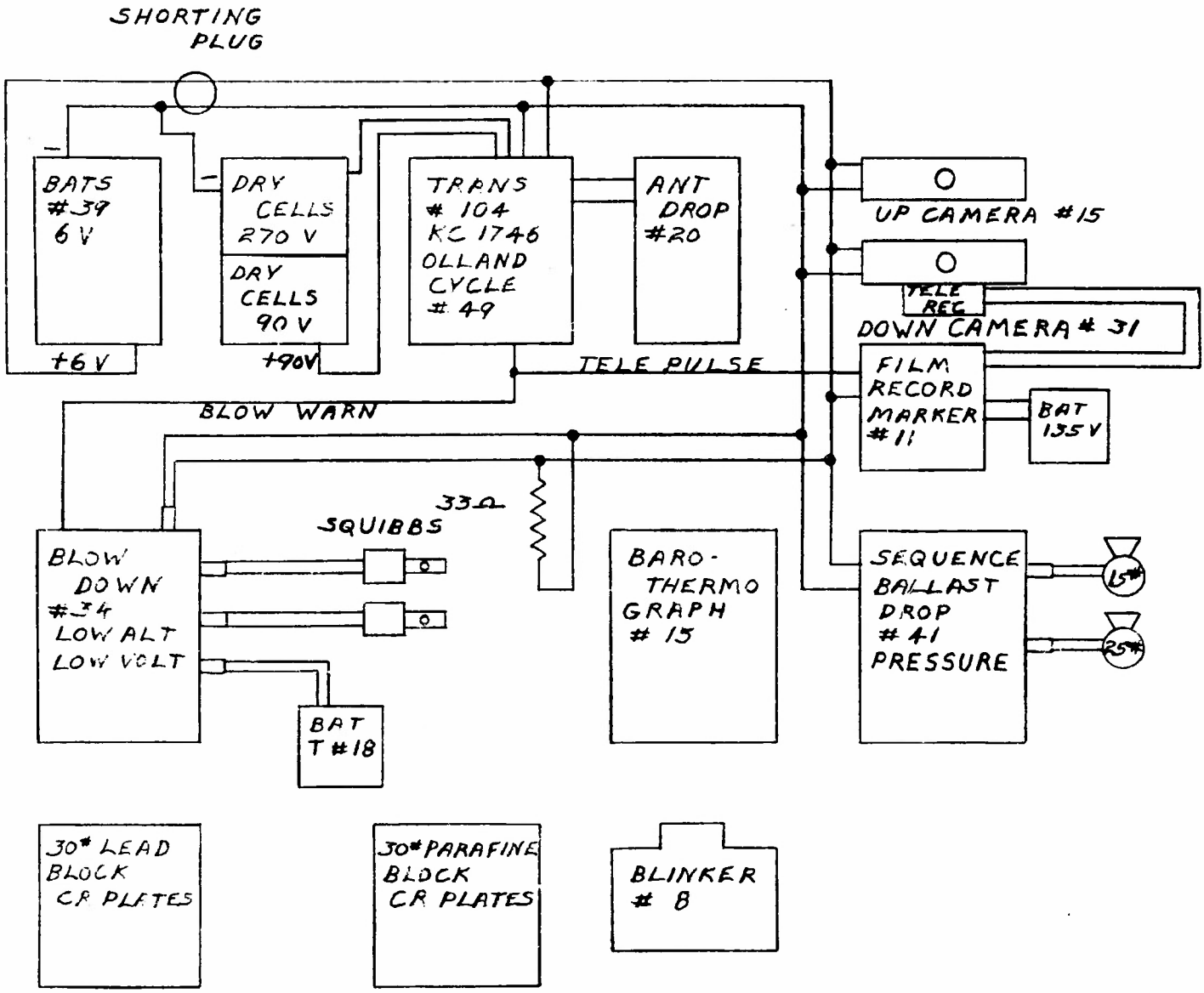

DEPT. OF PHYSICS U. OF MINN. BALLOON PROJECT SECT. INS.				
DWG. NO.	SHOP DWG. NO.	DRAWN BY	CHECKED BY	DATE
				10-17-52
FLIGHT # 44 GONDOLA # 13			MOD. 1	
			MOD. 2	
			MOD. 3	

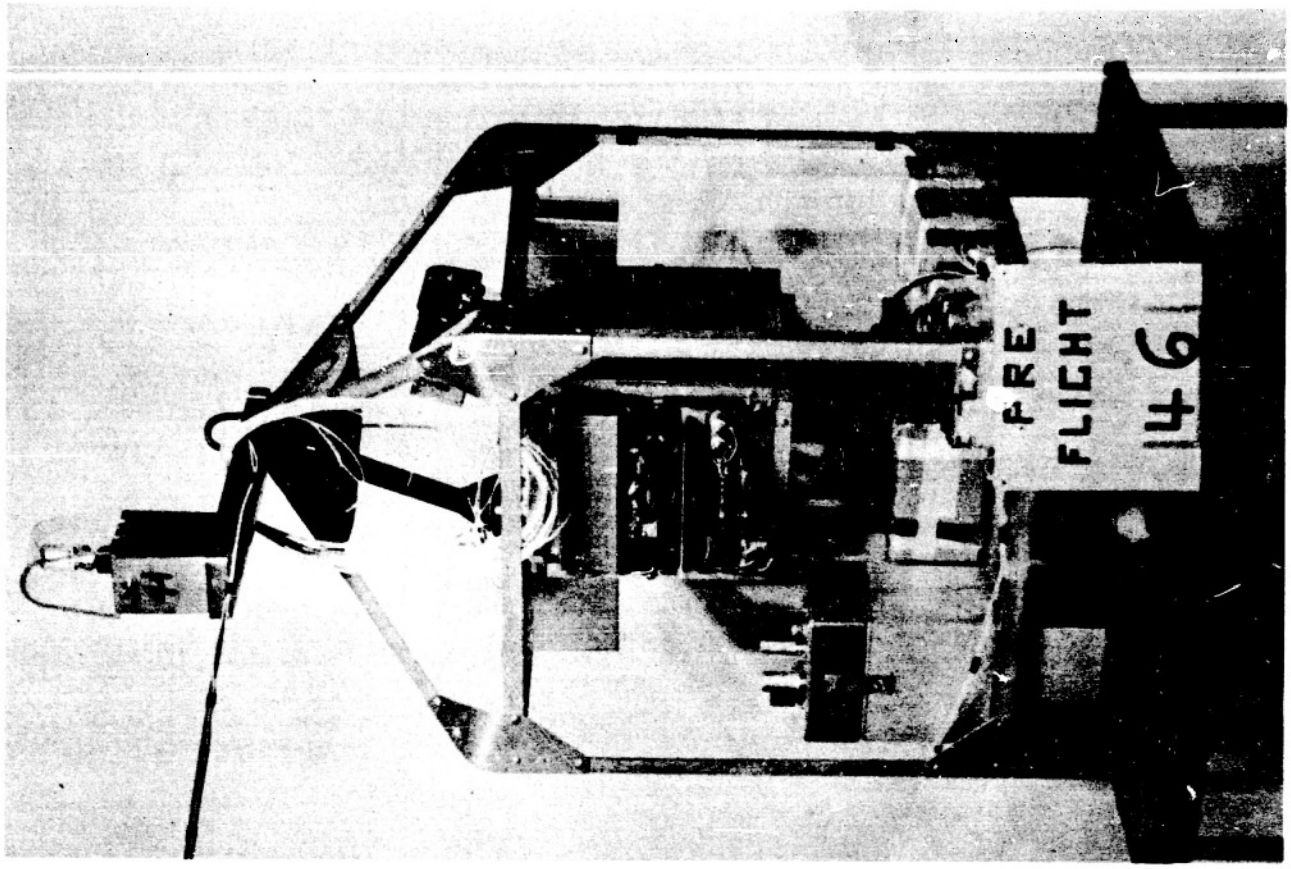
PRE
FLIGHT
461

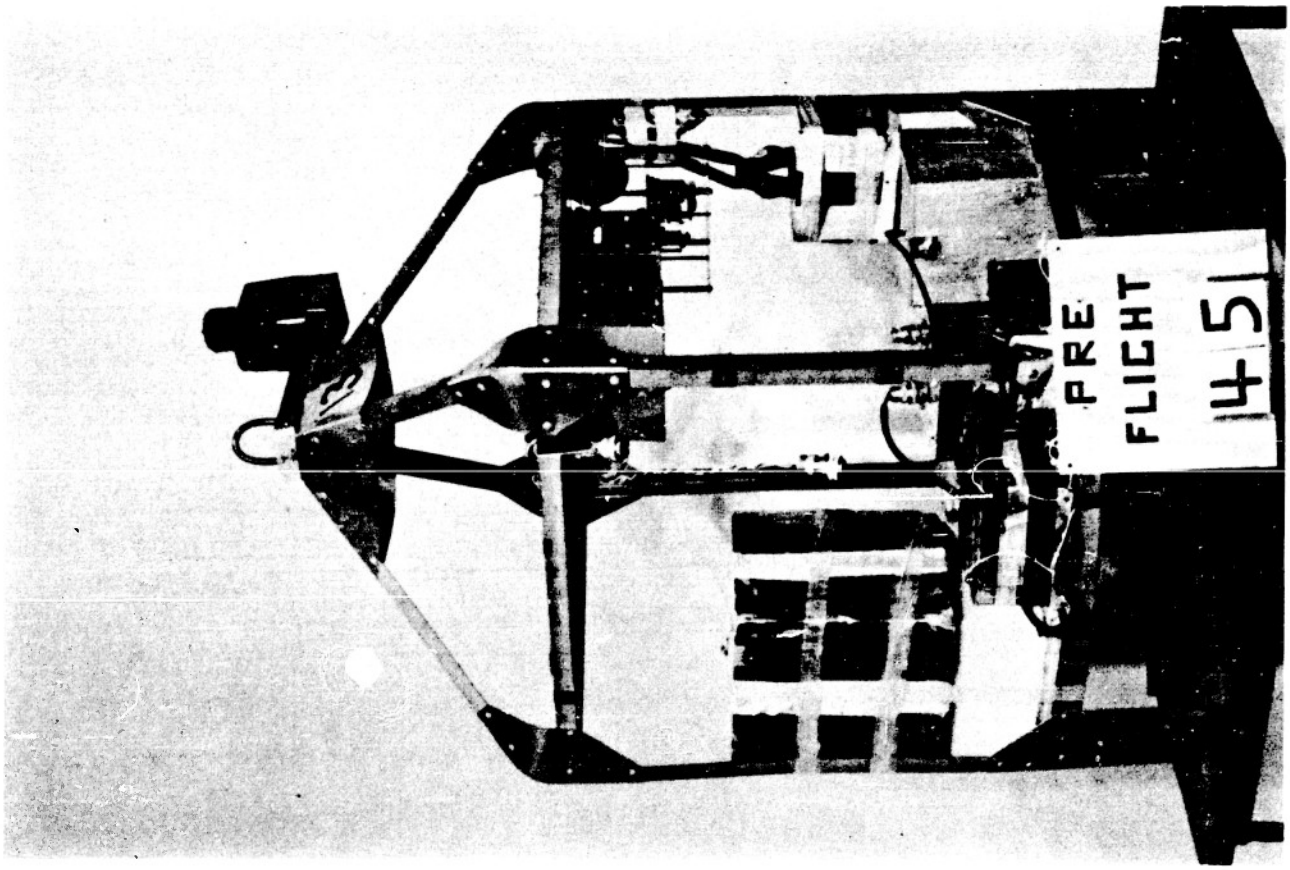
PRE
FLIGHT
451

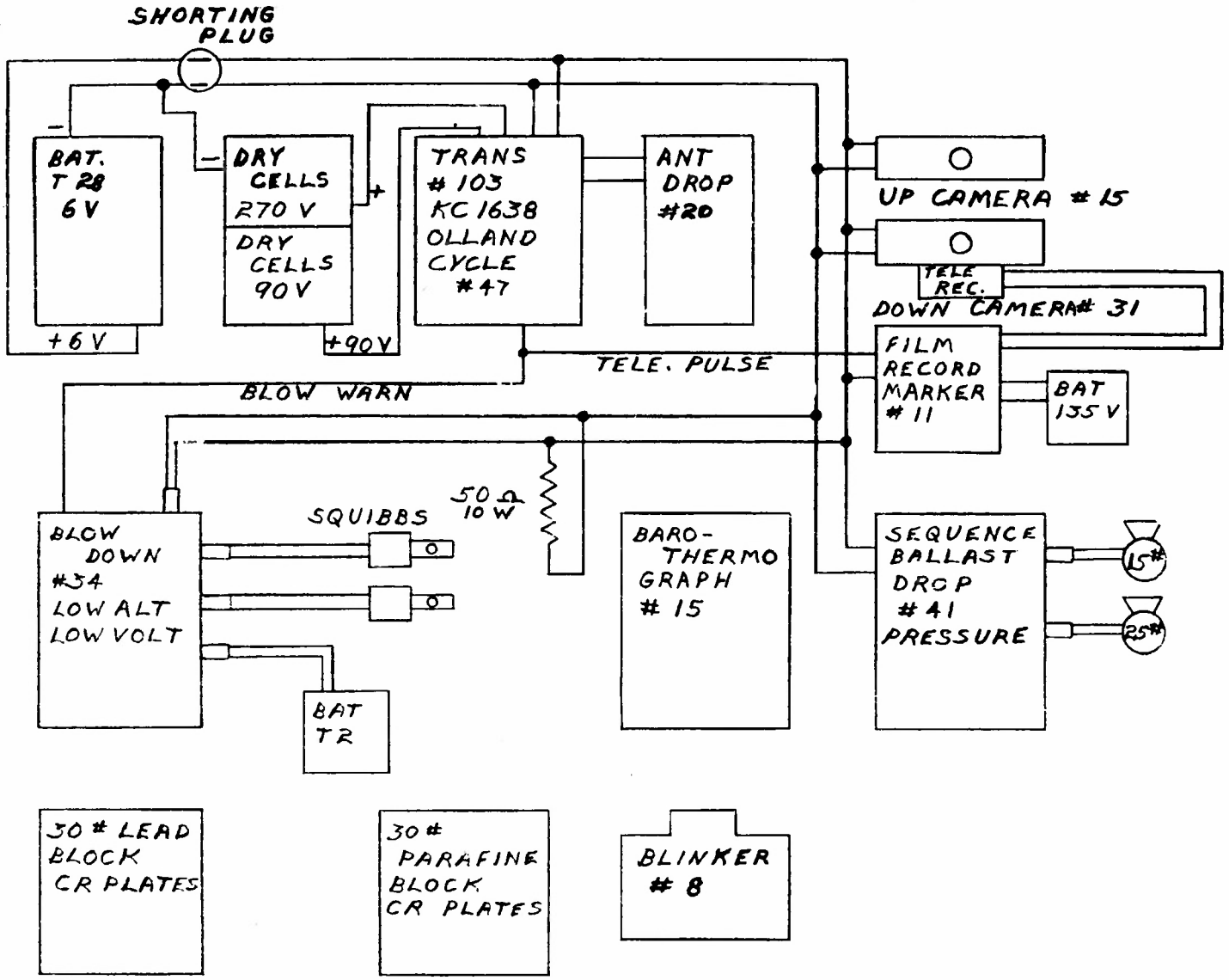

DEPT. OF PHYSICS U. OF MINN.
BALLOON PROJECT SECT. INS.

DWG. NO.	SUPERSEDES NO.	DRAWN BY	CHECKED BY	DATE
				10-21-58
			MOD. 1	
			MOD. 2	
			MOD. 3	

FLIGHT # 45
GONDOLA # 13

PAGE

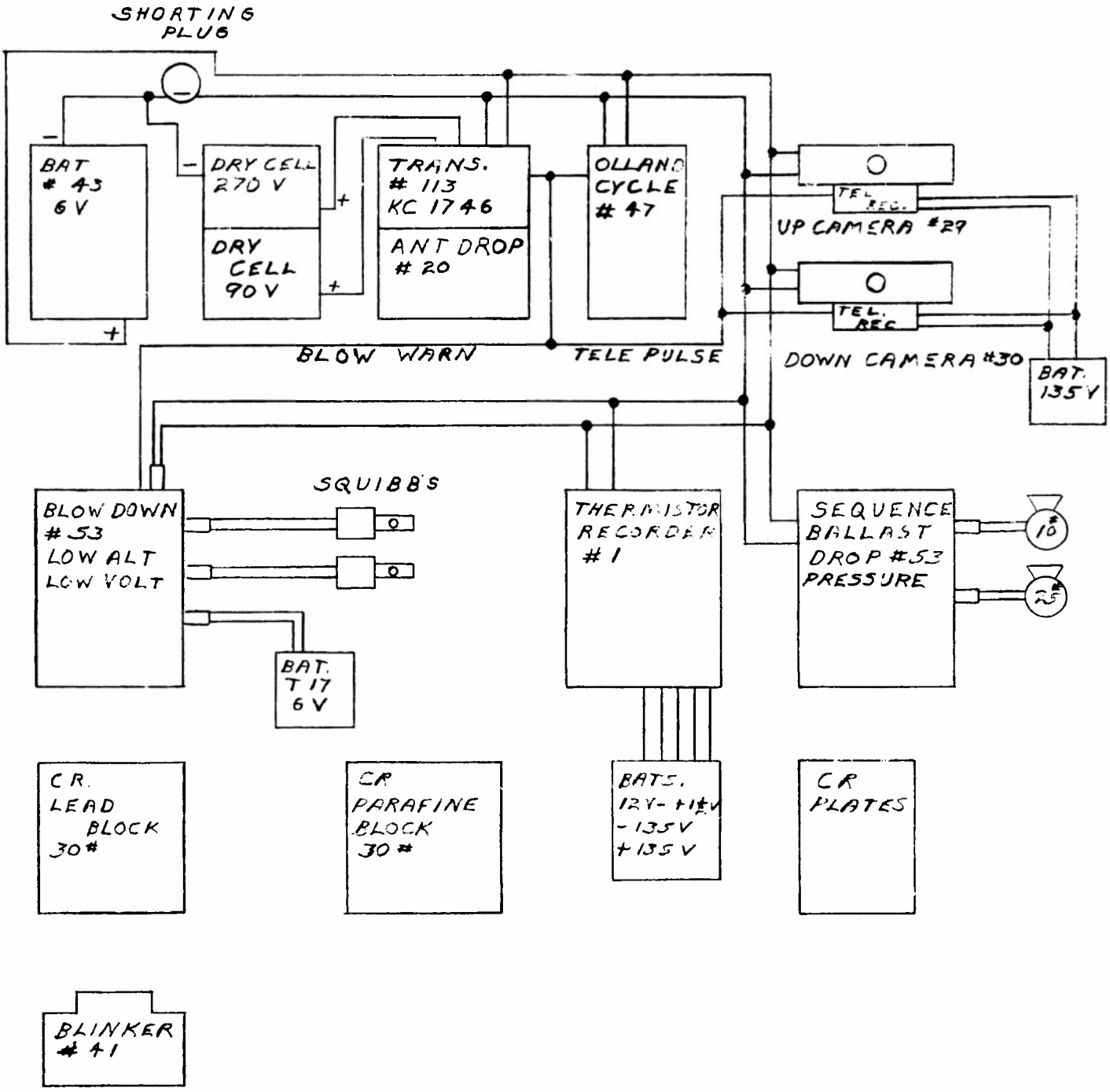

DEPT. OF PHYSICS U. OF MINN.				
BALLOON PROJECT			SECT. INS.	
DWG. NO.	SHOP DWG. NO.	DRAWN BY	CHECKED BY	DATE
		[illegible]	[signature]	11-3-52
FLIGHT # 46			MOD. 1	
GONDOLA # 15			MOD. 2	
Confidential Security Information			MOD. 3	

PAGE

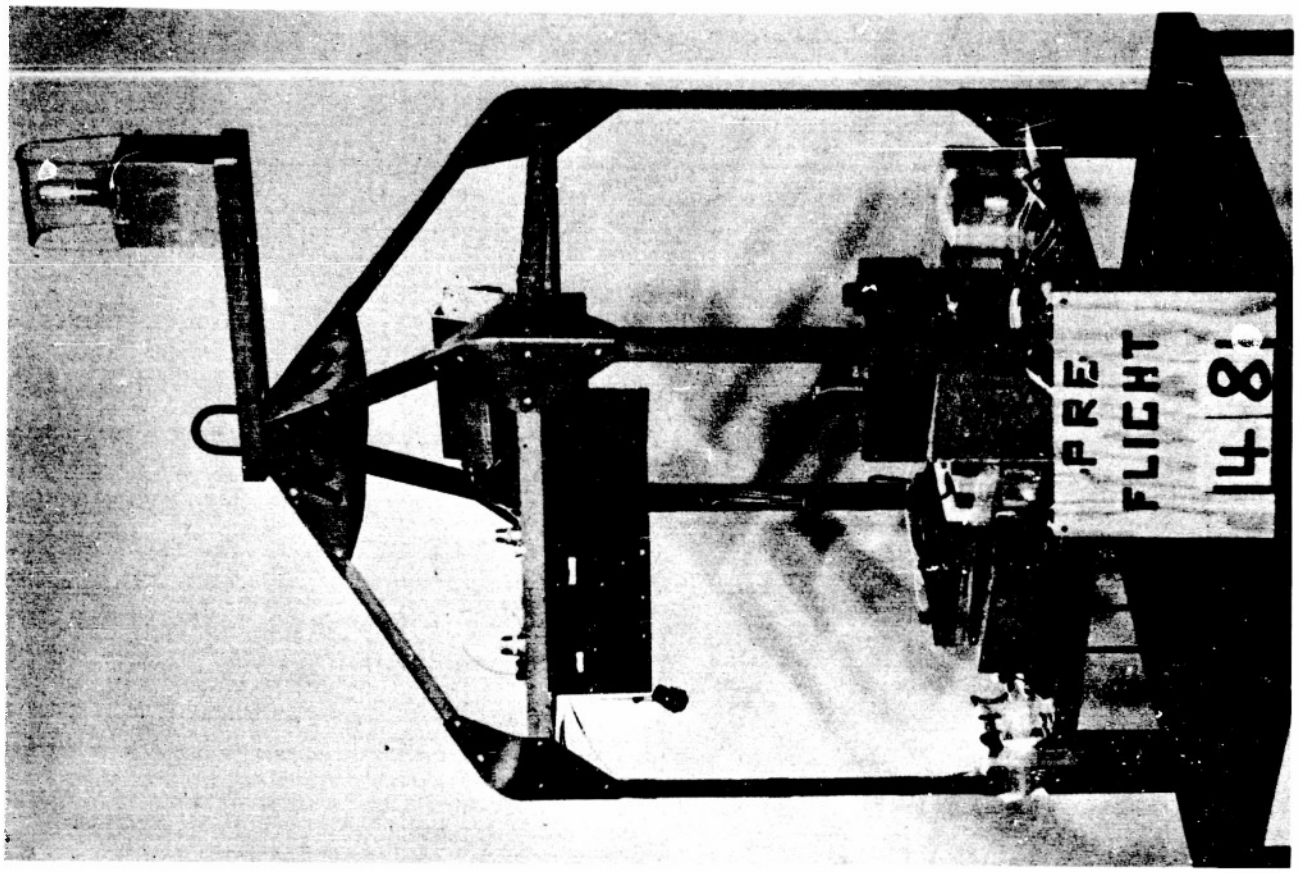
PRE
FLIGHT
4-8

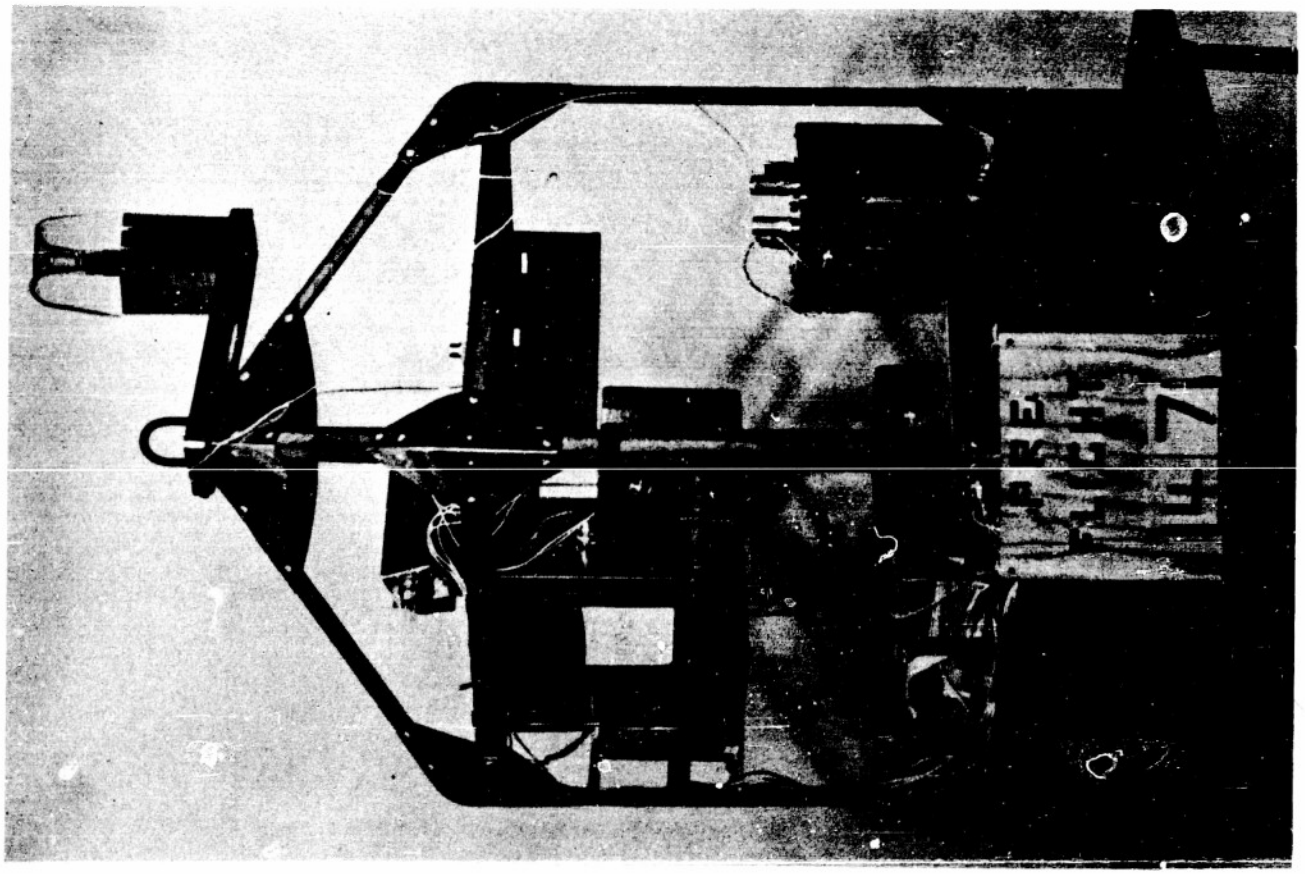

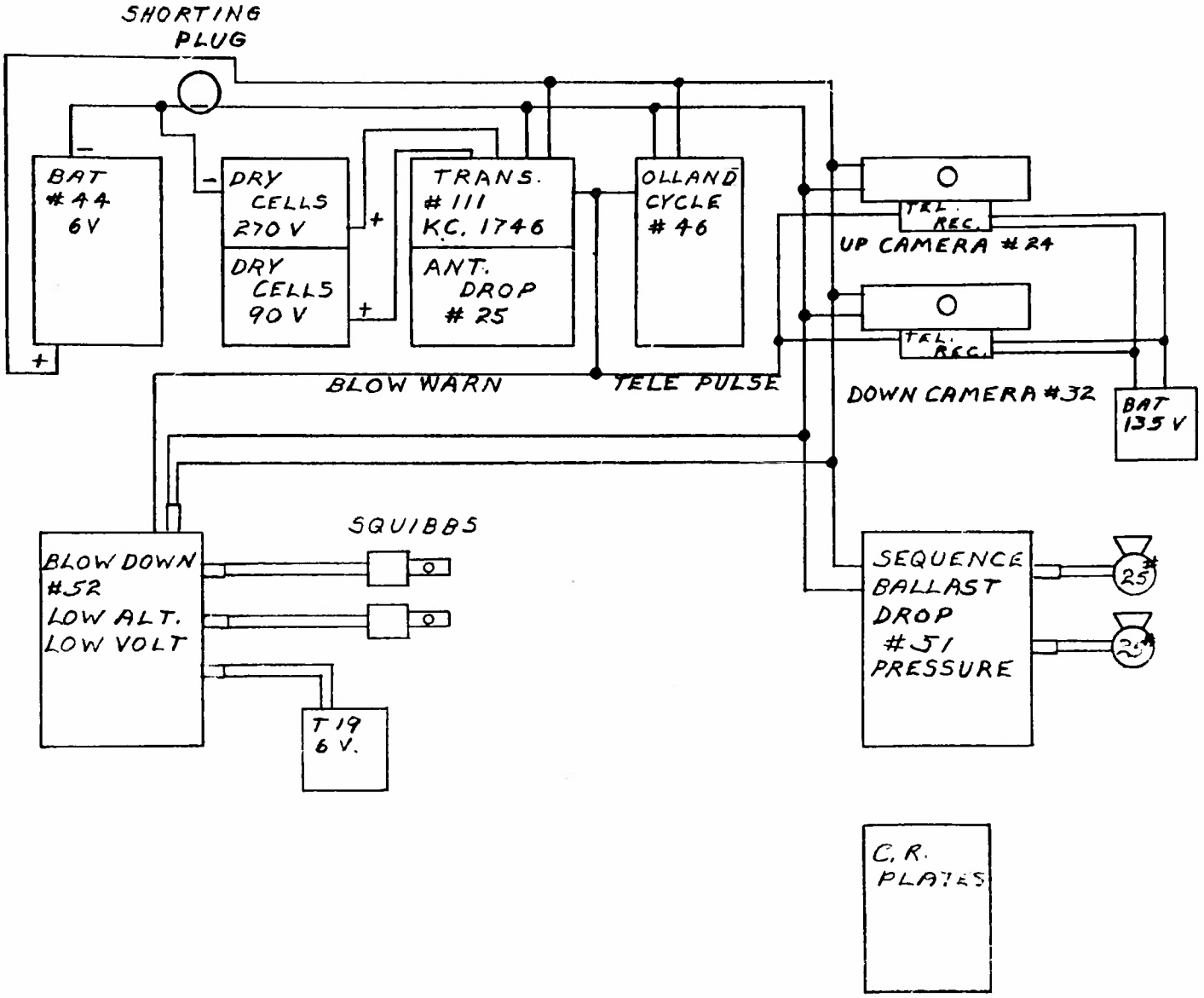

FLIGHT # 47
GONDOLA # 19

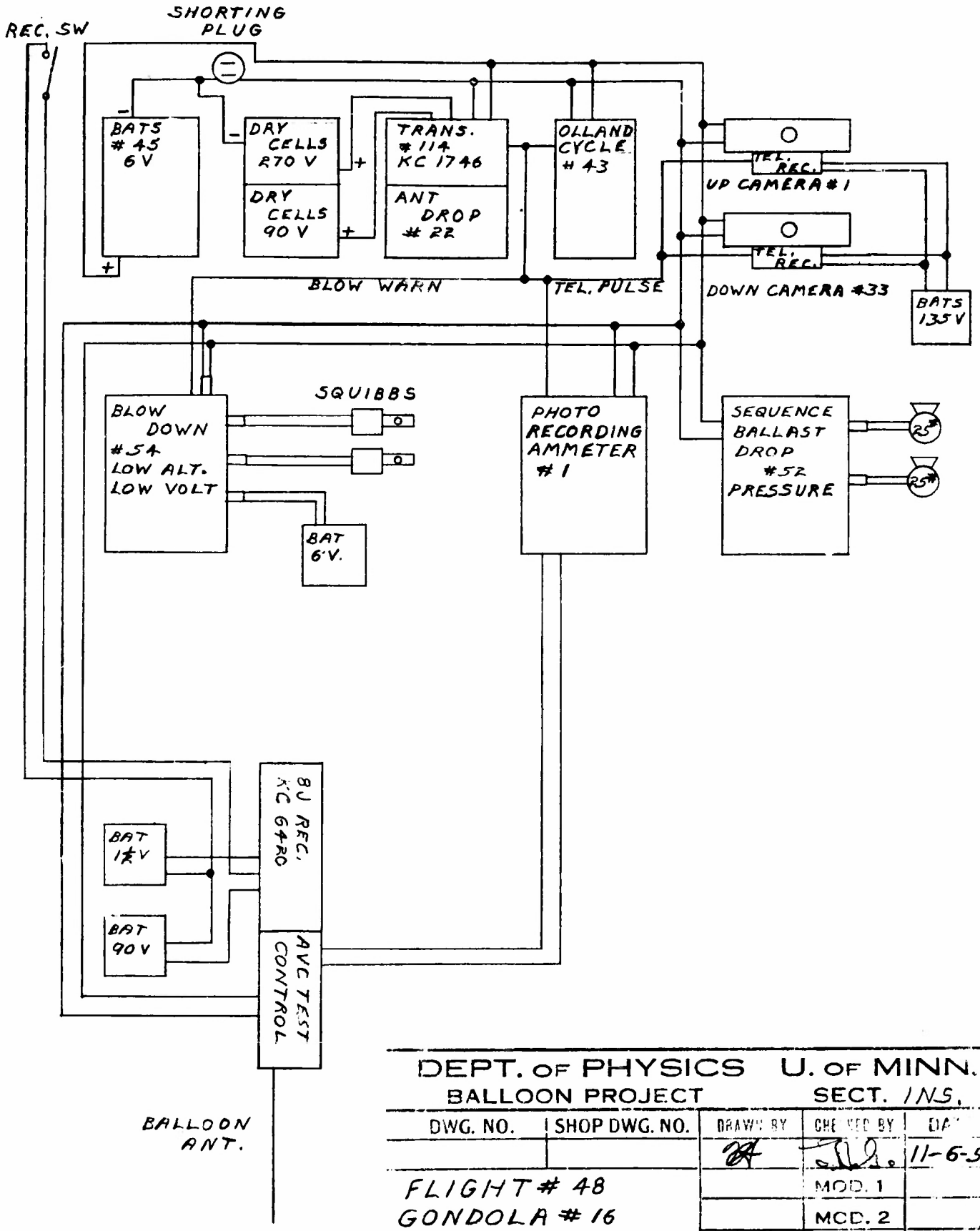

DEPT. OF PHYSICS U. OF MINN.
BALLOON PROJECT SECT. INS.

DWG. NO.	SHOP DWG. NO.	DRAWN BY	CHECKED BY	DATE
				11-6-52
FLIGHT # 48			MOD. 1	
GONDOLA # 16			MOD. 2	
PAGE			MOD. 3	

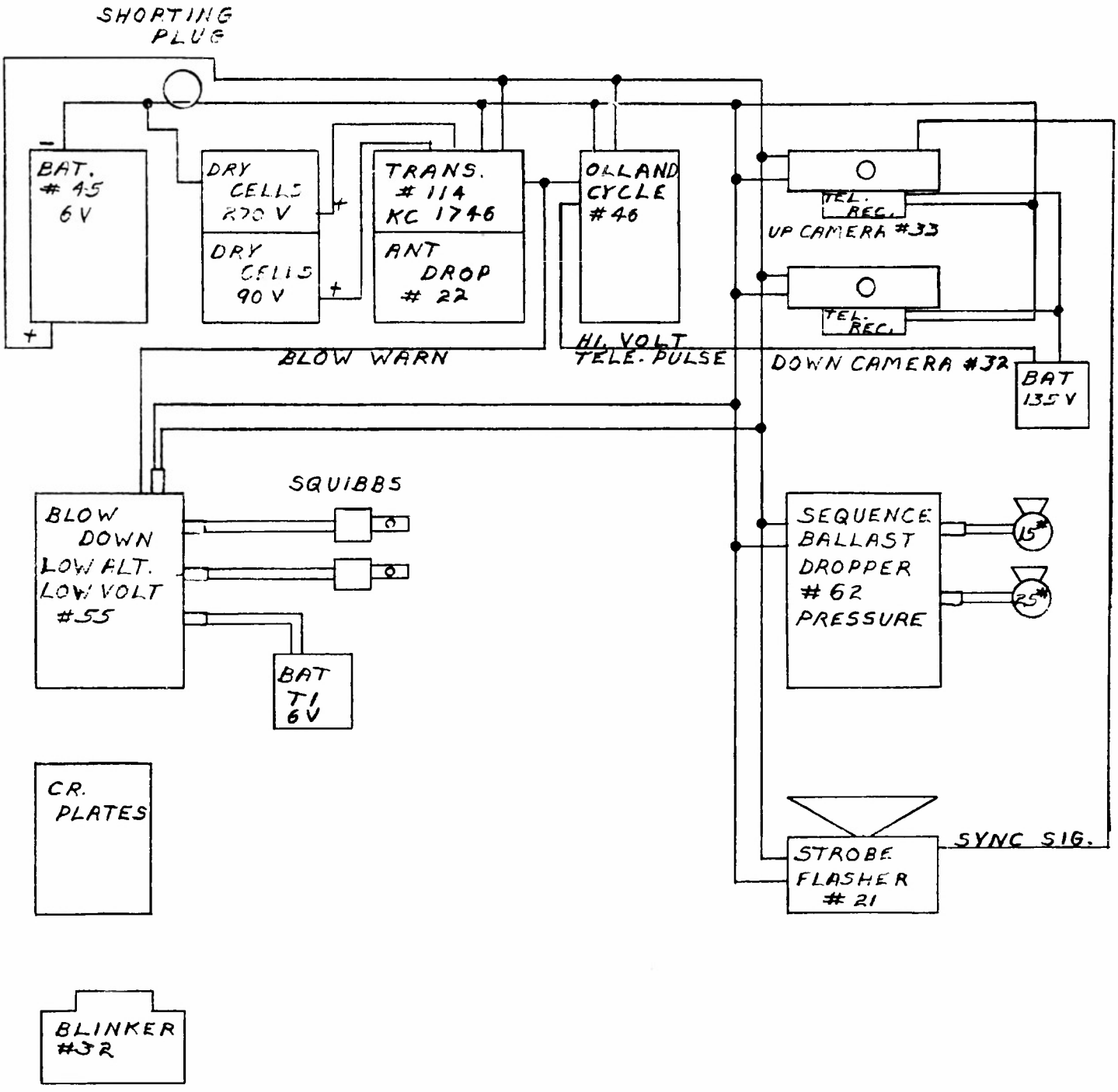

DEPT. OF PHYSICS U. OF MINN.				
BALLOON PROJECT			SECT. INS.	
DWG. NO.	SHOP DWG. NO.	DRAWN BY	CHECKED BY	DATE
		[illegible]	[illegible]	11-20-52
FLIGHT # 49			MOD. 1	
GONDOLA # 16			MOD. 2	
			MOD. 3	

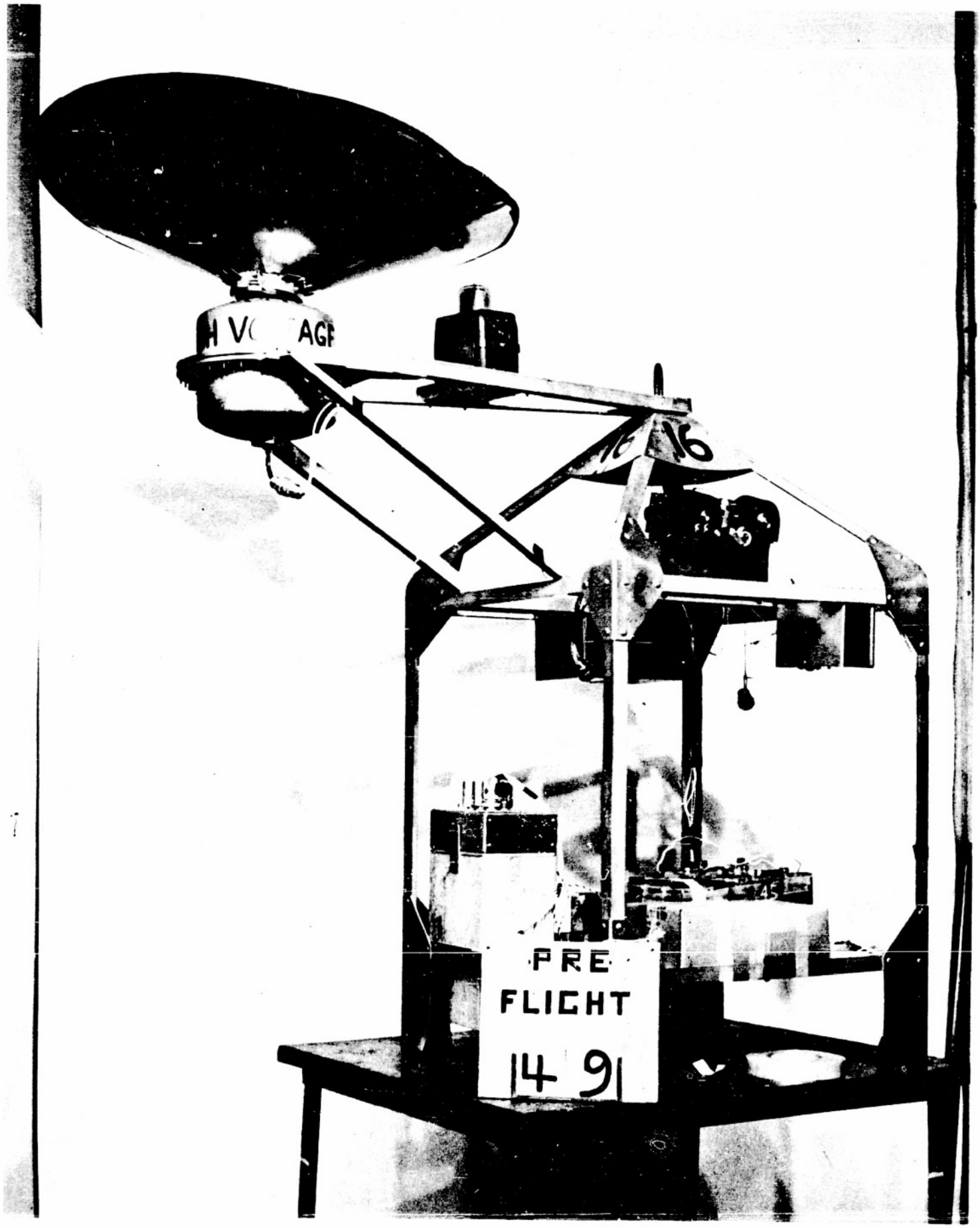
PRE
FLIGHT
14 9

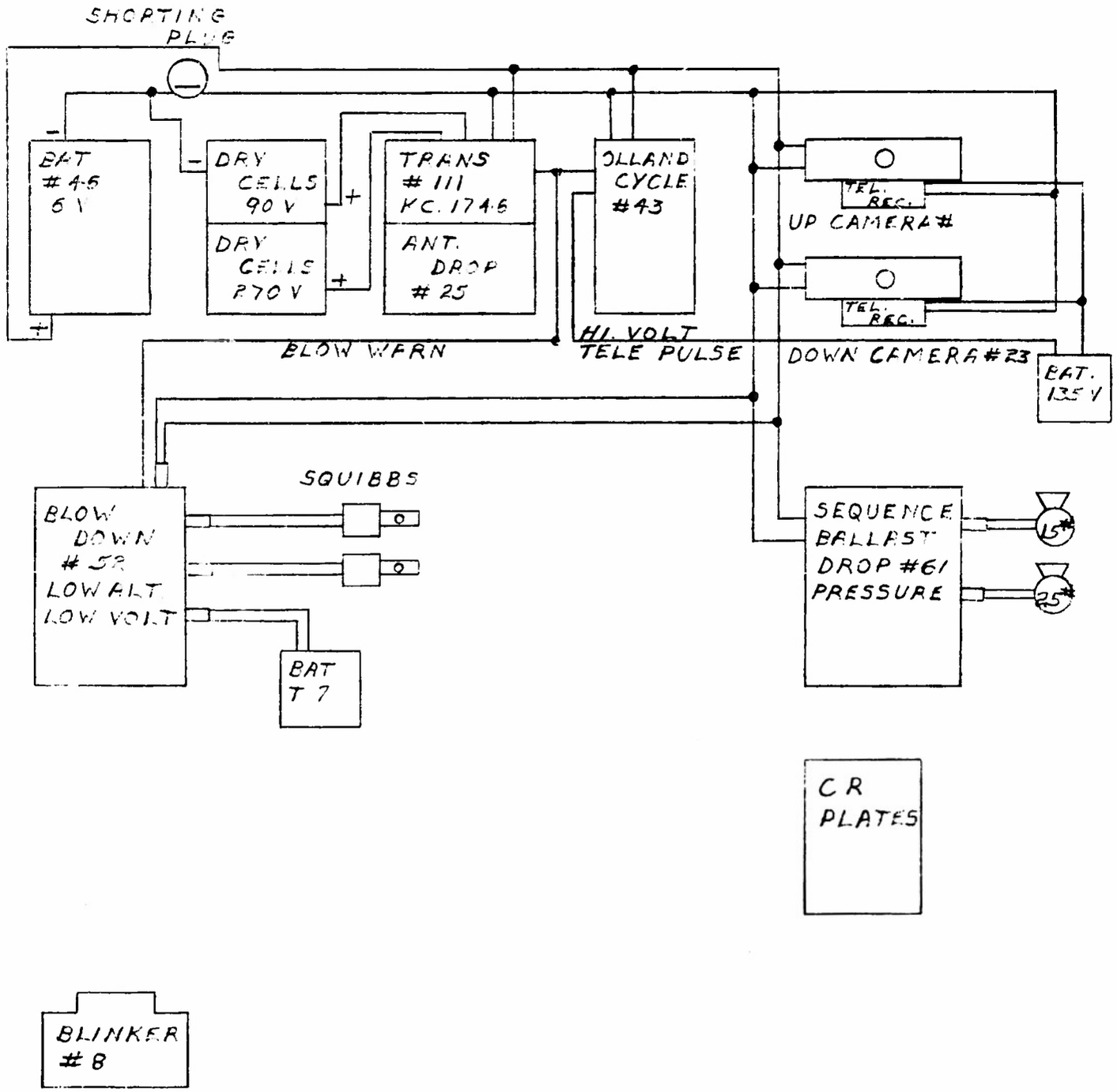

DEPT. of PHYSICS U. of MINN.
BALLOON PROJECT SECT. INS.

DWG. NO.	SHOP DWG. NO.	DRAWN BY	CHECKED BY	DATE
				11-22-52
			MOD. 1	
			MOD. 2	
			MOD. 3	

FLIGHT #50
GONDOLA #15
Confidential Security Information
PAGE

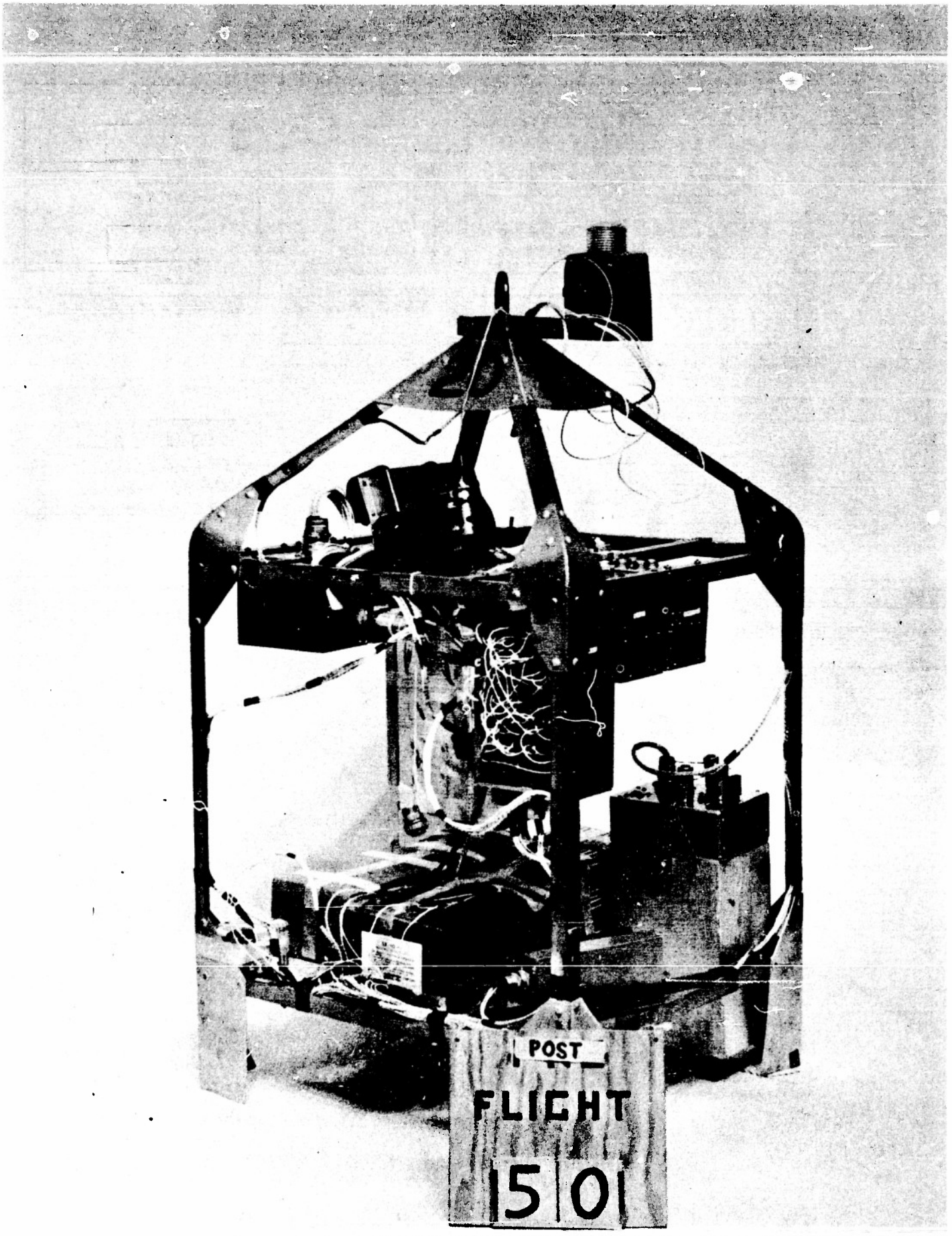
POST
FLIGHT
150

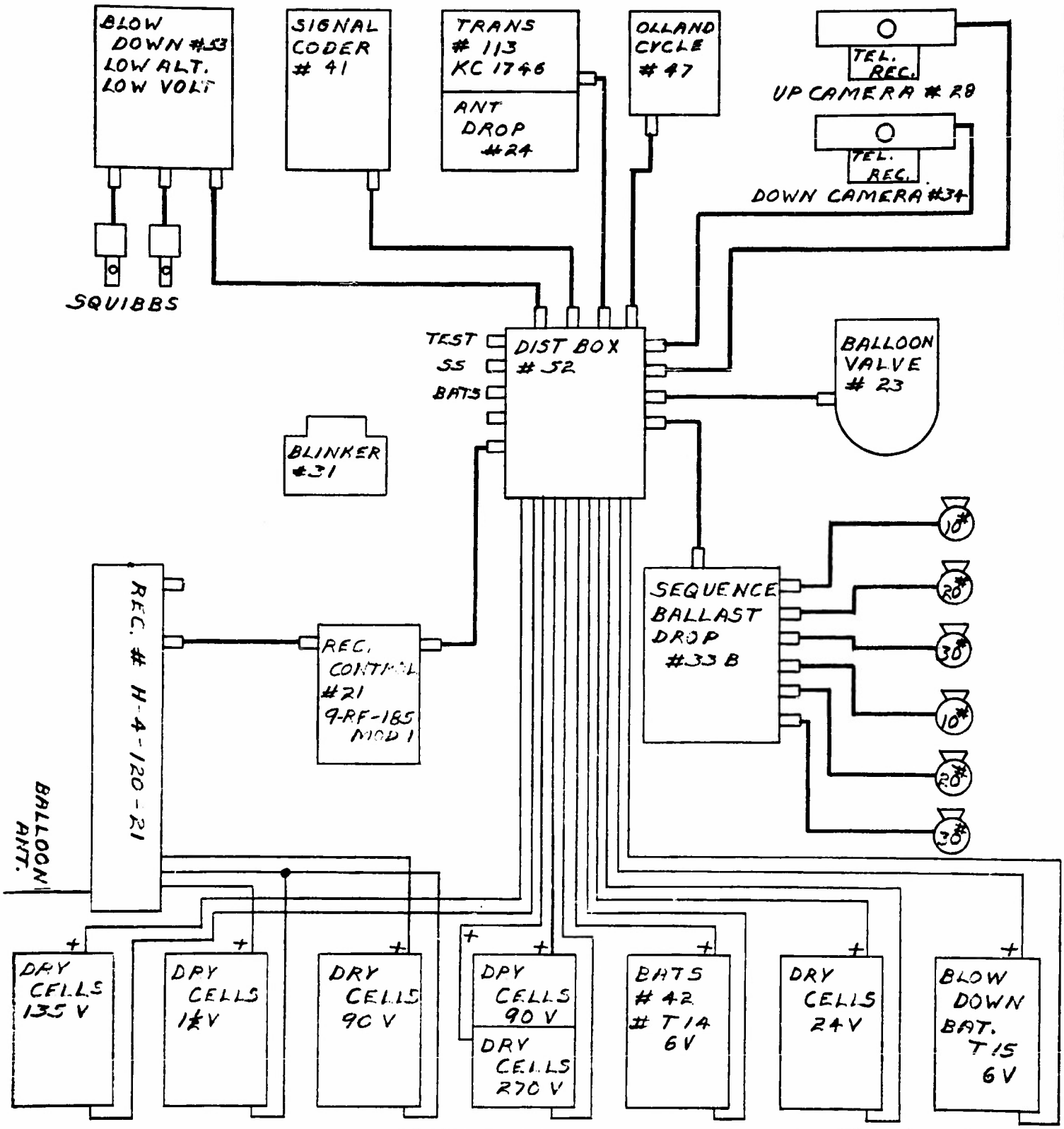

DEPT. OF PHYSICS U. OF MINN.

BALLOON PROJECT SCIENTIFIC INSTRUMENTS

	BY	DATE
	S.L.S.	11-24-5

FLIGHT #51

GONDOLA # 20

PAGE

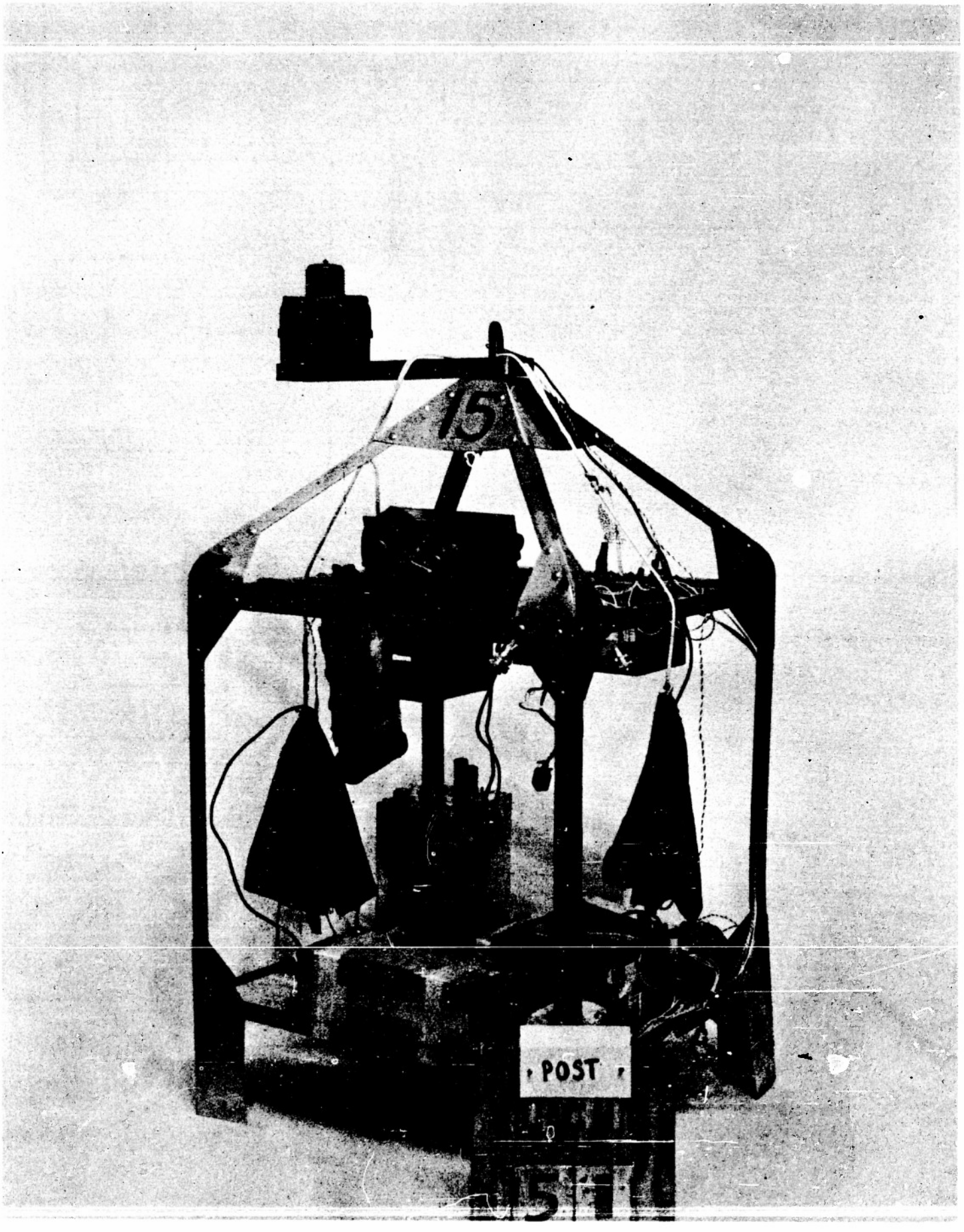
15
POST

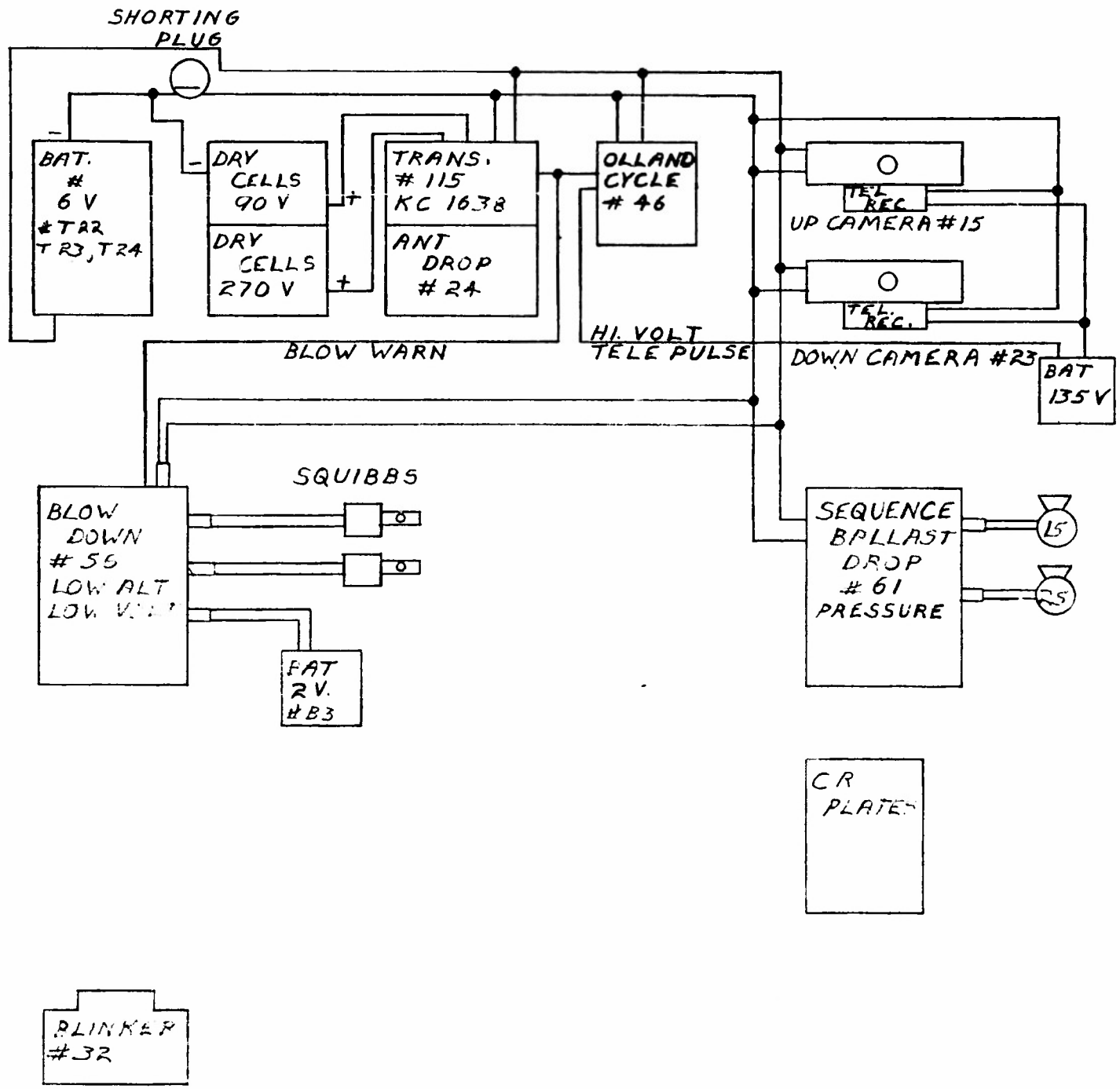

U. OF MINN.
SPOT. INS.

FLIGHT #52
GONDOLA #53

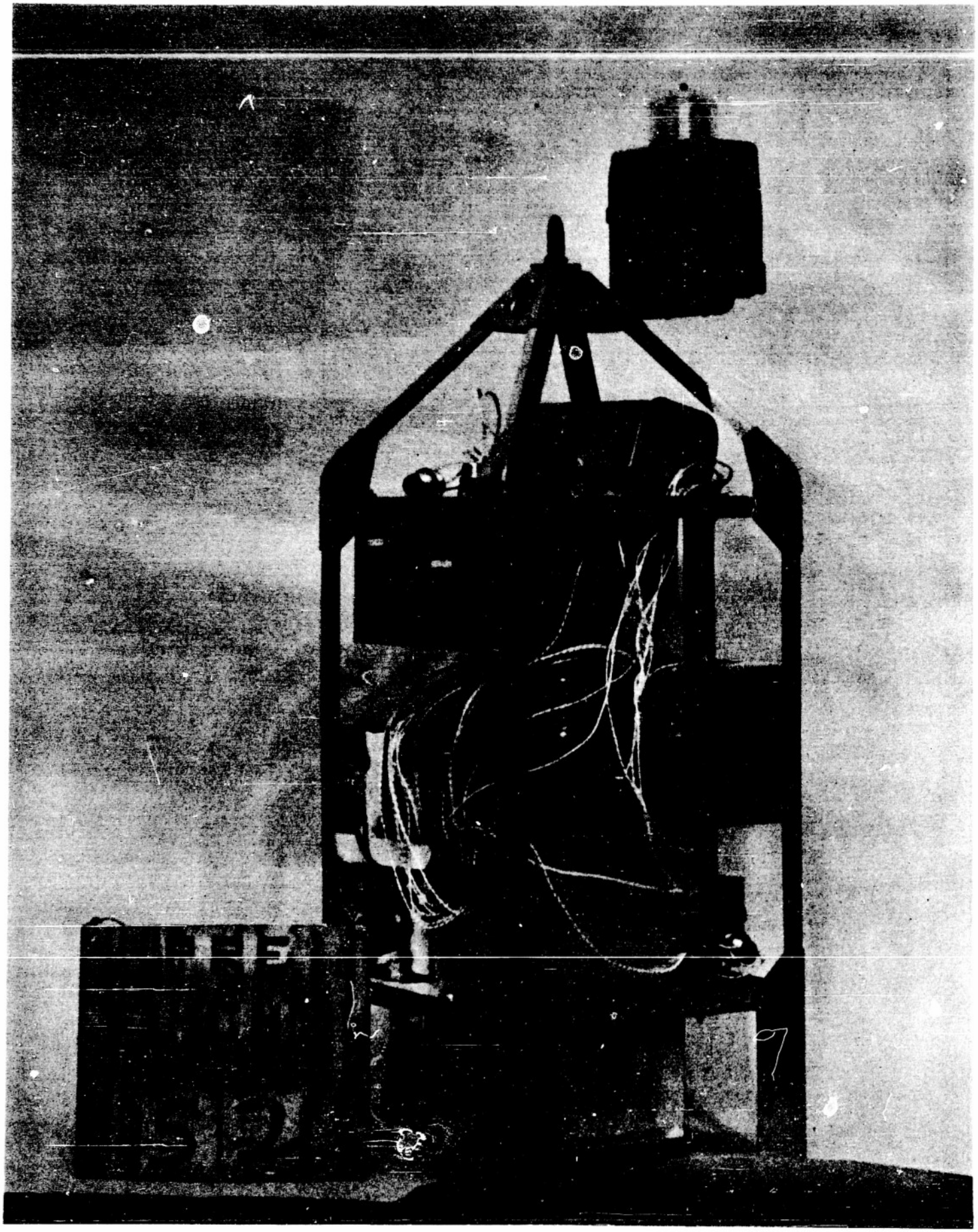

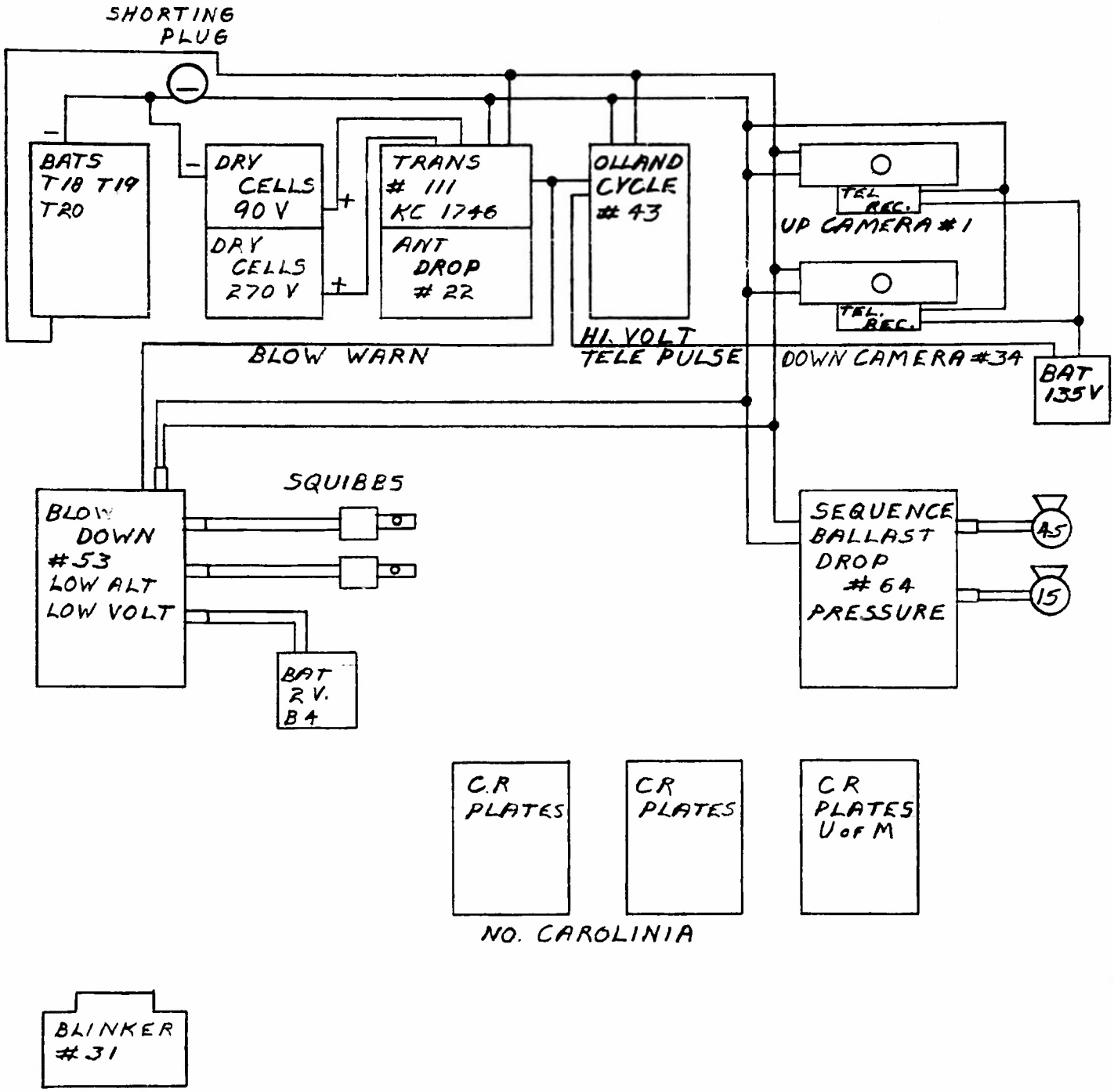

DEPT. OF PHYSICS U. OF MINN. BALLOON PROJECT			SECT. INS.	
DWG. NO.	SHOP DWG. NO.	DRAWN BY	CHECKED BY	DATE
				12-7-52
FLIGHT #53			MOD. 1	
GONDOLA #54			MOD. 2	
Confidential Security Information			MOD. 3	

PAGE

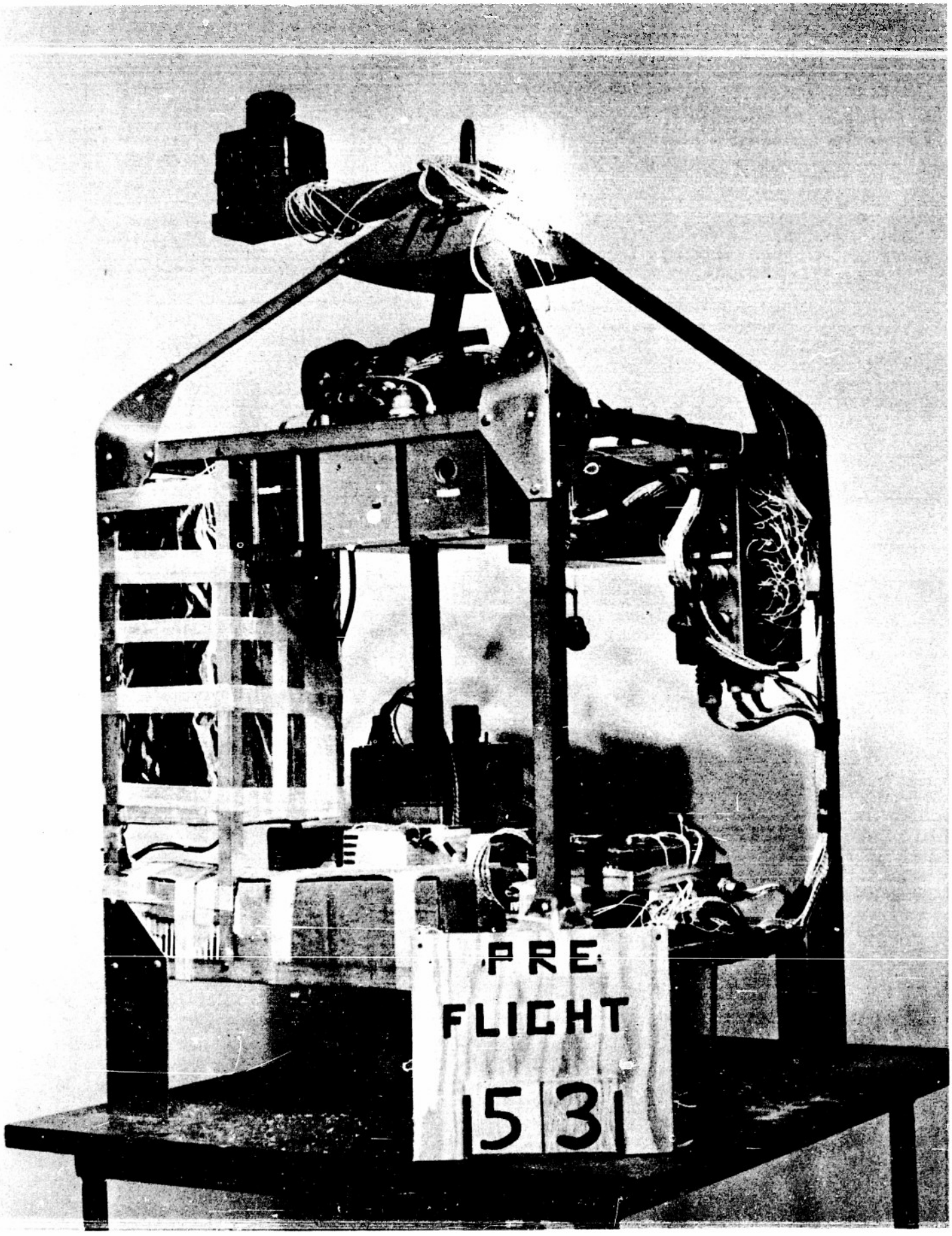
PRE
FLIGHT
53

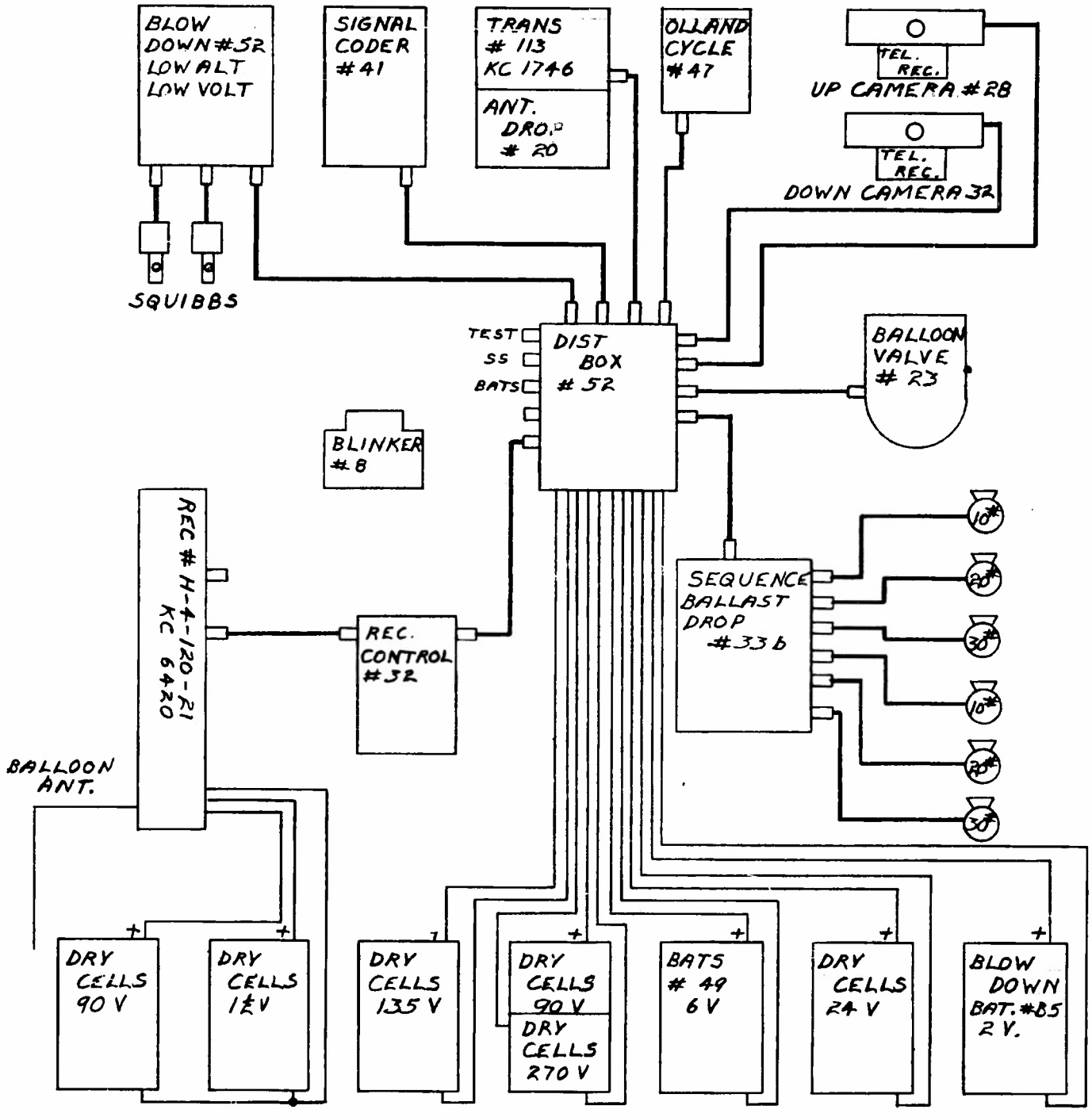

DEPT. OF PHYSICS U. OF MINN. BALLOON PROJECT			SECT. INS.	
DWG. NO.	SHOP DWG. NO.	DRAWN BY	CHECKED BY	DATE
				12-8-52
FLIGHT #54 GONDOLA #14			MOD. 1	
			MOD. 2	
			MOD. 3	

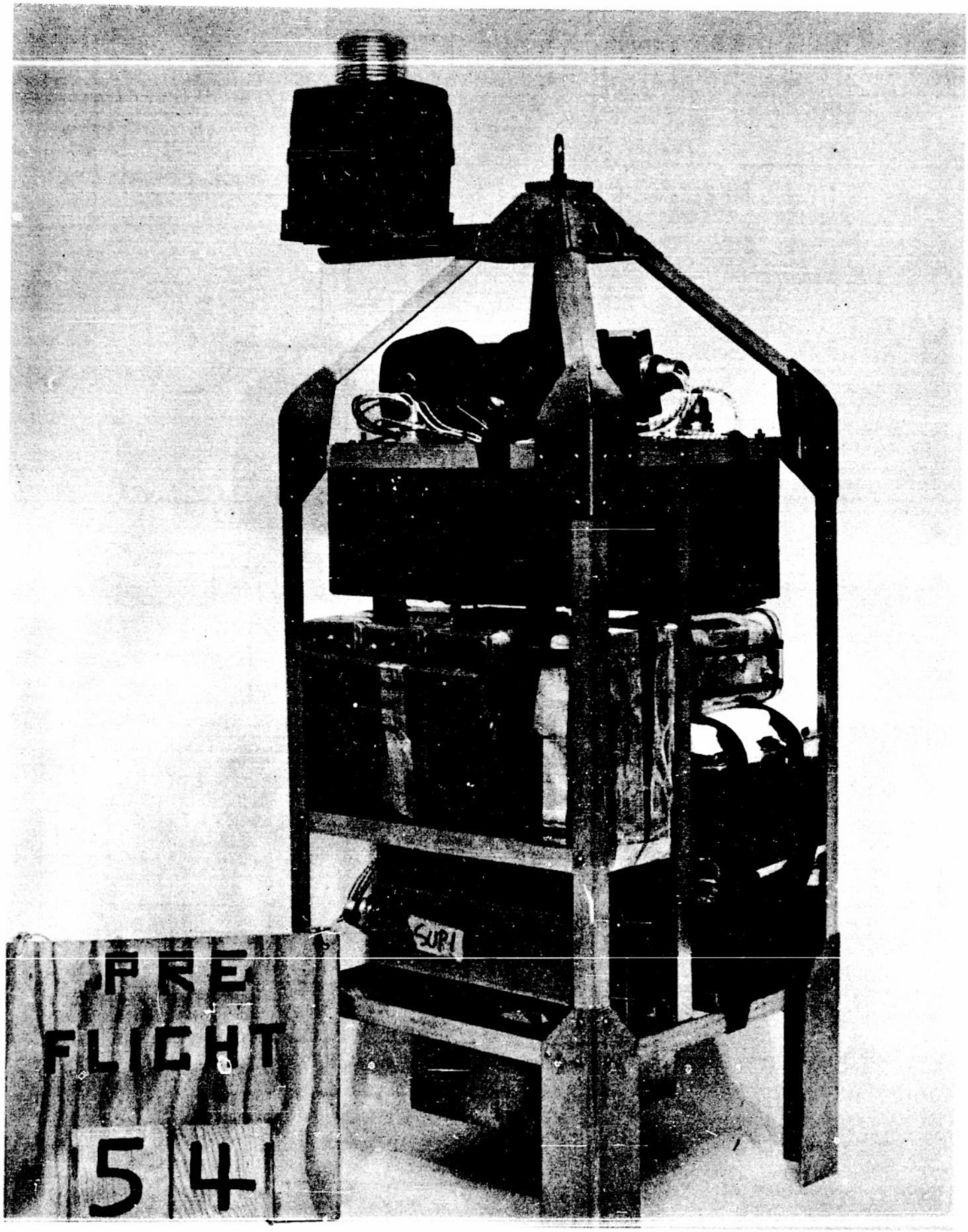
PRE
FLIGHT
541

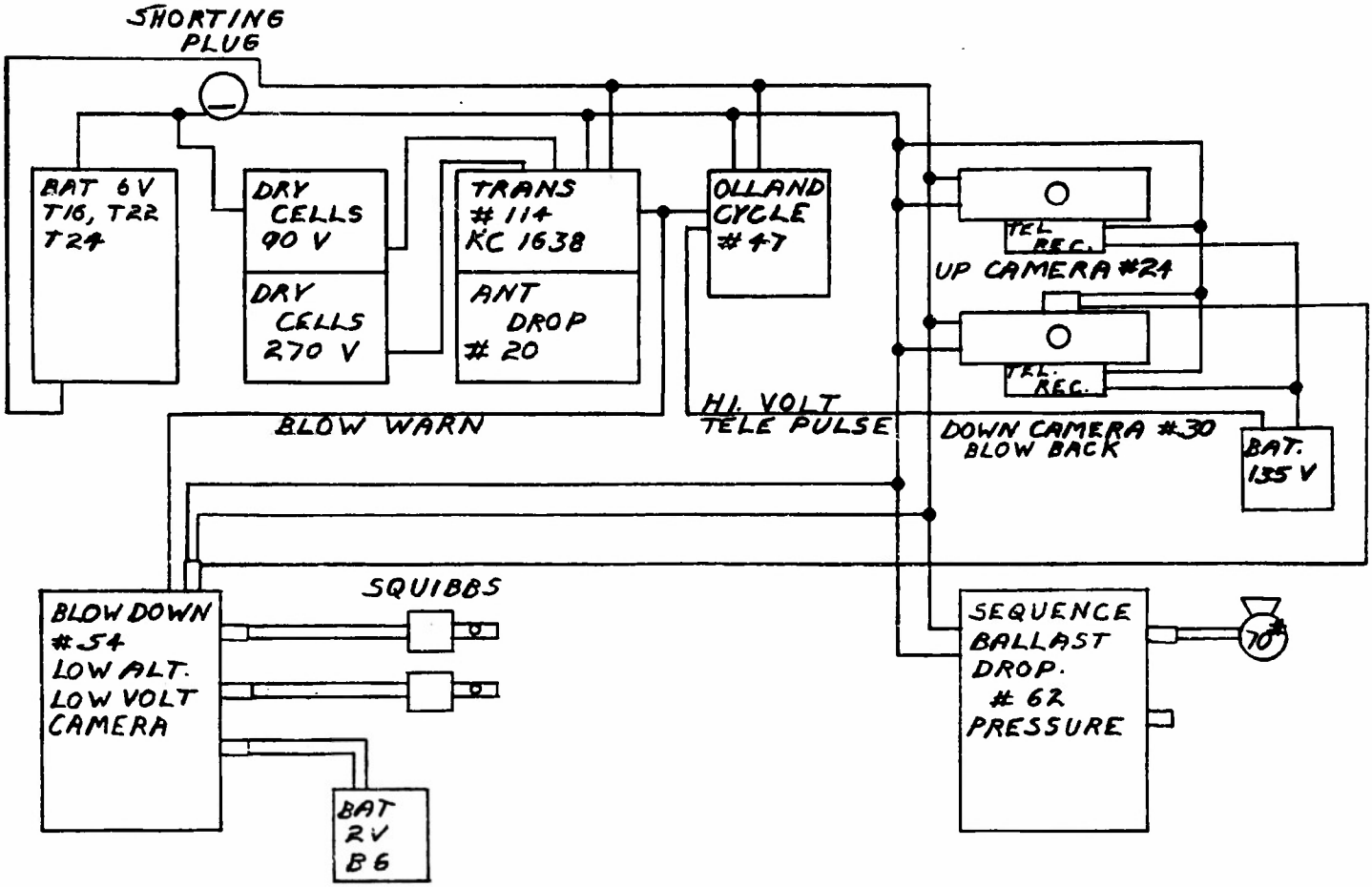

BLINKER # 7

DEPT. OF PHYSICS U. OF MINN.				
BALLOON PROJECT			SECT. INS.	
DWG. NO.	SHOP DWG. NO.	DRAWN BY	CHECKED BY	DATE
		BF	SMG	12-21-52
FLIGHT # 55			MOD. 1	
GONDOLA # 56			MOD. 2	
Confidential Security Information			MOD. 3	
PAGE				

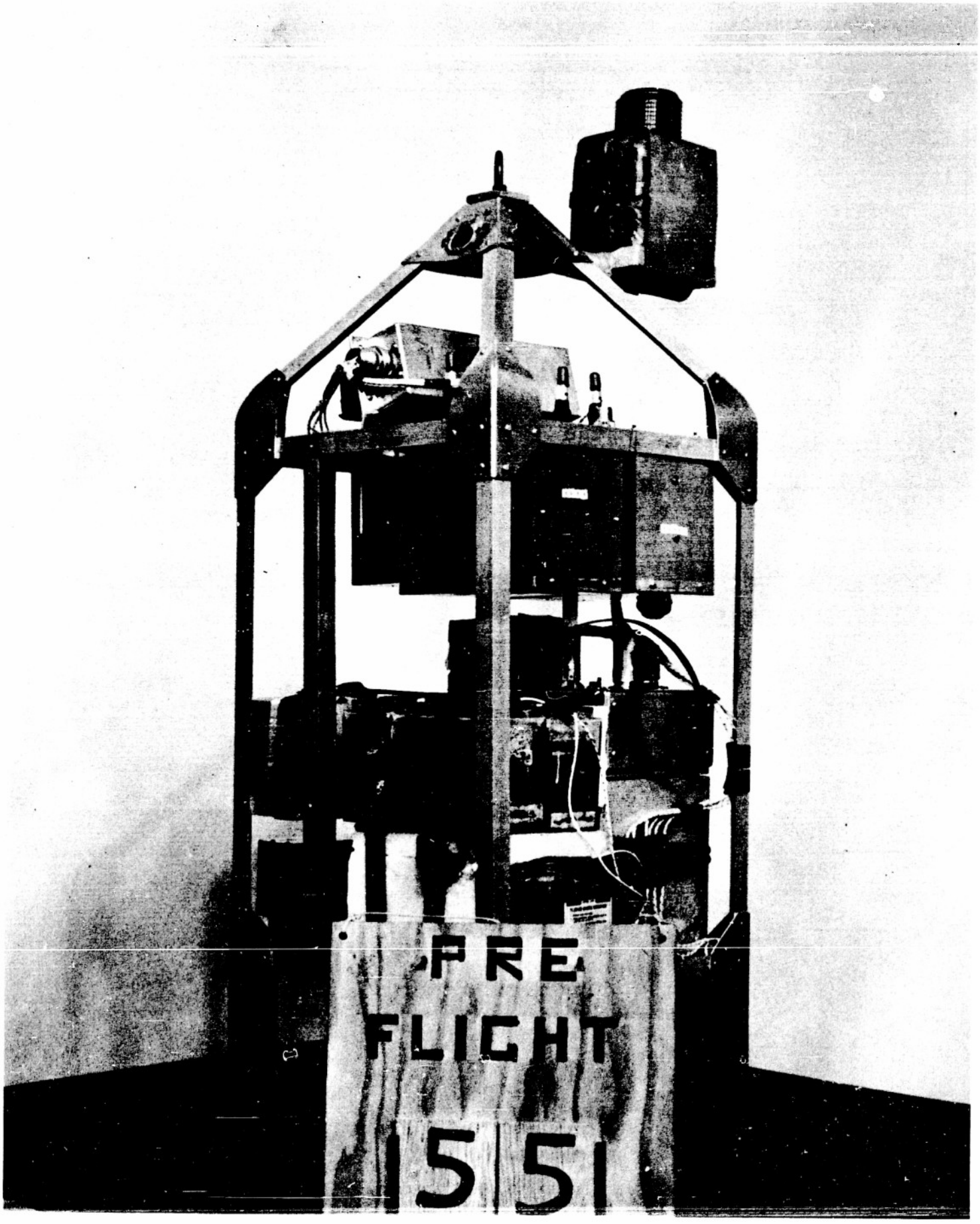
PRE
FLIGHT
1551

SECTION VIII

TELEMETERING

The principal consideration governing the development and design of telemetering equipment and systems has been to make such systems as simple as possible, to reduce the power drain of the flight equipment to a minimum, and yet to retain the flexibility needed for presentation of all the types of data required for the balloon experiments. An effort has been made to develop an efficient, compact beacon transmitter which is stable under varying conditions of temperature, pressure and applied voltages. A summary of the types of data telemetered during this series of flights is given in Figure 1.

A. Sub-Carrier System

This telemetering system was described in Section VI, Volume I, of the first Progress Report. This system of telemetering was used on flights #21 through #25 and #29. The use of this system was discontinued at this time for several reasons:

(a) The transmitters which were used in flight had low power efficiency. The power input to the transmitter was large compared to the amount of power radiated from the antenna. This power inefficiency is characteristic of amplitude-modulated systems.

(b) The audio-frequency of the sub-carrier was 2250 cycles and, therefore, the system as a whole required a band width of at least 4500 cycles. This necessarily meant that the service factor for this sub-carrier telemetering was essentially zero db as compared to radio telephone.

(c) It was decided that all the necessary data which would be telemetered could be carried on a narrow band system with higher power efficiency and a much better service factor.

Information Telemetered

Flight	(1) Olland Cycle Pressure Data	(2) Ballast Level Meter	(3) Command Indication: Ballast Drop Command Ind.	(4) Command Indication: Balloon Valve Command Ind.	(5) Operate Indication: Ballast Drop Operate Ind.	(6) Operate Indication: Balloon Valve Operate Ind.	(7) Flight Termination Warning	(8) Ballast* Unit Ind.
21	X							
22	X	X						
23	X							
24	X							
25	X	X	X				X	
26	X		X		X		X	
27	X		X		X		X	
28	X		X		X		X	
29	X	X		X			X	
30	X						X	
31	X		X	X	X	X	X	X
32	X		X	X	X	X	X	X
33	X						X	
34	X						X	
35	X		X	X	X	X	X	X
36	X						X	
37	X						X	
38	X		X	X	X	X	X	X
39	X		X				X	
40	X		X				X	
41	X		X	X	X	X	X	X
42	X						X	
43	X						X	
44	X						X	
45	X						X	
46	X						X	
47	X						X	
48	X						X	
49	X						X	
50	X						X	
51	X		X	X	X	X	X	X
52	X						X	
53	X						X	
54	X		X	X	X	X	X	X
55	X						X	

*Note: This indication is included in columns' 3 and 5.

SEC. VIII FIG. 1

B. Pulse-Interval System

The types of data which were transmitted by the pulse-interval telemetering system, which replaced the sub-carrier system, were:

(a) Olland Cycle pressure data which is a pulse-interval presentation

(b) Event information which indicates that a certain event has happened or is to happen. The event information was carried by coded symbols such as the standard Morse code for A, B, C or D. The events indicated were such things as package ballast drops, ballastmetered drops, balloon valving or flight termination.

(c) Metric information such as ballast weight in the tank. This metric information was necessarily changed into such a form that the measurement was presented as a space between pulses. In this case, the beacon transmitter was keyed by pulses from the ballast level coder mechanism. These pulses were distinguished from the Olland Cycle pulses by the characteristic frequency shift of the sub-carrier when this system was used or by their repetition rate and pulse length in the pulse-interval system.

In order to set a narrow band width on this system, certain characteristic pulse lengths had to be predetermined. The minimum pulse used in this system is approximately one second and the maximum pulse spacing is less than one minute. Therefore, the band width necessary in the receiving equipment is not greater than two cycles per second. With this bandwidth, the service factor as compared to radio telephone, three kc wide, is at least as great as 17 db. This service factor is that assigned to standard Morse code. The pulse-interval telemetering system was used on all of the flights in this series except those named above for the sub-carrier system.

The ground receiving equipment is an essential part of this telemetering system and special equipment was developed for the purpose of receiving this telemetered information. The receivers (Figures 2-a,b,c) used at present

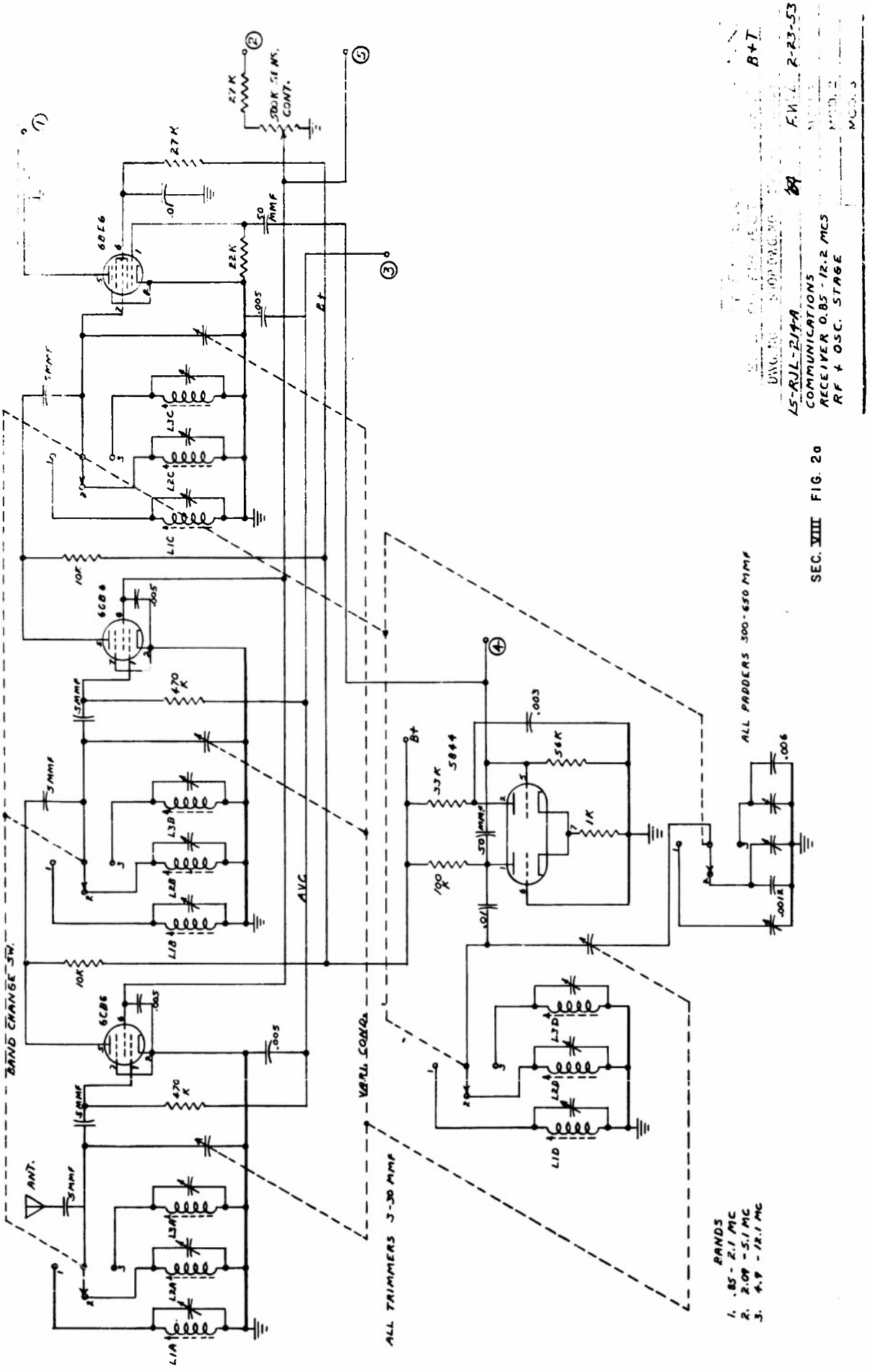
B+T
LS-RJL-214-A
COMMUNICATIONS
RECEIVER 0.85 - 12.2 MCS
RF & OSC. STAGE
F.W. 2-23-53
SEC. VIII FIG. 2a
ALL PADDERS 300-650 MMF
ALL TRIMMERS 3-30 MMF
VARI. COND.
BAND CHANGE SW.
AVC
B+
ANT.
BANDS
1. .85 - 2.1 MC
2. 2.09 - 5.1 MC
3. 4.9 - 12.1 MC

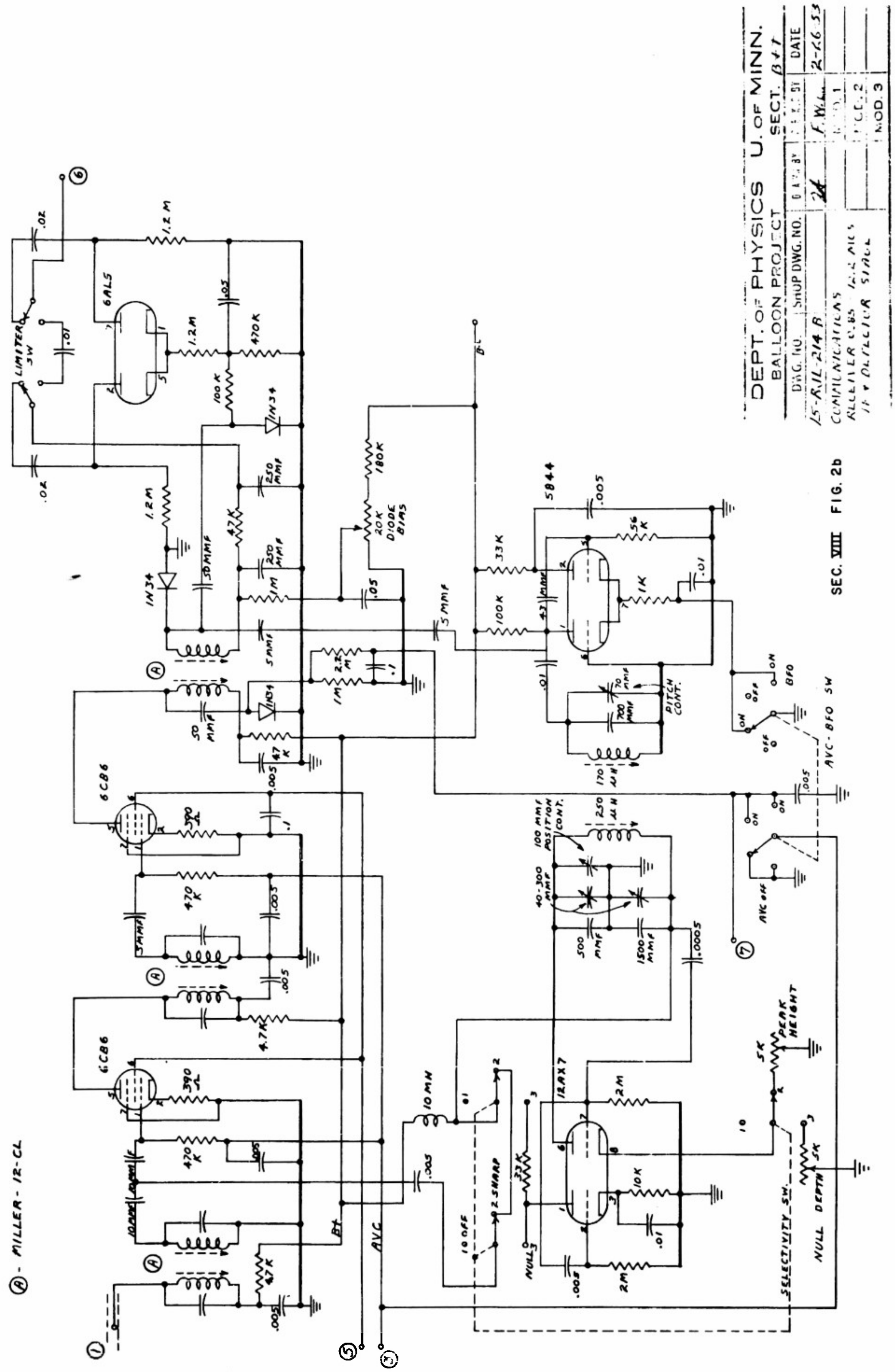

SEC. VIII FIG. 2b

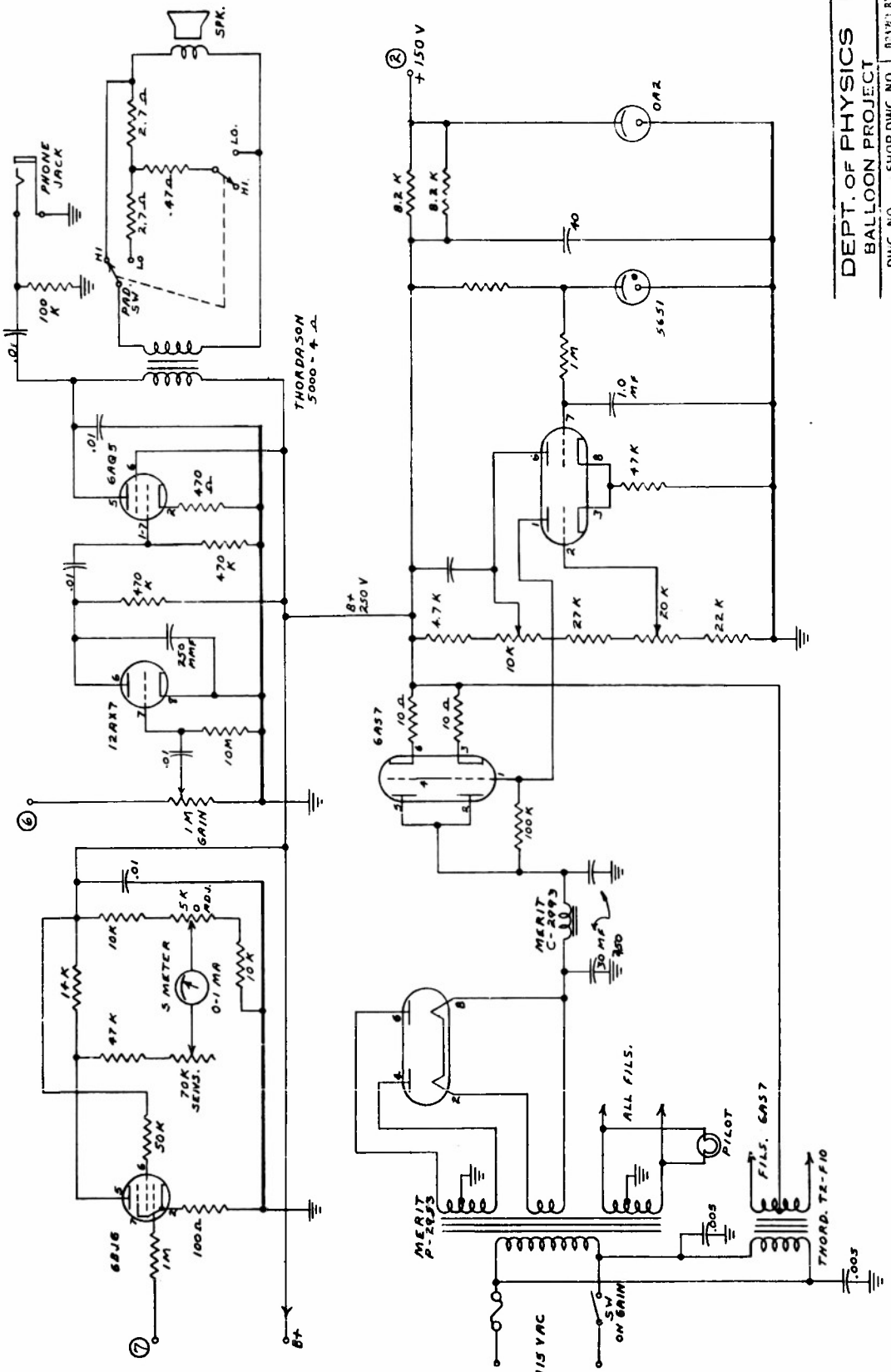
DEPT. OF PHYSICS U. OF MINN.
BALLOON PROJECT
SECT.
DWG. NO. | SHOP DWG. NO. | DRAWN BY | CHECKED BY | DATE
15-RJL-214 C1 | | | L.W.L. | 2-22-53
COMMUNICATIONS
RECEIVER -0.85 - 12.2 MCS
S METER AUDIO STAGE +
POWER SUPPLY
MOD. 1
MOD. 2
MOD. 3
SEC. VIII FIG. 2c
+150 V
8.2 K
8.2 K
.40
6AR
5651
1M
1.0 MF
47K
4.7K
10K
27K
20K
22K
8+ 250 V
6AS7
10Ω
10Ω
100K
MERIT C-2093
30 MF 350
ALL FILS.
PILOT
FILS. 6AS7
THORD. TZ-F10
.005
.005
115 VAC
SW ON GAIN
MERIT P-2093
THORDARSON S000-4-A
SPK.
PHONE JACK
100 K
.01
PAD SW
HI
LO
2.7Ω
.47Ω
2.7Ω
LO.
HI.
6AQ5
470 Ω
470 K
470 K
250 MMF
12AX7
10M
1M GAIN
6BJ6
50K
100Ω
1M
5K POT.
10K
14K
47K
70K SENS.
S METER
0-1 MA
10K

were developed and constructed in our shops and have several special features such as an electronic boost-null circuit in the intermediate frequency amplifier, which allows the operator to select the desired signal with ease and furnishes a large amount of rejection to unwanted signals. The receiver also features a diode clipper which allows the operator to cut out low level noise and obtain a better presentation of the data on the recorder and a noise limiter to clip sharp noise impulses. The receiver also contains a well regulated power supply which tends to prevent drift of oscillators and changes in gain and allows the boost-null circuit to remain on a fixed frequency. This is especially important in receiver design for narrow band work.

Another unit which is used with this telemetering system is a tunable audio amplifier (Figure 3). This unit contains a frequency selective filter which is entirely electronic and uses RC networks to obtain the desired filtering. This unit can be adjusted to almost the point of oscillation on a chosen frequency so that the selectivity is extremely great. The output of the frequency selective filter goes through a clipper circuit which is essentially a go, no-go amplitude discrimminator. This circuit is designed so that when the applied audio signal exceeds a predetermined level the gain at the amplifier is increased, resulting in a cumulative build-up to saturation level. This allows the presentation of the telemetered data in a much clearer form than would otherwise be possible. The final circuit in this amplifier is a direct coupled power amplifier which has been designed to operate the recorder system. The power amplifier also is provided with an external input to the second grid which allows other information to be fed in simultaneously with the telemetered data. This is used in some cases to put in timer marks or other such data.

C. Transmitters

All transmitters used in this series of flights were designed to operate over the medium frequency band which includes our assigned frequencies 1638, 1676, 1724 and 1746 kc. All of the transmitters were crystal controlled in order

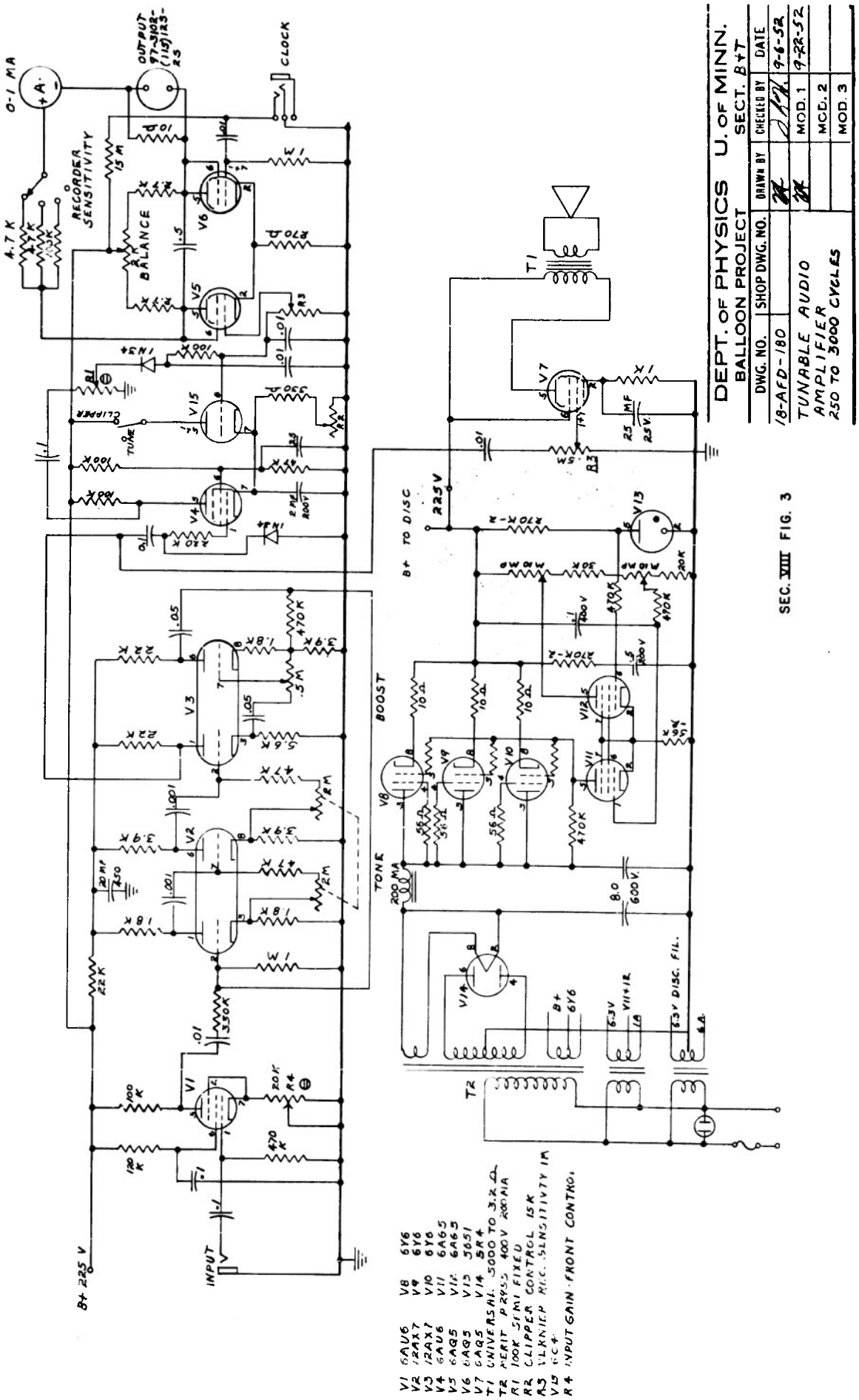
DEPT. OF PHYSICS U. OF MINN.
BALLOON PROJECT
SECT. B+T
DWG. NO. 18-AFD-180
SHOP DWG. NO.
DRAWN BY
CHECKED BY
DATE 9-6-52
MOD. 1 9-22-52
MOD. 2
MOD. 3
TUNABLE AUDIO AMPLIFIER 250 TO 3000 CYCLES
SEC. VIII FIG. 3
0-1 MA
OUTPUT 97-3102-(115)123-25
CLOCK
RECORDER SENSITIVITY
BALANCE
4.7 K
CLIPPER
TUNE
INPUT
B+ 225 V
B+ TO DISC
BOOST
TONE
T1
T2
V1 6AU6
V2 12AX7
V3 12AX7
V4 6AU6
V5 6AQ5
V6 6AQ5
V7 6AQ5
V8 6Y6
V9 6Y6
V10 6Y6
V11 6A65
V12 6A65
V13 3651
V14 5R4
T1 UNIVERSAL 3000 TO 3.2 Ω
T2 MERIT PR955 400 V 200 MA
R1 100K SEMI FIXED
R2 CLIPPER CONTROL 15K
R3 VERNIER REC. SENSITIVITY 1M
V15 6C4
R4 INPUT GAIN FRONT CONTROL

to achieve the stability necessary for narrow band telemetering. Crystal control is necessary to compensate for the large temperature and supply voltage changes encountered in balloon flights.

The transmitter used for the sub-carrier system which was described in the first report (Volume I, Section VI) is shown in Figure 4. This transmitter was used for the flights mentioned in the sub-carrier section.

The next transmitter (Figure 5) to be used was a transition model from the sub-carrier system to the pulse transmitter. It features high-and-low-power transmission with an associated frequency shift (LOFAM). The frequency shift and power change is obtained by shifting the cathode feed-back resistors. This transmitter was used for flights #26, #27, #28, #30, #31, #32, and #33. The power output was 5 W on maximum and approximately ½ W on minimum power. The telemetering decoding system used with this transmitter was the same equipment as used with the sub-carrier system. There was continuous power drain from the B supply and the total power efficiency was lower than desired.

The next transmitter (Figure 6) in the series was a high-low power transmitter. The idea behind the low power between pulses was that this was necessary for direction finding. However, it was found to be unsuitable because the low power signal was too weak to obtain good df bearings at long range. It was difficult to obtain a steady zero on the recorder, especially when the transmitter was at short range due to fading of the low power signal. This transmitter also put a continuous power drain on the battery supply and its power efficiency was again low. This transmitter was used on flights #34 through #45. Its power output was 4 W on maximum and approximately ½ W on minimum. The tunable audio amplifier (Figure 3) was used in the telemetering recording equipment starting with flight #34.

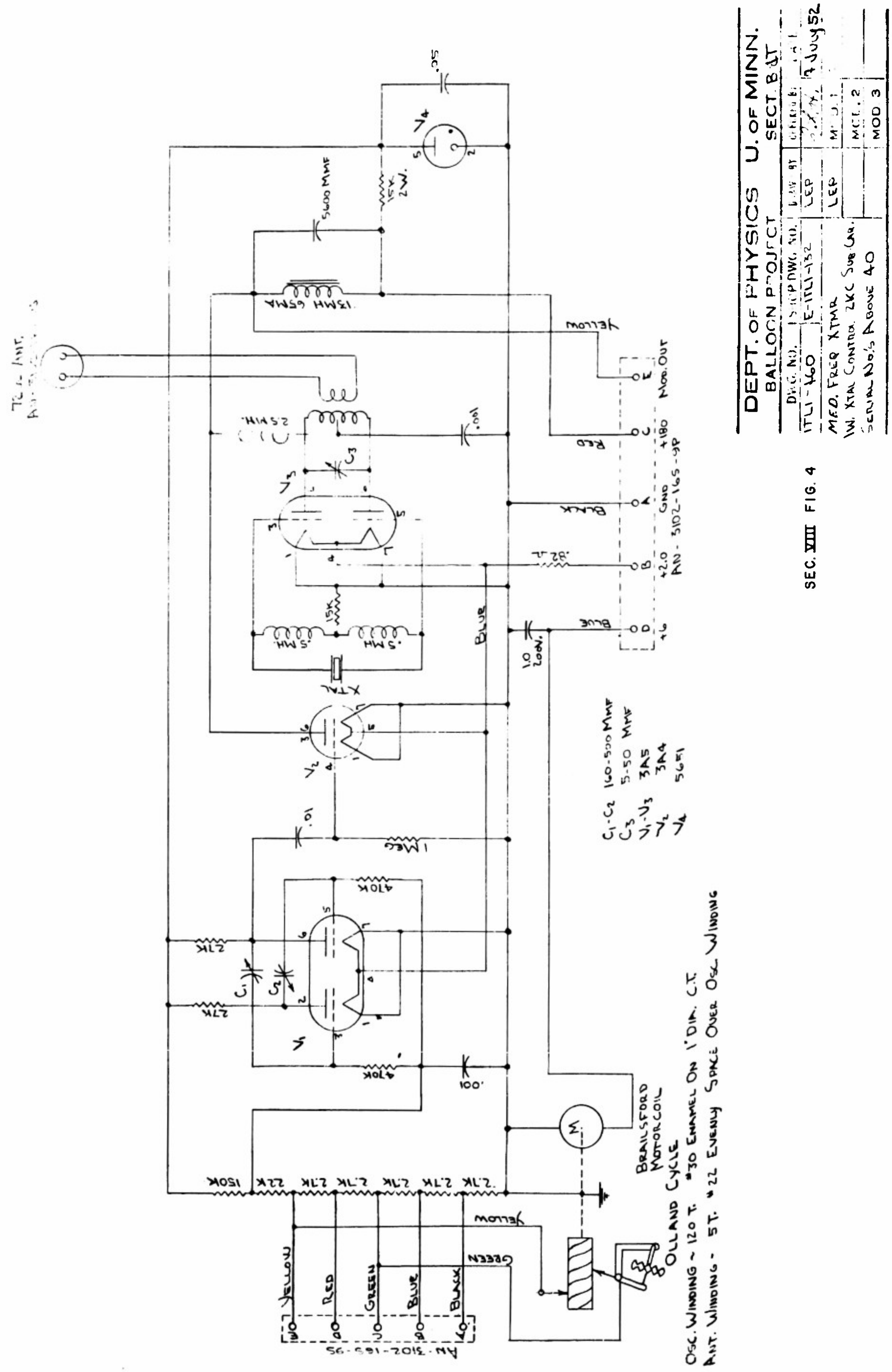

SEC. VIII FIG. 4

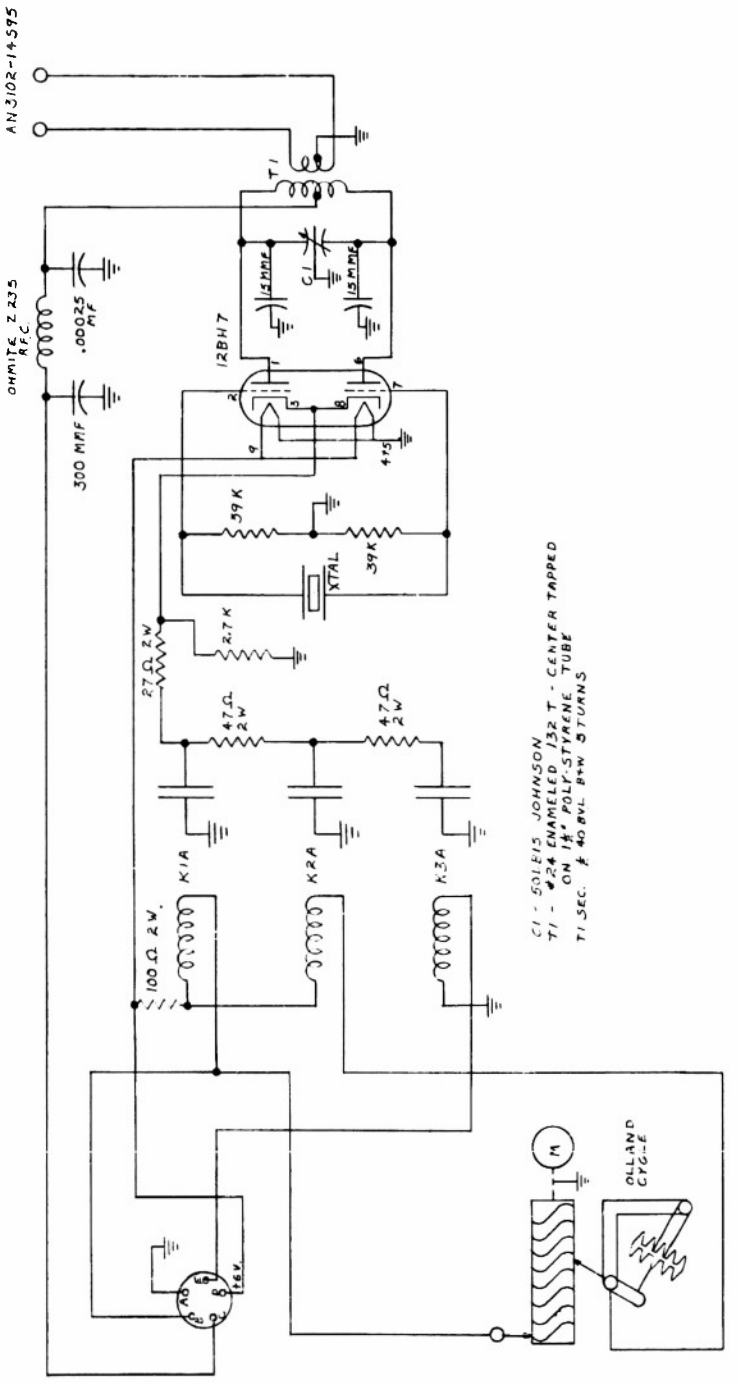

SEC. VIII FIG. 5

DEPT. OF PHYSICS U. OF MINN. BALLOON PROJECT			SECT. 8 Y 7
DWG. NO.	SHOP DWG. NO.	DRAWN BY	CHECKED BY	DATE
26-TL-170			R-L-H	8-9-52
MED. FREQ TRANSMITTER SERIAL OVER 60			MOD. 1	
			MOD. 2	
			MOD. 3	

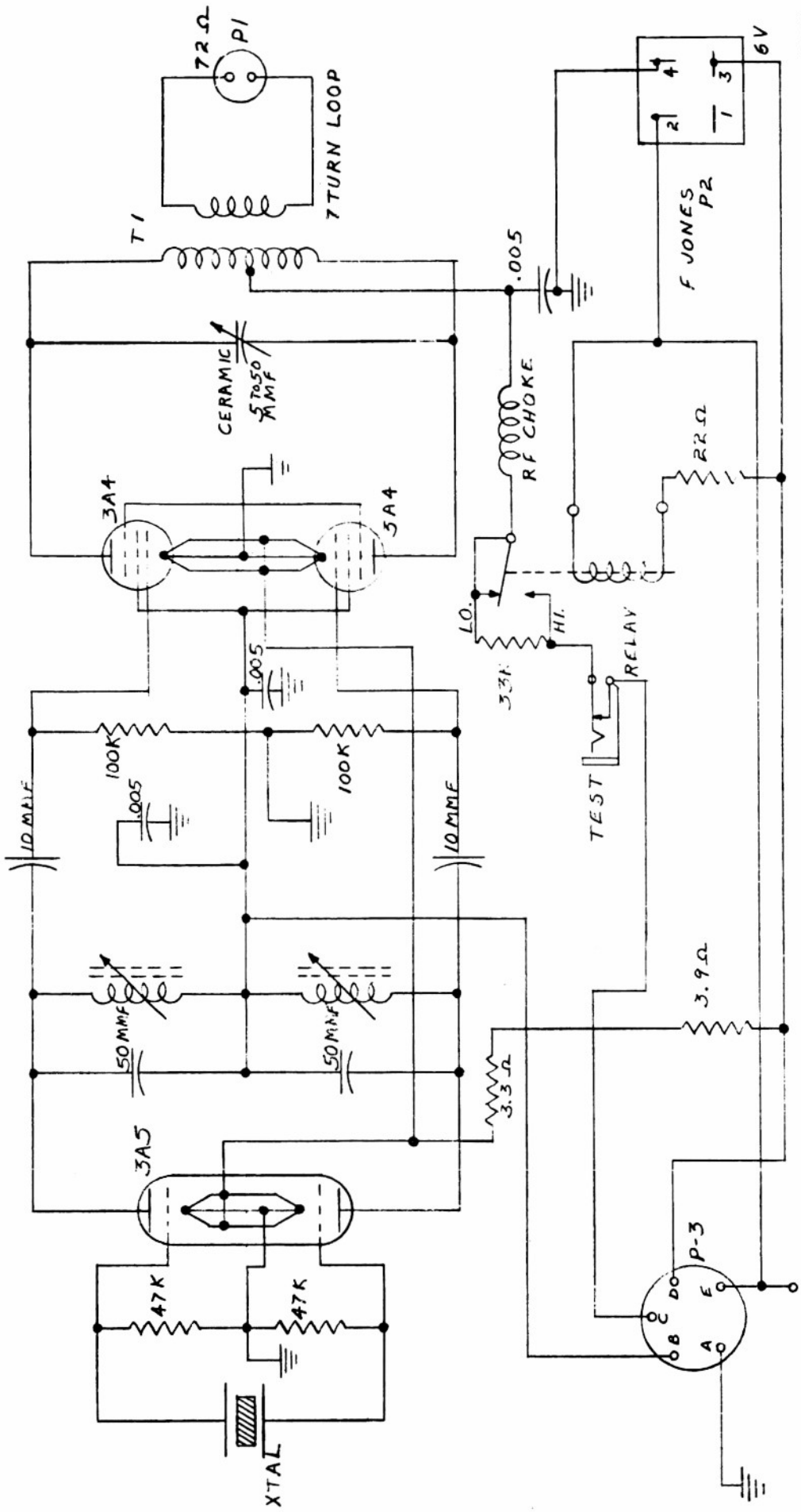

SEC. VIII FIG. 6

A pulse transmitter (Figure 7) with screen-grid keying was the next used in this series. This transmitter had a very low power output, a matter of a few milliwatts, except when pulsed. However, the power drain for the oscillator was continuous and this was an unnecessary power waste. This type of transmitter was used for flights #46 and #47. Its pulsed output was approximately 4 W.

The next transmitter was a pulse transmitter in which the negative terminal of the B supply was keyed (Figures 6, 9-a,b). This transmitter had no continous power drain from the B supply and therefore the power supply necessary for operation was reduced. It was found by laboratory experiments that the push-pull oscillator started reliably in extreme cold and with a very low battery supply. The filament supply used was a lead acid battery which does not drop in voltage appreciable before all of the available power is used. However, the dry cell batteries used for the B supply do show appreciable drop with use and with cold. The B battery supply for 24 hours operation weighs about five pounds. This type of transmitter was used for flights #48 through #55. Its power output was approximately 4 W.

The antennas used with these transmitters were of the Zepplin type in all of the flights of this series. This antenna is preferred as it is of the end-fed variety which permits the transmitter to be located in the gondola. The antenna is released by a dropper after launching. The antenna used for the first group of flights in this series consisted of a twisted pair of wires cut to approximately 1/4 wave at the frequency of the transmitter and a half-wave single wire antenna. This antenna was found* to have a severe power loss measured to be at least 20 db. At the time of this measurement, investigations were made into the properties of Zepplin antennas. It was shown by laboratory measurements that the twisted pair feed line had high attenuation at this frequency and had a characteristic impedance of around 70 ohms. This low impedance

*by General Mills, Inc.

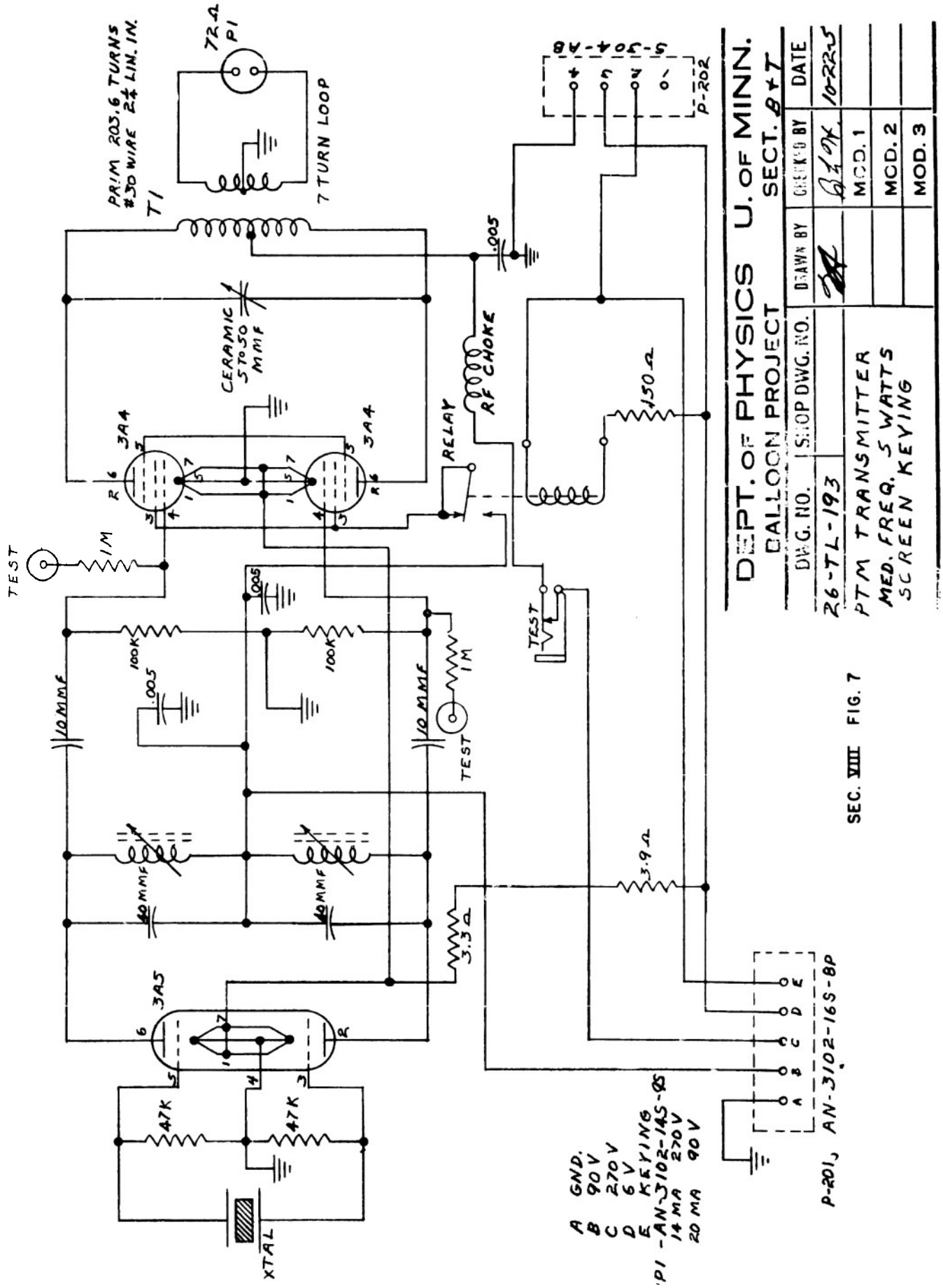

SEC. VIII FIG. 7

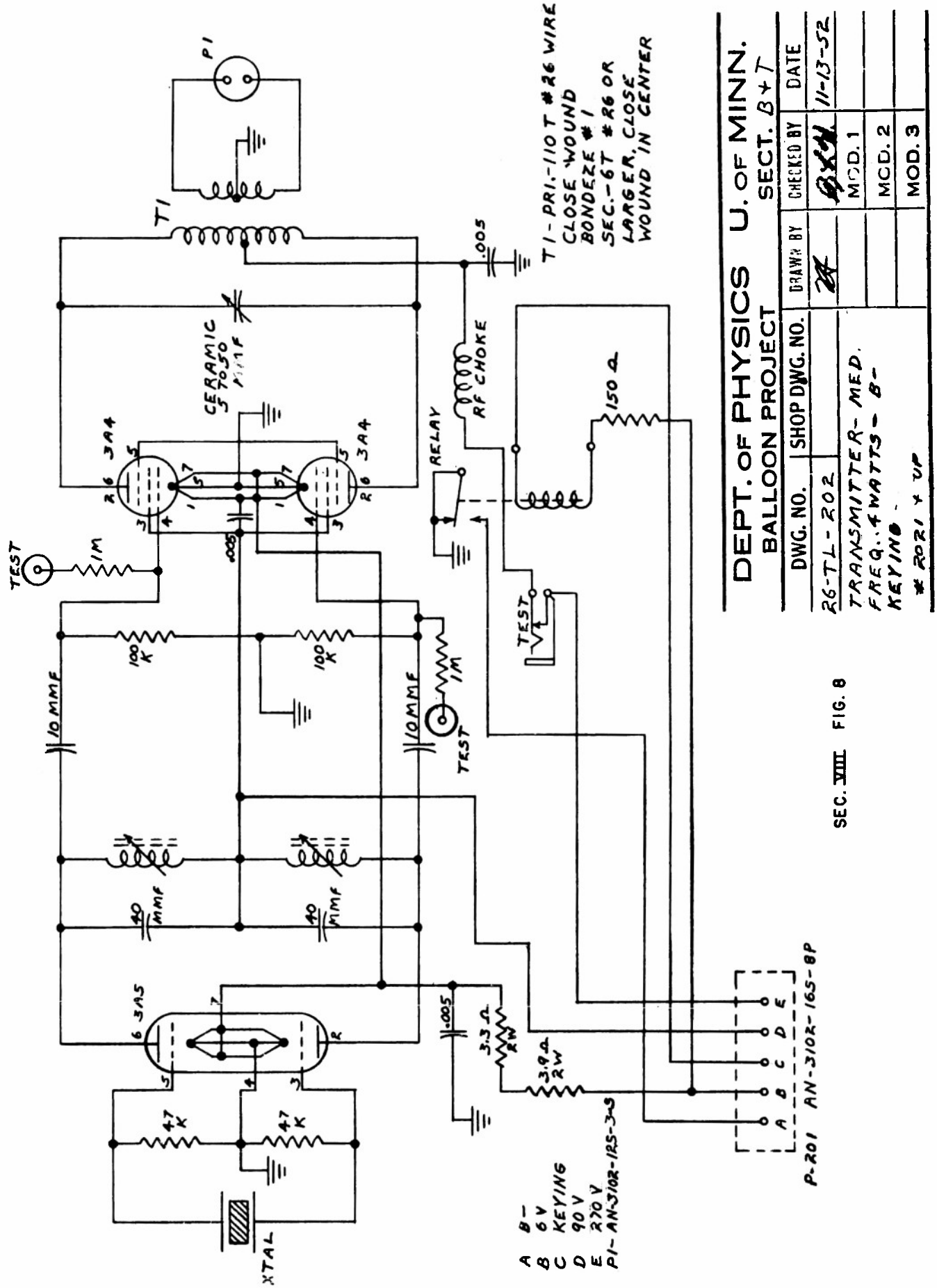

DEPT. of PHYSICS U. of MINN.
BALLOON PROJECT
SECT. B+T

DWG. NO.	SHOP DWG. NO.	DRAWN BY	CHECKED BY	DATE
26-TL-202				11-13-52
TRANSMITTER- MED. FREQ. 4 WATTS - B- KEYING -			MOD. 1	
* R201 + UP			MOD. 2	
			MOD. 3	

SEC. VIII FIG. 8

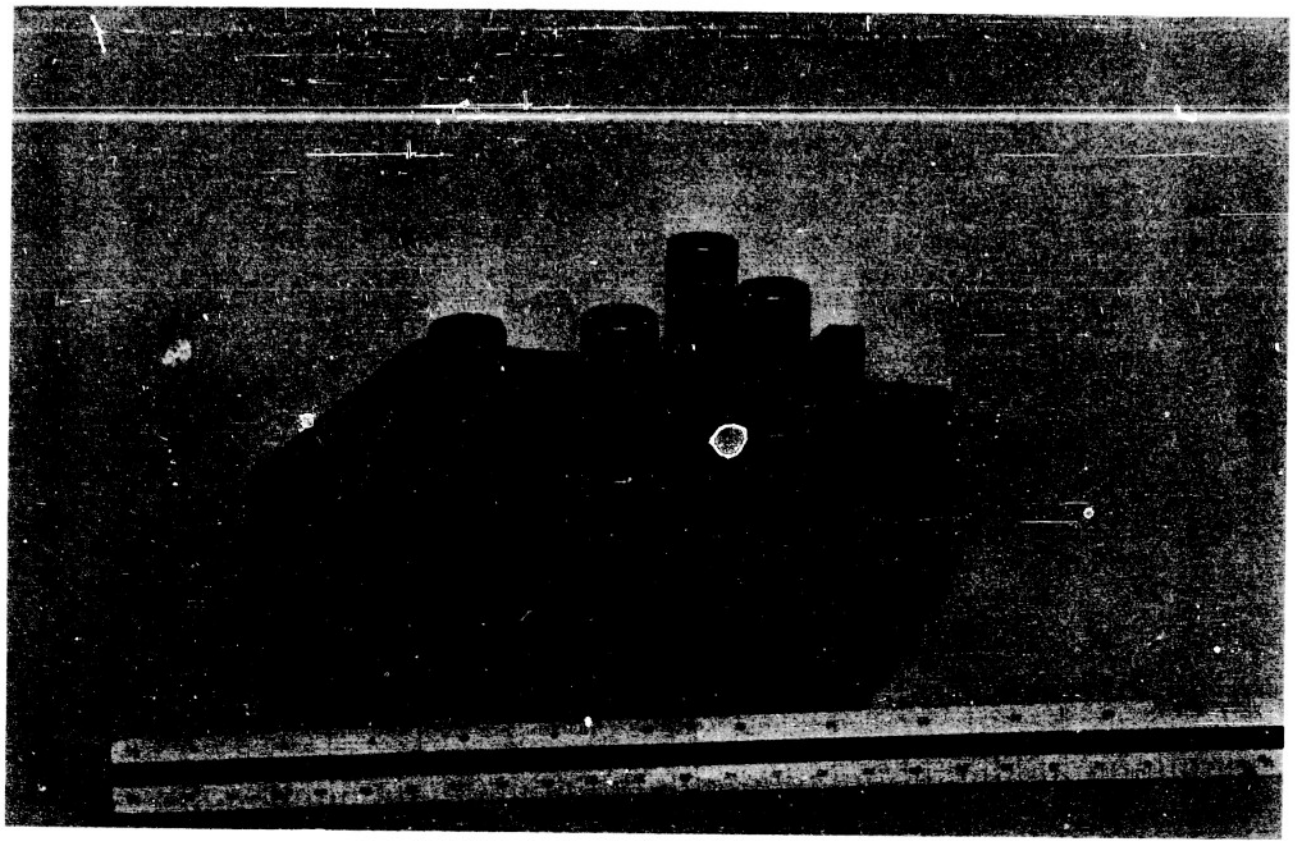

A. Top and side view.

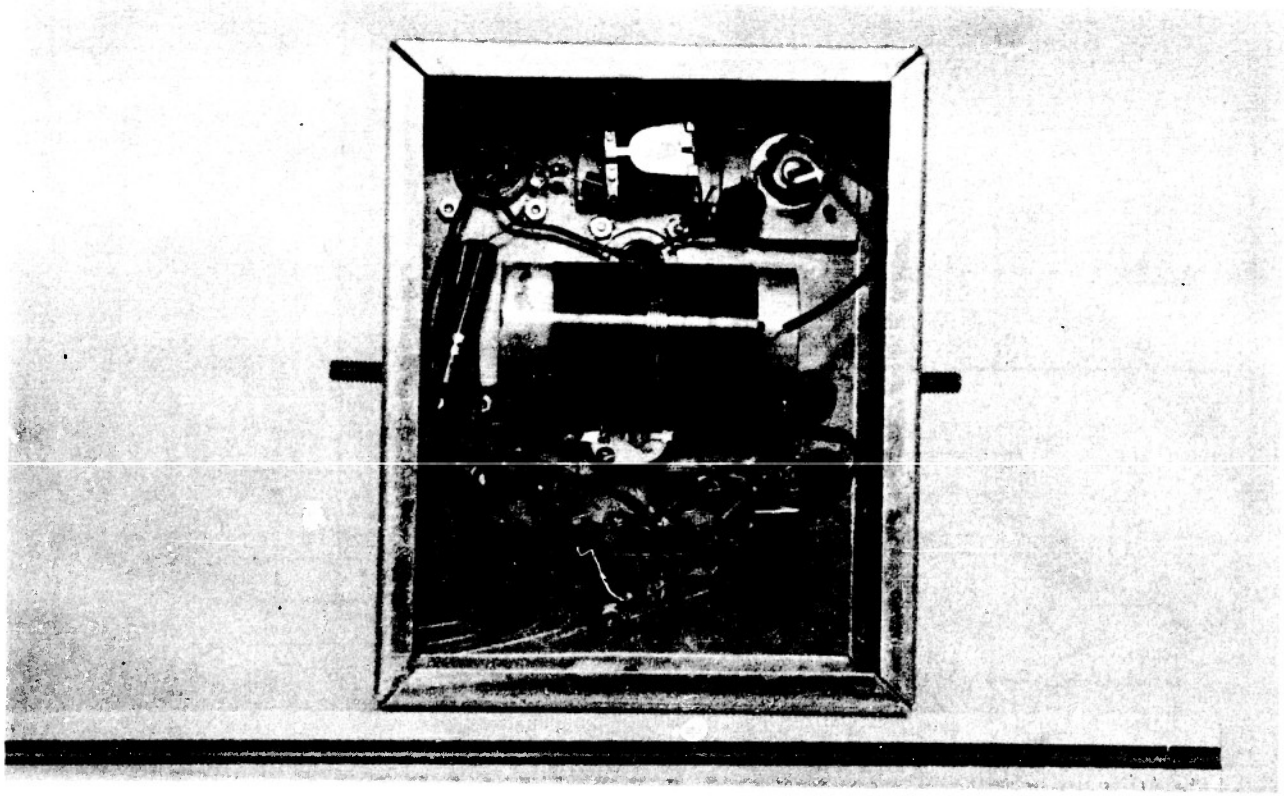

Sec VIII Fig 9. B. Bottom view. Medium frequency, 4 watt, pulse transmitter.

again contributed to the loss in this type of feed system as there was a high degree of mismatch. The type of antenna adopted from these experiments uses a transmission line of Columbia ATV-300R, 300 ohm twin lead. Careful measurements were made of its characteristics on the Q meter in the laboratory. It was found that the length which was necessary for the Zepplin transmission line was 27.6 meters for 1746 kc and 29.5 meters for 1638 kc. The radiating portion of the antenna is cut approximately 5% short of a half wave length to compensate for end effects. If we assume that the transmission line from the transmitter output to the antenna is feeding a 2400 ohm load, which is a good approximation for a half wave end-fed antenna, we find that the input impedance at 1700 kc is about 41.8 ohms. Therefore, the output transformer of the transmitter was designed to feed maximum power into an impedance of this value. For a theoretical lossless transmission line the input impedance would, in the same case, be 35.3 ohms. From these figures we can calculate the loss in this quarter wave transmission line to be equal to 0.735 db. This loss is rather insignificant and these antennas have been shown by use in flights to be efficient radiators. The transmitter performance has been as good as would be predicted for the power output since the use of this type of antenna was initiated.

D. Radio Propagation Predictions

As there are always considerable difficulties in telemetering from long range with low power transmitters, it was felt to be necessary to make a study of radio propagation. This work was carried on for several purposes. The radio propagation predictions can give the frequencies which are desirable for telemetering at the expected ranges. The predictions will also give a reasonable estimate of the required radiated power for the expected flight trajectory and allow equipment to be designed for use in these flights. They will also furnish data for determining the optimum launching time from a given place to obtain the best telemetering performance with a given transmitter freq-

quency and power output.

The radio predictions were based on the CRPL series D publications issued by the National Bureau of Standards. The methods used are described in Circular 462, US Department of Commerce, National Bureau of Standards. The following factors were considered in this work on radio propagation prediction:

(a) The atmospheric noise level at the receiving station

(b) The receiver noise

(c) Receiving antenna characteristics

(d) Predicted method of propagation based on distance and local time and the monthly ionospheric predictions (series D publications).

(e) The non-deviative absorption factor. This absorption occurs mostly in the D layer in daylight and is a function of the zenith angle of the sun, the time of year, and the number of sunspots. This absorption is at best a median value for a month and the absorption for any one day is very unpredictable.

(f) In flights where the great circle path from the balloon to the receiving station is through the auroral zone, the auroral attenuation factors are considered. The auroral attenuation is extremely large, especially at frequencies in the 2 mc range.

(g) The balloon altitude is a factor to be considered when calculating the line of sight range. The angle of incidence of radiation from the balloon transmitter on the ionosphere is less than would be calculated for a ground station at the same distance from the receiver. This effect can be approximated by assuming that the transmitter is located on the ground at a distance along the radius from the receiver equal to the geometrical line of sight. The balloon altitude is important only in determining the method of radio wave propagation and has little effect on the attenuation factors involved.

It is difficult to assign any definite degree of accuracy to these predictions as they are based on a large number of roughly predictable factors. According to Circular 462, Page 116, National Bureau of Standards, the value calculated for incident field intensity from a transmitter with a given power radiated is the median value for normal days of the month. These monthly median values are the ones used for computing the following prediction chart (Figure 10). The monthly median values are such that on 90% of the days of the month, the signal strength on a daily average will be greater than -6db and on 90% of the days the signal strength on a daily average will be less than + 6 db of the monthly median value.

We also encounter normal fading* of radio signals which is due to fluctuations of the ionsphere. As a result of this fading the instantaneous values of field intensity will be such that 90% of the time the signal strength is greater than -8.2 db and 90% of the time less than 5.1 db from the median daily value. Therefore the field intensity which the lowest instantaneous value of signal strength exceeds on 90% of the days of the month are found by taking the median monthly value times .195 (-14.2 db). Therefore on at least 90% of the days of the month it would be necessary to radiate at least 14 decibels above the predicted value of required effective radiated power in order to obtain a fixed value of field strength at the receiving antenna.

Another factor of importance in these predictions is the atmospheric noise which, of course, varies from time to time in a seemingly random fashion. This noise value, however, does vary with the season of the year and the transmission of this noise from the noise centers of the world, which are usually atmospheric storm centers, varies in the same manner as the transmission of any other electromagnetic radiation. Therefore atmospheric noise is much more important at night than in daytime as the attenuation is less at night.

*Pp 107-109, Circular 462, National Bureau of Standards

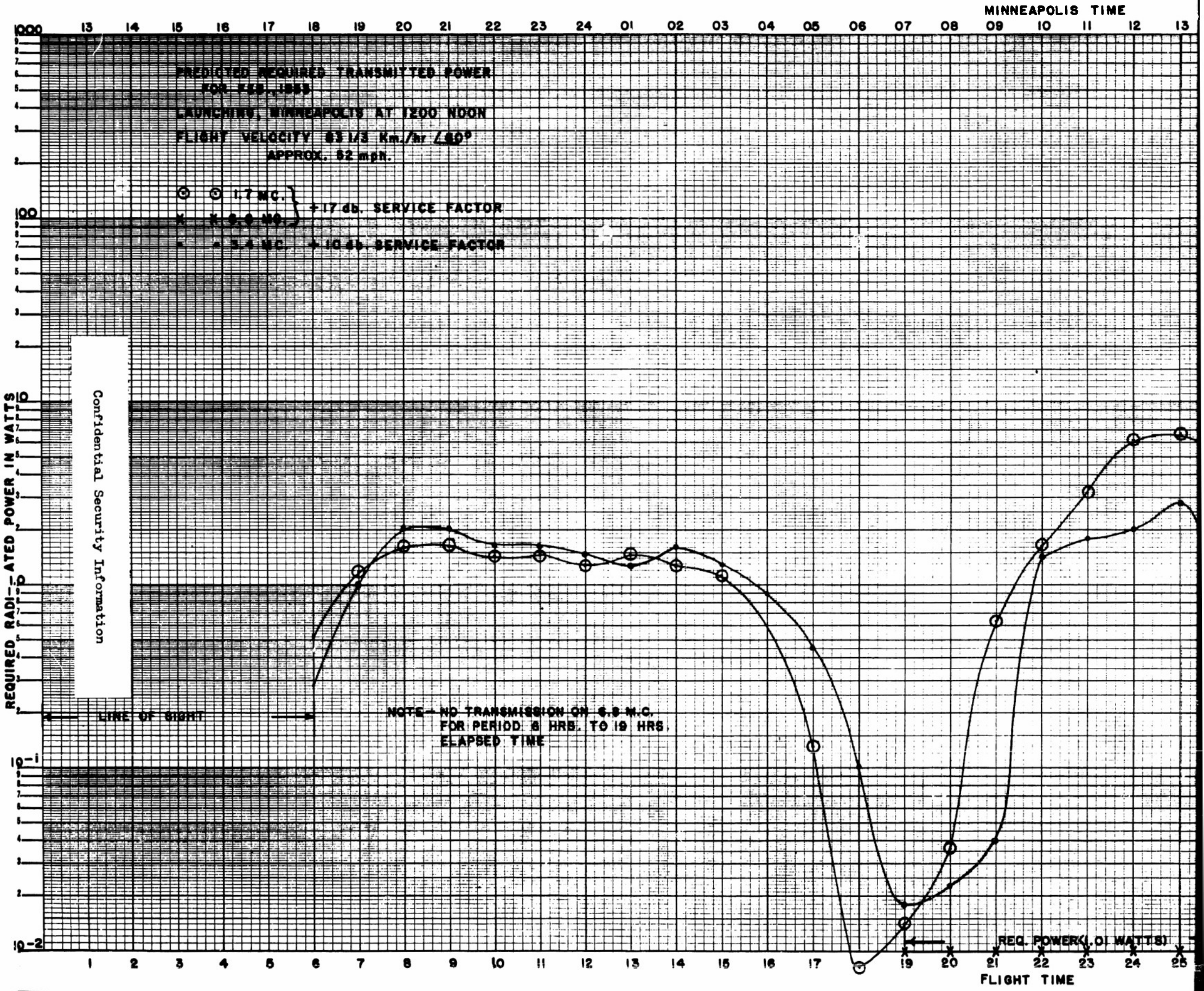
MINNEAPOLIS TIME
13 14 15 16 17 18 19 20 21 22 23 24 01 02 03 04 05 06 07 08 09 10 11 12 13
PREDICTED REQUIRED TRANSMITTED POWER
FOR FEB., 1955
LAUNCHING, MINNEAPOLIS AT 1200 NOON
FLIGHT VELOCITY 83 1/3 Km./hr ∠60°
APPROX. 52 mph.
⊙ ⊙ 1.7 MC. } +17 db. SERVICE FACTOR
× × 3.0 MC. }
• • 5.4 MC. +10 db. SERVICE FACTOR
REQUIRED RADIATED POWER IN WATTS
Confidential Security Information
LINE OF SIGHT
NOTE— NO TRANSMISSION ON 6.8 M.C.
FOR PERIOD 6 HRS. TO 19 HRS.
ELAPSED TIME
REQ. POWER(1.0 WATTS)
1 2 3 4 5 6 7 8 9 10 11 12 13 14 15 16 17 19 20 21 22 23 24 25
FLIGHT TIME

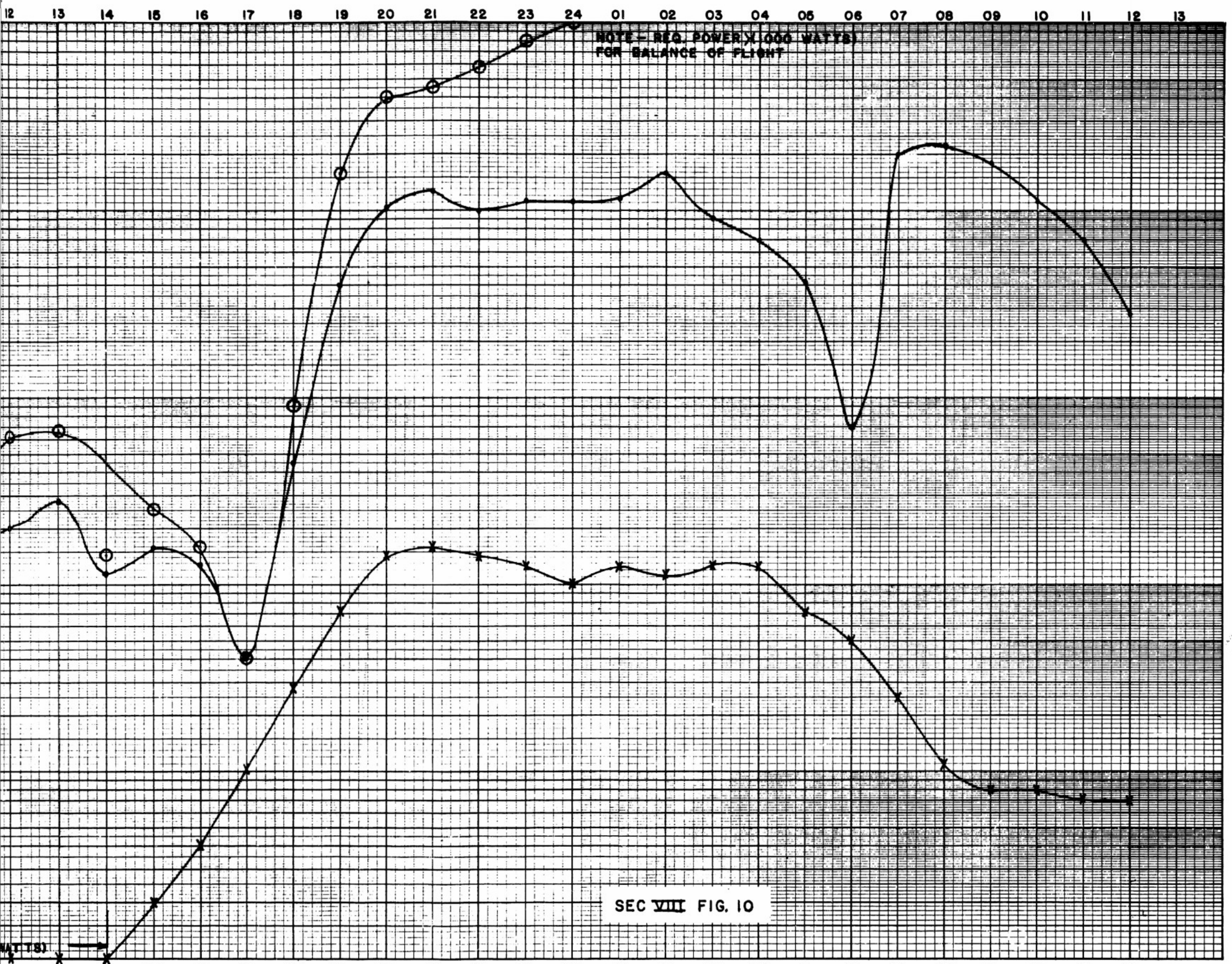

SEC VIII FIG. 10

A study made by the Central Radio Propagation Laboratory shows that 80% of the daily values for field intensity required to read a signal through atmospheric noise fall within a range of ∓ 6 db of the median values predicted. Therefore 6 db must be added to the figure given above of 14 db in order to insure radio communication or telemetering for at least 90% of the time. Consequently a transmission power of +20 db or 100 times the predicted median monthly value should be used.

An hour by hour prediction (Figure 10) of the median, required, effective radiated power for three frequencies and two types of radio communication (telemetering and audio frequency command) was made for an assumed flight trajectory during the month of February, 1953. The flight trajectory assumed was a reasonable value for winter months in this vicinity. The values given in this prediction chart are hourly median values based on the montly prediction for February 1953. The prediction data shows that the 1.7 mc band is useful, with moderate transmitter power, for approximately the first 24 hours of the flight. After the second sunrise this frequency should not be useful. This prediction was correlated by two flights in January in which a readable signal was received at the Minneapolis station continuously the first day and night in this frequency band and in which the signal faded below a useful intensity after sunrise on the following day. No data on performance of the 6800 kc band are available as yet although the plan is to fly transmitters on this frequency and to attempt a correlation between the radio performance and the predicted performance. Acccrding to the predictions a frequency in the 6-7 mc band should be useful for intermediate length flights for high balloon velocities such as 50 m/h. The radio propagation predictions do not indicate the amount of power necessary to read telemetered signals through interfering transmissions. The experience with the 1.7 mc band has shown that all of the assigned frequencies are subject to considerable radio interference, such as police network stations which interfere

with telemetering reception at night. There have been few cases of interference in daytime, but the night-time interference presents a serious problem when the balloon is at long range. With the narrow band system in use at present it is often possible to read the telemetered signal through voice transmissions and other interfering signals if the exact frequency of the interfering transmitter is as great as 200 cycles/sec from the telemetering transmitter.

RADIO COMMAND

A. Command Systems

Radio control of operation of various devices was used in a large number of flights in this series. In all of the command systems used in this series of flights resonant relays were used for the audio-selective filters and as elements in the control circuits. Our experience with the resonant relays has shown that the initial rejection of relays as received from the manufacturer is up to 50% and that of the remaining 50% a large amount of choosing is necessary to find relays which have high reliability. In many cases, equipment is operated for several hours and then the relays suddenly develop a condition in which they will no longer reliably operate the command system. The resonant relays are, in theory, an excellent method of obtaining extremely narrow band audio selectivity. The main difficulty lies in the mechanical unreliability of the existing relays. Radio control was used during this series of flights for operating the following:

(a) Ballast drop, both magnetic control of flow from a tank and package drop.

(b) Gas valving, with and without automatic cycling.

(c) Flight termination. A summary of radio command operation is shown in Figure 11.

One of the command control circuits used during this series of flights consisted of a resonant relay with a thermal-element time delay (Figure 12). The resonant relay controlled a small three-volt sensitive relay which in turn operated a 10-second time delay relay which operated the equipment commanded. This 10-second time delay was thought to be necessary to insure safety of the equipment against accidental operation. In this type of resonant relay control circuit, the command signal initiated a returning signal on the telemetering channel which indicated that command had been obtained on the control

Command Operations used in Flights

Flights	Magnetic Ballast Drop	Unit Ballast Drop	Balloon Valve	Direct Flight Termination	Sequence Flight Termination
22	X			X	
23		X		X	
24		X		X	
25	X			X	
26		X		X	
27		X		X	
28		X		X	
29	X		X		
31		X	X		X
32		X	X		X
35		X	X		X
38		X	X		X
39		X			
40		X			
41		X	X		X
51		X	X		X
54		X	X		X

SEC VIII FIG. II

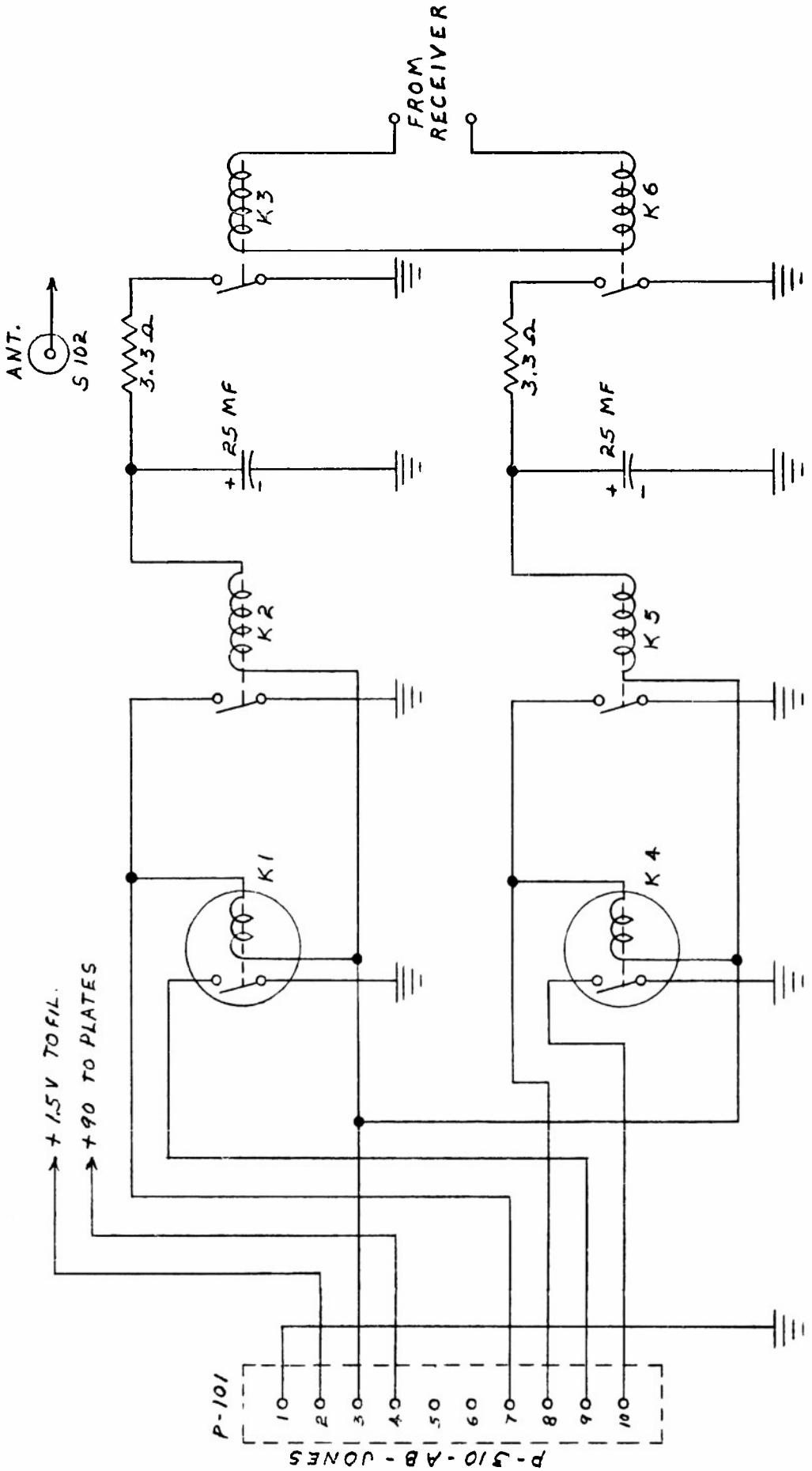

K1 TIME DELAY RELAY # 1 AMPERITE 6NO1OT
K2 OPERATING RELAY # 1
K3 RES. RELAY 210 CPS
K4 TIME DELAY RELAY # 2
K5 OPERATING RELAY # 2
K6 RES. RELAY 232 CPS

DEPT. OF PHYSICS U. OF MINN.
BALLOON PROJECT SECT. B+T

DWG. NO.	SHOP DWG. NO.	DRAWN BY	CHECKED BY	DATE
9-RF-183			BXK	9-15-52

COMMAND RECEIVING EQUIP
RES, RELAY CONT CKTS.

MOD. 1
MOD. 2
MOD. 3

SEC. VIII FIG. 12

channel in question. This indication of command was actuated by the closing of the three-volt relay. After the time delay had occurred, a different coded signal was telemetered to show that the commanded circuit had operated.

The second type of control circuit is shown in Figure 13. This unit used a resonant relay audio filter to actuate an amplifier tube-heater time delay. This unit consumed less power than the above control circuit and was found to be more reliable in operation and to require less adjustment. The time delay associated with this circuit was less than the 10-second time delay of the other circuit. It was found that with a time delay of 2 or 3 seconds the security of the operation was sufficient.

The command receiver antenna consisted of an 11-meter length of flexible wire which was attached to the balloon prior to packing. This antenna was connected to receiver at the time of launching. Two major types of command receivers were used during this series of flights. The first type was described in detail in the first report (Volume I, Section VI). The two receivers of this general type are shown in Figures 14, 15.

This type of receiver was flown in most of the command flights. The results of these operations showed that a strong signal in the vicinity of the command frequency, 6420 kc was capable of blocking this receiver. Subsequent laboratory measurements showed that it had rather poor selectivity ahead of the first RF amplifier and that it could be easily blocked by strong signals close to the operating frequency. A review of the radio command flights of this series shows that, in two flights (#35 and #41) the radio command operation was not completely successful due to inadequate radio frequency selectivity and resultant receiver blocking. In both of these flights the ballast dropping and flight terminating controls were operated. The difficulty appeared in the valving operation; in flight #35 as a result of interference from the valve motor and in flight #41 as a result of interference of the fourth harmonic of the 1638 kc telemetering transmitter.

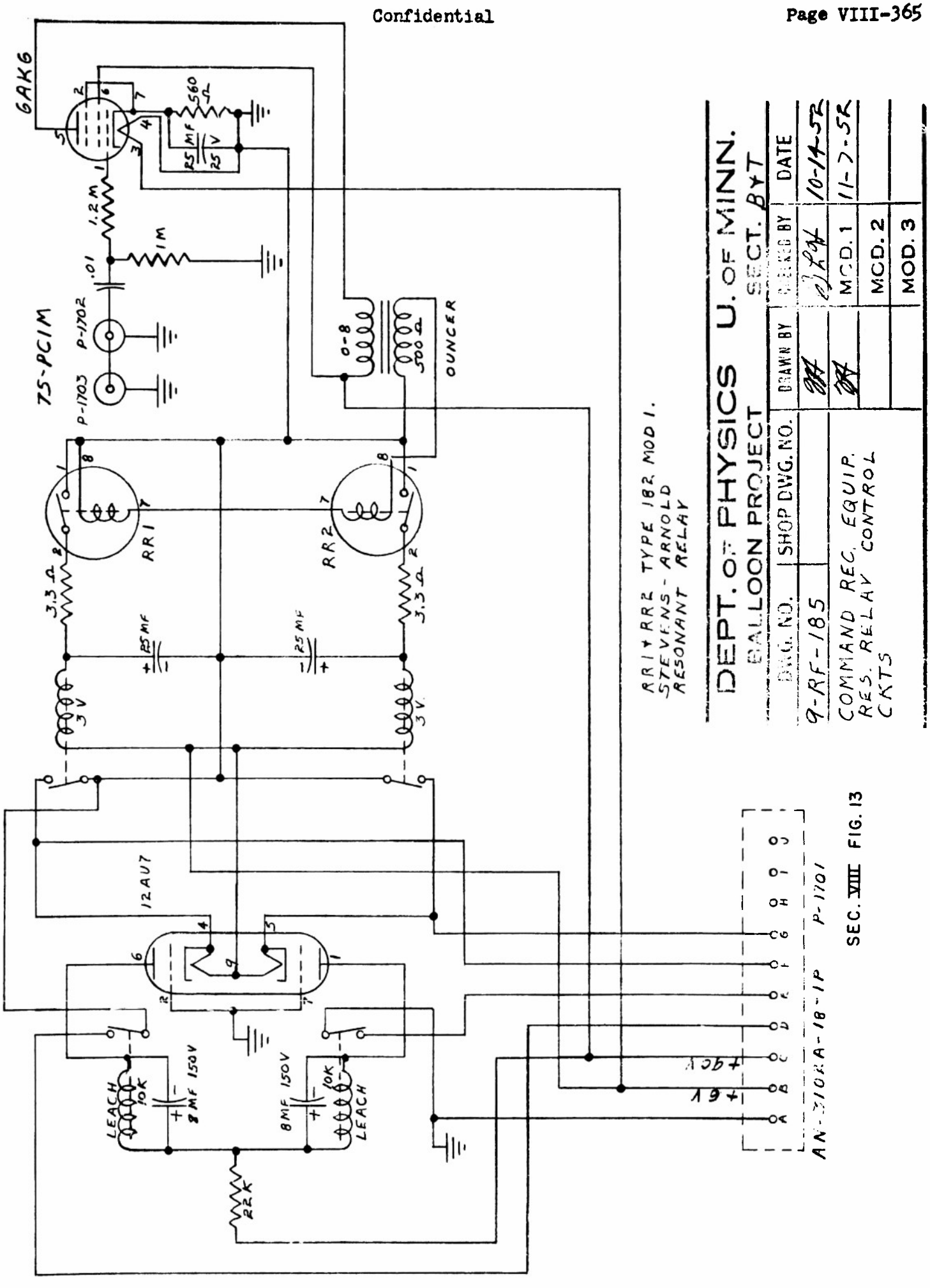

DEPT. OF PHYSICS U. OF MINN.
BALLOON PROJECT
SECT. BYT

DRG. NO.	SHOP DWG. NO.	DRAWN BY	CHECKED BY	DATE
9-RF-185				10-14-52
			MOD. 1	11-7-52
			MOD. 2	
			MOD. 3	

COMMAND REC. EQUIP.
RES. RELAY CONTROL
CKTS

SEC. VIII FIG. 13

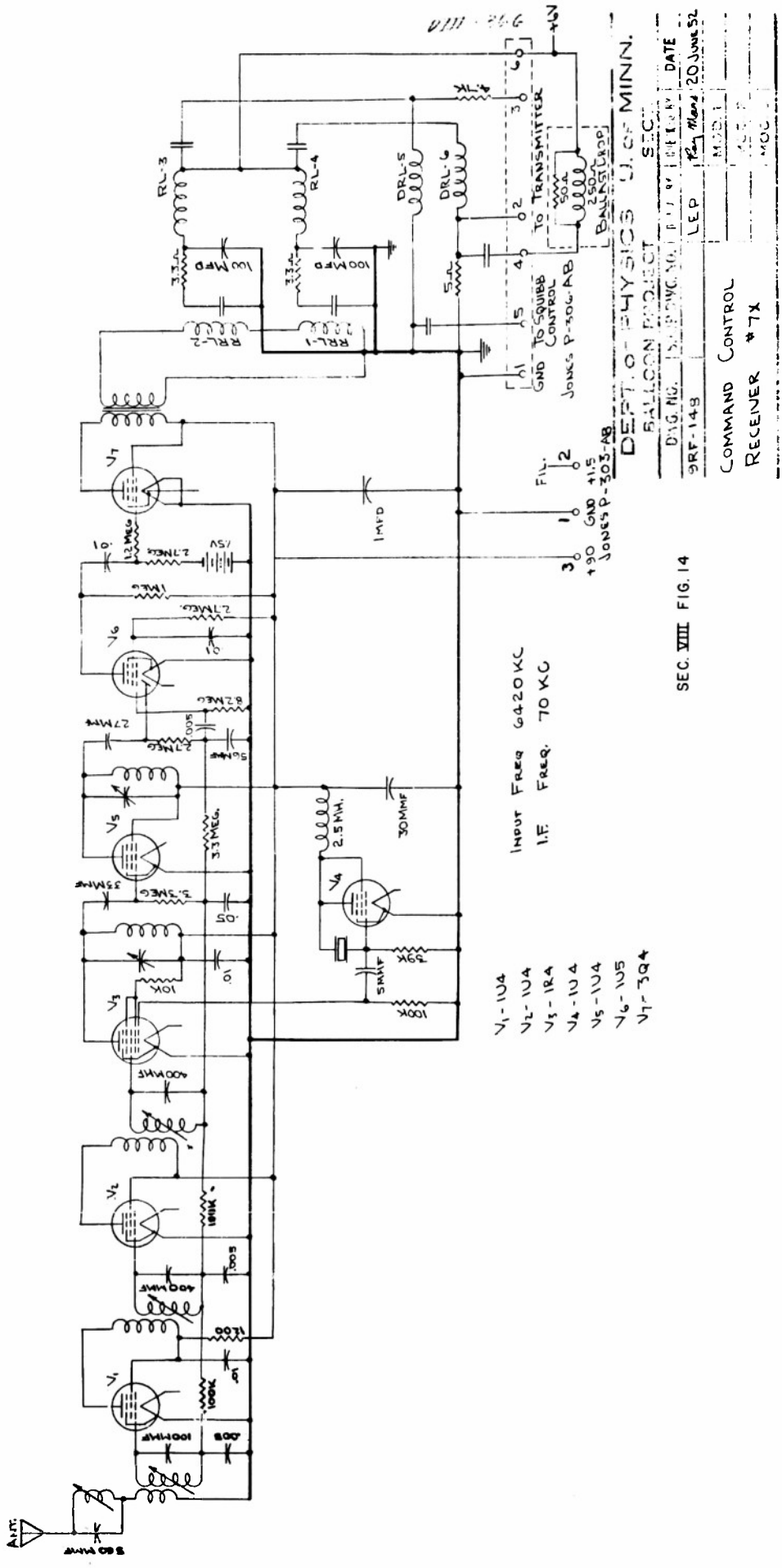
DEPT. OF PHYSICS U. OF MINN.
BALLOON PROJECT
DWG. NO. 9RF-148
DRAWN LEP
DATE 20 June 52
COMMAND CONTROL
RECEIVER #7X
SEC. VIII FIG. 14
INPUT FREQ 6420 KC
I.F. FREQ. 70 KC
V1 - 1U4
V2 - 1U4
V3 - 1R4
V4 - 1U4
V5 - 1U4
V6 - 1U5
V7 - 3Q4
TO TRANSMITTER
TO SQUIBB CONTROL
Jones P-306-AB
Jones P-303-AB
+90
+6V
ANT.

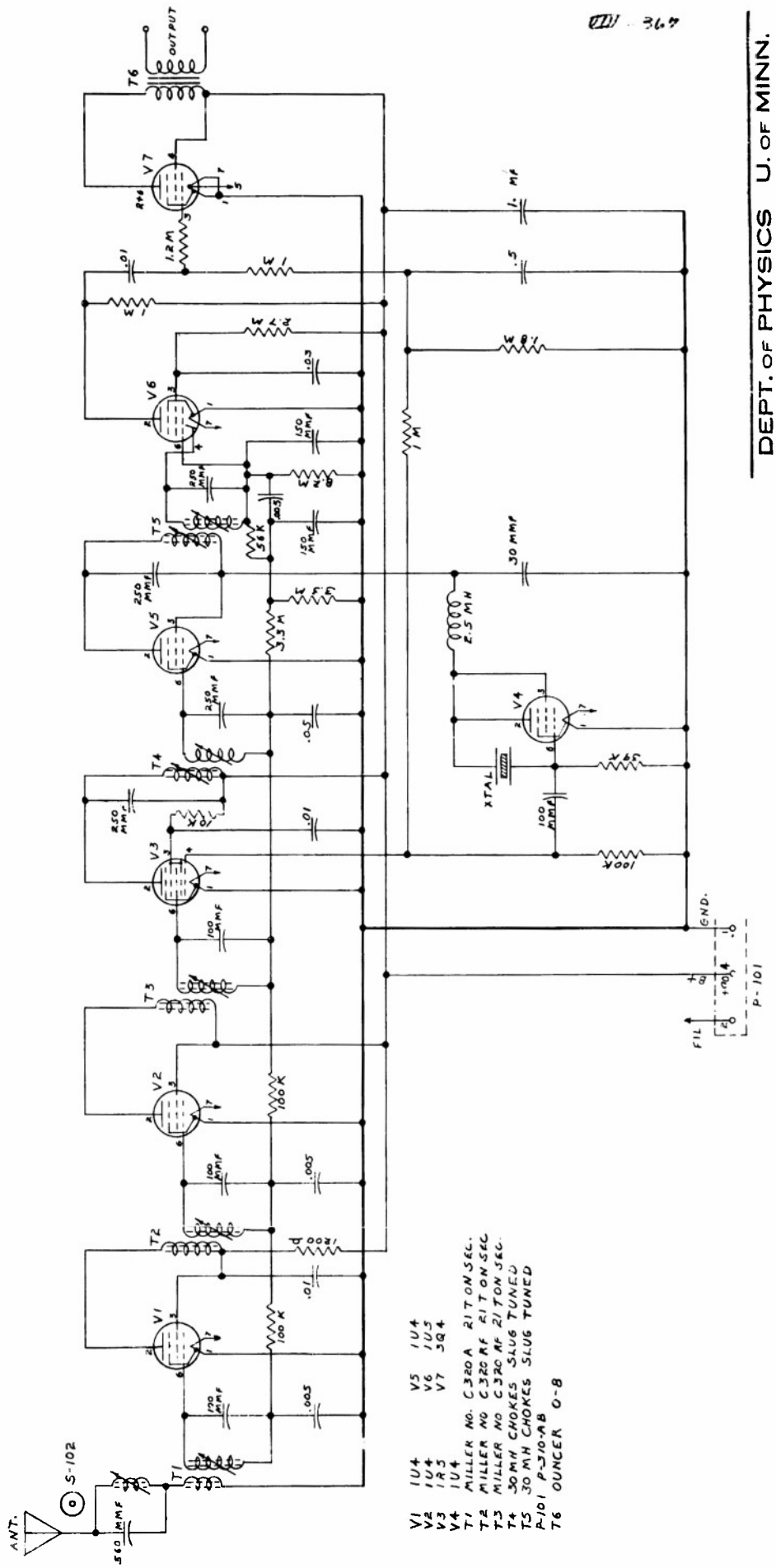
VIII 367
DEPT. OF PHYSICS U. OF MINN.
BALLOON PROJECT
SECT. INS.
DWG. NO. 9-RF-184
SHOP DWG. NO.
DRAWN BY
CHECKED BY
DATE 9-15-52
MOD. 1
MOD. 2
MOD. 3
COMMAND REC. EQUIP. BJ
RECEIVER
SEC. VIII FIG. 15
ANT.
S-102
560 MMF
T1
T2
T3
T4
T5
T6
OUTPUT
V1 1U4
V2 1U4
V3 1R5
V4 1U4
V5 1U4
V6 1U5
V7 3Q4
T1 MILLER NO. C320A 21 TON SEC.
T2 MILLER NO C320 RF 21 TON SEC
T3 MILLER NO C320 AF 21 TON SEC.
T4 30 MH CHOKES SLUG TUNED
T5 30 MH CHOKES SLUG TUNED
P-101 P-310-AB
T6 OUNCER 0-8
XTAL
END.
P-101

No indication of radio control was indicated on flights #24 and #40. In both cases, the first command attempt was made when the balloon was at a range of at least 200 miles and subsequent investigation showed that the power radiated from the ground station antenna, for command, was insufficient for proper operation of the control circuits in the balloon gondola. There were no other flights in this series which indicated receiver failure or improper design.

Therefore to obtain better RF selectivity a new receiver (Figures 16, 17-a,b) was developed. This receiver has a much larger amount of rejection before the first RF amplifier stage and therefore is not as subject to blocking by strong signals off the command frequency. The double-tuned RF coupling circuits are adjusted to be critically coupled which condition results in maximum signal with good frequency selectivity. The selectivity characteristics of a double-tuned RF coupling unit are shown in Figure 18. The intermediate frequency for this receiver was chosen to be 120 kc. The IF transformers are commercially obtainable and the frequency is low enough to obtain the narrow band pass which is necessary for good security of operation in this type of equipment. The audio-frequencies used for control are low, not over 500 cycles, and therefore it is not necessary to have a band pass of greater than 500 cycles. It is desirable, however, to have a low band pass from a standpoint of noise rejection.

The new type receiver was only used on two flights, #51 and #54, in this series. The command control system was not tested in flight due to balloon failures. However, the command system was operated on the ground at Pierre, South Dakota, by a 100 W transmitter at Minneapolis (a distance of 300 miles) and indications were that a good solid command resulted. This receiver, in laboratory checks apparently has the desired characteristics for a command receiver on this frequency range. The overall rejection or band pass characteristics of

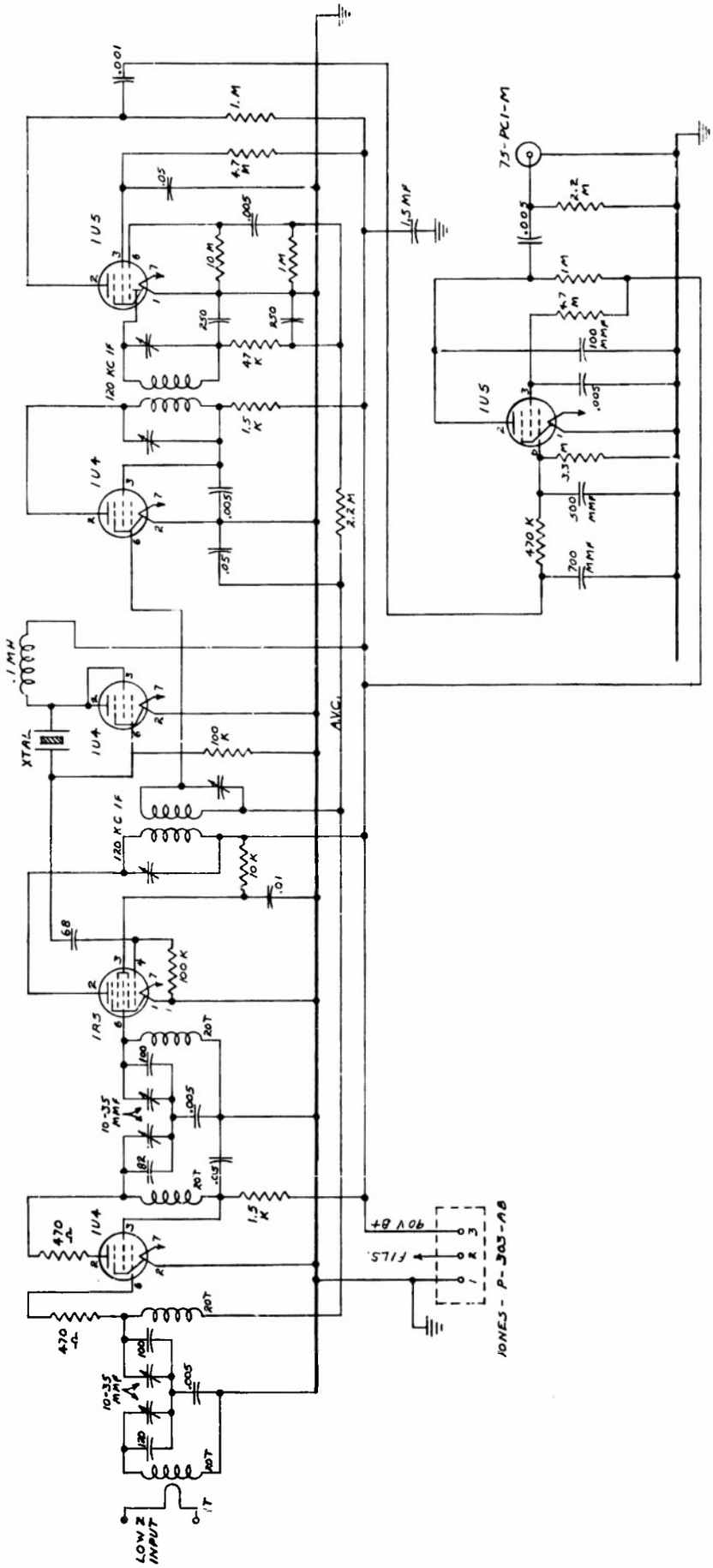
Y-RF-205
COMMAND RECEIVER
H-4-120-21
SEC. VIII FIG. 16
JONES - P-303-AB
LOW Z INPUT
XTAL
AVC
90 V B+
FILS.
120 KC IF
75-PC1-M
1U4
1U5
1R5

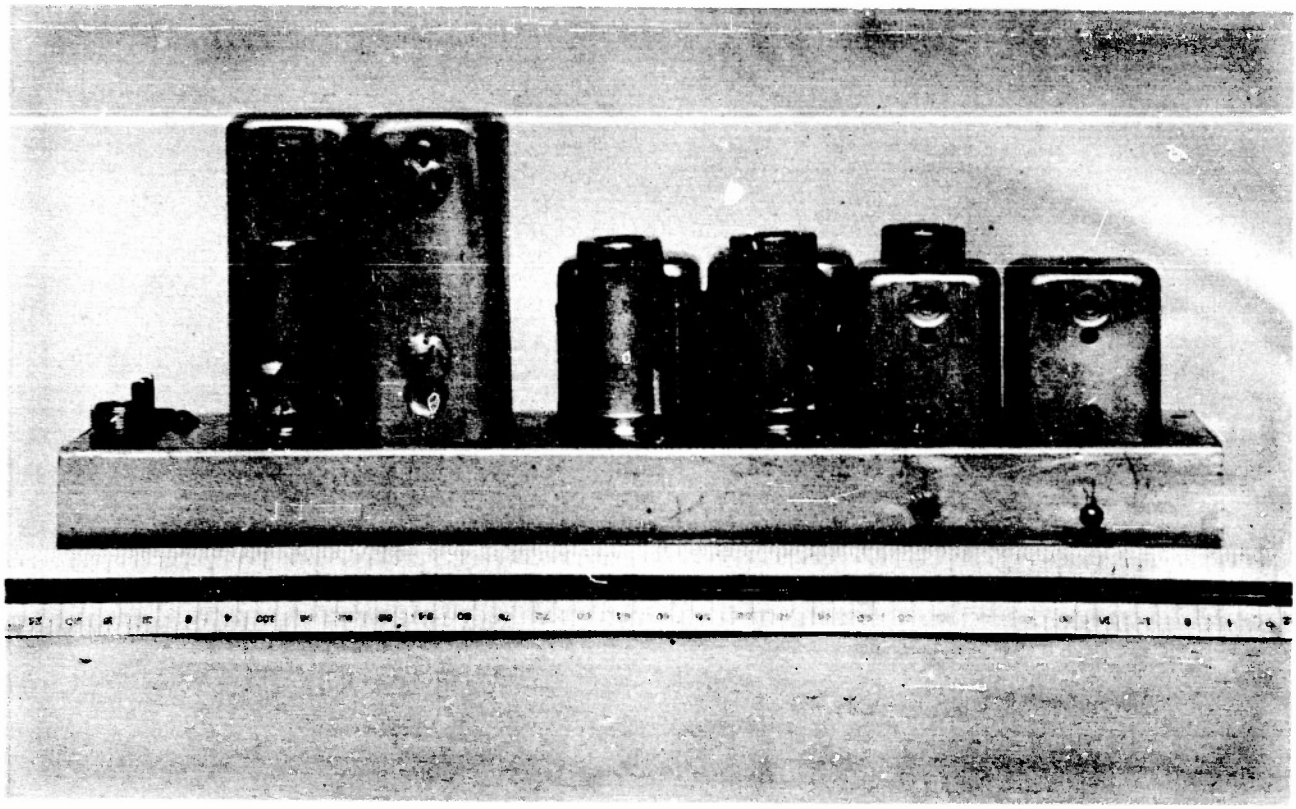

A. Side view

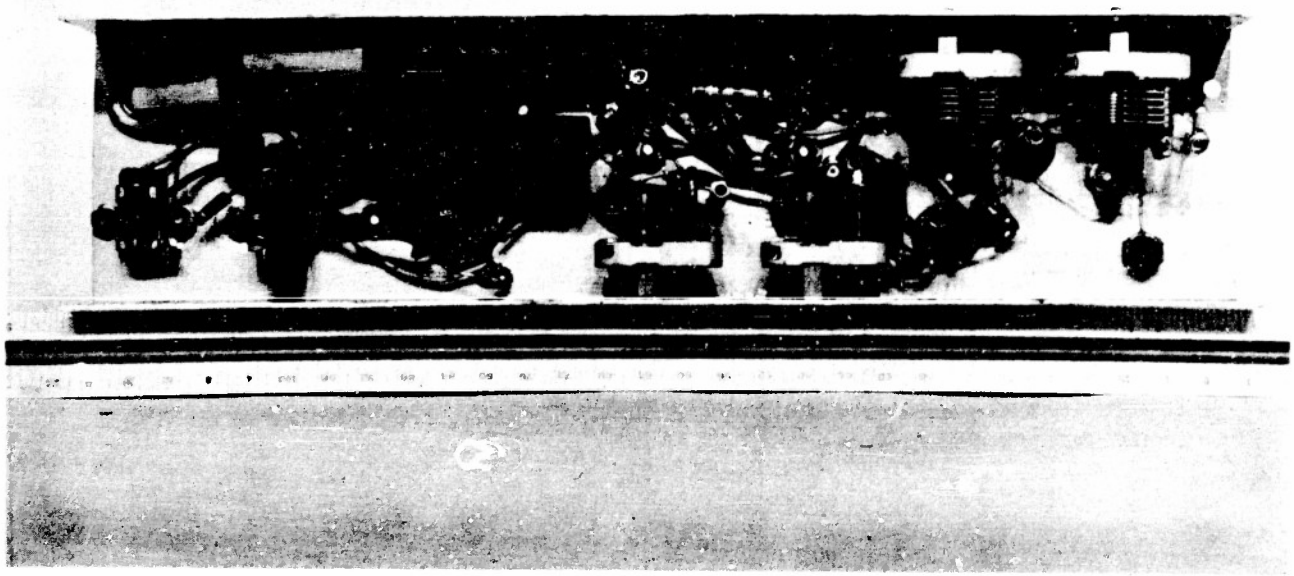

B. Bottom view

Sec VIII Fig 17. 6420 kc, command receiver with double tuned RF coupling.

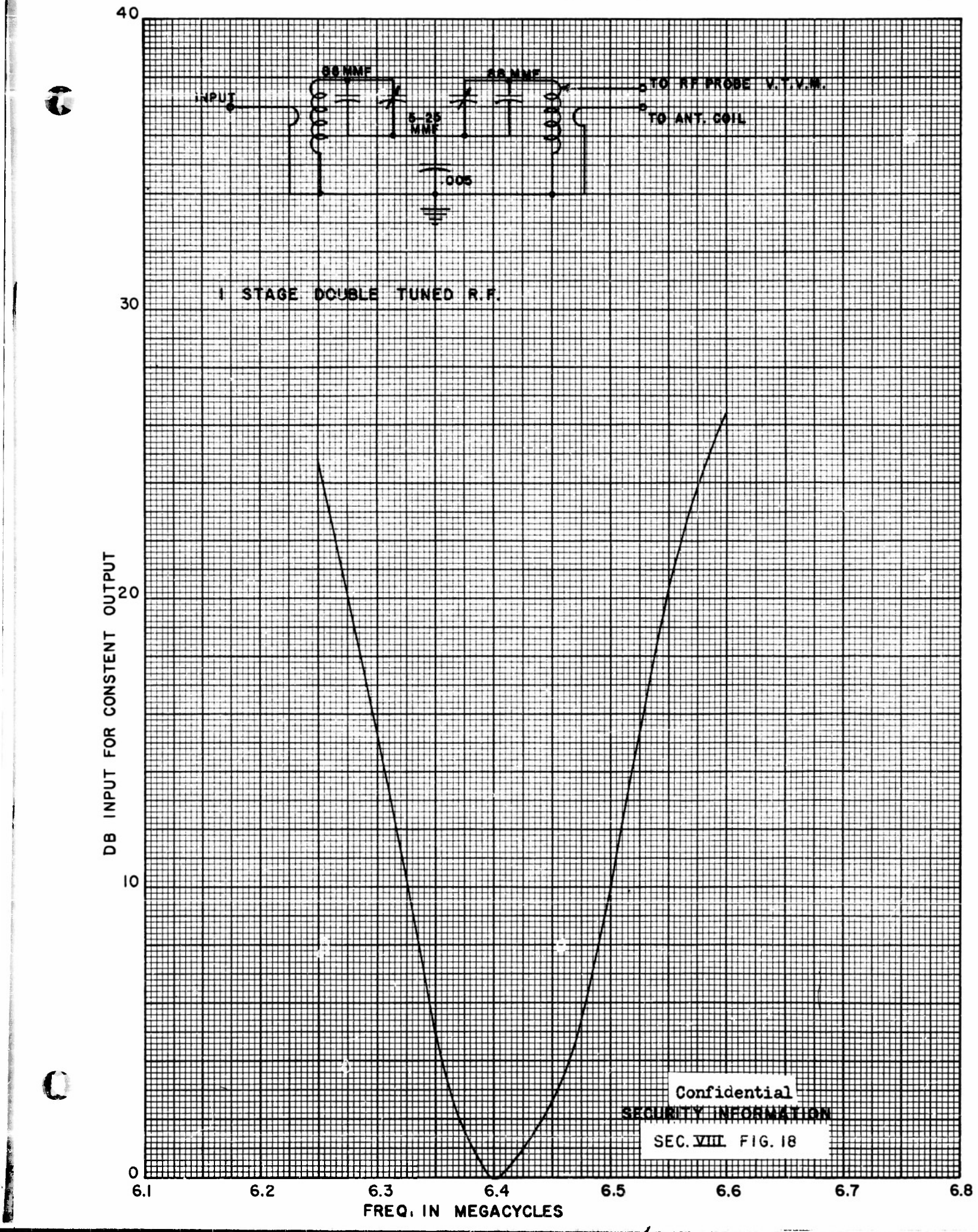
40
30
20
10
0
DB INPUT FOR CONSTENT OUTPUT
6.1
6.2
6.3
6.4
6.5
6.6
6.7
6.8
FREQ. IN MEGACYCLES
INPUT
68 MMF
5-25 MMF
.005
68 MMF
TO RF PROBE V.T.V.M.
TO ANT. COIL
1 STAGE DOUBLE TUNED R.F.
Confidential
SECURITY INFORMATION
SEC. VIII FIG. 18

this receiver are given in Figure 19.

COMMUNICATIONS AND TELEMETERING RECEIVING STATIONS AND EQUIPMENT

At the present time there are two semi-permanent stations which contain communications and receiving equipment. The main station is located at Anoka County Airport in the tower of the University Building. The equipment used at this location includes two receivers used for telemetering (Figures 2-a,b,c) and two communications receivers. One of the communications receivers is an National HRO-50T1 and the other receiver is a Hammerland Super-Pro. The telemetering receivers were constructed in the project with the special circuits described in the telemetering section.

There is also a U.S.N. type DAQ direction finder which is used in conjunction with tracking operations at this station. The DAQ presentation is apparently the only type which is suitable for operation with the pulse-interval telemetering system. AdCock type direction finders do not seem to be fast enough to df on this signal as the maximum pulse length is a matter of three or four seconds. The DAQ equipment, however, is suitable for direction finding and has been used on several occasions.

The transmitting equipment at the Anoka County Station consists of two 100 W transmitters. The modulating and power supply equipment is common to these two units. A transmitter control box in the control room allows the communications operator to choose one of the two assigned communications frequencies (3415 and 6420 kc). The operator is also able to choose the type of modulation by operation of control buttons and switches which choose either the microphone input CW or MCW transmission for code or he can switch in the command tone generator (Figure 20) for use in command operations. The command tone generator is connected into the main transmitter control unit so that the operator can select

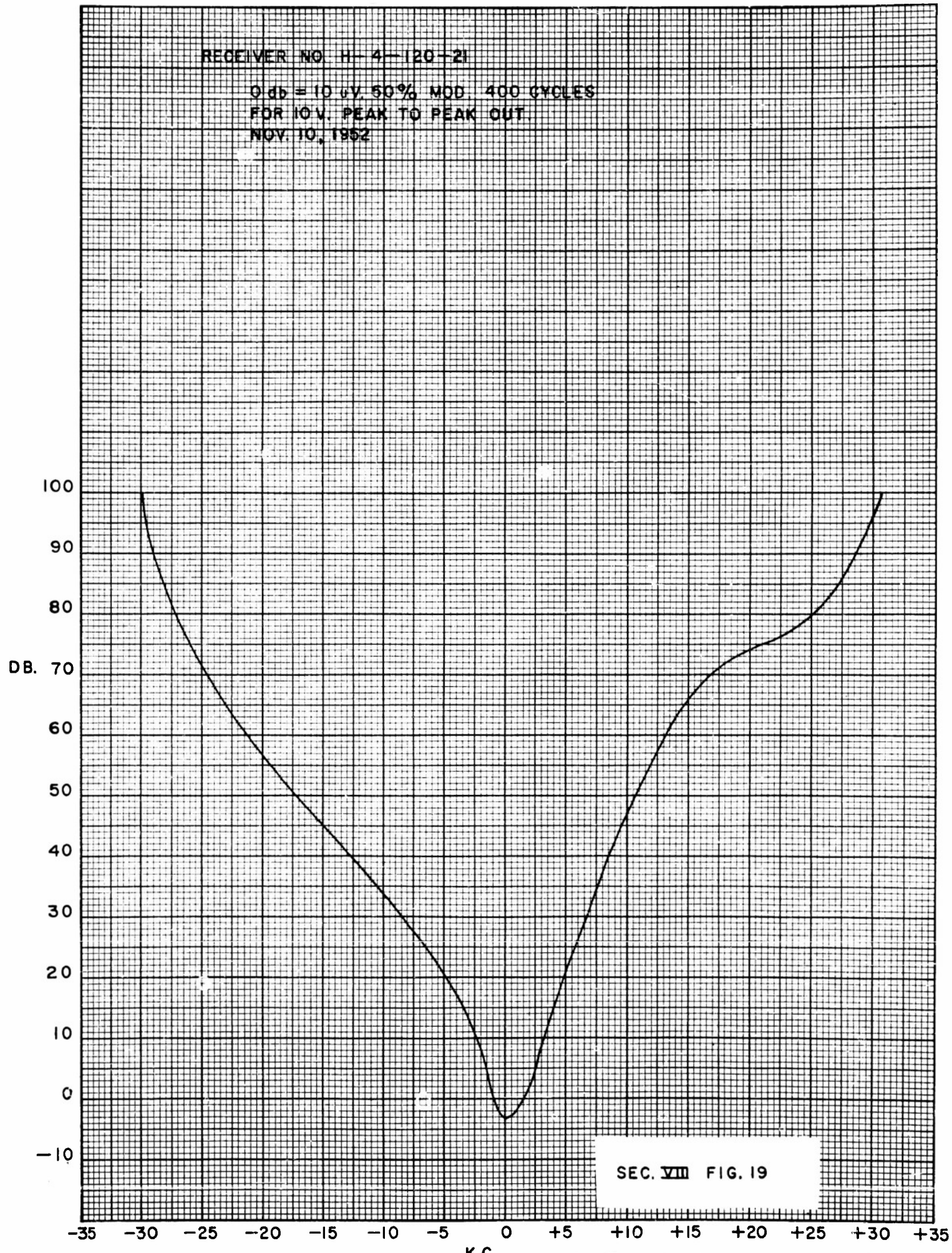
RECEIVER NO. H-4-120-21
0 db = 10 μV. 50% MOD. 400 CYCLES
FOR 10 V. PEAK TO PEAK OUT
NOV. 10, 1952
100
90
80
DB. 70
60
50
40
30
20
10
0
-10
-35 -30 -25 -20 -15 -10 -5 0 +5 +10 +15 +20 +25 +30 +35
KC
SEC. VIII FIG. 19

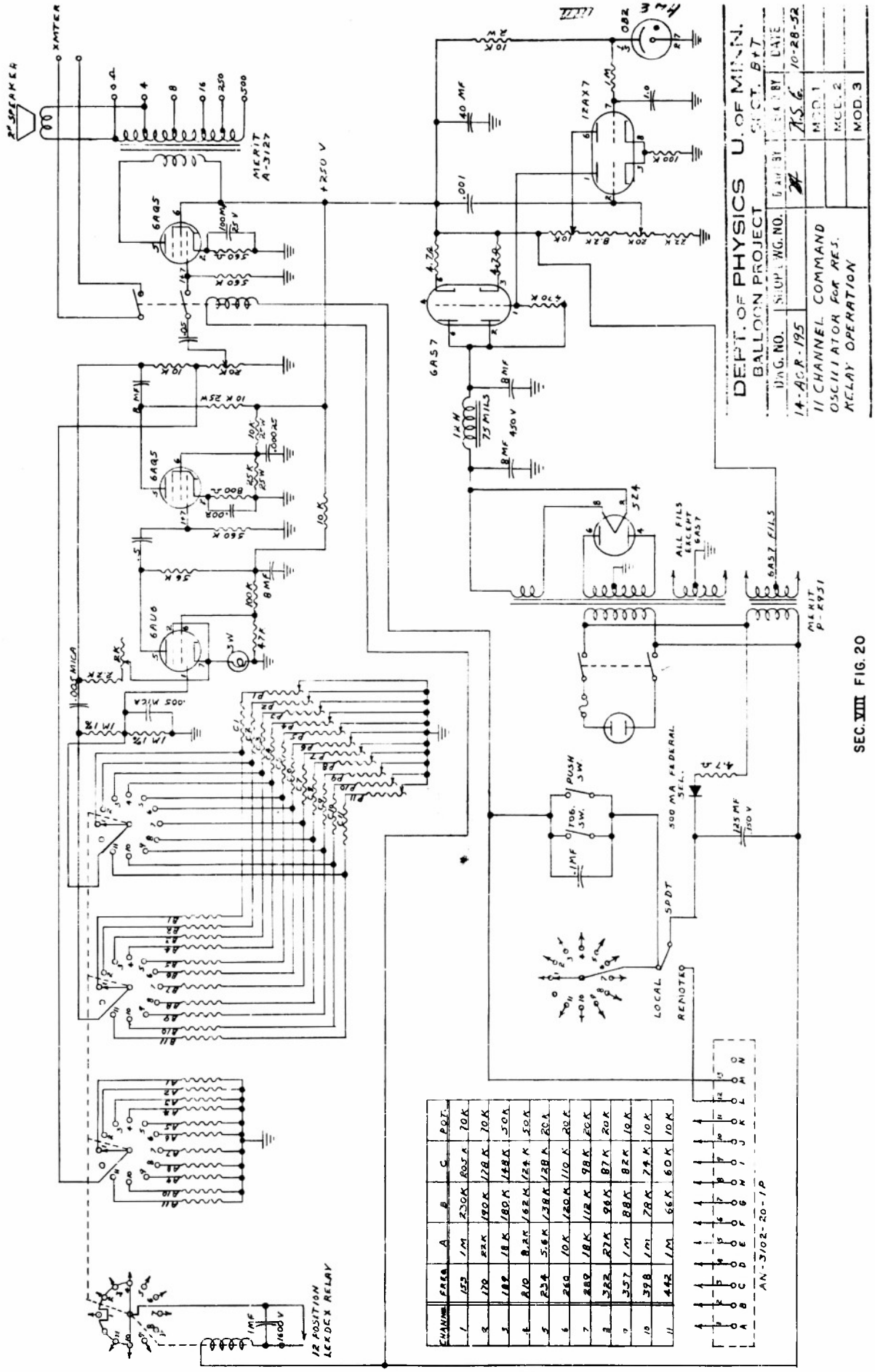

SEC. VIII FIG. 20

the desired audio tone by push-button.

It has been found that operations between Minneapolis and Pierre, South Dakota, require two radio frequencies to maintain a reasonably reliable communications network. The base line distance between Pierre and Minneapolis is so short that 6420 kc is unsuitable at night, due to the skip resulting from the high angle of incidence on the ionosphere. The alternate frequency 3415 kc is suitable from this standpoint for 24 hours a day, as far as ionospheric transmission is concerned, however, it is more subject to attenuation in daylight and the signal strength is normally lower during this period on 3415 kc than it is on 6420 kc. Therefore, both frequencies are necessary for good continuous communications.

The special equipment located at this station consists of the audio-frequency tunable filter (Figure 3) which is described earlier, a Leeds-Northrup Recorder, and a U.S.N. model RCD panoramic receiver which is used, at present, for checking the modulation pattern of the 100 W transmitters.

The other semi-permanent station in use at present is the communications trailor which has been located at Pierre, South Dakota, for a large part of the last series of flights. The receiving equipment in this trailor consists of two telemetering receivers, two communications receivers and a U.S.N. type ARN/7 automatic direction-finding receiver. This ADF unit is suitable for direction finding on our beacon signal if the operator switches from "automatic" to "antenna" when the signal is off and then, during the long pulse of the signal, switches again to "automatic". However, it is not as suitable as the DAQ equipment.

The transmitters installed in the communications trailor include a 750 W transmitter which can be tuned to 3415 or 6420 kc. The tuning from one frequency to the other takes about 15 minutes. There is also a small 3.5 W trans-

ceiver on 6420 kc which is used for testing gondolas and also for short range communication with the trailor. A 40 W emergency transmitter is located in the trailor. This equipment is capable of transmission on 3415 and 6420 kc.

The specialized equipment in this trailor includes the audio-frequency filter described before, a Magnecord tape recorder, a 60 cycle standard frequency generator which is used to run clocks and other timing devices. There is a Leeds-Northrup Speed-O-Max recorder for recording the telemetered data and a command tone generator (Figure 3). A transmitter control unit somewhat similar to that at the Anoka County Station is used in the communications trailor to control the transmitter.

The power supplies in the communications trailor consist of a 10 kw Onan generator which delivers 220 V, 60~,1ϕ. This generator is powered by a 4-cylinder gasoline engine. There is a 60 cycle to 400 cycle converter with an output of 100 W which is used to supply the necessary 400 cycle power for the ARN/7-ADF equipment. A zero to 50 V DC, 25 ampere, rectifier is also located in the trailor. This equipment is necessary for charging batteries and supplying filament voltages for the ARN/7.